REVISIONS TO MIL-F-8785B(ASG) PROPOSED BY CORNELL AERONAUTICAL LABORATORY UNDER CONTRACT F33615-71-C-1254

Charles R. Chalk
Dante A. DiFranco
J. Victor Lebacqz
T. Peter Neal

FOREWORD

This report was prepared for the United States Air Force by Calspan Corporation (formerly Cornell Aeronautical Laboratory, Inc. (CAL)), Buffalo, New York, in partial fulfillment of Contract F33615-71-C-1254, and describes the effort performed under that contract to formulate proposed revisions to MIL-F-8785B(ASG) and to document substantiation data in support of the recommended revision.

The investigation reported here was performed by the Flight Research Department of Calspan under sponsorship of the Air Force Flight Dynamics Laboratory, Wright-Patterson Air Force Base, Ohio, as part of Project 8219, Task 821905. The Air Force Project Engineer was Mr. Frank George (AFFDL/FGC).

This report represents the combined efforts of several members of the Flight Research Department. The project was performed under the supervision of Mr. Charles R. Chalk. The major contributions of each of the listed authors were as follows:

C. R. Chalk	Sections II, III, V, VI, Appendixes I, II
D. A. DiFranco	Section I
J. V. Lebacqz	Section VII
T. P. Neal	Section II

This report was submitted by the authors in August 1972, and is being published as Calspan Report No. BM-3054-F-1.

This report has been reviewed and is approved.

C. B. WESTBROOK
Chief, Control Criteria Branch
Air Force Flight Dynamics Laboratory

ABSTRACT

In August 1969, the Air Force and the Naval Air Systems Command adopted MIL-F-8785B(ASG) as the official Military Specification for Flying Qualities of Piloted Airplanes. Since that time effort has been sponsored by the Air Force to further improve the specification document and to increase its applicability in the development of future weapons systems. Results of a study performed by Calspan (formerly Cornell Aeronautical Laboratory) are presented in this report. Changes to the requirements of MIL-F-8785B(ASG) are suggested in the following areas:

1. Longitudinal maneuvering dynamics and control gradients.
2. Lateral-directional maneuvering dynamics and roll-sideslip coupling.
3. Atmospheric disturbance models.
4. Stall-spin characteristics.
5. Numerous miscellaneous corrections and changes.
6. Additions to Background Information and Users Guide for MIL-F-8785B(ASG).

Substantiation data for the recommended changes is also presented.

TABLE OF CONTENTS

LIST OF ILLUSTRATIONS

LIST OF ILLUSTRATIONS (con't.)

LIST OF ILLUSTRATIONS (con't.)

LIST OF ILLUSTRATIONS (con't.)

LIST OF ILLUSTRATIONS (con't.)

LIST OF ILLUSTRATIONS (con't.)

INTRODUCTION

In January of 1966, the Air Force Flight Dynamics Laboratory (AFFDL) contracted with Cornell Aeronautical Laboratory (CAL) to accomplish a major revision of the Military Specification MIL-F-8785, Flying Qualities of Piloted Airplanes. Reference 1 describes the program performed by CAL in accomplishing the specification revision.

CAL submitted a final draft of "Recommendations for Revision of MIL-F-8785(ASG), Military Specification - Flying Qualities of Piloted Airplanes" in May 1968. This document was modified by the Air Force and Navy to produce MIL-F-008785A(USAF), dated 31 October 1968, and after further minor modification it was subsequently published in August 1969 by the Aeronautical Standards Group as MIL-F-8785B(ASG) (Reference 2). In support of the new specification, CAL also submitted the final draft of Background Information and User Guide for Military Specification MIL-F-8785B(ASG), "Flying Qualities of Piloted Airplanes" in January 1969. The final version of this document was published in August 1969 as AFFDL-TR-69-72, Reference 3.

Since July 1969, FDL has continued in-house work on improving the content and accuracy of MIL-F-8785. In addition FDL has sponsored contract work with McDonnell-Douglas and Northrop Aircraft Corporations to compare the F-4 and the F-5 aircraft with the requirements of MIL-F-8785B(ASG). Contracts have also been awarded to Systems Technology, Inc. and CAL for further development of the specification document. The objective of these follow-on efforts is to:

a) Substantiate and refine existing requirements

b) Define requirements in new forms and in terms of new parameters where advantageous

c) Specify requirements that represent better than minimum acceptable characteristics

d) Replace qualitative requirements

e) Establish requirements that cover problem areas not presently included in the current specification to increase its applicability in the development of future weapon systems and to take into account the influence of expanded mission capabilities on flying qualities requirements.

Additionally, the results of experimental and analytical flying qualities investigations are continually becoming available.

This report documents the results of the work performed by CAL under Contract F33615-71-C-1254 during the period January 1971 through August 1972. A project planning document, Reference 4, was submitted to FDL in February 1971.

The work performed by CAL during this program was directed at the following areas:

1. Assist the Air Force in-house effort to revise the parts of MIL-F-8785 dealing with characteristics at high angle of attack associated with stall, post-stall and spin. Review the proposed specification MIL-S-83691 "Stall/Post-Stall/Spin Flight Test Demonstration Requirements for Airplanes."

2. Recommend specification changes related to several specific paragraphs discussed at the project planning meeting held on 11-12 February 1971.

3. Develop new requirements for longitudinal maneuvering dynamics that do not depend on identifying short period modal parameters and are applicable to airplanes with significant control system dynamics.

4. Develop a new analytical approach to piloted control of airplane flight path and airspeed during the Landing Approach Flight Phase (reported separately in Reference 5).

5. Compare recent lateral-directional flying qualities data with the requirements of MIL-F-8785B(ASG) and recommend revisions to these requirements. The majority of this effort was directed at the requirements that limit roll-sideslip coupling resulting from the pilot's use of aileron.

6. Propose corrections and additions to Section 3.7, Atmospheric Turbulence Disturbances, together with revisions of the substantiation material of Reference 3.

Part of the work accomplished during the project was documented in project memorandums, References 5, 6, and 7, which were submitted to the Air Force shortly after each study was completed.

Each major task undertaken is reported in the following sections of this report. Sections I through IX of the report are organized in parallel with the Table of Contents of MIL-F-8785B(ASG). Within each of these major sections, the material is arranged in the following form:

- List paragraph numbers from MIL-F-8785B(ASG) dated 7 August 1969 and note action recommended.
- List the proposed new paragraphs if changes are recommended.
- Introduction and motivation for recommended revisions.
- Discussion of the proposed requirements.
- Presentation of substantiation information and data.

Section I

PROPOSED REVISIONS TO 3.1, GENERAL REQUIREMENTS

Action Recommended for Subparagraphs to 3.1

No change to requirement. Addition to Background Information and User Guide.

Proposed New Requirements

None.

Introduction and Motivation for Recommended Action

Although no changes to the requirement paragraphs of Section 3.1 are being recommended, material is presented for incorporation in the Background Information and User's Guide for paragraph 3.1.10, Application of Levels. It is proposed that the material contained in the present discussion of Paragraph 3.1.10 in Reference 3 be retained with some minor modifications as indicated below. It is felt that this information is of general interest and useful in understanding the basic philosophy behind the Level concept and in general how it should be applied in airplane design. In addition, a considerable new body of background information is recommended for inclusion that should prove useful in applying Paragraph 3.1.10.2, Requirements for Airplane Failure States. The analysis of airplane Failure States, failure probabilities, degradations in flying qualities Levels, and the probability of encountering such degraded Levels is a complex problem. The new background material presents a specific outline for failure analysis that interrelates the many factors involved. Suggestions are also made on the "bookkeeping" required and the simplifications that are possible in a meaningful yet tractable analysis. Since these are proposed revisions to the Background Information and User's Guide, the references and reference numbers presented in the discussion are those in the User's Guide and not those that appear in this report.

Discussion and Substantiation

Concept

No changes.

Numerical Probabilities

No changes.

Implementation

Change the title of the discussion under "Implementation" from "Implementation" to "Implementation -- A General Discussion", and revise the discussion as follows.

Implementation -- A General Discussion

Implementation of the Level concept involves both reliability analyses (to predict failure probabilities) and failure effect analyses (to insure compliance with requirements). Both types of analyses are in direct accord with, and in the spirit of, MIL-STD-756A (reliability prediction) and MIL-S-38130A (safety engineering). These related specifications are, in turn, mandatory for use by all Departments and Agencies of the Department of Defense. Implementation of the flying qualities specification is, for the most part, a union of the work required by these related specifications with normal stability and control analysis.

Failure States influence the airplane configurations, and even the mission Flight Phases, to be considered. All failures must be examined which could have occurred previously, as well as all failures which might occur during the Flight Phase being analyzed. For example, failure of the wings to sweep forward during descent would require consideration of a wings-aft landing that otherwise would never be encountered. There are failures that would always result in an aborted mission, even in a war emergency. The pertinent Flight Phases after such failures would be those required to complete the aborted (rather than the planned) mission. For example, failure of the flaps to retract after takeoff might mean a landing with flaps at the take-off setting, with certain unexpended external stores; but supersonic cruises would be impossible. If the mission might be either continued or aborted, both contingencies need to be examined.

There are some special requirements pertaining to failure of the engines and the flight control system. For these special requirements the pertinent failure is assumed to occur (with a probability of 1), with other failures considered at their own probabilities. For all other requirements, the actual probabilities of engine and flight control system failure are to be accounted for in the same manner as for other failures.

Some specific Special Failure States (3.1.6.2.1) may be approved "a priori" by the procuring activity before any failure analysis is undertaken by the contractor. Additional Special Failure States may be approved based on their low probability of occurrence after preliminary and detailed failure analysis by the contractor. Special Failure States need not be considered in determining the probability of encountering degradation to Level 2, Level 3, or below Level 3. This allows particular failures to be considered based on their catastrophic effects, their probability of occurrence, or both. It also makes it possible to rationally limit the number of Failure States to be considered in analyzing failures and their effects on handling qualities. Requiring approval for each Special Failure State gives the procuring activity an opportunity to examine all the pertinent survivability, vulnerability, and probability aspects of each design. Survivability and vulnerability are important considerations, but it has not yet been possible to relate any specific flying qualities requirements to them.

A typical approach (but not the only one) for the system contractor is outlined in a general way below:

Initial Design: The basic airframe is designed for a Level 1 "target" in respect to most flying qualities in the Operational Flight Envelope. It may quickly become apparent that some design penalties would be inordinate (perhaps to provide sufficient aerodynamic damping of the short-period and Dutch-roll modes at high altitude); in those cases the basic-airframe "target" would be shifted to Level 2. In other cases it may be relatively painless to extend some Level 1 flying qualities over the wider range of the Service Flight Envelope. Generally the design will result in Level 1 flying qualities in some regions and, perhaps, Level 2 or Level 3 in others. Augmentation of one form or another (aerodynamic configuration changes, response feedback, control feedforward, signal shaping, etc.) would be incorporated to bring flying qualities up to Level 1 in the Operational Flight Envelope and to Level 2 in the Service Flight Envelope.

Initial Evaluation: The reliability and failure mode analyses are next performed to evaluate the nominal system design evolved above. All aircraft subsystem failures that affect flying qualities are considered. Failure rate data for these analyses may be those specified in the related specifications, other data with supporting substantiation and approval as necessary, or specific values provided by the procuring agency. Prediction methods used will be in accordance with related specifications. The results of this evaluation will provide: a) a detailed outline of design points that are critical from a flying qualities/flight safety standpoint, b) quantitative predictions of the probability of encountering Level 2 in a single flight within the Operational Envelope, Level 3 in the Operational Envelope, and Level 3 in the Service Envelope, and c) recommend airframe/equipment changes to improve flying qualities or increase subsystem reliability to meet the specification requirements. It should be noted that the flying qualities/flight safety requirements are concerned with failure mode effects, while other specifications provide reliability requirements per se (all failures regardless of failure effects). In the event of a conflict, the most stringent requirement should apply.

Re-evaluation: As the system design progresses, the initial evaluation is revised at intervals. This process continues throughout the design phase.

The results of the analyses of vehicle flying qualities/flight safety may be used directly to: a) establish flight test points that are critical and should be emphasized in the flight test program, b) establish pilot training requirements for the most probable, and critical, flight conditions, and c) provide guidance and requirements for other subsystem designs. Proof of compliance is, for the most part, analytical in nature as far as probabilities of failure are concerned. However, some equipment failure rate data

may become available during final design phases and during flight test, and any data from these or other test programs should be used to further demonstrate compliance. Stability and control data of the usual type (e.g., predictions, wind tunnel, flight test) will also be used to demonstrate compliance. Finally, the results of all analyses and tests will be subject to normal procedures of procuring agency approval.

In summary, the Level concept was evolved in recognition of the obvious fact that flying qualities, flight safety, and system reliability are all very much related in the development of current piloted aircraft. This interrelationship is being exploited to improve aircraft in terms of overall effectiveness. The net result can be system improvement with a minimum expenditure of effort. Examples of approaches to these interrelationships are presented in References J68, J69, J70 and J71.

Additional general insight into failures, failure probabilities, and their effects on the probabilities of encountering various degraded Levels of flying qualities is given in the Notes of Reference A1 (Paragraph 6.7). These are repeated here since they are of some significance to this general discussion.

"6.7 Application of Levels. Part of the intent of 3.1.10 is to ensure that the probability of encountering significantly degraded flying qualities because of component or subsystem failures is small. For example, the probability of encountering very degraded flying qualities (Level 3) must be less than specified values per flight.

"6.7.1 Theoretical compliance. To determine theoretical compliance with the requirements of 3.1.10.2, the following steps must be performed:

a. Identify those Airplane Failure States which have a significant effect on flying qualities (3.1.6.2).

b. Define the longest flight duration to be encountered during operational missions (3.1.1).

c. Determine the probability of encountering various Airplane Failure States, per flight, based on the above flight duration (3.1.10.2).

d. Determine the degree of flying qualities degradation associated with each Airplane Failure State in terms of Levels as defined in the specific requirements.

e. Determine the most critical Airplane Failure States (assuming the failures are present at whichever point in the Flight Envelope being considered is most critical in a flying qualities sense), and compute the total probability of encountering Level 2 flying qualities in the Operational Flight Envelope due to equipment failures. Likewise, compute the probability of encountering Level 3 qualities in the Operational Flight Envelope, etc.

f. Compare the computed values above with the requirements in 3.1.10.2 and 3.1.10.3. An example which illustrates an approximate estimate of the probabilities of encounter follows: if the failures are all statistically independent, determine the sum of the probabilities of encountering all Airplane Failure States which degrade flying qualities to Level 2 in the Operational Envelope. This sum must be less than 10^{-2} per flight.

If the requirements are not met, the designer must consider alternate courses such as:

a. Improve the airplane flying qualities associated with the more probable Failure States, or

b. Reduce the probability of encountering the more probable Failure States through equipment redesign, redundancy, etc.

Regardless of the probability of encountering any given Airplane Failure States (with the exception of Special Failure States) the flying qualities shall not degrade below Level 3.

"6.7.2 Level definitions. To determine the degradation in flying qualities parameters for a given Airplane Failure State the following definitions are provided:

a. Level 1 is better than or equal to Level 1 boundary, or number, given in section 3.

b. Level 2 is worse than Level 1, but no worse than the Level 2 boundary, or number.

c. Level 3 is worse than Level 2, but no worse than the Level 3 boundary, or number.

When a given boundary, or number, is identified as Level 1 and Level 2, this means that flying qualities outside the boundary conditions shown, or worse than the number given, are at best Level 3 flying qualities. Also, since Level 1 and Level 2 requirements are the same, flying qualities must be within this common boundary, or number, in both the Operational and Service Flight Envelopes for Airplane Normal States (3.1.10.1). Airplane Failure States that represent degradations to Level 3 must, however, be included in the computation of the probability of encountering Level 3 degradations in both the Operational and Service Flight Envelopes. Again degradation beyond the Level 3 boundary is not permitted regardless of component failures.

"6.7.3 Computational assumptions. Assumptions a and b of 3.1.10.2 are somewhat conservative, but they simplify the required computations in 3.1.10.2 and provide a set of workable ground rules for theoretical predictions. The reasons for these assumptions are:

a. '... components and systems are ... operating for a time period per flight equal to the longest operational mission time ...' . Since most component failure data are in terms of failures per flight hour, even though continuous operation may not be typical (e.g., yaw damper on during supersonic flight only), failure probabilities must be predicted on a per flight basis using a 'typical' total flight time. The 'longest operational mission time' as 'typical' is a natural result. If acceptance cycles-to-failure reliability data are available (MIL-STD-756), these data may be used for prediction purposes based on maximum cycles per operational mission, subject to procuring activity approval. In any event, compliance with the requirements of 3.1.10.2, as determined in accordance with Section 4, is based on the probability of encounter per flight.

b. '... failure is assumed to be present at whichever point ... is most critical ...'. This assumption is in keeping with the requirements of 3.1.6.2 regarding Flight Phases subsequent to the actual failure in question. In cases that are unrealistic from the operational standpoint, the specific Airplane Failure States might fall in the Airplane Special Failure State classification (6.1.6.2.1)."

For predicting failure, no account is taken of the likelihood of the different possible flight conditions. A given flight may be entirely within the Operational Flight Envelope or largely outside it, as with practice stalls. The flight may involve many Phases or only a few, as with practice approaches. In view of these factors and normal changes in operational use, it seems impractical in a design specification to apportion time among Flight Phases or other flight conditions for this purpose.

Paragraphs 3.1.10.2.1 through 3.1.10.3.3 enumerate special applications of the Level concept, tailoring it to some special kinds of requirements in Reference A1. Pertinent Requirement paragraphs of Reference A1 to which these special applications of the Level concept apply are listed below:

3.1.10.2.1 Requirements for specific failures.

3.3.9-3.3.9.5, 3.4.9, 3.4.10, 3.5.5-3.5.5.2, 3.4.2.4.1

3.1.10.3.1 Ground operation and terminal Flight Phases.

3.2.3.3-3.2.3.3.2, 3.2.3.4, 3.2.3.4.1, 3.3.7-3.3.7.3, 3.3.9-3.3.9.5, 3.4.1.2

3.1.10.3.2 When Levels are not specified.

Paragraphs too numerous to mention.

3.1.10.3.3 Flight outside the Service Flight Envelope.

3.2.3.6, 3.3.8, 3.4.1-3.4.3.

Implementation of Levels Concepts with Failure States -- A Specific Outline and Suggested Simplification

What has been said up to this point concerning the application of Levels, especially the requirements for airplane Failure States (Paragraph 3.1.10.2), has only been concerned with general concepts, some justification for the numerical probabilities used, and a general discussion of the important factors to be considered in the implementation of the Levels concepts with and without failures.

It is well at first to consider only the application of the Levels concept for airplane Normal States (Paragraph 3.1.10.1). A well planned analysis of flying qualities Levels for airplane Normal States is a basis for the more complex analysis with Failure States. Considering only airplane Normal States it becomes readily apparent that the task is far from trivial, although manageable. In general, each Flight Phase and Normal State of the airplane is associated with an Operational Flight Envelope and a Service Flight Envelope. As indicated by Paragraphs 3.1.7, the boundaries are three dimensional and defined in terms of speed, altitude, and load factor. For all points within the Operational Flight Envelopes, the airplane must be Level 1 for all the flying qualities requirements of Reference A1. Similarly, for points within the Service Flight Envelopes, the airplane must be Level 2.

Compliance with the specification for airplane Normal States must be based on selected design points. As stated in the Quality Assurance Section (Paragraph 4.1) of Reference A1, "the selected design points must be sufficient to allow accurate extrapolation to the other conditions at which the requirements apply." Table XV, Design and Test Conditions Guidelines, can be used as a guide, ..." but the peculiarities of the specific airplane design may require additional or alternate test conditions." In defining airplane Normal States; weights, moments of inertia, center of gravity positions, etc. are factors (see Table XVI in the discussion in Paragraph 3.1.6). Critical loading conditions such as "heaviest weight", "greatest moment of inertia," "most forward c.g.," and "most aft c.g." are suggested for particular requirements and Flight Phases in Table XV. Again, what conditions are likely to be critical from a flying qualities point of view will vary from one design to another, and good engineering judgment in selecting conditions to be evaluated is an essential ingredient.

In the Quality Assurance Section of Reference A1 suggestions are also made for altitudes and special conditions where flying qualities should be investigated for the airplane. These are quoted below as further suggestions on how the investigation of flying qualities in the Operational and Service Flight Envelopes can be bounded and still be adequate.

> "4.3 Design and test conditions
>
> 4.3.1 Altitudes. For terminal Flight Phases, it will normally suffice to examine the selected Airplane States at only one altitude below 10,000 feet (low altitude). For nonterminal Flight Phases, it will normally suffice to examine the selected Airplane

States at one altitude below 10,000 feet or at the lowest operational altitude (low altitude), the maximum operational altitude ($h_{o_{max}}$), and one intermediate altitude. When the maximum operational altitude is above 40,000 feet or when stability or control characteristics vary rapidly with altitude, more intermediate altitudes than shown in Table XV shall be investigated. When the Service Flight Envelope extends far above or below the Operational Flight Envelope, the service-altitude extremes must be considered.

4.3.2 Special conditions. In addition to the flight conditions previously indicated, the speed-altitude combinations that result in the following shall all be investigated, where applicable:

a. Maximum normal acceleration response per degree of elevator deflection

b. Maximum normal acceleration response per pound of stick force

c. Highest dynamic pressure and highest Mach number."

Some of the requirements in the specification are qualitative in nature and are characterized by such expressions as "objectionable flight characteristics," "realistic time delay," "normal pilot technique," etc. Such requirements cannot be tied to Levels and final determination of compliance with such requirements will be made by the procuring activity. Some requirements describe stability and control or flying qualities characteristics required or not permitted and to which no flying qualities Levels are attached. None of these requirements enter into a determination of flying qualities Levels for the airplane. They must be met regardless of whether the airplane is determined to be Level 1, Level 2, or Level 3.

If the analysis of airplane flying qualities for airplane Normal States is formidable, a similar determination for all the Failure States is even more so. For each Normal State the number of Failure States are likely to be many. In addition, each failure must be related to failure effects in terms of the degradation in flying qualities Levels and the probability of encountering degraded Levels in both the Operational and Service Flight Envelopes. A modern airplane design is likely to be extensively augmented through the use of a rather complex flight control system. Such a system will probably consist of considerable electronic, hydraulic, and mechanical equipment. As many as 100 Failure States for each Normal State is not an unlikely number. One might conclude therefore that flying qualities analysis in such a situation is likely to be 100 times more complex than the analysis for airplane Normal States. In addition, the probability of encountering each failure and each degraded flying qualities Level must also be determined to satisfy Paragraph 3.1.10.2. It may be that the 100 Failure States can be reduced to 10 Failure Modes, i.e., failures with the same effect on stability and control and flying qualities are combined into the same Failure Mode. A combination of only 10 Failure Modes, 50 flying qualities requirements to be checked, and 200 flight conditions within the Operational and Service Flight Envelopes will still result in 100,000 cases to be analyzed for failures and the effects of failures on the probability of encountering degraded Levels.

An outline of what is involved in meeting the requirement of Paragraph 3.1.10.2 on failures and failure effects is therefore desirable. Such an outline should consider all the factors involved, the "bookkeeping" that may be necessary, and what simplifications are possible in a reasonably thorough yet tractable failure investigation.

An analysis of failures and the effects of failures on flying qualities has many interrelated facets. It seems worthwhile, therefore, to prepare some block diagrams that exhibit the relationships between the important factors so that by glancing at them, an overall perspective can be maintained.

Figure 1 is an overall diagram outlining the conduct of flying qualities analysis. Note that application of MIL-F-8785B is central to this diagram. Briefly, it shows that a mission has certain Flight Phases and Flight Phase Categories associated with it. Each Flight Phase has an Operational Flight Envelope and at least one Normal State. For each Normal State there is an associated Service Flight Envelope. These envelopes and Normal States are necessary for applying MIL-F-8785B(ASG) which specifies that for Normal States flying qualities shall be Level 1 in the Operational Flight Envelopes and may be Level 2 in the Service Flight Envelopes. Failure analysis begins with a knowledge of the Normal States and involves the process of selecting Failure States for flying qualities analysis and grouping these failures into Failure Modes based on the effects of the failures. Certain failures are classified as Special Failure States and eliminated from further analysis. MIL-F-8785B is again applied and the Levels of flying qualities and the probabilities associated with the Failure Modes can be determined and organized so that the overall effects of failures on flying qualities are clearly evident.

Flying qualities below Level 3 (L3-) are not allowed by MIL-F-8785B(ASG) in either the Operational or Service Flight Envelopes. In addition, certain detrimental stability and control and flying qualities effects are not permitted by certain requirements. Figure 1 provides a means for tabulating the probability of occurrence of below Level 3 (L3-) and not permitted degradations in order to aid the contractor and procuring activity in assessing the acceptability of the overall design from all standpoints. What urgent actions may be required, if any, to make the design acceptable to the procuring activity will be a strong function of probability of occurrence of all Levels after failures and how they compare to the requirements in Paragraph 3.1.10.2. For example, failures that degrade handling qualities below Level 3 may be allowed by the procuring activity when their probability of occurrence is sufficiently small such that these failures are acceptable as Special Failure States.

Figure 2 elaborates on the block of Figure 1 titled "Failure Analysis". It indicates that a reasonable selection process should be carried out in order to determine which Failure States will be considered for flying qualities analysis. This process in general requires that both single and multiple Failure States within a given subsystem and between various subsystems should be evaluated against a rationale based on a combination of engineering judgment and the results of reliability analysis. A primary objective of this overall process is to select a sufficient number of Failure States to make a failure effects analysis valid while at the same time keeping the process tractable. It is not necessary

to consider each Failure State separately. Failure States will be combined into the same Failure Modes when the Failure effects in terms of flying qualities are the same. Each Failure Mode is then related to flying qualities by the application of MIL-F-8785B(ASG). Some Failure States may be designated as Special Failure States based on their low probability of occurrence per flight independent of the effects of the failures in flying qualities Levels.

Figure 3 elaborates on the block in Figure 1 titled "Application of MIL-F-8785B(ASG)". It indicates that with a basic knowledge of an airplane's Flight Envelopes and stability and control characteristics, it should be possible: (1) to select the more critical requirements and flight conditions applicable to a given Failure Mode and (2) to evaluate the Levels of flying qualities that result for each Failure Mode as determined by analysis.

An outline of a program for failure analysis, based on the block diagram, is now presented. This outline includes some items that are required by MIL-F-8785B in assessing the flying qualities of an airplane in general as well as an adequate assessment of flying qualities with Failure States. They are included here for completeness and to indicate the interrelationships of all aspects of flying qualities analysis, with and without failures. This outline includes some important details that are not evident from an examination of the block diagrams just presented. Some of these details will be elaborated upon after the outline is presented.

AN OUTLINE OF FAILURE AND FAILURE EFFECTS ANALYSIS TO MEET THE REQUIREMENTS OF PARAGRAPH 3.1.10.2

1.0 Define the basic missions of the airplane, and the Flight Phases associated with each mission.

1.1 Group Flight Phases in Category A, B, and C for each mission.

2.0 For each Flight Phase of a mission establish Flight Envelopes.

2.1 Establish Flight Envelopes (Operational, Service, and Permissible) in terms of velocity (Mach No.), altitude, and normal load factor.

3.0 Define the Normal States for all the Flight Phases of each Mission.

3.1 Normal States for each Flight Phase are determined by the airplane configuration as defined by State parameters such as weight, c.g., external stores, high lift devices, wing sweep, wing incidence, landing gear, speed brakes, bombing or cargo doors, stability augmentation, etc.

4.0 Group the Flight Phases into Flight Phase Categories with the same Normal States

4.1 Flight Phases in Category A grouped according to the same Normal States

4.2 Flight Phases in Category B grouped according to the same Normal States

4.3 Flight Phases in Category C grouped according to the same Normal States

5.0 Identification of Subsystems for Detailed Failure Analysis

5.1 For a given Flight Phase Category with the same Normal States, define the Subsystems to be used in Failure Analysis

5.1.1 Examples of Subsystems used in Failure Analysis

a. Fuel Sequencing Subsystem
b. Variable Sweep Mechanism Subsystem
c. Flap Actuation Subsystem
d. Engine Subsystem
e. Landing Gear Mechanism Subsystem
f. Flight Control Subsystem
   (1) Primary Flight Control System
   (2) Secondary Flight Control System

5.1.2 Define those Subsystems that are not to be considered in failure analysis, due to single or multiple failures in the subsystem - all failures of the Subsystem are therefore allowed as Special Failure States

a. Give reasons for selecting all failures of a given subsystem as Special Failure States

(1) Example

(a) Probability of occurrence of all failures per flight is extremely low ($<<$ 10^{-4}), or the probability is considered to be extremely low, but the numerical value is unknown

5.1.3 Prepare a block diagram of each Subsystem to be considered in Failure Analysis

a. On each block diagram show each component to be considered in failure analysis with its probability of failure per flight designated

6.0 Rationale for Selecting Complete Subsystems to be Considered in Failure Analysis

6.1 Determine Total Probability of Failures in any subsystem. Included in this total probability of failure of a subsystem are single failures and all possible combinations of multiple failures of components in the subsystem

6.1.1 Eliminate those subsystems that have a very low total probability of failures per flight, $<< 10^{-4}$, and therefore can justifiably be considered as Special Failure States

6.2 Based on Total Probability of Failure of each subsystem, determine the probability of the occurrence of Multiple-Subsystem Failures per flight, two or more subsystems

6.2.1 Eliminate those multiple subsystem failures that have a low probability of occurrence per flight, $<< 10^{-4}$, and therefore can justifiably be considered as Special Failure States

6.3 Categorize all single and multiple failures of subsystem combinations that should be considered in Failure Analysis

7.0 Rationale for Selecting Subsystem Components to be Considered in Failure Analysis

7.1 Determine single and multiple component failure probabilities within all subsystems

7.1.1 Eliminate those single and multiple component failures within any subsystem that have a very low probability of occurring per flight ($<< 10^{-4}$) and can be considered as Special Failure States

7.2 Categorize all single and multiple failure combinations within each subsystem that are to be considered in Failure Analysis

8.0 Selection of Failure Modes to be Considered in Analyzing the Effects of Failures on Flying Qualities

8.1 Arrange Failures according to Failure Modes based on failure effects -- Describe effects quantitatively

8.1.1 Examples of failure effects

a. Effect on c.g. location
b. Effect on Wing Sweep Position
c. Effect on Augmentation Gains
d. Effect on Control Authority
e. Effect on Control Rate
f. Effect on Control Hinge Moment
g. Effect on Symmetric and Asymmetric Control Motions

8.2 This tabulation will include no Failure Mode whose probability of occurrence per flight is $<< 10^{-4}$ and therefore can be considered a Special Failure State

8.3 Arrange Failure Modes in order of their probability of occurrence -- most probable first

8.4 Arrange Failure Modes according to their possible effects on Handling Qualities -- those Failure Modes with the greatest effects first

8.5 From a consideration of 8.2, 8.3, and 8.4, select those Failure Modes to be considered in determining the effects of Failures on handling qualities Levels.

9.0 For Each Failure Mode Applicable to a Particular Flight Phase Category, Define Those Flying Qualities Affected by the Failure

9.1 List the flying qualities affected by the failure in order of their importance

9.1.1 Flying qualities likely to degrade the most, in terms of Level, first

9.1.2 All other things being equal, quantitative requirements that can be easily checked before qualitative requirements

9.2 For a particular Failure Mode and Flight Phase, define the flying qualities to be used in analyzing the effects of failures on flying qualities and flying qualities Levels

10.0 For a Particular Failure Mode, Flight Phase Category, and Flying Quality, Define Those Parts of the Flight Envelope Where the Particular Flying Quality Requirement is to be Checked

10.1 Use the analysis of flying qualities for airplane Normal States within the Flight Envelopes, for that particular Flight Phase, as a guide

10.2 Example

a. A failure that affects the ability of the airplane to trim within the Operational Flight Envelope should probably be checked for Normal States with large gross weights and forward c.g. locations in those parts of the Flight Envelopes where the load factor is high

11.0 For a Particular Failure Mode, Determine the Degradation in Flying Qualities and the Probability of Occurrence Per Flight

11.1 Degradation to Level 2, or Level 3, or below Level 3 in the Operational Flight Envelopes

11.1.1 If any flying qualities examined are degraded to Level 2, or Level 3, or below Level 3 at one or more points within the operational Flight Envelopes of one or more Flight Phases, the probability of encountering Level 2 or Level 3, or below Level 3 in the Operational Flight Envelopes due to the failure is equal to the probability of encountering the failure per flight

11.2 Degradation to Level 3, or below Level 3 in the Service Flight Envelope

11.2.1 If any flying qualities examined are degraded to Level 3, or below Level 3 at one or more points within the Service Flight Envelopes of one or more Flight Phases, the probability of encountering Level 3, or below Level 3 in the Service Flight Envelopes due to the failure is equal to the probability of encountering the failure per flight.

11.3 Degradation in requirements not permitted

11.3.1 If any flying qualities requirements are degraded in the Operational or Service Flight Envelopes for one or more Flight Phases when such degradation is not permitted, the probability of encountering such prohibited degradation due to the failure is equal to the probability of the failure occurring per flight

12.0 Total Probability of Encountering Degraded Flying Qualities Per Flight Due to Failures

12.1 Total probability of encountering Level 2, Level 3, or below Level 3 in the Operational Flight Envelopes

12.1.1 The total probability of encountering Level 2 flying qualities per flight in the Operational Flight Envelopes is equal to the sum of the probabilities of encountering Failure Modes per flight that degrade flying qualities to Level 2 in the Operational Flight Envelopes. The same is true of Level 3 and below Level 3

12.2 Total probability of encountering Level 3, or below Level 3 in the Service Flight Envelopes

12.2.1 The total probability of encountering Level 3 flying qualities per flight in the Service Flight Envelopes is equal to the sum of the probabilities of encountering Failure Modes per flight that degrade flying qualities to Level 3 in the Service Flight Envelopes. The same is true of below Level 3

12.3 Total probability of encountering degradations not permitted by the requirements

12.3.1 The total probability of encountering degradations in flying qualities requirements, when such degradation is not permitted in the Operational or Service Flight Envelopes, is equal to the sum of the probabilities of encountering Failure Modes per flight that degrade requirements where no degradation is permitted in the Operational or Service Flight Envelopes.

Comments on the Outline of Failure and Failure Effects Analysis

Flying qualities requirements specified in MIL-F-8785B(ASG) are related to the Mission Flight Phases (Category A, B, or C) and the Flight Envelopes (Operational, Service, and Permissible) associated with each of the Flight Phases. The Flight Envelopes are defined in terms of velocity, altitude, and normal load factor. In addition, the Service Flight Envelopes in terms of speed, altitude, and load factors are a function of airplane Normal States, for example, the wing sweep position for an airplane with variable sweep.

The definition of Failure States is based on an adequate definition of Normal States. According to Paragraph 3.1.6.2 in MIL-F-8785B(ASG), Airplane Failure States "consist of Airplane Normal States modified by one or more malfunctions in airplane components or systems". Failure States will be the same when the Normal States are the same. To the extent that Flight Phases can be grouped together based on the same Flight Phase Categories and the same Normal States, they can be treated together in determining Failure States and the effects of failures on flying qualities Levels.

It is obvious that before adequate failure analysis can be performed, it is necessary to define all the subsystems to be considered in determining all the important Failure States of the airplane. These Failure States may include failures of combinations of subsystems as well as failures of components within any subsystem.

As examples, we can consider the following subsystems as being potentially pertinent to flying qualities analysis.

- Flight Control System (Primary and Secondary)
- Fuel Sequencing Subsystem
- Variable Sweep Subsystem
- Flap Actuation Subsystem
- Engine Subsystem
- Landing Gear Subsystem.

Each of these subsystems is pertinent because each can influence the forces and moments that act on the airframe.

Consider the Landing Gear Subsystem as an example. If the gear fails to retract following takeoff, the mission will no doubt be aborted and flying qualities considerations for Flight Phases subsequent to takeoff will not be of concern. If the gear fails to extend during the landing approach Flight Phase, a normal landing will obviously not be completed. Mission aborts and inability to land are of sufficient importance that the failure probabilities for the landing gear subsystem are likely to be established independently from flying qualities considerations. Thus, it would seem reasonable to classify landing gear failures as Special Failure States. As an additional comment, we can point out that gear up and gear down would be included in the definition of Normal States for the landing approach Flight Phase. Thus, an analysis of flying qualities for Normal States would automatically include the situation corresponding to a Failure State.

The above considerations for the landing gear subsystem are perhaps relatively simple compared to the kind of considerations that other subsystems would require. However, they exemplify the possibility of being able to eliminate certain Failure States from further consideration by application of engineering judgment and without a detailed knowledge of the subsystem's component reliability data.

Once failures of one or more subsystems are eliminated by considering such failures as Special Failure States, then block diagrams of each remaining subsystem should be prepared. The block diagram should show the components to be considered in failure analysis. The probability of failure of each component should also be indicated. Component reliability data is valuable because it provides the necessary information for a reduction in the Failure States to be considered within any Subsystem.

If the total subsystem failure probability is not very low, then an examination of the failure probability data for the individual components may still lead to a reduction in the number of Failure States that need be considered for flying qualities analysis. For example, even though total subsystem failure probability is relatively high, there still may be a number of individual components within the subsystem that have failure probabilities very much less than say 10^{-4} . The single and multiple Failure States determined by these components could therefore be neglected simply because of the very low probability of occurrence of these Failure States.

To summarize, we can say that the magnitude of total subsystem failure probabilities along with individual component failure probabilities appear to be a reasonable basis for rejecting certain Failure States for flying qualities analysis.

Assuming now that we have eliminated certain components using the above rationale, it may be possible to perform further simplifications. This further simplification would depend on knowing how the subsystem components operate. For example, certain components have similar effects on the performance of the overall subsystem.

To illustrate some of these points in a more concrete way, we will consider a few specific cases. Consider first single or multiple failures of components that will cause one or the other side of a horizontal stabilizer to be locked in place (Figure 4). A series string of such components is shown as Figure 4(a). Note that each component has the same probability of failure so that we cannot eliminate some and not the others on the basis of probability data. However, the probability that one or the other of these four components fail is $.056 \times 10^{-4}$. The probability of multiple failures of these components, two or more components, is extremely small, less than 10^{-10}. Thus multiple failures need not be considered since their failure probabilities are far less than $.056 \times 10^{-4}$. Since even $.056 \times 10^{-4}$ is small relative to 10^{-4} we could perhaps consider even this Failure State to be a Special Failure State. Because of the seriousness of the failure, we may choose not to consider $.056 \times 10^{-4}$ to be "extremely small" compared to 10^{-4}. In this case, since simplification is still possible by realizing that based on probability considerations these four components are equivalent to a single component with only one Failure State whose effect results in a jam of one side of the horizontal tail with a failure probability of $.056 \times 10^{-4}$ (Figure 4(b)). Thus, this single effective component defines the only significant Failure State in this case. This results in a large reduction from the 6 possible Failure States and their probabilities that could occur if we consider the different failure combinations for four components. It does not appear unreasonable to perform such lumping in determining Failure States and Failure Modes to be considered in failure analysis.

As a second example, which is somewhat more complicated than the previous two, we consider the Failure Modes associated with gain scheduling and a Control Air Data System (CADS) , in a particular design. Figure 5(a) shows a portion of the reliability diagram. Since failures in gain scheduling components and the CADS systems lead to different effects in the flight control system, "lumping" to define one effective component does not seem justified. Rather, a basic understanding of the functions performed by these components might lead to the desire to investigate at least the following two Failure Modes:

1. Loss of CADS, 1 dual side
2. Loss of gain scheduling, 1 dual side.

The probabilities associated with these two different Failure Modes would then be computed as indicated by the "reduced" reliability diagrams in Figure 5(b) and 5(c). Note that this reduction is very much dependent on the use of engineering judgment to select Failure States that appear to be significant as regards their effect on flying qualities.

Most of the previous discussion has emphasized consideration of failures within a single subsystem. However there may be some important Failure States defined by combinations of failures occurring in two or more subsystems. For example a wing sweep failure combined with a fuel sequencing failure could possibly result in having the c.g. located at an off design position. The rationale, however, for selecting multiple subsystem Failure States would still be based on the considerations previously discussed.

Assuming now that the process of selecting and rejecting Failure States has been completed, the flying qualities analysis phase can begin. Knowing the Failure States, it would be desirable to classify them as to their general effects on stability and control characteristics, that is, according to particular Failure Modes. For example, they could be grouped according to:

(a) effects on c.g. location
(b) effects on wing sweep
(c) effects on augmentation gains
(d) effects on control authority
(e) effects on control rate
(f) effects on control hinge moments
(g) effects on symmetric and asymmetric control motions.

Some Failure States could belong to more than one group. However, by having such a grouping it may be possible to select the more critical Failure Modes and flying qualities requirement that might be affected by the failure. Making such a selection is aided by having a certain amount of familiarity with the contents of MIL-F-8785B(ASG).

Once the Failure Modes to be considered are defined, it is necessary to relate each Failure Mode to the flying qualities and flying qualities Levels that exist after the failure in the Operational and Service Flight Envelopes. In order to do this, the effects of the failures must be interpreted in terms of the flying qualities requirements in MIL-F-8785B(ASG). Failure effects must first be described in terms such as the effects of the failure on c.g., wing sweep, augmentation gains, control authority, control rate, control hinge moments, etc.

Although many flying qualities requirements are likely to be affected by a particular failure, not all requirements are affected equally. The effects on some requirements are quite obvious and easy to check. The effects on other requirements are more subtle, qualitative, and very difficult if not impossible to determine. Sound engineering judgment will be of considerable importance in selecting those flying qualities requirements that will be degraded the most by a failure. A knowledge of how well a requirement is met for the Normal States, i.e., no component or system failures, will be of considerable assistance in making such judgments. Several Failure Modes in terms of failure effects, and the flying qualities likely to be degraded the most are presented here only as examples.

A. Failure Mode Effect

Maximum hinge moments can be reduced by 2/3.

Flying Qualities Requirements Most Affected

1) 3.2.3.1 Longitudinal control in unaccelerated flight.
2) 3.2.3.2 Longitudinal control in maneuvering flight.
3) 3.5.2.3 Rate of control displacement.

B. Failure Mode Effect

Pitch stability and control augmentation gains reduced 20%.

Flying Qualities Requirements Most Affected

1) 3.2.1.1 Longitudinal static stability with respect to speed.
2) 3.2.1.3 Flight-path stability.
3) 3.2.2.1.1 Short-period frequency and acceleration sensitivity.
4) 3.2.2.1.2 Short-period damping
5) 3.2.2.2.1 Control forces in maneuvering flight.

C. Failure Mode Effect

Increase in mechanical system friction - Increase in breakout forces and increase in force gradient.

Flying Qualities Requirements Most Affected

1) 3.2.2.1 Control forces in maneuvering flight.
2) 3.5.2.1 Control centering and breakout forces.
3) 3.2.2.3 Longitudinal pilot-induced oscillations.

For the Failure Mode Effect described in A, the first two requirements are easy to check and quantitative in nature. Flying qualities Levels due to the failure can be determined in the Flight Envelopes of the airplane. Requirement 3.5.2.3 is qualitative and difficult to check.

In the case of the Failure Mode Effect described in B, all the requirements are easy to check for the reduced gains. The effects of the failure can be determined quantitatively in terms of Levels.

In the case of the Failure Mode Effect described in C, the effects of the failure on the first two requirements can be determined once the increase in the mechanical friction due to the failure is described quantitatively. Requirement 3.2.2.3, although extremely important, is a qualitative requirement that will be difficult to evaluate in terms of the failure.

Once the flying qualities requirements that are most likely to be degraded by a particular failure are determined, they should be rated in their order of importance with the most important requirements first and quantitative requirements before qualitative requirements.

Failure Modes are tied to Flight Phases or Flight Phase Categories and the airplane Normal States. The effects of failures on flying qualities and flying qualities Levels are also associated with the flight conditions within the Flight Envelopes of the particular Flight Phase. Flying qualities requirements are likely to be degraded the most at particular flight conditions. If a failure applies to one or more Normal States, then the critical flight condition may also be a function of the Normal States, such as c.g. forward or aft, gross weight high or low, wing swept forward or aft, etc.

It cannot be overemphasized that the adequacy to which the degradation in flying qualities and flying qualities Levels can be assessed following a failure is a strong function of how complete the flying qualities have been determined for all Flight Phases, Normal States, and Flight Envelopes without failures. For example, in order to determine the critical flight conditions for a failure that reduces the control surface hinge moment or authority, the control surface hinge moments or authority required and available for the airplane Normal States throughout the Flight Envelopes must be determined.

The following are a few suggested examples of the interrelationships between Failure Modes and their effects, flying qualities, and the flight conditions and Normal States under which the requirements are likely to be affected the most.

1. Failure Modes that Reduce the Available Control Surface Hinge Moment

   a. Flying qualities most affected

      (1) Those flying qualities that require large control surface trim loads and control surface power in terms of loads and hinge moments.

   b. Critical Normal States and Flight Conditions

      (1) Forward c.g. locations, large gross weights, large normal load factors, and high dynamic pressures.

2. Failure Modes that Reduce Control Surface Authority

   a. Flying qualities most affected

      (1) Those flying qualities that require large control surface deflections for trim or those requirements that require large control power.

b. Critical Normal States and Flight Conditions

(1) Level flight trim at low speeds and high angles of attack with forward c.g.'s and high gross weights.
(2) Trim requirements in take-off and landing with forward c.g. and large gross weight.
(3) Trim and augmentation requirements with normal acceleration when the augmentation gains are high.
(4) Trim and control power, such as roll control, at low speeds and large gross weights and forward c.g. locations.

3. Failure Modes that Reduce Control Rate

a. Flying qualities most affected.

(1) Those flying qualities that require a large augmentation gain for the airplane Normal States.
(2) Those flying qualities that require rapid control surface response to pilot inputs.

b. Critical Normal State and Flight Conditions

(1) Those Normal States and Flight Conditions where the augmentation gains are high and the control authority required is high. Large gross weights, high normal accelerations, and high augmented frequencies or small augmented time constants.

The flight conditions specified are only a guide. The analysis of flying qualities of the airplane for Normal States will be the most important aid in establishing flight conditions to be examined for particular failures. For any given Failure Mode and flying qualities requirement, it should only be necessary to examine three or four combinations of Normal States and Flight Conditions within the Flight Envelopes to determine the degradation in Levels that can occur due to the Failure Mode.

Three or four flying qualities requirements and three or four flight conditions are likely to lead to between 9 and 16 combinations to be examined for an evaluation of the most critical effect of each Failure Mode in degrading flying qualities. The number of cases to be examined will of course vary with the Failure Mode. An adequate judgment should be based on the analysis of flying qualities without failures.

A matrix of Flying Qualities Requirements and Flight Conditions to be examined in determining the degradation in Levels resulting from a particular Failure mode might take the following tabular form:

TABLE 1
Flying Qualities Levels
(Failure Mode_____, Probability per flight____)

Flying Qualities Requirement No.	Flight Conditions			
	1A	1B	1C	etc.
a				
b				
c				
etc.				

If one or more combinations of Flying Qualities Requirements and Flight Conditions examined degrade flying qualities to Level 2, Level 3, or below Level 3 in the Operational Flight Envelopes, and Level 3 or below Level 3 in the Service Flight Envelopes, then the probability of the occurrence of the degraded Level due to the failure is equal to the probability of the occurrence of the failure per flight. Some flying qualities may be degraded in the Operational or Service Flight Envelopes when such degradation is not permitted. The probability of encountering prohibited degradation in requirements when they occur is also equal to the probability of encountering the failure per flight.

A limited or "bounded" analysis such as that just presented must be well thought out so that a sufficient number of critical requirements and flight conditions are examined in both the Operational and Service Flight Envelopes. It is only necessary to find one requirement and one flight condition that degrades flying qualities to Level 2, Level 3, or below Level 3 for the airplane flying qualities to be considered respectively Level 2, Level 3, or below Level 3.

The total probability of encountering degraded Levels of flying qualities in the Operational or Service Flight Envelopes can now be determined. Each Failure Mode analyzed will result in one or more of the flying qualities requirements examined being of one or more of the following Levels: Level 1, Level 2, Level 3, below Level 3, or a degradation that is not permitted in the Operational or Service Flight Envelopes.

The total probability of encountering degraded Levels, Level 2, Level 3, below Level 3, or degradations that are not permitted, is the sum of failure probabilities per flight of Failure Modes that degrade to these Levels. A given Failure Mode may degrade flying qualities to one or more of these Levels. In tabular form, the summation of failure probabilities for the various Levels may be presented as follows.

TABLE 2
Total Probability of Encountering Degraded Levels

Failure Mode No. & Probability	Operational Flight Envelopes			Service Flight Envelopes		Degradation not Permitted
	Level 2	Level 3	Below Level 3	Level 3	Below Level 3	
No. 1 Prob.__ No. 2 Prob.__						
. . .						
No. n-1 Prob.___ No. n Prob.___						
Total	$\sum P_2$	$\sum P_3$	$\sum P_{3-}$	$\sum P_3$	$\sum P_{3-}$	$\sum P_{NP}$

$\sum P_2$ = Summation of Failure Mode probabilities that degrade flying qualities to Level 2

$\sum P_3$ = Summation of Failure Mode probabilities that degrade flying qualities to Level 3

$\sum P_{3-}$ = Summation of Failure Mode probabilities that degrade flying qualities below Level 3

$\sum P_{NP}$ = Summation of Failure Mode probabilities that lead to flying qualities degradations not permitted.

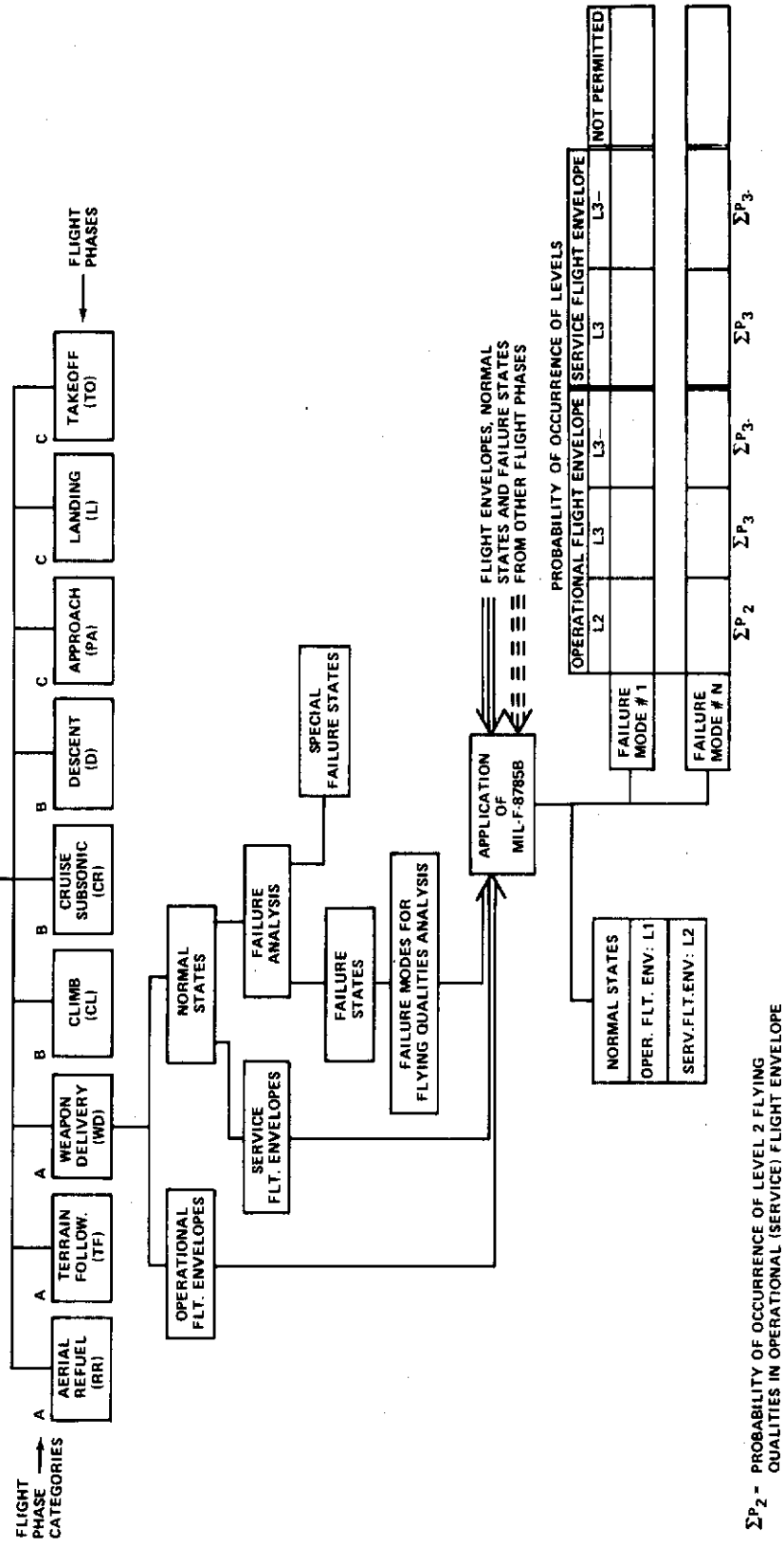

Figure 1 FAILURE AND FAILURE EFFECTS ANALYSIS FLOW DIAGRAM

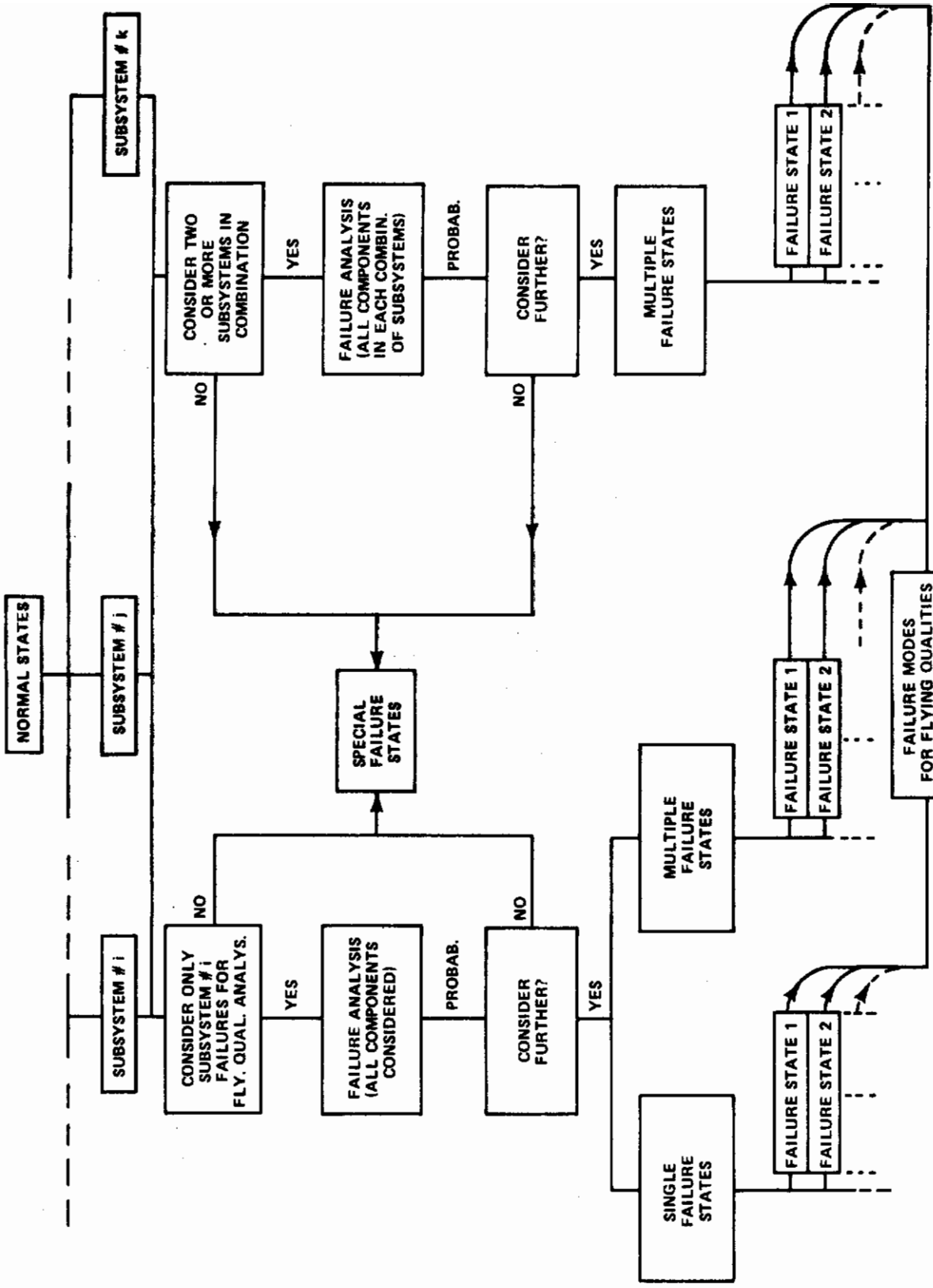

Figure 2 FAILURE ANALYSIS

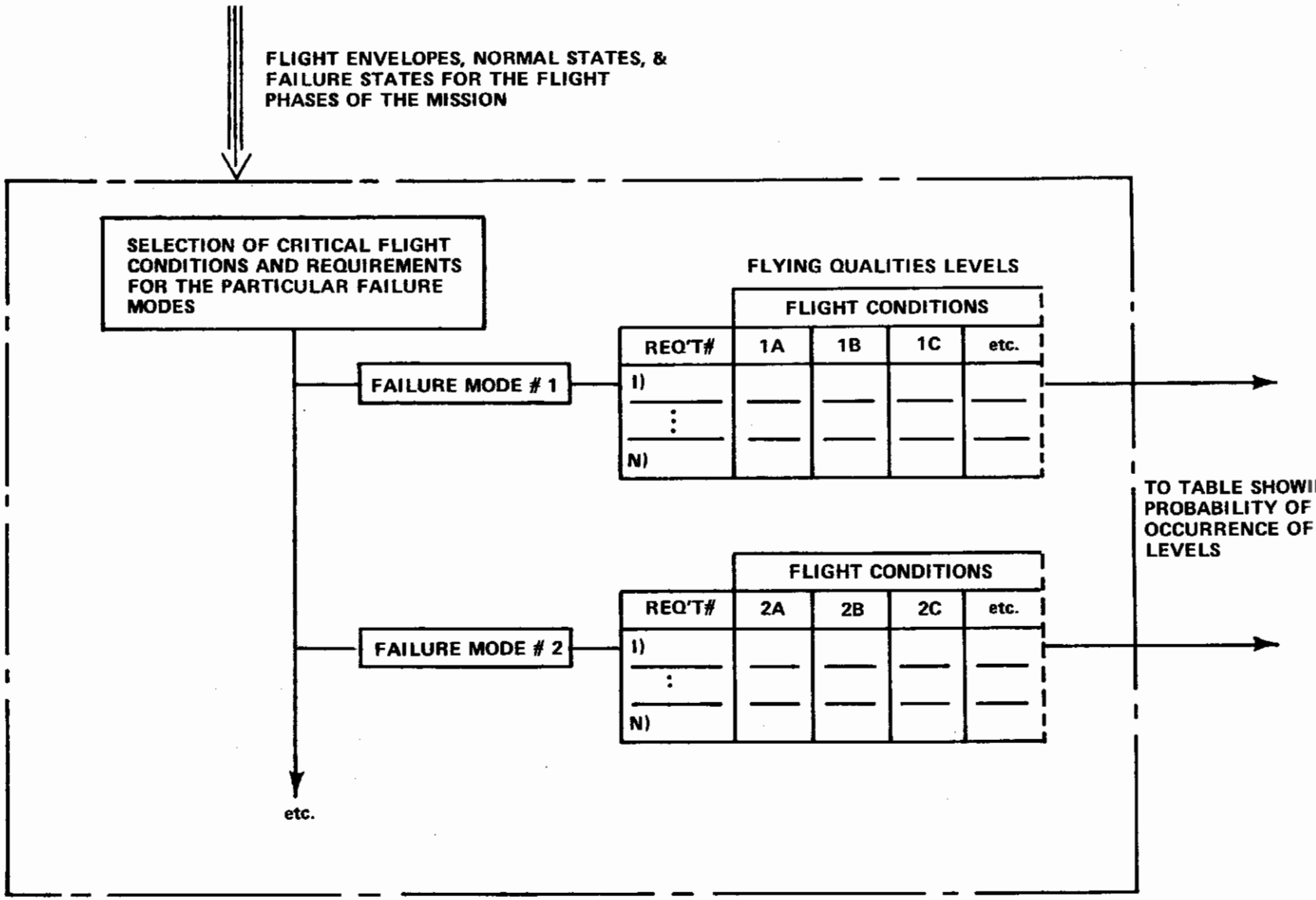

Figure 3 APPLICATION OF MIL-F-8785B(ASG)

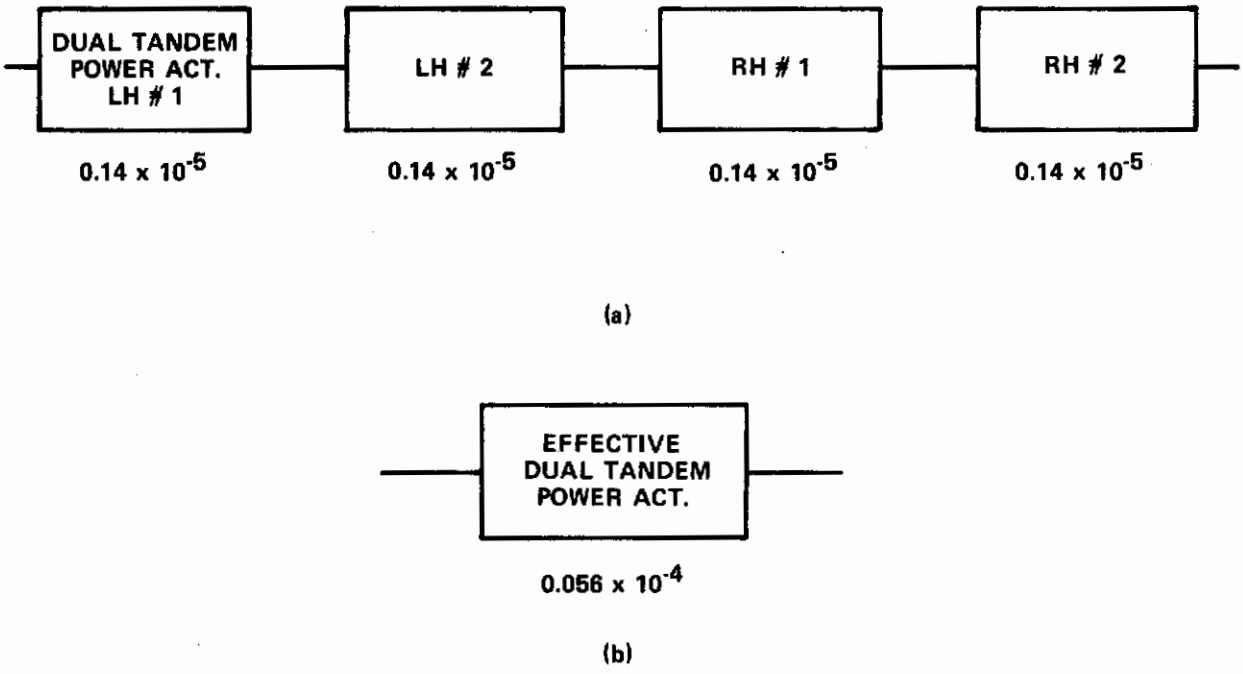

Figure 4 FAILURE MODE RESULTING IN JAM OF ONE SIDE OF HORIZONTAL TAIL

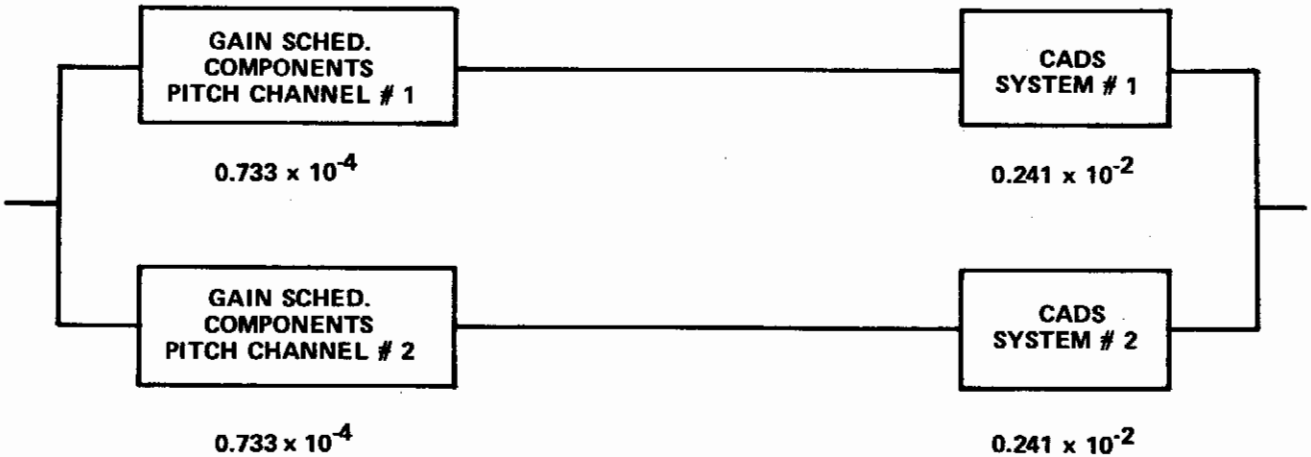

Fig. 5a

FAILURE MODE: LOSS OF CADS, ONE DUAL SIDE

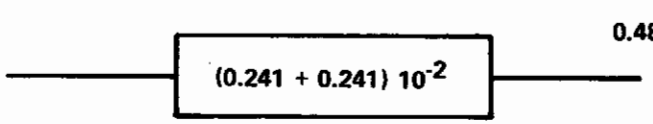

Fig. 5b

FAILURE MODE: LOSS OF GAIN SCHEDULING, ONE DUAL SIDE

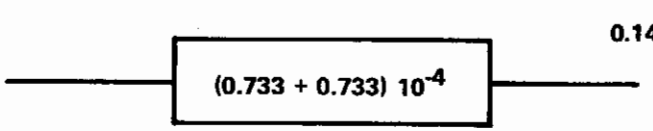

Fig. 5c

Figure 5 FAILURE MODES RESULTING IN LOSS OF CADS AND GAIN SCHEDULING

SECTION II

PROPOSED REVISIONS TO 3.2, LONGITUDINAL FLYING QUALITIES

Action Recommended for Subparagraphs to 3.2.1

3.2.1	Longitudinal stability with respect to speed
3.2.1.1	Longitudinal static stability - reviewed but no change
3.2.1.1.1	Relaxation in transonic flight - revise
3.2.1.1.2	Elevator control force variations during rapid speed changes - no change
3.2.1.2	Phugoid stability - no change
3.2.1.3	Flight path stability - no change

Proposed New Requirements

3.2.1.1.1 Transonic flight. In the transonic speed range, no local force gradient measured in 3.2.1.1 shall be more stable than the following:

	Stick Controllers	Wheel Controllers
Level 1	2.5 lb per .01M	5.5 lb per .01M
Level 2	4 lb per .01M	8.5 lb per .01M
Level 3	5.5 lb per .01M	12 lb per .01M

In addition, the requirements of 3.2.1.1 may be relaxed in the transonic speed range provided any divergent airplane motions or reversals in slope of elevator control force and elevator control position with speed are gradual and not objectionable to the pilot. In no case, however, shall the requirements of 3.2.1.1 be relaxed more than the following:

Maximum Unstable Gradient

	Stick Controllers	Wheel Controllers
Level 1	2.5 lb per .01M	5.5 lb per .01M
Level 2	4 lb per .01M	8.5 lb per .01M
Level 3	5.5 lb per .01M	12 lb per .01M

Maximum Unstable Force Change

	Stick Controllers	Wheel Controllers
Level 1	8 lb	17 lb
Level 2	16 lb	34 lb
Level 3	23 lb	49 lb

Introduction and Motivation for Recommended Action

Swedish engineers have apparently encountered a problem with one of their airplanes resulting from excessive static stability. Details of the problem encountered are not available but in general it is known that high static stability can cause problems related to high stick forces to change speed, high control sensitivity, or high stick force per g. The Swedish engineers have seen fit to limit their problem by placing upper limits on stick force gradients with speed (SAAB-SCANIA L-0-1-R10, Edition 2). CAL has reviewed the Swedish requirements for possible application to MIL-F-8785B. As a result of this review, we recommend that 3.2.1.1 be retained without change and 3.2.1.1.1 be replaced with the new requirement.

Discussion and Substantiation

The detailed reasoning behind these recommendations is discussed below.

The Swedish specification requires the maximum stable stick force gradient with speed to be less than the following:

Level 1	0.23 lb/knot
Level 2	0.46 lb/knot
Level 3	0.69 lb/knot

These requirements fail to recognize certain fundamental relationships between stick force per knot (F_s/u) and stick force per g (F_s/n). These relationships can be derived as follows:

$$\frac{F_s}{u} = \left(\left| \frac{u(s)}{\delta_e(s)} \right|_{ss} \frac{\delta_e}{F_s} \right)^{-1} = \left(\frac{\delta_e}{F_s} \right)^{-1} \left(\frac{M_w Z_u - Z_w M_u}{M_{\delta_e} Z_w - Z_{\delta_e} M_w} \right)$$

$$\frac{F_s}{n} = \left(\left| \frac{n(s)}{\delta_e(s)} \right|_{ss} \frac{\delta_e}{F_s} \right)^{-1} = - \left(\frac{\delta_e}{F_s} \right)^{-1} \frac{g}{V} \left(\frac{Z_w M_q - V M_w}{M_{\delta_e} Z_w - Z_{\delta_e} M_w} \right)$$

Now, most airplanes have relatively small M_u except in the transonic region or when they have downspring-type augmentation devices, Thus $|Z_w M_u| << |M_w Z_u|$ Also, for the high static stability cases we are interested in $|Z_w M_q| << |V M_w|$ Combining the two equations we then have:

$$\frac{F_s}{u} = -\left(\frac{Z_u}{g}\right)\left(\frac{F_s}{n}\right)$$

Since $Z_u \approx \frac{2g}{V}$, there results

$$\frac{F_s}{u} = -\frac{2}{V}\left(\frac{F_s}{n}\right)$$

Using this equation, it is interesting to determine F_s/u corresponding to the maximum F_s/n requirements of 3.2.2.2.1 for stick controllers. Using the T-33 as an example, and assuming $n_L = 7.0$, $(F_s/n)_{max}$ in lb/g is:

	Low n/α (150 kt)	High n/α (250 kt)
Level 1	28	9.3
Level 2	42.5	14.2
Level 3	56	56

These numbers result in the following values of F_s/u (lb/knot):

	150 kt	250 kt
Level 1	.38	.12
Level 2	.57	.19
Level 3	.75	.75

These numbers show that, for Levels 1 and 2, an airplane meeting the F_s/n requirements for high n/α will meet the Swedish F_s/u requirements. However, if this same airplane has F_s/n near the upper limits for low n/α , it will not meet the F_s/u requirements.

The point of this exercise is to show that the Swedish requirements are probably too stringent for low n/α situations, such as landing approach. In any case, requirements on F_s/u for situations where M_u is small are somewhat redundant if F_s/n limits are specified.

Properly designed requirements on F_s/u , however, could be used to limit the amount of M_u that the airplane has, such as might result from use of a downspring or due to flight in the transonic region. High M_u can indeed cause flying qualities problems, e.g., excessively high F_s/u gradients and poor turbulence response. CAL proposed requirements to limit M_u in its May 1967 recommended changes to MIL-F-8785:

> 3.2.1.1c Maximum force variations - It shall be possible to suddenly release the longitudinal control at any stabilized speed in the range of 3.2.1.1 without the change in normal acceleration exceeding the following limits:

Level 1 - 0.45 g's or $(300/V_{TRIM})$ g's, whichever is less

Level 2 - 0.60 g's or $(400/V_{TRIM})$ g's, whichever is less

Level 3 - no specific requirement

NOTE: V_{TRIM} is in knots.

These requirements are based on the previously derived relationship between F_s/u and F_s/n, but are re-arranged to avoid the necessity for having to know F_s/n. This can be seen by using the equation to derive the expression for n change resulting from a stick release at an off-trim speed:

$$\Delta n = \frac{\Delta F_s}{(F_s/n)} = \frac{(F_s/u)\,u}{(F_s/n)} = -\frac{2}{V}u$$

A study of estimated values of M_u for several different types of airplanes indicated that airplanes normally have only small positive values of M_u if any, and that F_s/u is seldom more than 20% higher than the value for $M_u = 0$. To limit M_u to reasonable values, therefore, it was decided to use:

$$\Delta n_{max} = -\frac{3}{V}u \quad \text{for Level 1}$$

$$\Delta n_{max} = -\frac{4}{V}u \quad \text{for Level 2}$$

When the speed ranges of paragraph 3.2.1.1 (±15 percent or ±100 knots at that time) are used to define the maximum excursions in u, the numbers of paragraph 3.2.1.1c are obtained.

The May 1967 requirements were criticized by many people, partially because of the form chosen for the criterion and partially because the numerical limits are not well supported. Most of the criticism of form could be remedied by directly expressing $(F_s/u)_{max}$ as a function of F_s/n Because of the lack of supporting data, however, the requirement was withdrawn. Since the data situation for M_u effects is not much improved since 1967, it is recommended that no requirements on maximum F_s/u be added at this time (with the exception of the transonic regime).

In the transonic regions, large changes in M_u can cause large stable and unstable gradients of F_s/u. Because large control force gradients with speed can cause piloting difficulties, it is necessary to set limits on these gradients.

The Swedish requirements on the allowable instabilities in the transonic region seem to be in the same ballpark as those of MIL-F-8785B and are apparently based on some data. For this reason, it is recommended that the Swedish requirements be adopted for stick controllers (after rounding off). For wheel controllers, the limits were arbitrarily multiplied by 2.15, in keeping with the philosophy of the F_s/n requirements.

The Swedish requirements on maximum stable gradients in the transonic region are rather confused because two different gradients are specified for each Level. One gradient is per .01M and one is per .05M. Since the intent appears to be the limiting of local gradients, the gradient per .05M is always slightly more stringent. Since there does not appear to be a need for having both gradients, the stable gradient limits per .01M are recommended, to be consistent with the unstable limits. Again, the limits for wheel controllers are higher by a factor of 2.15.

As a check on the practicality of the requirements on stable gradients, the limits were compared with the existing F_s/n requirements. Assuming that the transonic region will always result in reasonably high n/α, we can then determine the highest reasonable values of F_s/n which will still meet the F_s/n requirements:

Level	Stick (n_L = 4)	Wheel (n_L = 2.5)
1	18.5	80
2	28	121
3	56	240

Modifying the previously derived expression for F_s/u slightly, we have:

$$\left(\frac{F_s}{0.01M}\right) = \frac{a}{100}\left(\frac{F_s}{u}\right) = \frac{0.02}{M}\left(\frac{F_s}{n}\right)$$

Using the low end of the transonic speed range, say M = .85, (F_s/.01M) for each value of F_s/n listed above is as follows (for M_u = 0):

Level	Stick	Wheel
1	0.4 lb/.01M	1.9 lb/.01M
2	0.7 lb/.01M	2.9 lb/.01M
3	1.3 lb/.01M	5.6 lb/.01M

Since these gradients are well within the proposed limits, the limits allow a generous amount of stable M_u, and therefore seem quite reasonable.

Another check on the practicality of both the stable and unstable limits was made by quickly reviewing a number of AFFTC reports for forward c.g. configurations. For the cases examined, the gradients were well within the proposed Level 1 limits. The limits were also compared with Figure 19 (3.2.1.1) of McDonnell's F-4 evaluation of MIL-F-8785B. The McDonnell data compared quite well with the proposed limits, particularly when the crude nature of McDonnell's assigning of Levels to each data point is considered.

Action Recommended for Subparagraphs to 3.2.2

3.2.2	Longitudinal maneuvering characteristics
3.2.2.1	Short-period response - Delete
3.2.2.1.1	Short-period frequency and acceleration sensitivity - Delete
3.2.2.1.2	Short-period damping - Delete
3.2.2.1.3	Residual oscillations - Renumber (3.2.2.4)
3.2.2.2	Control feel and stability in maneuvering flight - Revise
3.2.2.2.1	Control forces in maneuvering flight - Revise
3.2.2.2.2	Control motions in maneuvering flight - Revise
3.2.2.3	Longitudinal pilot-induced oscillations - Renumber (3.2.2.5)
3.2.2.3.1	Transient control forces - Revise and renumber (3.2.2.3)

Proposed New Requirements

3.2.2 Longitudinal maneuvering characteristics

3.2.2.1 Pitch dynamic response in maneuvering flight. The frequency response of pitch attitude to elevator control force shall be such that the parameters $(\Delta n/\Delta F)_\theta$ and ΔF_θ are within the limits of figure 1, using the following reference frequency (ω_θ).

Levels 1 and 2:

Flight Phase Category	Class	ω_θ ~ rad/sec
A	I, IV	3.0
	II, III	2.0
B	ALL	1.2
C	ALL	1.2

Level 3:

Use ω_θ = 1.1 rad/sec for all Flight Phase Categories and Classes.

This requirement applies for responses of any magnitude that might be experienced in service use. In addition, the contractor shall show that the airplane has acceptable response characteristics in atmospheric disturbances.

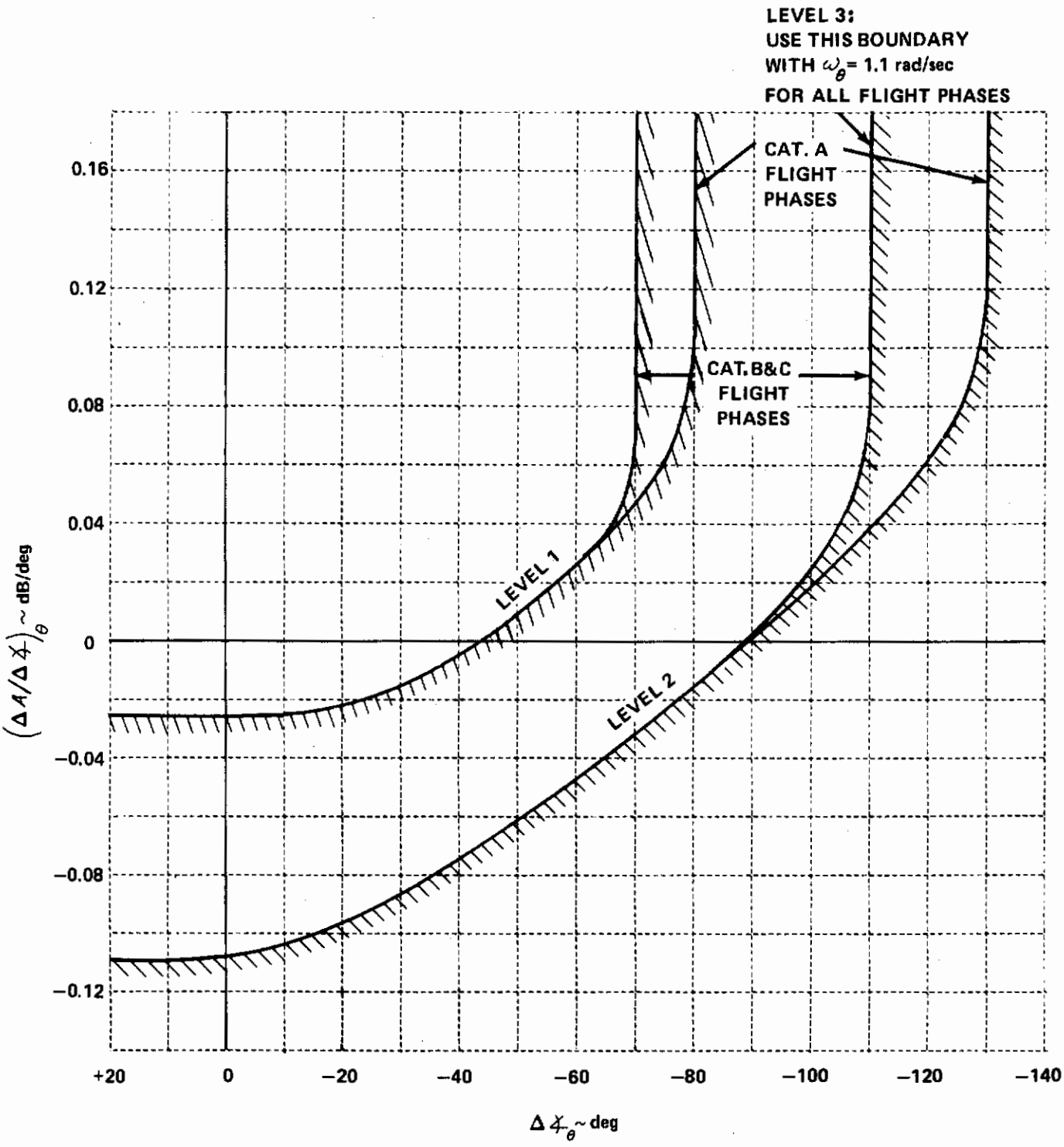

Figure 1 [OF MIL-F-8785B(ASG)] PITCH MANEUVER RESPONSE REQUIREMENTS

3.2.2.2 Compatibility of steady maneuvering forces and pitch sensitivity.

The product of the control force in steady maneuvering flight, F_s/n , and the maximum frequency-response-amplitude of pitch acceleration to elevator control force $|\ddot{\theta}/F_s|_{max}$, shall not exceed the following limits:

Level 1	$3.6 \frac{\text{rad/sec}^2}{\text{g}}$
Levels 2 and 3	$\frac{10.0 \text{ rad/sec}^2}{\text{g}}$

3.2.2.3 Dynamic control forces in maneuvering flight. The frequency response of normal acceleration at the c.g. to elevator control force shall be such that the inverse amplitude is greater than the following for all frequencies greater than 1.0 rad/sec. Units are pounds per g.

	Level 1	Level 2	Level 3
Center-Stick Controllers	$\frac{14}{n_L-1}$	$\frac{12}{n_L-1}$	$\frac{8}{n_L-1}$
Wheel Controllers	$\frac{30}{n_L-1}$	$\frac{25}{n_L-1}$	$\frac{17}{n_L-1}$

In addition, the cockpit control position shall not lead the elevator control force for any frequency or force amplitude.

3.2.2.4 Residual oscillations. (Same as present 3.2.2.1.3)

3.2.2.5 Longitudinal pilot-induced oscillations. (Same as present 3.2.2.3)

3.2.2.6 Control forces and displacements in steady maneuvering flight. In steady turning flight and in pullups at constant speed, incremental pull forces and aft displacements of the elevator control and airplane-nose-up deflection of the elevator surface are required to maintain increases in normal acceleration throughout the range of service load factors defined in 3.1.8.4. Incremental push force, forward control displacement, and airplane-nose-down deflection of the elevator surface are required to maintain reductions of normal acceleration in pushovers.

3.2.2.6.1 Control forces in steady maneuvering flight. At constant speed in steady turning flight, pullups, and pushovers, the variations in elevator-control force with steady-state normal acceleration shall be approximately linear. In general, a departure from linearity resulting in a local gradient which differs from the average gradient for the maneuver by more than 50 percent is considered excessive. All local force gradients shall be within the limits of table V. The term gradient does not include that portion of the force versus n curve within the preloaded breakout force or friction band.

TABLE V. Elevator Maneuvering Force Gradient Limits

Center Stick Controllers		
Level	Maximum Gradient, $(F_s/n)_{max}$, pounds per g	Minimum Gradient, $(F_s/n)_{min}$, pounds per g
1	$\frac{240}{n/\alpha}$ but not more than 28.0 nor less than $\frac{56}{n_L-1}$ *	The higher of $\frac{21}{n_L-1}$ and 3.0
2	$\frac{360}{n/\alpha}$ but not more than 42.5 nor less than $\frac{85}{n_L-1}$ *	The higher of $\frac{18}{n_L-1}$ and 3.0
3	56.0	The higher of $\frac{12}{n_L-1}$ and ~~3.0~~ 2.0
*For $n_L < 3$, $(F_s/n)_{max}$ is 28.0 for Level 1, 42.5 for Level 2.		

Wheel Controllers		
Level	Maximum Gradient, $(F_s/n)_{max}$, pounds per g	Minimum Gradient, $(F_s/n)_{min}$, pounds per g
1	$\frac{500}{n/\alpha}$ but not more than 120.0 nor less than $\frac{120}{n_L-1}$	The higher of $\frac{45}{n_L-1}$ and 6.0
2	$\frac{775}{n/\alpha}$ but not more than 182.0 nor less than $\frac{182}{n_L-1}$	The higher of $\frac{38}{n_L-1}$ and 6.0
3	240.0	The higher of $\frac{25}{n_L-1}$ and 6.0

3.2.2.6.2 Control displacements in maneuvering flight. The elevator-control displacement in maneuvering flight shall not be so large or so small as to be objectionable. For Category A Flight Phases, the average gradient of elevator-control force per inch of elevator-control displacement at constant speed shall be not less than 5 pounds per inch for Levels 1 and 2.

Introduction and Motivation for Recommended Action

The requirements of Subparagraphs to 3.2.2 were written in terms of classical aircraft dynamic parameters. This was done with full realization that there might be limitations in applying requirements so phrased to airplanes with flight control systems that introduce entirely new and significant modes of motion. At the time the revision was being formulated, however, there was insufficient experimental data concerning the effects of flight control systems on flying qualities to do otherwise. Thus in preparing the revision that was adopted in MIL-F-8785B(ASG), attention was devoted to development of requirements that accounted for the major factors found to be of importance through aircraft design experience and the large amount of flying qualities data that had been generated using variable stability airplanes. It was hoped that these requirements would be adequate but not overly restrictive and would encourage design of simple flight control systems with a minimum of complications such as high loop gains with adaptive gain changers and compensation networks. A great deal of momentum has been generated in the flight control system design community, however, and there has been recent emphasis on seeking ways to utilize the flight control system to reduce structural weight and limits on c.g. travel. Because of these factors, there is a need for flying qualities requirements that are stated in more general language than classical aircraft modal parameters. Since the publication of MIL-F-8785B(ASG) in 1969 there has been new experimental data generated concerning the effects of control system dynamics on longitudinal flying qualities, Reference 8. This data has been used to formulate a new approach to longitudinal flying qualities specification which makes use of amplitude ratio and phase information for the combined feel system, flight control system and the airplane.

The proposed new requirements are based upon considerations of the overall maneuvering response of the airframe/control-system combination, and appear to be applicable to airplanes having complex flight control systems (FCS), as well as to those whose dynamics can be adequately described by the short-period characteristics.

Also presented in this section is an alternate form of the pitch maneuvering requirement that is based on the transient response to a pilot input. The requirement is expressed as an equivalent system plus a time delay. This idea was presented in Reference 8 and was also used in an interim draft of the VTOL specification MIL-F-83300. Although the alternate requirement is not as generally applicable as the primary proposal it does appear to be an improvement over the existing requirements for aircraft with significant control system dynamics.

Discussion and Substantiation for 3.2.2

A. Philosophy of the Pitch Dynamic Requirements 3.2.2.1

The proposed pitch dynamic requirements, 3.2.2.1, represent an extension of the maneuver response criteria developed as part of the investigation reported in Reference 8. The basic criterion discussed in Reference 8 involved a closed-loop analysis of the pilot-airplane combination. A simplified version of this criterion, based on measurements made from the airplane response alone, was also presented. This simplified criterion was used to develop the proposed requirements, but was modified considerably to eliminate certain deficiencies. With this in mind, let us explain the theory behind the proposed requirements, beginning with the complete closed-loop analysis of Reference 8.

Precise control of pitch attitude is of critical importance in flying an airplane. This is particularly important for Category A Flight Phases where attitude control is often a primary task, and for Category C Flight Phases where attitude control is important as an "inner-loop" task. Since Reference 8 was primarily concerned with Category A Flight Phases, it was decided to analyze a simple mathematical model of pitch attitude tracking. Figure 6 shows the model used. To pick the values of the pilot model parameters, it is necessary to have some criteria for what the pilot might be looking for in the way of closed-loop performance. Good closed-loop performance would obviously be obtained if the closed-loop Bode amplitude was held near 0 dB and the phase near 0 degrees out to reasonably high frequencies. Using this idea, the performance standards used in the analysis are shown in Figure 7. The idea is to hold the closed-loop amplitude above -3 dB and the closed-loop phase above -90 degrees out to some frequency (we call this frequency for -90 degrees phase the bandwidth, ω_{θ}).

Physically, the bandwidth is a measure of how quickly the pilot wants to move the airplane's nose up to the target (if the closed-loop response were second-order, ω_{θ} would be equal to the natural frequency of the response). For a given task or flight phase, we have hypothesized that the pilot will try to achieve a closed-loop bandwidth which is equal to or greater than some minimum value. Thus, the minimum ω_{θ} can be expected to be a function of task or flight phase. Since the bandwidth that a pilot will strive for in a given experiment is a function of his experience and his interpretation of the task, there may be differences in the bandwidth used by different pilots. This may explain some of the differences in results between different experiments and different pilots.

Once the minimum bandwidth is determined for a given experiment, the pilot model parameters are chosen to just barely meet the performance standards of Figure 7. Pilot opinion should then be a function of the pilot compensation (τ_{p_1} and τ_{p_2} primarily) and any closed-loop resonance ($|\theta/\theta_c|_{max}$ on Figure 7) that might result. This closed-loop resonance is a measure of closed-loop oscillations (PIO's).

To convert the open-loop characteristics to closed-loop, a Nichols chart was used, which shows lines of constant closed-loop amplitude and phase on a grid of open-loop amplitude versus phase. Figure 8a is a Nichols chart with the performance standards of Figure 7 shown as hatched boundaries. Overlayed on this plot is an amplitude-phase curve for a low-frequency well-damped short-period configuration (top curve). This curve represents the airplane plus pilot with τ_{p_1} and τ_{p_2} equal to zero. The pilot gain K_p has been adjusted (by sliding the curve vertically) in an attempt to meet the performance standards (assuming a bandwidth of 3.0 rad/sec). Obviously the standards cannot be achieved without driving the closed-loop resonance to zero damping ($|\theta/\theta_c|_{max} = \infty$). Pilot lead compensation was then used and readjusted, resulting in the lower curve of Figure 8a. Now, we have met the performance standards (ω_θ = 3.0 rad/sec and droop = -3 dB) with a negligible closed-loop resonance. By analyzing airplane characteristics in this way, good correlation was obtained between pilot rating data and the pilot compensation plus closed-loop resonance.

The simplified version of this analysis was developed by observing that the pilot compensation and closed-loop resonance seemed to be strongly related to the open-loop slope and phase of the uncompensated amplitude-phase curve near $\omega = \omega_\theta$. Referring to Figure 8a, it can be seen that a steep positive slope near ω_θ will probably result in a low closed-loop resonance. Conversely, a flat or negative slope will cause large or unstable resonances. Also, the pilot compensation required is related to the open-loop phase of the uncompensated curve. Thus, the simplified criterion of Reference 1 was derived by correlating pilot rating data with this slope and phase angle.

With this background in mind, we can now discuss the modifications made to this criterion in developing the proposed requirements. Most of the problems with the original criterion occurred with configurations whose amplitude-phase curves are not as smooth as the one shown in Figure 8a. For example, Figure 8b shows the amplitude-phase curve for a configuration having low short-period frequency and damping ratio. It is clear that a bandwidth of 3.0 rad/sec will result in unstable PIO's even if pilot lead compensation is used, and the pilot ratings are poor for this type of configuration. However, it is obvious that the slope at ω = 3 on Figure 8b is considerably more positive than the slope of Figure 8a (on the uncompensated curves). Since a high positive slope should indicate no PIO tendencies, this slope is obviously not doing the job. The slope on Figure 8b which better indicates the size of the resonance is the average slope between ω_θ and the "knee" of the uncompensated curve (near ω = 1).

Another interesting configuration is one having moderate-frequency low-damped short-period configuration, as illustrated in Figure 8c. Here, we again have a problem with a large closed-loop resonance, even with pilot compensation (in this case, lag compensation is needed). The slope of the uncompensated curve at ω = 3 is very flat, which indicates a resonance problem, but does not account for the fact that the curve continues to swing upward at frequencies above 3. Thus, the most negative local slope between ω_θ and the frequency for which the phase is (-180) is a better indicator of the size of the closed-loop resonance.

With the above considerations in mind, the simplified criterion of Reference 8 was modified by using either the most critical (most negative) average slope between ω_θ and any lower frequency than ω_θ or the most negative local tangent between ω_θ and the frequency for which the phase is (-180°), whichever is more negative. Units are dB/deg.

Low values of $1/\tau_{\theta_2}$ can cause a different kind of difficulty, as shown in Figure 8d. In this case, the size of the closed-loop resonance is much larger than even the average amplitude-phase slope would indicate. The reason for this is that the "knee" of the curve is unusually far to the right, forcing the open-loop gain up to meet the 3 dB droop requirement. One way to account for this effect is to use the phase difference between the "knee" and ω_θ, instead of simply the phase at ω_θ. Since most configurations have only a small "knee" (near -90°), this phase difference is equivalent to the phase at ω_θ plus 90 degrees. However, configurations having a large "knee" are penalized by the phase difference measurement, to reflect the higher tendency toward closed-loop oscillations.

With the criterion in its final form, then, we call the most negative slope $(\Delta A/\Delta \angle)_\theta$, the phase difference $\Delta \angle_\theta$, and the bandwidth, ω_θ. For the four examples already discussed, the new slopes and phases for $\omega_\theta = 3$ are shown in Figure 6. The actual boundaries proposed in Figure 1 were determined by analyzing the pilot rating data discussed below.

B. Substantiating Data - Category A

The way in which the available flying qualities data was compared to the proposed requirements was to find the bandwidth (ω_θ) for each experiment which would result in the best correlation of the pilot ratings with the boundaries of Figure 1. This is a way to compensate for slight differences in task, pilots, etc. between the various experiments. The resulting values of ω_θ are then summarized for comparison between experiments.

The first set of data to be analyzed for Category A Flight Phases is that of Reference 8, which was obtained for a wide range of short-period and control-system dynamics. The results are shown in Figures 9a and 9b for $\omega_\theta = 3.5$ rad/sec. It will be noted that a number of configurations lying inside the Level 1 boundaries are rated worse than 3.5. The pilot comments indicate that either high stick force per g or high pitch control sensitivity are responsible for the degraded ratings for most of these cases. These configurations are discussed in detail along with other data in Subsections E & D which contain substantiating data for 3.2.2.2.

Also discussed in Reference 8 are two special T-33 flights. The data from these flights are presented in Figure 10 for $\omega_\theta = 3.0$ rad/sec. Data for three configurations that were evaluated in the experiment of Reference 9 are shown in Figure 11. The airplane dynamics are identified as follows:

Config.	ω_{sp}	ζ_{sp}	n/α	F_s/n_γ	$\left\|\frac{\ddot{\theta}}{F_s}\right\|_{max}$
1	7.7	.48	22	5.4	0.55
2	10.1	.30	22	5.3	1.49
3	12.3	.17	22	5.0	3.80

Configurations 2 and 3 have sufficiently high short period frequency that even though the damping ratio is low they satisfy the requirement of 3.2.2.1. These configurations which have high values of pitch acceleration gain will be discussed in more detail in Subsections F & G.

The next set of data to be analyzed was all the Category A short-period data of the specification backup document (Reference 3). For each experiment used in Reference 3, the parameters of Figure 1 were measured for a matrix of frequency/damping combinations (an attempt was made to account for the control-system dynamics in each experiment.) In this way, a frequency/damping grid could be overlayed on the boundaries of Figure 1. An example of such a grid is shown in Figure 12. The intersections of the grid with the boundaries were then picked off and plotted on the frequency/damping plane for each experiment, as in Figure 13 from Reference 10. The results of the same procedure for the other experiments (References 11-16) are shown in Figures 14 through 21. It can be seen that the boundaries derived in this way do not discriminate against configurations having high short period frequencies. In general, these configurations are downrated because of high stick force per g or high control sensitivity.

Another experiment providing data on the effects of control system dynamics is the T-33 higher-order system program of Reference 16. Figure 22 presents the "up and away" portion of the data for ω_θ = 2.5 rad/sec. It can be seen that the correlation of the data with the proposed boundaries is rather poor. No way could be found to account for these discrepancies, and the same type of problem was encountered in Reference 8 using the more complete closed-loop criterion. In fact, this particular set of data has eluded a unified explanation ever since it was first generated: even the flying qualities parameters examined in the project report (Reference 16) failed to correlate all the data successfully. Perhaps the problem is related to the fact that very few satisfactory configurations were evaluated during the experiment. In fact, 60% of the configurations were rated unacceptable (PR worse than 6.5). The fact that the experiment was so heavily weighted with poor configurations was an unexpected result, but the lack of a uniform mix of flying qualities may have caused the evaluation pilots to lose their "calibration" and evaluate somewhat erratically.

It should be noted that the F-86 data shown in Figure 14 are only for the part of the experiment of Reference 11 in which the control system dynamics are reasonably fast. Another part of that same experiment studied the effects of a first-order lag in the control system. In this part, the pilot was allowed to select the "optimum" value of the lag for each short-period configuration. An attempt was made to compare these data with Figure 1. However, information as to the exact value of the lag for each configuration is not presented in Reference 11; only faired curves of constant lag on a plot of

short-period frequency versus damping are shown. Upon checking with one of the authors of Reference 11, it was determined that there was "considerable scatter" in these curves, but the detailed data on which the curves were based is no longer readily accessible. Viewing the data as a whole, however, the results show that the evaluation pilot preferred some lag for all configurations, except those having very low short-period frequency. In fact, even for moderate short-period frequencies, rather large amounts of lag produced improved pilot ratings. This result is diametrically opposed to the results of Reference 8, in which even small amounts of control-system lag degraded pilot opinion in all cases except when the short-period frequency was very high. For example, a comparison of comparable configurations for the two experiments shows the following:

	(no lag)	lag time constant $\approx$ 0.3 sec
Reference 8	PR $\approx$ 5	PR $\approx$ 8.5
Reference 11	PR $\approx$ 4	PR $\approx$ 3

Note: $\omega_{sp} \approx 5$ rad/sec, $\zeta_{sp} \approx 0.3$ $\quad 1/\tau_{\theta_2} \approx 1.2$

In spite of the fact that Reference 11 uses the Cooper rating scale and Reference 8 uses the latest Cooper-Harper scale, there is a glaring conflict between the two experiments which cannot be resolved because of lack of detailed information concerning the F-86 program.

The ω_θ values used in the data correlations described above are summarized in Figure 23. With the exception of the B-26 program, the values of ω_θ vary between 2.5 and 3.5 rad/sec. The tasks evaluated in the B-26 program are more representative of a Class II airplane than a fighter, and this may explain the lower value of ω_θ . To a lesser extent, the same statement applies to the T-33 wheel program. Thus, the proposed requirements have different values of ω_θ as a function of Class, for Category A Flight Phases.

C. Substantiating Data - Category C

The correlation of available data with the proposed Category C boundaries of Figure 1 began with analysis of the experiments used in the specification backup document (Reference 3). The approach used was similar to that outlined in the Category A data, and the results are presented in Figures 24 and 25.

The T-33 HOS program (Reference 16) provides some data on the effects of control system dynamics in landing approach. These data are presented in Figure 26 for ω_θ = 1.8 rad/sec. It should be noted that this value of ω_θ is considerably higher than the values used to obtain data correlation in Figures 24 and 25. This is probably due to the fact that the tasks evaluated for the configurations of Figure 26 involved more than landing approaches. Several Category A tasks were evaluated for each configuration before the landing appraoch was begun. Thus pilot rating was influenced by these more demanding tasks.

There are two moving-base ground simulator experiments which provide considerable data in the low $1/T_{\theta_2}$, low ω_{sp} area (Reference 21 and some unpublished Grumman results used in the specification backup document). However, there were many flying qualities parameters being varied in these experiments, such as short-period frequency and damping, $1/T_{\theta_1}$, n/α, stick force per g, and control sensitivity. The only hope for sorting out which parameters are causing the pilot rating degradation for a given configuration is to carefully analyze the pilot comments. Unfortunately, detailed pilot comment data are not reported for either experiment. Therefore, it is impossible to decide which configurations could appropriately be used to compare with the proposed requirements of Figure 1.

The results of the data correlations discussed above are summarized in Figure 27. Based on this figure, $\omega_\theta = 1.2$ was used in the proposed requirements.

It should be mentioned that a study was begun to validate the proposed maneuver response requirements for low static stability situations such as might occur at aft c.g. positions. Although there is some limited data available in this area (e.g. Reference 22), most of the data is presented as if the airplane's response were second-order. That is, only the least stable and most stable real roots are identified. Since the airplane is actually a minimum of fourth order, two roots are not identified. The low-frequency pitch attitude zero is not identified either. It was determined that the locations of the two missing roots and attitude zero for low-static-stability configurations can have a strong effect on the shape of the amplitude-phase curves used in the proposed requirements. Therefore, the low-static-stability area was not pursued, due to lack of definitive data.

Between the time the above study was performed and the time the final draft of this report was submitted, data from the X-22A variable stability program became available for which the complete θ/F_s transfer function could be approximated.

An experimental investigation of longitudinal dynamics typical of STOL vehicles was performed by Cornell Aeronautical Laboratory using the Variable Stability X-22A airplane, Reference 23. A number of the configurations from this experiment were briefly analyzed for the proposed requirement using the complete three-degree-of-freedom pitch attitude transfer function. The result of this preliminary analysis indicated that in general the requirement can be applied, however, slight modifications to the definitions of $(\Delta A/\Delta \phi)_\theta$ and $\Delta \phi_\theta$ were considered necessary to avoid confusion in interpreting the amplitude-phase plots when the low frequency transfer function terms are included. Time did not permit a thorough analysis or incorporation of the data from Reference 23 in this report. Further analysis of the X-22A data together with data from the TIFS flight programs should be performed to validate the proposed requirement and to develop interpretation of the low frequency portion of the θ/F_s amplitude-phase plots.

D. Substantiating Data - Category B

It is clear that precise control of pitch attitude is very important for Category A and C Flight Phases. While it is also important for Category B Flight Phases, it is not clear how critical attitude control might be in this situation. The only data available for Category B are from the XB-70 experiment supersonic cruise situation; it is somewhat shaky to associate the pilot ratings only with the short-period characteristics. Also, it is necessary to know the value of $1/T_{\theta_2}$ to generate the parameters needed for comparison with the proposed requirements. Because the XB-70 is essentially a tail-less airplane, $1/T_{\theta_2}$ is probably strongly dependent on L_{δ_e} as well as L_α. Since no information on L_{δ_e} is given in Reference 24, $1/T_{\theta_2}$ must be computed using L_α alone.

With these problems kept in mind, the data were compared with the proposed boundaries, as shown in Figure 28. This correlation was obtained with ω_θ = 1.2 rad/sec, and this value is therefore used in the proposed requirements. It should be mentioned that data for configurations having $1/T_{\theta_2}$ less than 0.5 sec^{-1} were not used in this correlation. This was done because it was felt that the approximation $1/T_{\theta_2} = L_\alpha$ becomes increasingly subject to question at low values of L_α, for an airplane like the XB-70.

Although the data correlation shown in Figure 28 is quite good, the use of ω_θ = 1.2 for Category B Flight Phases should be regarded somewhat preliminary until more data become available.

E. Substantiation of the Level 3 Limit for 3.2.2.1

The Level 3 limit for pitch dynamic response in maneuvering flight is not thoroughly substantiated by data but it is considered to be a reasonable representation of the available data and together with the other requirements in 3.2.2 should be an adequate definition of Level 3 flying qualities.

As defined in 1.5, Levels of flying qualities, the Level 3 limit should provide:

> Flying qualities such that the airplane can be controlled safely, but pilot workload is excessive or mission effectiveness is inadequate, or both.

Based primarily on the above definition, it was decided to make the Level 3 specification boundary the same as the Level 2 boundary in Figure 1 and to make ω_θ slightly less than the value chosen for Level 2 Flight Phase Categories B and C, i.e., ω_θ = 1.1 rather than 1.2.

The resulting Level 3 boundary has not been calculated for each set of data presented. The Level 2 boundary shown on the Boeing C-5A simulation data in Figure 24 and on the T-33 landing data in Figure 25 corresponds to the proposed definition of Level 3 and shows how this boundary varies for two different values of $1/T_{\theta_2}$. The Level 2 boundary for the T-33 data in Figure 25

can be transferred to the NASA F-86 data in Figure 14 to get an idea how the Level 3 boundary would be placed on that data set. This is approximately correct because the $1/\tau_{\theta_2}$ values are nearly equal and the control system dynamics were not a large consideration for either set of data.

F. Philosophy of the Requirement for Compatibility of Steady Maneuvering Forces and Pitch Sensitivity 3.2.2.2

The requirements on compatibility of steady maneuvering forces and pitch control sensitivity are primarily designed to limit problems due to high short-period frequencies. For these configurations, the proposed maneuver response criteria predict a good airplane, even for reasonably low values of short-period damping ratio, yet the pilot comments often indicate tendencies to oscillate or "bobble" on target. The bobbles are generally higher in frequency than the type of closed-loop oscillations which result from low short period frequency, low short period damping, and large lags in the control system. These latter problems are well covered by the pitch dynamic response requirement of 3.2.2.1.

The high frequency oscillations or "bobbles" occur when the pilot attempts precise attitude tracking or makes abrupt inputs. The closed-loop analysis performed in Reference 8 does indicate a second or higher frequency closed-loop resonance (see Figure 29) but the relative amplitude calculated is smaller than what is observed in flight. The problem appears to be strongly related to pitch control sensitivity but it is also influenced by the relative values of the pitch sensitivity at high frequency and the steady forces required to maneuver. The parameters used in the requirement are the steady stick force per g for which there are requirements in 3.2.2.6.1 and the maximum-amplitude-ratio of pitch acceleration response to pilot-applied elevator-control force, $\left|\frac{\ddot{\theta}}{F_s}\right|_{max}$. Consideration was given to establishing independent limits on F_s/n_γ and $\left|\frac{\ddot{\theta}}{F_s}\right|_{max}$ but this would have required separate values to be established for each of these parameters for each type of cockpit controller. It was noted that the available data (presented in following sections) could be fit equally well by bounds on stick force per g and by bounds on the product $\frac{F_s}{n_\gamma} \times \left|\frac{\ddot{\theta}}{F_s}\right|_{max}$. The limits on $\frac{F_s}{n_\gamma} \times \left|\frac{\ddot{\theta}}{F_s}\right|_{max}$ are independent of the type controller.

The proposed requirement 3.2.2.2 takes recognition of the fact that an airplane has multiple degrees of freedom and requires that the control gain for the various airplane responses must be compatible. It further recognizes that the control gain of importance for one response variable may be in a different frequency band than the control gain of importance to another response variable. The stick force per g referenced is the steady state value (assuming constant speed) and the pitch acceleration gain is that occurring at the short period frequency or, if there are lightly damped control system modes, at the frequency which has the largest amplitude ratio. The need for compatibility of these two gains is somewhat intuitive if one thinks of

controlling attitude precisely while also holding the stick force required to pull steady maneuvering load factor.

These two control gains can become incompatible in the sense that the pitch control sensitivity is too high relative to the stick force per g for the following situations.

1. Very high short period frequency.

2. High short period frequency and low short period damping.

3. Large lead in the flight control system.

4. Airplanes with poorly designed bobweight systems that cause the stick-free short period frequency to be much higher than the stick-fixed short period frequency. This causes large amplification of the elevator surface response to pilot applied stick force at frequencies above the stick fixed short period frequency. Examples follow in subparagraph G.

The following paragraphs present substantiation data for the proposed requirement 3.2.2.2.

G. Substantiating Data for Paragraph 3.2.2.2

It was noted in Subsection B above that a number of the configurations from Reference 8 that are in the Level 1 area of Figures 8 and 9 were rated worse than 3.5. All the configurations from the Level 1 area of Figures 8 and 9 are plotted on Figure 30 in terms of F_s/n_γ and $\left|\frac{\ddot{\theta}}{F_s}\right|_{max}$ for each pilot. Also shown on Figure 30 are the present Level 1 stick force per g limits of 3.2.2.6.1 and the proposed control compatibility parameter limits of 3.2.2.2. From Figure 30 it can be seen that a number of configurations fall outside the F_s/n_γ limits and others exceed the proposed limits on $\frac{F_s}{n_\gamma} \times \left|\frac{\ddot{\theta}}{F_s}\right|_{max}$. It It should also be noted that both the pilot ratings and comments from Reference 8 indicate problems when stick force per g exceeds 7 lb/g, and therefore this value is also indicated on Figure 30. The points in the Level 1 area on Figures 8 and 9 have been tagged to indicate which ones violate the boundaries on Figure 30.

Configurations 14, 13, 8A and 3A are identified as the ones that exceed the proposed Level 1 limit of $\frac{F_s}{n_\gamma} \times \left|\frac{\ddot{\theta}}{F_s}\right|_{max} = 3.6 \frac{\text{rad/sec}^2}{\text{g}}$. The values of $\left|\frac{\ddot{\theta}}{F_s}\right|_{max}$ and F_s/n_γ selected by the pilots have been calculated for all the configurations in Groups 3, 5, 8 and the sets 9, 10, 11 and 12, 13, 14 from Reference 8. These data are presented in Figures 31 through 34 together with brief pilot comments. The purpose of these figures is to indicate the different nature of the pilot comments and ratings as the value of the control compatibility parameter is changed from a low value to a high value by variations in either the airplane short period dynamics or the control system dynamics.

For low values of $\frac{F_s}{n_z} \times \left|\frac{\ddot{\theta}}{F_s}\right|_{max}$ the comments are:

"Initial forces high, sluggish initial response. Must overdrive it in pitch. Forces heavy initially then lighten. Load factor control is poor. Tends to dig in. Can't predict the response. PIO in aggressive maneuvers and tight tracking."

Comments of this nature result for configurations with low short period frequency, low short period damping, and excessive control system lag. The proposed criteria of paragraph 3.2.2.1, pitch dynamic response in maneuvering flight, will screen out or prohibit airplanes with these problems.

For high values of $\frac{F_s}{n_z} \times \left|\frac{\ddot{\theta}}{F_s}\right|_{max}$ the comments are:

"Sensitivity around trim. Light initial forces; heavy steady forces. Good control of normal acceleration but poor attitude control. Initial response too abrupt; airplane described as nervous. Tends to bobble on target unless pilot uses low gain. Pilot must smooth his control inputs. Sensitive to external disturbances."

Figure 35 contains similar data and comments for several configurations from the experiment of Reference 9 for which the value of $\frac{F_s}{n_z} \times \left|\frac{\ddot{\theta}}{F_s}\right|_{max}$ was very high. The comments for Case 3 in this group are quite severe.

Figures 36, 37, 38 are taken from Reference 3 (BIUG for 8785) and illustrate data from Reference 15. The plots have been modified by changing the definition of the ordinate scale from M_{F_s} to $\left|\frac{\ddot{\theta}}{F_s}\right|_{max}$ and by adding points from the experiment of Reference 15 for which the short period damping ratio was low. These points are identified on each plot. The pilot rating and PIO rating, together with a footnote to indicate the type of PIO problem encountered, is noted for a number of points. The PIO rating scale is defined in Figure 39. Comparisons between Figures 19, 20, 21 and Figures 36, 37, 38 will indicate that this set of data is quite well screened by the combination of the proposed 3.2.2.1 and 3.2.2.2 requirements. The low frequency cases and low damping cases with low to moderate frequency are screened by the requirement of 3.2.2.1. The high frequency cases and high frequency cases with low damping are screened by the requirement of 3.2.2.2.

It should be realized that for the case of high short period damping ratio, and negligible control system dynamics

$$M_{F_s} = \left|\frac{\ddot{\theta}}{F_s}\right|_{max}$$

and

$$\frac{F_s}{n_\gamma} \times \left|\frac{\ddot{\theta}}{F_s}\right|_{max} = \frac{F_s}{n_\gamma} M_{F_s} = \frac{\omega_{sp}^2}{n/\alpha}$$

For high short period frequency cases with low short period damping or significant control system dynamics, $\left|\frac{\ddot{\theta}}{F_s}\right|_{max} = k M_{F_s}$

$$\frac{F_s}{n_\gamma} \times \left|\frac{\ddot{\theta}}{F_s}\right|_{max} = k \frac{\omega_{sp}^2}{n/\alpha}$$

where k is an amplification or attenuation factor. For the case of negligible control system dynamics, the amplification factor is related to the short period damping ratio. $k = \frac{1}{2\zeta_{sp}}$ for $\zeta_{sp} < 0.2$ and $k = 1$ for $\zeta_{sp} > 0.7$. Thus, the suggested limits on $\frac{F_s}{n_\gamma} \times \left|\frac{\ddot{\theta}}{F_s}\right|_{max}$ are equivalent to the high frequency limits on $\frac{\omega_{sp}^2}{n/\alpha}$ in paragraph 3.2.2.1 of MIL-F-8785B(ASG) for high short period damping ratio and negligible control system dynamics. For low short period damping ratio, however, the new requirement limits the maximum short period frequency to lower values than MIL-F-8785B(ASG). Assuming negligible control system dynamics, the proposed Level 1 requirement $\frac{F_s}{n_\gamma} \times \left|\frac{\ddot{\theta}}{F_s}\right|_{max} = 3.6 \frac{\text{rad/sec}^2}{g}$ maps on the ω_{sp}-ζ_{sp} plane as indicated by the dashed lines in Figures 13 through 21, 24, 25.

In Figures 40 through 47, time histories are shown which indicate the dynamic character of the pilot-airplane-Flight Control System combination for configurations 14, 13, 8A, 3A and 5A from Reference 8. These time histories illustrate various examples of the problems described by the pilots when evaluating configurations with high values of $\frac{F_s}{n_\gamma}\left|\frac{\ddot{\theta}}{F_s}\right|_{max}$. All the time histories shown are taken from flights on which pilot M of Reference 1 was the evaluation pilot.

Configuration 14 was evaluated on Flight 1054. The PR = 6, the PIO rating = 3. The control gain was adjusted such that $\frac{F_s}{n_\gamma} = 5.4$ lb/g and $\left|\frac{\ddot{\theta}}{F_s}\right|_{max} = 1.53 \frac{\text{rad/sec}^2}{\text{lb}}$. The record shown in Figure 40 was taken from the discrete-error pitch-attitude tracking task. The pilot was required to drive the pitch attitude error to zero as rapidly and accurately as he considered necessary. The pitch attitude error indicator was driven by the difference between a command and actual pitch attitude. Discrete step commands occurred at random times and were random in magnitude and direction. Figure 40 shows the pilot correcting two of these commands in rapid succession. The transient behavior is considerably different in the two cases. In the first case two dynamic modes are indicated, one with a frequency of about 16.3 rad/sec and the other with a frequency of about 7.5 rad/sec. This is roughly consistent with the closed-loop analysis of Reference 8 as illustrated in Figure 29.

Figure 29 shows the closed-loop system characteristics for two cases, one assuming pilot lead-lag compensation as required to meet the closed-loop performance criteria of Reference 1 and the other showing the closed-loop characteristics resulting if the loop gain is adjusted to meet only the droop requirement. This is perhaps representative of the closed-loop system if the pilot were to attempt to fly the airplane without providing any lead-lag compensation.

In correcting the second command in Figure 40, the pilot-airplane combination exhibits a very lightly damped oscillation of about 16.3 rad/sec with little indication of the lower frequency resonance predicted by the closed-loop analysis. This high frequency oscillation is an example of the problem encountered by the evaluation pilot when attempting rapid transitions from one visual target to another and when attempting precise attitude tracking. The problem was especially troublesome when the airplane was also being disturbed by a random noise input to the elevator. The pitch accelerations experienced are quite large.

Configuration 13 was first evaluated by pilot M on Flight 1053. The PR = 7 and the PIOR = 3. The control gain was adjusted such that $\frac{F_s}{n_z} = 6.0 \frac{lb}{g}$ and $\left|\frac{\ddot{\theta}}{F_s}\right|_{max} = .75 \frac{rad/sec^2}{lb}$. Figure 41 shows the pilot responding to a series of step attitude commands. The transient during the first two commands is pretty well behaved with a small overshoot. The transient for the third command which was pitch down in direction is quite slow and may indicate a reluctance on the part of the pilot to be very abrupt in accomplishing pushover maneuvers because of the susceptibility of certain configurations, such as No. 13, to develop oscillations when push forces are required.

Configuration 13 was evaluated a second time on Flight 1066. The PR = 5.5 and PIOR = 2.5 for this evaluation. The control gain was adjusted such that $\frac{F_s}{n_z} = 8.1$ and $\left|\frac{\ddot{\theta}}{F_s}\right|_{max} = .53 \frac{rad/sec^2}{lb}$. Figure 42 shows the airplane responding to an electrical step elevator command which is removed about midway through the record. Shortly thereafter the evaluation pilot resumed control of the airplane and proceeded to recover to level flight. During this pushover maneuver, a lightly damped closed-loop oscillation developed which typifies the pilot's complaint of small amplitude, high frequency oscillations resulting from his control efforts. For Configuration 13 this problem was most evident when the pilot was attempting precise attitude control with visual reference to the outside world.

Configuration 8A was evaluated on Flight 1028. The PR = 5 and PIOR = 2.5. The control gain was adjusted such that $\frac{F_s}{n_z} = 6.3$ lb/g and $\left|\frac{\ddot{\theta}}{F_s}\right|_{max} = .84 \frac{rad/sec^2}{lb}$. Three records are shown for this configuration in Figures 43, 44, and 45. The record shown in Figure 43 illustrates the pilot responding to step attitude commands. The pilot had evidently decided to apply a pull force to the stick just about the time the command for a pitch-down step occurred. The pilot made a rapid reversal of the stick force and set off a small amplitude, high frequency, lightly damped closed-loop oscillation.

The record shown in Figure 44 shows the pilot responding to a pitch-up command. In this case the transient response is relatively free of high frequency oscillations. Figure 45 shows a section of a tracking record where the pilot is trying to follow a continuous randomly varying pitch attitude command. This record illustrates the high frequency closed-loop oscillation typical of configurations with high values of $\frac{F_s}{n_\gamma} \times \left|\frac{\ddot{\theta}}{F_s}\right|_{max}$.

Configuration 3A was evaluated on Flight 1044. The PR = 4 and PIOR = 1.5. The control gain was adjusted such that F_s/n_γ = 5.4 lb/g and $\left|\frac{\ddot{\theta}}{F_s}\right|_{max}$ = .99 $\frac{\text{rad/sec}^2}{\text{lb}}$. Figure 46 shows the pilot responding to a series of step pitch attitude commands. The transient response is fast with essentially no overshoot. The pitch acceleration resulting from the applied stick force is relatively large as compared with other configurations and is probably the cause of the pilot comment about the abruptness of the initial response and high pitch sensitivity.

Configuration 5A was evaluated on Flight 1026. The PR = 7 and PIOR = 3. The control gain was adjusted such that F_s/n_γ = 10 lb/g and $\left|\frac{\ddot{\theta}}{F_s}\right|_{max}$ = .4 $\frac{\text{rad/sec}^2}{\text{lb}}$. Figure 47 shows the pilot responding to a pitch-down command first and later to a pitch-up command. In responding to the pitch-down command it is clear that the pilot initially misinterpreted the command and applied a pull force. He quickly reversed the elevator input but, in so doing, he set off a lightly damped closed-loop oscillation. An oscillation is also evident in the transient following the pitch-up command. The closed-loop transient response for this configuration is quite similar to that calculated in Reference 8 from the closed-loop analysis. This configuration fails to meet the proposed dynamic response requirement of paragraph 3.2.2.1 and also fails to meet the proposed Level 1 requirement on $\frac{F_s}{n_\gamma} \times \left|\frac{\ddot{\theta}}{F_s}\right|_{max}$.

H. Comparison of A4D and T-38 Airplanes with Proposed Requirements

The A4D and T-38 airplanes both encountered pilot-induced oscillation (PIO) problems at low-altitude high-speed flight conditions with the original flight control systems. In each case, modifications to the flight control system were required to alleviate the problem. References 25 and 26 contain information describing these airplanes and their flight control systems. Based on the information in these reports, the block diagram of Figure 48 and mathematical models have been developed to represent the feel system, elevator servo and airframe. The significant parameters for each airplane are listed in Table I. Frequency response plots have been calculated for elevator deflection in response to pilot applied stick force for each airplane in the configuration that had the PIO problem and for the modified control systems. These Bode diagrams are plotted on Figures 49, 50, 51 and 52. The unmodified (PIO) control systems both exhibit large amplitude magnification in the frequency band $5 < \omega < 25$ rad/sec together with phase lead around $5 < \omega < 10$ rad/sec. The modified control systems both show considerable reduction in the amplitude magnification and elimination of the phase lead. They also indicate a decrease in damping ratio of the control system mode at $\omega \approx 19$ rad/sec for the A4D and 24 rad/sec for the T-38.

TABLE I

Low Altitude (Sea Level - 10,000 ft)

Airplane			STI T.M. 239-3 T-38, aft c.g.		Douglas LB-25452 A4D-2, c.g. slight aft	
Control System Configuration:			orig.	mod.	orig.	mod.
Airframe Parameters:						
stick fixed	ω_{sp}	rad/sec	7.0		7.94	
	ζ_{sp}		.40		.40	
stick free	ω'_{sp}	rad/sec	9.8	7.5	8.8	4.8
	ζ'_{sp}		.10	.28	.16	.34
	n/α		94	94	69	69
	τ_{θ_2}	sec	.315		.44	
	τ_{n_1}	sec	.0509		.040	
	τ_{n_2}	sec	-.0506		-.038	
	K_θ	rad/sec/deg	-.86		-.026	
	n_z/δ_e	g's/deg	-2.54		-.79	
	V	ft/sec	950		980	
	M/h	ft	.85/SL		.91/1000	
Control System Parameters						
(on ground)	ω_{FS}	rad/sec	18.0	$\approx$ 25	13.7	10.7
	ζ_{FS}		.18	$\approx$ .13	.45	.62
	τ_{ES}	sec	.05		.04	
(in flight)	ω'_{FS}	rad/sec	17.7	24	18.4	19.2
	ζ'_{FS}		.23	.17	.22	.14
	τ'_{ES}	sec	.046	.046	.031	.029
	(δ_s/F_T)	in./lb	.20	.10	.314	.294
	(δ_e/δ_s)	deg/in.	-1.0		-2.41	
	(δ_e/δ_s)	in./lb	.098	.085	.105	.146
	$K_{b_{\ddot{\theta}}}$	lb/rad/sec^2	.80	.40	2.48	5.38
	K_{b_n}	lb/g	2.0	1.0	3.01	1.56
	(F_s/n_z)	lb/g	4.0	4.6	4.6	3.3

Frequency response plots have also been calculated for pitch acceleration in response to pilot applied stick force for these airplanes. These Bode diagrams are presented in Figures 53, 54, 55 and 56. The unmodified (PIO) configurations both exhibit large $\left|\frac{\ddot{\theta}}{F_s}\right|$ in the frequency band $5 < \omega < 25$ rad/sec. The modified configurations have a factor of five reduction in the amplitude ratio in the frequency band near $\omega = 10$ rad/sec. The control system resonance of the A4D at $\omega \approx 19$ rad/sec is evident in the plot on Figure 54.

The amplitude vs phase plot specified in 3.2.2.1 has been calculated for each of the A4D and T-38 configurations and the measures $\Delta\phi_{\omega=3}$ and $\frac{\Delta A}{\Delta\phi}\Big|_{\omega=3}$ have been calculated. The amplitude-phase plots are presented in Figures 57, 58, 59, and 60. These specification measures are plotted in Figure 61 to illustrate how these airplanes compare with the proposed requirement. In the original configurations both airplanes are in the Level 2 region near the Level 2 limit. The modified configurations are also in the Level 2 region but near the Level 1 boundary indicating a quite substantial improvement in the pitch control characteristics.

In Figure 62, the stick force per g and the maximum pitch sensitivity for these airplanes have been plotted. The unmodified airplanes are both outside the Level 1 boundary and the modified airplanes are both well within that boundary. It should be realized in reviewing calculations such as those just described that they may not represent the real airplanes very accurately. At best, they represent linearized descriptions of control systems that have significant nonlinearities such as friction, preload, nonlinear gearing and nonlinear spring gradients with stick deflection. In the case of the T-38, for example, there is considerable difference in the stick force per g information quoted in References 25, 27 and 28. These differences are indicated in Table II. The frequency response calculations presented above were based on the information contained in Reference 25 and may not represent the actual T-38 airplane very accurately; however, general observations should be valid.

TABLE II
COMPARISON OF F_s/n_z INFORMATION IN
REFERENCES 25 AND 27 FOR THE T-38

Reference	Airplane Configuration	$\left\|\frac{F_s}{n_z}\right\|$ steady state	$\left\|\frac{F_s}{n_z}\right\|$ minimum dynamic
25	Baseline	4.0 lb/g	0.7 lb/g
	Modified	4.6	2.9
27	Baseline	4.3 lb/g	1.3 lb/g
	Modified	6.4	3.8

I. Philosophy of the Requirement for Dynamic Control Gain in Maneuvering Flight 3.2.2.3

The requirement should be viewed primarily as an additional motivation for the designer to either provide adequate damping of the short period and control system dynamic modes or to increase the steady stick force per g. The paragraph is included in 3.2.2 as one of the set of requirements expressed in frequency response terminology, designed to achieve good maneuvering response and to avoid PIO tendencies. The requirement should prevent undesirable phase relationship between control force and stick displacement.

J. Discussion and Substantiation

Basically, the new requirement is the same as 3.2.2.3.1 of MIL-F-8785B (ASG). The title and wording have been changed to clarify the intent without specifying a flight-test technique. The word dynamic has been substituted for transient in the title to avoid any connotation of a direct ratio of force to normal acceleration in a transient response to a step or pulse force input. The requirement wording now clearly indicates the frequency response of normal acceleration measured at the c.g. to elevator control force. The requirement is made applicable to frequencies greater than 1.0 rad/sec to avoid confusion with the phugoid mode.

The requirement that the stick deflection not lead the stick force at any frequency of force application has been retained primarily to discourage improperly designed feel systems such as the bobweight systems originally in the A4D and T-38 airplanes. See Figures 49 and 51.

The old requirement 3.2.2.3.1 in MIL-F-8785B(ASG) did not specify different values for the dynamic control force for different Levels. Because of the ground rule in paragraph 3.1.10.3.2 of MIL-F-8785B(ASG), when Levels are not specified in a requirement, the requirement applies for all conditions of system failure except approved Airplane Special Failure States. This ground rule makes the requirement too severe and therefore the new requirement 3.2.2.3 specifies separate values of dynamic control force per g for Levels 1, 2 and 3.

The values specified for the dynamic stick force per g are expressed in terms of formulas involving limit load factor as is done in Table V of MIL-F-8785B for steady maneuvering gradients. The constants in the formula are defined such that for an airplane with classical modal parameters and negligible control system dynamics, the maximum short period damping ratio required is $\zeta_{sp} \approx .35$. This value is arrived at by considering the following combinations of circumstances.

Center Stick

Level	Steady State F_s/n	Dynamic F_s/n	Ratio	Equivalent ζ'_{sp}
1	$\frac{21}{n_L-1}$	$\frac{14}{n_L-1}$	1.5	.35
2	$\frac{18}{n_L-1}$	$\frac{12}{n_L-1}$	1.5	.35
3	$\frac{12}{n_L-1}$	$\frac{8}{n_L-1}$	1.5	.35

Wheel

Level				
1	$\frac{45}{n_L-1}$	$\frac{30}{n_L-1}$	1.5	.35
2	$\frac{38}{n_L-1}$	$\frac{25}{n_L-1}$	1.5	.35
3	$\frac{25}{n_L-1}$	$\frac{17}{n_L-1}$	1.5	.35

Other implications of the requirement are explored in the following examples.

Assume an airplane with center stick and $n_L = 7.0$ is designed to have the minimum Level 1 steady stick force per g.

$$\frac{F_s}{n} = \frac{21}{7-1} = 3.5 \text{ lb/g}$$

Next assume that it has a washed out pitch-rate feedback to increase short period damping. If this pitch damper failed, the specification would permit the dynamic stick force per g to decrease to 2 lb/g for Level 2 and to 1.33 lb/g for Level 3. The steady state stick force would probably not change as a result of such a failure, thus the ratio of steady state to dynamic stick force per g is

Level 2

$$\left.\frac{F_s}{n}\right|_{ss} \div \left.\frac{F_s}{n}\right|_{dynamic} = \frac{21}{(n_L-1)}\frac{(n_L-1)}{12} = 1.75 \qquad \zeta = 0.29$$

Level 3

$$\frac{21}{(n_L-1)}\frac{(n_L-1)}{8} = 2.62 \qquad \zeta = 0.19$$

(From Fig. 1(3.2.2.3.1) of Reference 3)

If the airplane had been designed to have the maximum Level 1 stick force per g permitted for high n/α, then

$$\frac{F_s}{n} = \frac{56}{6} = 9.33 \text{ lb/g}$$

In this case the specification would permit the following Level 2 and Level 3 damping ratios

Level 2

$$\left.\frac{F_s}{n}\right|_{ss} \div \left.\frac{F_s}{n}\right|_{dyn} = \frac{56}{12} = 4.66 \; ; \; \zeta_{sp} = 0.107$$

Level 3

$$\left.\frac{F_s}{n}\right|_{ss} \div \left.\frac{F_s}{n}\right|_{dyn} = \frac{56}{8} = 7.0 \; ; \; \zeta_{sp} = 0.071$$

The trends and values of stick force per g and short period damping ratio are quite consistent with the data for center sticks in Figures 2 - 6 (3.2.2.3.1) in Reference 3, reproduced here as Figures 63 through 67.

The corresponding situations for wheel controllers result in the following damping ratio values. For the case where steady stick force is on minimum Level 1 limit:

Level 2

$$RATIO = \frac{45}{25} = 1.8 \; ; \; \zeta_{sp} = 0.28$$

Level 3

$$RATIO = \frac{45}{17} = 2.65 \; ; \; \zeta_{sp} = 0.19$$

For the case where the steady stick force is on the maximum Level 1 limit for high n/α :

Level 2

$$RATIO = \frac{120}{25} = 4.9 \; ; \; \zeta_{sp} = 0.10$$

Level 3

$$RATIO = \frac{120}{17} = 7.06 \; ; \; \zeta_{sp} = 0.071$$

The discussion under 3.2.2.3, pilot-induced oscillations, on pages 135-163 of Reference 3 covers the effect of control system dynamics resulting from devices such as bobweights and elevator hinge moments. The following general transfer function for airplanes with such devices is shown on page 141 of Reference 3.

$$F_s \rightarrow \boxed{\frac{\omega_{cs}^2 \; \frac{\delta_e}{F_{cs}} \left(s^2 + 2\zeta_{sp}\omega_{n_{sp}} s + \omega_{n_{sp}}^2\right)}{\left(s^2 + 2\zeta'_{cs}\omega'_{cs} s + \omega'^2_{cs}\right)\left(s^2 + 2\zeta'_{sp}\omega'_{sp} s + \omega'^2_{sp}\right)}} \rightarrow \delta_e \rightarrow \boxed{\frac{(AIRFRAME\ NUMERATOR)}{s^2 + 2\zeta_{sp}\omega_{n_{sp}} s + \omega_{n_{sp}}^2}} \rightarrow AIRFRAME\ RESPONSE$$

The frequency response for elevator to stick force can look like the sketch on page 141 of Reference 3 if the stick free short period frequency is higher than the stick fixed short period frequency. Examples of this situation are illustrated in Figures 49 and 51 for the A4D and T-38 airplanes. It should be noted that the gain at frequencies higher than $\omega_{n_{sp}}$ (stick fixed short period) is increased because of two factors. First, there are resonant peaks at the stick free short period and at the stick free control system natural frequency. These are a result of low damping ratio in these roots.

A second cause of increased gain results from the stick free short period frequency being higher than the stick fixed value. If we next look at airplane responses to control force inputs, it is observed that the pitch acceleration and the normal acceleration frequency responses are modified as indicated in the following sketches. See Figures 53 and 55 also.

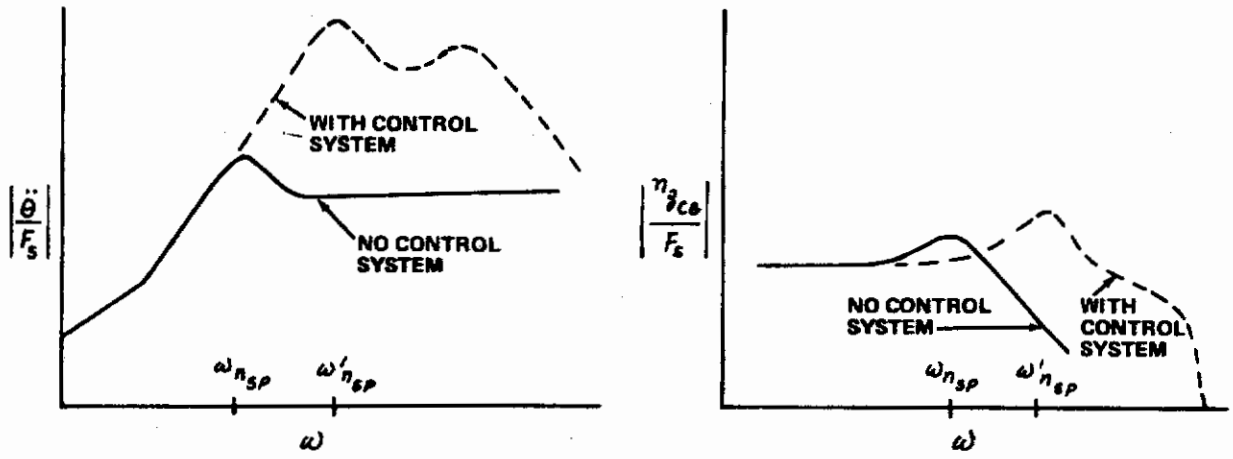

From these sketches it is seen that the effect of the control system on the normal acceleration frequency response is to extend the frequency range, perhaps alter the short period damping ratio and to exhibit additional higher frequency modes. The requirement on minimum dynamic stick force per g of 3.2.2.3 is seen to be primarily a limit on the relation between steady stick force per g and stick free damping ratio.

In contrast the pitch acceleration frequency response is directly affected by both the damping ratio and the relative values of $\omega_{n_{sp}}$ and $\omega'_{n_{sp}}$ i.e., "stick-fixed" and stick-free short period frequency. Therefore it is concluded that the requirement of 3.2.2.2 is probably more sensitive to the type of problem caused by improper control system design than the requirement of 3.2.2.3. Both are believed to be necessary together with 3.2.2.1 to ensure good maneuver dynamics and to minimize the possibility of encountering pilot-induced oscillations of either the "low" frequency type or the "high" frequency type described in Subparagraph F.

K. Philosophy of Requirements 3.2.2.4, Residual Oscillations, and 3.2.2.5, Pilot-Induced Oscillations

These two requirements are identical to MIL-F-8785B(ASG). They have been reunumbered and grouped with the other requirements for longitudinal maneuvering characteristics.

L. Philosophy of Requirements on Control Forces and Displacements in Steady Maneuvering Flight, 3.2.2.6

The philosophy of this set of requirements 3.2.2.6, 3.2.2.6.1 and 3.2.2.6.2 is the same as the old paragraphs 3.2.2.2, 3.2.2.2.1, and 3.2.2.2.2. They establish the sense or sign of control force and displacement gradients in steady maneuvering flight and put limits on the gradient magnitudes.

M. Discussion and Substantiation for 3.2.2.6

The titles of the paragraphs have been changed to more explicitly describe their content. The words "feel" and "stability" have been eliminated because they can have dynamic connotations that are not really addressed in the requirements. The word "steady" has been introduced to call attention to the fact that the gradients referenced are for steady turns or based on the constant speed assumption.

The wording changes introduced by the 31 March 1971 revision to MIL-F-8785B(ASG) are incorporated in the paragraphs, i.e., "motion" and "deflection" are replaced by "displacement", and "increase" is replaced by "incremental".

The sentences in 3.2.2.2.1 that make reference to the old short period frequency requirement have been eliminated in the new 3.2.2.6.1.

Consideration was given to changing the linearity requirement in 3.2.2.6.1 but it was concluded that the requirements are appropriate and should be retained until more definitive data become available.

The most significant change to paragraph 3.2.2.6.1, however, is the change proposed in Table V for the minimum stick force per g limits. The changes proposed are:

Center Stick Controllers

Make minimum gradient a function of n_L and reduce the absolute limit from 3 lb/g to 2 lb/g.

Make Level 3 the higher of $\frac{12}{n_L - 1}$ and 2.

Wheel Controllers

Make minimum gradient a function of n_L.

Make Level 3 the higher of $\frac{25}{n_L - 1}$ and 6.

These recommendations are discussed in more detail below.

Linearity

The French have recently brought up the old argument about the need (or lack of need) for linearity in the gradient of stick force with load factor. Many people feel that the gradient should be greater at high load

factor than at 1.0 g, to provide g-limiting. Others feel that the gradient should be significantly higher around 1.0 g for making small, precise maneuvers, than be reduced at high load factors to allow gross maneuvers to be performed without undue pilot effort. Both groups think that a gradient change of more than 50 percent is no problem, as long as the transition is smooth.

On the subject of gradient shape, paragraph 3.2.2a of CAL's recommended revisions to MIL-F-8785 (dated May 1967) contained the following statement:

> "In addition, the force versus normal acceleration plot shall be linear, or smooth and concave downward; and the ratio of the maximum local gradient shall never exceed 2.0."

This statement drew considerable criticism; here are some examples:

- FDCC and SEG - "Maybe concave upward is O.K."
- R.J. Woodcock - "Why should we insist on prohibiting any upward concavity at all for $n < .85\ n_L$?"
- G.D./Fort Worth - "It is believed that the "concave downward" requirement may be difficult to meet due to $C_m \sim C_L$ nonlinearities. Considering constant elevator effectiveness, this requirement stipulates that $C_m \sim C_L$ should have a constant, stable slope or an increasingly stable slope up to approximately 89 percent limit load factor."
- Fairchild-Hiller - "The last sentence in this paragraph should be eliminated. There are many airplanes which have a "convex" stick force/load factor relationship and it is not regarded as a deficiency."
- LTV - "The wording is contradictory. The gradient can't be linear and also concave downward or change value by a factor of 2. The main criteria should be that the variations are smooth and an increasing force accompany an increasing load factor. As written, this paragraph would outlaw certain feel systems in present day airplanes that are considered acceptable."
- NAA/LAD - "Clarify concave downward. This seems contrary to our past experience."
- NASA - "The forces versus normal acceleration should be linear or preferably concave upward, not downward. A concave downward variation promotes overshoots in rapid maneuvers. Furthermore, allowing the ratio of the maximum local gradient to the minimum local gradient to be as high as 2.0 might permit the local gradients to fall below the minimum desired. It would appear that a more definitive requirement on the minimum local gradient is needed."

These comments indicate that "concave upward" is good, and may even be desirable. On the other hand, many satisfactory production airplanes have "concave downward" gradients. These thoughts led to the conclusion that not enough is known about gradient nonlinearities to specify desired shape. Therefore, the "concave downward" requirement was abandoned. Even today there does not appear to be evidence that any particular type of nonlinearity shape is necessarily bad, as long as the magnitude of the nonlinearity is not too large.

Concerning the magnitude of the allowable nonlinearity, a number of people have criticized the 50 percent nonlinearity limit of 3.2.2.2.1, primarily on the grounds that it is unrealistic. McDonnell, in its F-4 comparison with MIL-F-8785B, is one company that shares this opinion. They suggest that any amount of nonlinearity is satisfactory as long as the gradient is reasonably smooth and all local gradients are within the numerical limits of 3.2.2.2.1. This certainly seems reasonable, but the 50 percent requirement of 3.2.2.2.1 is worded in such a way that the procuring activity can exercise judgment in its enforcement. In view of this, it is recommended that the requirement remain unchanged to force each contractor to justify why his nonlinear gradient is satisfactory.

Minimum Level 3 Gradient

In their comparison of the F-4 with MIL-F-8785B, the McDonnell people show data which indicate Level 3 flying qualities for values of stick force per g as low as 1.0 lb/g. On this basis, they recommend that the minimum Level 3 limit of 3.2.2.2.1 be reduced from 3.0 lb/g to 2.0 lb/g.

The F-4 data presented is entirely consistent with the T-33 data used to establish the requirements of 3.2.2.2.1. Figure 1 (3.2.2.2.1) of the backup document shows that the USAF pilot of Reference D3 had values of stick force per g as low as 1.0 lb/g. Examination of Reference D3 shows that his pilot ratings never went below PR = 7, even at these low values of force gradient. Also, the CAL B-26 demonstration programs regularly show that an airplane can be controllable with the c.g. at the maneuver point, i.e., with zero stick force per g.

Even though existing data show that very small values of stick force per g can result in a controllable airplane under the proper conditions, the old MIL-F-8785 minimum value of 3.0 lb/g was retained as a conservative measure. This was done as a hedge against any "combination of bads" situation that might accompany low stick force per g. This philosophy seems valid, but the exact minimum value used is rather arbitrary. In view of these facts, it is concluded that reducing the minimum Level 3 limit for stick controllers to 2.0 lb/g is reasonable for high load factor airplanes. Because center stick controllers are being considered for low load factor airplanes, it is considered necessary to make the Level 3 minimum stick force gradient a function of n_L. It is proposed that the Level 3 lower limit for center stick controllers be changed to read: the higher of $\frac{12}{n_L - 1}$ and 2 lb/g. Similarly the Level 3 lower limit for wheel controllers should be changed to read: The higher of $\frac{25}{n_L - 1}$ and 6 lb/g.

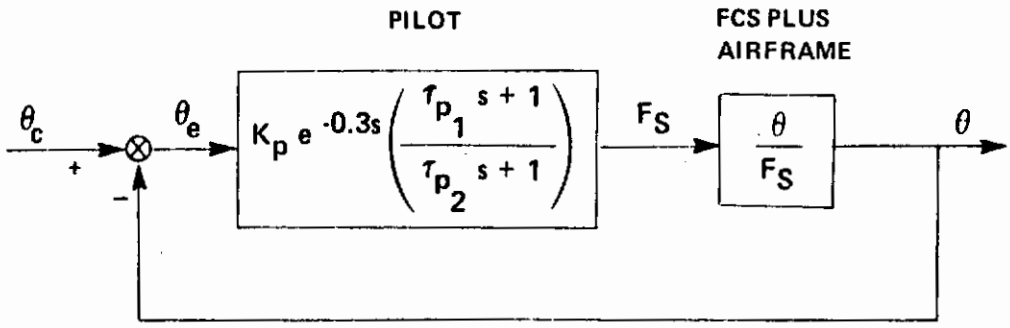

Figure 6 MATHEMATICAL MODEL OF PITCH ATTITUDE TRACKING

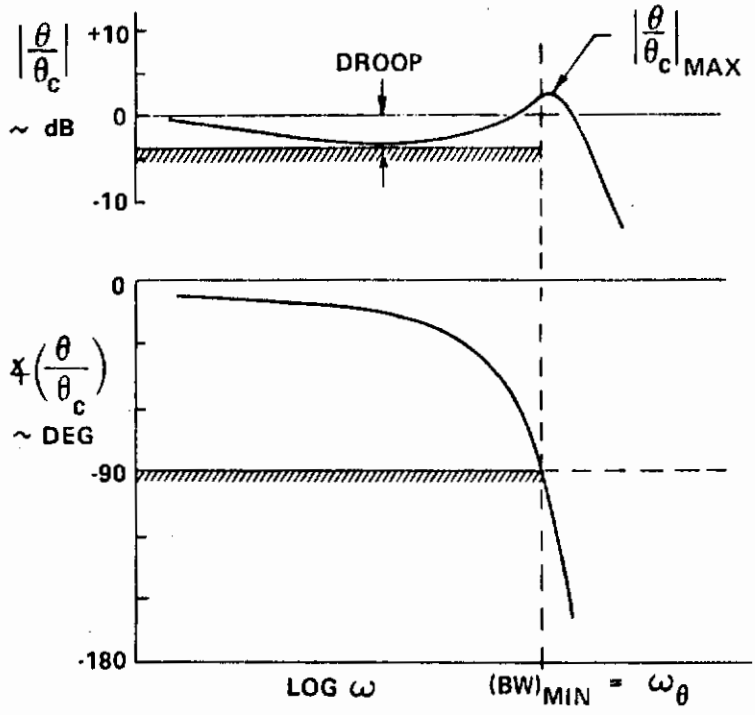

Figure 7 TRACKING PERFORMANCE STANDARDS USED IN THE ANALYSIS

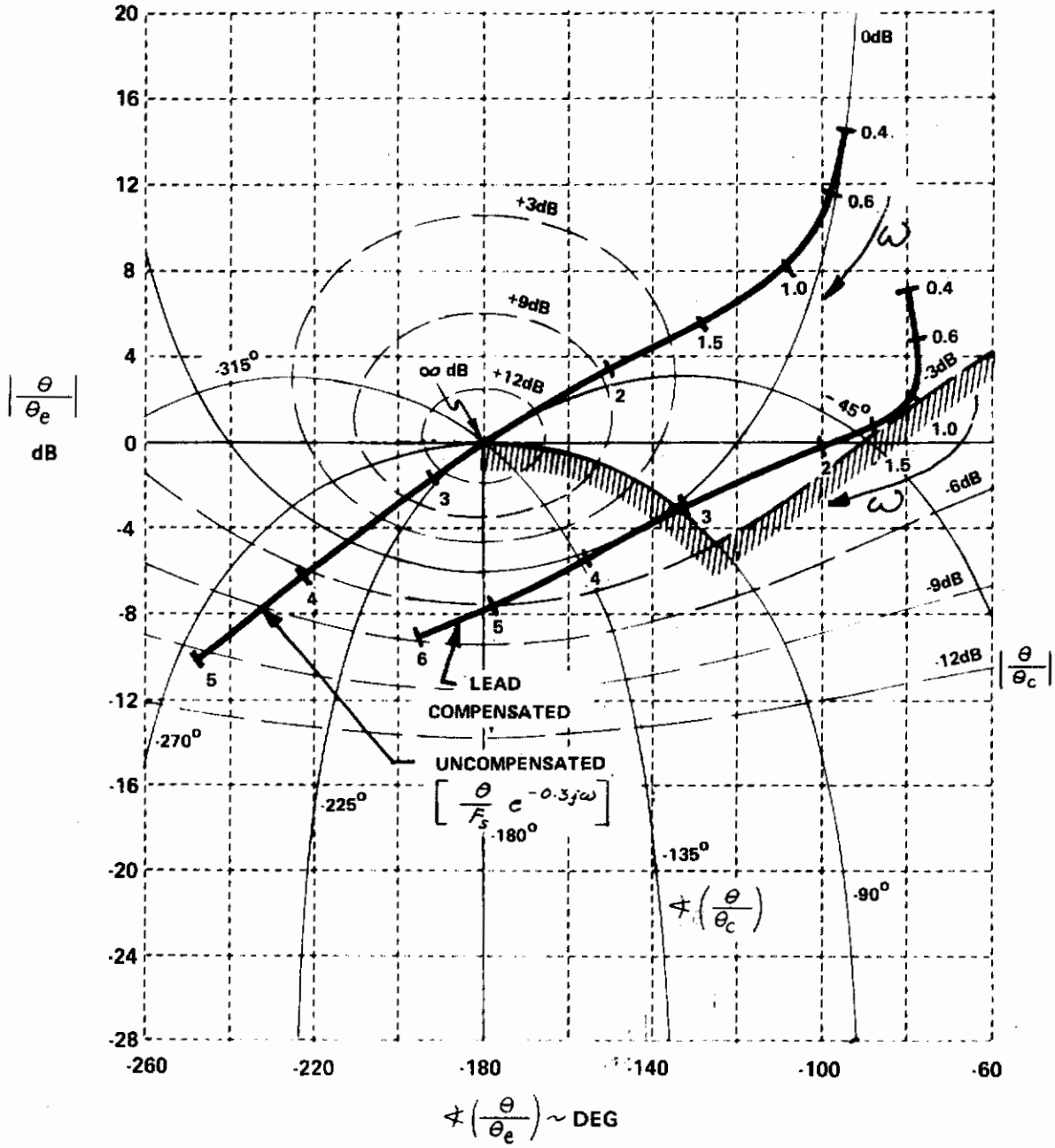

Figure 8a LOW ω_{SP}, WELL-DAMPED SHORT PERIOD CONFIGURATION

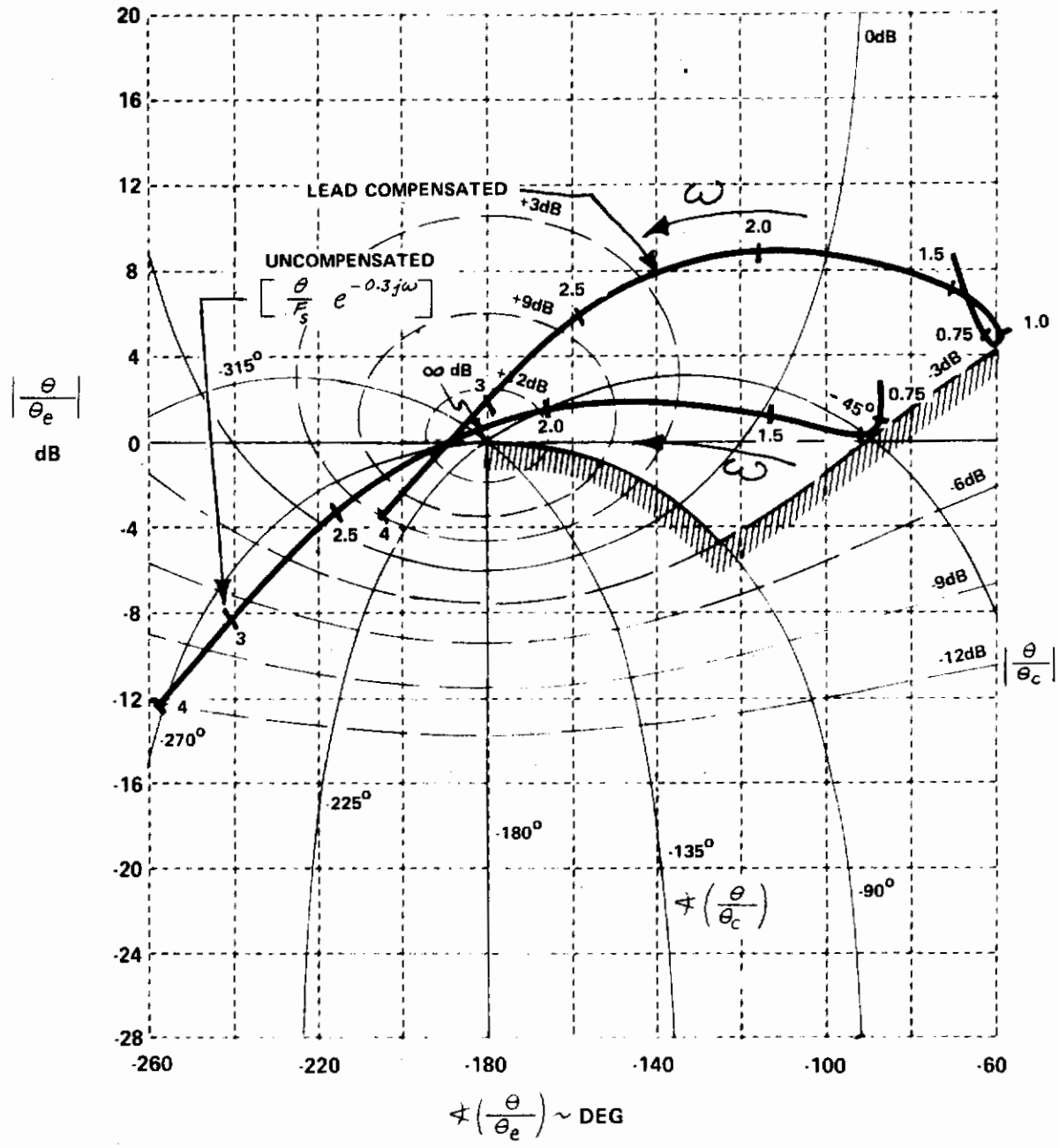

Figure 8b LOW ω_{sp}, LOW ζ_{sp} SHORT PERIOD CONFIGURATION

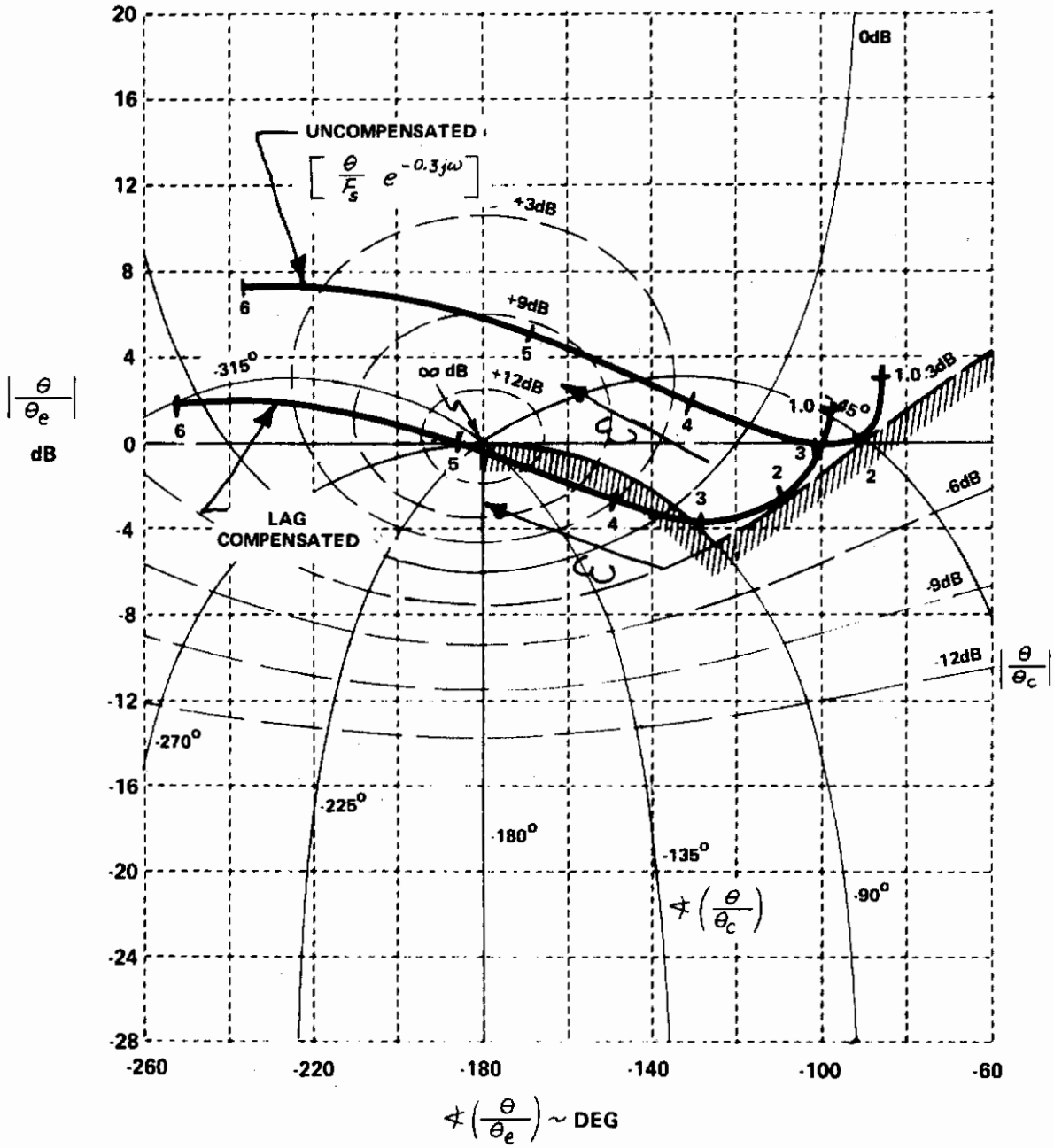

Figure 8c MODERATE ω_{sp}, LOW ζ_{sp} SHORT PERIOD CONFIGURATION

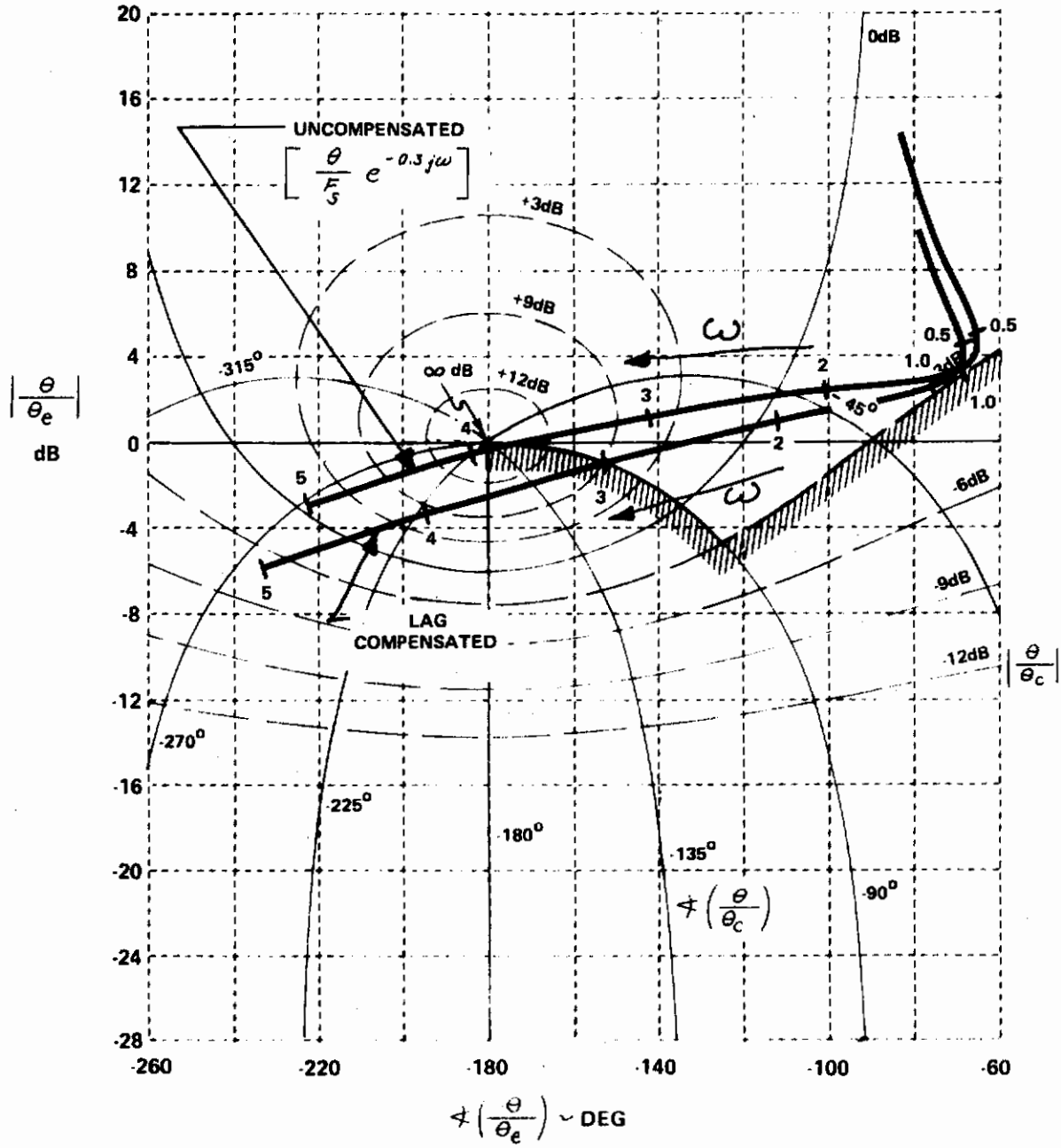

Figure 8d LOW $1/\tau_{\theta_2}$, GOOD ω_{SP}, GOOD ζ_{SP} SHORT-PERIOD CONFIGURATION

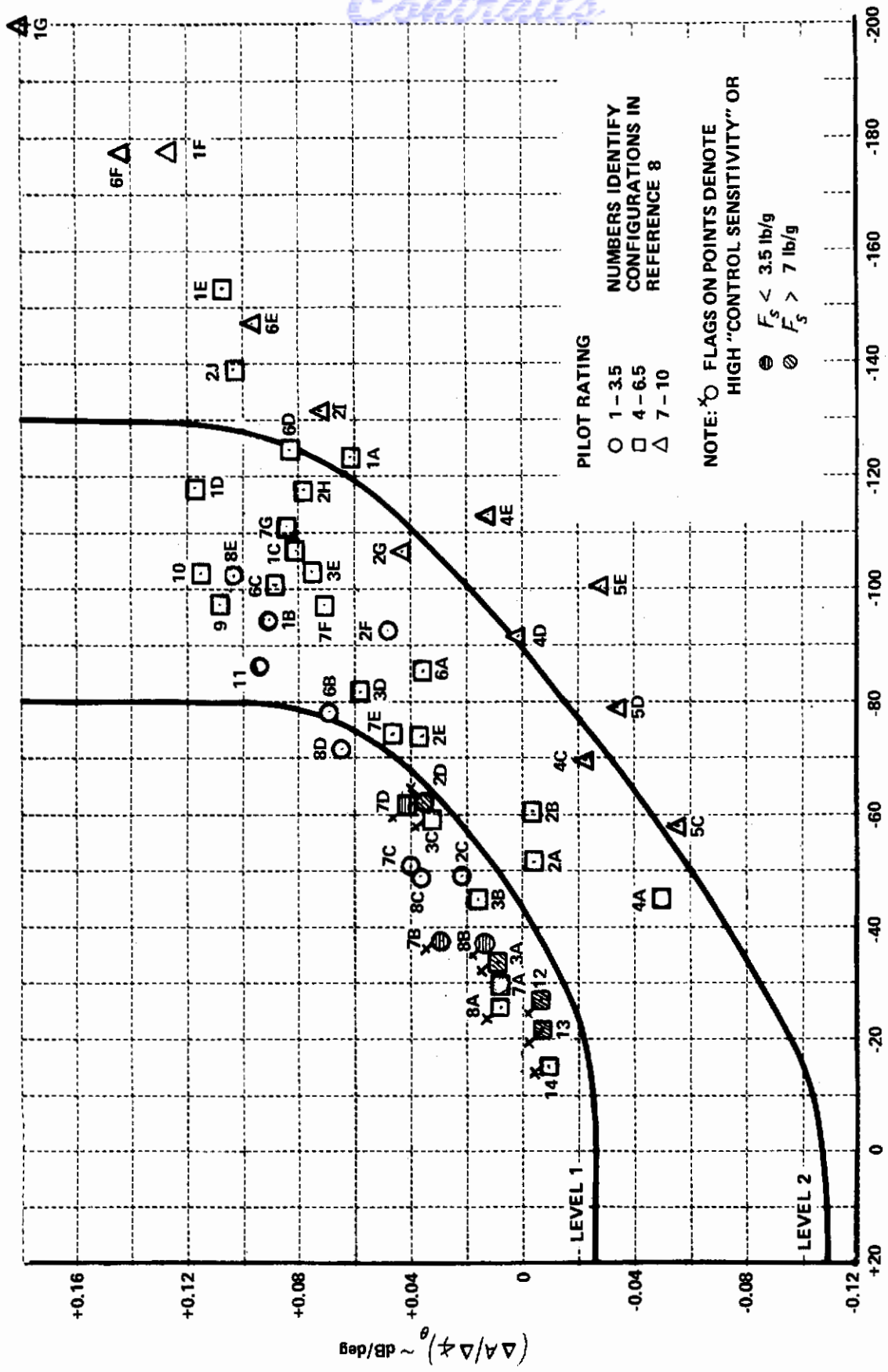

Figure 9a T-33 FCS PROGRAM (REFERENCE 8) ω_θ = 3.5, PILOT M

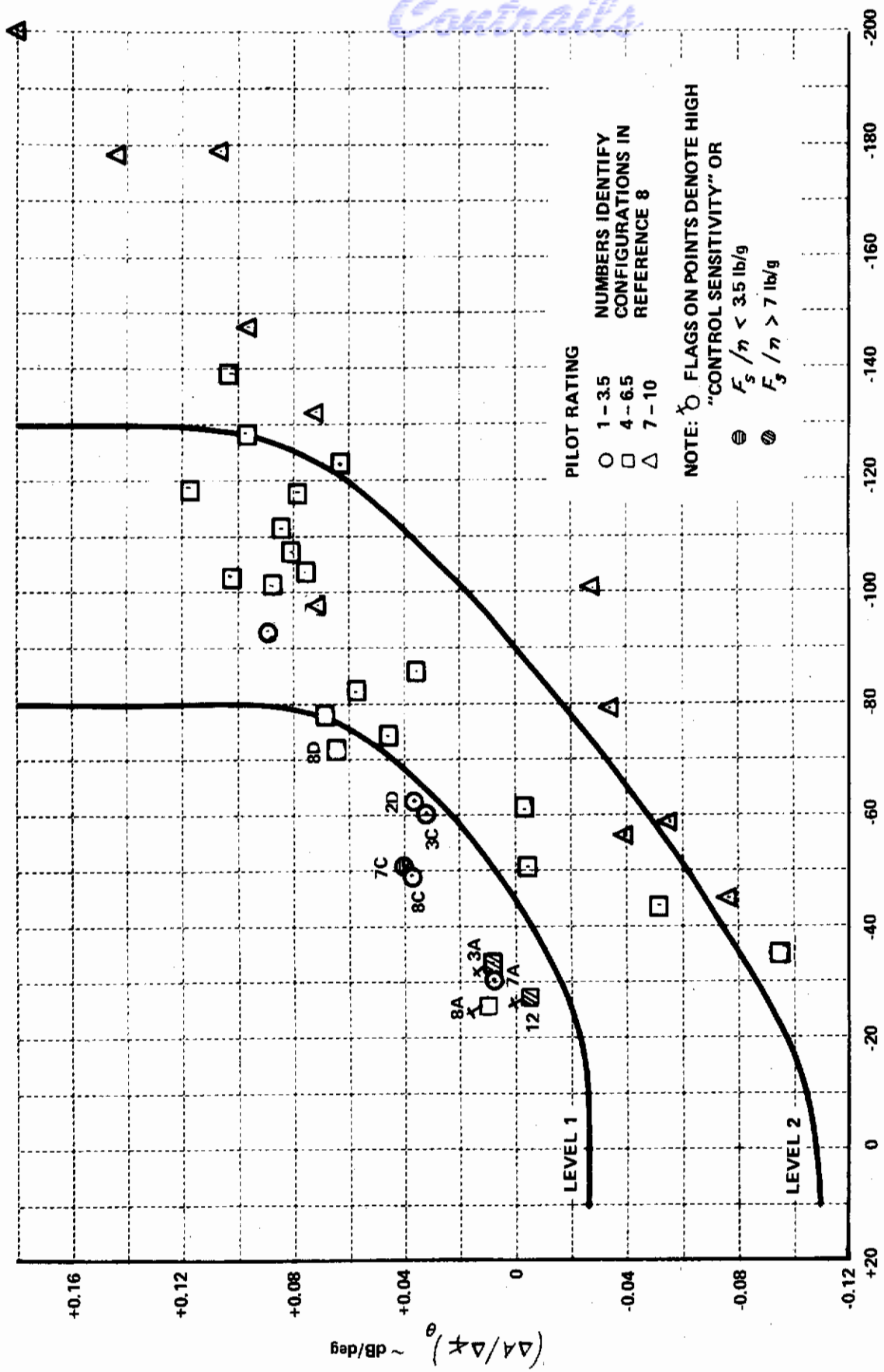

Figure 9b T-33 FCS PROGRAM (REFERENCE 8) ω_θ = 3.5, PILOT W

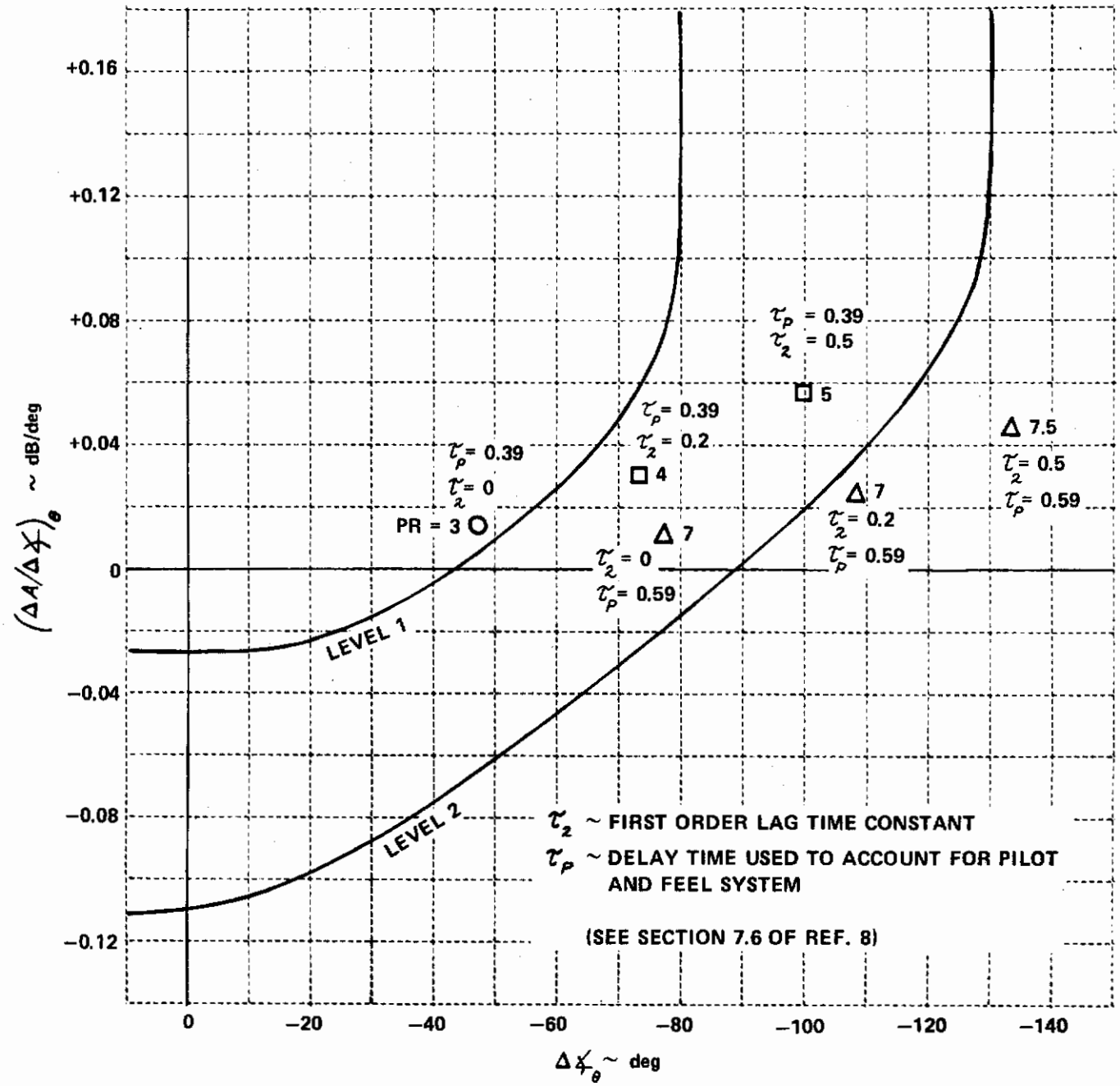

Figure 10 SPECIAL T-33 FLIGHTS (REFERENCE 8), ω_θ = 3.0

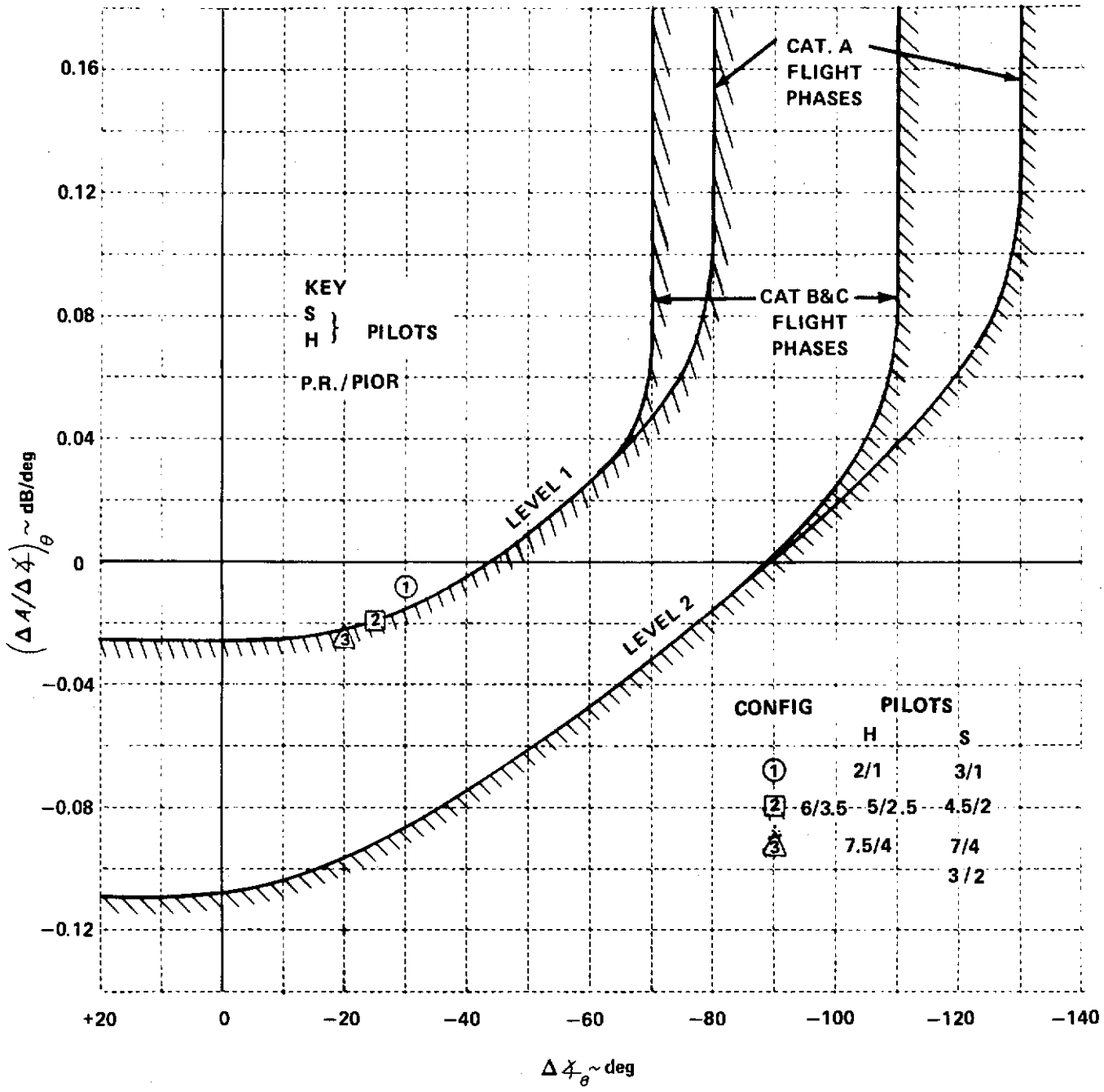

Figure 11 T-33 BOBWEIGHT PROGRAM (REFERENCE 9), ω_θ = 3.0

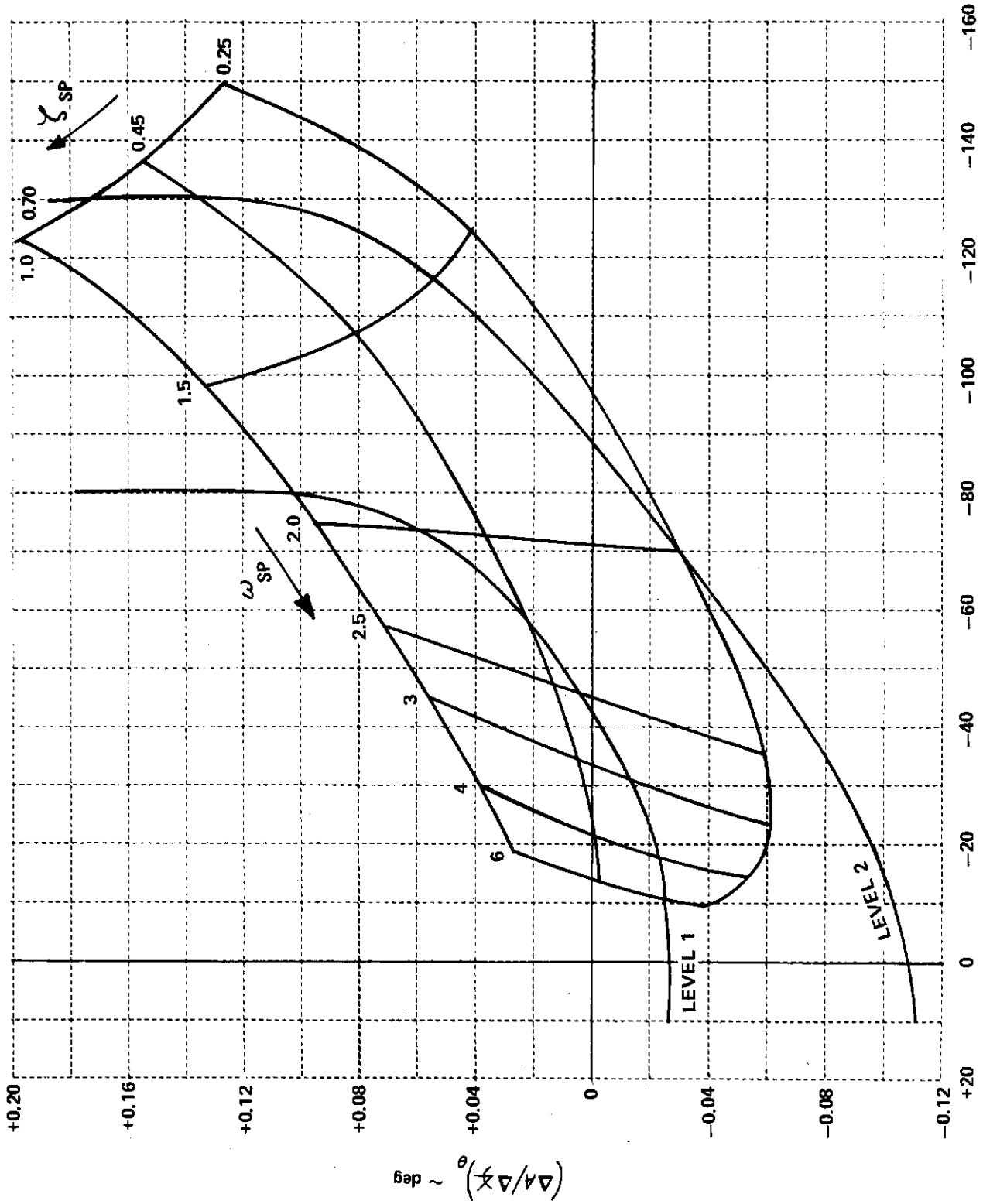

Figure 12 B-26 PROGRAM, $1/\tau_{\theta_2}$ = 1.2, ω_θ = 1.9

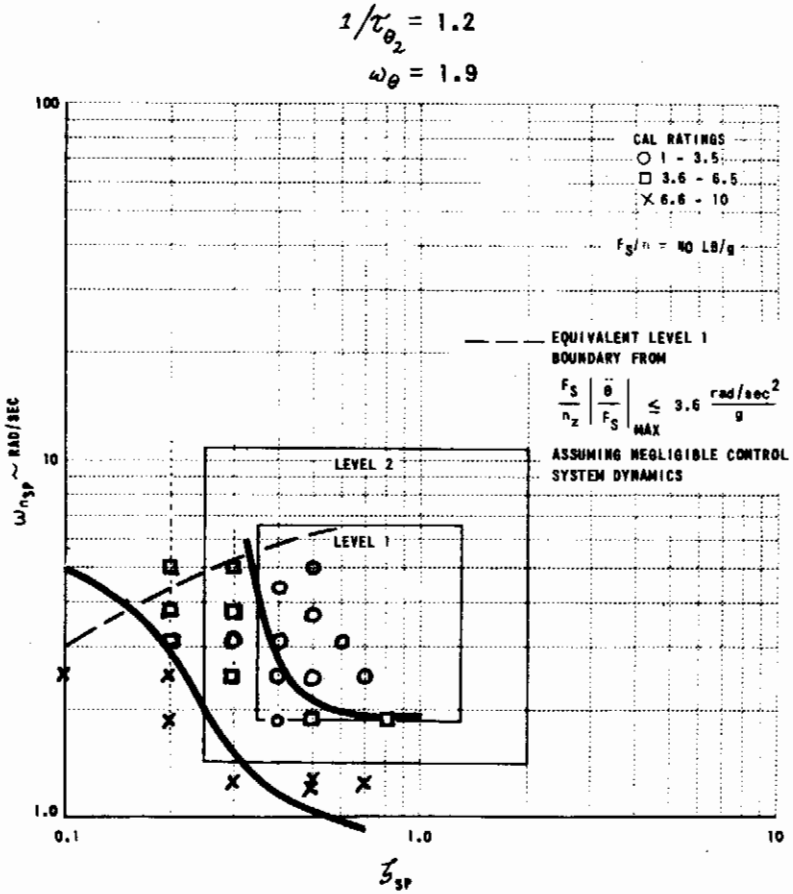

CATEGORY A FLIGHT PHASES
B-26 AVG. OF ALL PILOTS, LONG-LOOK

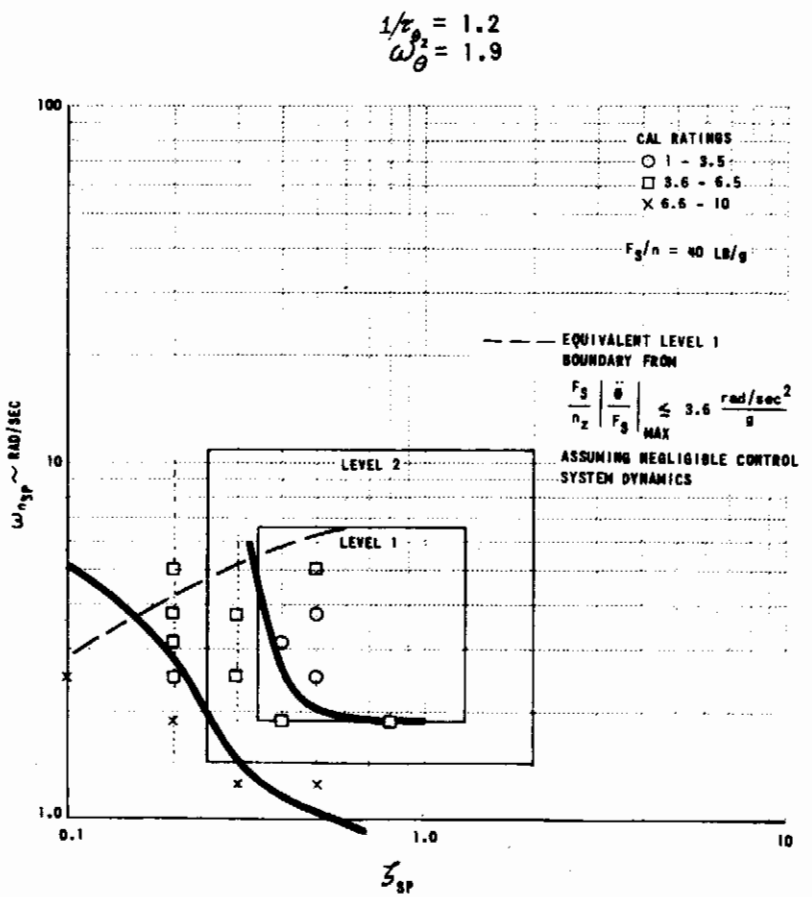

CATEGORY A FLIGHT PHASES
B-26, AVG. OF ALL PILOTS, SHORT-LOOK

Figure 13 REFERENCE 10 DATA

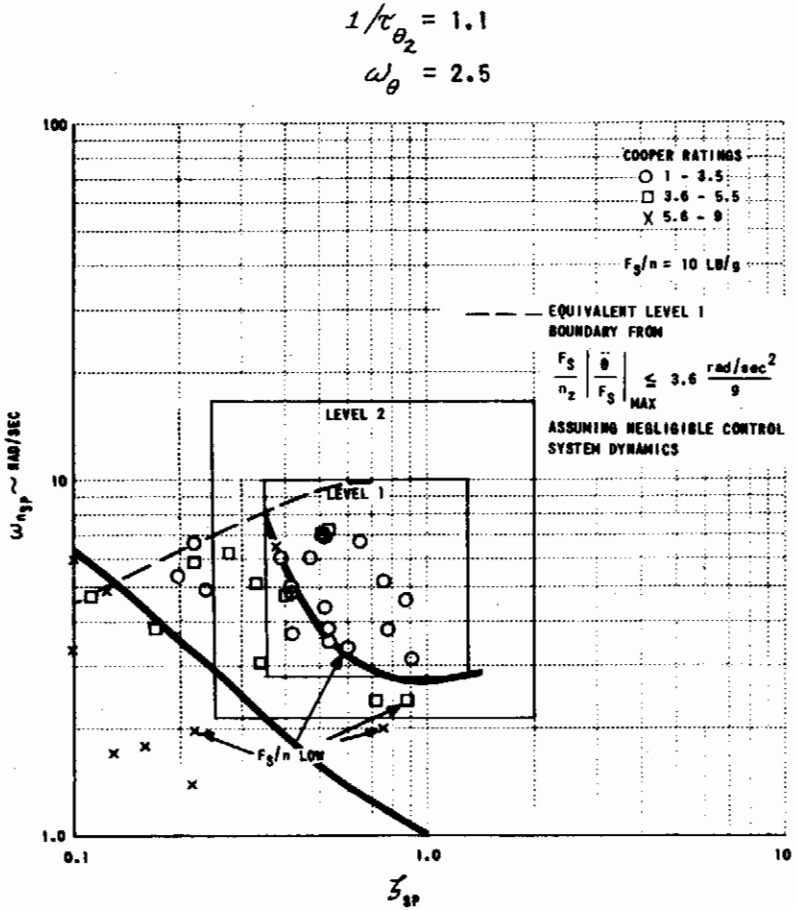

NASA F-86 (NO CONTROL SYSTEM ELECTRIC LAG)
(CATEGORY A) (REF.11)

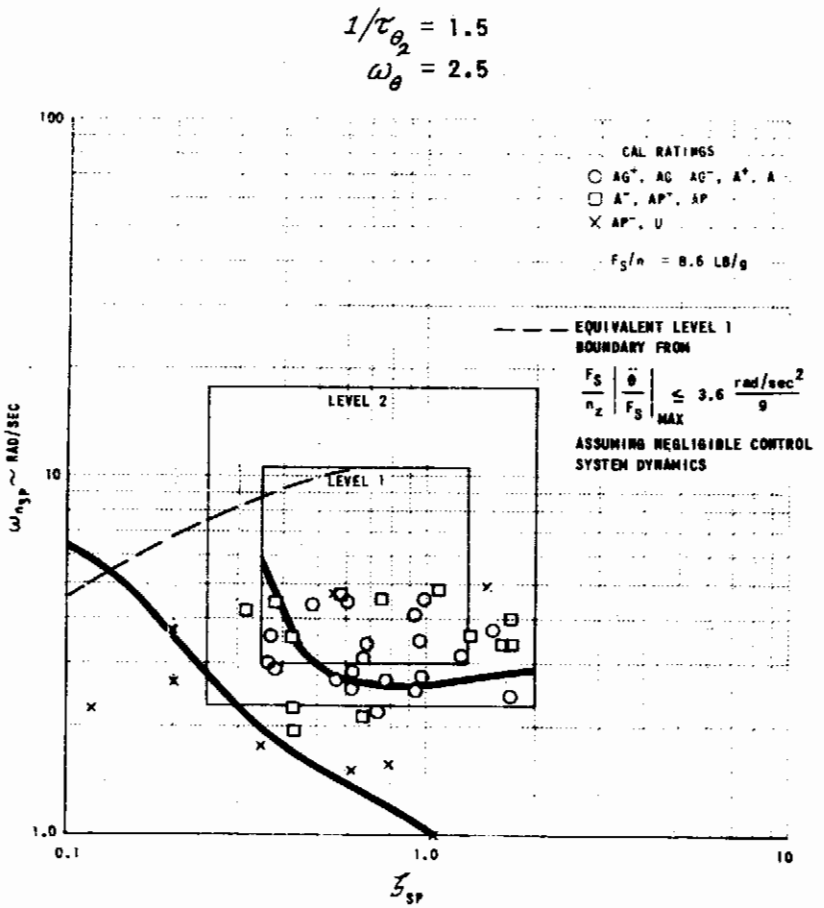

F-94 FIRST PROGRAM
(CATEGORY A) (REF.12)

Figure 14 REFERENCE 11 AND 12 DATA

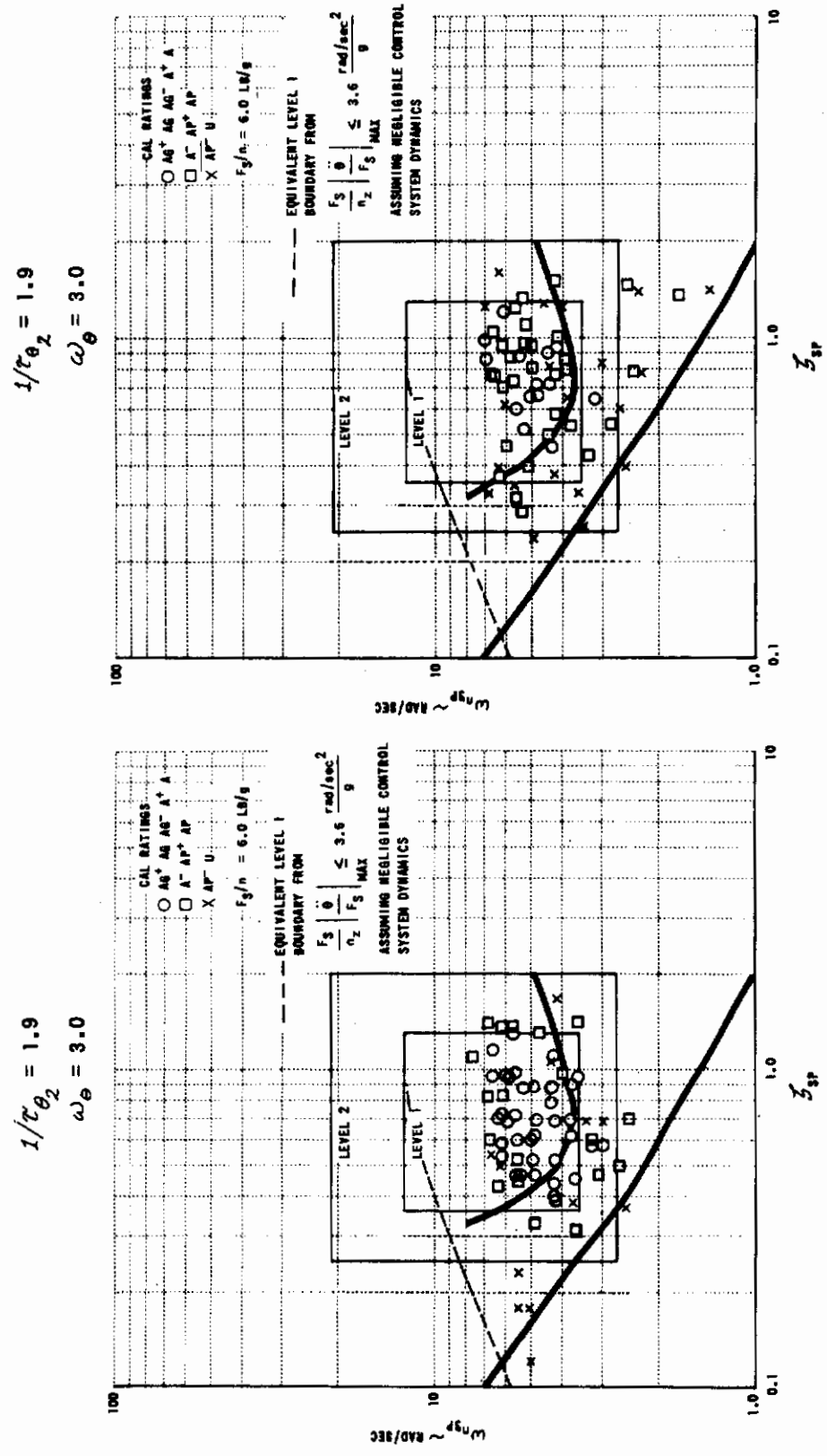

Figure 15 F-94 SECOND PROGRAM (CATEGORY A) (REFERENCE 13)

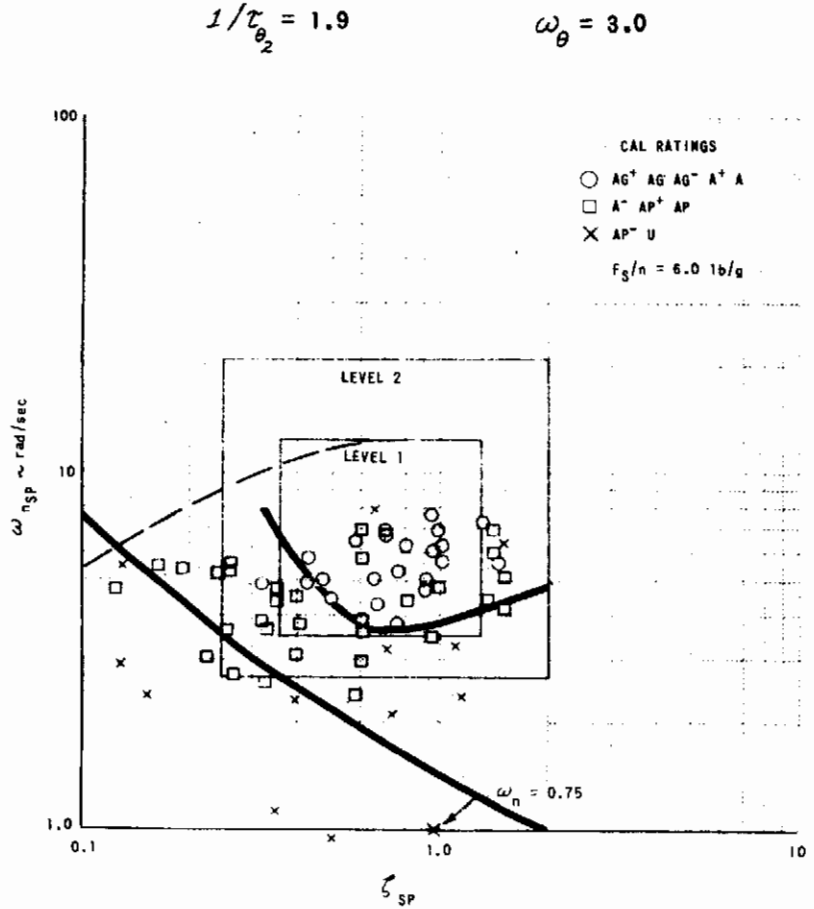

2nd USAF PILOT

Figure 16 F-94 SECOND PROGRAM (CATEGORY A) (REFERENCE 13)

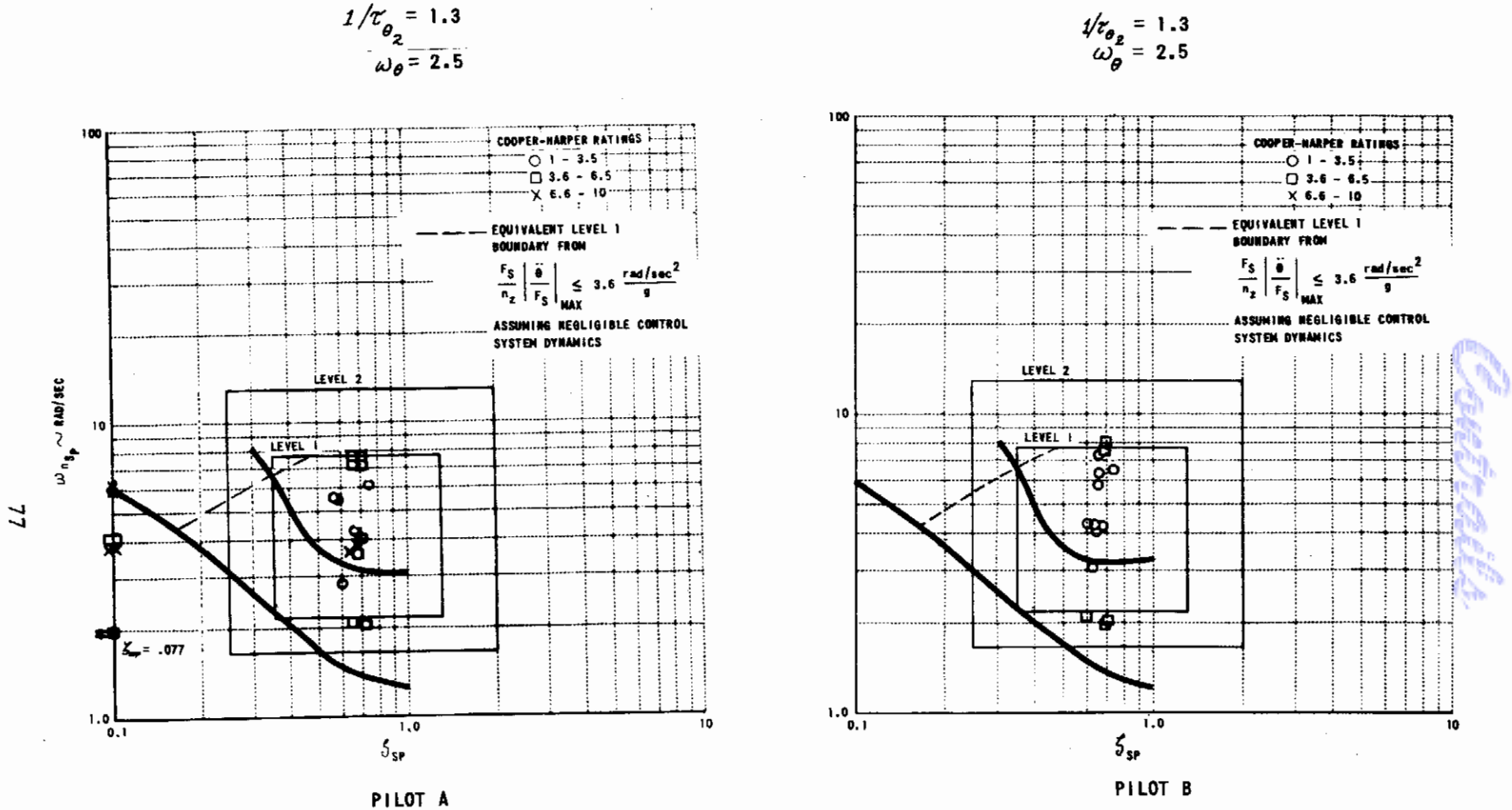

Figure 17 T-33 WHEEL PROGRAM (CATEGORY A) (REFERENCE 14)

$1/\tau_{\theta_2} = 2.7$

$\omega_\theta = 2.5$

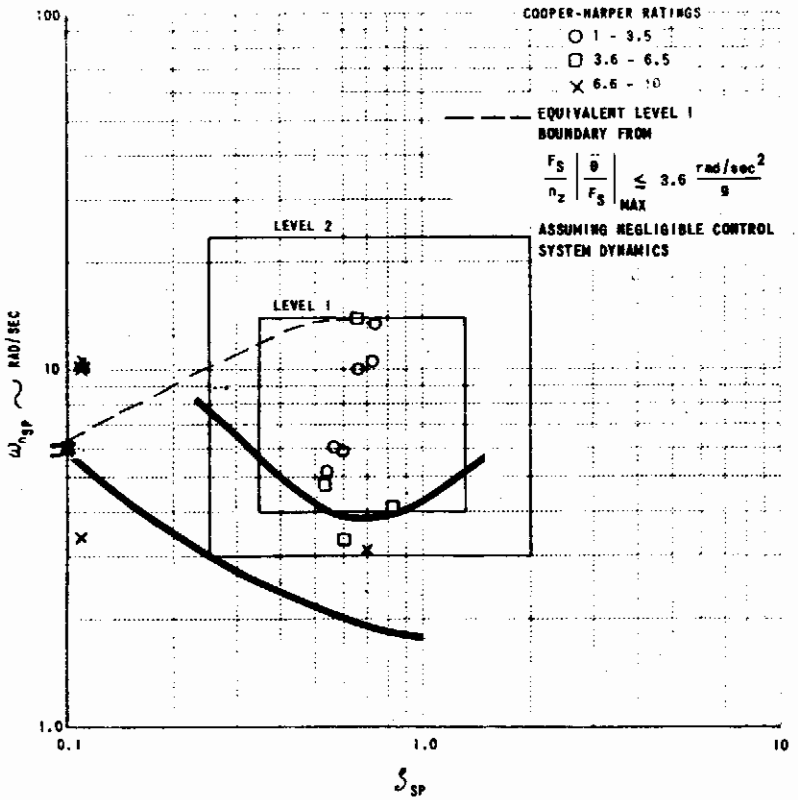

PILOT A

$1/\tau_{\theta_2} = 2.7$

$\omega_\theta = 2.5$

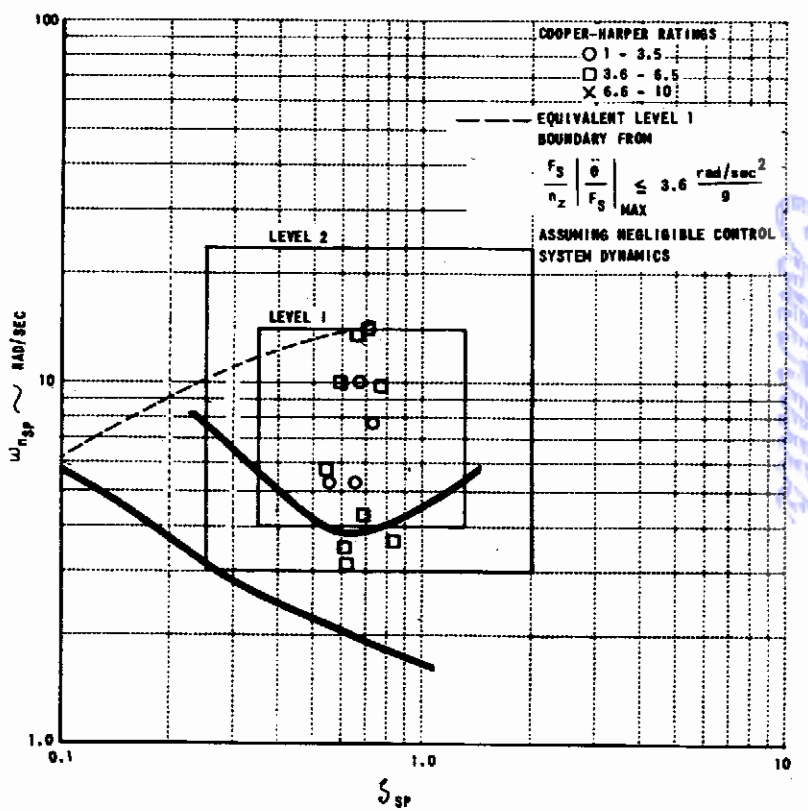

PILOT B

Figure 18 T-33 WHEEL PROGRAM (CATEGORY A) (REFERENCE 14)

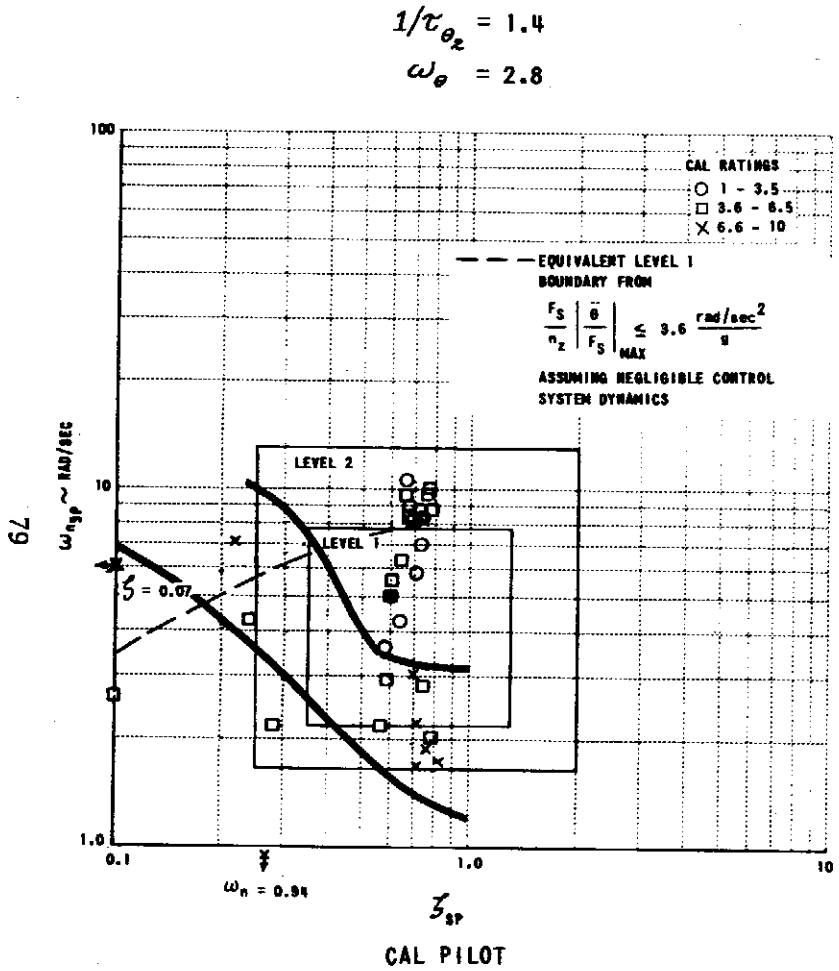

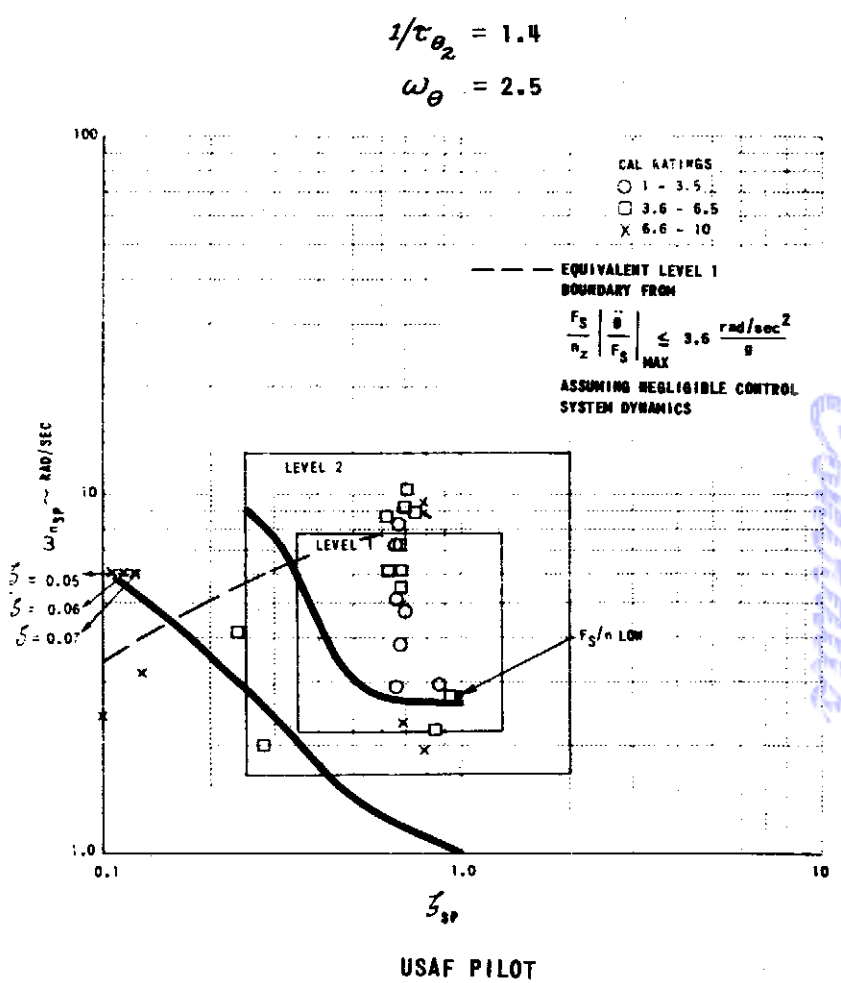

Figure 19 T-33 SHORT PERIOD AND PIO (CATEGORY A) (REFERENCE 15)

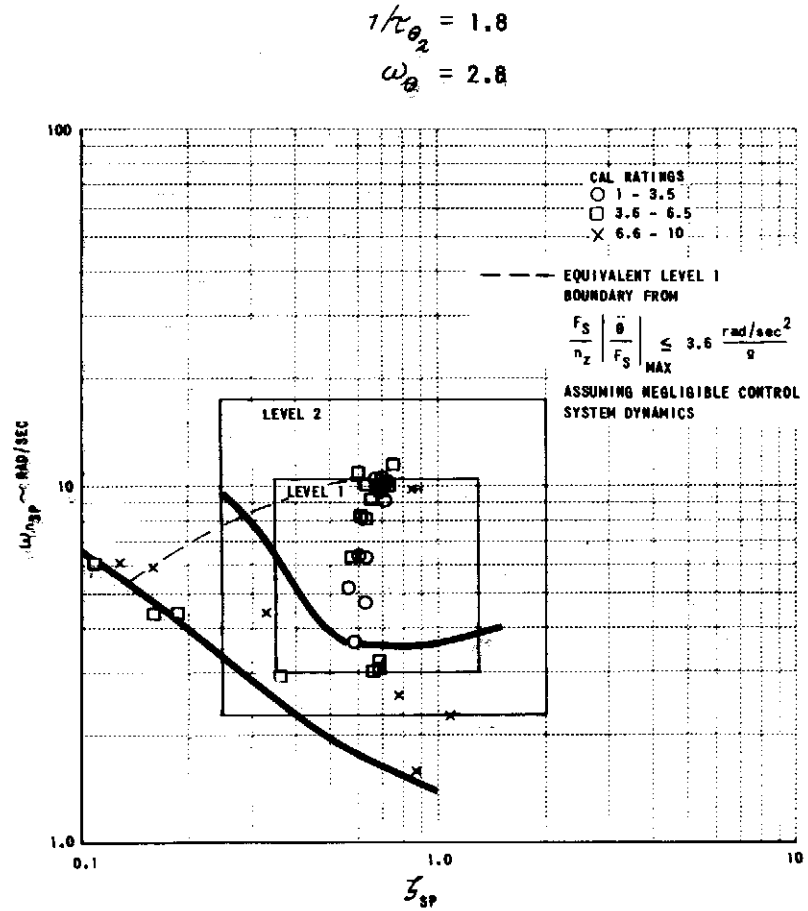

CAL PILOT

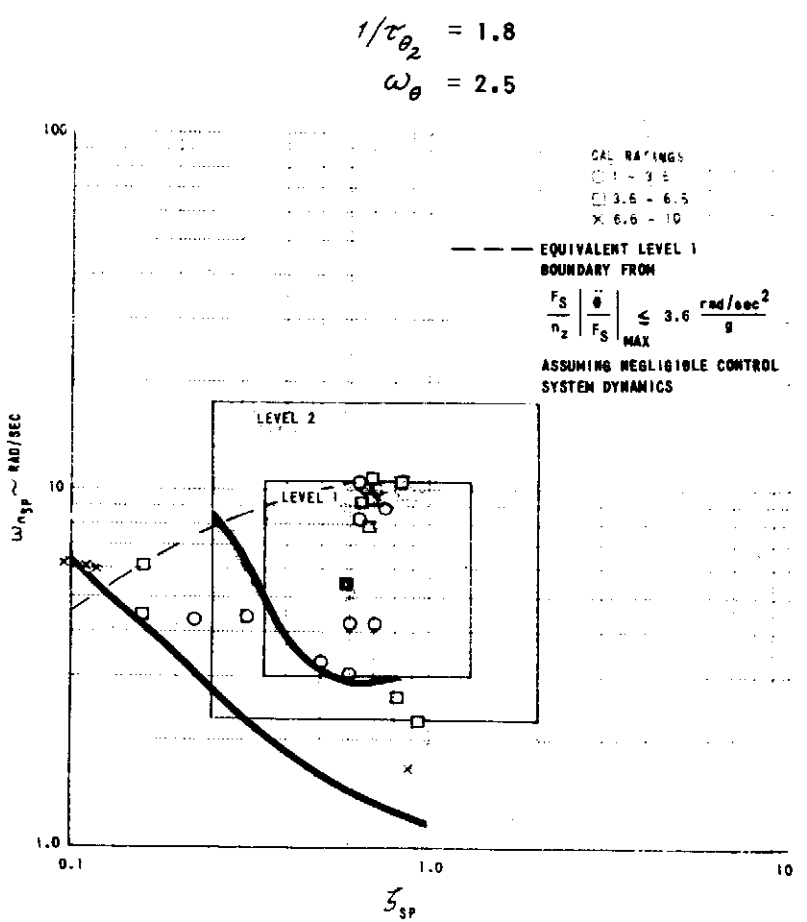

USAF PILOT

Figure 20 T-33 SHORT PERIOD AND PIO (CATEGORY A) (REFERENCE 15)

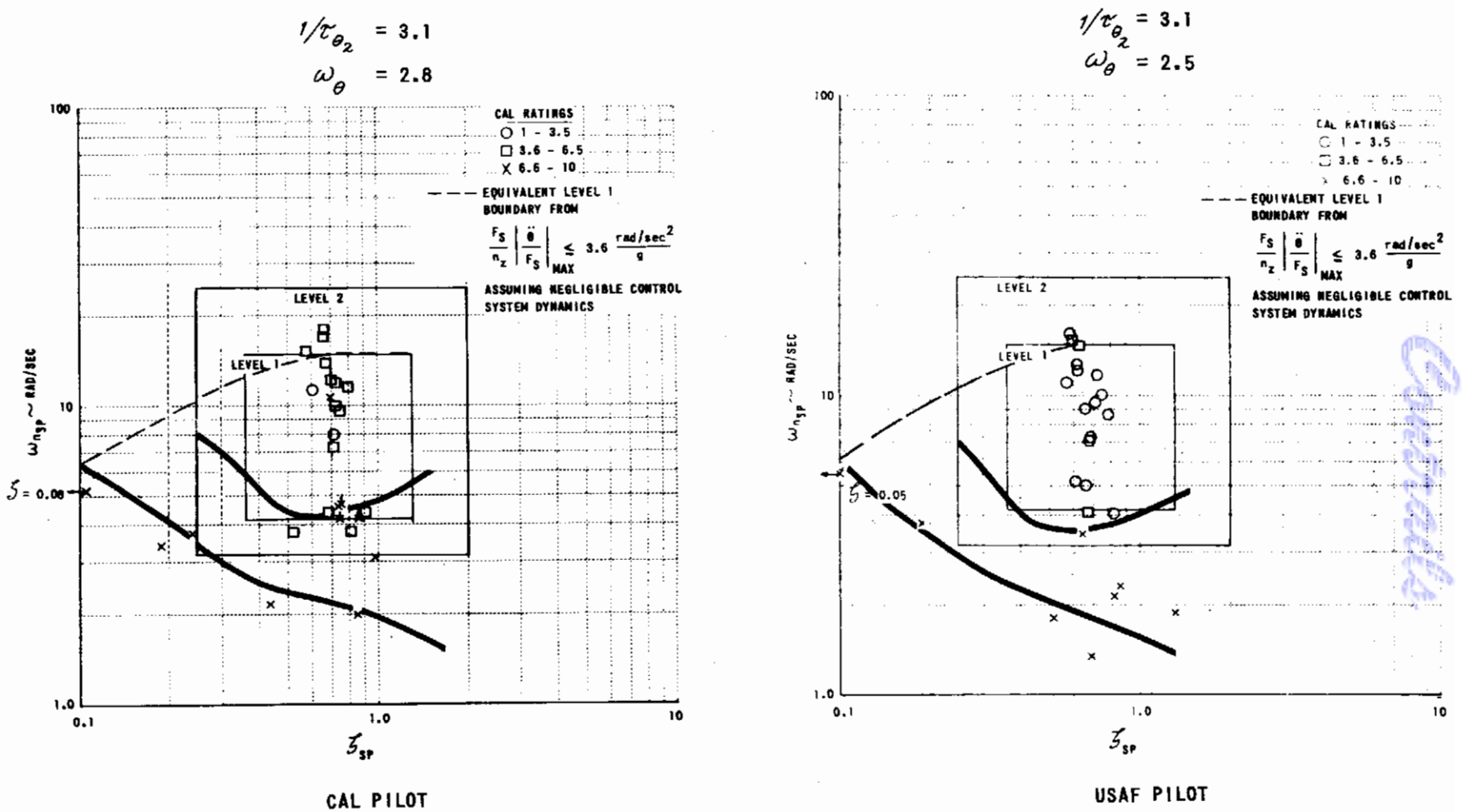

Figure 21 T-33 SHORT PERIOD AND PIO (CATEGORY A) (REFERENCE 15)

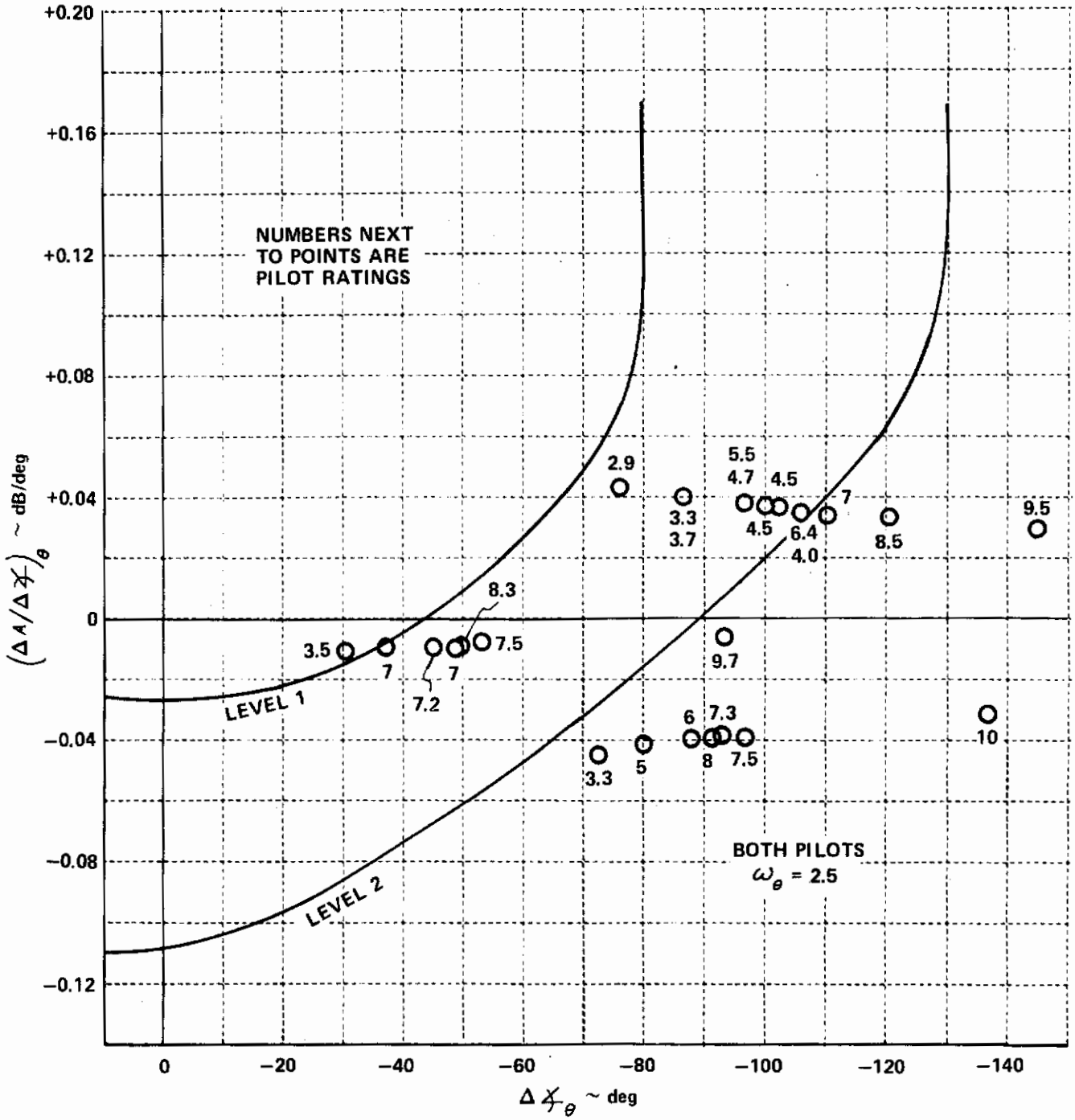

Figure 22 T-33 HIGHER ORDER SYSTEM DATA (REFERENCE 16)

PROGRAM	$1/\tau_{\theta_2}$ rad/sec	ω_θ rad/sec
B-26 LONG-LOOK/SHORT-LOOK (REFERENCE 10)	1.2	1.9
T-33 WHEEL CONTROLLER (REFERENCE 14)	1.3, 2.7	2.5
F-94 FIRST PROGRAM (REFERENCE 12)	1.5	2.5
NASA F-86 (REFERENCE 11)	1.1	2.5
T-33 HOS PROGRAM (REFERENCE 16)	1.2	2.5
T-33 S. P. & PIO (REFERENCE 15)	1.4, 1.8, 3.1	2.8 (CAL PILOT) 2.5 (USAF PILOT)
SPECIAL T-33 FLIGHTS (REFERENCE 8)	1.3	3.0
F-94 SECOND PROGRAM (REFERENCE 13)	1.9	3.0
T-33 FCS CRITERIA (REFERENCE 8)	1.3, 2.4	3.5

Figure 23 SUMMARY OF DATA CORRELATION WITH PROPOSED MANEUVER RESPONSE REQUIREMENTS - CATEGORY A FLIGHT PHASES

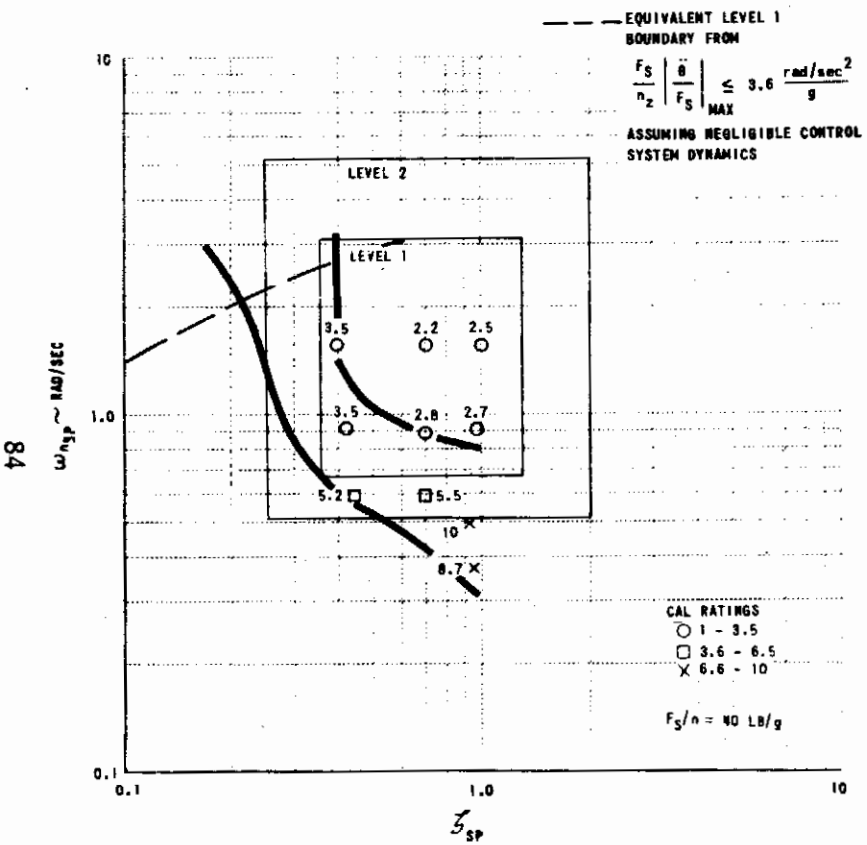

BOEING C-5A SIM. (REF. 17)

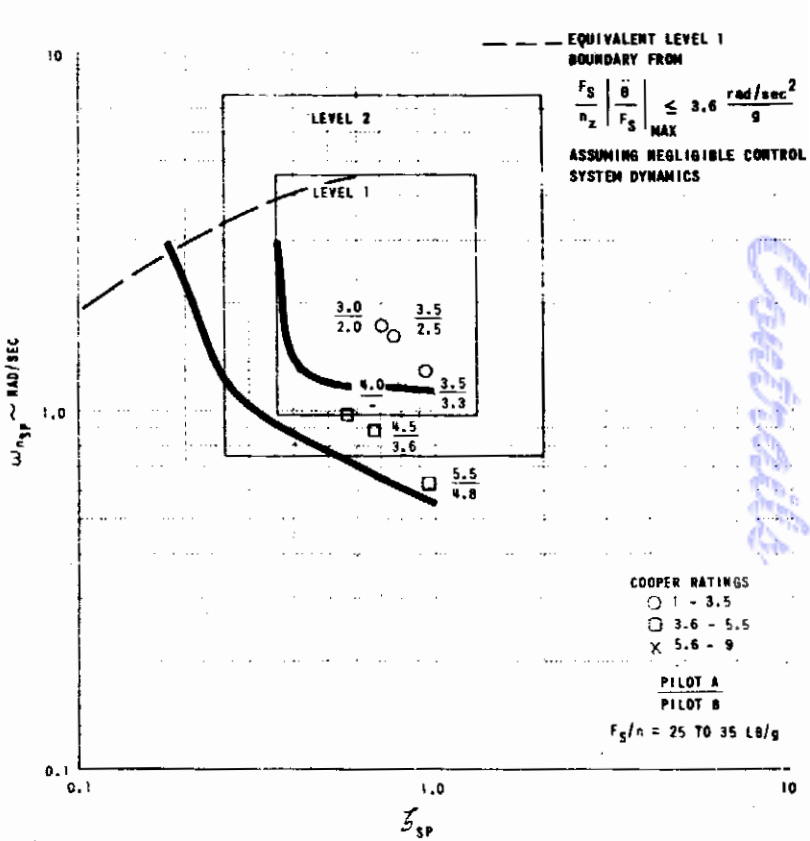

BOEING SST SIM. (REF. 18)

Figure 24 BOEING SIMULATIONS (CATEGORY C) (REFERENCES 17 AND 18)

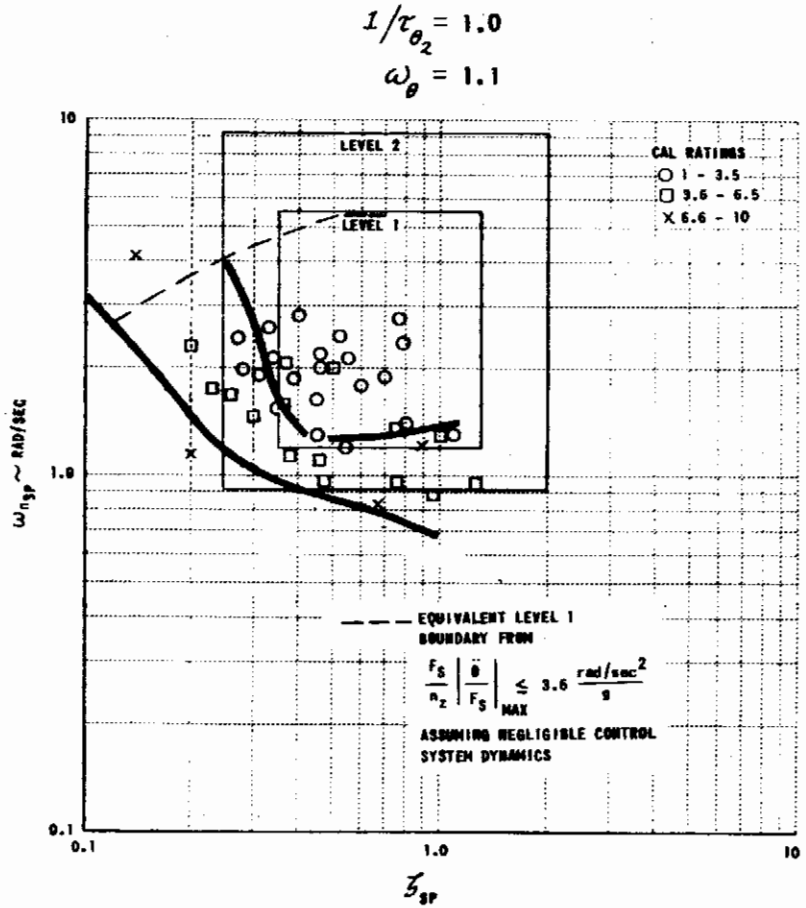

FIRST T-33 LANDING (REF. 19)

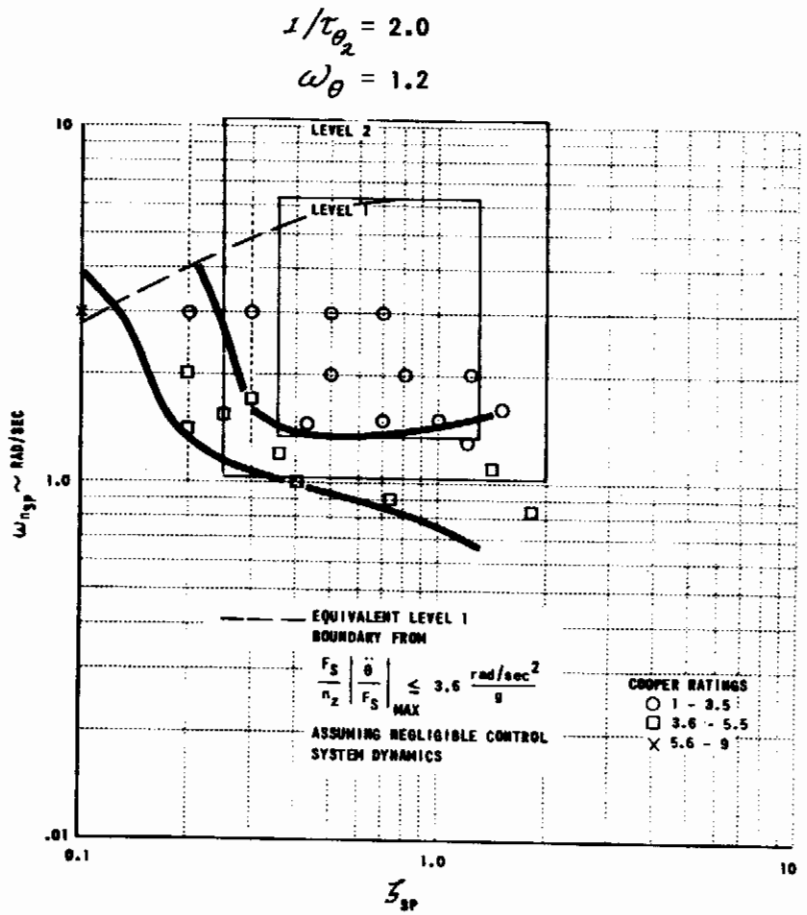

PRINCETON NAVION (REF. 20)

Figure 25 CATEGORY C DATA (FROM REFERENCES 19 AND 20)

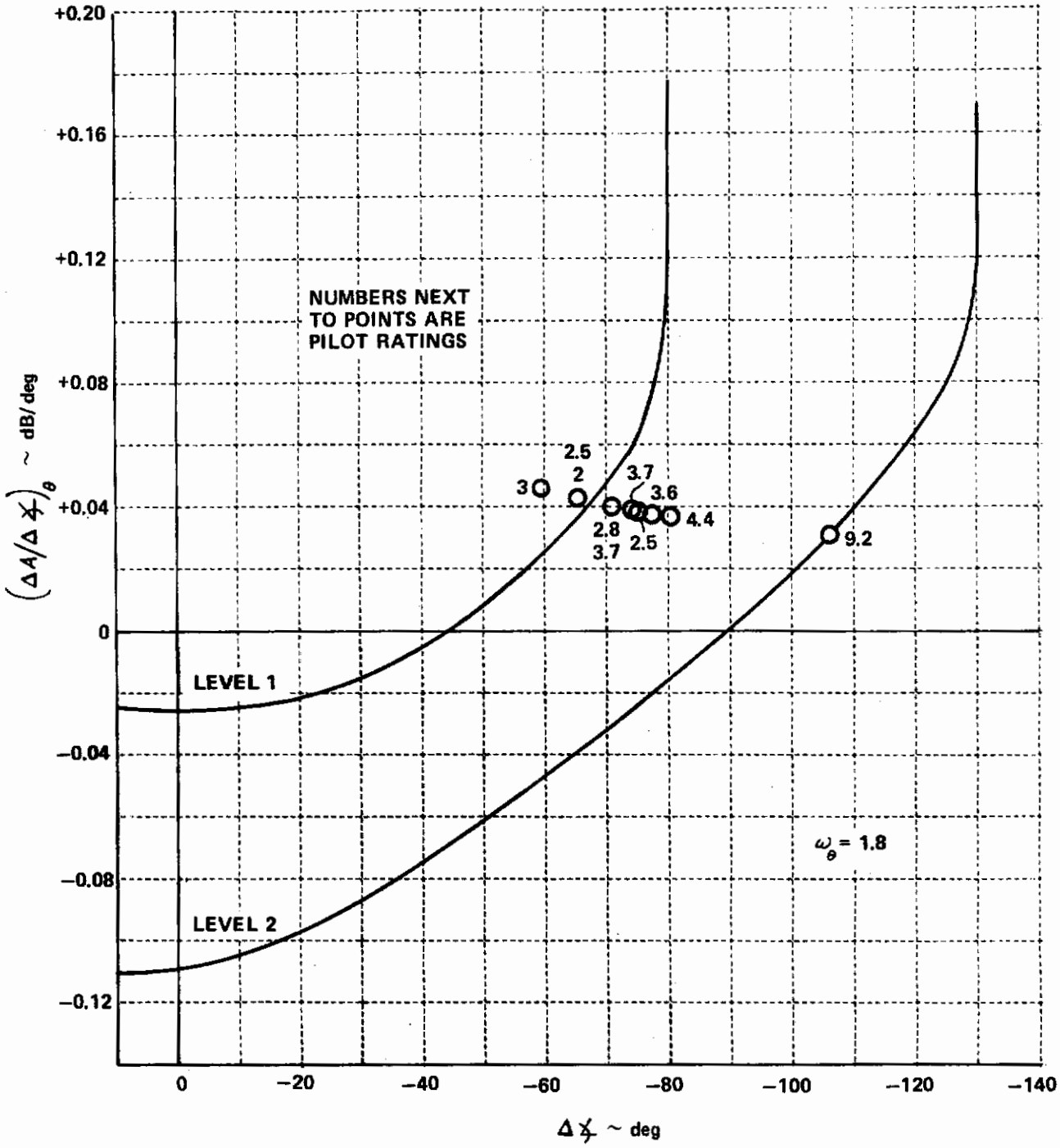

Figure 26 T-33 HIGHER ORDER SYSTEM DATA (REFERENCE 16)

PROGRAM	$1/\tau_{\theta_2}$ rad/sec	ω_θ rad/sec
BOEING C-5A SIMULATION (REFERENCE 17)	0.45	1.1
FIRST T-33 LANDING (REFERENCE 19)	1.0	1.1
PRINCETON NAVION (REFERENCE 20)	2.0	1.2
BOEING SST SIMULATION (REFERENCE 18)	0.8	1.3
T-33 HOS LANDING (REFERENCE 16)	0.8	1.8*

*THE EVALUATION TASKS FOR THIS "LANDING APPROACH" DATA INCLUDED CATEGORY A TASKS AS WELL AS CATEGORY C.

Figure 27 SUMMARY OF DATA CORRELATION WITH PROPOSED MANEUVER RESPONSE REQUIREMENTS - CATEGORY C

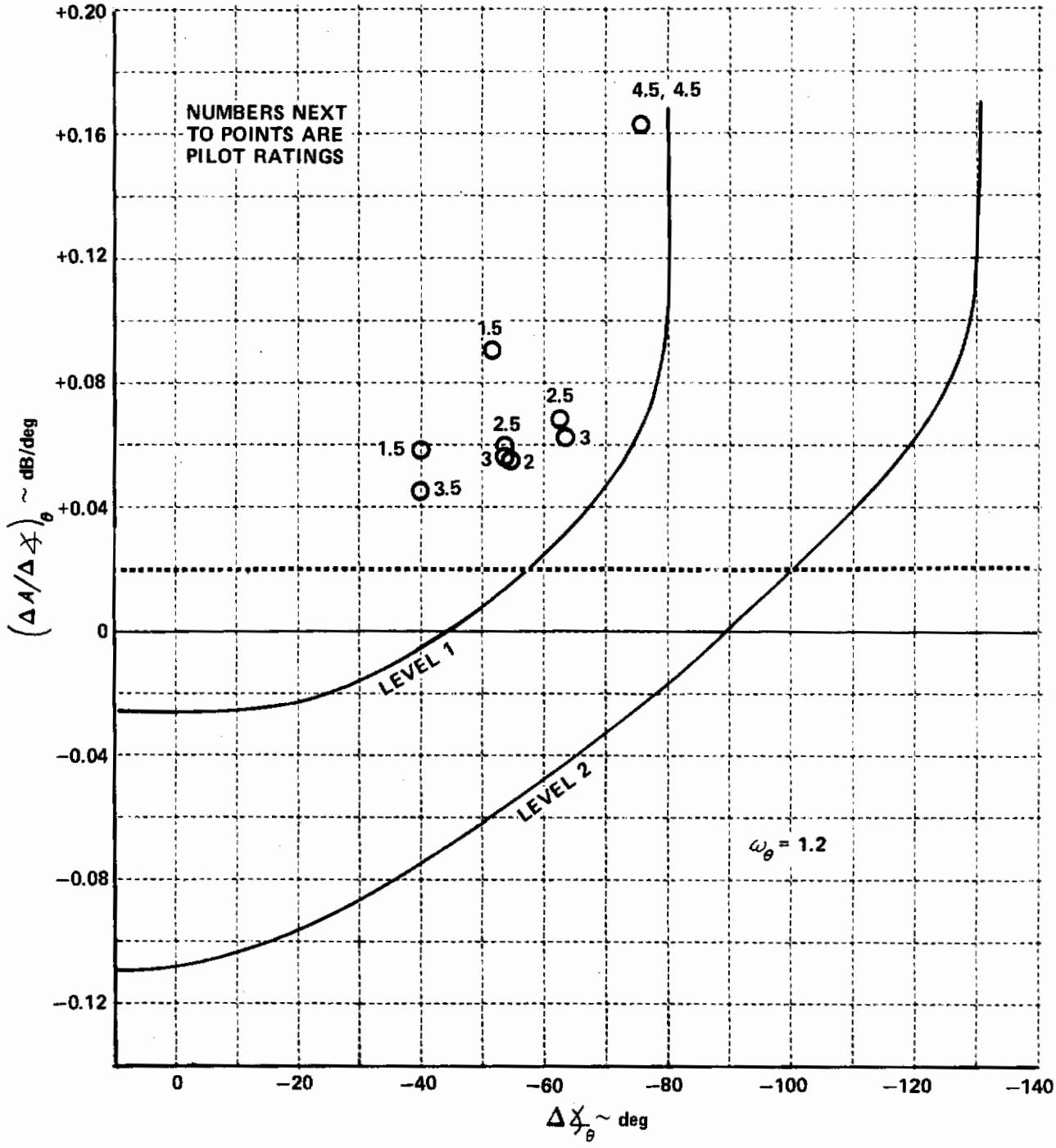

Figure 28 XB-70 DATA (REFERENCE 24)

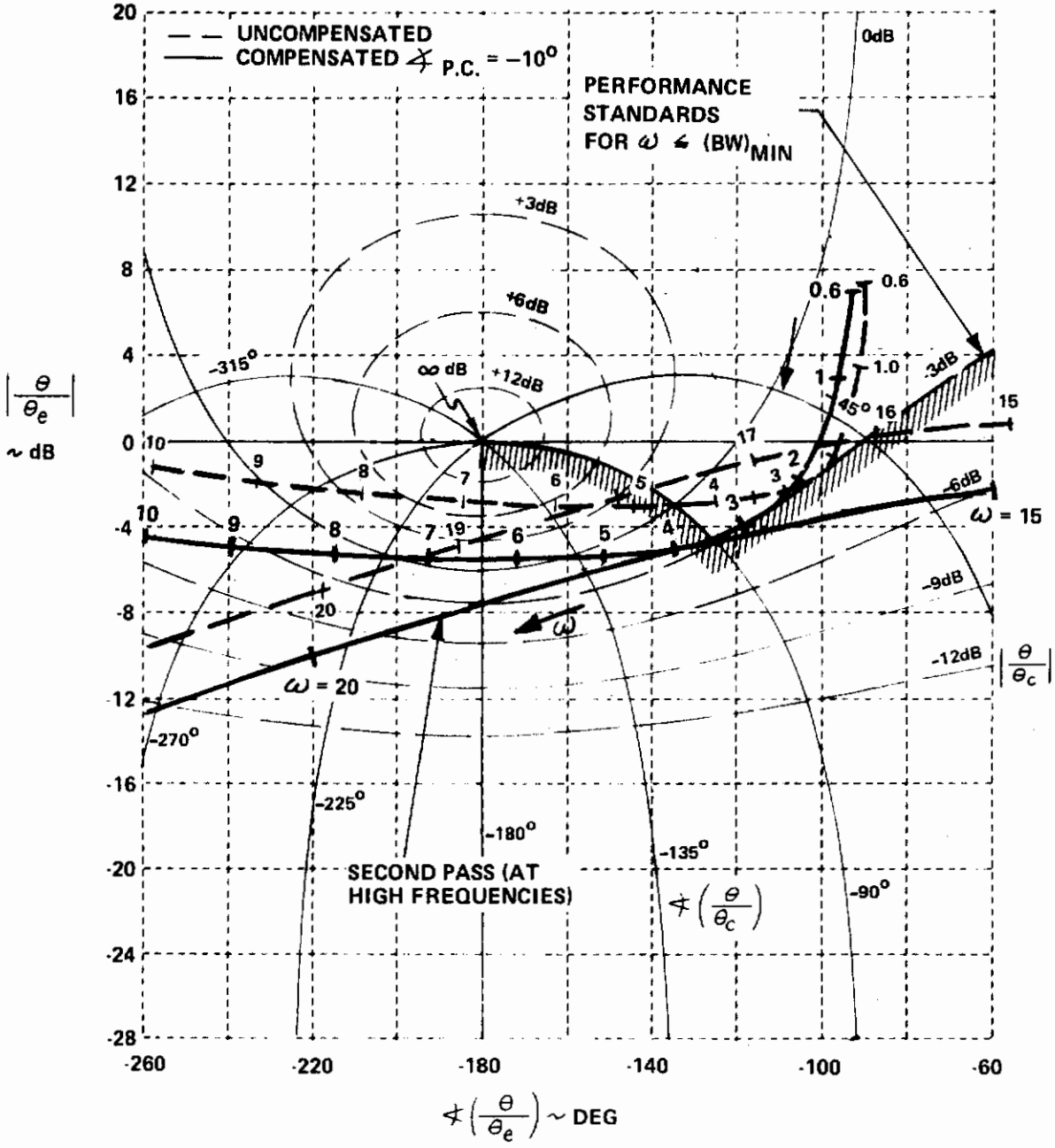

Figure 29 COMPENSATED AND UNCOMPENSATED AMPLITUDE-PHASE PLOT FOR CONFIGURATION 14, SHOWING THE CAUSE OF THE HIGH FREQUENCY RESONANCE.

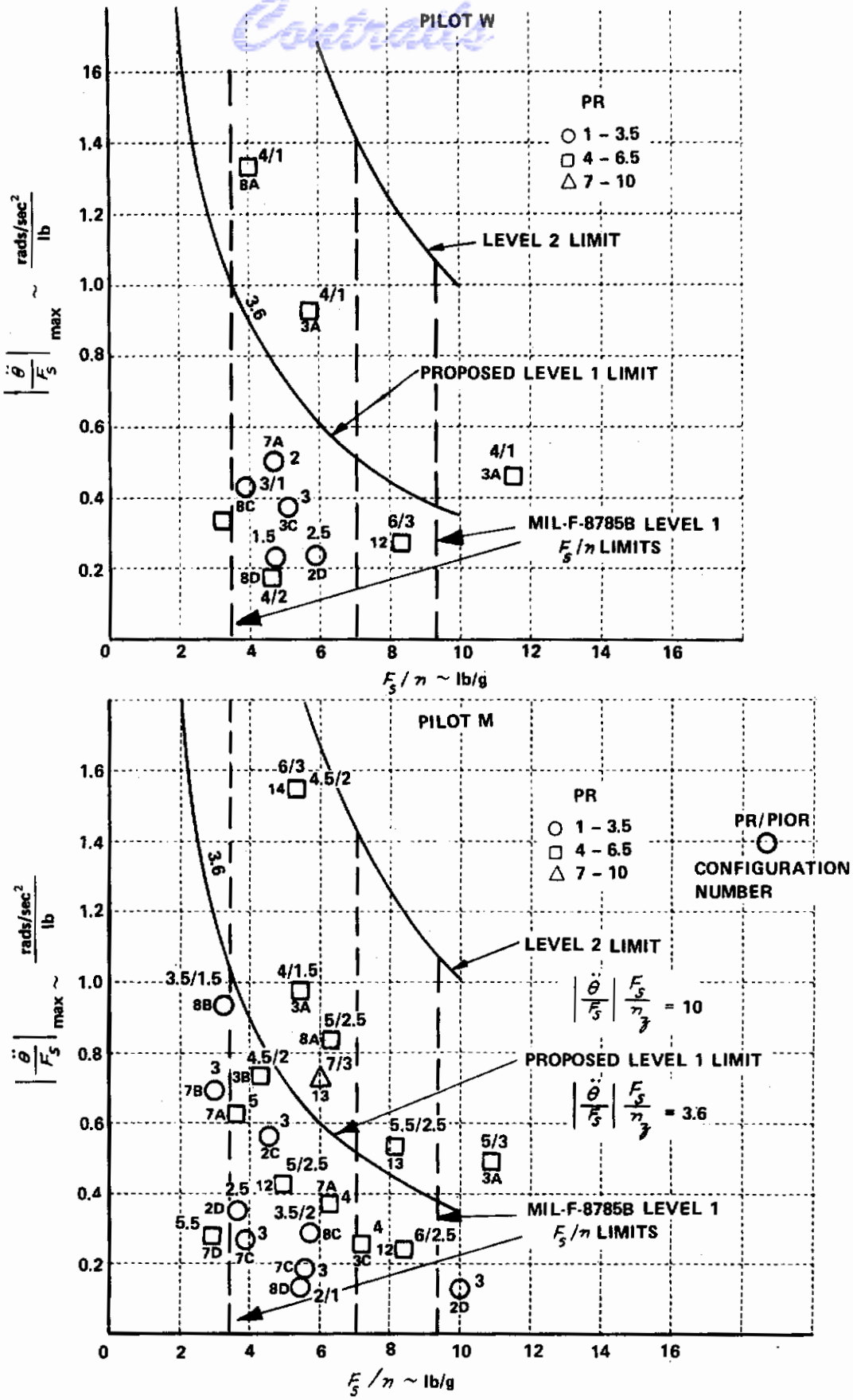

Figure 30 CONTROL SENSITIVITY DATA FOR T-33 FCS PROGRAM (REFERENCE 8)

AIRPLANE CONFIG. 3
CONTROL SYSTEM:

PILOT COMMENTS

A INITIALLY ABRUPT, TOO SENSITIVE. BOBBLES ON TARGET, HOLD STICK LIGHTLY.

B USE SMOOTH INPUTS. TENDENCY TO OVERCONTROL, BOBBLES ON TARGET

C NO COMPROMISE IN GEARING SELECTION. SLIGHT TENDENCY TO DIG IN. OSCILLATES ON TARGET.

D SLOW INITIALLY. OVERDRIVE AND CHECK. FORCE LIGHTENS. OVERSHOOTS.

E INITIALLY HEAVY THEN LIGHTENS. INITIAL DELAY.

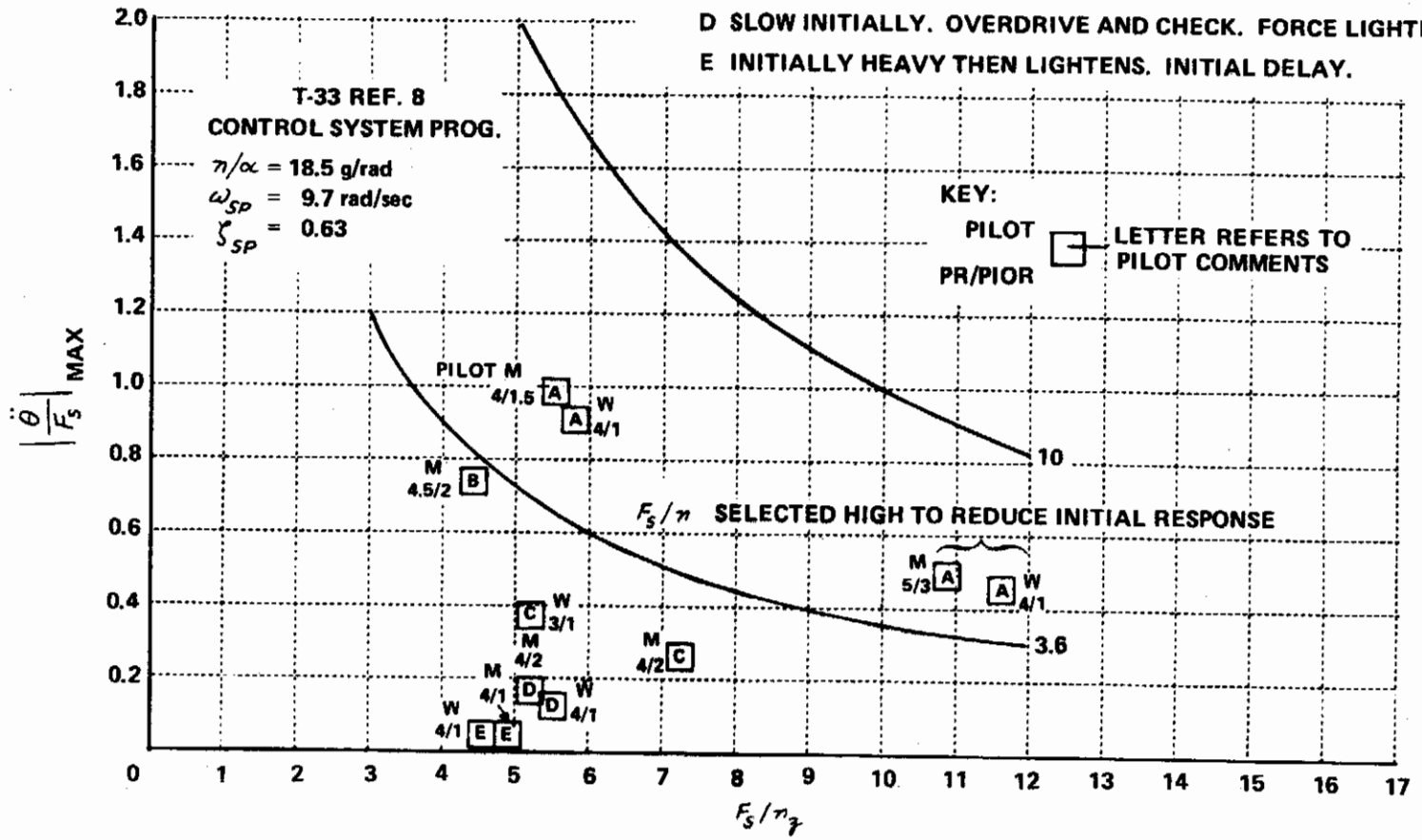

Figure 31 CONTROL SENSITIVITY DATA FOR GROUP 3 (REFERENCE 8)

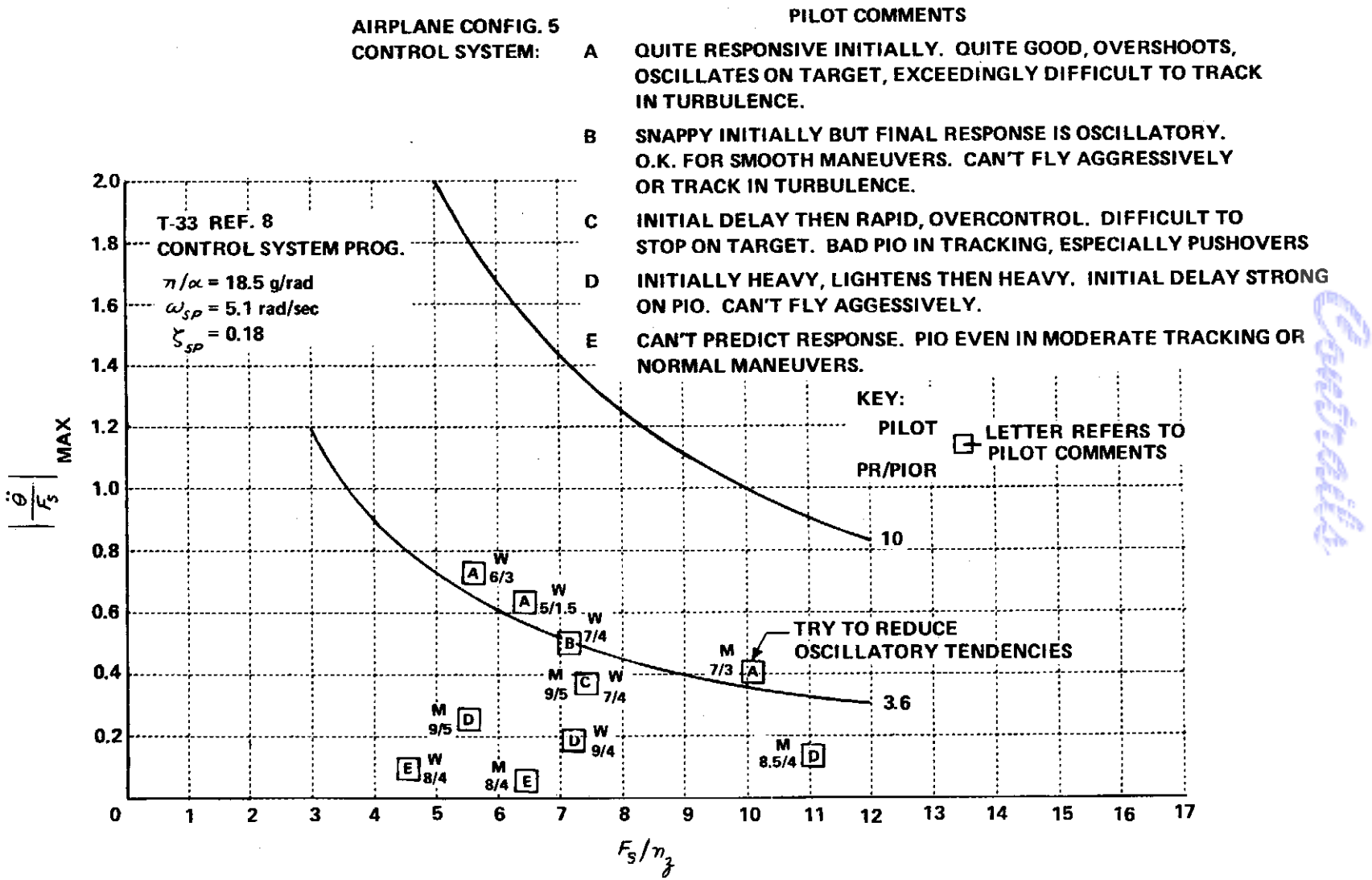

Figure 32 CONTROL SENSITIVITY DATA FOR GROUP 5 (REFERENCE 8)

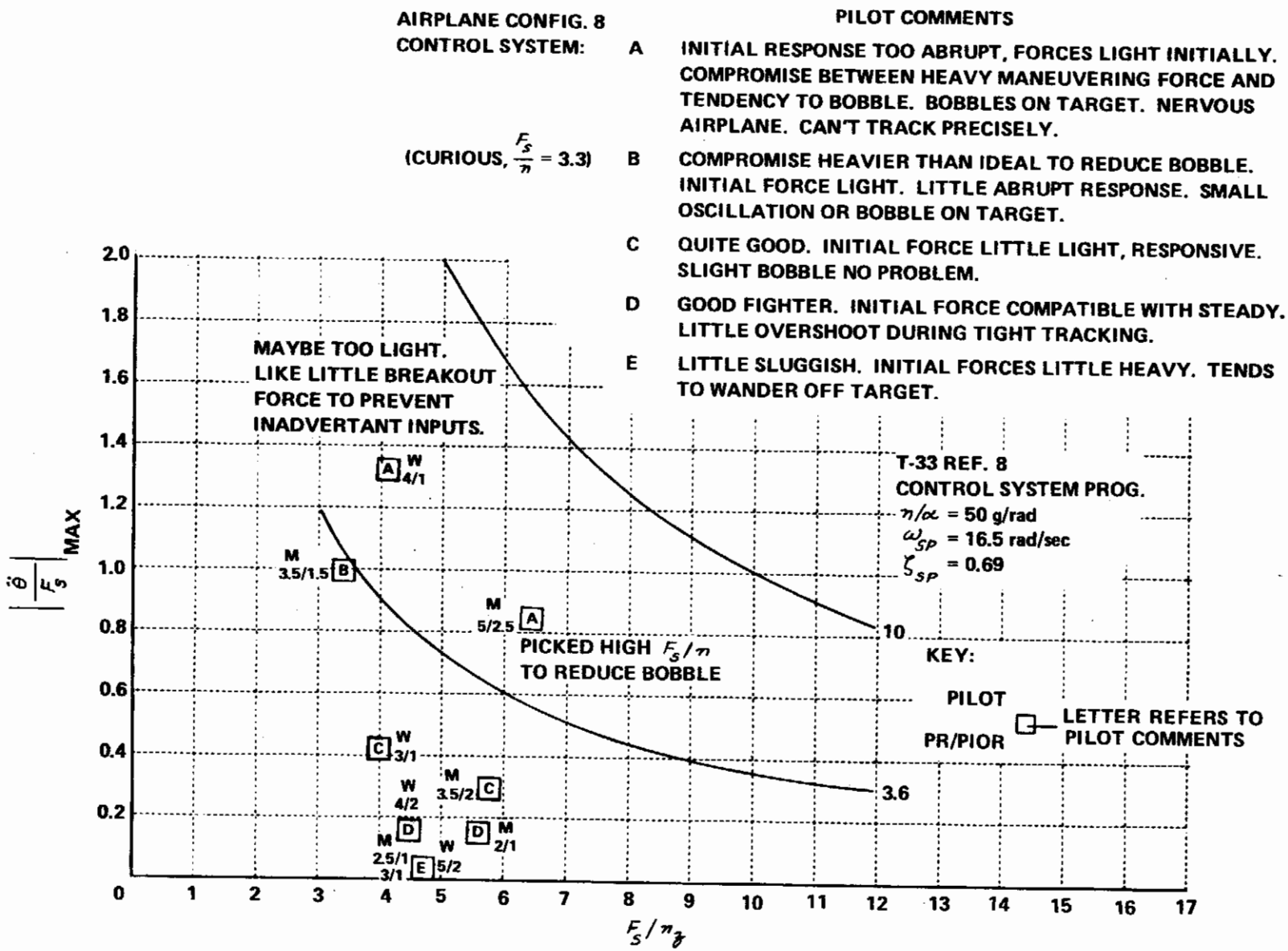

Figure 33 CONTROL SENSITIVITY DATA FOR GROUP 8 (REFERENCE 8)

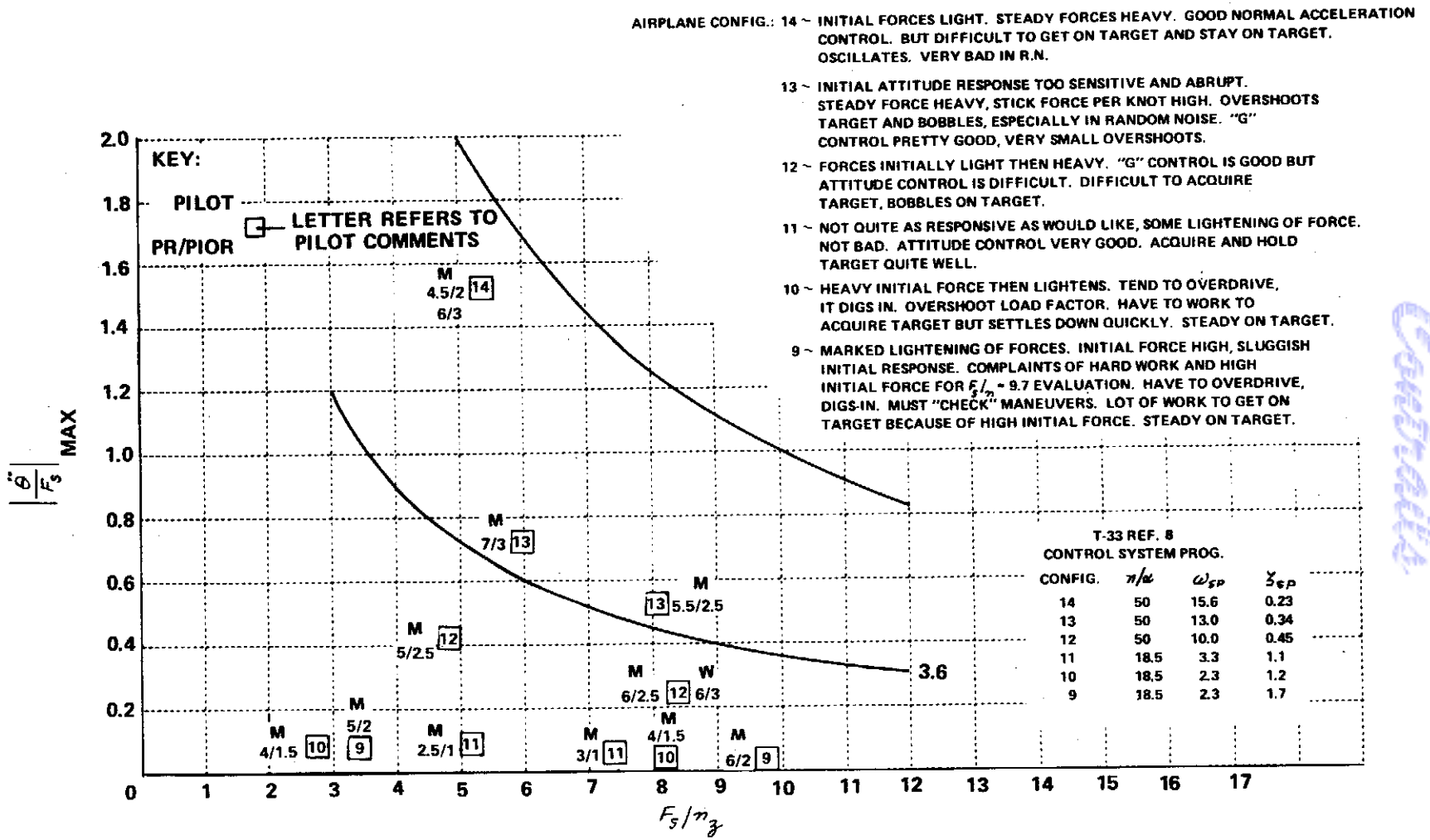

Figure 34 CONTROL SENSITIVITY DATA FOR CONFIGURATION 9, 10, 11 12, 13 AND 14 (REFERENCE 8)

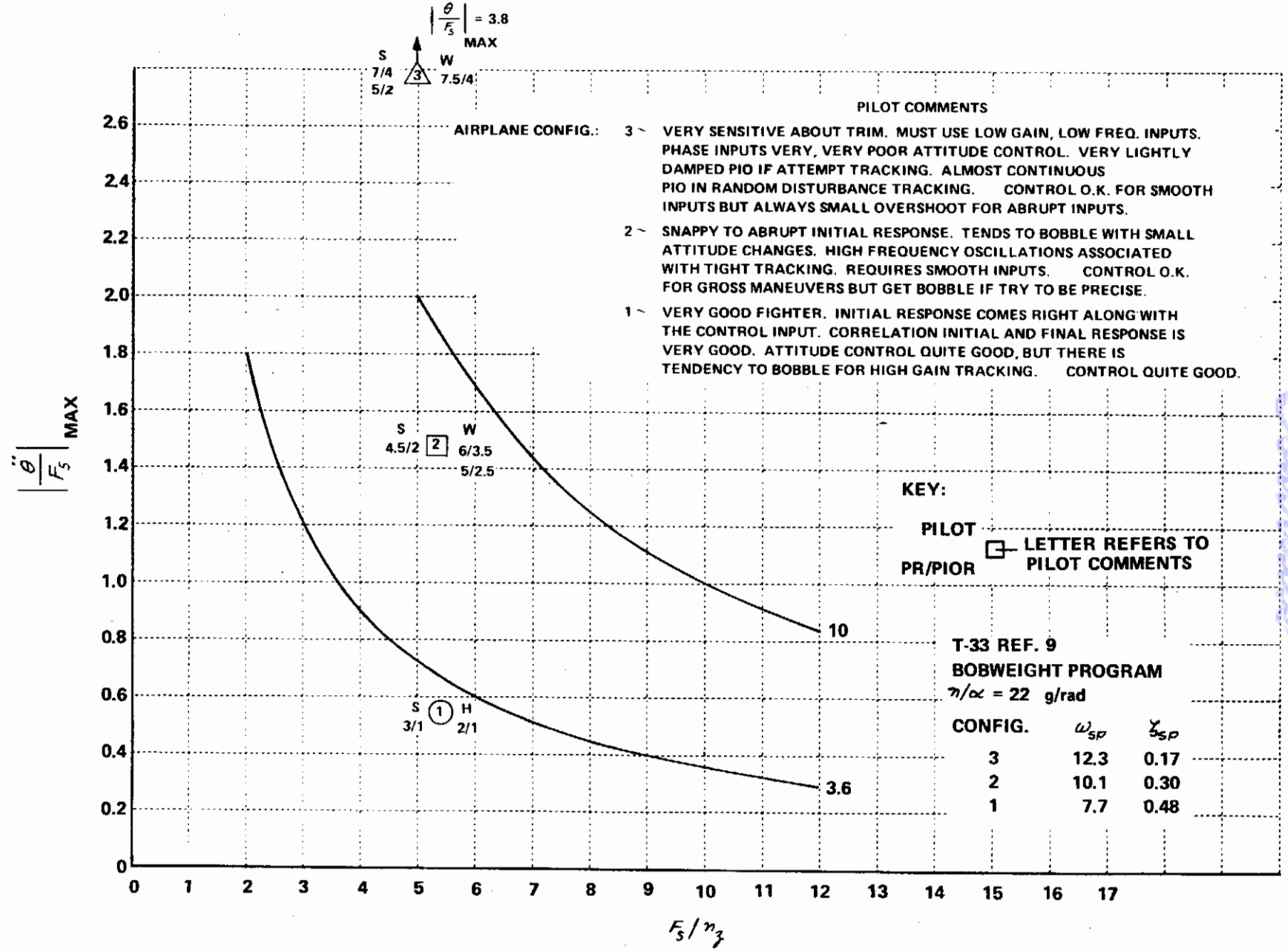

Figure 35 CONTROL SENSITIVITY DATA FOR CONFIGURATIONS 1, 2 and 3 (REFERENCE 9)

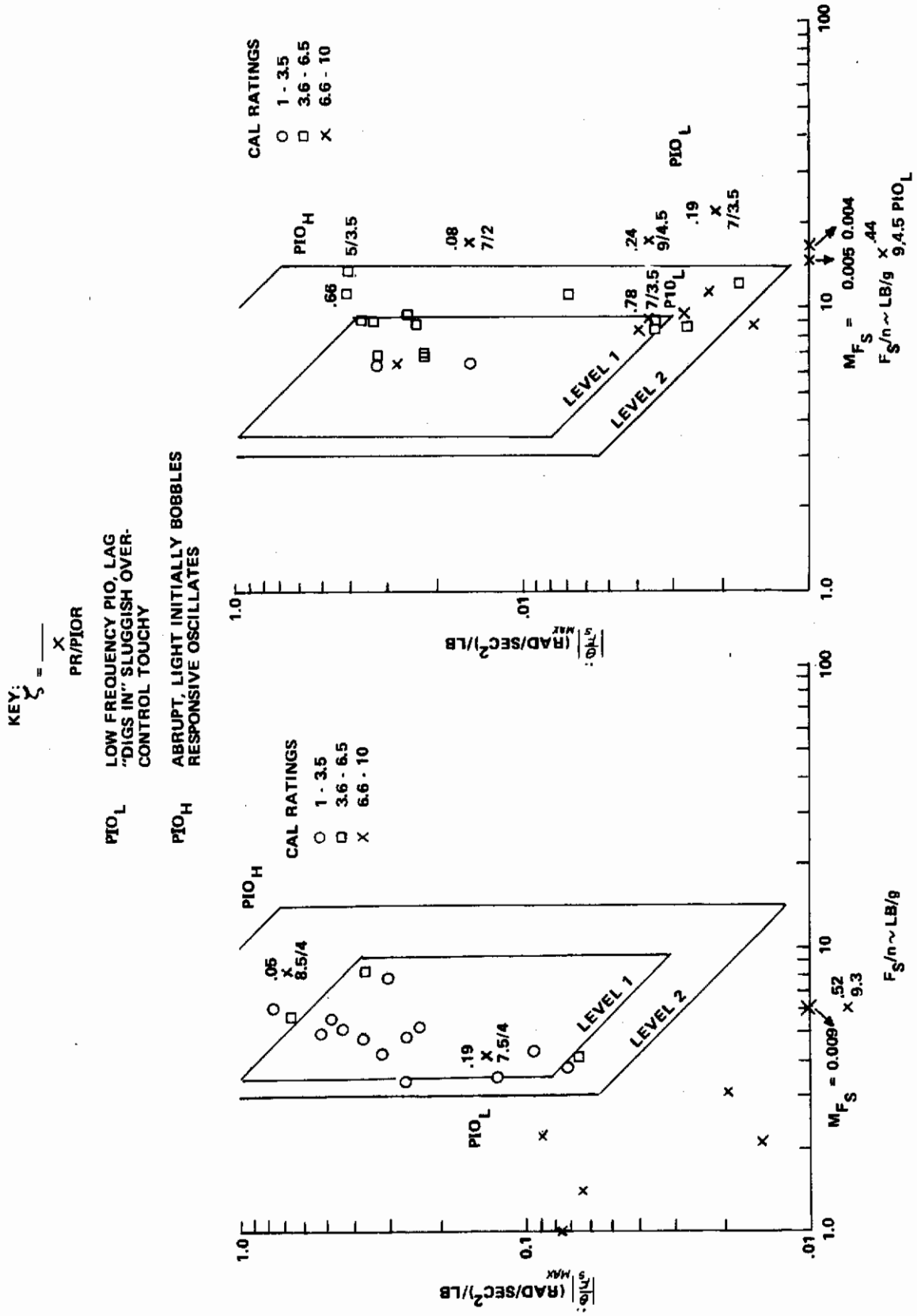

Figure 36 CONTROL SENSITIVITY DATA FOR η/α = 61.5 (REFERENCE 15)

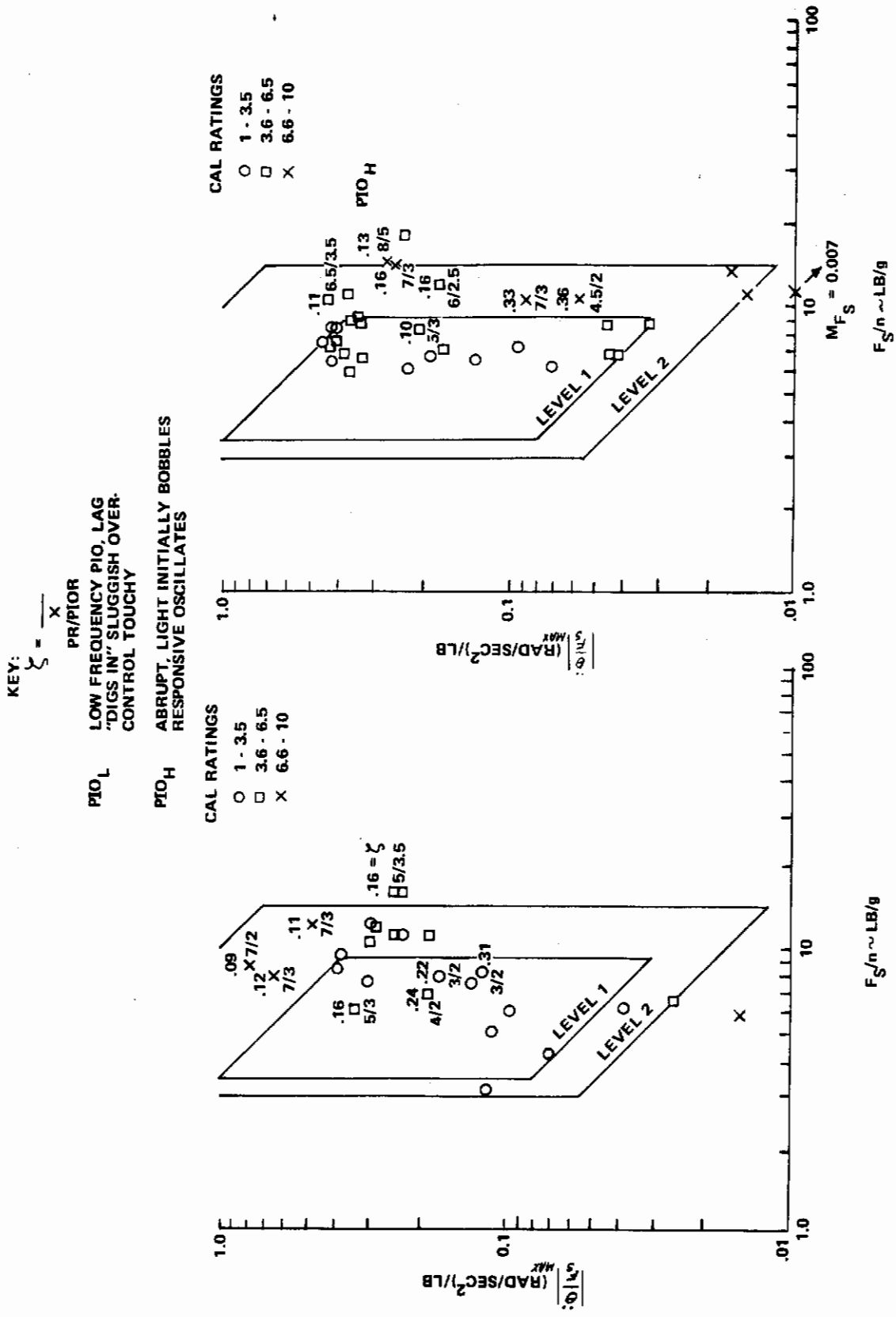

Figure 37 CONTROL SENSITIVITY DATA FOR n/α = 30.1 (REFERENCE 15)

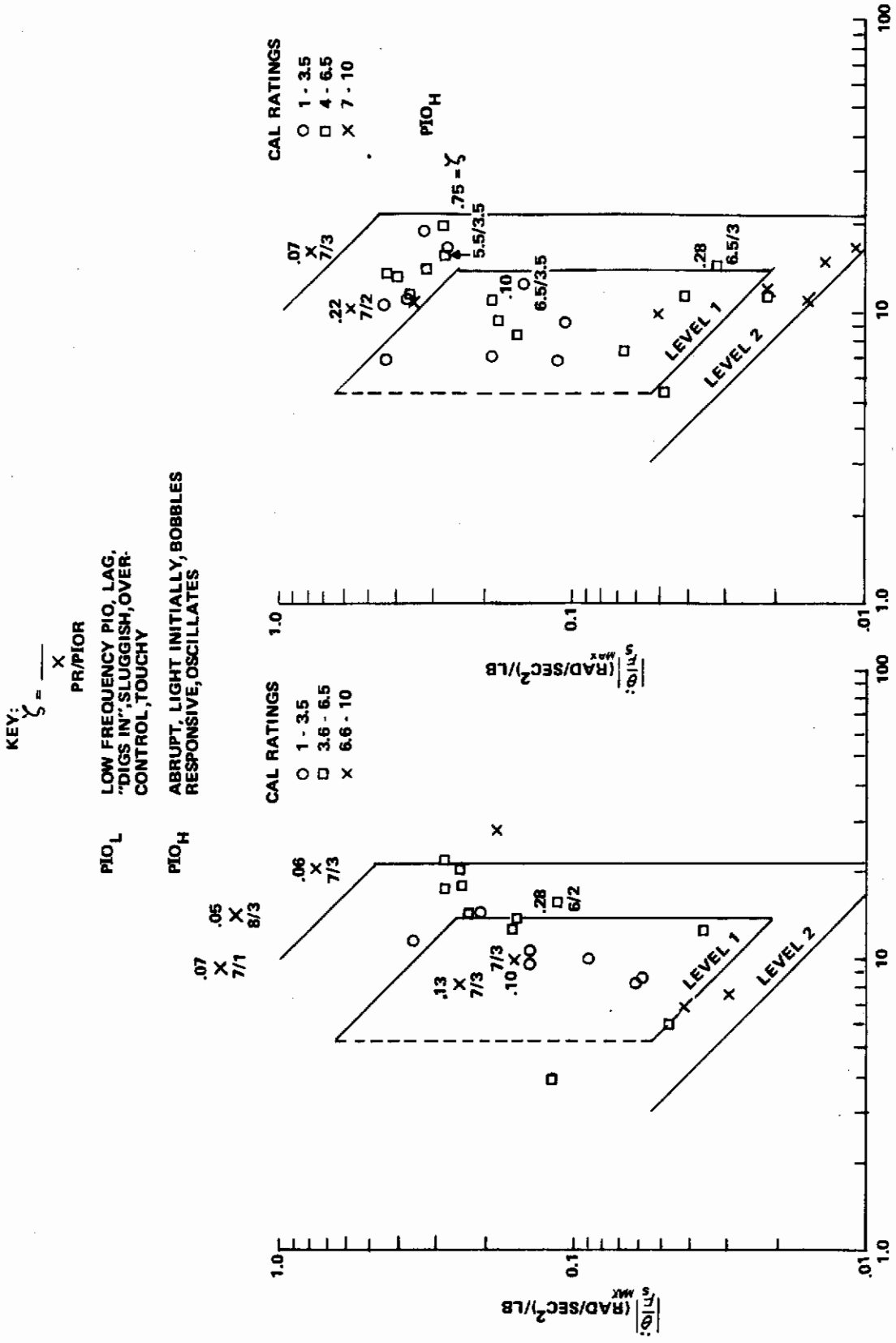

Figure 38 CONTROL SENSITIVITY DATA FOR η/α= 16.9 (REFERENCE 15)

DESCRIPTION	NUMERICAL RATING
NO TENDENCY FOR PILOT TO INDUCE UNDESIRABLE MOTIONS	1
UNDESIRABLE MOTIONS TEND TO OCCUR WHEN PILOT INITIATES ABRUPT MANEUVERS OR ATTEMPTS TIGHT CONTROL. THESE MOTIONS CAN BE PREVENTED OR ELIMINATED BY PILOT TECHNIQUE.	2
UNDESIRABLE MOTIONS EASILY INDUCED WHEN PILOT INITIATES ABRUPT MANEUVERS OR ATTEMPTS TIGHT CONTROL. THESE MOTIONS CAN BE PREVENTED OR ELIMINATED BUT ONLY AT SACRIFICE TO TASK PERFORMANCE OR THROUGH CONSIDERABLE PILOT ATTENTION AND EFFORT.	3
OSCILLATIONS TEND TO DEVELOP WHEN PILOT INITIATES ABRUPT MANEUVERS OR ATTEMPTS TIGHT CONTROL. PILOT MUST REDUCE GAIN OR ABANDON TASK TO RECOVER.	4
DIVERGENT OSCILLATIONS TEND TO DEVELOP WHEN PILOT INITIATES ABRUPT MANEUVERS OR ATTEMPTS TIGHT CONTROL PILOTMUST OPEN LOOP BY RELEASING OR FREEZING THE STICK.	5
DISTURBANCE OR NORMAL PILOT CONTROL MAY CAUSE DIVERGENT OSCILLATION. PILOT MUST OPEN CONTROL LOOP BY RELEASING OR FREEZING THE STICK.	6

Figure 39 PIO TENDENCY RATING SCALE

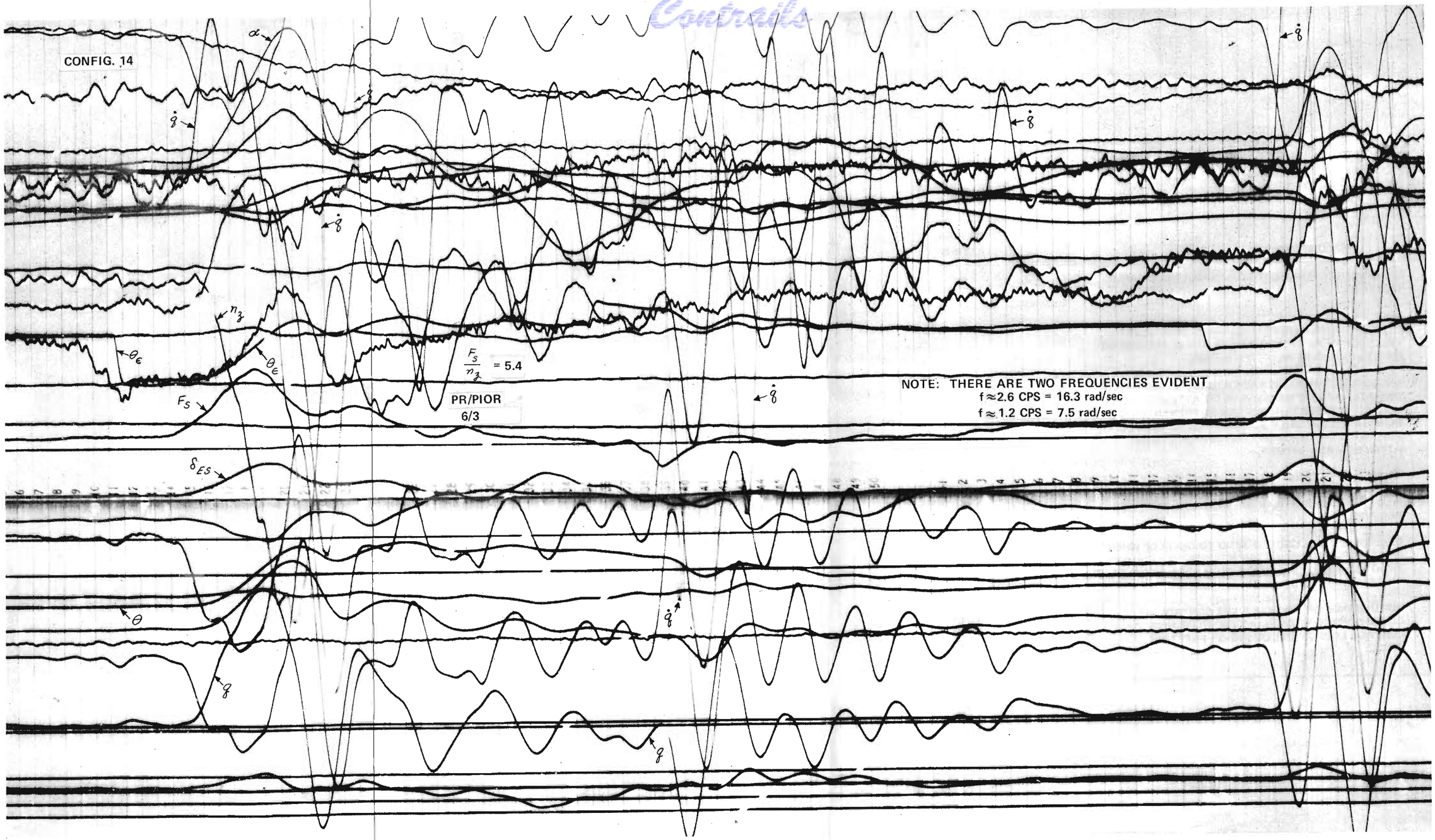

Figure 40 TIME HISTORY OF CONFIGURATION 14 (REFERENCE 8)

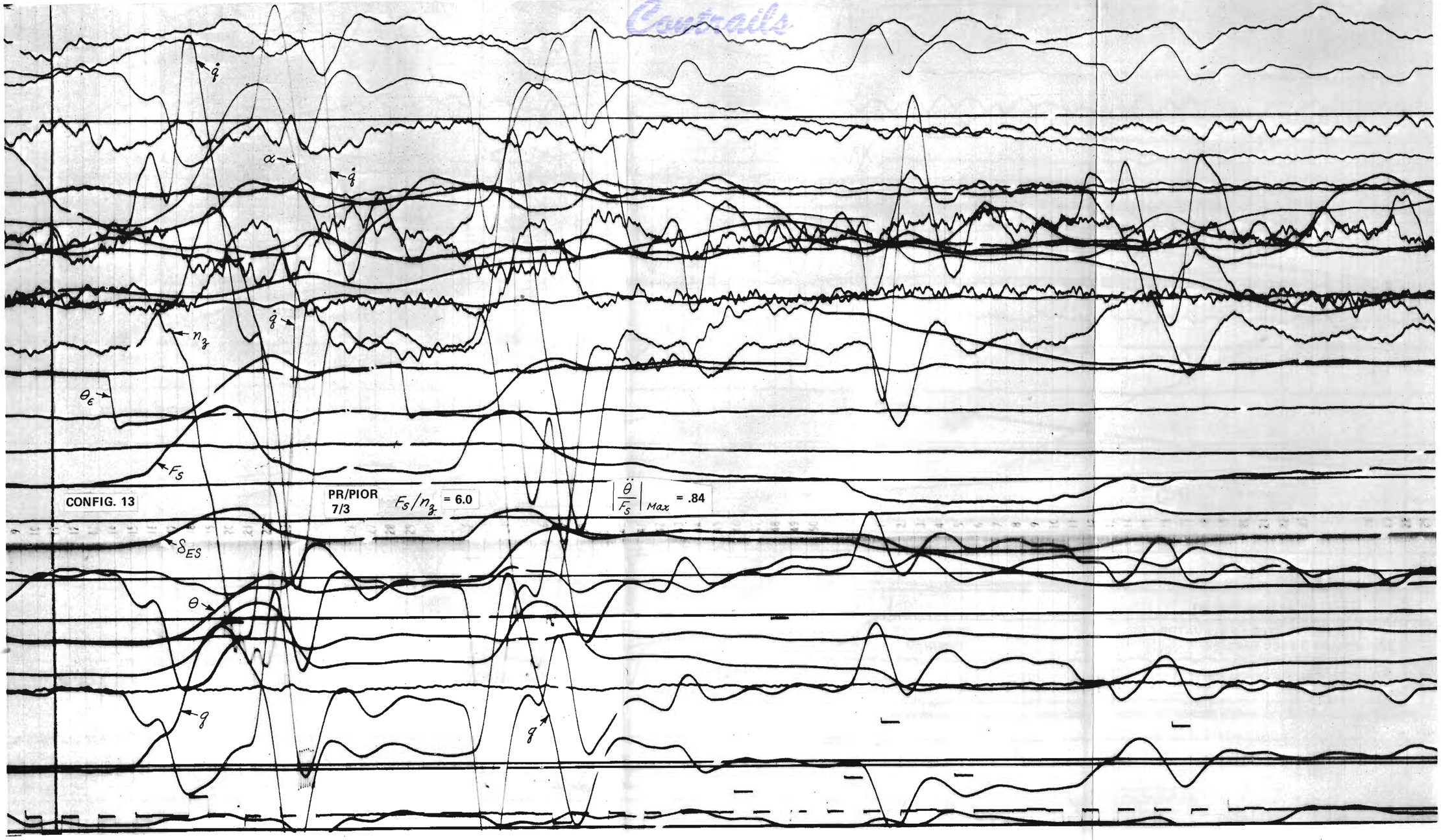

Figure 41 TIME HISTORY OF CONFIGURATION 13 (REFERENCE 8)

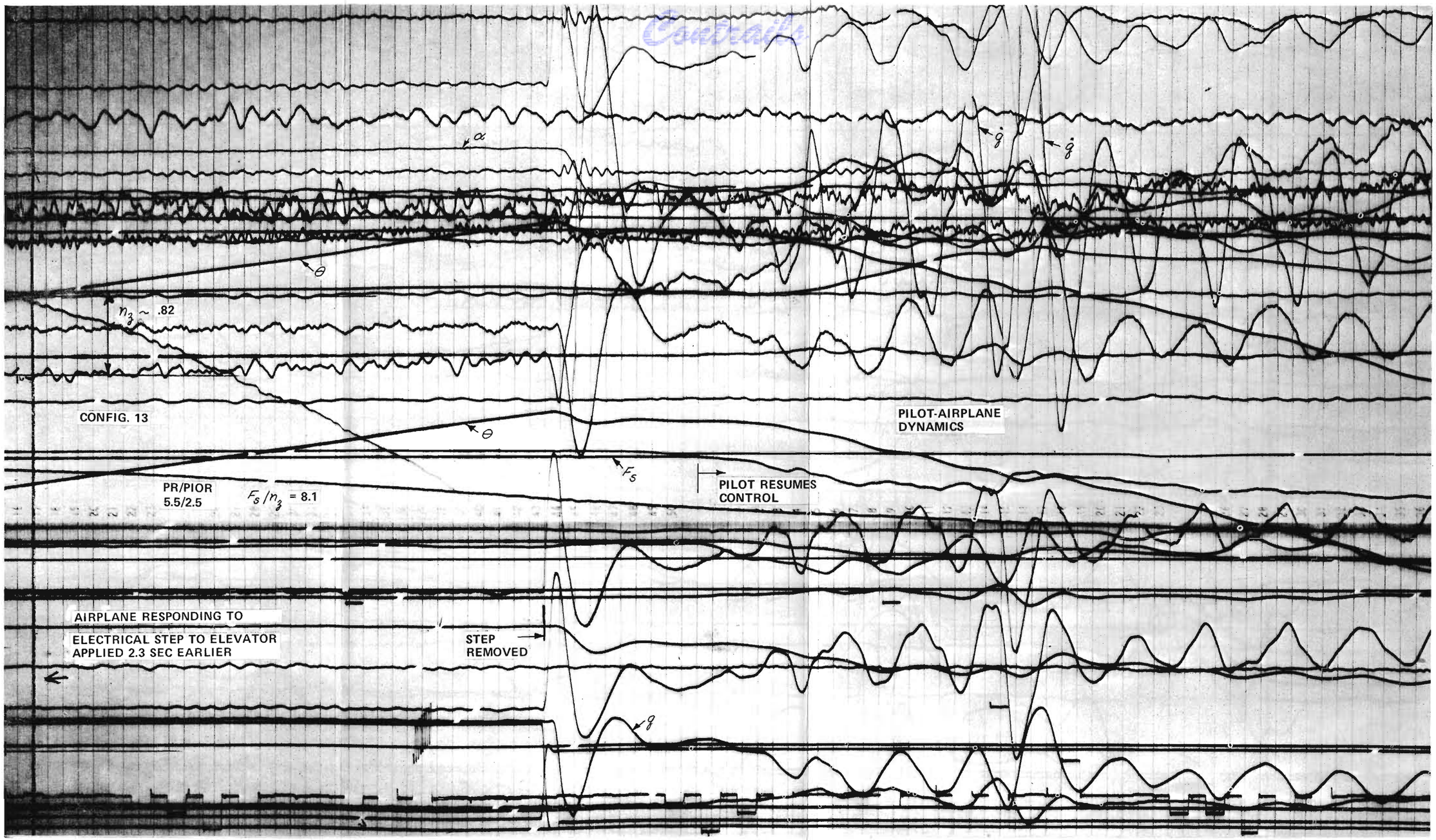

Figure 42 TIME HISTORY OF CONFIGURATION 13 (REFERENCE 8)

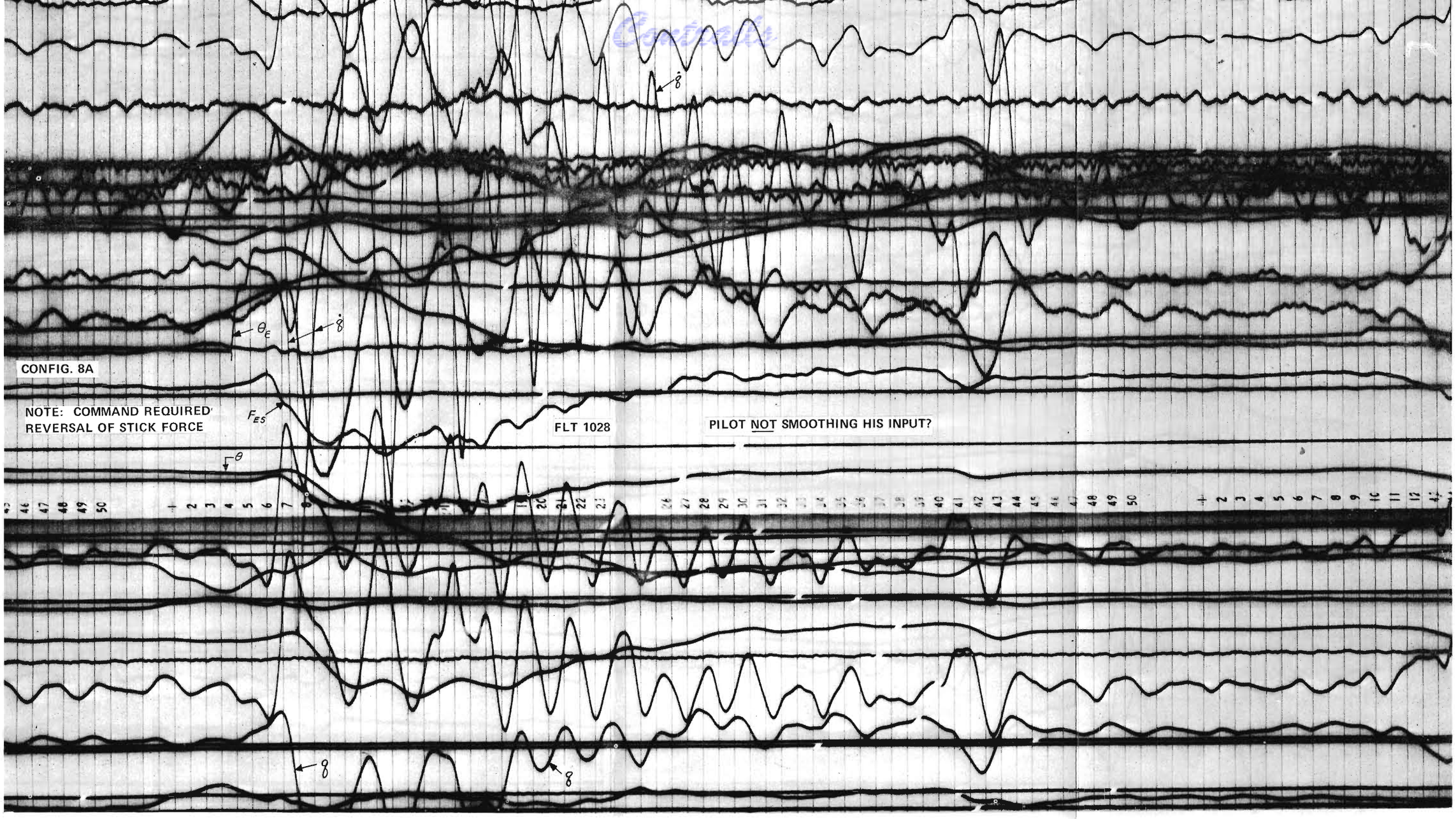

Figure 43 TIME HISTORY OF NO.1 CONFIGURATION 8a (REFERENCE 8)

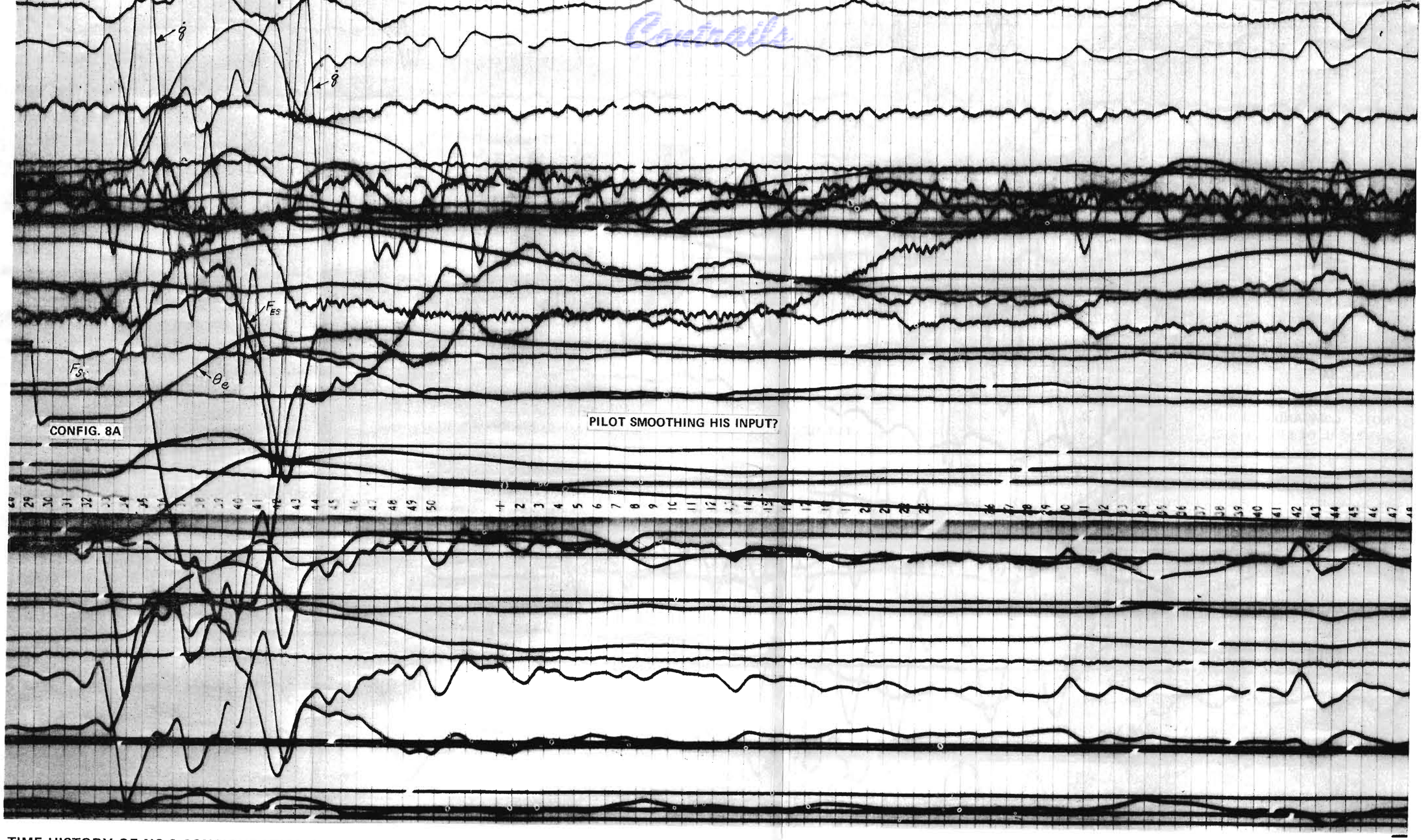

Figure 44 TIME HISTORY OF NO.2 CONFIGURATION 8a (REFERENCE 8)

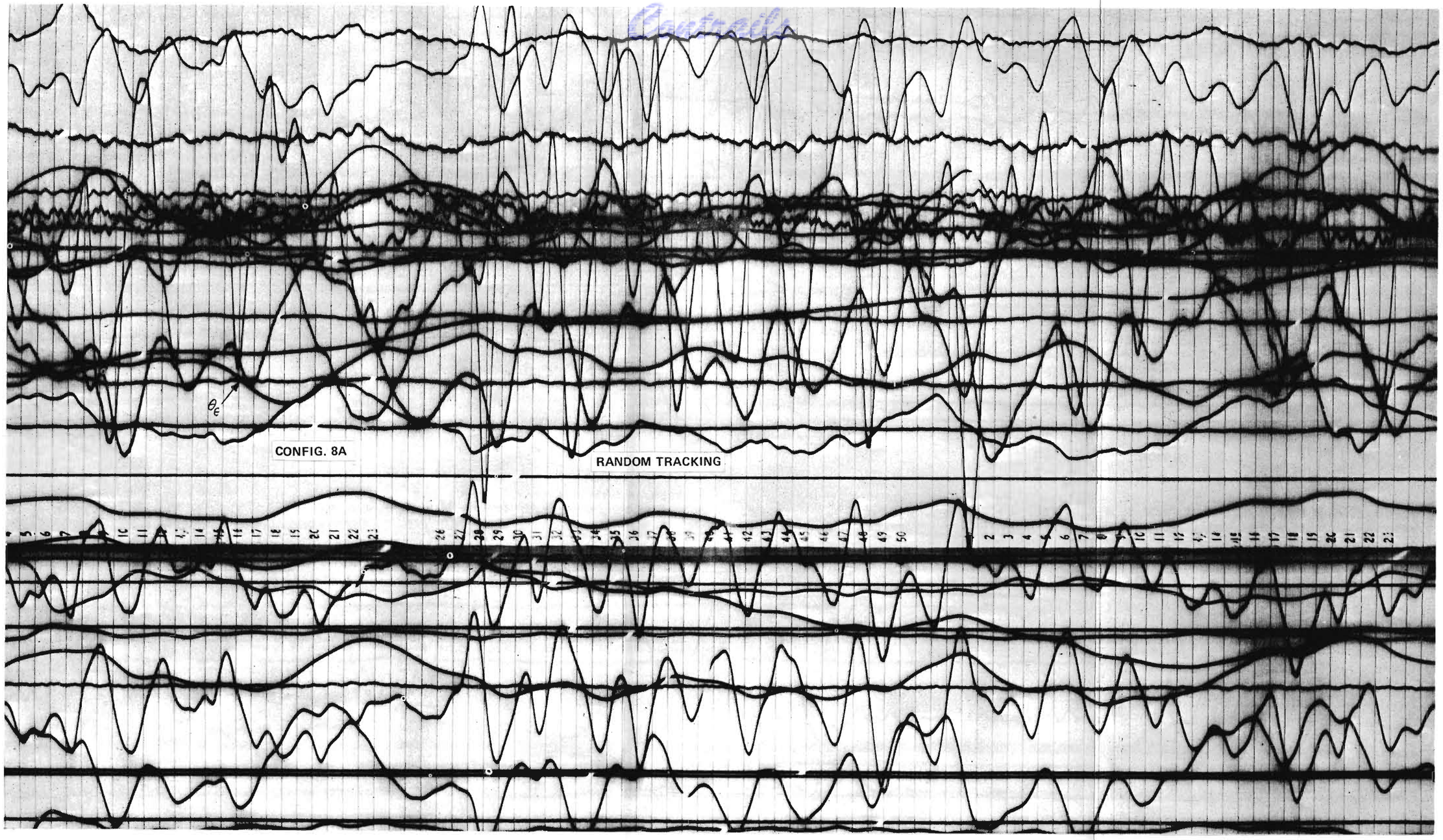

Figure 45 TIME HISTORY OF NO. 3 CONFIGURATION 8a (REFERENCE 8)

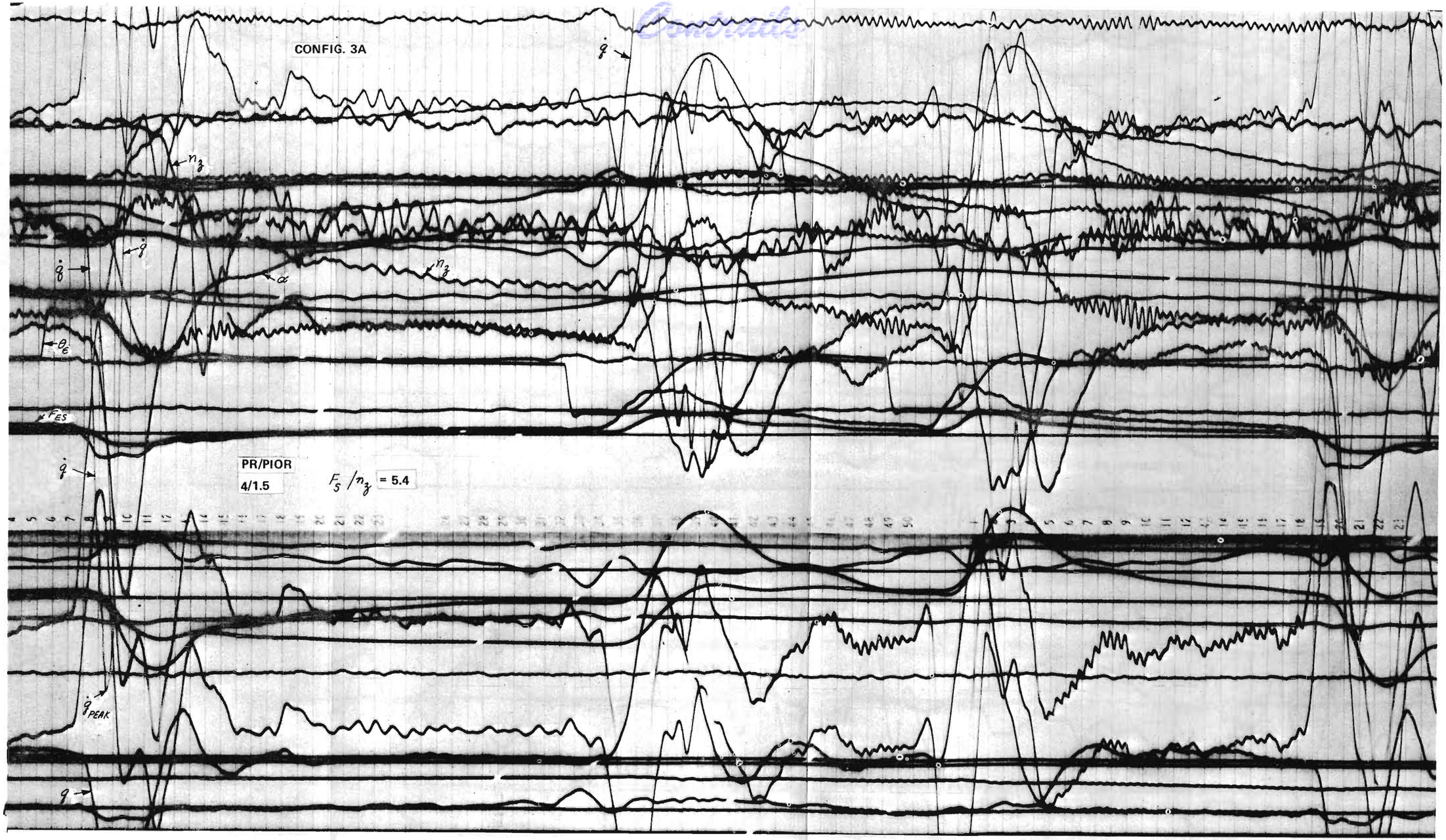

Figure 46 TIME HISTORY OF CONFIGURATION 3a (REFERENCE 8)

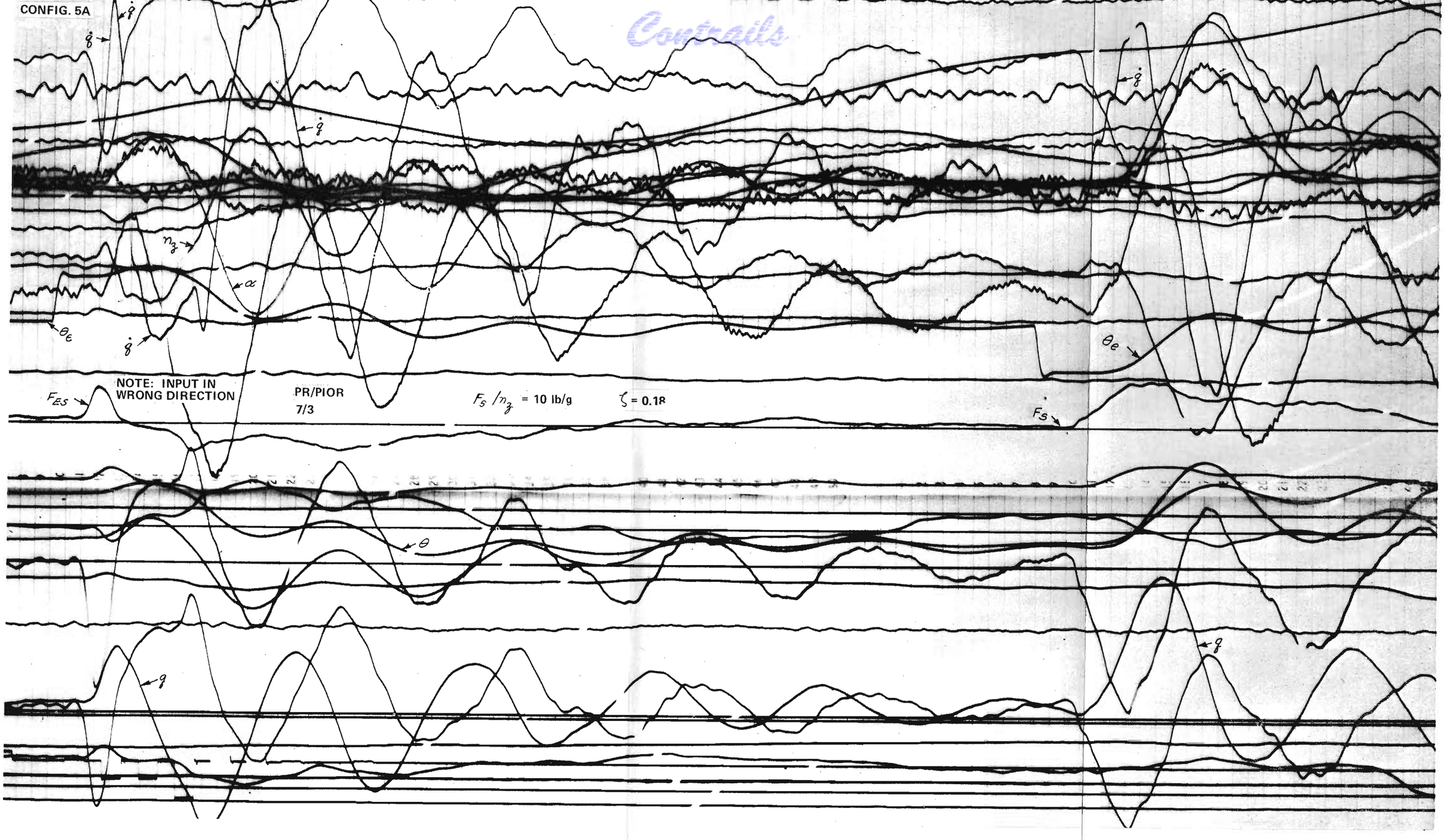

Figure 47 TIME HISTORY OF CONFIGURATION 5a (REFERENCE 8)

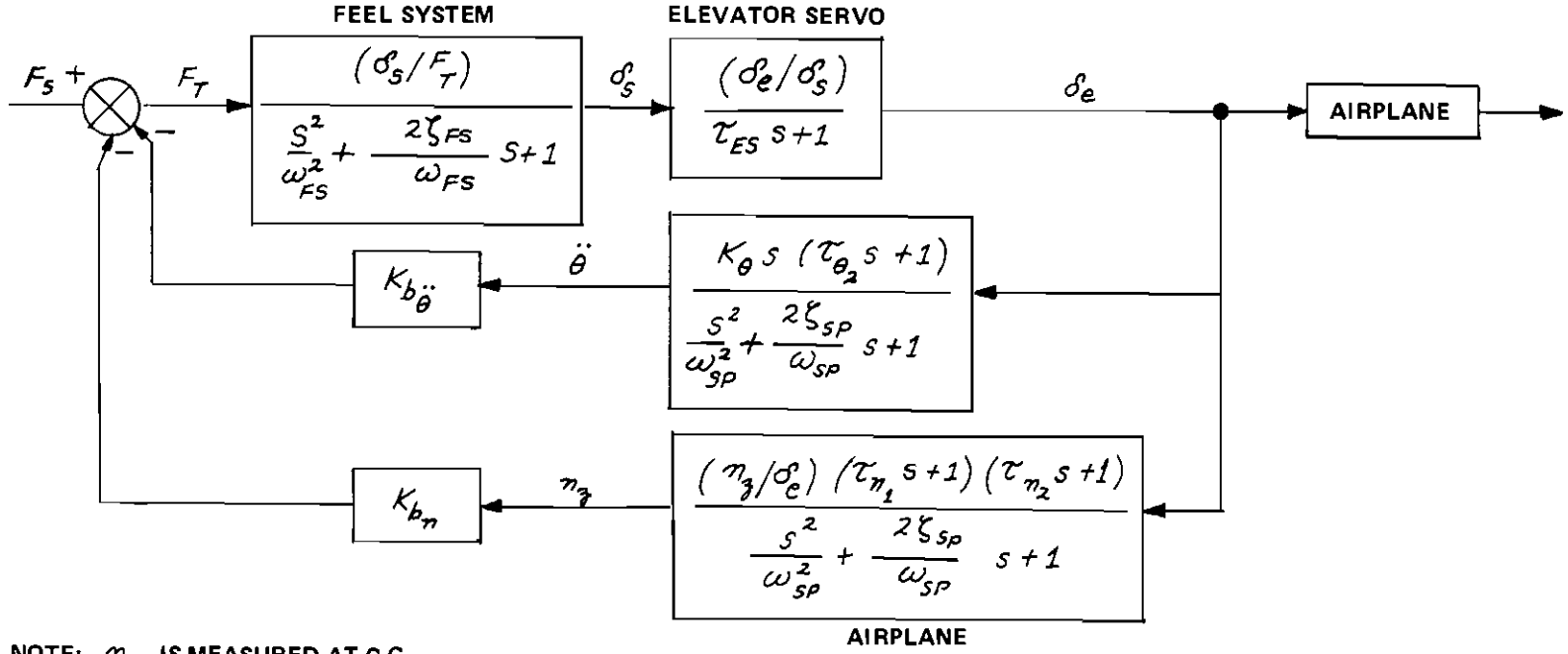

NOTE: n_z IS MEASURED AT C.G.

BOBWEIGHT LOOP CLOSED (PRIMED PARAMETERS REPRESENT CLOSED-LOOP VALUES, UNPRIMED PARAMETERS ARE OPEN-LOOP VALUES)

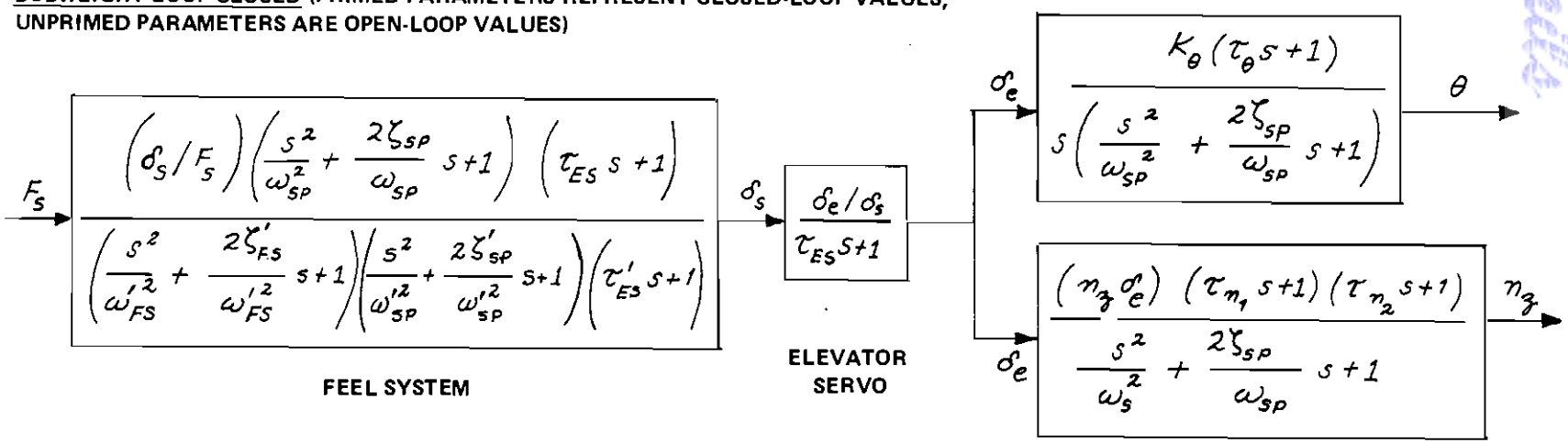

Figure 48 BASIC DYNAMIC CHARACTERISTICS

$$\frac{\delta_e}{F_s} = \frac{\frac{\delta_s}{F_s}\,\frac{\delta_e}{\delta_s}\left(\frac{s^2}{\omega_{sp}^2} + \frac{2\zeta_{sp}}{\omega_{sp}}s + 1\right)}{\left(\tau'_{es}s + 1\right)\left(\frac{s^2}{\omega'^2_{F_s}} + \frac{2\zeta'_{F_s}}{\omega'^2_{F_s}}s + 1\right)\left(\frac{s^2}{\omega'^2_{sp}} + \frac{2\zeta_{sp}}{\omega'_{sp}}s + 1\right)}$$

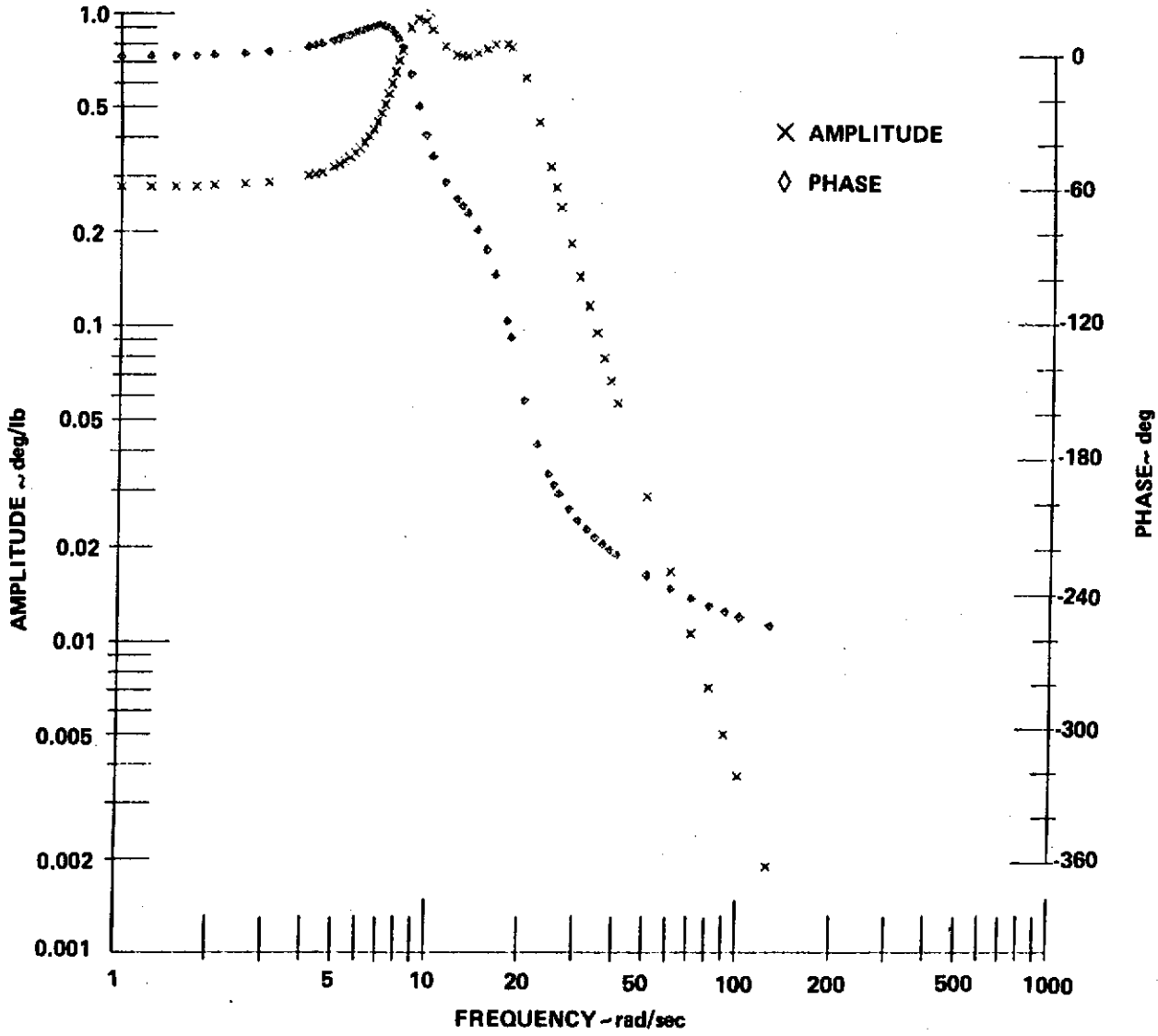

Figure 49 FREQUENCY RESPONSE OF ELEVATOR TO STICK FORCE, $A4D_{PIO}$

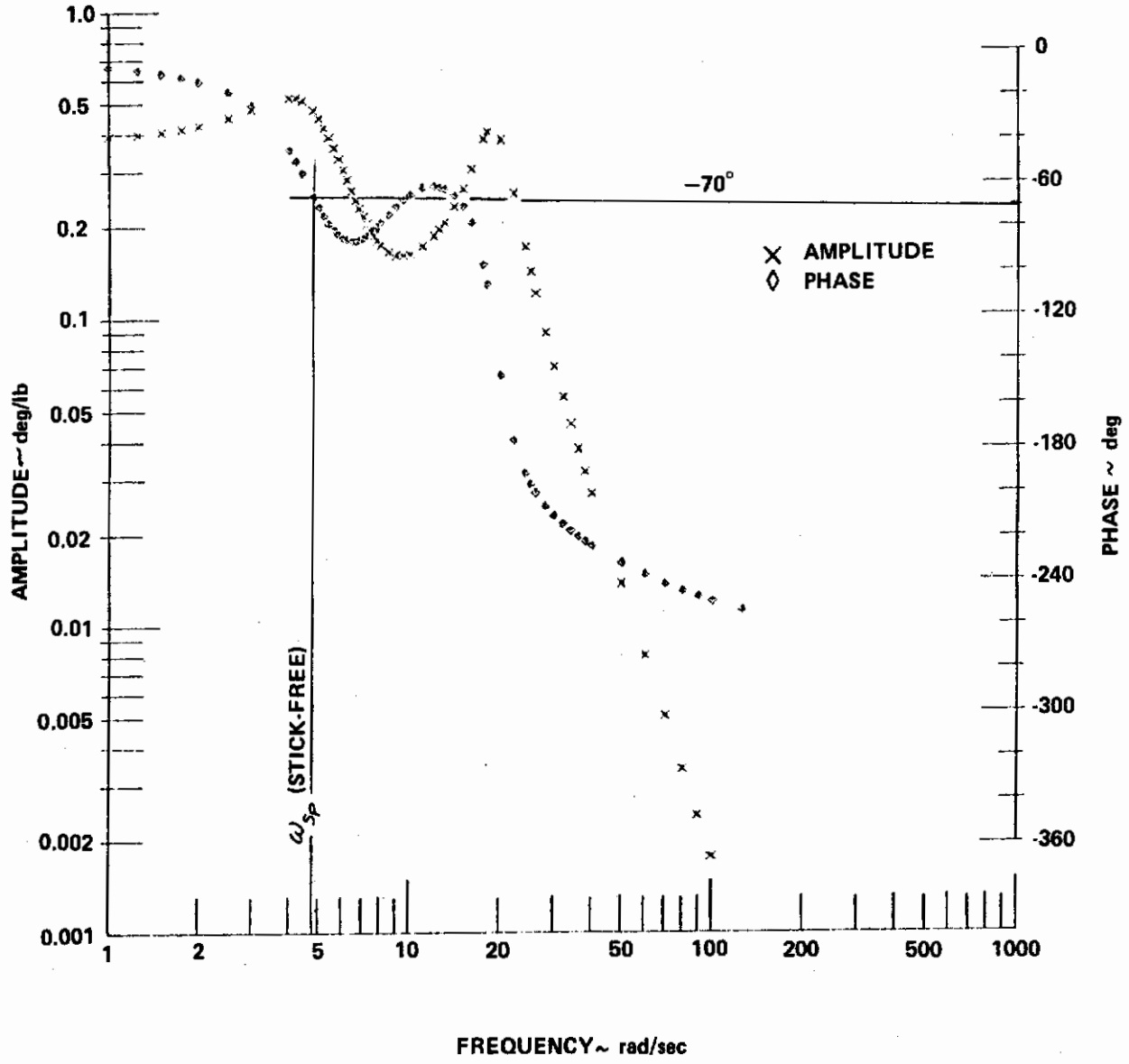

Figure 50 FREQUENCY RESPONSE OF ELEVATOR TO STICK FORCE, $A4D_M$

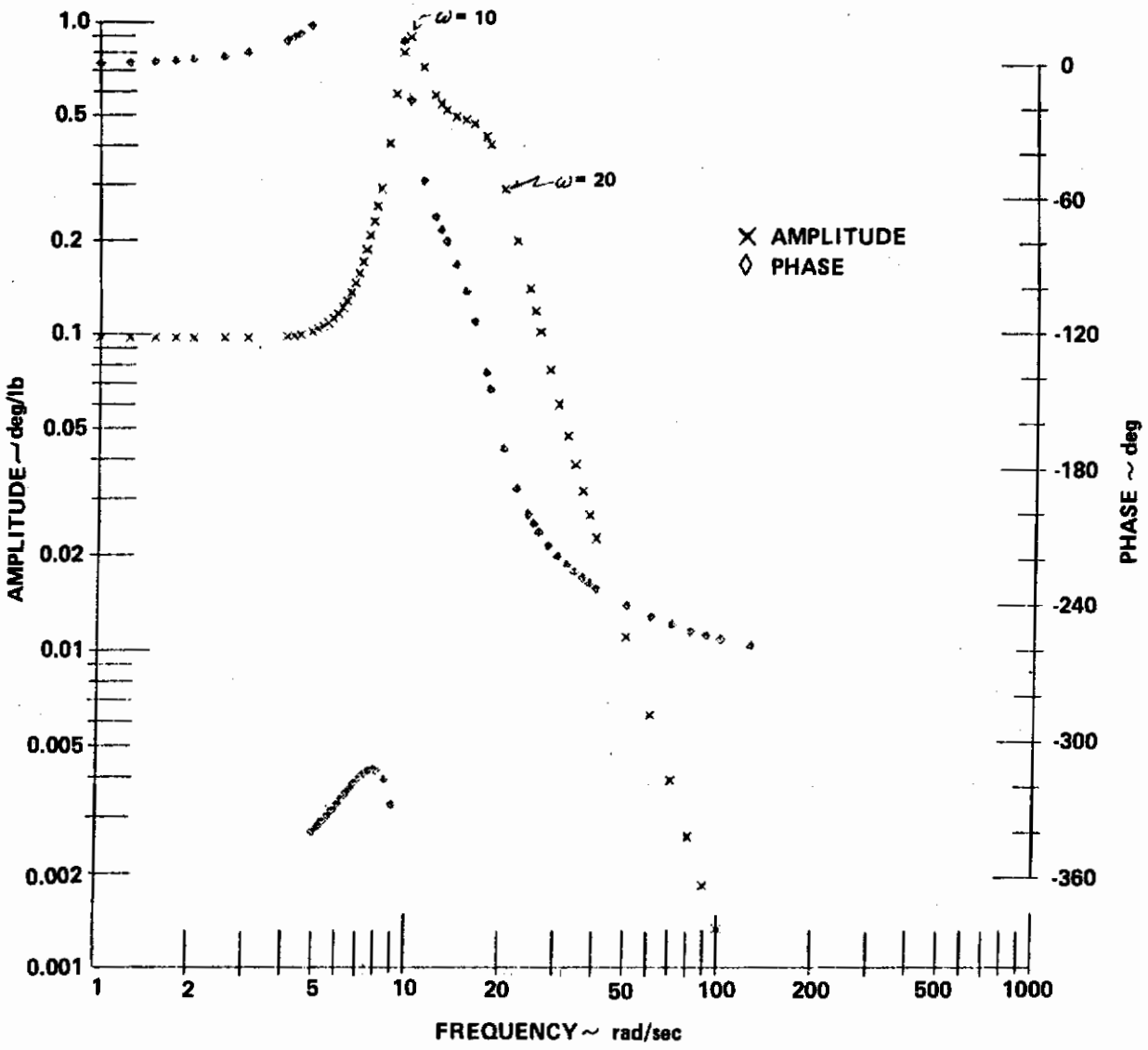

Figure 51 FREQUENCY RESPONSE OF ELEVATOR TO STICK FORCE, T-38$_{PIO}$

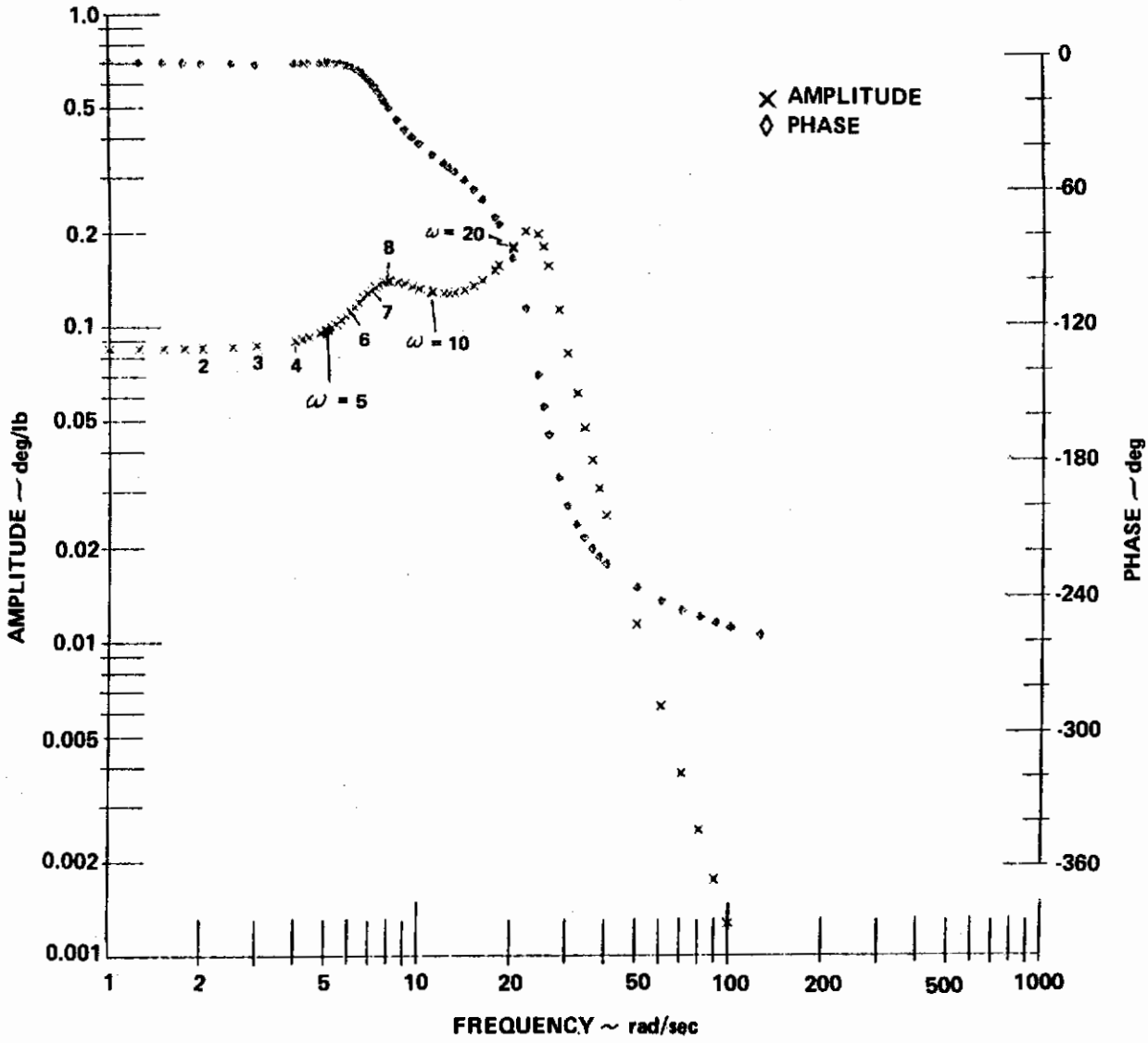

Figure 52 FREQUENCY RESPONSE OF ELEVATOR TO STICK FORCE, $T\text{-}38_M$

$$\frac{\ddot{\theta}}{F_S} = \frac{\frac{\delta_S}{F_S}\,\frac{\delta_e}{\delta_S}\,K_\theta\, s\left(\tau_\theta s + 1\right)}{\left(\tau'_{ES} s + 1\right)\left(\frac{s^2}{\omega'^2_{F_S}} + \frac{2\zeta'_{F_S}}{\omega'_{F_S}} s + 1\right)\left(\frac{s^2}{\omega'^2_{SP}} \frac{2\zeta_{SP}}{\omega'_{SP}}\, s + 1\right)}$$

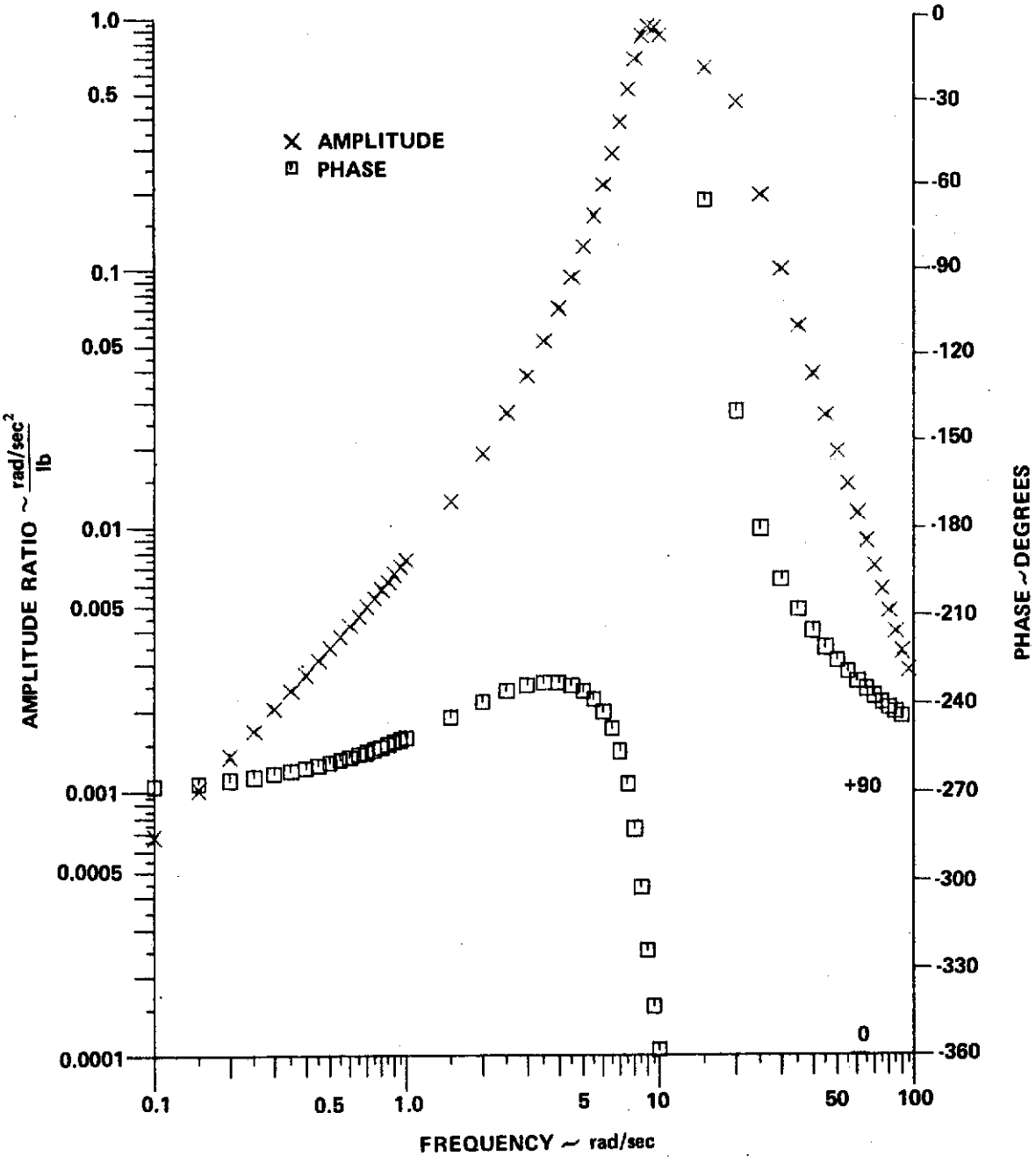

Figure 53 FREQUENCY RESPONSE OF PITCH ACCELERATION TO STICK FORCE, $A4D_{PIO}$

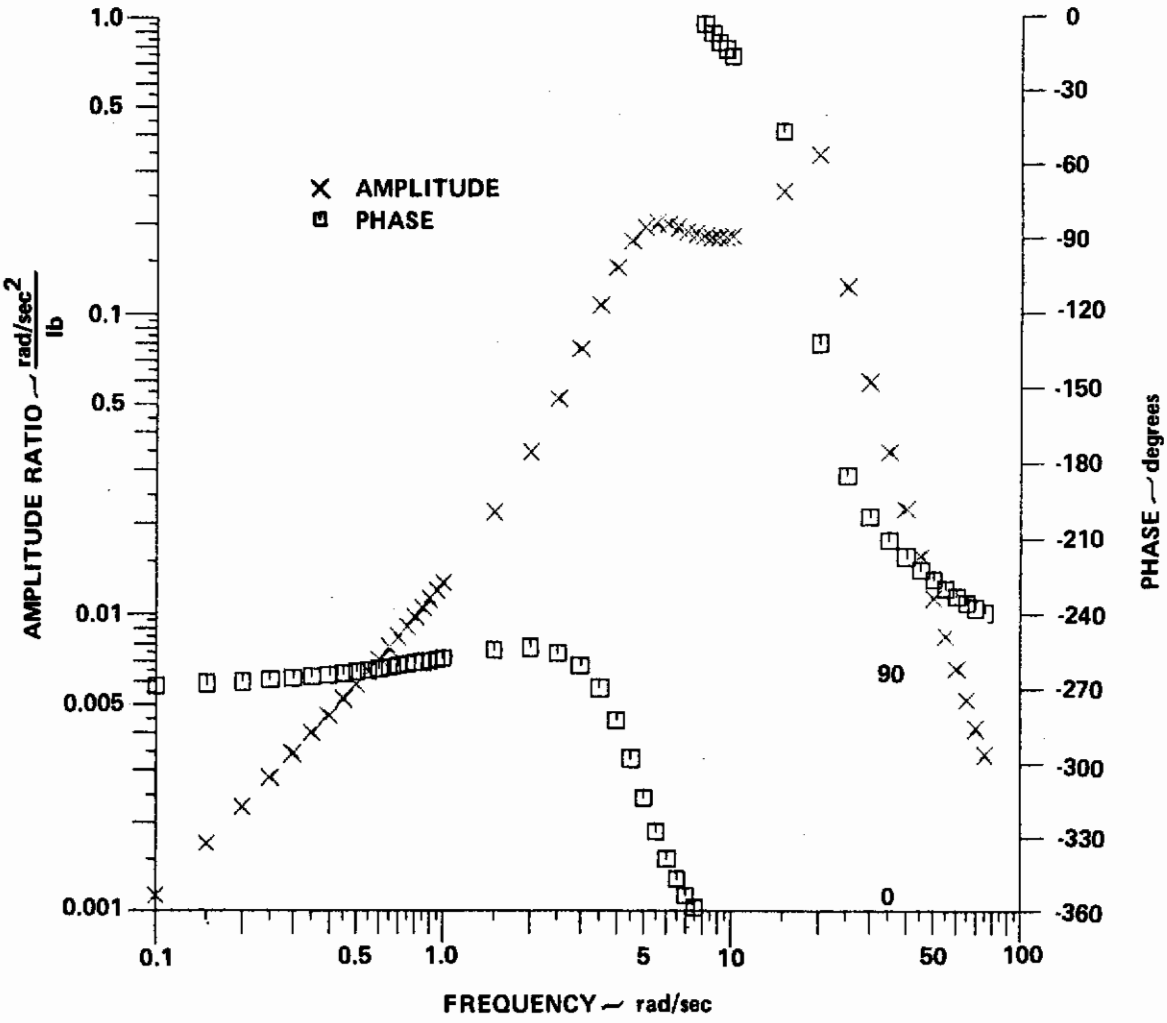

Figure 54 FREQUENCY RESPONSE OF PITCH ACCELERATION TO STICK FORCE, $A4D_M$

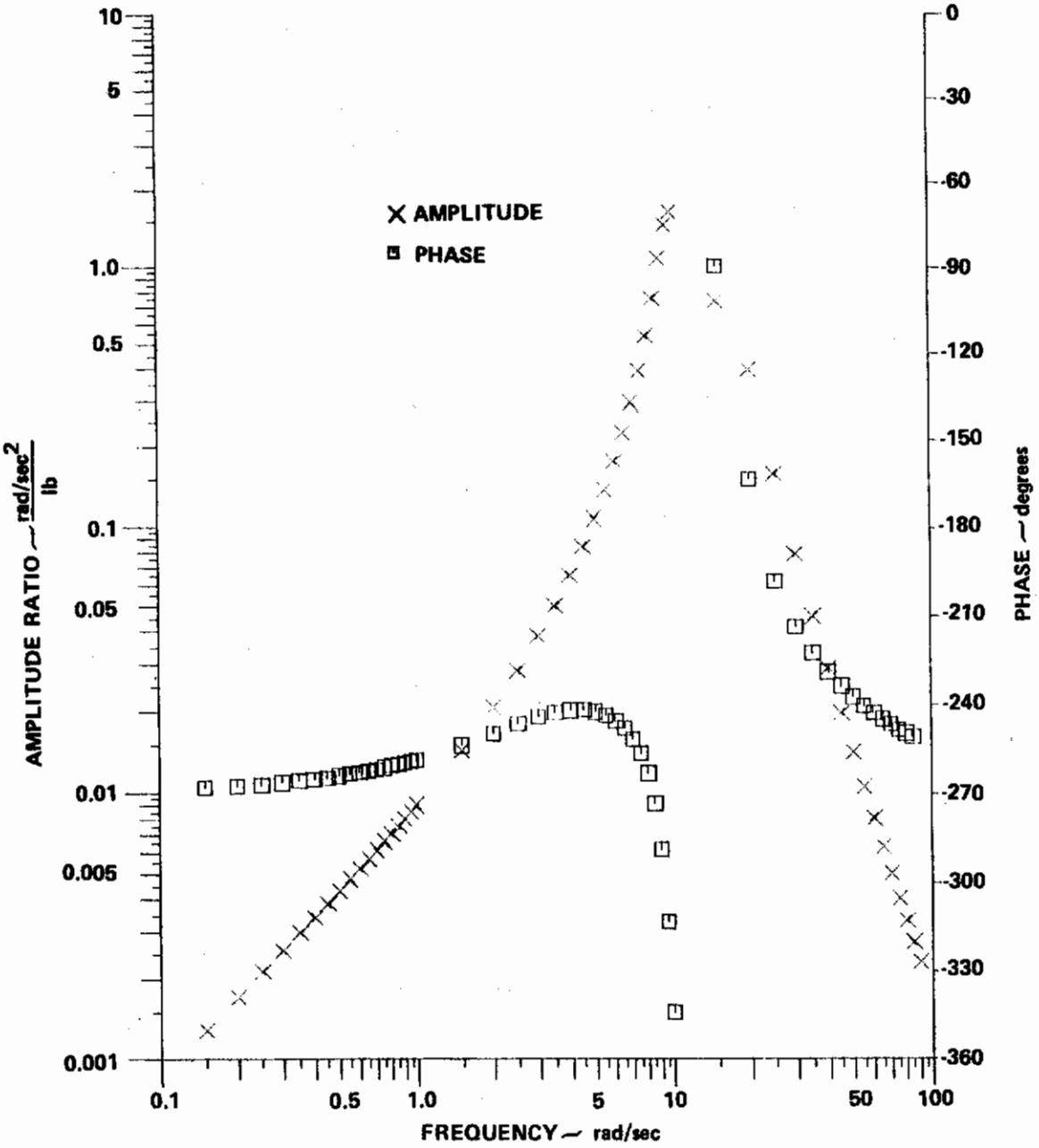

Figure 55 FREQUENCY RESPONSE OF PITCH ACCELERATION TO STICK FORCE, T-38$_{PIO}$

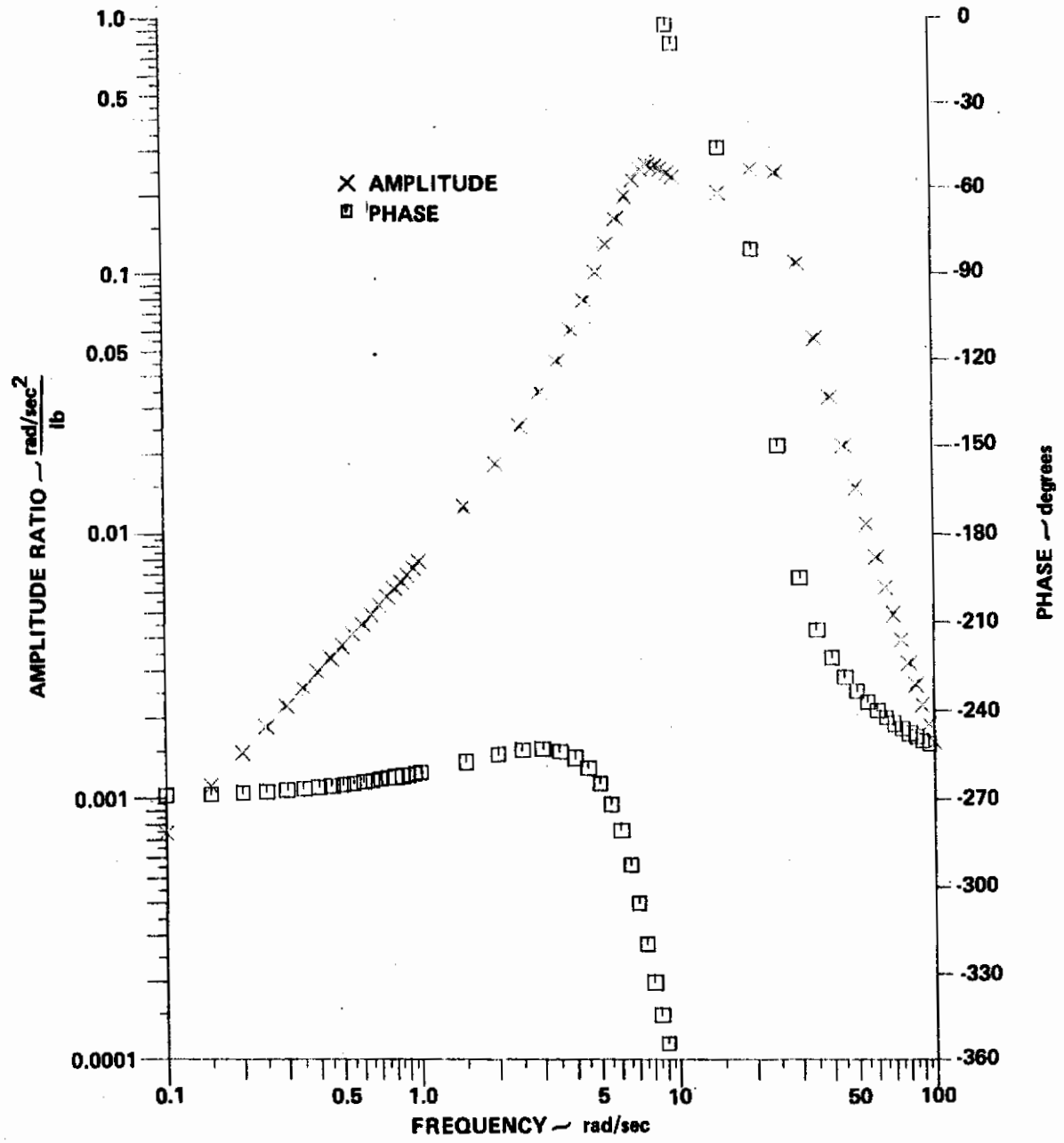

Figure 56 FREQUENCY RESPONSE OF PITCH ACCELERATION TO STICK FORCE, $T\text{-}38_M$

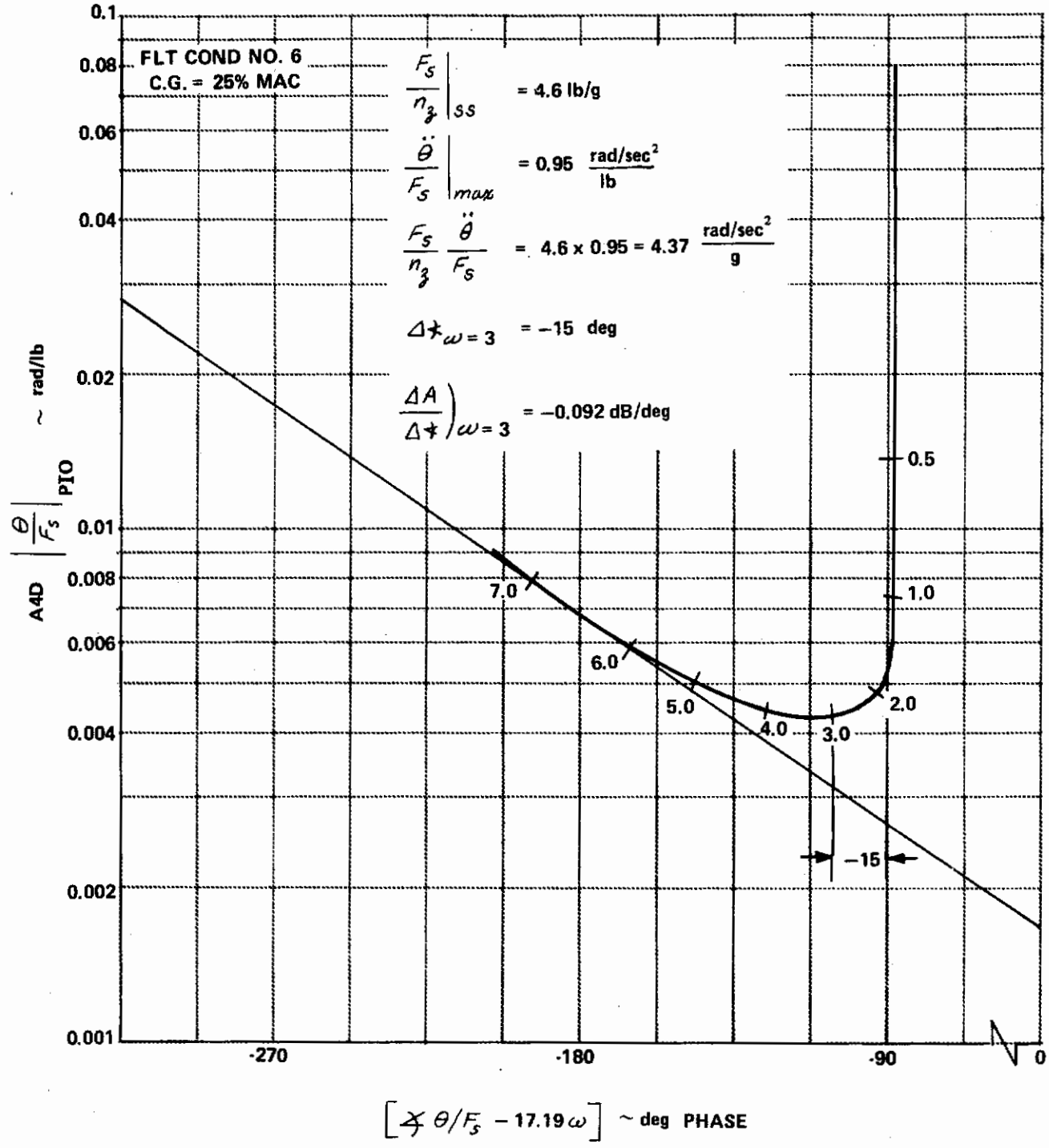

Figure 57 FREQUENCY RESPONSE OF PITCH TO STICK FORCE, $A4D_{PIO}$

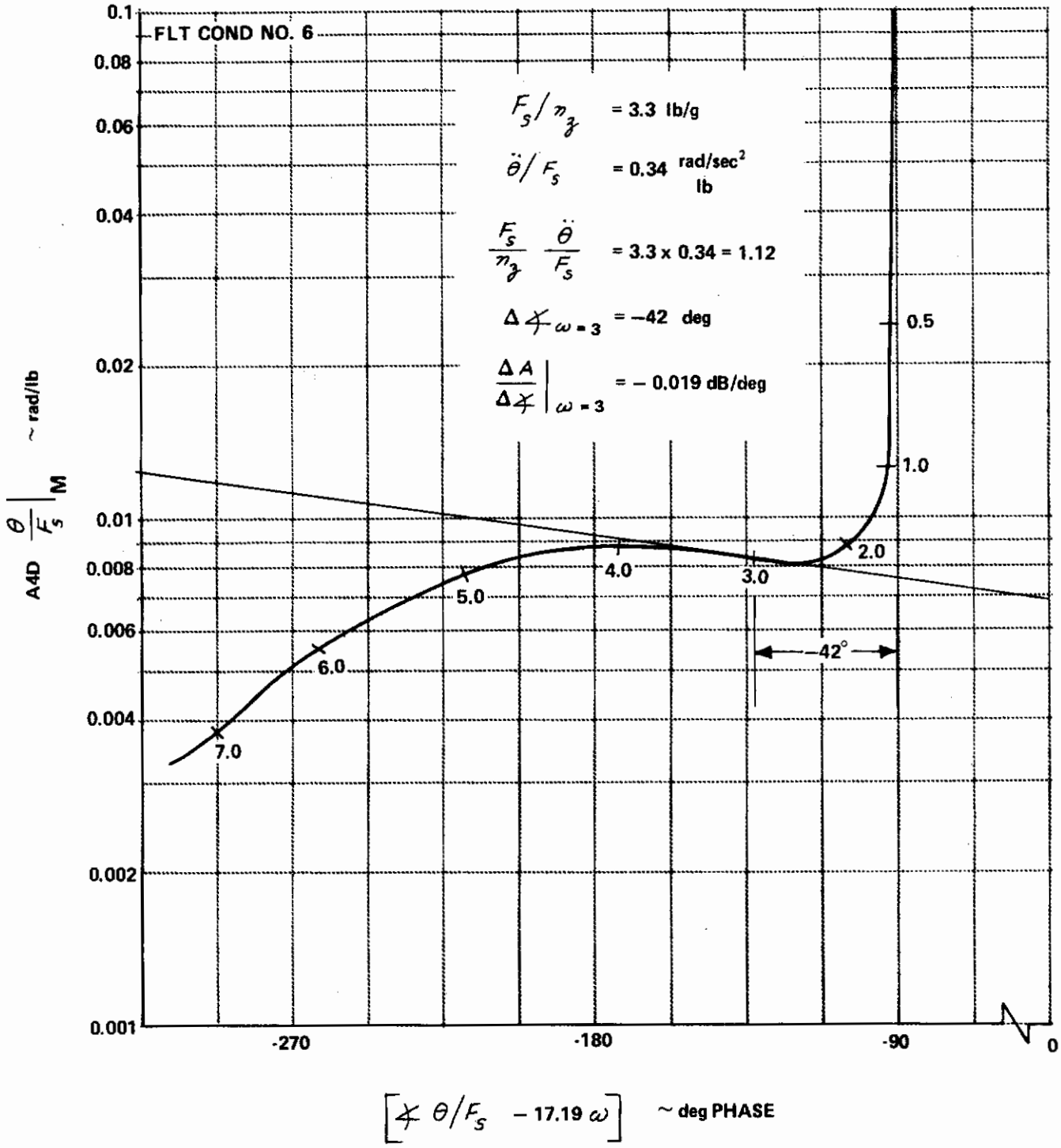

Figure 58 FREQUENCY RESPONSE OF PITCH TO STICK FORCE, $A4D_M$

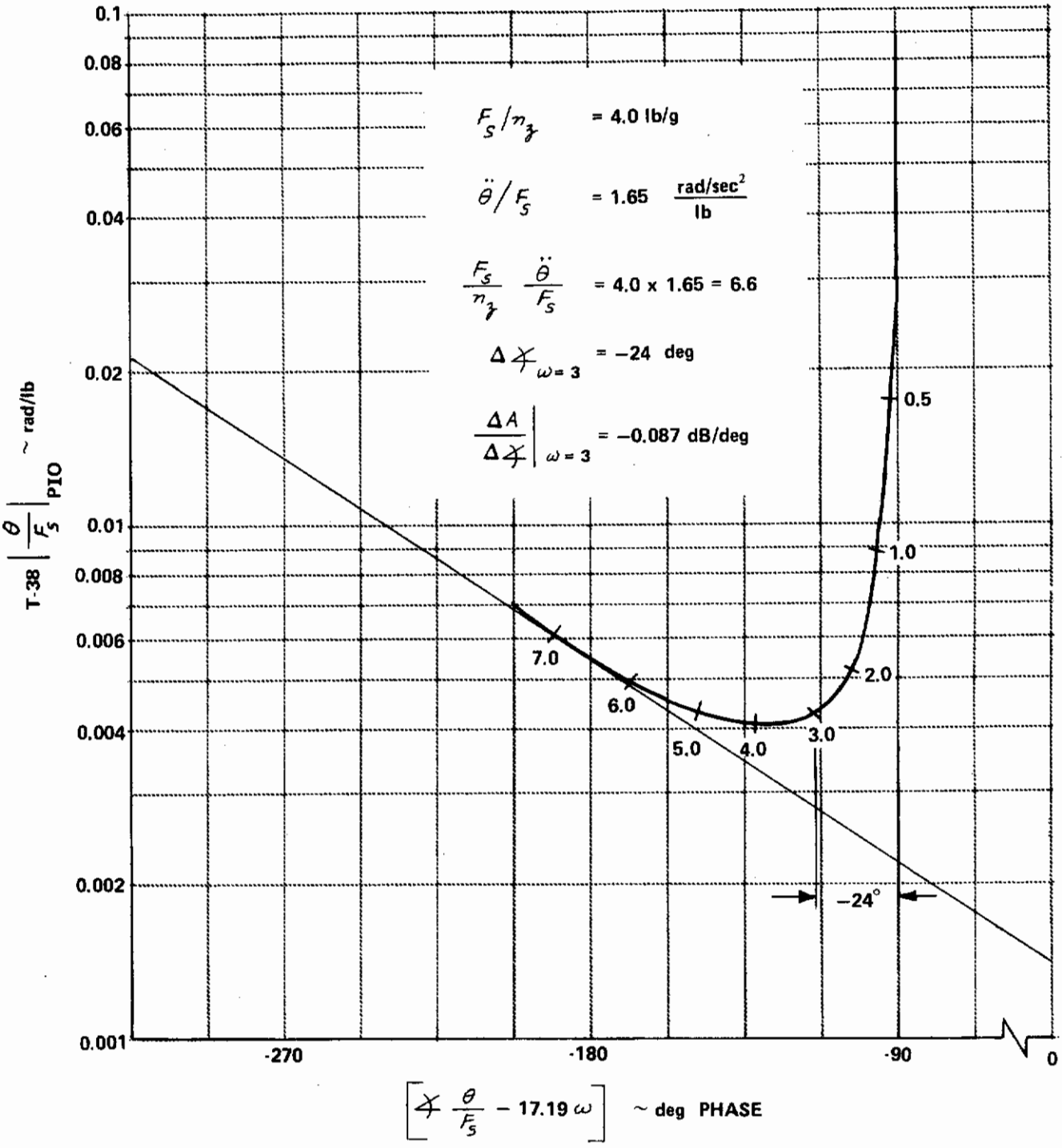

Figure 59 FREQUENCY RESPONSE OF PITCH TO STICK FORCE, T-38$_{PIO}$

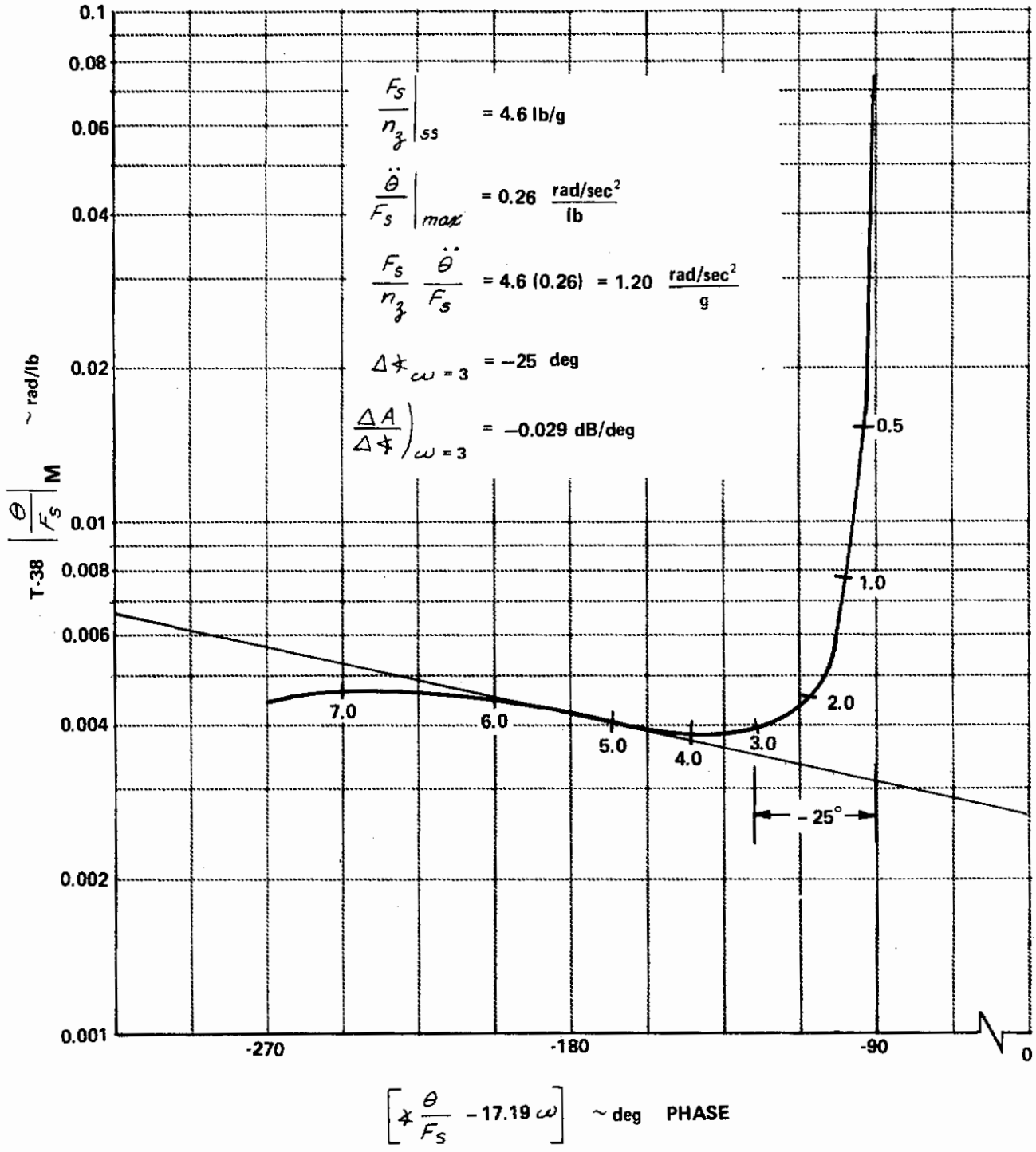

Figure 60 FREQUENCY RESPONSE OF PITCH TO STICK FORCE, T-38$_M$

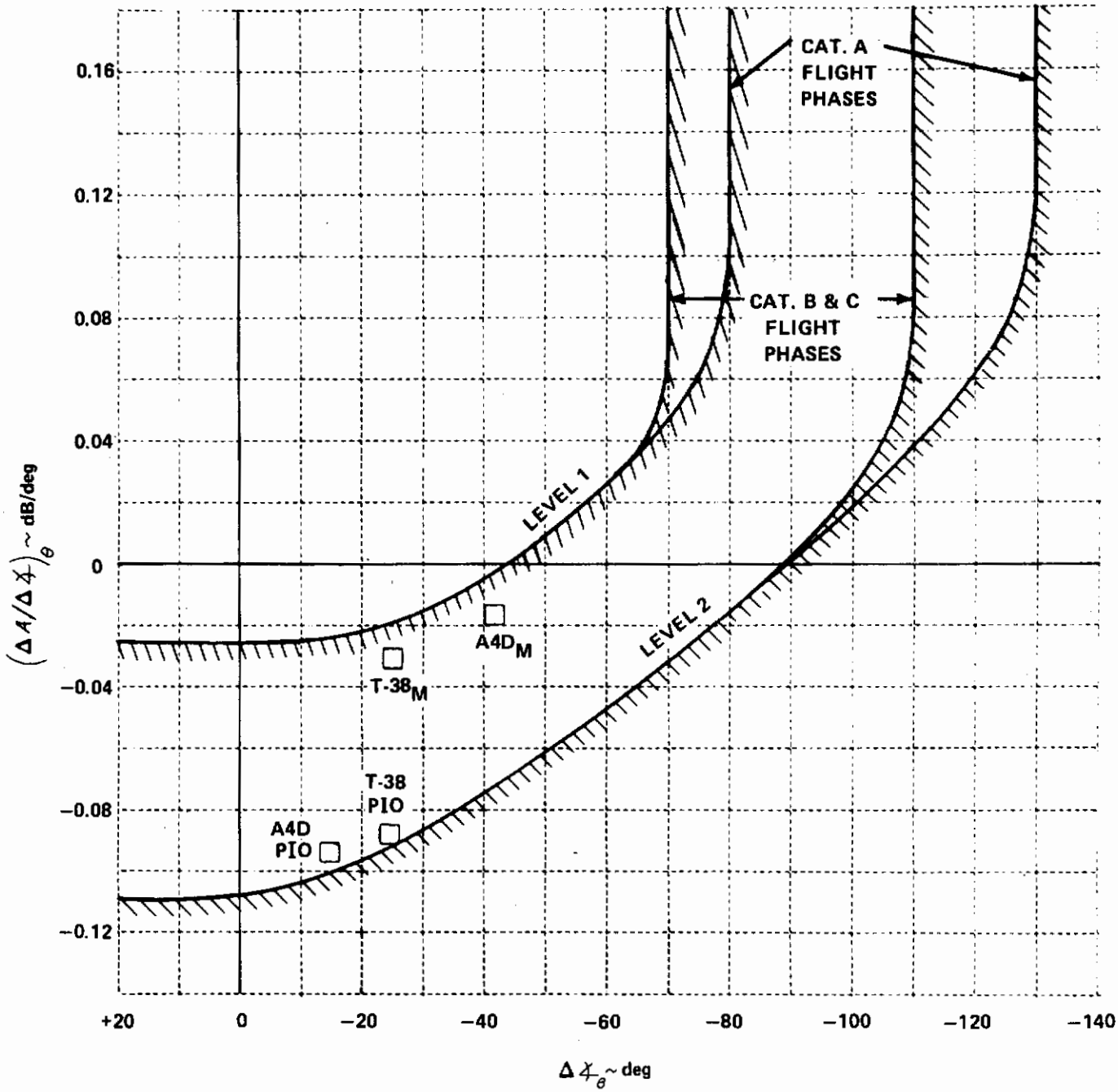

Figure 61 PITCH MANEUVER RESPONSE CHARACTERISTICS OF THE A4D AND T-38 AIRPLANES

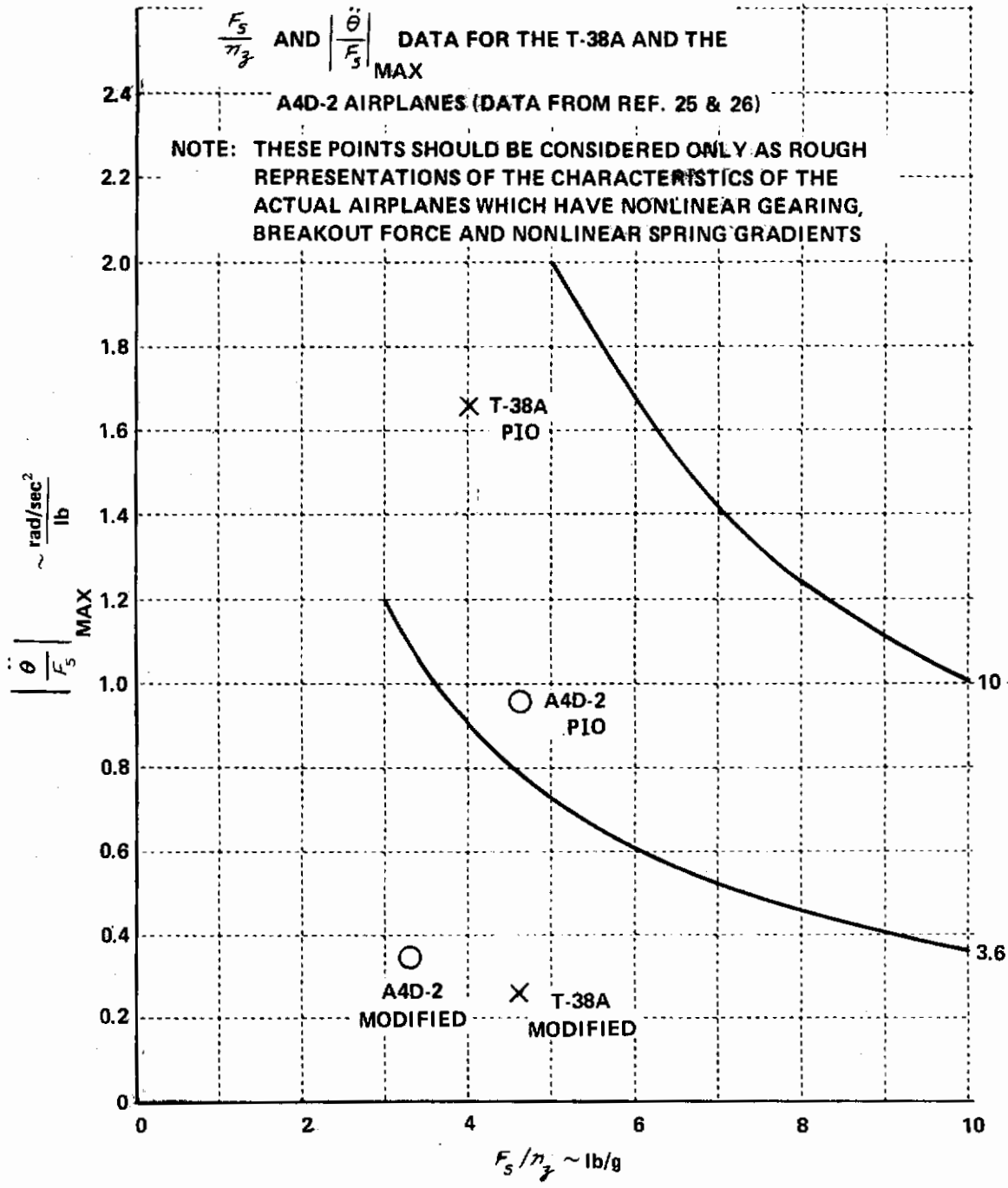

Figure 62 CONTROL SENSITIVITY DATA FOR A4D AND T-38 AIRPLANES

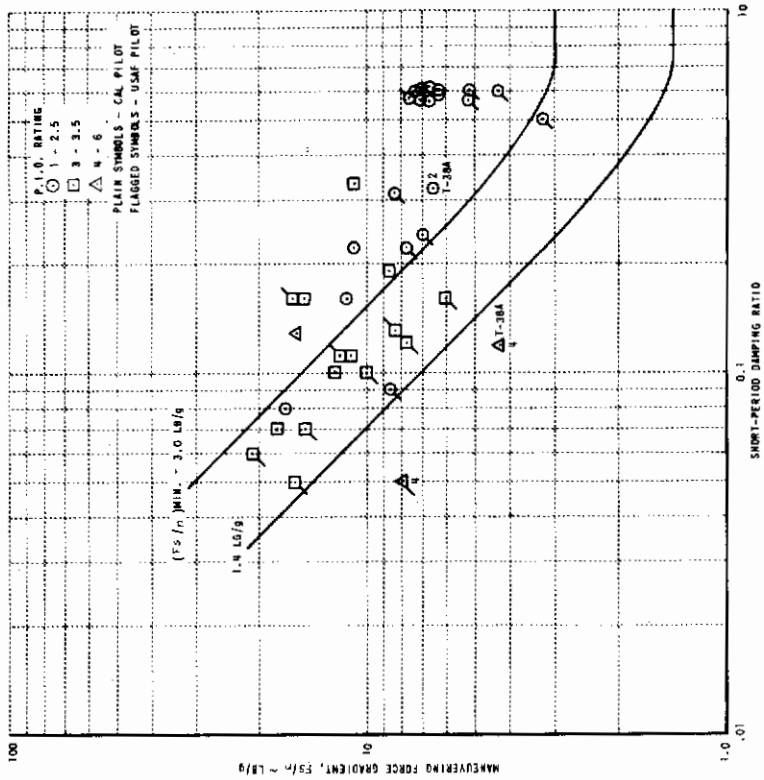

Figure 64 T-33 FLIGHT PROGRAM OF REFERENCE D3 (of Ref. 3)

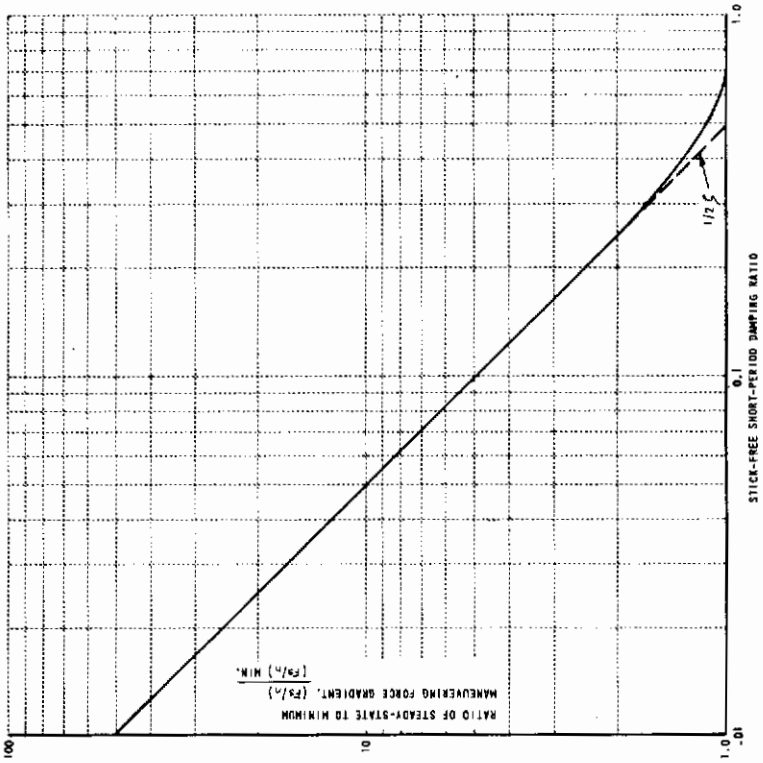

Figure 63 THE RATIO $(F_s/n)/(F_s/n)_{min}$ VS. ζ_{sp}

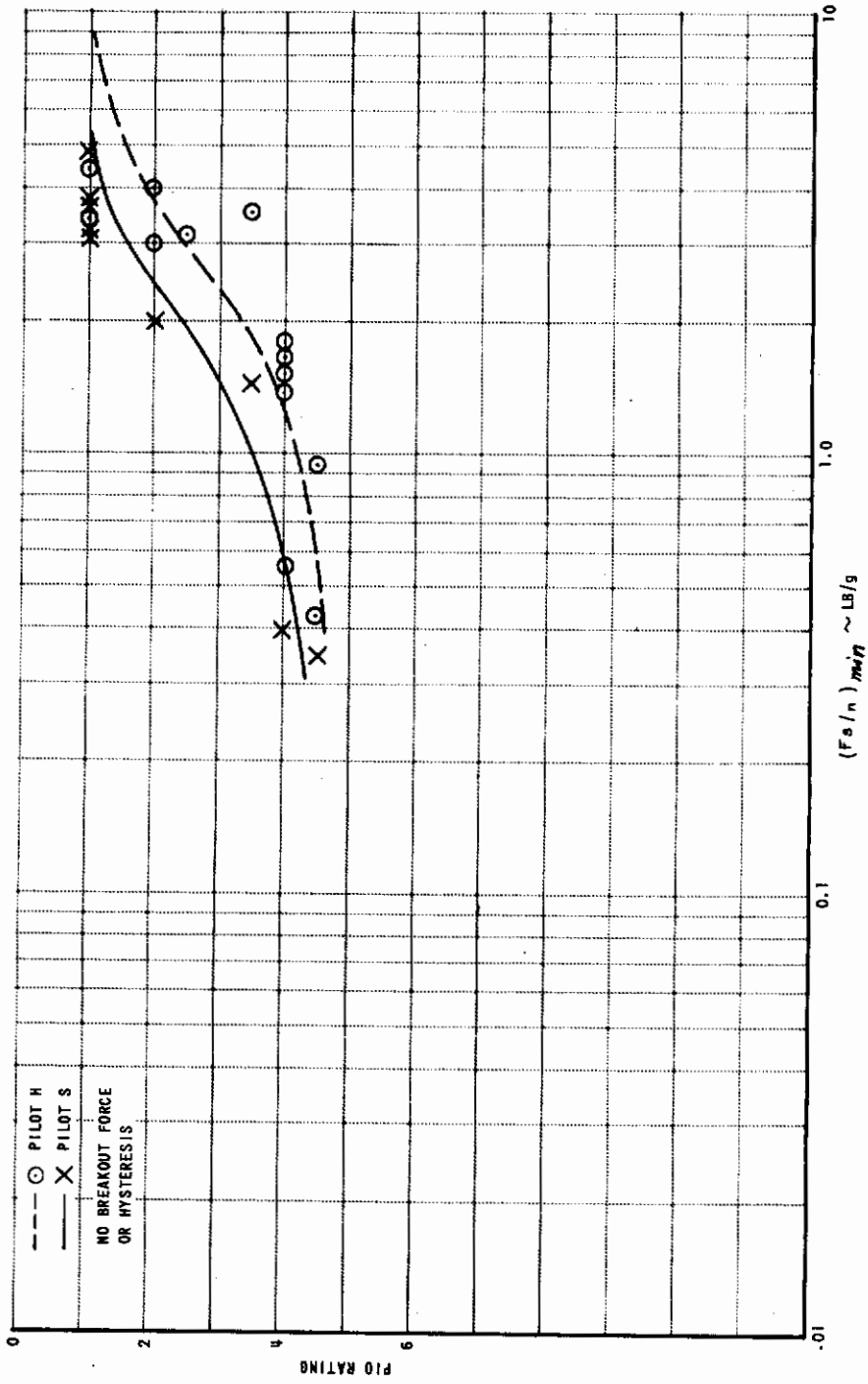

Figure 65 T-33 FLIGHT PROGRAM OF REFERENCE J60 (of Ref. 3)

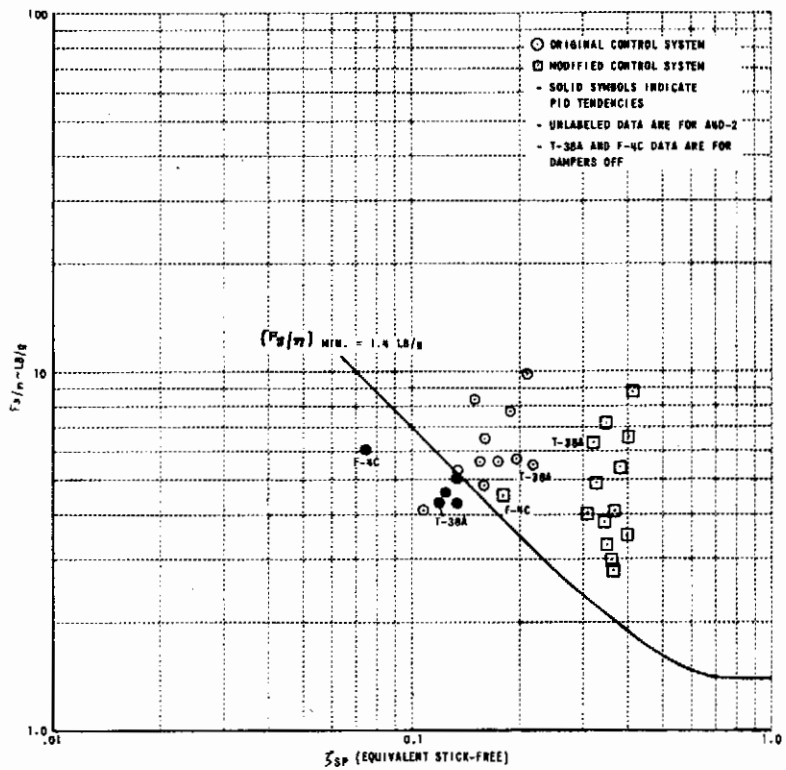

Figure 66
PIO CHARACTERISTICS OF A4D-2, T-38A, F-4C (REFERENCES H11, H5, P2 OF REFERENCE 3)

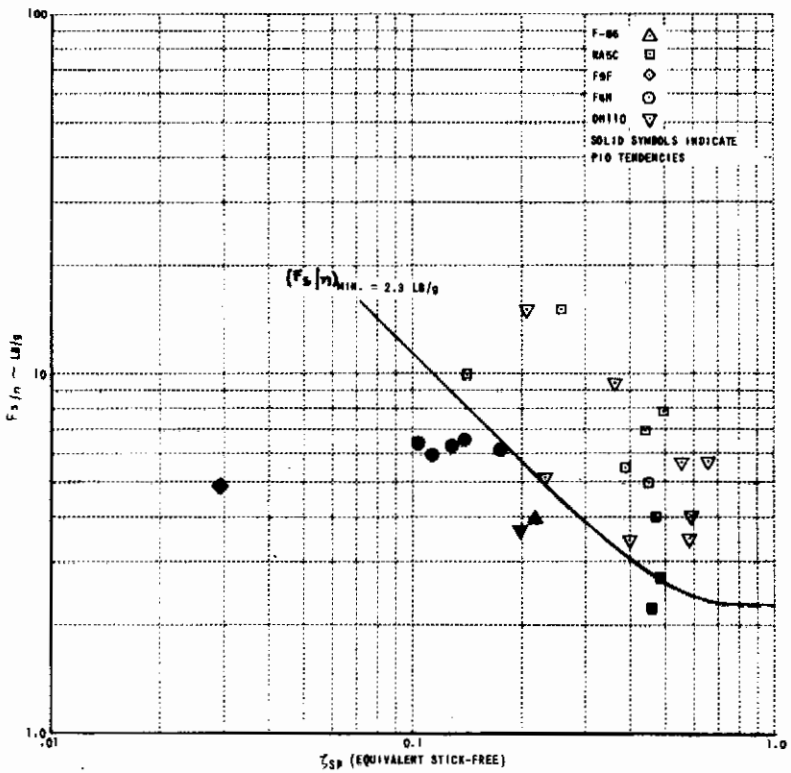

Figure 67
PIO CHARACTERISTICS OF AIRPLANES DESCRIBED IN REFERENCE H2 OF REFERENCE 3

Action Recommended for Subparagraphs to 3.2.3

3.2.3.1	Longitudinal Control in Unaccelerated Flight - No change
3.2.3.2	Longitudinal Control in Maneuvering Flight - No change
3.2.3.3	Longitudinal Control in Takeoff - Correction to BIUG
3.2.3.3.1	Longitudinal Control in Catapult Takeoff - No change
3.2.3.3.2	Longitudinal Control Force and Travel in Takeoff - No change
3.2.3.4	Longitudinal Control in Landing - No change
3.2.3.4.1	Longitudinal Control Forces in Landing - No change
3.2.3.5	Longitudinal Control Forces in Dives - Service Flight Envelope - No change
3.2.3.6	Longitudinal Control Forces in Dives - Permissible Flight Envelope - No Change
3.2.3.7	Longitudinal Control in Sideslips - No change

Proposed New Requirement

No change in the requirement is proposed.

Introduction and Motivation for Recommended Action

The equations and free-body diagram on page 168 in Reference 3 for this paragraph are in error. The summation of moments about the c.g. does not include the pitching moment resulting from thrust. Omission of this effect results in errors in nose wheel or tail wheel lift-off speed calculated.

Discussion and Substantiation

Revise equations and free-body diagram on page 168 of Reference 3 as indicated on the next page.

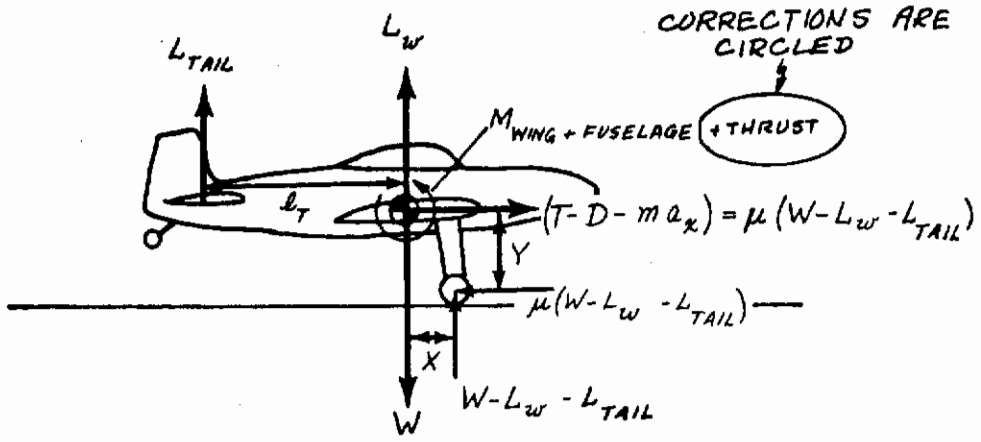

- From ΣM_{CG}, $$L_{TAIL} = \frac{M_{W+F} \oplus T + (X-\mu Y)(W-L_W)}{l_T + X - \mu Y}$$

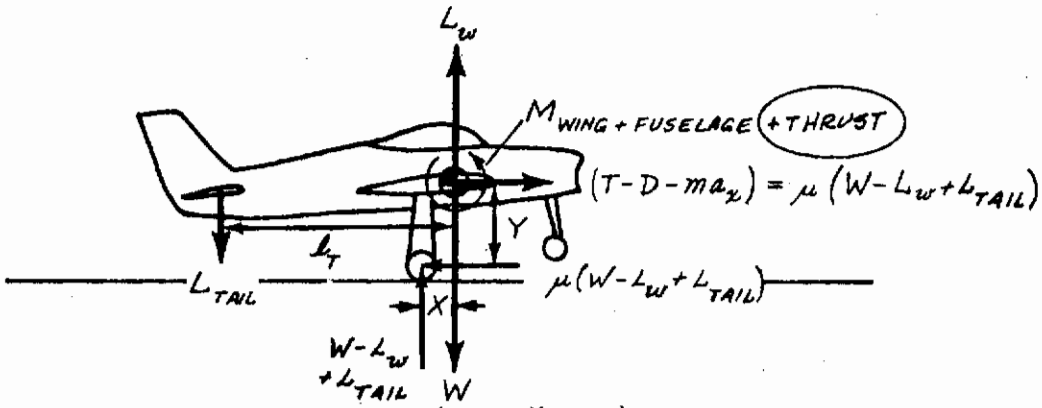

$$L_{TAIL} = \frac{-M_{W+F} \oplus T + (X+\mu Y)(W+L_W)}{l_t - X - \mu Y}$$

Alternate Proposal for Revision of 3.2.2, Longitudinal Maneuvering Characteristics

Action Recommended for Subparagraphs to 3.2.2

3.2.2 Longitudinal maneuvering characteristics

3.2.2.1 Short-period response - No change

3.2.2.1.1 Short-period frequency and acceleration sensitivity - Revise notation

3.2.2.1.2 Short-period damping - Revise notation

3.2.2.1.3, 3.2.2.2, 3.2.2.3 - Same action as primary proposal

Proposed New Requirements

3.2.2 Longitudinal maneuvering characteristics

3.2.2.1 Short-period response Same as MIL-F-8785B(ASG)

3.2.2.1.1 Short-period frequency and acceleration sensitivity. The equivalent short period undamped natural frequency, $[\omega_{n_{SP}}]_E$, shall be --- (Same Wording as MIL-F-8785B) --- lower bounds on $[\omega_{n_{SP}}]_E$ and n/α of figure 3 ----- (Note change $\omega_{n_{SP}}$ to $[\omega_{n_{SP}}]_E$ on figure 3)

3.2.2.1.2 Short-period damping. The equivalent short period damping ratio, $[\zeta_{SP}]_E$, shall be within the limits of table IV.

Table IV (no change)

3.2.2.1.3 Initial Time Delay. The equivalent time delay in the maneuvering response, a_E, shall not exceed the limits shown below.

	$a_E \sim$ SECONDS	
Level	Cat. A Flight Phases	Cat. B and C Flight Phases
1	0.12	0.30
2	0.25	0.48
3	0.33	0.59

3.2.2.2 Revise same as primary proposal

3.2.2.3 Revise same as primary proposal

3.2.2.4 Revise same as primary proposal

3.2.2.5 Revise same as primary proposal

3.2.2.6 Revise same as primary proposal

3.2.2.6.1 Revise same as primary proposal

3.2.2.6.2 Revise same as primary proposal

6.2.5 Longitudinal Parameters

$[\omega_{n_{sp}}]_E$, $[\zeta_{sp}]_E$ - The equivalent short-period natural frequency and damping ratio, when the airplane's response to elevator control-force inputs is matched with simple constant speed transfer functions, plus a time delay. For example, the angle of attack response would be matched with the following transfer function:

$$\frac{\alpha}{F_s} = \left[\frac{K e^{-a_E s}}{\frac{s^2}{(\omega_{n_{sp}})_E^2} + \frac{2(\zeta_{sp})_E}{(\omega_{n_{sp}})_E} s + 1} \right]$$

The matching process can be accomplished either by analog matching the time response to a step force input, or by curve-fitting the frequency response amplitude and phase. Units are rad/sec and nondimensional, respectively.

a_E - The equivalent time delay in the matching process used to obtain $(\omega_{n_{sp}})_E$ and $(\zeta_{sp})_E$, seconds. In the case of the time response to a non-ideal step, a_E shall be measured from the time that the force input has reached 50% of its total change.

Introduction and Motivation for Recommended Action Same as given in the Primary Proposal for Revision

Philosophy of the Requirements

These requirements are based primarily upon the ideas in Appendix II of Reference 8. In that study it was found that the effects of control-system dynamics and other "nonairplane-like" response characteristics could be at least crudely accounted for by matching the actual response to pilot inputs with a "normal" airplane constant-speed transfer function plus a pure time delay. The approach used in Reference 8 was to analog-match step responses of pitch rate with the following transfer function:

$$\frac{\ddot{\theta}}{F_s} = \left[\frac{K e^{-a_E s}(\tau_{\theta_2} s + 1)}{\frac{s^2}{(\omega_{n_{sp}})_E^2} + \frac{(2\zeta_{sp})_E}{(\omega_{n_{sp}})_E} s + 1} \right]$$

Obviously, this transfer function would be appropriate to match any "classical" airplane response if the numerator were modified. For example:

$$\frac{\alpha}{F_s} = \left[\frac{K e^{-a_E s}}{\frac{s^2}{(\omega_{n_{sp}})_E^2} + \frac{(2\zeta_{sp})_E}{(\omega_{n_{sp}})_E} s + 1} \right]$$

It is felt that the equivalent short-period parameters obtained by such a matching process can then be compared with the existing short-period requirements of MIL-F-8785B, provided that a separate limit is placed on a_E. This criterion shows promise, but it suffers from two major drawbacks:

- The matching process is not unique, whether matching time histories or frequency responses. This can lead to considerable uncertainty in the measured value of a_E.
- The matching process can totally break down for airplanes with very significant control system dynamics, e.g., the situation with low ζ_{sp} and a low-frequency first-order control system lag.

Substantiating Data

The data used to derive the requirements are the two T-33 experiments of References 8 and 16. In both cases, pilot rating was plotted versus a_E only for those configurations whose equivalent short-period characteristics fall within the present short-period requirements for Level 1.

Figure 68 shows the data from Appendix II of Reference 8. Those configurations having large amounts of control-system lead were not used because the matches achieved were somewhat questionable. Figure 69 presents the Category A data of Reference 16 (short-period configurations A and C were the only configurations having the short-period characteristics within the Level 1 limits of MIL-F-8785B). The faired curve on both figures is the final curve judged to be the best fit to both sets of data.

Figure 70 shows the Category C data of Reference 16. It should be noted that the evaluation procedure for these data included some Category A tasks as well as landing approaches. Thus, the values of a_E proposed for Category C may be somewhat too stringent.

The Category B requirements were arbitrarily set equal to the Category C values because of lack of data. This may be too stringent.

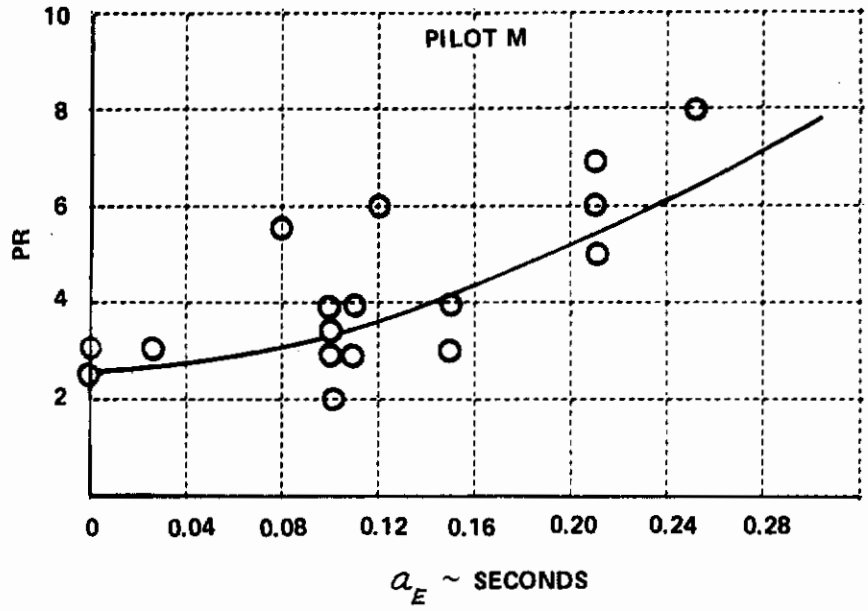

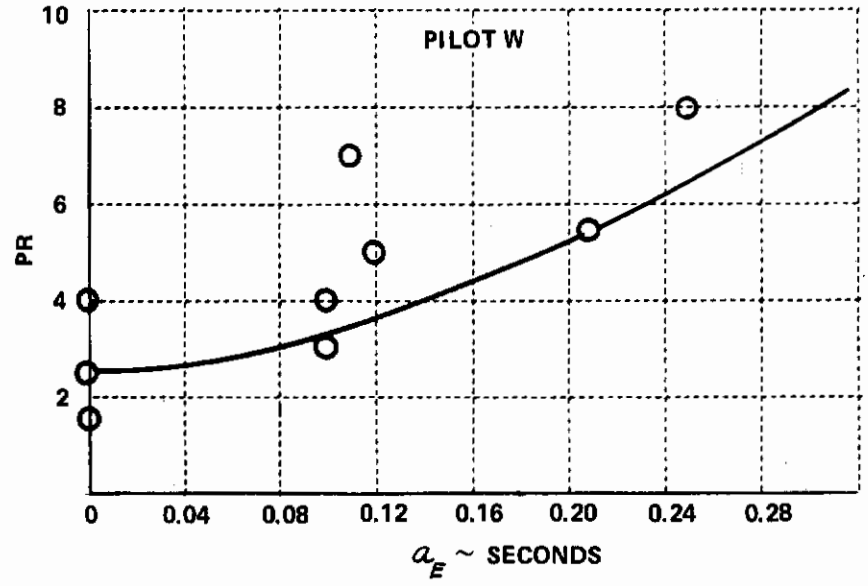

Figure 68 EQUIVALENT TIME DELAY - CATEGORY A DATA (REFERENCE 8)

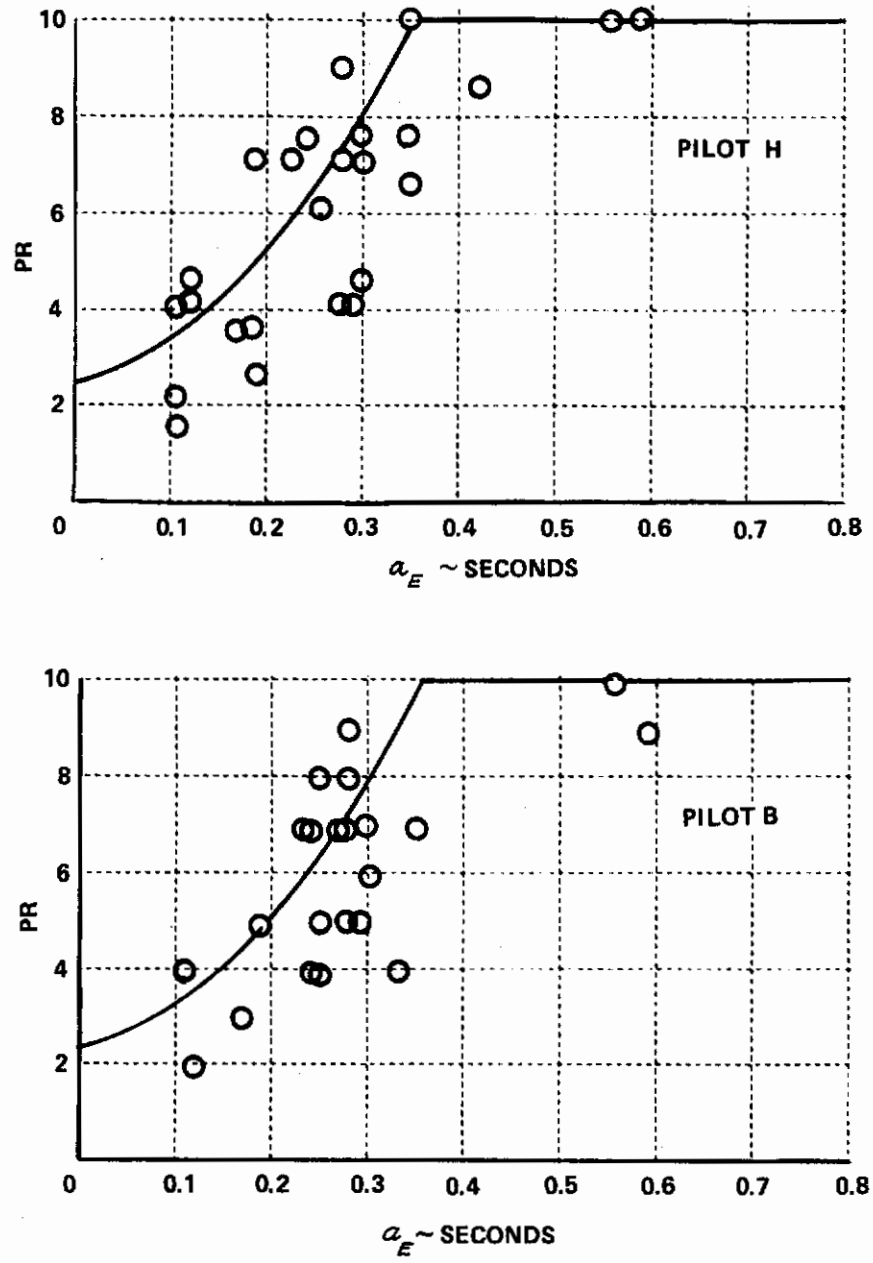

Figure 69 EQUIVALENT TIME DELAY - CATEGORY A DATA (REFERENCE 16)

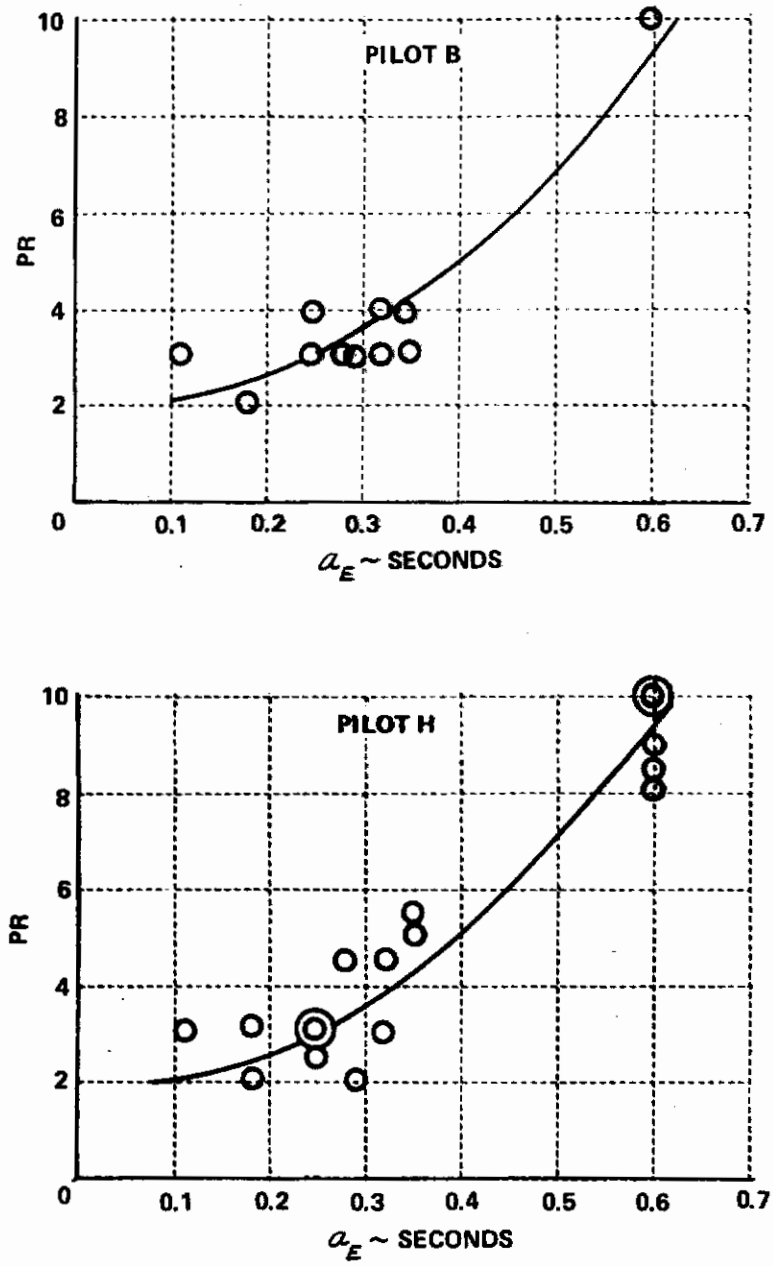

Figure 70 EQUIVALENT TIME DELAY - CATEGORY C DATA (REFERENCE 16)

SECTION III

PROPOSED REVISIONS TO 3.3, LATERAL-DIRECTIONAL FLYING QUALITIES

Action Recommended for Subparagraphs to Lateral-Directional Mode Characteristics 3.3.1

3.3.1.1	Lateral-directional oscillations (Dutch roll) - revise
3.3.1.2	Roll damping - revise
3.3.1.3	Spiral stability - revise
3.3.1.4	Coupled roll-spiral oscillation - revise

Proposed New Requirements

3.3 Lateral-directional flying qualities

3.3.1 Lateral-directional mode characteristics

3.3.1.1 Lateral-directional oscillations (Dutch roll). The frequency, ω_{n_d}, and damping ratio, ζ_d, of the lateral-directional oscillations following a rudder disturbance input shall exceed the minimums in table VI. The requirements shall be met with cockpit controls fixed and with them free, in oscillations of any magnitude that might be experienced in operational use. If the oscillation is nonlinear with amplitude, the requirement shall apply to each cycle of the oscillation. Residual oscillations may be tolerated only if the amplitude is sufficiently small that the motions are not objectionable and do not impair mission performance. For Category A Flight Phases, angular deviations shall be less than ±3 mils. With the control surfaces fixed, the airplane shall always be directionally stable.

TABLE VI. Minimum Dutch Roll Frequency and Damping

Level	Flight Phase Category	Class	Min ζ_d *	Min $\zeta_d \omega_{n_d}$ *, rad/sec.	Min ω_{n_d}, rad/sec.
1	A	I, IV	0.19	0.35	1.0
		II, III	0.19	0.35	(0.5)
	B	All	0.08	0.15	(0.5)
	C	I, II-C, IV	0.08	0.15	1.0
		II-L, III	0.08	(0.10)	(0.5)
2	All	All	0.02	0.05	(0.5)
3	All	All	(0)		(0.4)

*The governing damping requirement is that yielding the larger value of ζ_d.
( ) indicates changes recommended.

3.3.1.2 Roll mode. The roll-mode time constant, τ_R, exhibited by the airplane in response to pilot commands shall be no greater than the appropriate value in table VII.

TABLE VII. Maximum Roll-Mode Time Constant

Flight Phase Category	Class	Level		
		1	2	3
A	I, IV	1.0	1.4	
	II, III	1.4	3.0	
B	ALL	1.4	3.0	10
C	I, II-C, IV	1.0	1.4	
	II-L, III	1.4	3.0	

3.3.1.3 Spiral stability. The combined effects of spiral stability, flight-control-system characteristics, and rolling moment change with speed shall be such that following a disturbance in bank of up to 20 degrees, the time for the bank angle to double will be greater than the values in table VIII. This requirement shall be met with the airplane trimmed for wings-level, zero-yaw-rate flight with the cockpit controls free.

TABLE VIII. Spiral Stability - Minimum Time to Double Amplitude

Flight Phase Category	Level 1	Level 2	Level 3
A & C	12 sec	8 sec	4 sec
B	20 sec	8 sec	4 sec

3.3.1.4 Coupled roll-spiral oscillation. A coupled roll-spiral mode will not be permitted for Category A Flight Phases. A coupled roll-spiral mode will be permitted for Category B and C Flight Phases provided the frequency and damping ratio exceed the following requirements:

Flight Phase Category	Level	$\omega_{n_{RS}}$	ζ_{RS}
B & C	1	0.4 rad/sec	0.35
	2 & 3	0.3	0.20

Motivation and Background for Action Recommended for 3.3.1

MIL-F-8785B(ASG) has been criticized as being inadequate in its treatment of flying qualities in turbulence. Thus as a first step toward responding to this criticism it is recommended that paragraph 3.3.2.1, Lateral-directional response to atmospheric disturbances, be expanded to contain lateral-directional dynamic requirements specifically directed at ensuring good flying qualities

in turbulence. It is recommended that the additional damping requirement be moved from 3.3.1.1 to 3.3.2.1 where it more properly belongs.

Other changes recommended for the subparagraphs to 3.3.1 are of the nature of refining the numbers in the requirements based on additional data and re-examination of the data in the BIUG.

The prohibition of coupled roll-spiral mode has been re-examined and modified to permit certain types of coupled modes. The original requirement was based on experience with lifting body research vehicles, Reference 29, and ground simulator data in Reference 30. In many of these examples, the coupled roll spiral was the result of low roll damping, high dihedral effect and high yaw due to roll rate. These vehicles exhibited very low frequency coupled roll-spiral roots and truly have undesirable flying qualities. In several examples, higher frequency coupled roll-spiral roots resulting from roll and yaw rate feedback to the aileron and rudder have exhibited acceptable flying qualities.

Coupled roll-spiral roots can also result from introducing roll attitude stabilization. In this case it should be possible to have adequate or desirable flying qualities for Flight Phases classed in Categories B and C and for some Category A Flight Phases. Thus it is proposed that the absolute prohibition of a coupled roll-spiral mode be revised.

Discussion and Substantiation for Lateral-Directional Mode Characteristics 3.3.1

A. Lateral-directional oscillations (Dutch roll) 3.3.1.1

Three proposed changes to the Dutch roll frequency and damping requirement of MIL-F-8785B(ASG) are recommended. It is recommended that:

1. The minimum Level 1 $\zeta_d \omega_{n_d}$ requirement for Class II-L and Class III airplanes, Category C Flight Phases be reduced from 0.15 to 0.10 rad/sec. The Level 3 requirement be reduced from ζ_d = .02 to ζ_d = 0.

2. The minimum ω_{n_d} value for Levels 1 and 2 be increased from 0.4 to 0.5 rad/sec and the footnote permitting exception to this requirement eliminated.

3. The additional damping requirement be removed from 3.3.1.1 and reintroduced in paragraph 3.3.2.1.1 which addresses response to atmospheric disturbances.

The minimum Dutch roll damping ratio and frequency boundaries in MIL-F-8785B(ASG) were not well substantiated in Reference 3 for frequencies below ω_{n_d} = 1.0 rad/sec. Since publication of Reference 3, the experiment of Reference 31 has been performed. Data from this experiment indicated that

when aileron excitation of the Dutch roll mode was small, then configurations with ω_{n_d} = 1.0 rad/sec and ζ_d = .1 or $\zeta_d \omega_{n_d}$ = 0.10 were satisfactory for the Landing Approach Flight Phase. The new data tabulated in Figure 71 show that 23 evaluations all resulted in pilot ratings of 3.5 or better for this Dutch roll value. Also shown in Figure 71 are data from Reference 32 for ω_{n_d} = .8 and ζ_d = .1. These are configurations 207 and 209 of that reference. Configuration 207 had L'_β = 0, was evaluated 6 times, and received an average rating of 5.5. Configuration 209 had L'_β = -16, was evaluated 13 times, and received an average rating of 4.5. These new data are considered sufficient justification for reducing the minimum $\zeta_d \omega_{n_d}$ limit for Class II-L and III from 0.15 to 0.10 sec^{-1}.

The requirement for positive damping for Level 3 seems unsupported by any of the available data. In fact, slightly negative or zero ζ_d seems consistent with a large body of data for pilot ratings in the neighborhood of 6.5 to 7. Furthermore, for some designs this requirement, especially if applied to high-altitude flight, could lead to unnecessary configuration compromises or to fail-operational yaw dampers where neither is required. Thus it is recommended that the Level 3 value of ζ_d be reduced from ζ_d = .02 to ζ_d = 0.

The proposal to increase the minimum ω_{n_d} boundary from ω_{n_d} = 0.4 to 0.5 rad/sec for Level 1 and Level 2 is based on data reported in References 33 and 34 together with an increasing conviction by the author that directional stability is a highly desirable characteristic and should be encouraged by the specification. The elimination of the footnote pertaining to exception from the minimum ω_{n_d} requirement is to lend emphasis to this point of view.

The purpose of the recommendation to remove the additional damping requirement from paragraph 3.3.1.1 and to put it in paragraph 3.3.2.1 is to call attention to the fact that the requirement is primarily intended to ensure good flying qualities in turbulence. This requirement is treated further in the discussion for paragraph 3.3.2.1.

B. Roll mode

The wording has been changed to include the phrase "exhibited by the airplane in response to pilot commands." This was done to permit differentiation between response to pilot commands and response to external disturbances. The former is specified by this requirement, 3.3.1.2, and the latter is specified by the new requirement in paragraph 3.3.2.1.2. The wording in these two requirements is intended to permit designs using both feedback and feedforward techniques to reduce response to external disturbances without sacrificing response to pilot commands.

C. Spiral mode

The requirements on time to double amplitude of the spiral mode have been simplified by removing the breakdown by airplane Class, Flight Phase Category C has been grouped with Category A rather than B and the Level 2 limit has been reduced from 12 sec to 8 sec. Eliminating the breakdown by Class is a simplification that is more consistent with the available data.

Grouping Category C Flight Phases with Category A Flight Phases is based on the consideration that during Category A and C Flight Phases the pilot is in more continuous control of the airplane than in Category B Flight Phase and is therefore less concerned about long-term attitude characteristics. This point was demonstrated in the TIFS Phase I landing approach experiments reported in Reference 35. Spiral roots with time to double of 9.6 sec were hardly noticed and a case with time to double of 6.4 sec, although noted, was not considered reason for downgrading the evaluation. Based on these data together with the extensive data in Reference 36 and re-examination of the data in Reference 33, it is recommended that the Level 2 limit on T_2 be reduced from 12 sec to 8 sec. Even this limit is a conservative interpretation of the data in Reference 36 which could be used to support a value of T_2 = 6 sec for Level 2. The gradient of pilot rating with time to double is steep, however, and a conservative interpretation is believed justified.

Data in Reference 37 for unstable real roots resulting from reduced directional stability also indicate T_2 = 6 sec as a reasonable limit for cruise flight. A limit of 2.7 sec for landing approach is also indicated in this report but this value is regarded as too fast and inconsistent with other data to be accepted. The data in this report does lend support for the decision to group Category C with Category A rather than Category B.

D. Coupled Roll-Spiral Oscillation, 3.3.1.4

The coupled roll-spiral requirement of MIL-F-8785B(ASG) was based primarily on the data in References 30 and 31 and the analysis of Reference 38. Reference 39 documents additional experience with the M-2 lifting body research vehicle and Reference 40 reports the results of a ground simulator study of the effects of a coupled roll-spiral oscillatory mode on flying qualities for the Cruise and Landing Approach Flight Phases. Also, there are a few points in Reference 29 that were evaluated in the T-33 variable stability airplane used as a ground-based simulator. These points were set up to represent the augmented M2-F2 vehicle before it was flight tested.

The above referenced data have been plotted on Figure 72 (Figure 1 (3.3.1.4) from the BIUG). Examination of these data together with the comments available in the various reports indicates that a coupled roll-spiral oscillatory mode can be acceptable provided the frequency and damping are above certain minimums. The less than satisfactory ratings obtained for coupled roots in this best area are due primarily to pilot objections to "spiral stability" and lack of roll control effectiveness and high steady forces in turning flight. This is particularly true of the data in Reference 40. In this experiment the roll control gearing and feel system characteristics were set to be compatible with the base configuration for each Flight Phase and were not varied during the experiment as the roll spiral was changed. This constraint is probably the cause of complaints about lack of roll control effectiveness.

The data from Reference 39 do not have pilot ratings associated with each point but the report indicates that control problems were encountered when the angle of attack was near zero or negative for the augmented M2-F2 and that the M2-F3 exhibited improved flying qualities but also had a similar trend for deterioration for negative angles of attack. Data are also shown for the M2-F2 with the SAS turned OFF. This data correlates fairly well with the proposed boundaries considering the fact that the Dutch roll mode is also affected by the angle of attack change.

It should be noted that the coupled roll-spiral cases studied in all of the above experiments were the result of combinations of normal stability derivatives that have taken on rather unusual values. In general the coupled roll spiral results from fairly large L'_β, large N'_p/L'_p, and large N'_r. If L'_p is low, the coupled roll spiral will be low frequency and the airplane is likely to be difficult to control.

It is possible to have a coupled roll-spiral mode as a result of introducing roll attitude stabilization. In this case the roll damping need not be low and L'_β need not be large for the mode to exist, thus the flying qualities may be quite satisfactory for Flight Phases that do not require rapid maneuvering. This should be especially true if proper attention is given to feel system gradients and roll control gain so that they are compatible with the attitude command response that results.

Action Recommended for Subparagraphs to Lateral-Directional Dynamic Response Characteristics, 3.3.2

3.3.2	Lateral-directional dynamic response characteristics - change to the new paragraph numbers in text
3.3.2.1	Lateral-directional response to atmospheric disturbances - delete
3.3.2.2	Roll rate oscillations - delete
3.3.2.2.1	Additional roll rate requirements for small inputs - delete
3.3.2.3	Bank angle oscillations - delete
3.3.2.4	Sideslip excursions - delete
3.3.2.4.1	Additional sideslip requirement for small inputs - delete
3.3.2.5	Control of sideslip in rolls - renumber (3.3.2.4)
3.3.2.6	Turn coordination - revise

Proposed New Requirements

3.3.2 Lateral-directional dynamic response characteristics. Lateral-directional dynamic response characteristics are stated in terms of response to atmospheric disturbances and in terms of allowable roll rate and bank oscillations, sideslip excursions, aileron stick or wheel forces, and rudder pedal forces that occur during specified rolling and turning maneuvers. The requirements of 3.3.2.2, 3.3.2.3, and 3.3.2.4 apply for both right and left aileron commands of all magnitudes up to the magnitude required to meet the roll performance requirements of 3.3.4 and 3.3.4.1.

3.3.2.1 Lateral-directional response to atmospheric disturbances. The combined effect of the airplane modal parameters (ω_{n_d}, ζ_d, τ_R, $|\phi/\beta|$, etc.), gust sensitivity, control authority, and flight control system characteristics shall be such that the airplane will have acceptable response and controllability characteristics in atmospheric disturbances. In particular, the roll acceleration, rate and displacement responses to side gusts and cross winds shall be investigated for airplanes with large rolling acceleration due to side velocity.

3.3.2.1.1 Additional damping requirement for lateral-directional oscillatory mode. The minimum damping of the lateral-directional oscillatory mode shall exceed both the values of 3.3.1.1, table VI, and the values resulting from the following equations.

Level

1 $\zeta_d \omega_{n_d} \geq 11.1 \left[\frac{\omega_{n_d}^2}{V_T} \left|\frac{\phi}{\beta}\right|_d\right] - 0.15$

2 $\zeta_d \omega_{n_d} \geq 5.15 \left[\frac{\omega_{n_d}^2}{V_T} \left|\frac{\phi}{\beta}\right|_d\right] - 0.15$

3 $\zeta_d \omega_{n_d} \geq 3.10 \left[\frac{\omega_{n_d}^2}{V_T} \left|\frac{\phi}{\beta}\right|_d\right] - 0.15$

where

ω_{n_d} ~ rad/sec

V_T ~ ft/sec true

The governing damping requirement is that yielding the larger value of ζ_d except that ζ_d need not exceed 0.7.

3.3.2.1.2 Roll mode time constant for external disturbances. The roll mode time constant, τ_{R_E}, exhibited by the airplane in response to a step rolling acceleration about the x stability axis shall be less than the value resulting from the following equations.

Level

1 $\tau_{R_E} \leq 1.90\, e^{-\frac{135}{V_T \omega_{n_d}} \left|\frac{\phi}{\beta}\right|_d}$

2 $\tau_{R_E} \leq 3.90\, e^{-\frac{88}{V_T \omega_{n_d}} \left|\frac{\phi}{\beta}\right|_d}$

3 $\tau_{R_E} \leq 7.50\, e^{-\frac{45}{V_T \omega_{n_d}} \left|\frac{\phi}{\beta}\right|_d}$

3.3.2.2 Bank angle oscillations. The value of the parameter $\hat{\phi}_{osc}/\hat{\phi}_1$ following a rudder-pedals-free impulse aileron control command shall be within the limits in figure 4 for Levels 1 and 2. The impulse shall be as abrupt as practical within the strength limits of the pilot and the rate limits of the aileron control system. For all Levels, the change in bank angle shall always be in the direction of the aileron control command.

3.3.2.2.1 Additional roll rate requirement for small step inputs. The value of the parameter $\hat{p}_{osc}/\hat{p}_1$ following a rudder-pedals-fixed step aileron command shall be within the limits shown on figure 4 for Levels 1 and 2. This requirement applies for step aileron control commands up to the magnitude which causes a 60 degree bank angle change in 1.7 τ_d seconds. For all Levels, the change in bank angle shall always be in the direction of the aileron control command.

3.3.2.3 Sideslip excursions. Following a rudder-pedals-fixed step aileron control command, the sideslip increment, $\Delta\beta$, shall be less than the values specified herein. The aileron command shall be held fixed until the bank angle has changed at least 90 degrees.

Level	Flight Phase Category	
1	A	6 degrees
	B&C	10 degrees
2	All	15 degrees

3.3.2.3.1 Additional sideslip requirement. The amount of [sideslip] (rate of change of sideslip) following a rudder-pedals[-free] (-fixed) [impulse] (step) aileron control command shall be within the limits shown on figure 5 for Levels 1 and 2. The impulse shall be as abrupt as practical within the strength limits of the pilot and the rate limits of the aileron control system. The requirement shall apply for step aileron control commands up to the magnitude which causes a 60-degree bank angle change within τ_d seconds.

3.3.2.4 Control of sideslip in rolls. In the rolling maneuvers described in 3.3.4, but with the rudder pedals used for coordination for all Classes, directional-control effectiveness shall be adequate to maintain zero sideslip with a rudder pedal force not greater than 50 pounds for Class IV airplanes in Flight Phase Category A, Level 1, and 100 pounds for all other combinations of Class, Flight Phase Category and Level.

3.3.2.5 Turn coordination. With the airplane trimmed for wings-level straight flight, it shall be possible to maintain steady coordinated turns in either direction, using 60 degrees of bank for Class IV airplanes, 45 degrees of bank for Class I and II airplanes, and 30 degrees of bank for Class III airplanes, with a rudder pedal force not exceeding 40 pounds and with an aileron stick force not exceeding 4 pounds or an aileron wheel force not exceeding 6 pounds. These requirements constitute Levels 1 and 2.

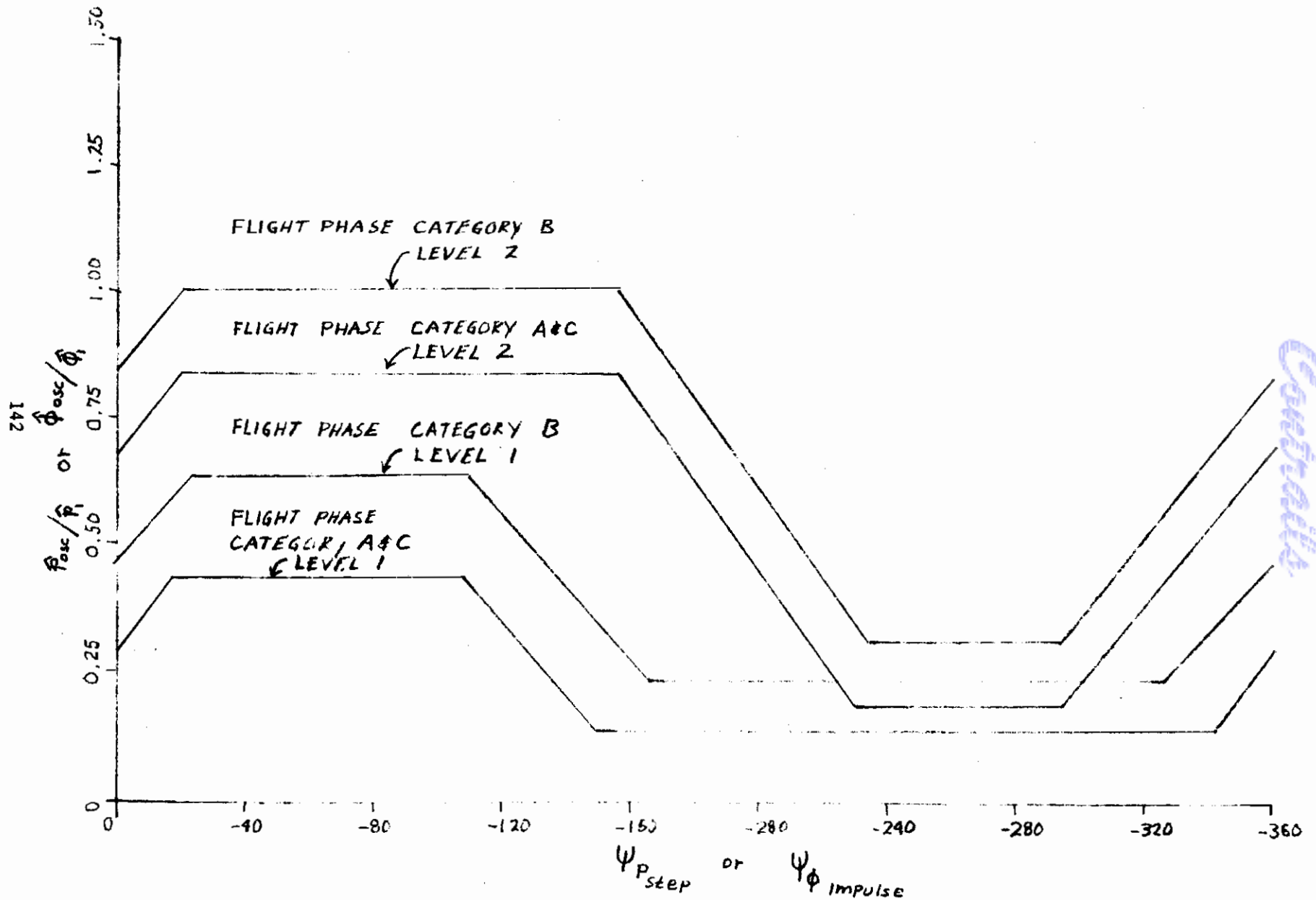

FIGURE 4 ROLL RATE AND BANK ANGLE OSCILLATION LIMITATIONS

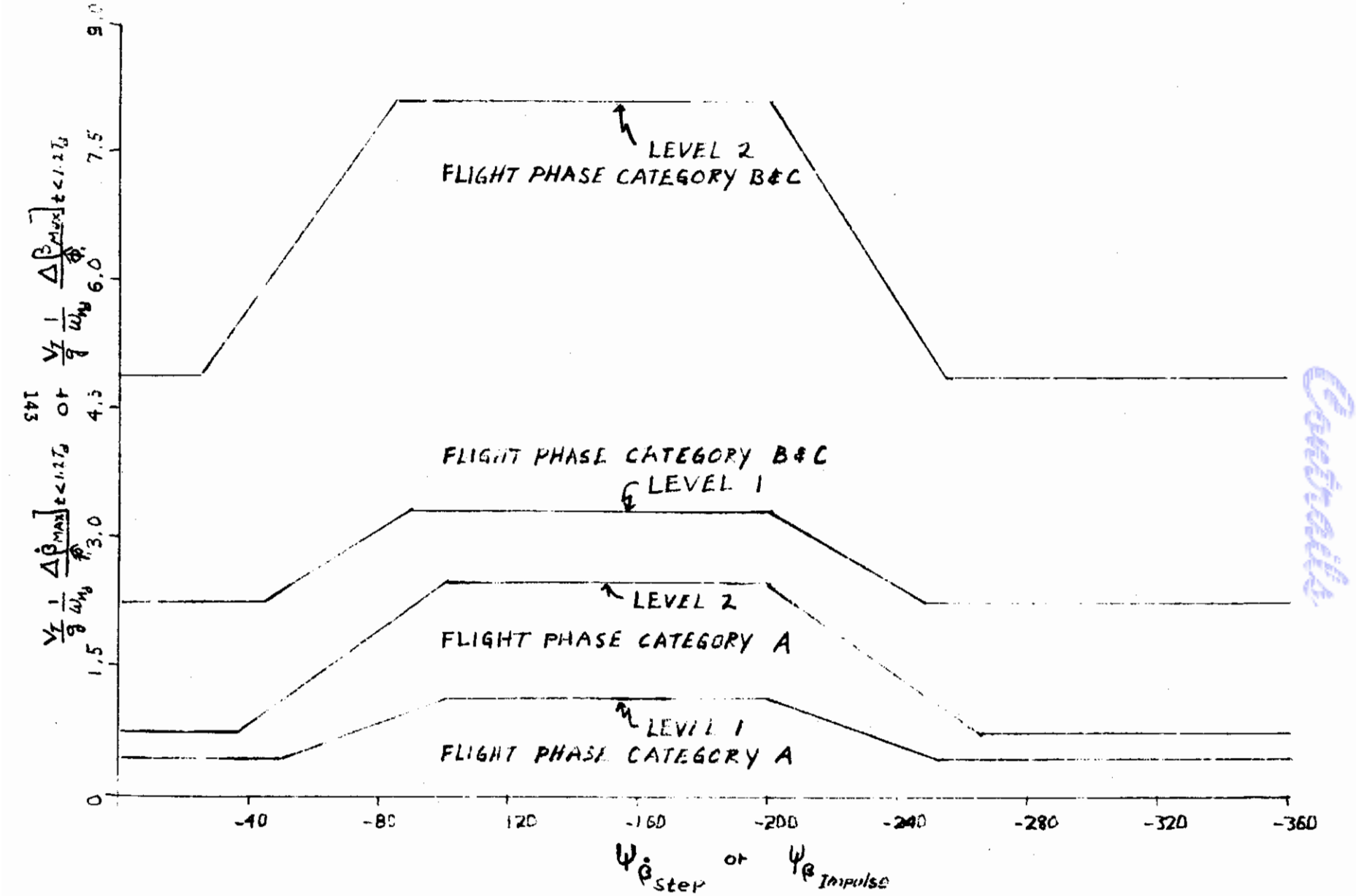

FIGURE 5 SIDESLIP EXCURSION LIMITATIONS

Motivation and Background for Action Recommended as 3.3.2, 3.3.2.1, 3.3.2.1.1 and 3.3.2.1.2

That MIL-F-8785B(ASG) is inadequate in its treatment of flying qualities in turbulence is well recognized.

To understand the complexity of the gust and turbulence response problem, it is beneficial to examine the analysis given in Reference 29. Although this was a study of causes underlying the severe response to gusts of certain re-entry configurations, the results are of general applicability. From this study (presented in a slightly modified form in Appendix VA of Reference 3), it can be seen that parameters such as Dutch roll natural frequency, roll damping, and the stability derivative L_β, as well as Dutch roll damping ratio, all contribute significantly to the roll response due to side gusts. Pilots tend to downrate otherwise acceptable configurations with high $|\phi/\beta|_d$ because of sensitivity to turbulence. ($|\phi/\beta|_d$ is discussed in detail in Appendix VC of Reference 3.)

This, however, does not tell the whole story. The ability of a pilot to control an aircraft in the presence of atmospheric disturbances depends not only on the response of the aircraft to atmospheric disturbances, but also on the closed-loop controllability characteristics of the pilot/aircraft combination. Since the latter is influenced by factors such as roll-sideslip coupling characteristics, the overall problem of controllability in the presence of atmospheric disturbances is extremely complex. For this reason, the qualitative requirement of 3.3.2.1 must be given serious attention.

There is considerable evidence in the literature that the lateral-directional flying qualities of airplanes which have large roll acceleration response to side gusts can be significantly improved by increases in roll damping and Dutch roll oscillatory damping.

In MIL-F-8785B(ASG), an increment in Dutch roll damping, $\zeta_d \omega_{n_d}$ is specified when $\omega_{n_d}^2 |\phi/\beta|_d$ exceeds $20/sec^2$. This requirement was suggested in Reference 41 based on the analysis in Reference 42 of the data contained in Reference 43. This data has been re-examined and a new requirement has been formulated which is similar in form to the additional damping requirement of 3.3.1.1 of MIL-F-8785B(ASG). The new requirement, however, interprets the data of Reference 43 in terms of a different parameter, $\frac{\omega_{n_d}^2}{V_T} |\frac{\phi}{\beta}|_d$, which is thought to be more directly related to the airplane's response to turbulence, i.e., the turbulence environment is better expressed in terms of velocity components rather than in terms of the gust induced sideslip angle. The latter is related to the turbulence velocity components by the aircraft velocity. The new requirement is applied separately from the basic Dutch roll damping requirement of 3.3.1.1 rather than as an increment to be added to the requirement of 3.3.1.1. The details of the new requirement are discussed with the substantiation data in a following section.

After examination of data in References 29, 30, 32, 36 and 44, it was concluded that a requirement relating roll damping to a measure of the roll response to lateral gusts was justified. Figures 73 through 78 illustrate the strong interacting effect on pilot rating of dihedral, roll damping and roll control authority for flight in turbulence.

Figure 73 (from Reference 32) shows the degradation in pilot rating resulting from large values of L_β and reduced roll damping or large values of τ_R . The degradation noted was the result of increased difficulty of control in turbulence.

Figure 74 (from Reference 44) shows the effect of roll damping on pilot rating and roll control authority for various levels of turbulence for an airplane with $L_\beta = -6.4$. Data are also presented in Reference 44 for other values of L_β and airplane dynamics.

Figures 75, 76, and 77 (from Reference 36) show the degradation in pilot rating resulting from an increase in $|\phi/\beta|_d$ and a decrease in roll damping. Figure 78 (from Reference 30) shows a general degradation in pilot rating for high $|\phi/\beta|_d$ configurations and a more rapid degradation with reduced roll damping than was found by other experimenters for lower values of $|\phi/\beta|_d$.

The need for a requirement relating minimum roll damping to a measure of the roll response to lateral gusts is established by these data. The development of quantitative requirements is discussed in the following sections.

Discussion and Substantiation for 3.3.2, 3.3.2.1, 3.3.2.1.1 and 3.3.2.1.2

A. Lateral-directional dynamic response characteristics, 3.3.2

This paragraph is introductory to the subparagraphs that follow. The only changes made were to correct the paragraph references to reflect changes made in the subparagraphs that follow.

B. Lateral-directional response to atmospheric disturbances, 3.3.2.1

This paragraph is a qualitative requirement for the designer to give serious consideration to the flying qualities of the pilot-airplane combination. The paragraph was reworded to include mention of control authority and to reflect the quantitative requirements that have been added.

C. Additional damping requirement for lateral-directional oscillatory mode, 3.3.2.1.1

The purpose of this paragraph is essentially the same as the additional damping part of 3.3.1.1 of MIL-F-8785B(ASG); however, the statement of the requirement and the parameters in the equations have been changed. In addition, a maximum value of $\zeta_d = 0.7$ which need not be exceeded has been stated.

The additional damping requirement of 3.3.1.1 of MIL-F-8785B(ASG) was based on the data of Reference 43 as interpreted by the author of Reference 42. These two reports have been reviewed in detail along with Reference 37 to formulate the proposed new requirement recommended in paragraph 3.3.2.1.1.

The requirement in 3.3.1.1 of MIL-F-8785B(ASG) specifies that an increment in $\zeta_d \omega_{n_d}$ be added to the basic $\zeta_d \omega_{n_d}$ required by the paragraph for the particular Class, Flight Phase and Level. The increment to be added is calculated from equations involving the parameter $\omega_{n_d}^2 \left|\frac{\phi}{\beta}\right|_d$. The equations in MIL-F-8785B(ASG) are derived from the general curve fitted rating equation developed in Reference 43. The equations used in the requirement in 3.3.1.1 of MIL-F-8785B(ASG) are modified in that only the slope of $\zeta_d \omega_{n_d}$ with $\omega_{n_d}^2 \left|\frac{\phi}{\beta}\right|_d$ required to maintain a constant rating is used. The intercepts of the straight lines were arbitrarily changed from the actual curve fit developed in Reference 43 and defined to be $\omega_{n_d}^2 \left|\frac{\phi}{\beta}\right|_d = 20$. The validity of this interpretation of the data is questioned and therefore it has not been used in the new requirement in paragraph 3.3.2.1.1. In the new requirement, it is assumed that the basic damping requirements in 3.3.1.1 are adequate for airplanes performing tasks appropriate to the Class, Flight Phase and Level specified. It is further assumed that these values of Dutch roll damping are adequate for flight in turbulence unless the airplane has particular sensitivity to turbulence. In the latter case the damping required by 3.3.2.1.1 may exceed that required by the basic requirement of 3.3.1.1 and in this situation the designer must design to 3.3.2.1.1 rather

than 3.3.1.1. It is also recognized that a point of diminishing returns is reached where further increases in Dutch roll damping will do little to improve the flying qualities. Thus a maximum value of the minimum Dutch roll damping is established as $\zeta_d = 0.7$.

Examination of Reference 43 indicates that the author tried several correlating parameters before settling on $\zeta_d \omega_{n_d}$ vs. $\omega_{n_d}^2 \left|\frac{\phi}{\beta}\right|_d$. It is also evident that a contest of sorts was being held at that time regarding the validity of the parameter, $\left|\phi/v_e\right|_d$, proposed in Reference 37. Although it now seems evident that the major cause of degradation in the rating data in Reference 10 can be accounted for by ϕ_{osc}/ϕ_{AV} type requirements for the response to aileron commands, there is no doubt that as the dihedral effect and $\left|\phi/\beta\right|_d$ increase, the flying qualities in turbulence can be degraded.

The idea expressed in both References 37 and 43 of requiring increased Dutch roll damping as a function of the airplane's sensitivity to turbulence is considered valid and is implemented in the requirement of 3.3.2.1.1. In developing this requirement it was reasoned that the requirement should be referenced to gust velocity rather than gust induced sideslip, i.e., L'_v rather than L'_β, or $\left|\phi/v\right|_d$ rather than $\left|\phi/\beta\right|_d$, should be tried as the correlating parameter. The reasons expressed in Reference 37 for using equivalent airspeed rather than true airspeed in the parameter ϕ/v_{e_d} were also reviewed. The following quotation from Reference 37 gives the background for the choice of $\left|\phi/v_e\right|_d$ used in that report.

> "A plot of $1/C_{1/2}$ against $|\phi|/|\beta|$ (one of the possible criteria suggested in Reference 3) was found to give good results for a given flight condition (landing approach or cruising), but the results for the two flight conditions were not in agreement. When $|\phi|/|\beta|$ was converted to $|\phi|/|v|\left(v = \frac{\beta V}{57.3}\right)$ and plotted against $1/C_{1/2}$, the results of separating tolerable configurations from intolerable ones agreed very well for the two flight conditions. It is realized, of course, that the airplane was not rated for the same uses in the two flight conditions; however, it seems logical that the oscillatory rolling characteristics would affect the pilots' ratings in the same manner during a landing approach as during cross-country flying or gunnery runs. Also, it seems logical to use $|\phi|/|v|$ because side-gust disturbances do not occur in the form of changes in β, but rather they occur in the form of changes in v.
>
> "One objection to $|\phi|/|v|$ as a criterion, however, is the value of $|\phi|/|v|$ for a specific airplane lacks the feature of growth with altitude for a constant indicated airspeed. The altitude was kept constant during this investigation. However, evidence exists

> in the literature (see Reference 4) that pilots often notice an objectionable increase in the rolling motion in rough air as the altitude is increased. This has been substantiated by unpublished pilots' comments made during flight tests at the Ames Laboratory of a swept-wing operational fighter.
>
> "If $|\phi|/|v|$ is divided by the square root of the density ratio, it becomes $|\phi|/|v_e|$, where v_e is the equivalent side velocity. In general, $|\phi|/|v_e|$ does increase with altitude. Such a change in variable seems on the surface, to be strictly arbitrary, but support for such a change is found in atmospheric gust data. Reference 5 presents statistical information which shows that the effective gust velocity does not vary with altitude in turbulent air conditions, and the effective gust velocity referred to is in the form of an equivalent airspeed."

From this quotation it is seen that although success in correlating data had been obtained using $|\phi/v|_d$, the authors decided to change the variable from $|\phi/v|_d$ to $|\phi/v_e|_d$ to account for "an objectionable increase in the rolling motion in rough air as altitude is increased." This observation was a general one based on experience outside the data taken in the experiment reported in Reference 37. It is believed that this effect was probably a result of decreased roll and Dutch roll damping with altitude and possibly an increase in L'_β and N'_{δ_a} at higher angle of attack.

The evidence cited indicating that gust velocity, expressed as equivalent airspeed, was constant with altitude is not consistent with the description of σ_w vs. altitude in Figure 79 [Figure 8 of MIL-F-8785B(ASG)]. This curve is for w expressed as true gust velocity. The shape of the curve for true velocity as a function of altitude for constant equivalent velocity is shown on Figure 79.

Thus it seems that both of the reasons cited in Reference 37 for changing from $|\phi/v|$ to $|\phi/v_e|$ were invalid. With this review in mind it was decided to plot the data of Reference 43 in terms of $\zeta_d \omega_{n_d}$ vs. $\omega_{n_d}^2 |\phi/v|_d$ or $\frac{\omega_{n_d}}{V_T}\left|\frac{\phi}{\beta}\right|_d$. The resulting correlation is shown on Figure 80. The parameter $|\phi/\psi|_d$ was used in Reference 18 because the sideslip measurements were unreliable.

The data shown on Figure 80 are quite systematic and can be separated into four regions by straight lines radiating from the point (0, -.15).

The three straight lines used to divide the data correspond to pilot ratings of 3.5, 6.5 and about 8.5 on the rating scale used in Reference 43. This rating scale is quite similar in definition to the current Cooper-Harper scale. Several points which fall in the wrong region on Figure 80 were also troublesome for the rating equation developed in Reference 43. The calculated ratings are noted on Figure 80 in parentheses. Although a point by point comparison was not made to determine whether $\omega_{n_d}^2 \left|\frac{\phi}{\psi}\right|_d$ or $\frac{\omega_{n_d}^2}{V_T}\left|\frac{\phi}{\psi}\right|_d$ gives the best correlation, it is believed that the correlation indicated on Figure 80 is good enough to justify using the data to substantiate the requirement of 3.3.2.1.1.

Although the data of Reference 43 are self consistent and are being used as the primary basis for the requirement of paragraph 3.3.2.1.1, it is in order to raise some questions about the way the data were taken. The XF-88 airplane was equipped with a servo control system with yaw rate and sideslip feedback to the rudder and sideslip feedback to the aileron. The evaluations performed by the pilot consisted of setting the feedback gains, trimming the airplane and then kicking the rudder and observing the resulting uncontrolled motions. His rating was an overall opinion of the Dutch roll motion *only*, as felt and observed by him, taking into account considerations of discomfort, gunnery, instrument flight, contact flight, etc. The report does not give any information on how the pilot sized the rudder kick; therefore, the effect of changes in amount of sideslip resulting from the rudder input as the flight condition and especially the feedback gain settings were changed cannot be judged. To interpret this data as validly representing the response of the configurations to side gusts is an assumption. The data could be interpreted as representing the effect of miscoordination of the rudder but one suspects that the magnitude of the inputs used was perhaps too large to represent other than intentional misuse of the rudder.

In any event the data are the most extensive available and the correlation of $\zeta_d \omega_{n_d}$ with the parameter $\frac{\omega_{n_d}}{V_T}\left|\frac{\phi}{\beta}\right|_d$ is quite good.

D. Roll mode time constant for external disturbances, 3.3.2.1.2

In the Motivation and Background section for this requirement, data from a number of reports were presented to establish that degradation of flying qualities in turbulence results from the combination of low roll damping and large dihedral or $|\phi/\beta|_d$. Data from References 29, 30, 31, 32, 33, 36, 44 have been used to formulate the quantitative requirement establishing the maximum roll mode time constant to be permitted for responses to external disturbances. Care has been taken in stating the requirement in 3.3.1.2 so that it applies to the response to pilot commands whereas the requirement of 3.3.2.1.2 is stated such that it applies to the response of the airplane to externally applied disturbances such as atmospheric gusts, weapon release or control surface deflections as opposed to cockpit control deflections. The separate statement of the requirements should permit freedom to design separately for response to cockpit controls and response to external disturbances.

A number of parameters were tried as correlating parameters for the data from the various experiments. The parameter τ_R was plotted vs. the following parameters: L'_β, $\frac{L'_\beta}{V_T \omega_{n_d}}$, $\frac{L'_\beta}{V_T \omega_{n_d}^2}$, $\frac{1}{V_T}\left|\frac{\phi}{\beta}\right|_d$, $\frac{\omega_{n_d}}{V_T}\left|\frac{\phi}{\beta}\right|_d$ and finally $\frac{1}{V_T \omega_{n_d}}\left|\frac{\phi}{\beta}\right|_d$. The data considered are listed in Table III.

The most success in correlating the data from the seven widely different experiments was obtained for τ_R vs. $\frac{1}{V_T \omega_{n_d}}\left|\frac{\phi}{\beta}\right|_d$. The data are presented in this form on Figure 81. The data are presented in terms of pilot ratings on Figure 81 but the detailed pilot comments were used, when available, in interpreting the influence of the roll response to turbulence on the pilot rating. In some cases the configurations were given ratings both in smooth air and in simulated turbulence; in other cases a separate rating of the effect of turbulence on the flying qualities was given.

It must be appreciated that the simulation of turbulence in the different experiments was far from standard in either spectral content or rms intensity. In some of the in-flight experiments, actual turbulence and high crosswinds were experienced for part of the configurations. For experiments where gust intensity was a variable, the data for σ_v = 5 ft/sec was used. In the various ground simulation experiments, some were fixed base and others were done with washed-out motion. In view of these considerations it is thought that the degree of correlation achieved in Figure 81 is reasonably good and can be used as the basis for the requirement of 3.3.2.1.2. The equations in paragraph 3.3.2.1.2 are for straight lines radiating from a point at τ_R = 15, $\frac{1}{V_T \omega_{n_d}}\left|\frac{\phi}{\beta}\right|_d$ = -0.0153 with τ_R plotted on a log scale.

The data listed in Table III show that values of L'_β from -1.5 sec^{-2} to -102.2 sec^{-2} were simulated and true airspeeds from V_T of 84.5 ft/sec to 1190 ft/sec were simulated. The two points near τ_R = .25 and $\frac{1}{V_T \omega_{n_d}}\left|\frac{\phi}{\beta}\right|_d$ = .0175 had L'_β values of -5.79 and -40 sec^{-2}.

Thus although the L'_β values differ by a factor of 7 the pilot ratings are nearly the same and the two points plot at the same location on the τ_R vs. $\frac{1}{V_T \omega_{n_d}}\left|\frac{\phi}{\beta}\right|_d$ plane. The point from the NRC variable stability helicopter experiment needs some explanation as to why it is listed with a pilot rating of 5 when Reference 33 lists the configuration as being evaluated six times and rated 8.5, 10, 5, 10, 10, 9. The pilot comments reveal that the very bad ratings resulted from inadequate roll control authority to counter the simulated crosswind and to execute the sidestep maneuver. For portions of the evaluation task not involving these factors, the pilot rating is indicated to be 6-6.5 by one pilot. Another pilot gave the configuration a rating of 5. This case is reviewed to lend emphasis to the point that the flying qualities and controllability in turbulence of airplanes with large dihedral effect is highly dependent on having adequate roll control authority to trim steady sideslip and to counter gust induced roll disturbances. This point is discussed further in the section dealing with roll performance requirements.

Referring to the analysis of roll response to side gusts in Appendix VA of the BIUG, the following two forms of the transfer function can be written. The spiral root is assumed to be at the origin and approximations have been assumed in simplifying the numerator.

$$\frac{\phi(s)}{v_g(s)} = \frac{-\frac{1}{V_T} L'_\beta \, s}{\left(s + \frac{1}{\tau_R}\right)\left(s^2 + 2\zeta_d \omega_{n_d} s + \omega_{n_d}^2\right)}$$

$$\frac{\phi(s)}{v_g(s)} = -\tau_R \frac{L'_\beta}{V_T \omega_{n_d}^2} \frac{s}{(\tau_R s + 1)\left(\frac{s^2}{\omega_{n_d}^2} + \frac{2\zeta_d}{\omega_{n_d}} s + 1\right)}$$

The first form shows that the gain at high frequency is proportional to $\frac{1}{V_T} L'_\beta$ while the second form shows that the gain at low frequency is proportional to $\tau_R \frac{L'_\beta}{V_T \omega_{n_d}^2}$. The latter form suggests plotting pilot rating data on a plane of τ_R vs. $\frac{L'_\beta}{V_T \omega_{n_d}^2}$. The experimental data are plotted in this way on Figure 82. Lines of $\tau_R \frac{L'_\beta}{V_T \omega_{n_d}^2} = C$ do a fairly good job of separating the points into good and bad regions on Figure 82.

The transient response of the uncontrolled airplane to side gust inputs for variations in L'_β is illustrated by time histories in Figure 83 from Reference 29. The effect of variation of roll mode time constant is illustrated by the time histories in Figure 84 from Reference 36. These time histories illustrate the response of the configurations to the abrupt step input sketched on Figure 83. The responses in Figure 84 are also for this input, although in Reference 36 they are erroneously identified as responses to a pulse input. Examination of Figure 83 shows that the roll response is greatly different for the high $\left|\phi/\beta\right|_d$ cases, (A-7, A-8, A-9) compared with low $\left|\phi/\beta\right|_d$ (A-1, A-2, A-3).

Examination of Figure 84 shows very little difference between the responses for high roll damping and the responses for low roll damping but the pilot rating data in Figure 77 indicate a strong pilot preference for the high roll damping cases. (It should be noted that the recording scales are different on Figures 83 and 84.)

In both Figures 83 and 84, the Dutch roll mode has been excited by the abrupt input and it dominates the transient response. It seems obvious from these time histories that the response to abrupt inputs can be reduced by increasing the Dutch roll damping as is required by 3.3.2.1.1. It is also suggested by the transient responses that the response ratio $\left|\phi/v\right|_d$ or $\frac{1}{V_T}\left|\frac{\phi}{\beta}\right|_d$ may be the best indicator of the amplitude in roll of the resulting Dutch roll oscillation. The initial slope of the roll rate response is proportional to $\frac{1}{V_T} L'_\beta$ but the amplitude of the Dutch roll oscillation in bank angle is proportional to $\frac{1}{V_T}\left|\frac{\phi}{\beta}\right|_d$. With this in mind the data from the various experiments were

plotted on the γ_R vs. $\frac{1}{V_T}\left|\frac{\phi}{\beta}\right|_d$ plane, γ_R vs. $\frac{\omega_{n_d}}{V_T}\left|\frac{\phi}{\beta}\right|_d$ plane and γ_R vs. $\frac{1}{V_T \omega_{n_d}}\left|\frac{\phi}{\beta}\right|_d$ plane. The best correlation was obtained for the last plotting scheme and is illustrated in Figure 81. The division by ω_{n_d} was arrived at empirically but the operation is suggested from inspection of a Bode diagram of the ϕ/v_g transfer function. For all other factors constant, an increase in Dutch roll frequency will reduce the transfer function gain at low frequency. These effects are illustrated by Figure 85 from page 642 of Reference 29.

It should also be recognized that we do not know to what combination of ϕ, p, and $\dot{p}$ the pilot is sensitive nor do we know whether or not he is sensitive to each of these parameters in different frequency bands. The asymptotic slope of the amplitude ratio of ϕ/v_g with frequency is +1 at low frequency and -2 at high frequency. The slope of the amplitude ratio of p/v_g with frequency is +2 at low frequency and -1 at high frequency. The slope of the amplitude ratio of $\dot{p}/v_g$ with frequency is +3 at low frequency and 0 at high frequency. The best correlation of the experimental data, however, resulted from γ_R vs. $\frac{1}{V_T \omega_{n_d}}\left|\frac{\phi}{\beta}\right|_d$.

Table III-1 DATA FOR τ_{R_E} VS $\frac{1}{V_T \omega_{n_d}} \left|\frac{\phi}{\beta}\right|_d$ REQUIREMENT

CONFIGURATION	τ_R	ω_{n_d}	ζ_d	V_T	L'_β	$\left\|\frac{\phi}{\beta}\right\|_d$	$\frac{1}{V_T}\left\|\frac{\phi}{\beta}\right\|_d$	$\frac{\omega_{n_d}}{V_T}\left\|\frac{\phi}{\beta}\right\|_d$	$\frac{L'_\beta}{V_T \omega_{n_d}}$	$\frac{1}{V_T \omega_{n_d}}\left\|\frac{\phi}{\beta}\right\|_d$	P.R.	$\frac{L'_\beta}{V_T \omega_{n_d}}$
AFFDL-TR-70-145 (REF. 31) GROUP 4	0.4	2.02	0.10	245	-19.4	3.14	0.0128	0.0258	-0.0392	0.00635	3.5	-0.0194
9	0.4	1.09	0.12	↓	-8.91	3.11	0.0127	0.0139	-0.0332	0.0116	5	-0.0304
10	0.4	1.03	0.25		-7.3	2.90	0.0118	0.0121	-0.0290	0.0115	3.5	-0.0282
15	0.95	1.13	0.09		-4.39	3.50	0.0143	0.0162	-0.0158	0.0127	5	-0.0140
16	2.0	1.00	0.11		-1.5	1.55	0.0065	0.0065	-0.0061	0.0065	4	-0.0061
FAA DS 69-13 (REF. 36) τ_R HI $\left\|\frac{\phi}{\beta}\right\|$	1.51	1.90	0.046	541	-11.3	3.01	0.00555	0.0105	-0.011	0.00293	5.5	-0.0058
τ_R LO $\left\|\frac{\phi}{\beta}\right\|$	1.58	1.85	0.053		-6.2	1.74	0.00321	0.00595	-0.0062	0.00173	2.5	-0.00335
τ_R HI $\left\|\frac{\phi}{\beta}\right\|$	0.50	1.96	0.046	↓	-16.4	3.06	0.00565	0.0111	-0.0155	0.00289	3.0	-0.00792
As 303 (REF. 44) R	0.66	1.46	0.15	203	-12.8	4.4	0.022	0.0324	-0.043	0.015	3.5	-0.0294
R	0.71	1.47	0.15	↓	-6.4	2.1	0.0103	0.0070	-0.0215	0.0070	3.5	-0.0146
R	0.38	1.46	0.15		-6.4	1.4	0.0069	0.0047	-0.0215	0.0047	3.0	-0.0147
J	0.578	2.07	0.054	236	-24.5	4.53	0.019	0.0394	-0.050	0.0092	5	-0.0241
L	0.93	2.45	0.147	304	-16.2	2.6	0.0085	0.0208	-0.0217	0.0035	3.5	-0.00885
NRC (REF. 33) HH 103+29+29	0.25	1.0	0.3	84.5	-5.79	1.5	0.018	0.018	-0.068	0.018	5	-0.0680
P.U. 11 (REF. 8)	0.25	1.8	0.1	178	-40	5.7	0.0321	0.0575	-0.125	0.0178	4.4	-0.0695
	1.00	1.8	0.1	178	-16	1.81	0.0102	0.0184	-0.050	0.0057	3.9	-0.0278
AFFDL-TR-65-39 (REF. 30) 1	1.03	2.08	0.2	1190	-50	10.8	0.0091	0.019	-0.0202	0.00436	5.5	-0.00973
2	3.21	2.10	0.2		-50	11.3	0.0095	0.020	-0.0200	0.0045	7.5	-0.00953
8	1.39	2.14	0.2		-30	6.38	0.00536	0.0115	-0.0118	0.0025	6.5	-0.00552
14	3.72	2.11	0.05		-30	6.61	0.00556	0.0117	-0.0119	0.00263	8.5	-0.00564
25	8.94	2.11	0.2		-42	9.3	0.0079	0.0166	-0.0167	0.0037	9.5	-0.00792
26	0.655	2.08	0.2		-42	8.3	0.0070	0.0146	-0.0170	0.00335	3.5	-0.00816
43	0.294	2.10	0.2		-30	3.85	0.00324	0.0068	-0.0120	0.00183	3.5	-0.00572
57	5.55	2.14	0.14		-30	6.54	0.0055	0.0118	-0.0178	0.00256	8	-0.00552
59	2.18	2.15	0.1		-30	6.48	0.00545	0.0117	-0.0117	0.00253	6	-0.00544
60	1.79	2.17	0.07		-30	6.41	0.0054	0.0117	-0.0116	0.00248	6	-0.00534
62	2.38	2.12	0.025	↓	-30	6.33	0.0053	0.0112	-0.0119	0.00259	6	-0.00561
NASA CR-778 (REF. 29) A-1, 2, 3	0.321	2.20	0.099	612	-5.36	0.89	0.0011	0.00242	-0.00398	0.0005	2	-0.00181
A-4, 5, 6	0.311	2.10	0.18	↓	-77.1	9.70	0.015	0.0315	-0.0600	0.0070	3.5	-0.0286
A-7, 8, 9	0.446	2.41	0.12		-102.2	14.7	0.0212	0.0510	-0.0692	0.0094	4	-0.0288

REFERENCE 31 HALL-BOOTHE; CLASS II-L; CATEGORY C

GROUP 6 ω_d = 1.0 ζ_d = .11

PR = 2.5, 2.5, 2.0

GROUP 11 ω_d = 1.00 ζ_d = .11

PR = 2.5, 3.5, 1.0, 2.0, 2.0, 2.0, 3.0

GROUP 13 ω_d = 1.00 ζ_d = .099

PR = 3.0, 3.0, 3.0, 3.0

GROUP 14 ω_d = 1.01 ζ_d = .10

PR = 2.0, 1.0, 3.0, 3.0, 3.0, 2.0, 2.0, 2.0, 2.5

REFERENCE 32 SECKEL; PU-797; CARRIER LANDING

CONFIGURATION 207 ω_d = .8 ζ_d = .1 $\angle_\beta$ = 0

PR = 5.5 6 EVALUATIONS

CONFIGURATION 209 ω_d = .8 ζ_d = .1 $\angle_\beta$ = 16

PR = 4.5 13 EVALUATIONS

Figure 71 DUTCH ROLL DATA FOR ω_{n_d} NEAR 1.0 RAD/SEC

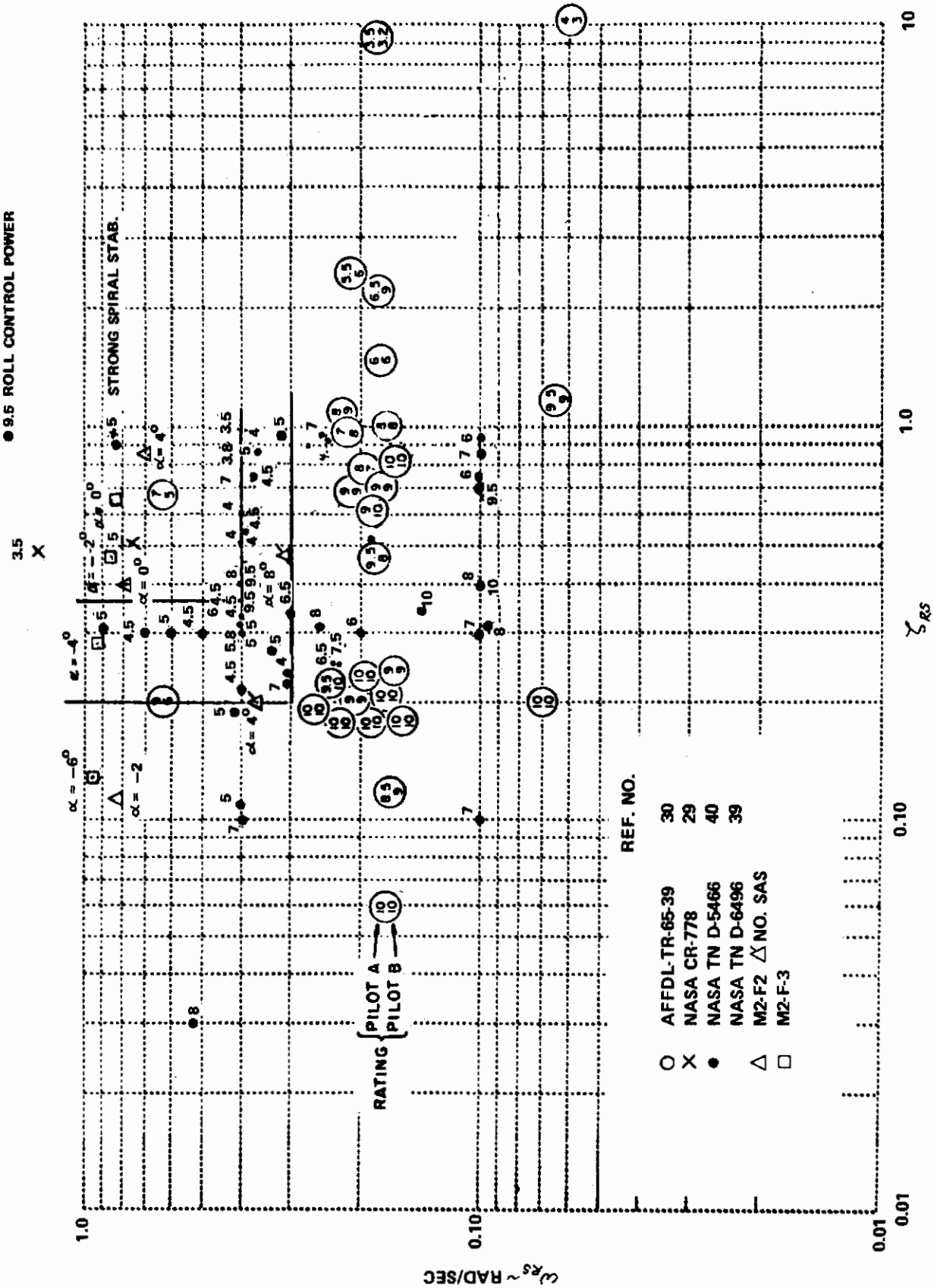

Figure 72 $\omega_{n_{RS}}$ VS ζ_{RS} FOR CONVERGENT DUTCH ROLL (Figure 1 (3.3.1.4) of Reference 3)

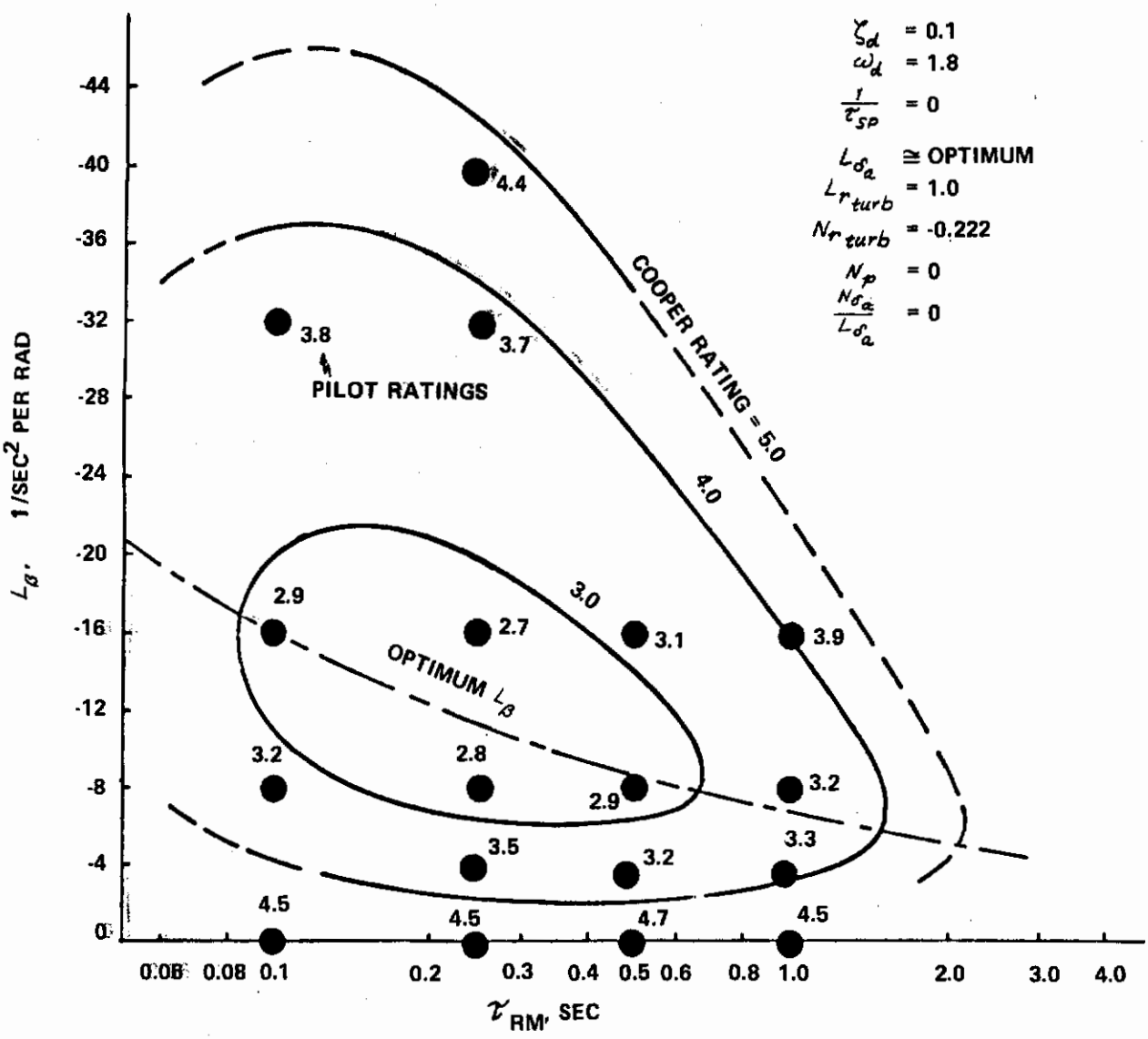

Figure 73 EFFECT OF NON-OPTIMUM DIHEDRAL (Figure 16 of Reference 32)

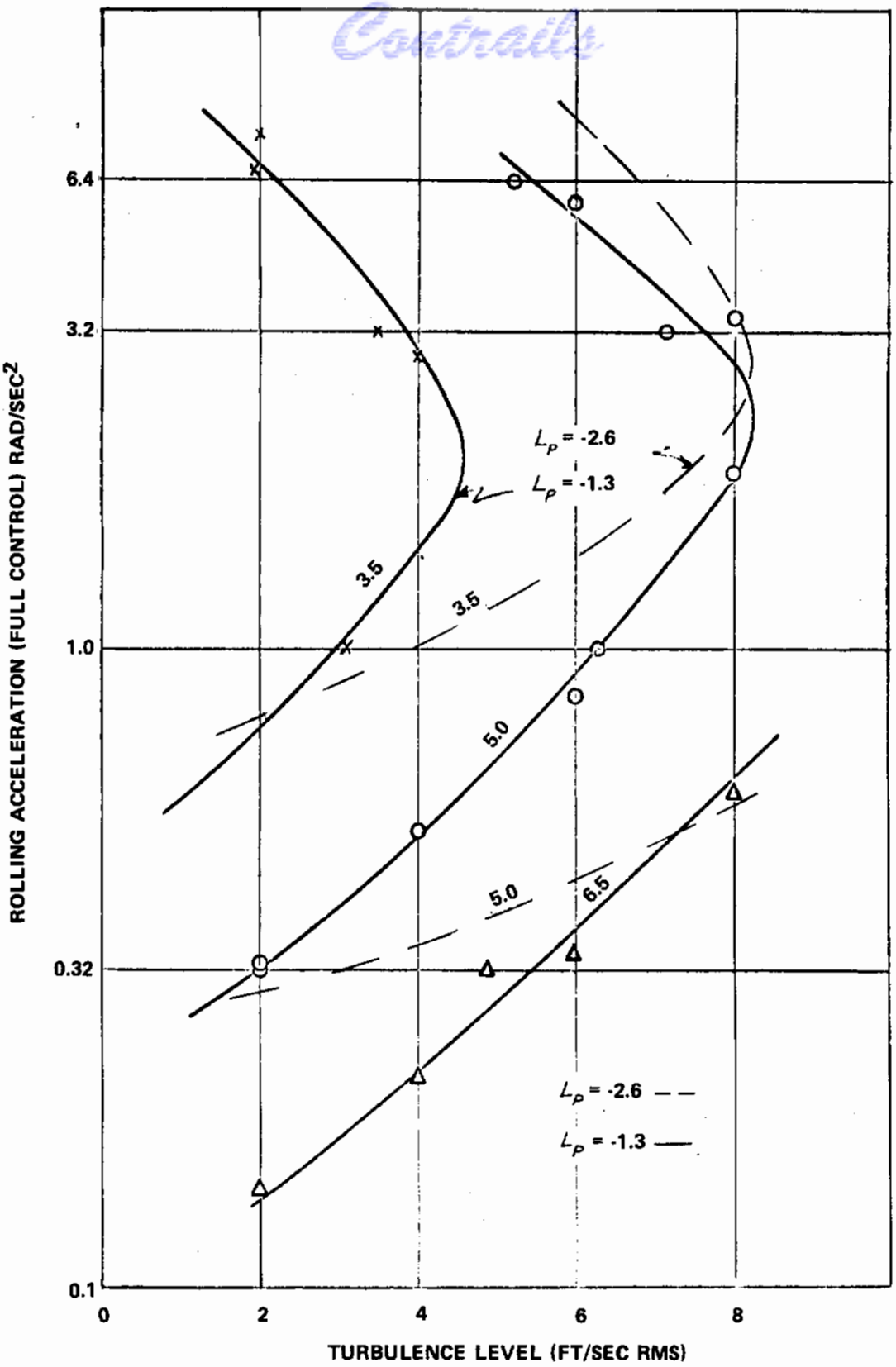

Figure 74 PILOT OPINION BOUNDARIES (From Reference 44)

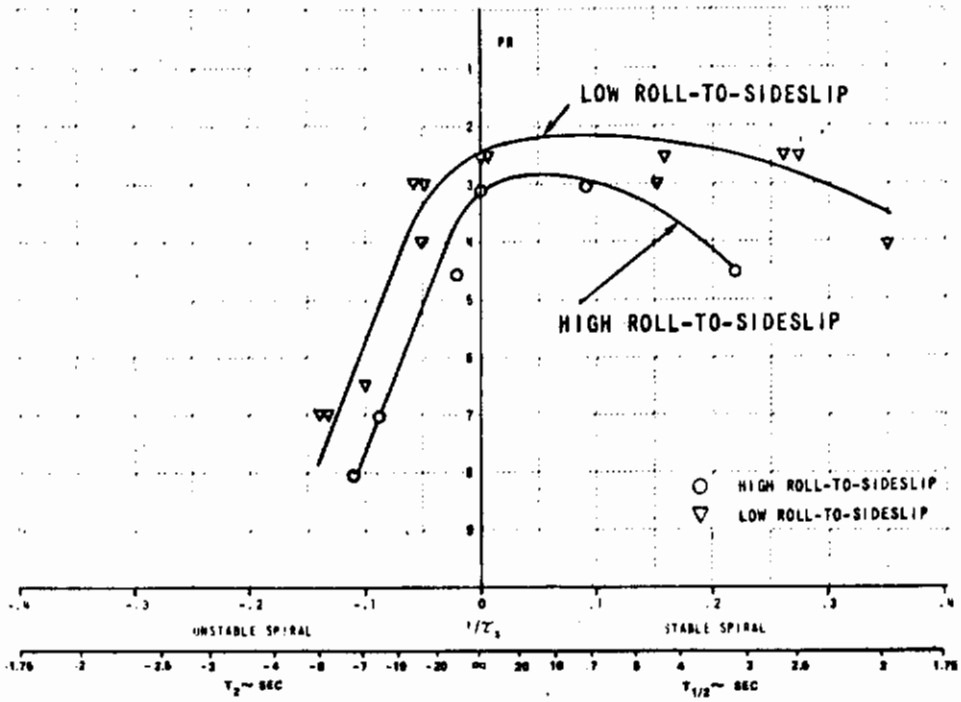

I **Figure 75 COMPARISON OF PILOT RATING DATA FOR THE HIGH ROLL DAMPING, LOW AND HIGH ROLL-TO-SIDESLIP CONFIGURATIONS (From Reference 36)**

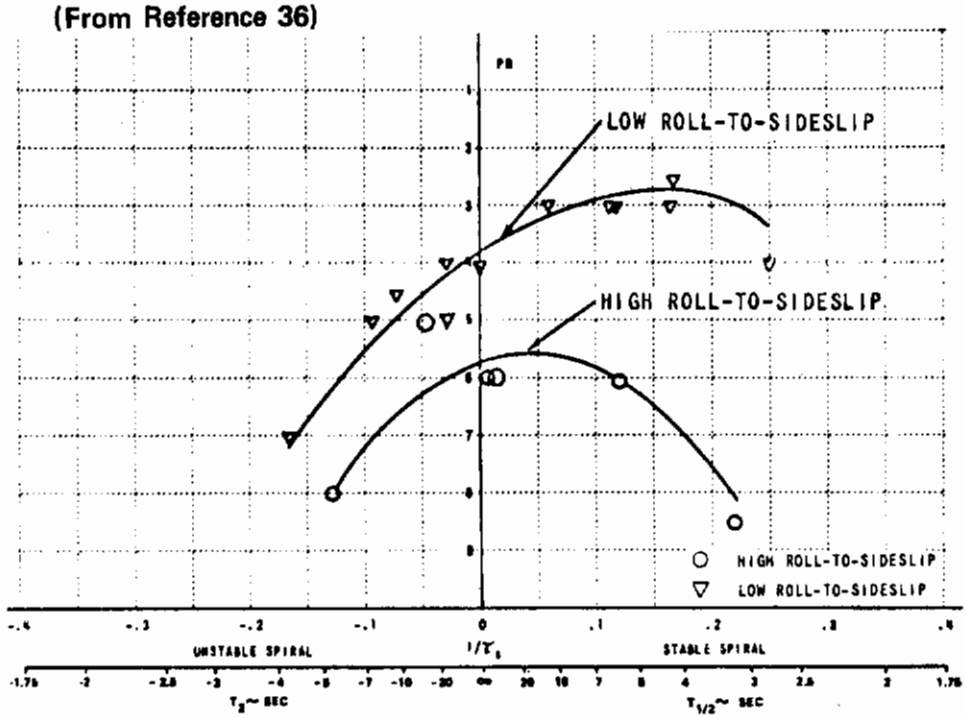

Figure 76 COMPARISON OF PILOT RATING DATA FOR THE LOW ROLL DAMPING, HIGH AND LOW ROLL-TO-SIDESLIP CONFIGURATIONS (From Reference 36)

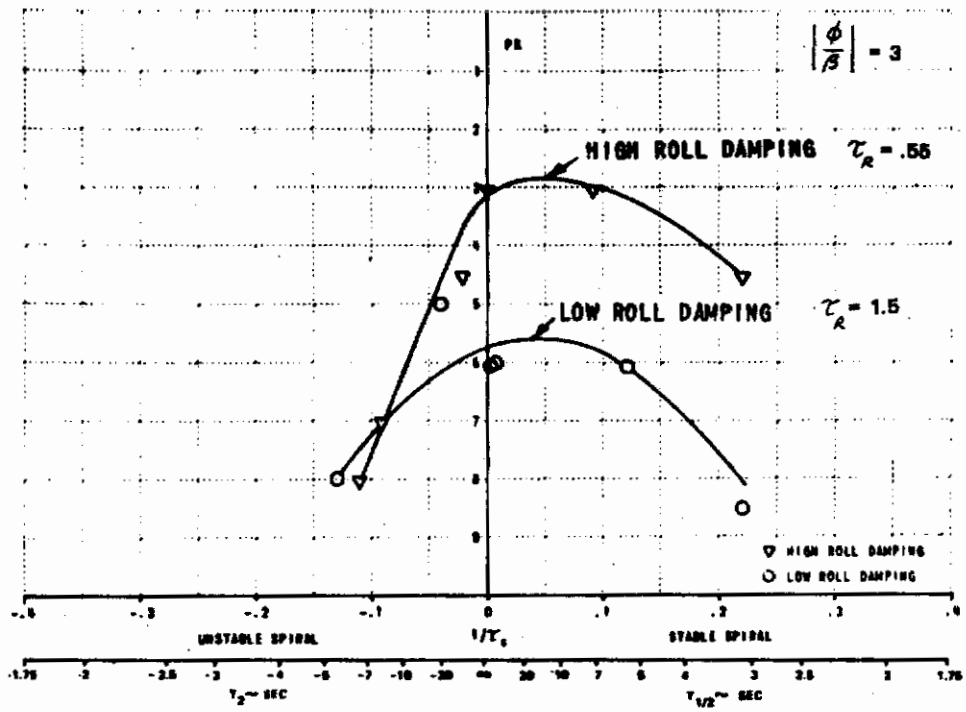

Figure 77 COMPARISON OF PILOT RATING DATA FOR THE HIGH ROLL-TO-SIDESLIP, LOW AND HIGH ROLL DAMPING CONFIGURATIONS (From Reference 36)

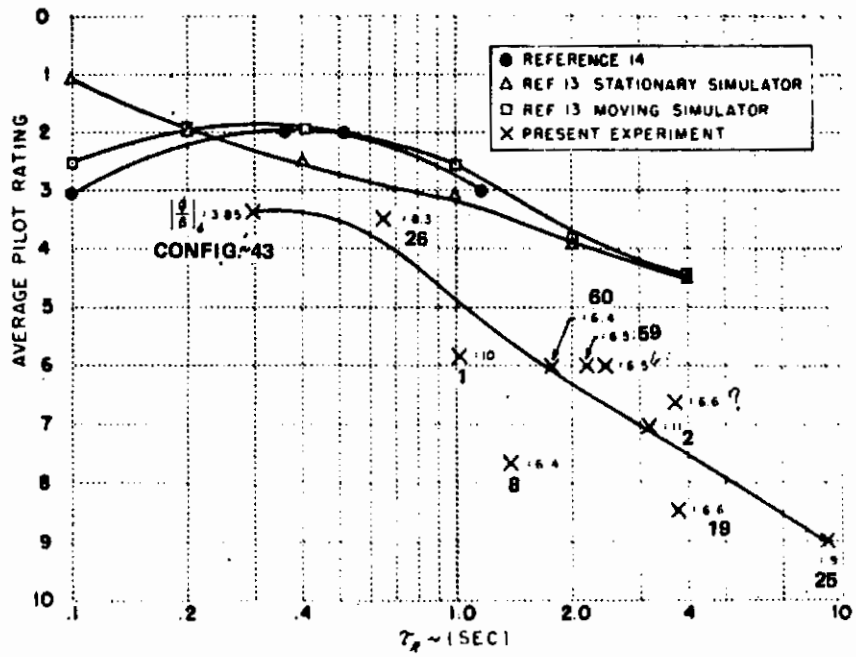

Figure 78 AVERAGE PILOT RATING OF ROLL MODE TIME CONSTANT (From Reference 30)

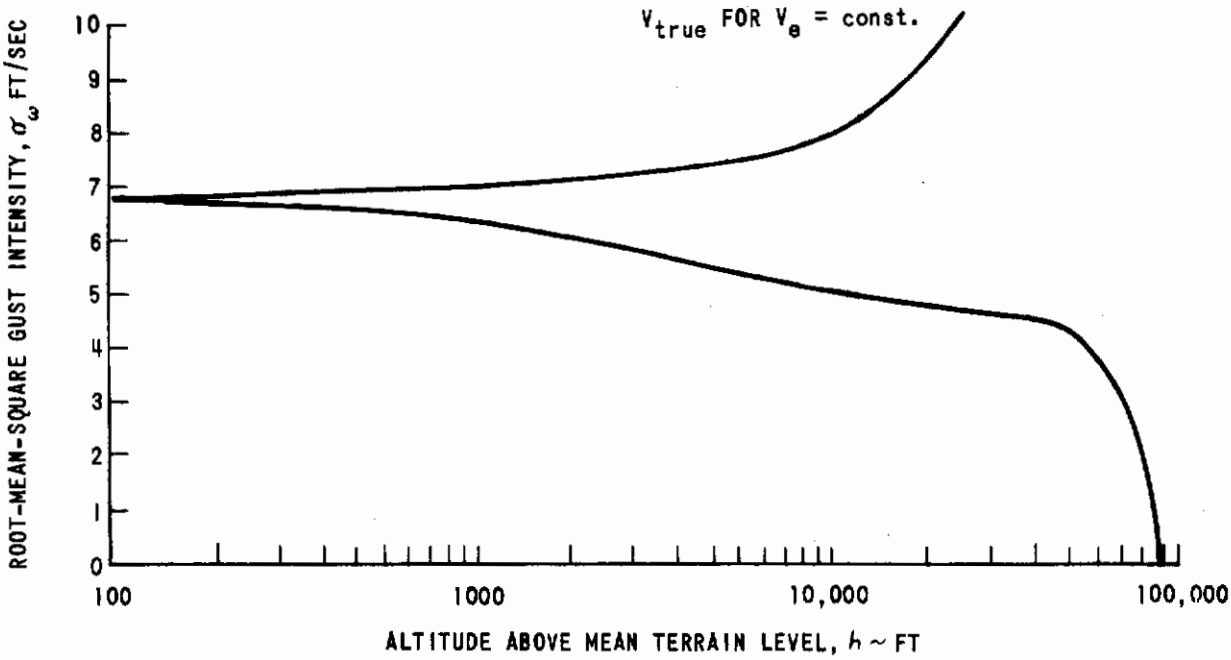

Figure 79 INTENSITY OF CLEAR AIR TURBULENCE (Figure 8 of MIL-F-8785B (ASG))

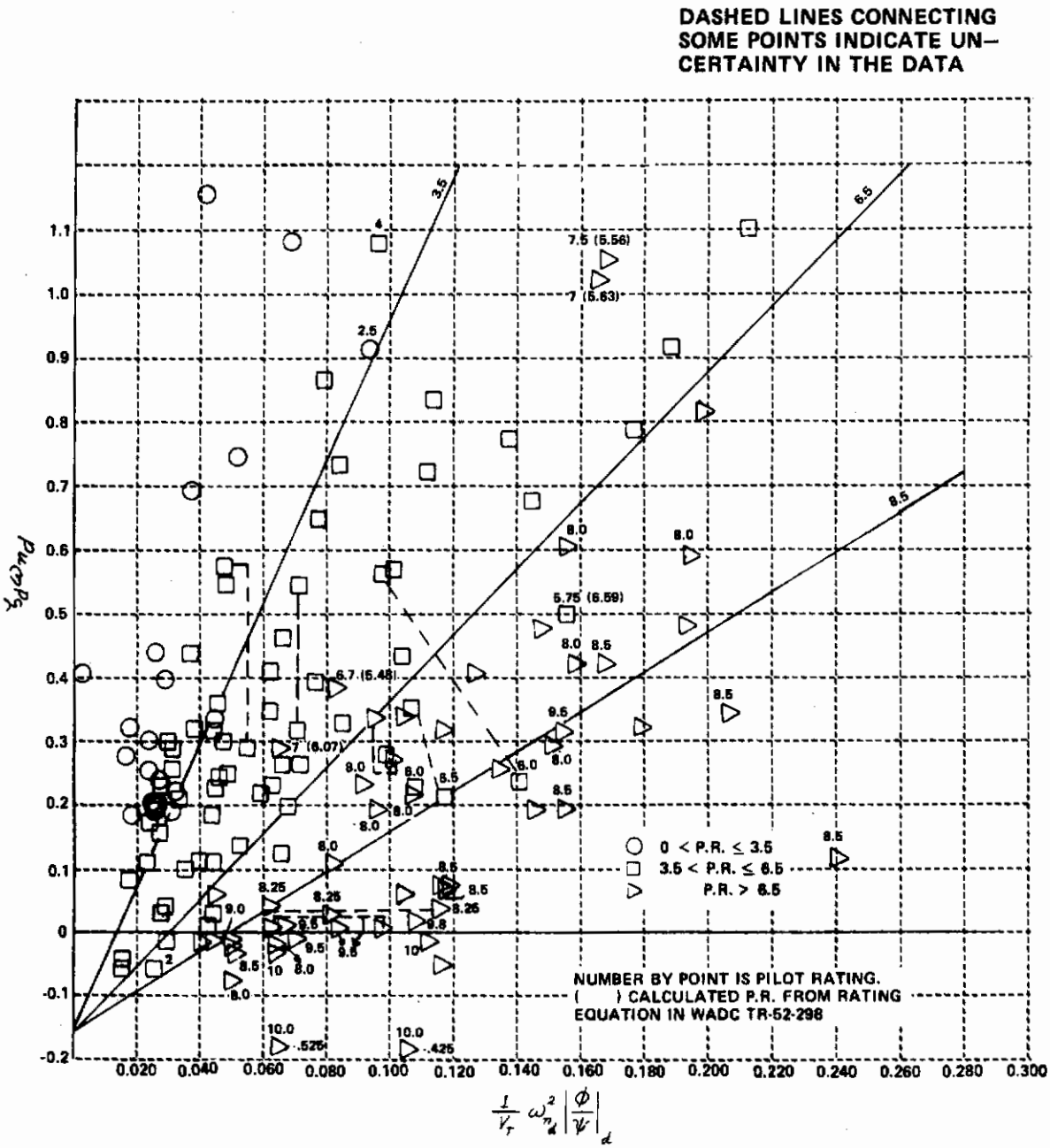

Figure 80 $\zeta_\phi \omega_{n_\phi}$ **AS A FUNCTION OF** $\frac{1}{V_T}\omega_{n_d}\left|\frac{\phi}{\psi}\right|_d$

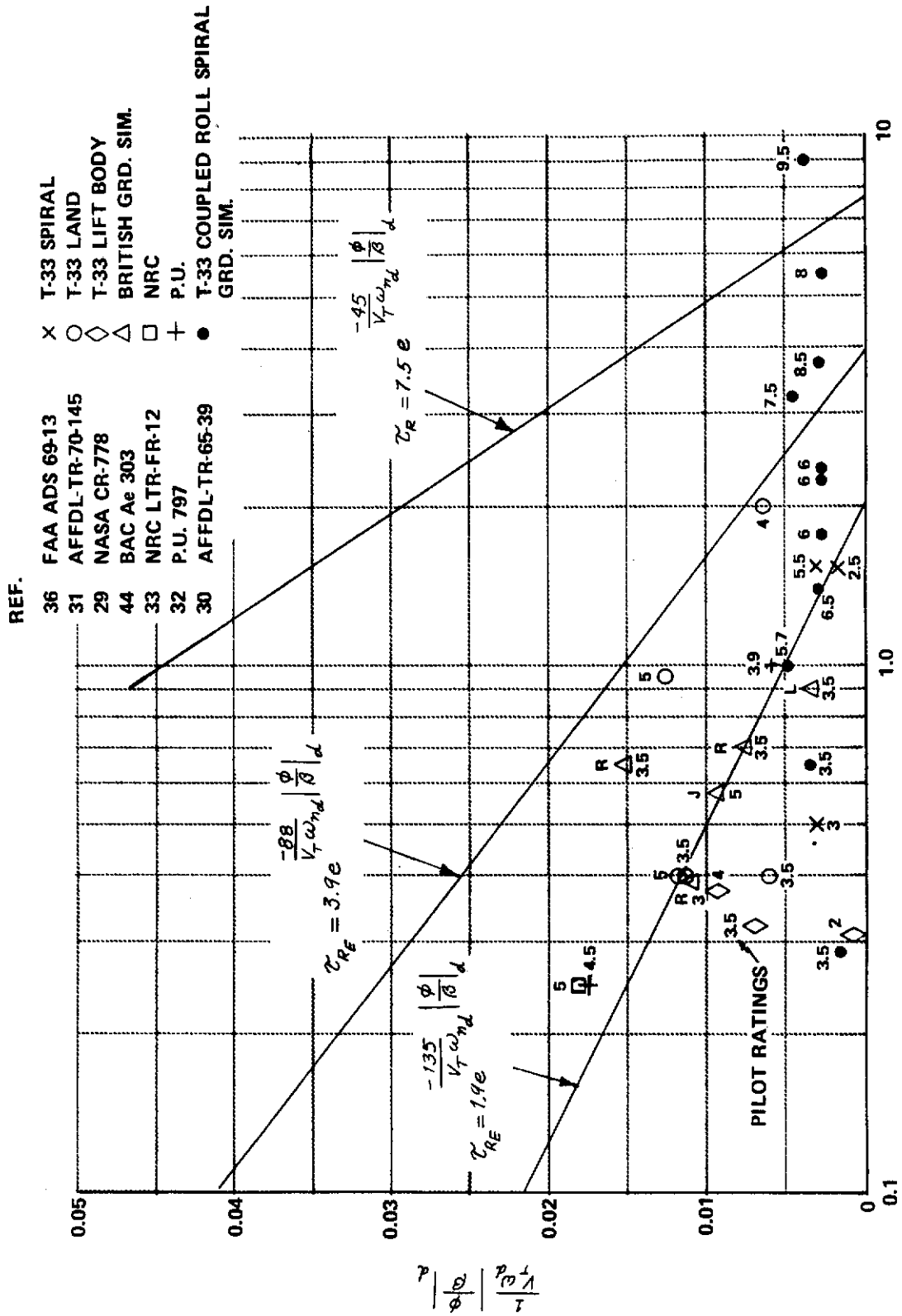

Figure 81 ROLL MODE TIME CONSTANT AS A FUNCTION OF $\frac{1}{V_T\omega_{n_d}}\left|\frac{\phi}{\beta}\right|_d$

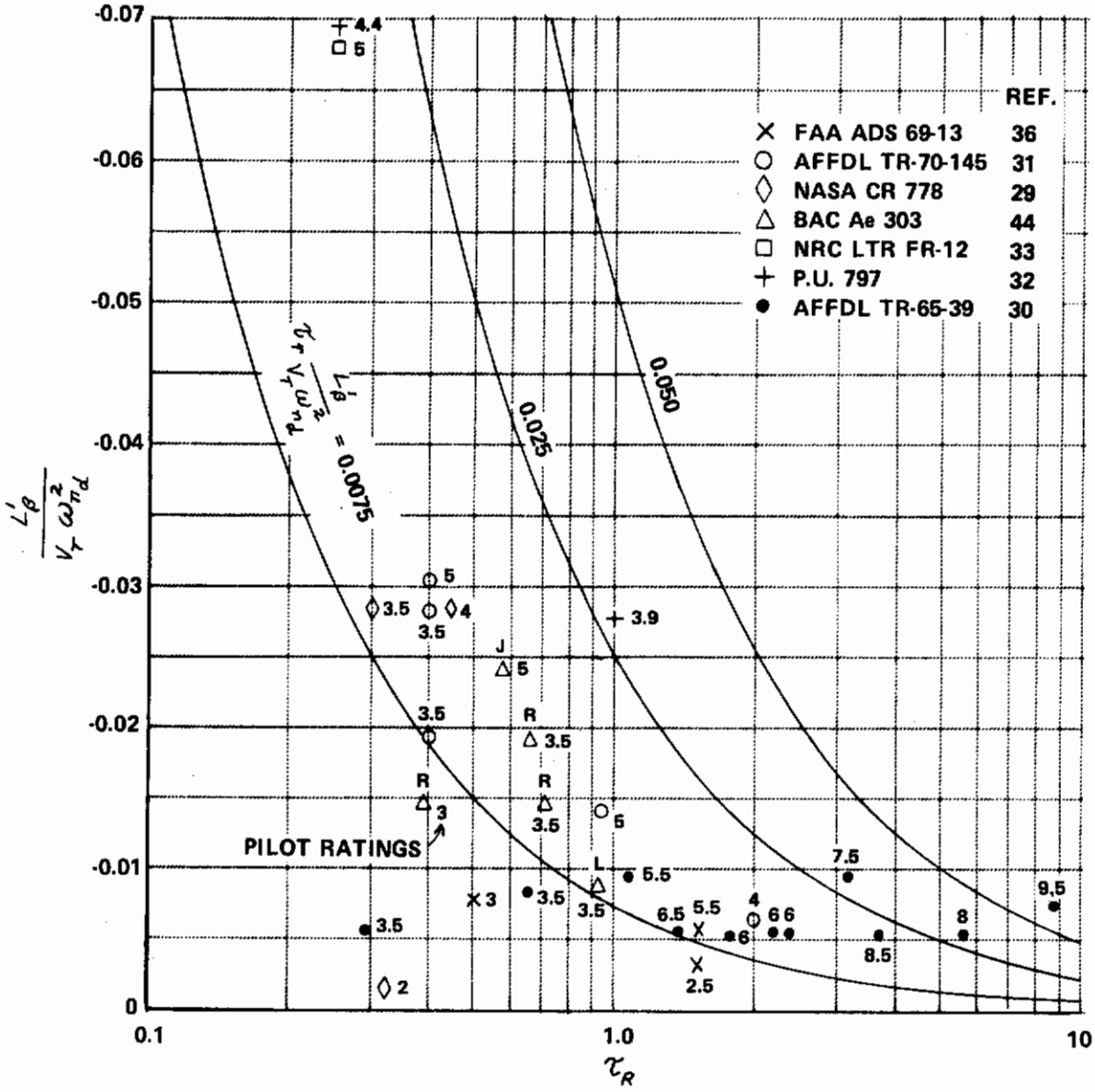

Figure 82 ROLL MODE TIME CONSTANT AS A FUNCTION OF $\frac{L'_\beta}{V_T \omega_{n_d}^2}$

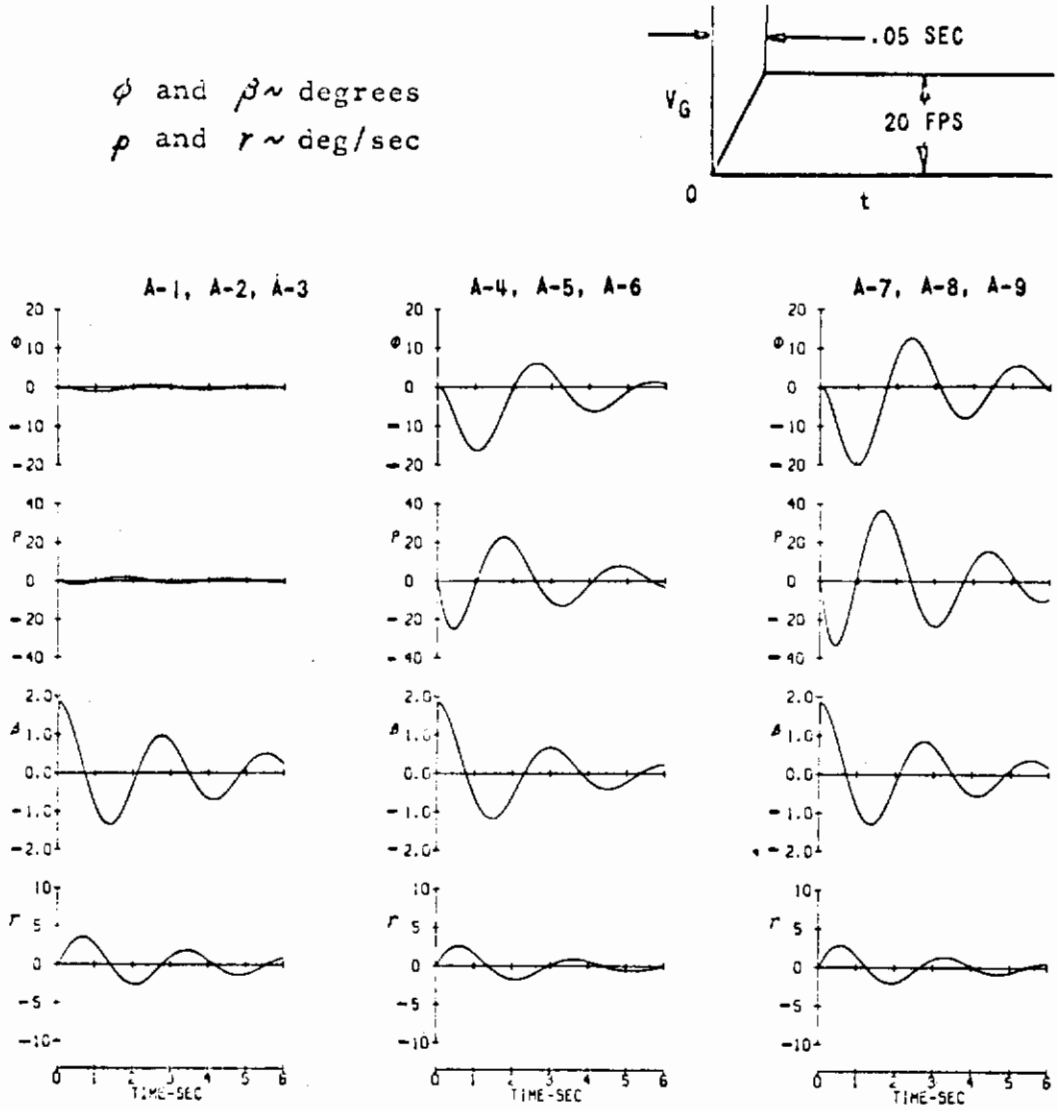

Figure 83 TRANSIENT RESPONSES TO SIDE GUST CALCULATED FROM PSEUDODERIVATIVES (From Reference 29)

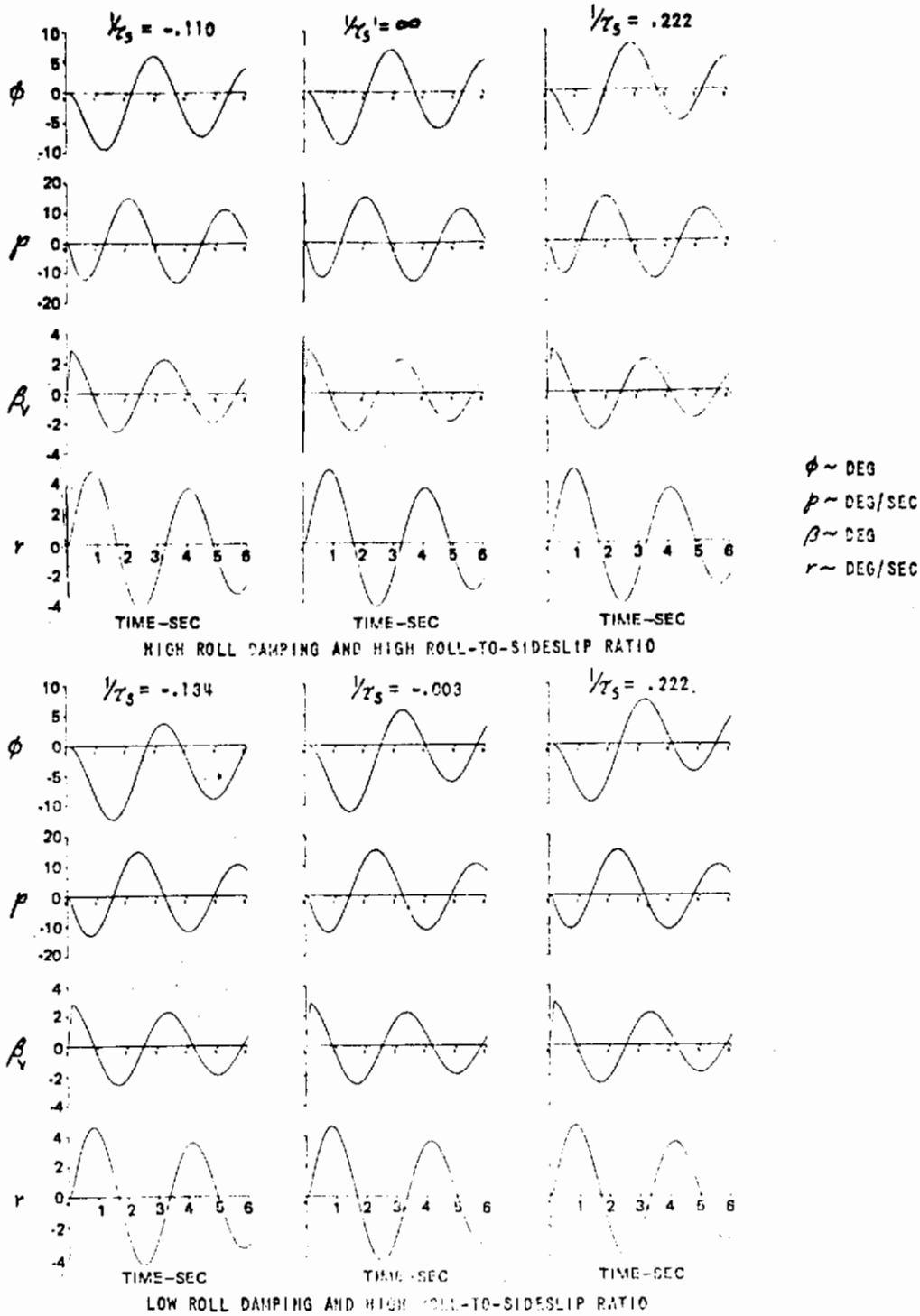

Figure 84 **COMPARISON OF THE GUST RESPONSE FOR THE HIGH ROLL-TO-SIDESLIP CONFIGURATIONS WITH HIGH AND LOW ROLL DAMPING (From Reference 36)**

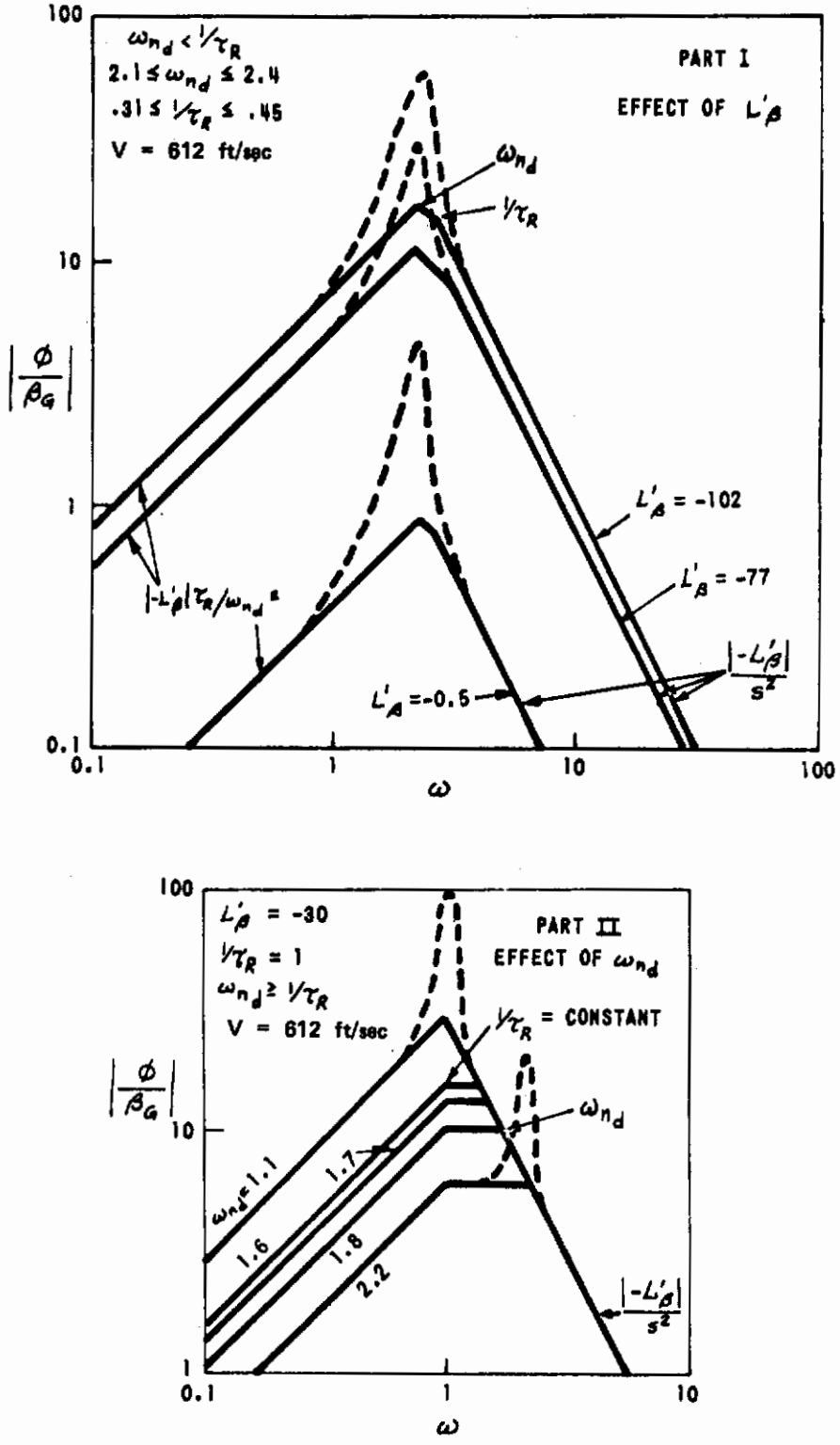

Figure 85 $|\phi/\beta_G|$ **FREQUENCY-RESPONSE ASYMPTOTES, WITH EFFECT OF LIGHT DUTCH ROLL DAMPING INDICATED (From Reference 29)**

Motivation and Background for Action Recommended (New Paragraphs 3.3.2.2 and 3.3.2.2.1)

The requirements to limit bank angle and roll rate oscillations resulting from the pilot's use of aileron were introduced in MIL-F-8785B(ASG). These requirements have now been tested by additional data and have been subjected to the test of application. From this experience it is concluded that the requirements are basically valid and certainly should be retained, but certain problems in the present statement of the requirements have come to light which should be rectified.

1. It has been found that certain combinations of stability derivatives result in $\not\propto \frac{p}{\beta}$ of the Dutch roll mode between 180° and 270°. Because of this, the use of two ψ_β scales in the requirement and the rule for deciding which scale is to be used based on $\not\propto \frac{p}{\beta}$ has been re-examined and found to be an inadequate feature of the requirement. Both this problem and the problem identified in Item 2 can be remedied by using ψ_p rather than ψ_β in the requirement.

2. When $|\phi/\beta|_d$ is large, the amplitude of the Dutch roll oscillation in sideslip is quite small and measurement of the phase angle ψ_β is difficult and inaccurate.

3. When the spiral root is not at the origin, the measures ϕ_{osc}/ϕ_{AV} and p_{osc}/p_{AV} are severely distorted and do not correlate with the flying qualities rating. This problem can be remedied by removing the spiral mode contribution to the ϕ and p time histories.

4. The symmetrical shape of the requirement boundary is inaccurate; additional data permit defining the boundary more accurately.

5. The requirements on roll rate oscillations require step aileron inputs to be held for 1.7 T_d sec in one case and until bank angle has changed 90° in another case. To avoid extreme roll attitude at the end of the test it is desirable to start the maneuver from banked turning flight in one direction and to roll through wings level to bank in the opposite direction. The requirement that the rudder pedal be free during this maneuver prevents setting up zero-sideslip initial conditions or if the rudder is used to zero initial sideslip and is then released when the aileron step is applied, the resulting response is not to the aileron input alone. This problem can be remedied by specifying that the rudder pedal be held fixed for the requirements that are based on aileron step inputs.

6. The large difference in the magnitude of p_{osc}/p_{AV} permitted by the requirement for $\Psi_p = -240°$ relative to that permitted for $\Psi_\beta = -40°$ is primarily a result of the fact that p_{AV} tends to zero for large adverse yaw due to aileron. This causes p_{osc}/p_{AV} to tend to infinity, but the pilot rating does not degrade nearly so rapidly, thus the gradient of pilot rating with p_{osc}/p_{AV} is shallow, making location of Level 2 boundaries imprecise. This situation can be alleviated by changing the denominator of the ratio to $\hat{p}_1$ and $\hat{\phi}_1$ respectively in the definitions of $\hat{p}_{osc}/\hat{p}_1$ and $\hat{\phi}_{osc}/\hat{\phi}_1$.

7. The formula using two peaks to calculate p_{osc}/p_{AV} and ϕ_{osc}/ϕ_{AV} has been found to have a characteristic which results in lack of discrimination for certain $\Psi_{p_{STEP}}$ or $\Psi_{\phi_{IMPULSE}}$ phase angles. For some combinations of poles and zeros the time history of roll rate for a step aileron has the following character. (see cases 3 and 4 on Figure 27 (3.3.2.2) and 28 (3.3.2.2) of Reference 3).

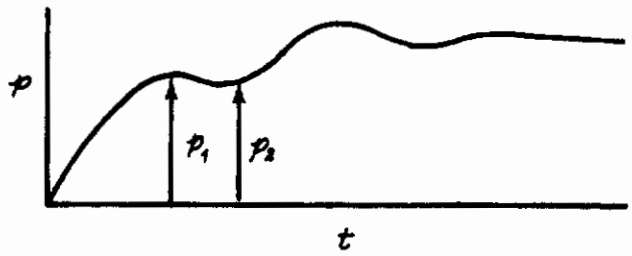

$$\frac{p_{osc}}{p_{AV}} = \frac{p_1 - p_2}{p_1 + p_2}$$

The phase of the Dutch roll component can always be shifted (by choice of the angular locations of the zeros) such that $p_1 - p_2$ is very small, regardless of how far the zeros are from the Dutch roll pole. Thus there will always be a set of zero locations for which $p_1 - p_2$ is very small even though the excitation of the Dutch roll mode is large. As a result the formula using two peaks defines a region on the s plane that looks as follows:

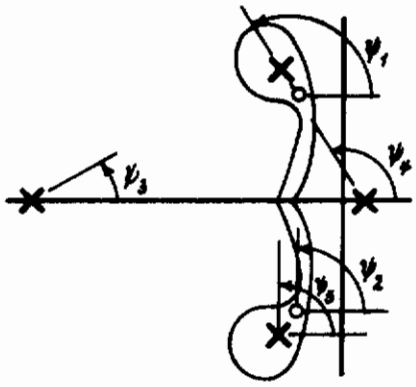

$\psi_p = \psi_1 + \psi_2 - \psi_3 - \psi_4 - \psi_5 = \text{constant}$

$\psi_1 + \psi_2 = \text{constant}$

For zeros on $\zeta = \zeta_d$ line but very small distance from the pole,

$\psi_1 = 90 + \sin^{-1}\zeta_d$, $\psi_2 = 90°$.

And for zeros coincident on real axis,

$\psi_1 = \psi_2 = 1/2\ (180 + \sin^{-1}\zeta_d)$.

This situation can be avoided by using a formula based on three peaks for all damping ratios. When ζ_d is high and there is no third peak, $p_3 = p_2$.

In the following paragraphs the first three problems are examined in detail and proposed remedies are developed. In a following section the substantiation data for the modified requirements is presented.

The sections under paragraphs 3.3.2.2, 3.3.2.2.1, 3.3.2.3 and Appendix VC in the BIUG for MIL-F-8785B(ASG) present an extensive discussion of the theory and development of the roll rate and bank angle oscillation requirements.

As part of this development it was established that there are areas around the Dutch roll pole in which the zeros of the bank angle to aileron transfer function can be located for a good airplane. It was tacitly assumed in the development that the allowable areas were best described by the relative angle ψ_1 and a measure of the amplitude of the Dutch roll oscillation relative to the average roll rate. Consideration was then given to how the relative angle ψ_1 could best be determined from time history information. The phase angle ψ_p was considered but rejected because it was not a unique indicator of ψ_1, i.e., the location of the roll mode and spiral mode roots also influences ψ_p. Next it was discovered that the phase angle ψ_β was, under certain assumptions, a quite good indicator of ψ_1.

In Appendix VC of the BIUG, the assumptions and circumstances under which ψ_1 and ψ_β are related were examined. It was concluded that for nearly all practical cases the correspondence between ψ_1 and ψ_β was sufficiently unique to permit using ψ_β as the phase angle metric in the requirement. It was found necessary, however, to include two ψ_β scales on the requirement plot along with a rule to define which scale should be used in a given case.

New data in Reference 35 have called attention to the fact that configurations with low values of L'_β and large values of L'_r can violate some of the approximations and assumptions made in Appendix VC regarding probable values of $\angle \frac{p}{\beta}$ and the unique relation between ψ_1 and ψ_β. Instead of $\angle \frac{p}{\beta}$ lying between 90° - 180° or 270° - 360° as was reasoned in Appendix VC, many of the configurations in Reference 35 had values of $\angle \frac{p}{\beta}$ in the range 180 - 270°. Also, the approximate equations relating ψ_1 and ψ_β are given in Appendix VC.

$$\psi_\beta \approx \psi_1 - \sin^{-1} \zeta_d + 90° \text{ for } 45° < \angle \frac{p}{\beta} < 225°$$

and

$$\psi_\beta \approx \psi_1 - \sin^{-1} \zeta_d - 90° \text{ for } 225° < \angle \frac{p}{\beta} < 405°$$

were found to be invalid for many of the configurations in Reference 35 for which L'_β was small.

These observations have forced a review of the development of the requirement, identification of assumptions involved and examination of approximations used. It is concluded that a primary assumption had been made in the BIUG that ψ_1, the relative angular location of the zero and the pole in the roll transfer function, was a unique indicator of desirable characteristics. Following this assumption much of the development in the BIUG deals with a search for and justification of the use of another parameter, ψ_β, as a reliable indicator of ψ_1. It is now proposed that the phase angle ψ_p should be used instead of ψ_β in the roll oscillation requirements. The following observations are presented to support substitution of this parameter for ψ_β.

1. The data correlation obtained is equally good or better than that obtained using ψ_β.

2. The relative locations of all the roll transfer function poles and zeros are important to the acceptability of the pilot-airplane dynamic system. It is suggested that the departure angle of the Dutch roll root along its root locus path for ϕ to δ_a feedback is a more significant feature than the angle ψ_1. The departure angle and the phase angle ψ_p can be shown to be interrelated.

The data correlation obtained is of course the most meaningful substantiation for using a particular parameter. Plots of pilot rating on the p_{osc}/p_1 vs. $\psi_{p_{STEP}}$ plane are presented in a following section and are the primary substantiation for the requirement revision.

The interrelation between ψ_p and the relative location of the ϕ/δ_a transfer function factors is discussed next.

Consider the following nominal s plane plot of the roll rate transfer function factors for a step input.

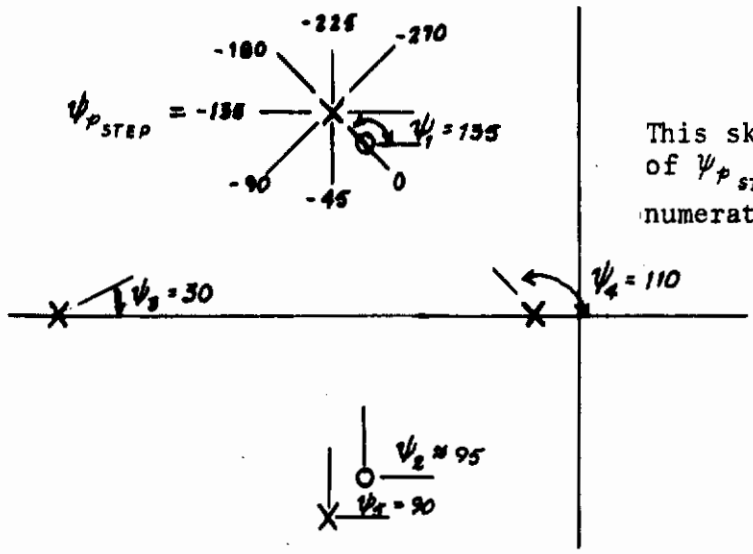

This sketch shows the relationship of $\psi_{p_{STEP}}$ and the location of the numerator zeros.

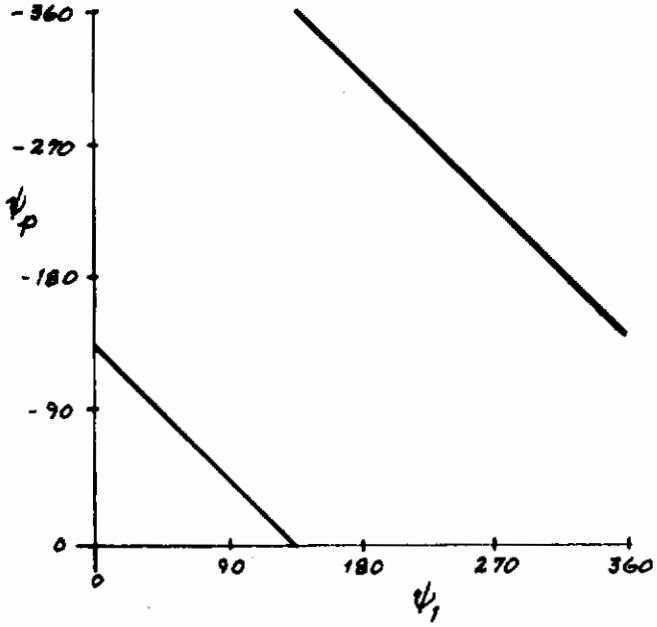

This sketch shows a nominal relation between ψ_p and ψ_1

$$\psi_p = \psi_1 + \psi_2 - \psi_3 - \psi_4 - \psi_5$$

$$= \psi_1 + \psi_2 - 30 - 110 - 90$$

$$= \psi_1 + \psi_2 - 230$$

If the zeros are moved around the Dutch roll pole, ψ_1 ranges from 0 to 360° and ψ_p ranges from 0 to -360°.

With this general orientation in mind it is interesting to see what shift of the zero location would be required to keep ψ_p constant for different roll mode root locations and for different Dutch roll frequencies.

The left hand sketch below illustrates how the zero would have to move for three roll mode root locations to keep ψ_p constant.

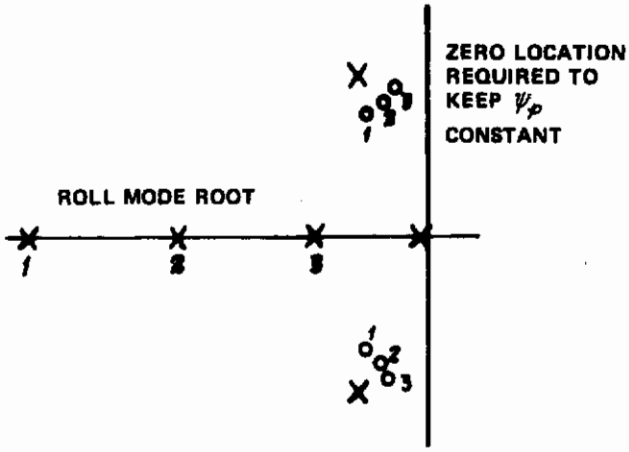

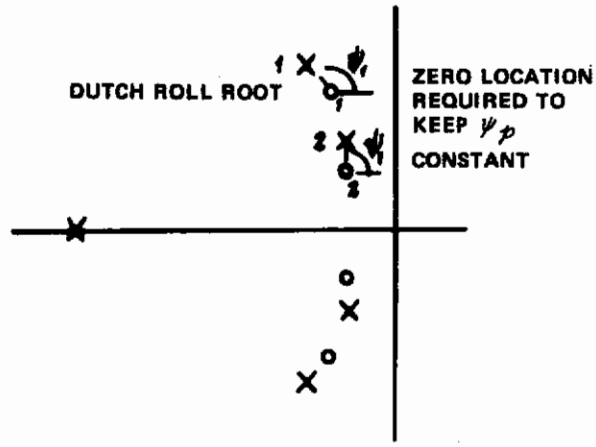

The right hand sketch illustrates how the zero would have to move to keep ψ_p constant for two different Dutch roll frequencies. From these sketches it is seen that as the roll mode root moves toward the origin (less roll damping) the zero must move counter-clockwise around the pole and as the Dutch roll frequency is reduced, the zero must move clockwise around the pole to keep ψ_p constant.

It is also instructive to examine how the departure angle of the Dutch roll root changes as a function of the roll mode root location and the zero location. The departure angle can be computed from the following equation and sketch.

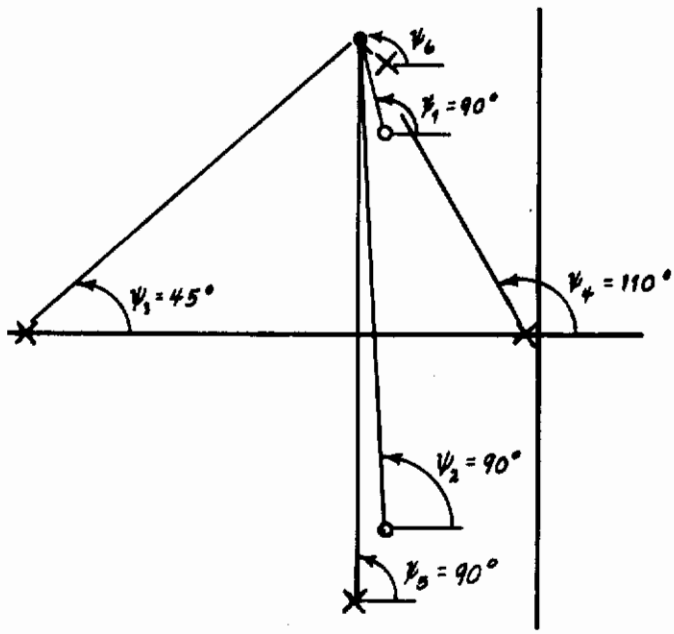

For the point to be on the root locus, it must satisfy the following equation

$$\psi_1 + \psi_2 - \psi_3 - \psi_4 - \psi_5 - \psi_6 = (2n+1)180$$

$$\psi_p - \psi_L = (2n+1)180$$

Assume the following values for the angles

$$90 + 90 - 45 - 110 - 90 - \psi_6 = (2n+1)180$$

$$\psi_6 = -245° \text{ or } 115°$$

Next assume that the roll root is moved toward the origin such that it is at $\lambda_R = \zeta_d \omega_{n_d}$, for example, and $\psi_3 = 90°$. Now solve for the zero location that will keep the departure angle $\psi_6 = 115°$.

$$\psi_6 = \psi_p - (2n+1)\,180 = 115°$$

therefore, $$\psi_p = \psi_1 + \psi_2 - \psi_3 - \psi_4 - \psi_5 = \text{constant}$$

and since ψ_4 and ψ_5 are constant in this example, then $\psi_1 + \psi_2 - \psi_3 =$ constant, and if ψ_3 increases then $\psi_1 + \psi_2$ must also increase. Thus it is seen that as the roll mode root moves toward the origin, the zero must be moved counter-clockwise around the pole to keep the departure angle constant, i.e., $\psi_6 = 115°$ for this example. This is similar to the result obtained when ψ_p was kept constant as the roll damping was reduced. Thus moving the zero counter-clockwise around the pole as the roll mode root moves toward the origin will result in constant ψ_p and constant departure angle of the Dutch roll root locus for ϕ to δ_a feedback. A similar result will be observed for the effect of reducing the Dutch roll frequency, i.e., if the Dutch roll frequency is reduced at constant ζ_d, and the zero is moved clockwise around the pole, the phase angle ψ_p will remain constant and the departure angle of the Dutch roll root will remain constant.

Although these arguments cannot be used as proof that the phase angle ψ_p will correlate the data better than ψ_β, they do illustrate that an erroneous assumption was made in the BIUG about the overriding significance of ψ_1.

In Appendix VC of the BIUG it is recognized that the approximate equations relating ψ_β and ψ_1 become invalid if L'_β is small but it was assumed that when L'_β was small there would not be any problems with bank angle or roll rate oscillations so it didn't matter what the phase angle was. This assumption is not valid unless L'_r is also small. The data in Reference 35 illustrate that the zero of the roll transfer function can be quite far from the Dutch roll pole (i.e. large Dutch roll residue) if L'_r and N'_{δ_a} are large. This situation can exist in the landing approach for a straight wing airplane with high lift devices. For Cases P-1, 2, 3, 4 and S-1, 3, 5 from Reference 35 the value of L'_β was small but L'_r was large. Variations in N'_{δ_a} resulted in the relative locations of the zero and pole illustrated in Figures 86 and 87 from Reference 35. From these figures it can be seen that the zero moves nearly horizontally for variations of N'_{δ_a} when L'_r is large and L'_β is small whereas it moves nearly vertically when L'_β is large and L'_β is small.

The $\angle \frac{p}{\beta}$ for these cases was in the region 180° to 270°.

P-1, 2, 3, 4	$\angle p/\beta = 229°$
S-1, 3, 5	$\angle p/\beta = 243°$

Phase angles in this region were considered improbable in the development in Appendix VC. This is illustrated in Figure 88 (Sketch 4 from the BIUG).

After becoming aware of the above described details, consideration was given to defining a continuous variation of the ψ_β scale in the requirements as a function of $\angle \frac{p}{\beta}$ rather than having two scales shifted by 180°, i.e., $\frac{p_{osc}}{p_{AV}}$ versus $\psi_\beta + f\left(\angle \frac{p}{\beta}\right)$. The following sketch illustrates the idea.

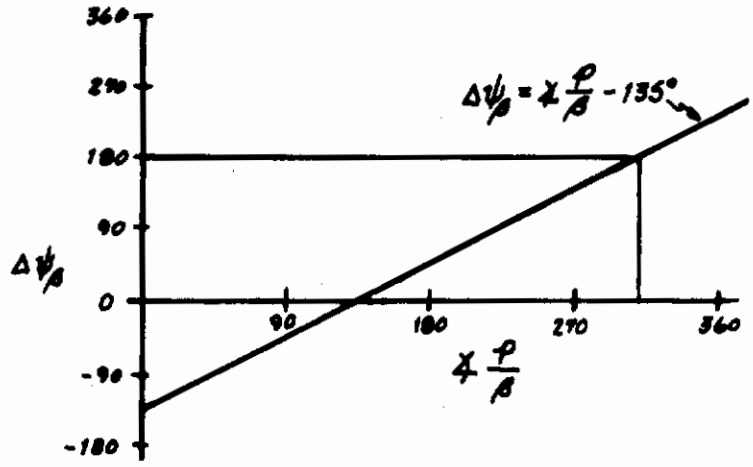

In this case the p_{osc}/p_{AV} requirement would be plotted for

$$\psi_\beta + \Delta\psi_\beta = \psi_\beta + \angle\frac{p}{\beta} - 135°$$

It was recognized, however, that $\psi_p = \psi_\beta + \angle\frac{p}{\beta}$ and therefore ψ_p and ($\psi_\beta + \Delta\psi_\beta$) would be different only by a constant. This of course suggests the use of ψ_p directly in the requirement rather than going to all the complication of measuring both ψ_β and $\angle\frac{p}{\beta}$. This also gets away from the measurement difficulties encountered in trying to measure ψ_β from flight records for configurations with high $|\phi/\beta|_d$. In these circumstances the Dutch roll component of the sideslip trace may be of small amplitude and the trace may exhibit a ramp or non-zero steady state making accurate measurement of ψ_β very difficult.

Because of the above described considerations it was decided to plot the ϕ_{osc}/ϕ_{AV} data vs. $\psi_{\phi_{pulse}}$ and the p_{osc}/p_{AV} data vs. $\psi_{p_{step}}$. The data are discussed in the substantiation section for the revised requirements.

The problem listed as Item 3 at the beginning of this section deals with the distorting effects of the spiral mode on the ϕ_{osc}/ϕ_{AV} and p_{osc}/p_{AV} measurements from time histories. Figure 89 illustrates this effect for a

wide range of stable and unstable spiral modes. Measurement of p_{osc}/p_{AV} from these time histories is not possible in extreme cases because there are no peaks in the time history but even when there are peaks, the measure of p_{osc}/p_{AV} is "distorted" by the spiral effect. This distortion will be a function of the relative characteristic times of the Dutch roll and spiral modes. The p_{osc}/p_{AV} measure for each case is plotted vs. τ_d/τ_s on Figure 90 which shows the sensitivity of the measure for the example time histories of Figure 89. It should be noted that the value of p_{osc}/p_{AV} is increased for stable spiral roots and is decreased for unstable spiral roots. This is the reverse of what one would hope for in that it would encourage permitting the spiral root to be unstable to help pass the p_{osc}/p_{AV} requirement. This problem was considered to be a serious shortcoming of the roll oscillation requirements. For example, many of the configurations in the data of Reference 35 could not be checked against this requirement because of the effect of the unstable spiral root on the time histories. It was decided to investigate ways to eliminate the spiral effect on the time history of roll and roll rate to pulse and step inputs. Initially a factoring method was considered but it was realized that when the Dutch roll root was of low frequency, this method resulted in distortion of the magnitude and phase of the Dutch roll component. Because of this, it was decided to also investigate methods for subtracting the spiral residue from the total time history. The two methods are developed below.

First the factoring approach is illustrated. Consider the general roll rate to aileron transfer function for a step aileron input

$$p(s) = \frac{s(As^2+Bs+C)}{(s+\lambda_s)(s+\lambda_R)(s^2+2\zeta_d\omega_{n_d}s+\omega^2_{n_d})} \quad \frac{\delta_{AS}}{s}$$

Multiply both sides by $\frac{s+\lambda_s}{s}$

$$\hat{p}(s) = p(s) + \frac{\lambda_s}{s}p(s) = \frac{As^2+Bs+C}{s(s+\lambda_R)(s^2+2\zeta_d\omega_{n_d}s+\omega^2_{n_d})}$$

Taking the inverse Laplace transform

$$\hat{p}(t) = p(t) + \lambda_s \phi(t) = \delta_{AS}\left[\hat{K}_{ss} + \hat{K}_R e^{-\lambda_R t} + \hat{K}_D e^{-\zeta_d\omega_{n_d}t}\cos(\omega t + \psi_{\hat{p}})\right]$$

where $\omega = \omega_{n_d}\sqrt{1-\zeta_d^2}$

This approach gives the result that $\hat{p}(t)$ can be calculated by adding the roll rate response to the bank angle response weighted by the value of the spiral root. The Dutch roll component of the response will be modified slightly and

perhaps significantly if the Dutch roll root is low frequency. The method does have some attractive features, however, because the $\hat{p}(t)$ variable can be formed simply by weighting and adding two time histories. If data is on magnetic tape this would be a very simple operation.

If the flight record is processed by the analog matching method described in Appendix VB of the BIUG, the $\hat{p}(t)$ time history could be generated by setting the plot labeled 2 or $1/\tau_s$ in Figure 8 (Appendix VB) to zero after the matching procedure was completed and running another response.

The method for subtracting the spiral mode from the total time history is described below.

Consider the roll rate transfer function for a step input

$$p_s = \frac{s(As^2 + Bs + C)}{(s+\lambda_s)(s+\lambda_R)(s^2 + 2\zeta_d\omega_{n_d} s + \omega_{n_d}^2)} \quad \frac{\delta_{AS}}{s}$$

The time response can be expressed as follows

$$p(t) = \delta_{AS}\left[K_s e^{-\lambda_s t} + K_R e^{-\lambda_R t} + K_D e^{-\zeta_d\omega_{n_d} t}(\cos\ \omega t + \psi_p)\right]$$

Add $K_s\delta_{AS}$ to both sides and subtract $K_s e^{-\lambda_s t}\delta_{AS}$ from both sides

$$p(t) + K_s\left(1 - e^{-\lambda_s t}\right)\delta_{AS} = \delta_{AS}\left[K_s + K_R e^{-\lambda_R t} + K_D e^{-\zeta_d\omega_{n_d} t}\cos(\omega t + \psi_p)\right]$$

This method does not alter the values of K_D or ψ_p but it may not be as easy to calculate as the factoring method. The difference in coefficients for the two methods is indicated by the following expressions.

$$K_s = \frac{A\lambda_s^2 - B\lambda_s + C}{(\lambda_R - \lambda_s)\left[(\zeta_d\omega_{n_d} - \lambda_s)^2 + \omega^2\right]} \qquad \hat{K}_{ss} = \frac{C}{\lambda_R\,\omega_{n_d}^2}$$

$$K_R = \frac{A\lambda_R^2 - B\lambda_R + C}{(\lambda_s - \lambda_R)\left[(\zeta_d\omega_{n_d} - \lambda_R)^2 + \omega^2\right]} \qquad \hat{K}_R = -\frac{A\lambda_R^2 - B\lambda_R + C}{\lambda_R\left[(\zeta_d\omega_{n_d} - \lambda_R)^2 + \omega^2\right]}$$

$$K_D = \frac{A}{\omega}\sqrt{\frac{\omega^2\left(\frac{B}{A} - 2\zeta_d\omega_{n_d}\right)^2 + \left[\frac{C}{A} - \frac{B}{A}\zeta_d\omega_{n_d} + \left(\zeta_d\omega_{n_d}\right)^2 - \omega^2\right]^2}{\left[\left(\zeta_d\omega_{n_d} - \lambda_s\right)^2 + \omega^2\right]\left[\left(\zeta_d\omega_{n_d} - \lambda_R\right)^2 + \omega^2\right]}}$$

$$\hat{K}_D = \frac{A}{\omega}\sqrt{\frac{\omega^2\left(\frac{B}{A} - 2\zeta_d\omega_{n_d}\right)^2 + \left[\frac{C}{A} - \frac{B}{A}\zeta_d\omega_{n_d} + \left(\zeta_d\omega_{n_d}\right)^2 - \omega^2\right]^2}{\left(\zeta_d\omega_{n_d}{}^2 + \omega^2\right)\left[\left(\zeta_d\omega_{n_d} - \lambda_R\right)^2 + \omega^2\right]}}$$

$$\psi_p = \psi_1 + \psi_2 - \psi_3 - \psi_4 - 90 \qquad \psi_{\hat{p}} = \psi_{\hat{1}} + \psi_{\hat{2}} - \psi_{\hat{3}} - \psi_{\hat{4}} - 90$$

$$\psi_1 = \psi_{\hat{1}} \; ; \qquad \psi_2 = \psi_{\hat{2}} \; ; \qquad \psi_4 = \psi_{\hat{4}}$$

$$\psi_3 = 180 - \tan^{-1}\frac{\omega}{\zeta_d\omega_{n_d} - \lambda_s} \qquad \psi_{\hat{3}} = 180 - \tan^{-1}\frac{\omega}{\zeta_d\omega_{n_d}}$$

All the above algebra can be illustrated in the following sketches.

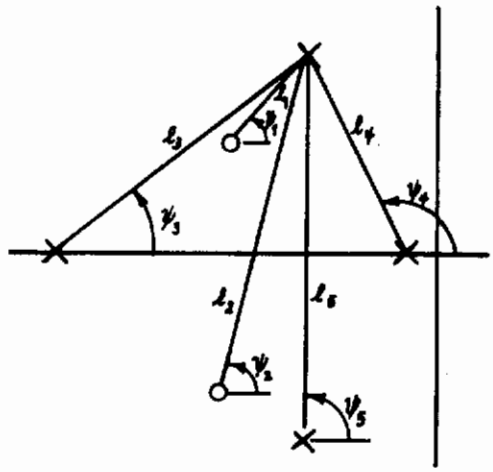

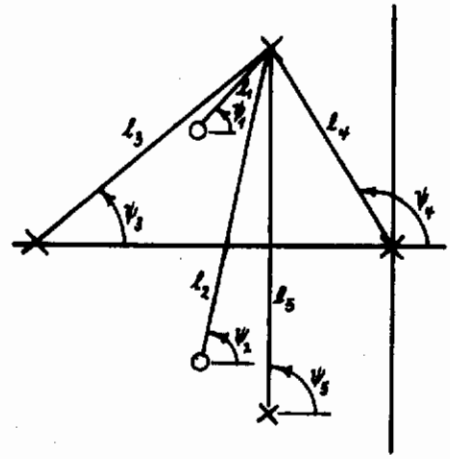

The residue of the Dutch roll mode is the ratio of the products of the directed line segments and the phase angle ψ_p is the sum of the angles ψ_1 through ψ_5 . It can be seen that ℓ_4 and ψ_4 are the only components that are different in the two cases. Thus the factoring approach differs from the subtracting approach by very little if the Dutch roll root is far from the spiral root but the difference can be significant for extreme spiral root locations and low frequency Dutch roll roots.

The discussion in the beginning of Appendix VB of the BIUG describes a graphical method for identifying and subtracting the spiral component from the total time history of roll rate for a step aileron input.

Analytically the reduced time history can be computed from the following equation

$$\hat{p}(t) = p(t) + K_s\left(1 - e^{-\lambda_s t}\right)\delta_{AS}$$

where δ_{AS} represents the magnitude and sign of the control input and K_s is computed from the expression given earlier.

It is recommended that the requirements be stated in terms of measurements taken from the reduced time histories $\hat{p}$ and $\hat{\phi}$ and that the subtraction method be used to obtain the reduced time histories.

In the preceding discussion the phase angle $\psi_{\hat{p}}$ is seen to be the sum of the angles of the lines connecting the zeros to the Dutch roll root minus the angles of the lines connecting the roll, spiral and the conjugate Dutch roll root to the Dutch roll root for which the residue is being evaluated. For a zero damped oscillation $\psi_{\hat{p}_{STEP}}$ can be calculated from the $\hat{p}$ time history by measuring the time to a positive peak and by ratioing this time to the period of the oscillation. When the oscillation is damped, however, the time to the peak will not give the same value of $\psi_{\hat{p}_{STEP}}$ as is obtained through summing angles on the s plane plot. This is because the phase as measured from the s plane and as defined in $e^{-\zeta_d \omega_{n_d} t}\cos\left(\omega t + \psi_{\hat{p}_{STEP}}\right)$ corresponds to the point of tangency between the exponential envelope and the cosine wave in the time history. The point of tangency lags the peak of a damped oscillation by the damping angle $\sin^{-1}\zeta_d$. This phenomenon is discussed in Appendix VB of the BIUG and is illustrated by the following sketch.

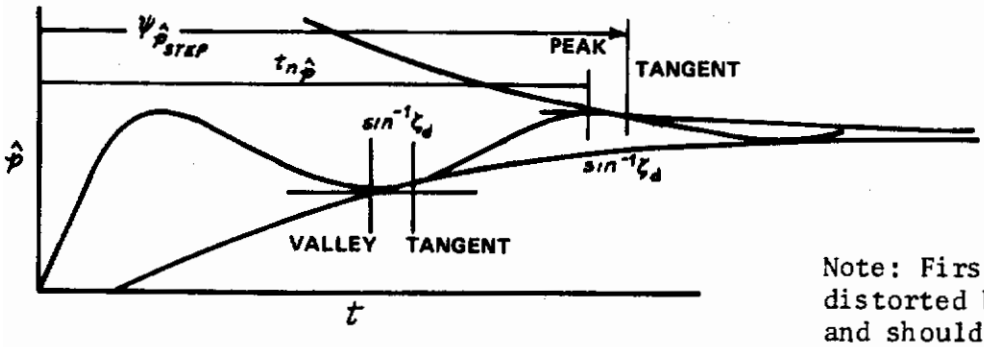

Note: First peak is distorted by roll mode and should not be used to determine $\psi_{\hat{p}}$. Should use peaks after $3\tau_R$.

$$\psi_{\hat{p}_{STEP}} = -\left[360\,\frac{t_{n\hat{p}}}{T_d} + \sin^{-1}\zeta_d\right] + (n-1)\,360$$

It is proposed that the definition of $\psi_{\hat{p}_{STEP}}$ and the corresponding phase angles for other variables be changed to this form so that analytical and time history definitions are consistent.

It was noted in item 6 at the beginning of this section that the shape of the requirement curves in Figures 4 and 5 of MIL-F-8785B are largely a result of the denominator ϕ_{AV} or ϕ_{AV} tending to zero for "adverse yaw" cases. Since the definitions of ϕ_{osc}/ϕ_{AV} and ϕ_{osc}/ϕ_{AV} were empirically established, there is no reason to prevent suggestion of alternate definitions that may be better behaved, i.e., have less difference in value for "proverse" and "adverse" yaw cases. The following alternate definitions are proposed which are graphically illustrated by the following sketch. The spiral residue is assumed to have been removed from the time history.

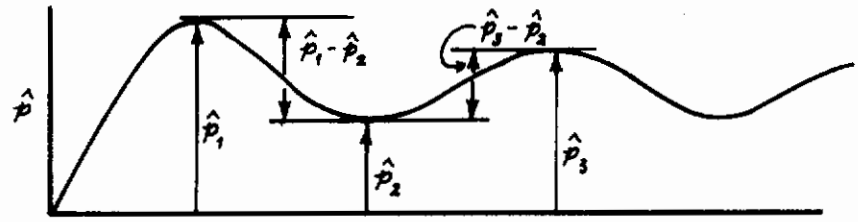

$$\hat{p}_{osc} \equiv \frac{1}{2}\left[(\hat{p}_1 - \hat{p}_2) + (\hat{p}_3 - \hat{p}_2)\right]$$

This definition of $\hat{p}_{osc}$ consists of the average peak-to-valley amplitude of the oscillation measured over one cycle following the first peak. This measure of the oscillatory component is ratioed to the amplitude at the first peak to form the proposed new flying quality parameter $\hat{p}_{osc}/\hat{p}_1$ which

can be written as follows:

For step aileron stick input

$$\hat{p}_{osc}/\hat{p}_1 = \frac{\hat{p}_1 + \hat{p}_3 - 2\hat{p}_2}{2\hat{p}_1} \qquad \text{for all } \zeta_d$$

For impulse aileron stick input

$$\hat{\phi}_{osc}/\hat{\phi}_1 = \frac{\hat{\phi}_1 + \hat{\phi}_3 - 2\hat{\phi}_2}{2\hat{\phi}_1} \qquad \text{for all } \zeta_d$$

$\hat{p}_1$ and $\hat{\phi}_1$ are used as the denominator in the proposed new parameters to get away from the problems caused by p_{AV} going to zero. $\hat{p}_1$ will always be greater than zero for positive aileron stick inputs.

For the reasons noted in item 7 at the beginning of this section, the definitions of the new parameters $\hat{p}_{osc}/\hat{p}_1$ and $\hat{\phi}_{osc}/\hat{\phi}_1$ are based on three peaks for all cases regardless of Dutch roll damping ratio. This definition avoids "discontinuities" or "singularities" that can occur at certain phase angles when the parameters are defined using only two peaks.

The sensitivity of the new parameter $\frac{p_1 + p_3 - 2p_2}{2p_1}$ (note p not $\hat{p}$) to the spiral root not being located at the origin was checked by calculating the value of the parameter from the time histories in Figure 89. The results are plotted on Figure 90 for comparison with the old parameter $\frac{p_1 + p_3 - 2p_2}{p_1 + p_3 + 2p_2}$. It is seen that the new parameter form is much less sensitive to spiral root effects than the old one was. This is a fortunate aspect because for practical values of τ_d/τ_s it may not be necessary to remove the spiral residue from the p time history before evaluating the flying qualities parameters.

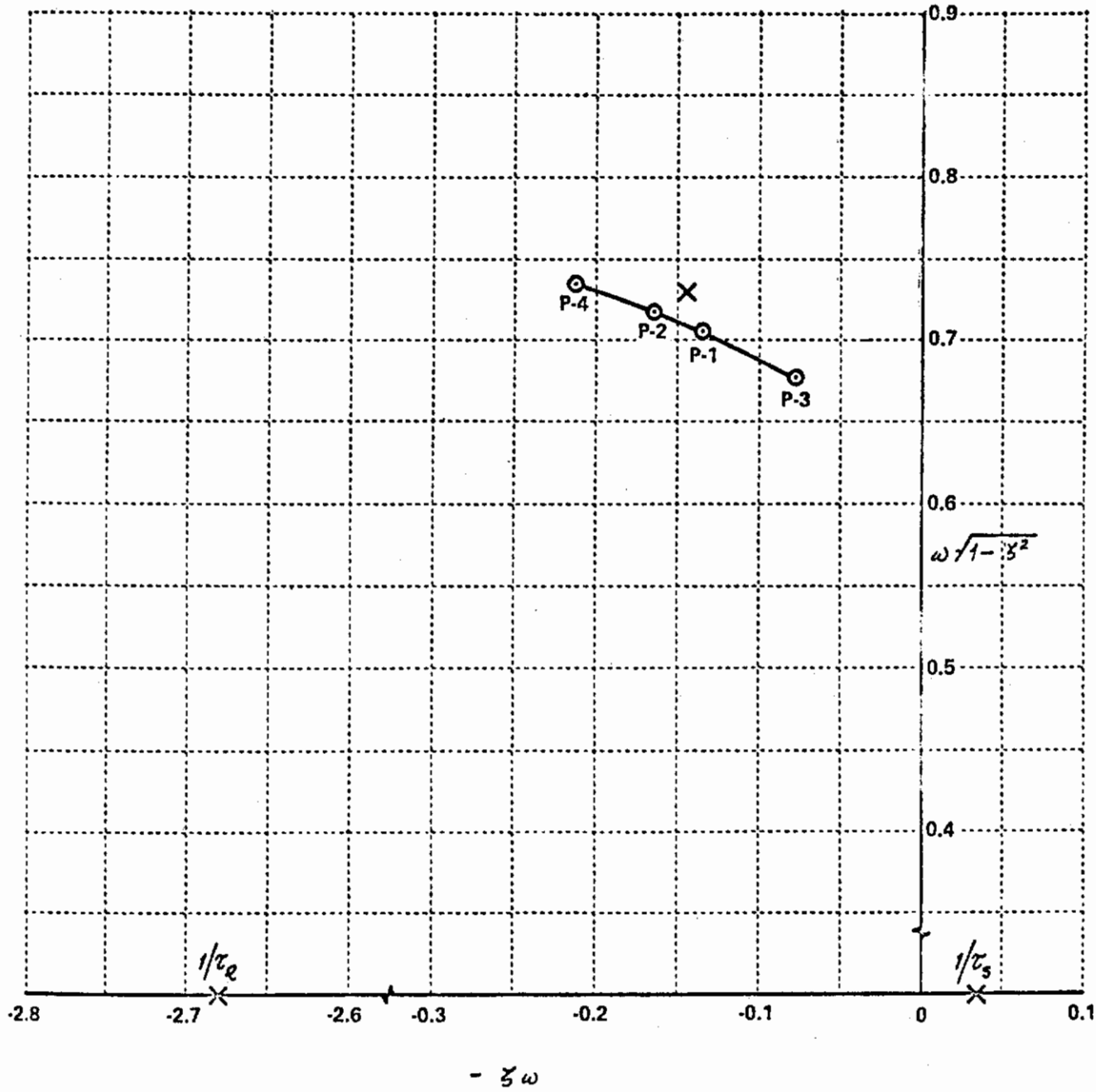

Figure 86 EFFECT OF VARIATIONS IN $C_{n_{\delta_a}}$ ON THE ϕ/δ_a NUMERATOR ZEROS FOR THE BASELINE CONFIGURATION (From Reference 35)

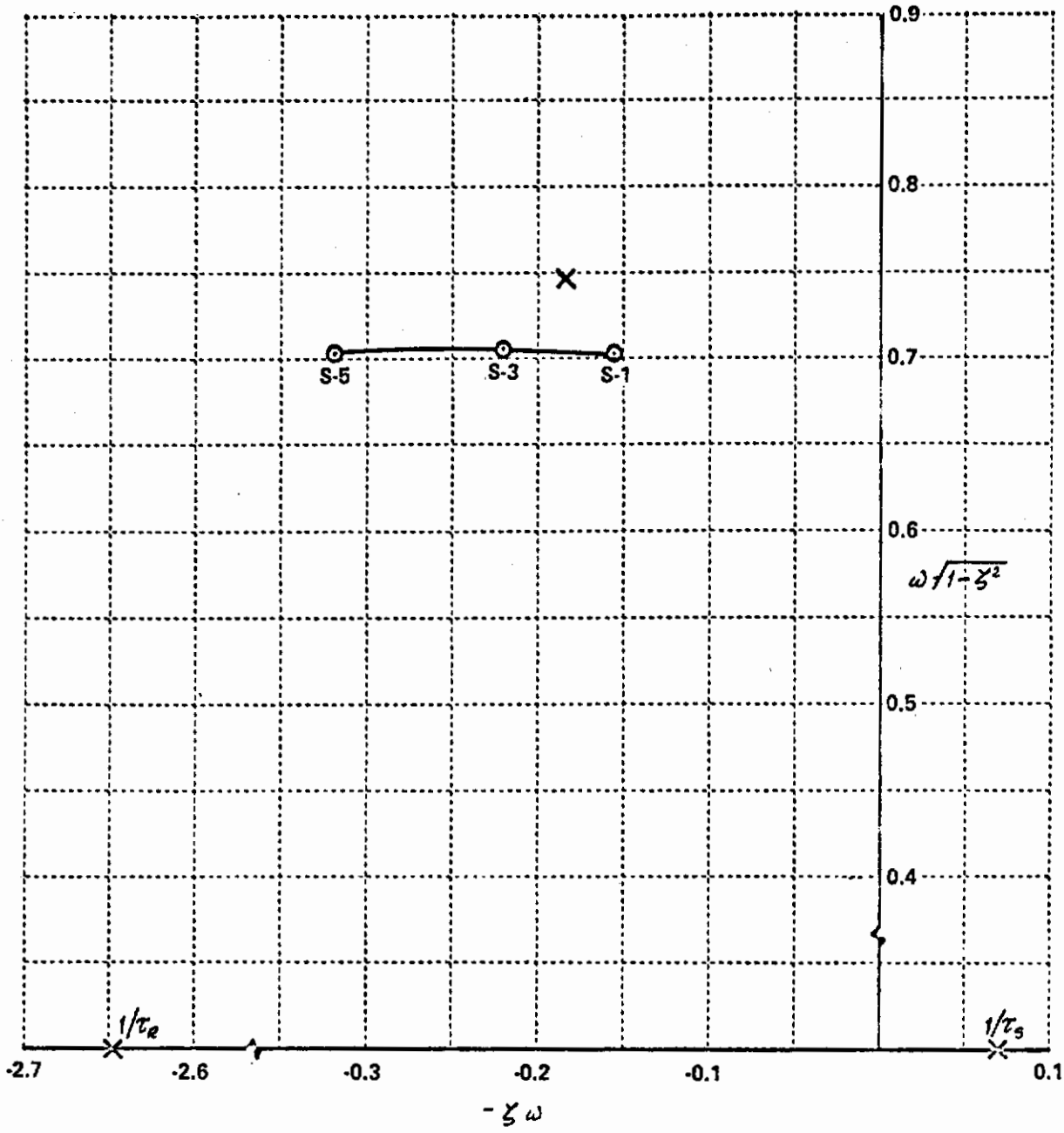

Figure 87 EFFECT OF VARIATIONS IN $C_{n_{\delta_a}}$ ON THE ϕ/δ_a NUMERATOR ZERO FOR THE BASELINE CONFIGURATION WITH INCREASED N'_{δ_a} (From Reference 35)

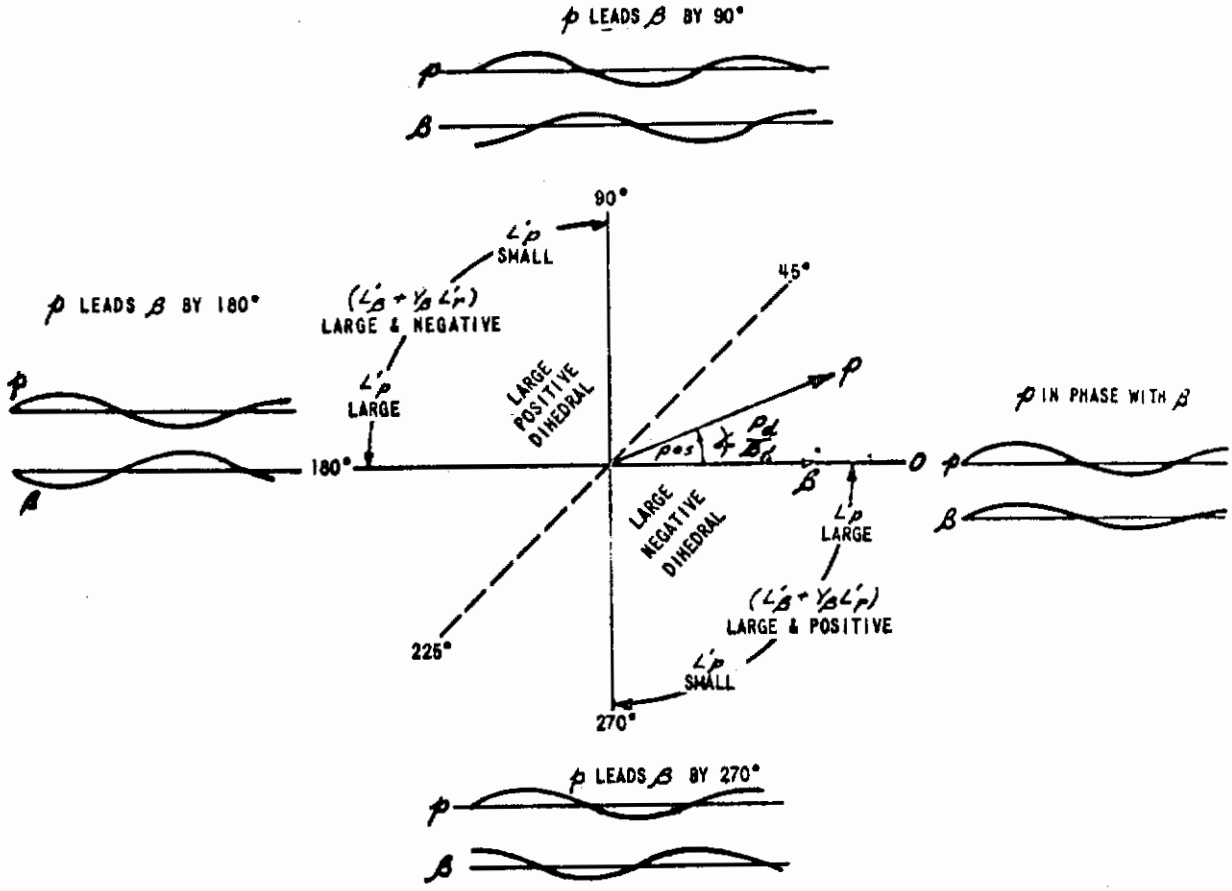

Figure 88 EFFECT OF DIHEDRAL AND ROLL DAMPING ON ROLL-SIDESLIP PHASING IN THE DUTCH ROLL MODE (From REF. 3)

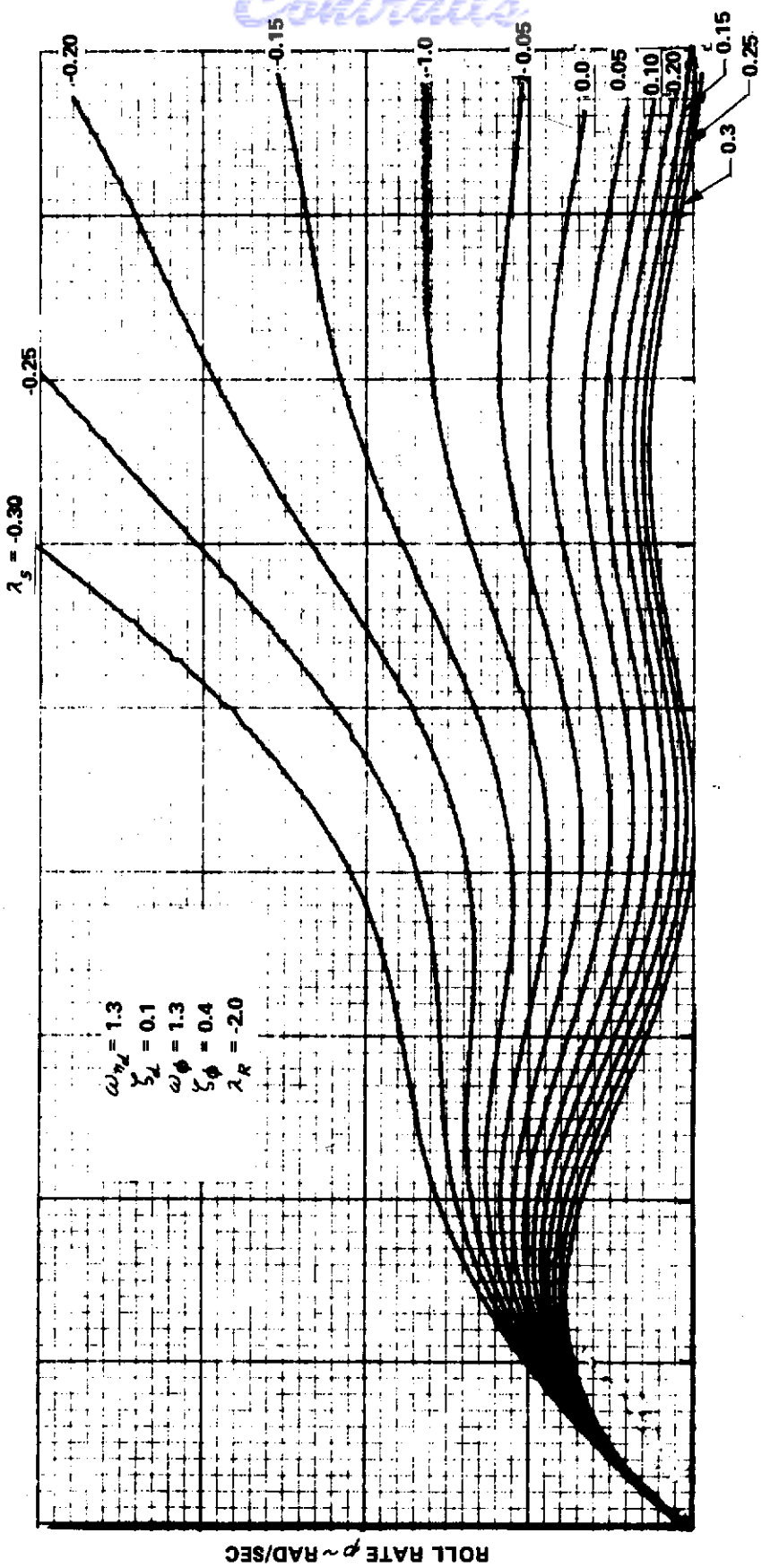

Figure 89 ROLL RATE RESPONSE TO STEP AILERON INPUT FOR STABLE AND UNSTABLE SPIRAL ROOT

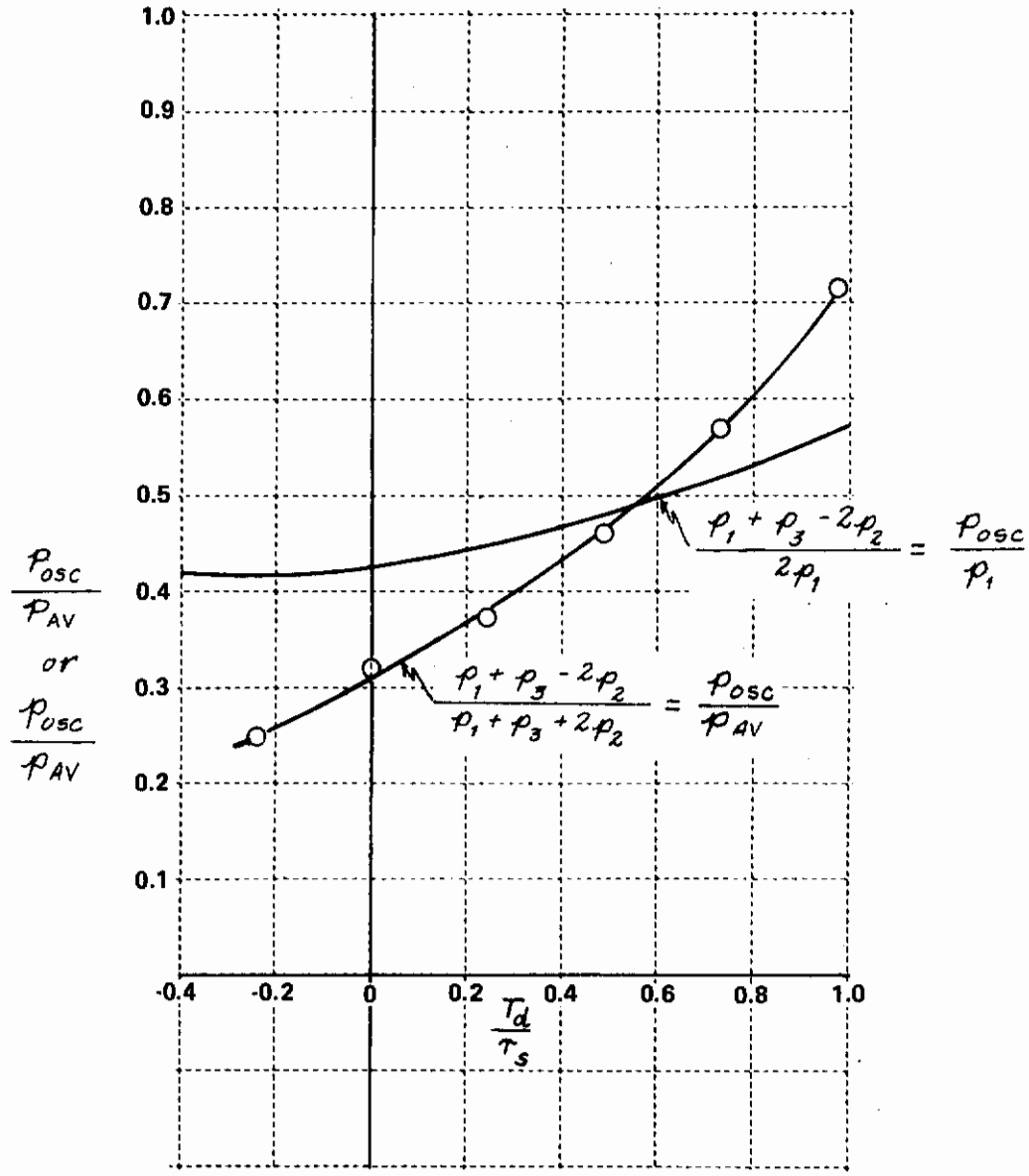

Figure 90 $\frac{P_{osc}}{P_{AV}}$, $\frac{P_{osc}}{P_1}$ **AS A FUNCTION OF THE RATIO OF DUTCH ROLL PERIOD AND SPIRAL ROOT TIME CONSTANT**

Discussion and Substantiation for 3.3.2.2 and 3.3.2.2.1

Lateral-directional data for various Flight Phases and Classes of airplanes are available in the following fifteen reports.

Ref. No.	Report	Author	Flt. Phase Category	Class	Simulation Equipment	Figures	
45	AFFDL-TR-67-98	Meeker-Hall	A	IV	T-33	92	109
46	AFFDL-TR-72-36	Boothe-Parrag	A	IV	T-33	93	110
47	NASA TND-1141	Vomaske-Sadoff	A	IV	F-86	94	111
29	NASA CR-778	Meeker	B	Reentry	T-33	95	112
48	NASA CR-1718	Franklin	B	I	Navion	96	113
36	FAA ADS-69-13	Hall	B	II	T-33	97	114
49	WADC TR-61-147	Harper	B	Reentry	T-33	98	115
50	NASA TND-3910	McNeill-Innis	C	III	Ames-Ground Simulation	99	116
51	NASA CR-2017	Stapelford	C	III	Ames-FSAA	100	117
35	AFFDL-TR-71-164 Vol. 1	Wasserman	C	III	TIFS	101	118
31	AFFDL-TR-70-145	Hall-Boothe	C	II	T-33	102	119
33	NRC LTR-FR-12	Doetsch	C	STOL	H-13	103	120
52	PU 727	Seckel	C	IV or I	Navion	104	121
53	FAA 70-65 Part 2	Ellis	C	I	Navion	105	122
54	FAA 71-118 Part 4	Ellis	C	I	Navion	106	123

In the following paragraphs each report is discussed briefly and the data from each report used in this analysis is identified.

AFFDL TR-67-98

A flight program performed in the T-33 variable stability airplane simulating Flight Phase Category A tasks of a fighter or Class IV airplane. Flight records were matched to identify the stability derivatives listed in the report. Body axis angle of attack was small so rotation of axis system was not necessary. The Cornell rating scale was used. Data is presented for one Dutch roll root with $\zeta_d = .10$. This value does not meet the Level 1 requirement in MIL-F-8785B, however, ratings better than 3.5 were obtained for configurations with small values of yaw due to aileron and yaw due to roll rate. There are fifteen groups of data in this report

consisting of combinations of $\omega_{n_d}, \zeta_d, \tau_R, |\phi/\beta|_d$ and N'_p. In each group several values of yaw due to aileron were evaluated. Groups identified as CB-1, CB-2 and CB-3 have not been included because the pilot comments indicate the roll damping was too low.

AFFDL TR-72-36

A flight program performed in the T-33 variable stability airplane simulating Flight Phase Category A task of Class IV airplanes. Flight records were matched to identify the stability derivatives listed in the report. Body axis angle of attack was small so rotation of axis system was not necessary. Cooper-Harper rating scale was used. Data is presented for five Dutch roll root locations and two values of $|\phi/\beta|_d$. For one Dutch roll root, evaluations were made for a third value of $|\phi/\beta|_d$. For each combination of Dutch roll root and $|\phi/\beta|_d$, several values of yaw due to aileron were evaluated. For two combinations of Dutch roll root and $|\phi/\beta|_d$, both N'_p and $N'_{\delta_{AS}}$ were varied. A small number of configurations with negative dihedral were also evaluated. Groups 6 and 12 are not included because the combination of low Dutch roll damping ratio and high $|\phi/\beta|$ resulted in poor response to turbulence.

NASA TN D-1141

A flight program performed in the F-86 variable stability airplane and a NASA ground simulator. The evaluation task simulated Flight Phase Category A tasks of a Class IV airplane. Stability derivatives listed in the report were estimated. Modal parameters from flight records compare reasonably well with calculated values. Pilot rating data from Figure 5 of the Reference, for various values of yaw due to aileron, have been used for cases with $\zeta_d = .22$ and $\zeta_d = .10$. No angle of attack information is listed but it is estimated that the trim angle of attack at h_p = 10,000 ft and V = 170 kt IAS would be small. The original Cooper scale was used in the experiment.

NASA CR-778

A flight program performed with the T-33 variable stability airplane used both as an in-flight and as a ground based simulator. Flying tasks thought to be representative of re-entry vehicles were simulated. Interpreted here as Flight Phase Category B tasks. The flight data is not completely defined in terms of stability derivatives, but since the ground simulator data shows the same general trends as the flight data, the ground simulator data has been used in this analysis. Only data from Part 1 of this report has been used. The trim angle of attack was small so rotation of the axis system was not necessary. The Cornell pilot rating scale was used in this experiment.

NASA CR-1718

A flight program performed in the Navion variable stability airplane to study turbulence simulation models. The tasks simulated were typical of Flight Phase Category B in a Class I light airplane. The pilot ratings used are the averages for the turbulence models 8, 26, 27, 31 and 52 from that report. The trim angle of attack is assumed to be small. The Cooper-Harper rating scale was used.

FAA ADS-69-13

A flight program performed in the T-33 variable stability airplane to investigate effect of spiral stability on Flight Phase Category B tasks in Class II airplanes. Flight records were matched to identify the stability derivatives listed in the report. The stability derivatives L'_p and L'_ϕ were primary variables used to control spiral and roll modes. Only cases with the spiral root between zero and 0.17 1/sec stable for groups without control system friction have been selected. Trim angle of attack was small. The Cornell pilot rating scale was used in this experiment.

WADC TR-61-147

A flight program performed in the T-33 variable stability airplane. Flying tasks thought to be representative of re-entry vehicles were simulated. Interpreted here as Flight Phase Category B tasks. Stability derivatives were estimated from flight records using the equations of motion method. The following configurations have been omitted from this analysis.

Configuration	Reason
12, 14, 16	Unstable directionally
67-70, 91-94, 99-102	Errors suspected
75-78, 83, 86, 124, 125, 127, 128	Low Dutch roll damping
1, 107, 108, 109	Low control gain
5, 113, 114, 115	High control gain
116-129	Poor short period dynamics
106a, 106b	Pilot rating degraded because of response to random noise input to rudder.

The trim angle of attack was small so rotation of axis system was not necessary. The Cornell pilot rating scale was used in this program.

NASA TN D-3910

A ground simulator program performed at Ames Research Center to study effects of yaw coupling parameters on the lateral-directional handling qualities of a supersonic transport at landing approach airspeed. Variations

were made in N_β, N_r, N_p, and N_{δ_a}. The task simulated was an instrument landing approach. Considered here as Flight Phase Category C for Class III airplanes. The pilot ratings of pilots A and B were averaged using the ratings given for control using aileron and rudder. The original Cooper rating scale was used in this program. The trim angle of attack listed in the report for the ground simulation was 4 degrees, therefore this data should be transformed to stability axes before calculating the flying qualities parameters involving yaw rate. This was not accomplished in this study, however, the effect on roll oscillation and sideslip parameters should be negligible.

NASA CR-2017

A ground simulator program performed by Systems Technology Inc. on the NASA Ames FSAA facility. The program was directed at flying qualities of space shuttle orbiter vehicles in the terminal flight phase. Considered here as Flight Phase Category C for a Class III airplane. The pilot ratings for all pilots were averaged using rating for evaluations made using both rudder and aileron for control. The Cooper-Harper rating scale was used in this program. The data are presented in primed dimensional form referenced to stability axes. The emphasis of the program was on factors affecting heading control in the approach.

AFFDL-TR-71-164, Vol. 1

A flight program performed in the TIFS variable stability airplane. The program was performed to evaluate the lateral-directional landing approach characteristics of design variations of the B-1 airplane. Considered here as Flight Phase Category C for a Class III airplane. The pilot ratings from the various pilots were averaged for each configuration. The Cooper-Harper rating scale was used in this program. The trim angle of attack was small so the data can be considered to be in stability axes. The configurations consisted of variations of C_{l_r}, C_{n_p}, $C_{n_{\delta_a}}$ and C_{n_β}. Configurations with low C_{l_β} and high C_{l_r} resulted in unstable spiral mode and unusual phase relation of roll rate and sideslip in the Dutch roll mode.

AFFDL TR-70-145

A flight simulation experiment performed in the T-33 variable stability airplane. The program was performed to evaluate lateral-directional flying qualities for Class II airplanes in the landing approach. Emphasis was placed on crosswind approaches. The data is considered as Flight Phase Category C for a Class II airplane. The Cooper-Harper pilot rating scale was used in this program. Flight records were matched to identify the stability derivatives listed in the report. The trim angle of attack was large enough that the data should be transformed to stability axes for analysis of

flying qualities parameters involving yaw rate. This was not done in this analysis. All data were analyzed except groups 1, 3 and 8 which had low Dutch roll damping ratio. Also data for configurations with limited roll control authority were not considered in this analysis. The pilot ratings used were "averaged" values taken from smooth curves faired through the data for evaluations using the wheel controller.

NRC-LTR-FR-12

A flight simulation program performed in the variable stability H-13 helicopter. The program was performed to evaluate lateral-directional flying qualities for a 6 degree approach path at STOL approach speed V=50 kt IAS. The data is considered as Flight Phase Category C for a STOL airplane of undefined class. The interim Cooper-Harper rating scale was used in this experiment. The data are listed in stability axes. The 52 configurations selected for analysis are cases with

$$\omega_{n_d} = 1.0 \text{ and } 0.5 \text{ rad/sec}$$

$$\zeta_d = 0.1,\ 0.2,\ 0.3$$

$$|\phi/\beta|_d = 0.2$$

Extreme values of the stability derivatives N'_p and $N'_{\delta_{AS}}/L'_{\delta_{AS}}$ were evaluated in this program. Configurations with values of $|\phi/\beta| = .75$ and 1.5 were not included in this analysis because the pilot ratings for these configurations reflect the lack of sufficient roll control authority to counter the simulated crosswind and turbulence. The stability derivatives listed in the report are referenced to stability axes.

Princeton University Report 727

A flight simulation experiment performed in the Navion variable stability airplane. The program was performed to evaluate lateral-directional flying qualities for the landing approach of carrier based airplanes with closure speed of V = 105 kt IAS. The data is considered as Flight Phase Category C for a Class IV or I airplane. The original Cooper scale was used in this program. The data is listed as dimensional stability derivatives for stability axes. The following configurations were analyzed: 1-23, 53, 65, 75, 81-84, 86, 101-104, 106-110, 112, 113, 115-123, 126-128, 130, 132-134.

FAA 70-65 Part 2 and FAA-7-118 Part 4

Flight simulation experiments performed in the Navion variable stability airplane. The programs were performed to evaluate lateral-directional flying qualities for the landing approach of light airplanes. The data is considered as Flight Phase Category C for a Class I airplane.

The Cooper-Harper rating scale was used in these programs. The data is listed as dimensional stability derivatives for stability axes.

Data from these references have been analyzed in the current program and are presented in the following discussion. The stability derivative data in each report was used together with the equations of motion to compute time histories of ϕ, p, r, $\dot{r}$, β and $\dot{\beta}$ for a step aileron input. The resulting time histories were used to calculate the values of the various flying qualities parameters discussed in the Motivation and Background Section for 3.3.2. The flying qualities parameters calculated are listed in tables contained in Appendix III.

The data for $\hat{p}_{osc}/\hat{p}_1$ versus $\psi_{p\ STEP}$ are presented in Figures 92 through 106. The data in this form are identical with what would be obtained for $\hat{\phi}_{osc}/\hat{\phi}_1$, versus $\psi_{\phi\ IMPULSE}$ if an ideal impulse input had been used. The step input was used because some of the requirements in MIL-F-8785B (ASG) are based on roll rate and sideslip responses to a step aileron input. By using a step input and recording ϕ, p, r, $\dot{r}$, β and $\dot{\beta}$, all the proposed measures can be made on the resulting time histories.

Figure IV-12 from Reference 53 is reproduced here as Figure 91 to illustrate the effect on p_{osc}/p_{AV} of removing the spiral component from the roll rate time history and then calculating $\hat{p}_{osc}/\hat{p}_{AV}$. The two low frequency configurations, 1 and 13, which had stable spiral roots are affected by the removal of the spiral root component. Both points move into regions of better correlation as a result. The two points labeled "1" in Figure 91 have the same value of $\psi_{\beta\ STEP}$ but they have different values of $\psi_{p\ STEP}$. The high frequency configuration has $\psi_{p\ STEP}$ =-127° and the low frequency configuration has $\psi_{p\ STEP}$ =-101°. This difference in phase angle causes the points to be separated on Figure 105 which permits discerning between them in the $\hat{p}_{osc}/\hat{p}_1$ vs $\psi_{p\ STEP}$ parameter plane. This example is cited to illustrate the differences between the proposed requirement and the requirement in MIL-F-8785B(ASG).

The proposed requirement boundaries drawn on Figures 92 to 106 were established through iterative trials with attention given to the data in each separate experiment and in many cases to individual data points and the associated pilot comments. The data for $\hat{p}_{osc}/\hat{p}_1$ and the data for the sideslip parameter, $V_T/g\ \ 1/\omega_{n_d}\ \Delta\beta_{MAX}/\hat{\phi}_1$, must be considered simultaneously in determining the best boundaries. This is because the individual boundaries on a given parameter plot are necessary conditions but they are not sufficient conditions. For example, all the data in Reference 53 fall within the Level 1 sideslip excursion requirement boundary on Figure 122 even though some points are rated PR = 6.5 or 7. This is perfectly alright because the problem in these cases was not the magnitude of sideslip generated but rather the roll oscillation and bank angle control problem. These points violate the $\hat{p}_{osc}/\hat{p}_1$ boundaries and are properly screened out by that requirement.

Overall the correlation is considered to be quite good, especially when it is observed that data for V = 84 ft/sec to 586 ft/sec is included from simulation experiments performed in a variety of simulation facilities and for a variety of cockpit locations and aircraft classes.

In the following paragraphs the data will be discussed in three sets associated with each of the three Flight Phase Categories A, B and C. No attempt was made to further subdivide the data and requirements as a function of airplane Class because there is insufficient data for the various Classes of airplanes.

It was found that the $\hat{p}_{osc}/\hat{p}_1$ data from experiments for Flight Phase Categories A and C could be fit with common boundaries. The data for $\hat{p}_{osc}/\hat{p}_1$ from experiments for Flight Phase Category B was barely adequate to define the Level 1 boundary. The suggested Level 2 boundary is arbitrarily shaped like the Level 2 boundary for Flight Phase Categories A and C. The maximum amplitude permitted for adverse yaw cases was arbitrarily limited to $\hat{p}_{osc}/\hat{p}_1 = 1.0$ for Flight Phase Category B Level 2.

The shape of the $\hat{p}_{osc}/\hat{p}_1$ boundaries is primarily a result of $\hat{p}_1$ being smaller for $\omega_\phi < \omega_{n_d}$ and $\hat{p}_1$ being larger for $\omega_\phi > \omega_{n_d}$. Because $\hat{p}_1$ is in the denominator of the parameter $\hat{p}_{osc}/\hat{p}_1$ it has the effect of increasing the magnitude of the ratio for cases with $\psi_{p\,STEP}$ near -90° and it decreases the magnitude of $\hat{p}_{osc}/\hat{p}_1$ for cases with $\psi_{p\,STEP}$ near -270°. Explanation of the detail differences in the requirement boundaries for the different Levels and Flight Phase Categories requires more involved arguments. For example, the difference between the Level 2 and Level 1 boundaries for $\psi_{p\,STEP} = -270°$ is much less than the difference between the boundaries for $\psi_{p\,STEP} = -90°$. This is because pilots find the rudder activity required to keep sideslip constrained is very complex for $\psi_{p\,STEP} = -270°$, whereas for $\psi_{p\,STEP} = -90°$ the sideslip can be controlled through "normal" rudder usage, i.e., essentially a stick to pedal interconnect. As a result the difference between the Level 1 and 2 boundaries for $\psi_{p\,STEP} = -270°$ reflects only the decrease in bank angle control precision that the pilot is willing to accept when controlling the airplane with aileron only. The difference between the Level 1 and 2 boundaries for $\psi_{p\,STEP} = -90°$ is a reflection of the fact that the pilot can compensate for roll-sideslip coupling and yaw due to aileron by "coordinating" rudder with aileron.

The Level 1 boundary for Flight Phase Category B crosses the Level 2 boundary for Flight Phase Categories A and C in the region of $\psi_{p\,STEP} = -270°$. This is a reflection of the differences in the task requirements for rapid and precise bank angle control. The configurations with $\psi_{p\,STEP}$ near -270° are down graded because of the control difficulties that result when aggressive and precise bank angle control is attempted. If the airplane can be flown in more gradual maneuvers and without the need for precise bank angle tracking the configurations with $\psi_{p\,STEP}$ near -270° are more acceptable.

A number of data points in References 45 and 46 (Figures 92 and 93) do not correspond exactly with the proposed requirement boundaries. These points are listed below along with observations that tend to account for the discrepancies.

Reference 45 AFFDL TR-67-98 Meeker-Hall

Case IBM Sheet	P. R.	Report Configuration	Comment
19	7	AB-1-5	Calculated sideslip response for step aileron is somewhat smaller than the flight record.
20	8	AB-1-6	
35	8	AB-3-6	Calculated time history for β & r is not real good match. Flight record sideslip is larger than the computed value.
38	7	BB-1-3	Rating inconsistent with rest of BB-1 group. Should be $\approx$ 5.0.
41	8	BB-1-6	No obvious reason other than variability. This one is very close to boundary.
54	7	BB-2-5	
65	7	CB-1-4	The CB-1, 2 and 3 groups do not satisfy Dutch roll damping requirement for cases with high $\lvert\phi/\beta\rvert$ and ω_{n_d}. ζ_d should be greater than .24 for Level 2 according to new requirements in 3.3.2.1.1.
71	8	CB-2-4	
74	8	CB-3-4	
48	5	BA-2-7	The BA-1, 2 and 3 sets have quite high roll damping which helps to counter the roll disturbances from sideslip whether from random inputs or pilot rudder miscoordination. These groups are well under the Level 1 boundary in Figure 81.
97	5.5	BA-3-4	

Reference 46 AFFDL TR-72-36 Boothe-Parrag

Case IBM Sheet	P. R.	Report Configuration Group	Comment
111	7	1(+.09)	Very close to boundary. Pilot debated rating 6.5.
148	7	7(-.20)	Down rated because of roll and yaw response to turbulence and inability to coordinate the fast Dutch roll, ω_{n_d} =4.3 rad/sec. May indicate simple division by ω_{n_d} in the sideslip parameter is not adequate.

Reference 46 AFFDL TR-72-36 Boothe-Parrag (Cont.)

Case IBM Sheet	P.R.	Report Configuration Group	Comment
152	8	8(-.05)	Pilot comments lost. Sideslip control was major problem, point is fairly close to Level 2 boundary of Fig. 110. Gradient of pilot rating with $N'_{\delta_{AS}}/L'_{\delta_{AS}}$ is very steep as indicated in Fig. 16 of Ref. 46.
167 176	7 7	11(+.08) 11B(+.08)	Initial impression was not too bad but tight roll attitude control leads to roll oscillations that could not be coordinated with the rudder. These ratings must be weighed against favorable ratings obtained in Ref. 45 for the same phase angle $\psi_{p_{STEP}}$. The data in Fig. 31 of Ref. 46 suggest these two points may have been rated severely.
182 187	7 8	13(-.10) 13(.12)	Does not meet the Level 1 Dutch roll damping ratio required by new paragraph 3.3.2.1.1 $\zeta_d = .24$ rather than $\zeta_d = .43$. Bank angle control in turbulence was major problem.
155 161	4 4	8(+.02) 9(+.06)	Both these configurations have a low frequency Dutch roll and small proverse yaw due to aileron. The proverse yaw causes the Dutch roll mode to be phased so the sideslip is initially proverse. The residue of the spiral mode causes the sideslip to grow in the adverse direction. The net result is that aileron inputs do not cause much sideslip initially and the adverse sideslip that grows after a time is relatively easy to control with "normal" rudder application. The rating of case 161 is inconsistent with other ratings in Group 9 of Ref. 46. P.R. = 5.5 would be more consistent.

Reference 47 NASA TND-1141 Vomaske-Sadoff

Case IBM Sheet	P.R. Cooper	Report Configuration	Comment
190	6	ζ_d =.22, N_{δ_a} = 2.31	Note that the original Cooper rating scale was used in this experiment. The boundary between the square symbol and the delta symbol on the pilot rating plots was defined to be P.R. = 5.5 for the original Cooper scale. It could be argued that the division should be at P.R. = 6.0 in which case the delta symbols would be squares on Figures 94 and 111 and the correlation would be improved.
194	6	ζ_d = .10, N_{δ_a} = 2.31	

The above review of individual configurations is presented as an example of the attention to detail that is necessary in arriving at the "best fit" set of requirement boundaries. Similar attention has been given to the data in the other references in arriving at the recommended requirement boundaries indicated on Figures 4 and 5 of the proposed revision.

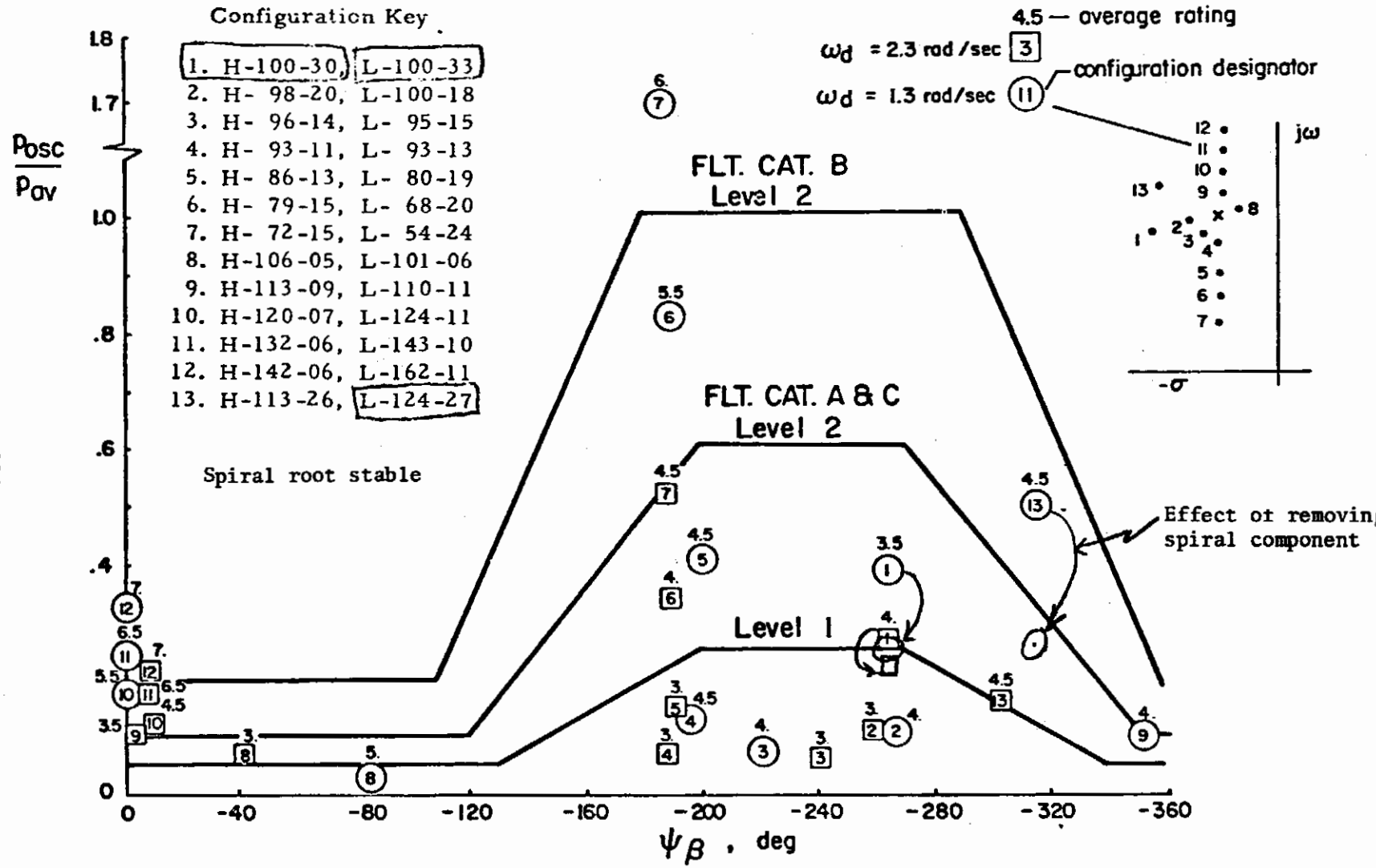

Figure 91 DATA COMPARISON WITH MIL-F-8785B (ASG) ROLL RATE OSCILLATION LIMITATIONS (Figure IV-12 of Reference 33)

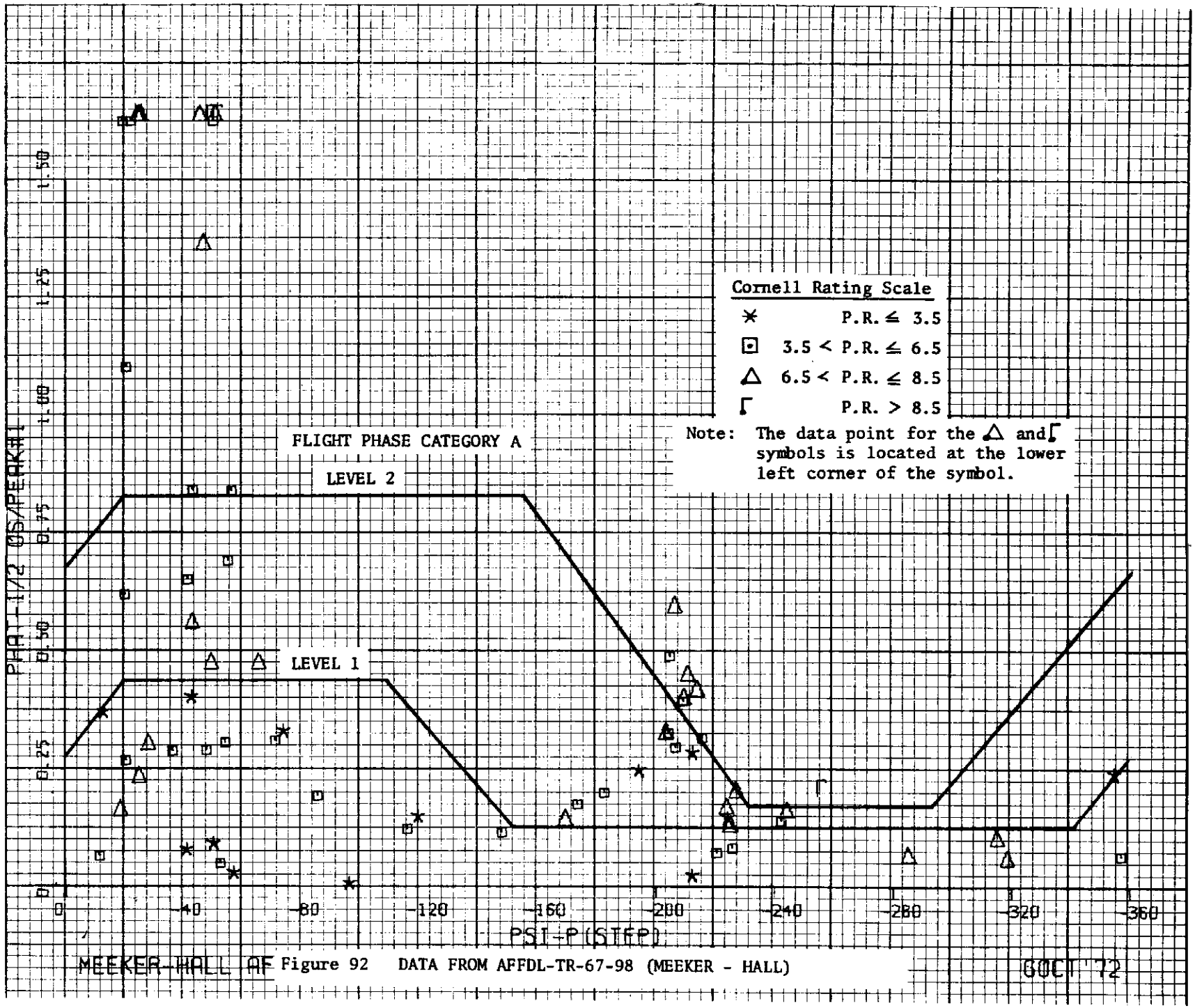

MEEKER-HALL AF Figure 92 DATA FROM AFFDL-TR-67-98 (MEEKER - HALL) 60CT 72

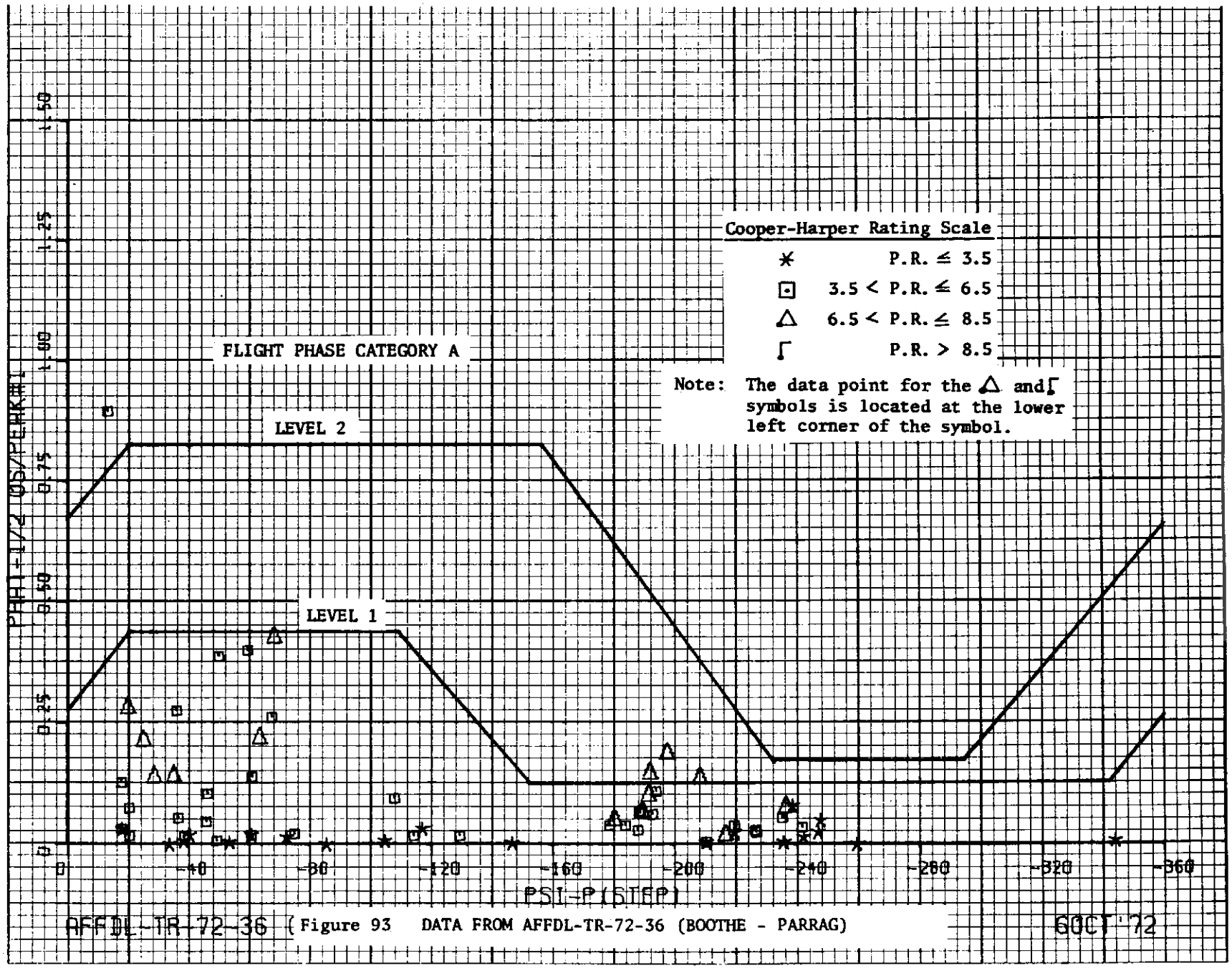

AFFDL-TR-72-36 (Figure 93 DATA FROM AFFDL-TR-72-36 (BOOTHE - PARRAG) 60CT 72

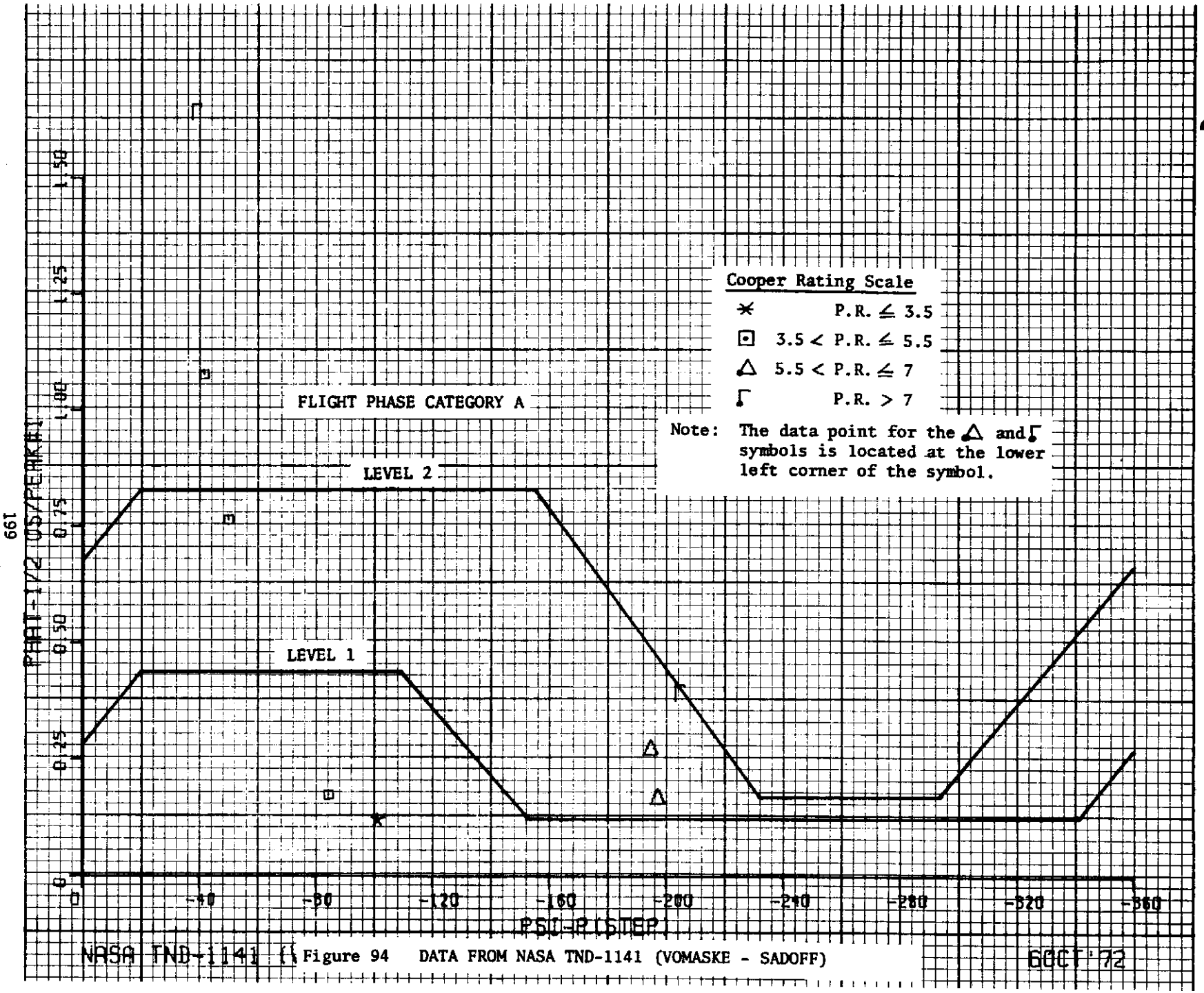

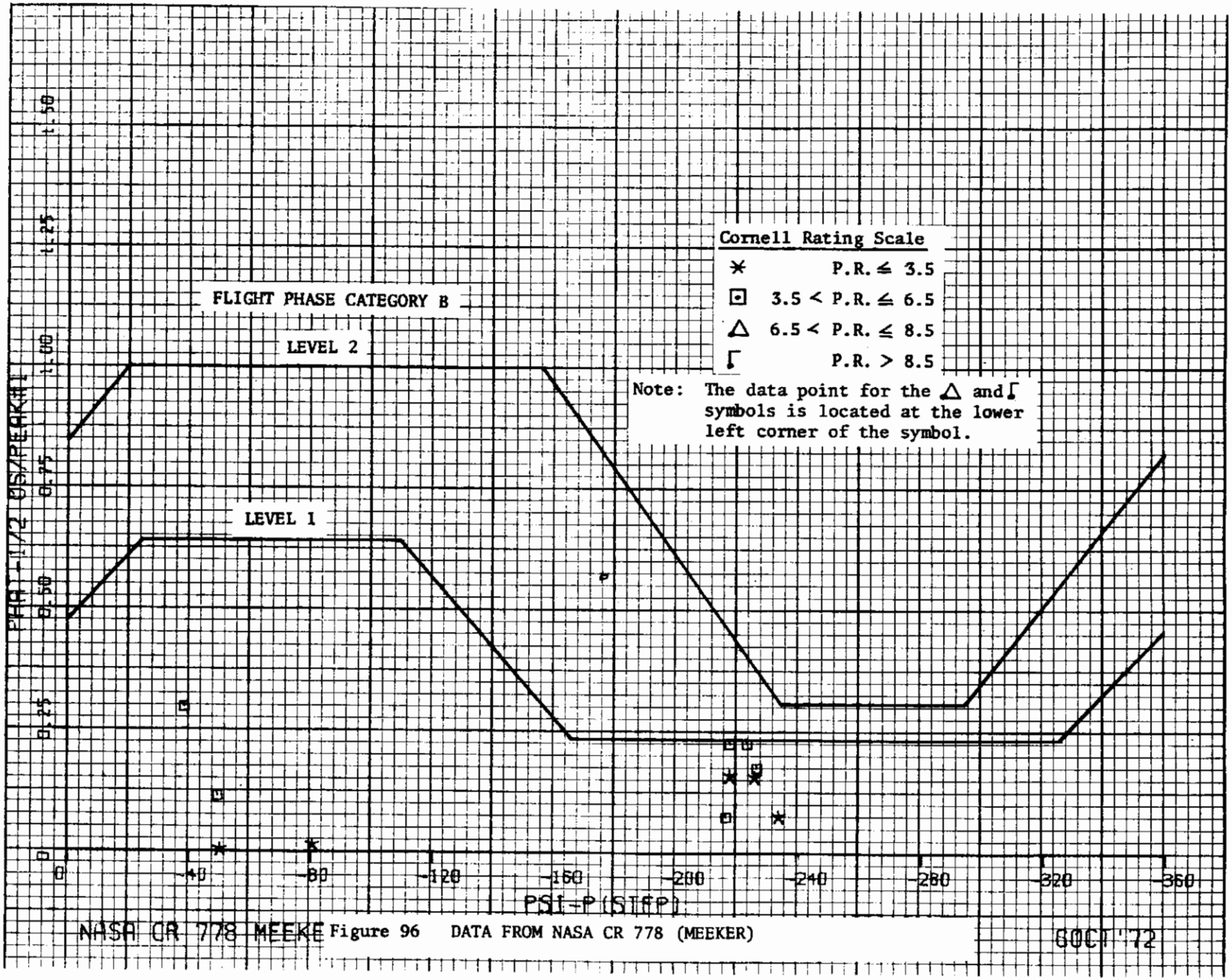

Figure 96 DATA FROM NASA CR 778 (MEEKER)

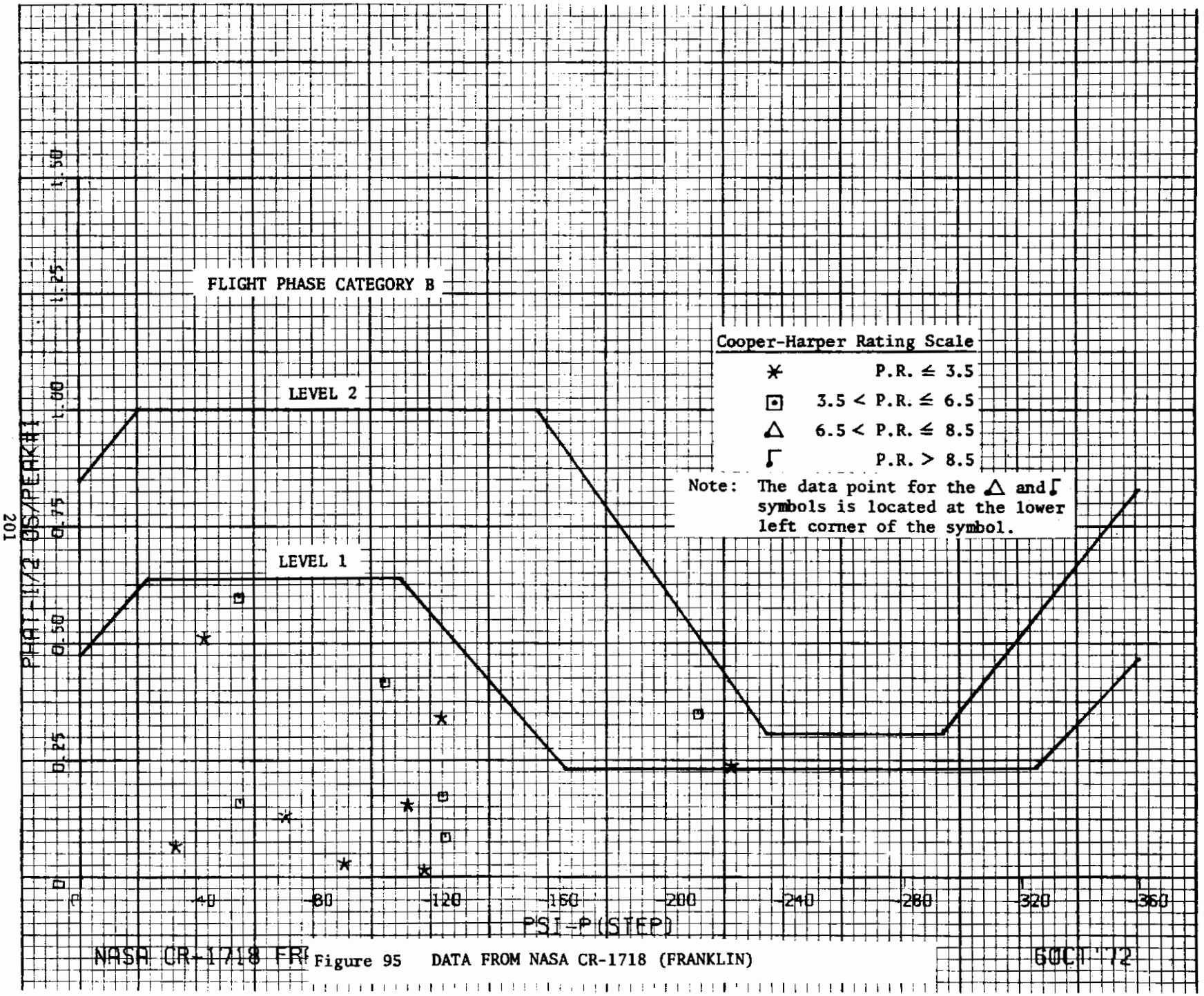

Figure 95 DATA FROM NASA CR-1718 (FRANKLIN)

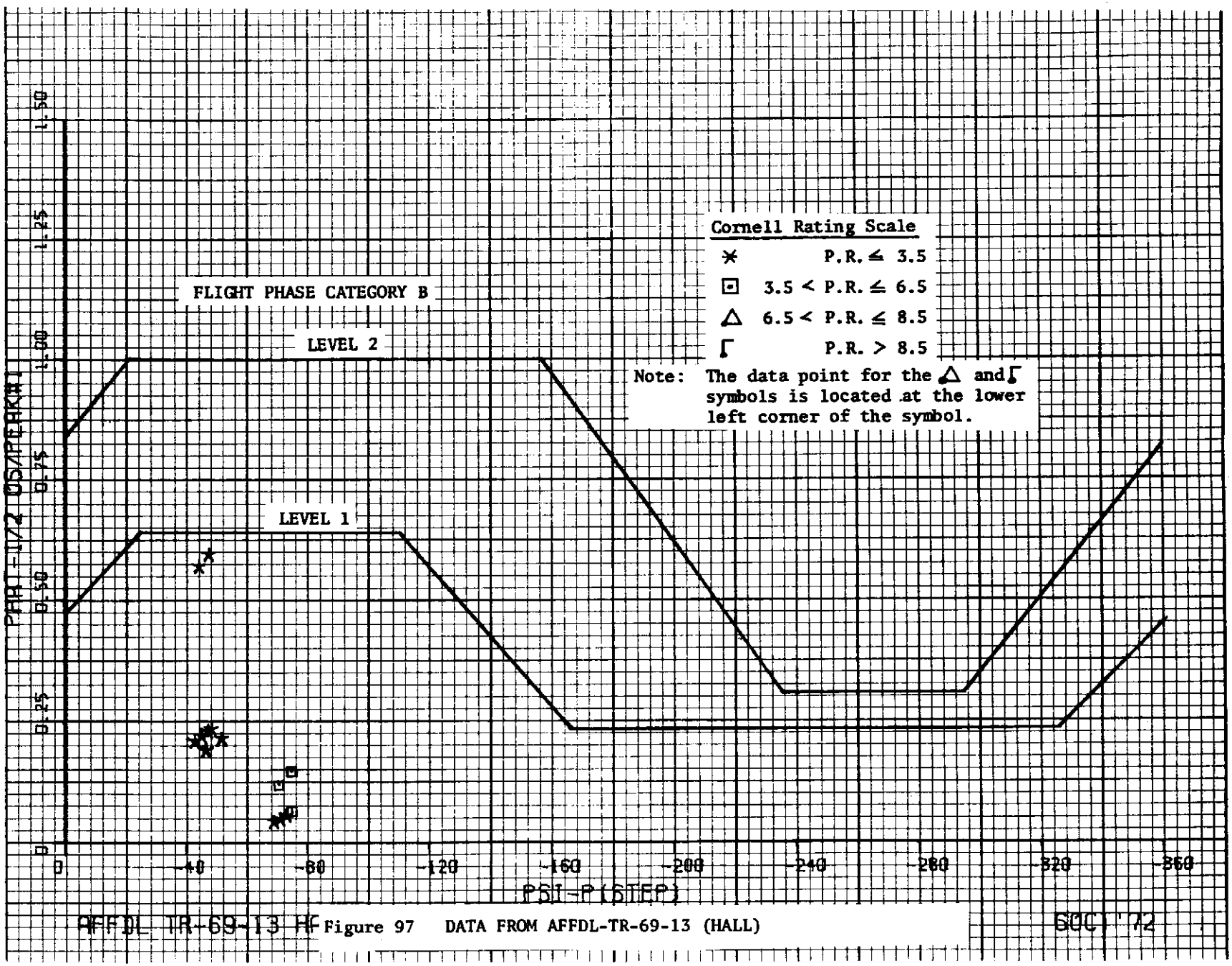

AFFDL TR-69-13 HF Figure 97 DATA FROM AFFDL-TR-69-13 (HALL)

SCC '72

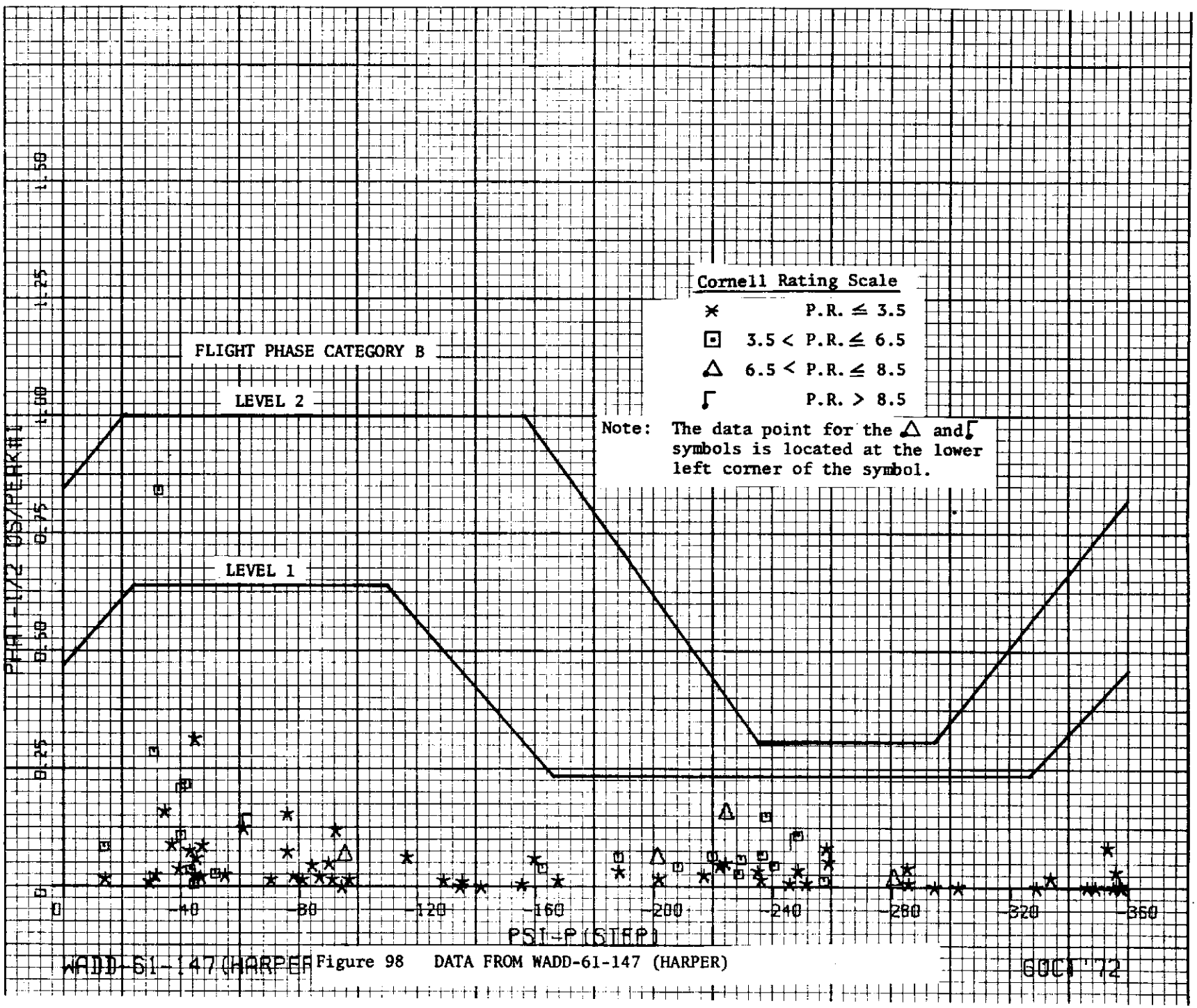

Figure 98 DATA FROM WADD-61-147 (HARPER)

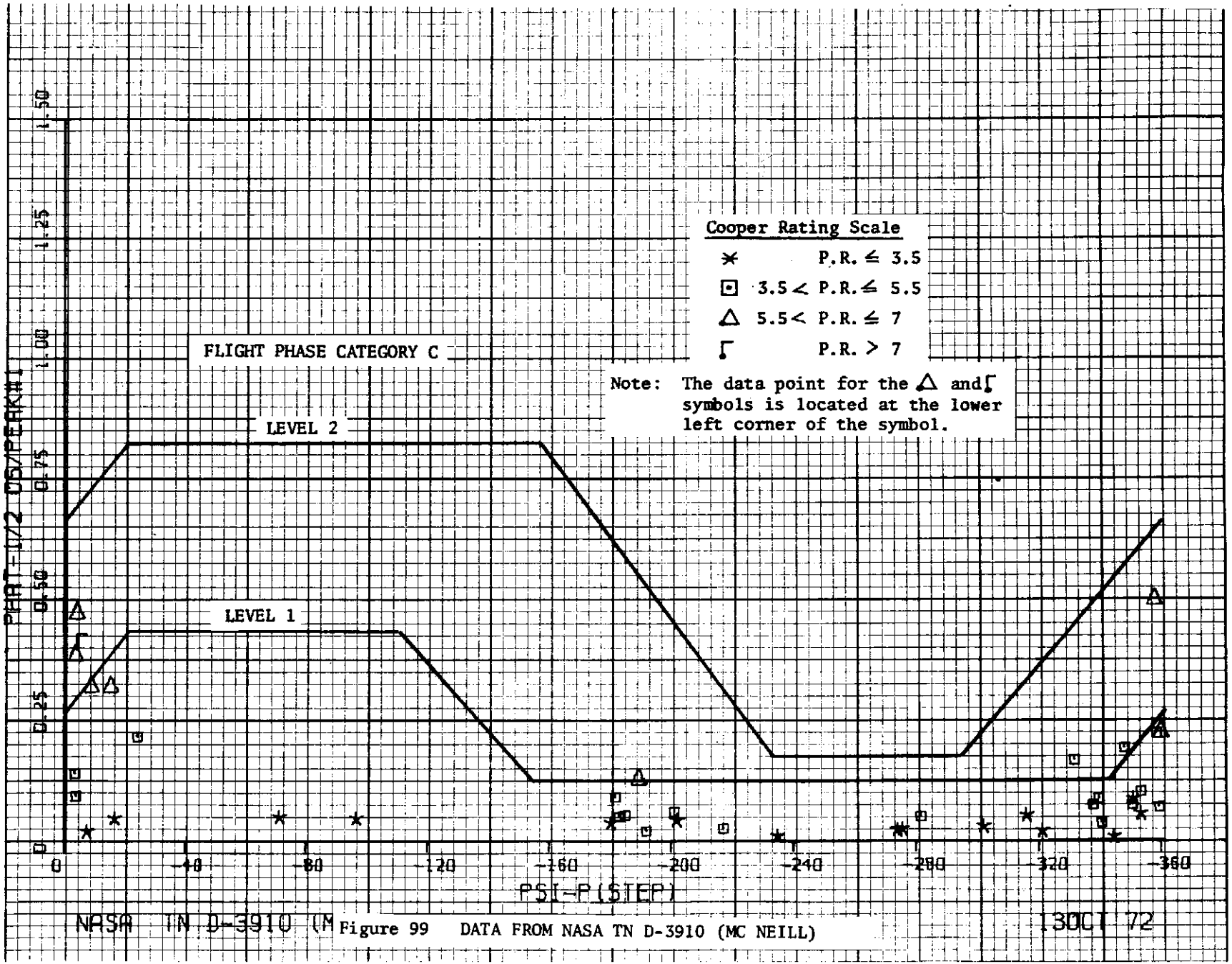

Figure 99 DATA FROM NASA TN D-3910 (MC NEILL)

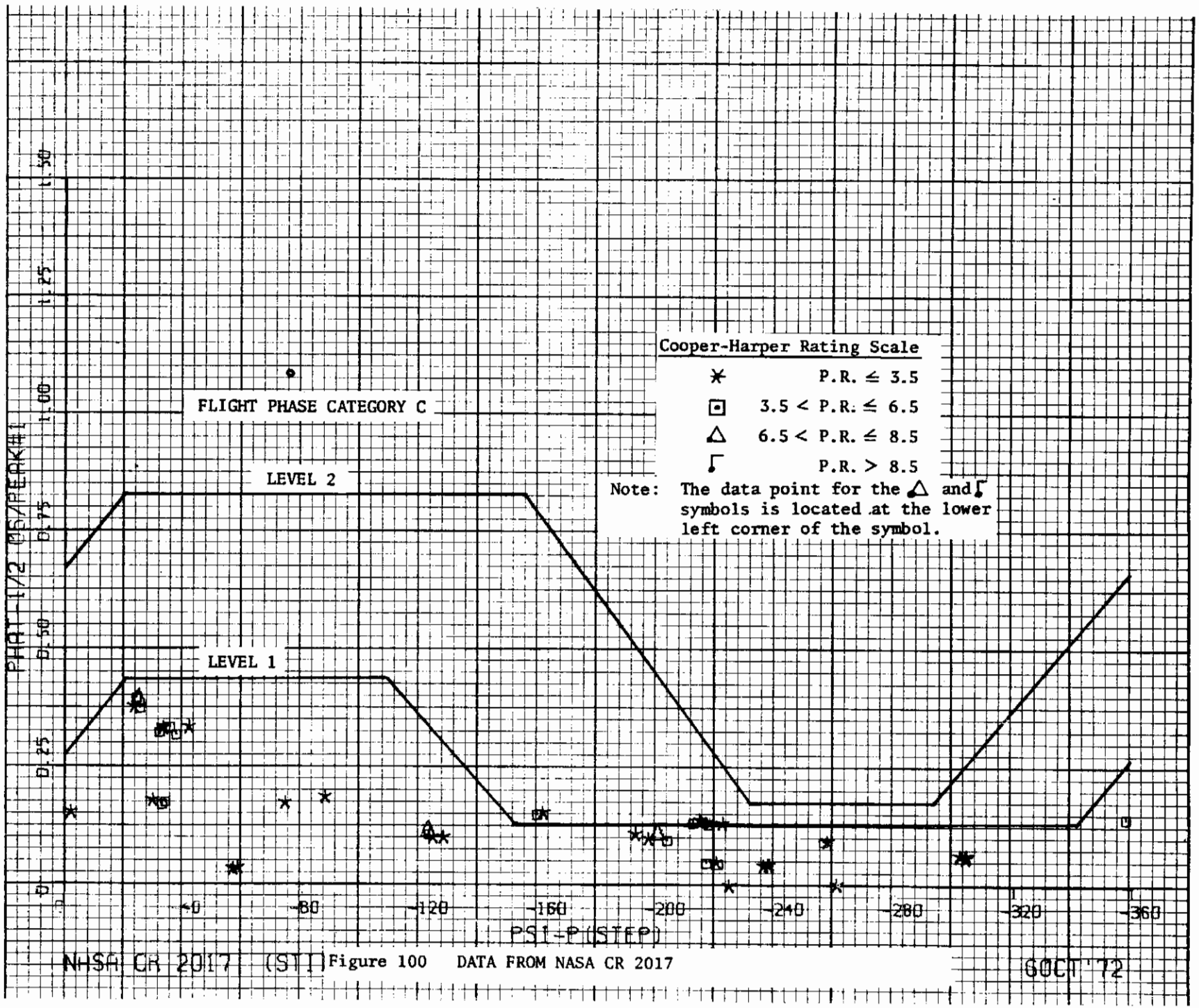

205

NHSA CR 2017 (ST) Figure 100 DATA FROM NASA CR 2017

60CT'72

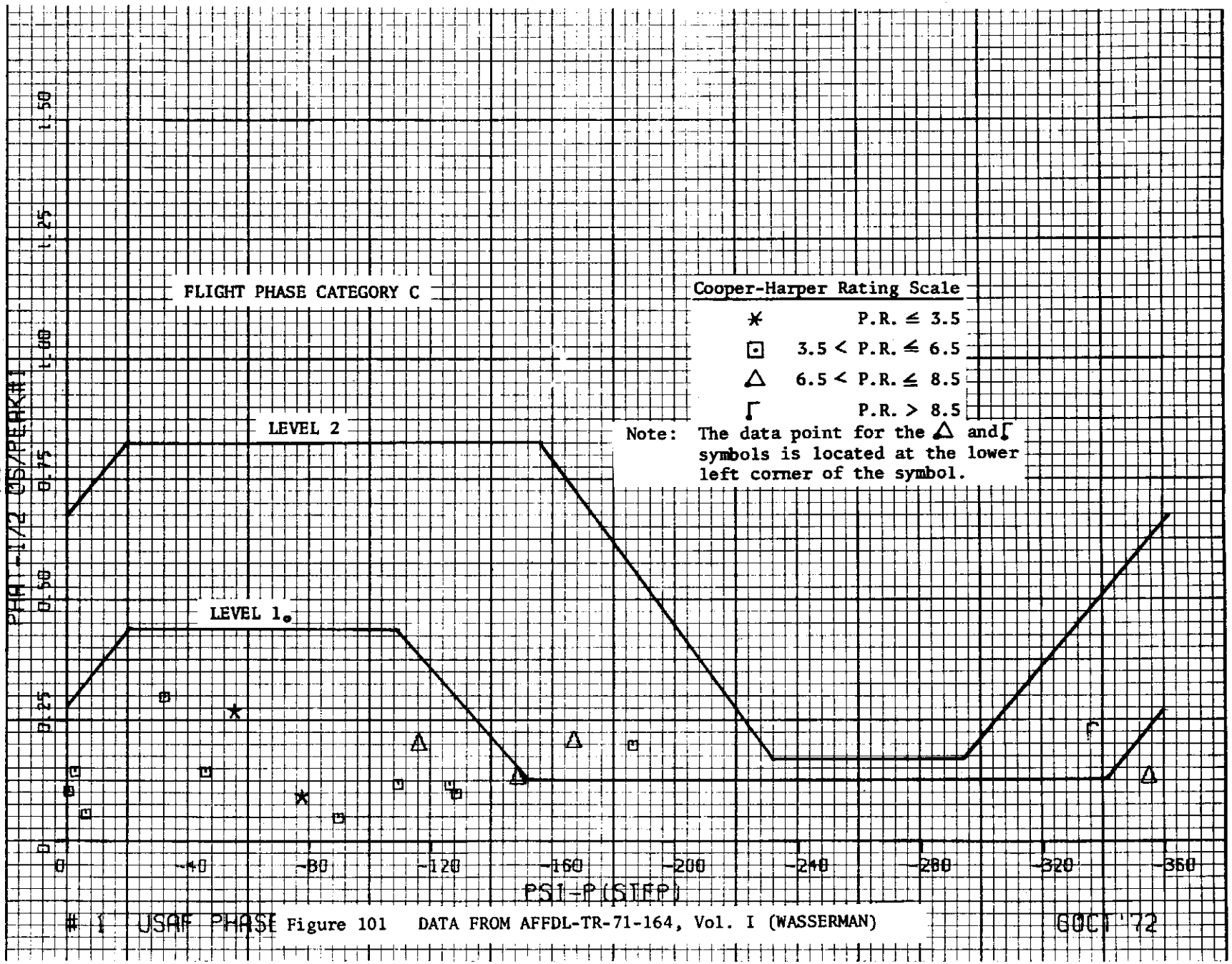

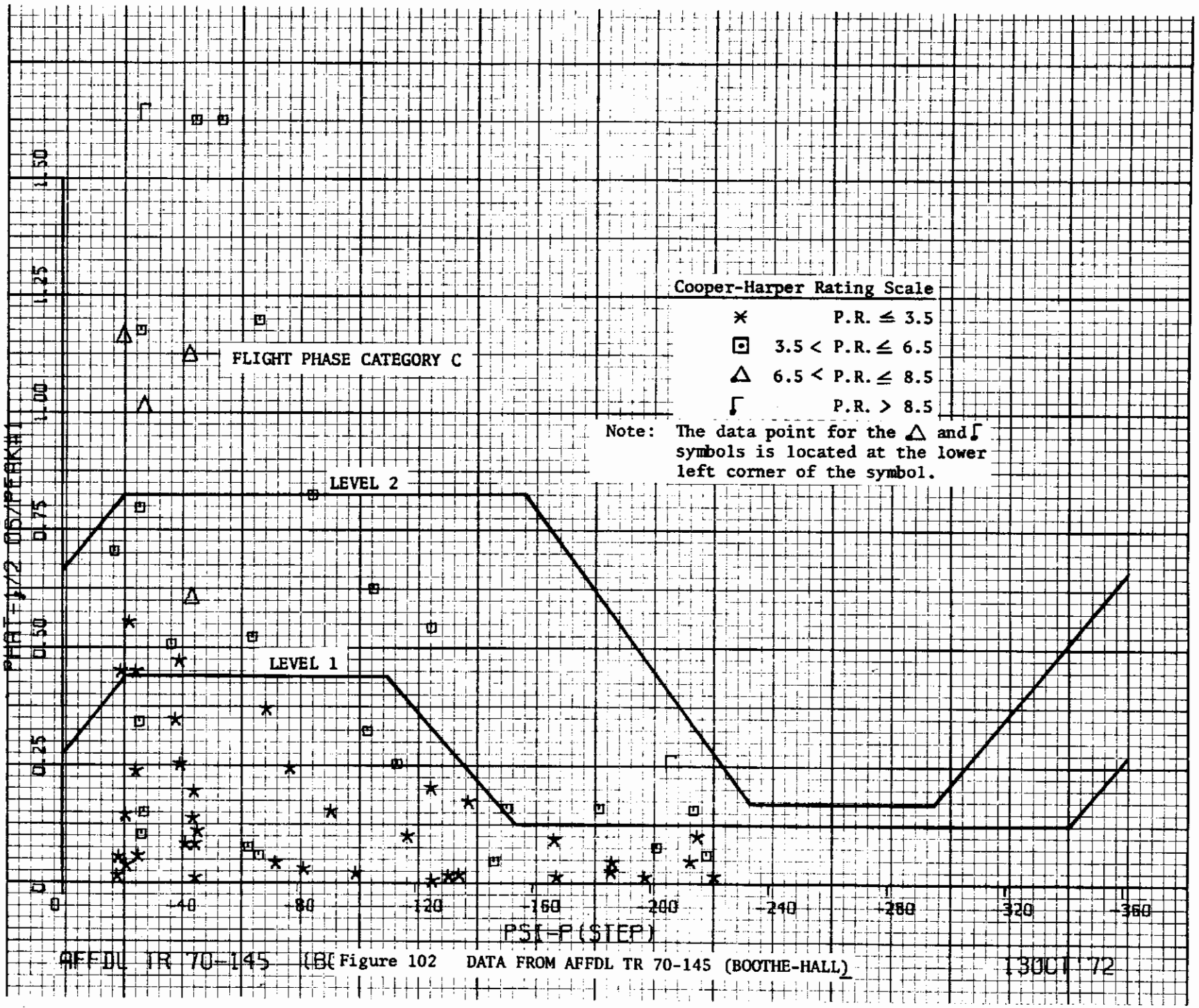

Figure 102 DATA FROM AFFDL TR 70-145 (BOOTHE-HALL)

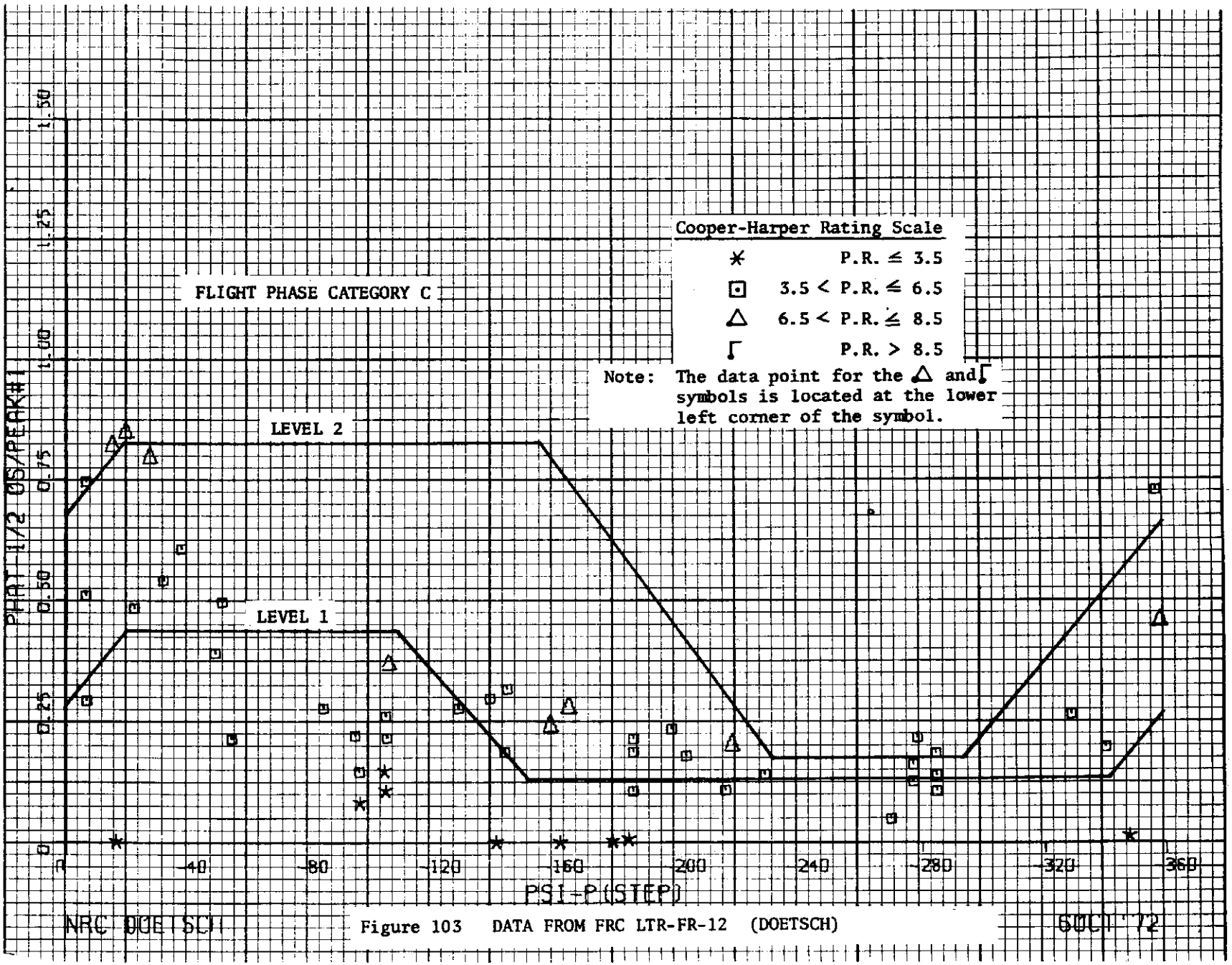

Figure 103 DATA FROM FRC LTR-FR-12 (DOETSCH)

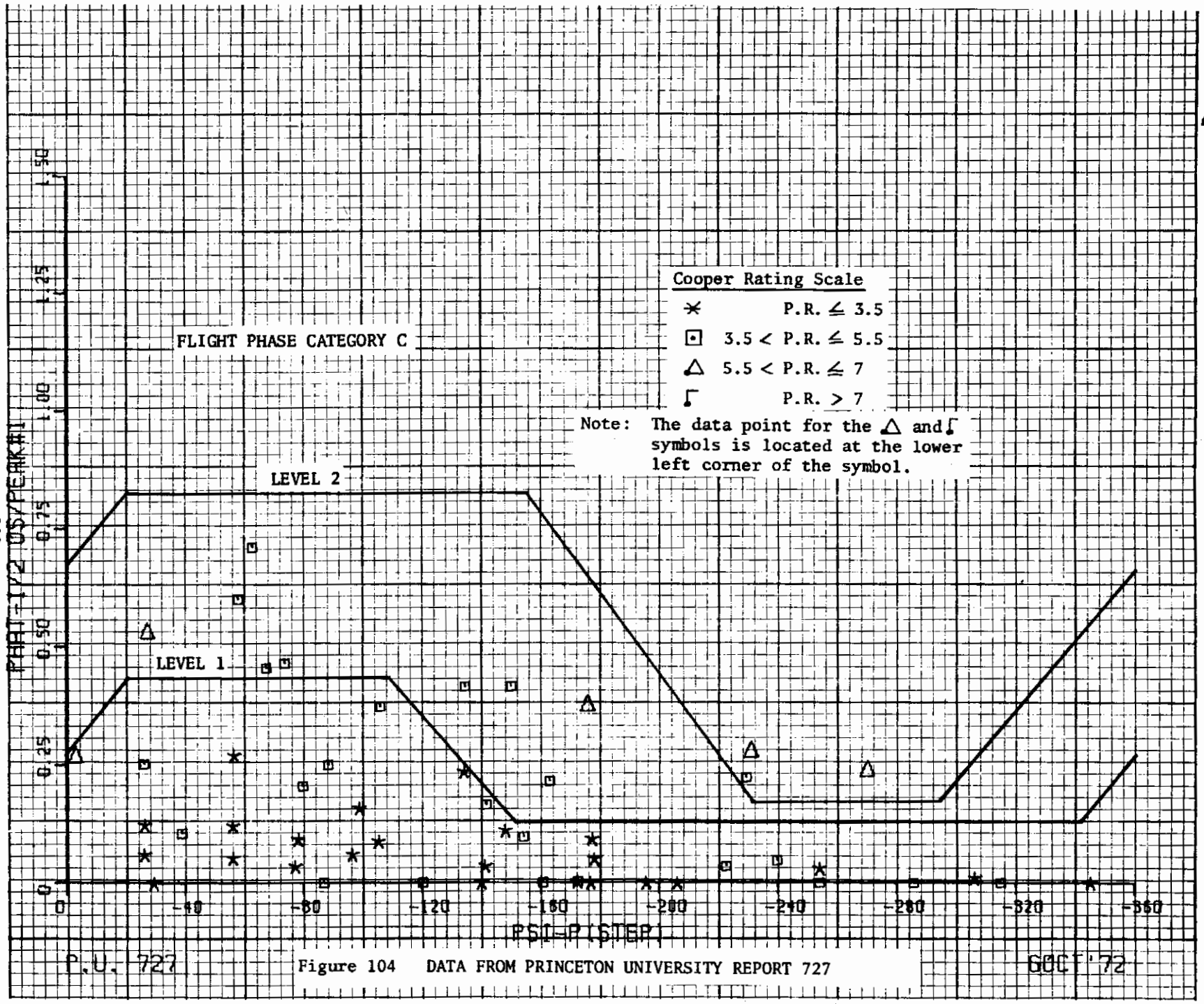

Figure 104 DATA FROM PRINCETON UNIVERSITY REPORT 727

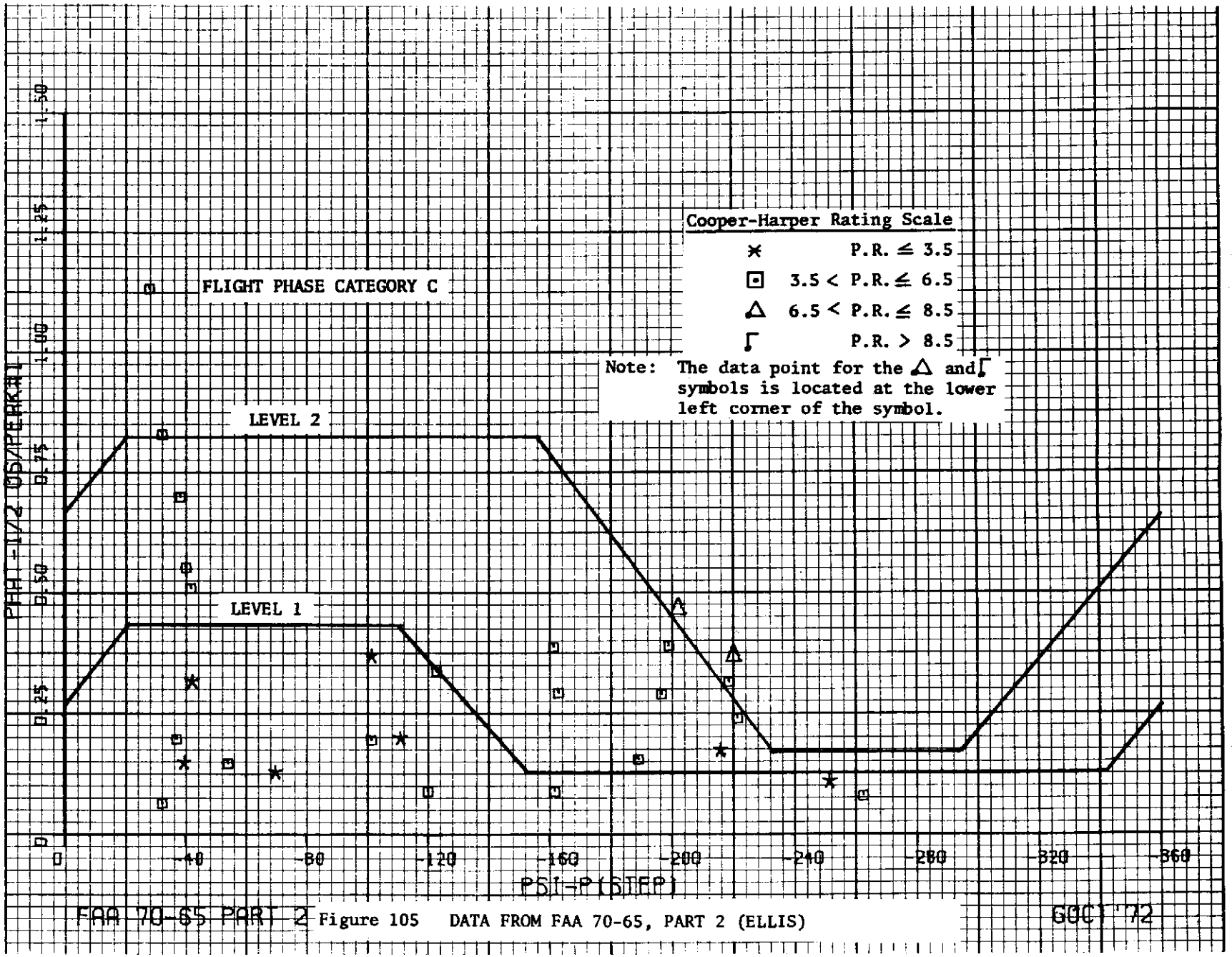

FAA 70-65 PART 2 Figure 105 DATA FROM FAA 70-65, PART 2 (ELLIS)

GOCT 72

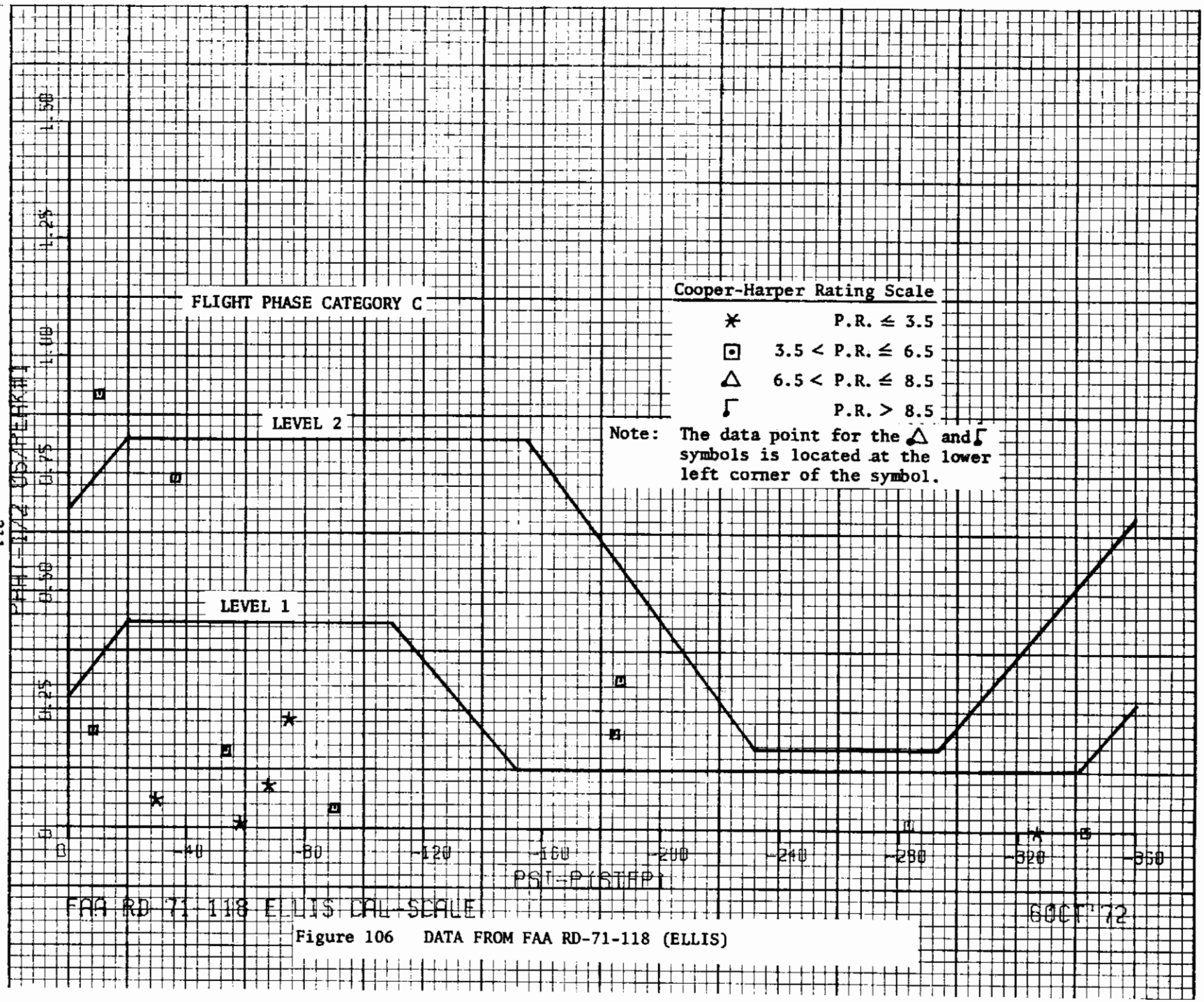

Figure 106 DATA FROM FAA RD-71-118 (ELLIS)

Motivation and Background for Action Recommended (New Paragraphs 3.3.2.3 and 3.3.2.3.1)

New Paragraph 3.3.2.3

The requirement of 3.3.2.3 is intended to limit the amount of sideslip resulting from large aileron control inputs. Because large inputs and at least 90° bank angle changes are required, it is necessary for nearly all classes to start the maneuver from banked turning flight in one direction so that the airplane can roll through wings level to banked flight in the opposite direction. It is desirable to start the maneuver from trimmed initial conditions. If the airplane does not have rudder trim it will be necessary to hold sideslip zero with the rudder pedals. It is desirable therefore to state the requirement for rudder pedals fixed rather than rudder pedals free. This permits trimming sideslip to zero in turning flight and holding this rudder position as the aileron input is applied and the roll rate and bank angle develop.

The different values of sideslip permitted for adverse and proverse sideslip are not considered to be adequately justified for large open loop aileron commands and it is recommended that the requirement be simplified to only one set of numbers, those listed for adverse sideslip. The parameter $k = \frac{\phi_t \text{ command}}{\phi_t \text{ required}}$ has been eliminated from the requirement. The aspects of closed-loop control are considered to be adequately covered by the requirements of 3.3.2.2, 3.3.2.2.1, and 3.3.2.3.1. The requirement of 3.3.2.3 is intended to limit the sideslip resulting from large amplitude abrupt roll maneuvers that are intermediate in severity between normal maneuvering and the gross maneuvers addressed by the roll-pitch-yaw coupling requirement of 3.4.4.

New Paragraph 3.3.2.3.1

The roll oscillation requirements are quite effective in limiting Dutch roll excitation resulting from roll control, roll rate and bank angle when the roll coupling derivatives L'_r and L'_β are significant. When these derivatives are small, however, the roll oscillation requirements are ineffective in limiting the Dutch roll excitation which will be manifested as a yawing oscillation with little roll. The flying qualities problems for configurations of this type are most serious if the Dutch roll frequency is low and the damping is light. For the situation of low roll-yaw coupling it is important to limit the excitation of the Dutch roll mode in sideslip and yaw rate resulting from the pilot's use of aileron to control roll rate, bank angle and heading.

In MIL-F-8785B(ASG) the parameter $\Delta\beta_{max}/k$ versus $\psi_{\beta_{STEP}}$ was introduced to limit the Dutch roll excitation in sideslip resulting from a step aileron input. This requirement has several undesirable features.

1. The requirement is based on step aileron inputs up to the magnitude that causes 60 degree bank change in a time of 2 sec or T_d sec, whichever is longer. For low

frequency Dutch roll roots it is necessary to restrict the size of the aileron input to quite small values.

2. For some configurations the maximum sideslip occurring within 1/2 T_d results from the residue of the spiral mode rather than the Dutch roll mode. For landing approach data the resulting sideslip does not correlate with pilot rating data.

3. The definition of the parameter $k = \frac{\phi_{t\ \text{command}}}{\phi_{t\ \text{requirement}}}$ involves the roll performance requirement. Thus, the validity of the sideslip requirement depends on the validity of the roll performance requirements.

4. Permitting use of rudder to determine $\phi_{t\ \text{command}}$ in a requirement based on rudder-pedal-free aileron inputs leads to confusion and additional work. This is a cumbersome aspect of the requirement because it requires a series of tests or analyses to define the roll performance as a function of aileron input amplitude and a separate series of tests or analyses to determine the sideslip excursions as a function of aileron input amplitude. For analytical checks of the requirement there is no guidance as to how to calculate $\phi_{t\ \text{command}}$. This aspect of the requirement is not substantiated in the BIUG because none of the data presented was treated in that way. The data were reduced in the form $\Delta\beta_{max}/\phi_{t=1}$ for step aileron inputs and then multiplied by what was considered to be the appropriate $\phi_{t=1}$ requirement for each experiment with no consideration being given to use of rudder to prevent adverse yaw.

5. Because the ϕ_t required values are different for Levels 1 and 2 it is necessary to calculate two separate values of $\Delta\beta_{max}/k$ for each data point to be compared with the requirements, one for Level 1 which is compared with the Level 1 boundary and one for Level 2 which is compared with the Level 2 boundary. This "double relaxation" of the requirement, i.e., lower required roll performance and a separate Level 2 boundary in the $\Delta\beta_{max}/k$ versus $\dot{\psi}_\beta$ plane, is involved and cumbersome and is not shown to be necessary by the available data.

6. Although Figure 6 of paragraph 3.3.2.4.1 only has three boundaries, one for Level 2 and two for Level 1 as a function of Flight Phase Category, the requirement is actually the most complex and finely defined requirement in the entire specification. This is because the parameter k depends on the roll performance requirements of paragraph 3.3.4 and 3.3.4.1 which are specified as a function

of Class, Flight Phase and Level. In the BIUG the parameter k is discussed as being the ratio of roll performance attainable from a specific aileron input to roll performance required by the specification and is presented as a replacement for the scaling rule in MIL-F-8785, paragraph 3.4.9. In 3.4.9 the sideslip resulting from a given input was scaled by the ratio of aileron deflection used to the aileron deflection required to meet roll performance requirements.

If the $\Delta\beta_{max}/k$ parameter is written as $\phi_{t_{required}} \frac{\Delta\beta_{max}}{\phi_{t_{command}}}$ it seems that a better interpretation is that the ratio $\Delta\beta_{max}/\phi_{t_{command}}$ must be multiplied by a weighting constant $\phi_{t_{required}}$ which makes the requirement a function of Class, Flight Phase, and Level. In other words the requirement could have been written such that the measurement $\frac{\Delta\beta_{max}}{\phi_{t_{command}}}$ is compared with a new Figure 6 which would have about 45 different curves on it, one for each $\phi_{t_{required}}$ value in 3.3.4 and 3.3.4.1. Some of the 45 curves would be coincident with Class I, Flight Phase Category A, Level 2 would be coincident with Class I, Flight Phase Category B, Level 1 because $\phi_{t_{required}}$ is 60° in 1.7 sec for both situations. If the sideslip excursion requirement had been presented in the latter format it would no doubt have received much more criticism.

In MIL-F-83300 the requirements to limit sideslip excursions resulting from use of aileron are stated in terms of the response to a pulse aileron command. This form of input was specified because it permits using larger commands without encountering excessive bank angle changes. In addition the pulse input eliminates the ramping of sideslip that occurs for some configurations when step inputs are used. The requirements are stated in terms of the parameter $\Delta\beta/\phi_1$ and $\frac{\Delta\beta}{\phi_1}\left|\frac{\phi}{\beta}\right|_d$ versus ψ_β. The requirements use two ψ_β scales based on the value of $\not\propto p/\beta$ as in the roll oscillation requirements.

The parameters used in MIL-F-83300 were developed primarily to accommodate the data from Reference 3. When the data from other experiments are compared with the boundaries in MIL-F-83300 for $\Delta\beta/\phi_1$ the data usually fall way below the boundary. This observation probably indicates that the parameter $\Delta\beta/\phi_1$ should be scaled by some factor that is different between experiments. Measuring the sideslip excursion for an impulse aileron input occurring within 1/2 T_d results in amplitude measures that can be different by a factor of two depending on the phase of the Dutch roll mode. Since the $\Delta\beta/\phi_1$ requirement is stated as a function of Dutch roll phase angle this is not a critical shortcoming, because the requirement boundary as a function of ψ_β can be shaped as required to fit the experimental data. It is best to realize these artifacts of the measurement rules, however, because it aids in interpreting the information being handled. The following sketch illustrates the point.

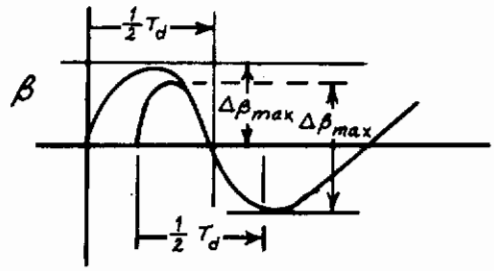

For the first case the amplitude measured would be from zero to one peak. For the second case where the Dutch roll phase is shifted, the $\Delta\beta$ measured would be from peak to peak.

Further study of the parameter $\frac{\Delta\beta}{\phi_1}\left|\frac{\phi}{\beta}\right|_d$ leads to the conclusion that this parameter is essentially a variation of the ϕ_{osc}/ϕ_{AV} versus $\psi_{\beta\,PULSE}$ requirement. To appreciate that this is true consider the following rough interpretations.

ϕ_{osc} ~ Measure of Dutch roll double amplitude

ϕ_{AV} ~ Measure of steady state roll change

$\Delta\beta$ ~ Measure of Dutch roll double amplitude

ϕ_1 ~ Measure of steady state roll change plus single amplitude Dutch roll

$|\phi/\beta|_d$ ~ Ratio of Dutch roll double amplitude in bank angle and sideslip

Thus

$$\frac{\phi_{osc}}{\phi_{AV}} \sim \frac{\text{D.R. OSCILL. IN } \phi}{\text{STEADY STATE } \phi} \qquad \frac{\Delta\beta}{\phi_1}\left|\frac{\phi}{\beta}\right|_d \frac{\text{D.R. OSCILL. IN } \beta}{\phi\sim\text{STEADY STATE+D.R.}} \qquad \frac{\text{D.R. OSCILL. IN } \phi}{\text{D.R. OSCILL. IN } \beta}$$

$$\sim \frac{\text{D.R. OSCILL. IN } \phi}{\phi\sim\text{STEADY STATE+D.R.}}$$

For proverse yaw cases the value of ϕ_{AV} and the value of ϕ_1 will be nearly equal in magnitude but for adverse yaw ϕ_1 may be relatively large compared to ϕ_{AV}. Thus the two requirements are quite similar for proverse yaw cases but differ for adverse yaw because ϕ_{AV} goes to zero for large adverse yaw due to aileron while ϕ_1 is still positive.

$$\phi_{AV} = \frac{\phi_1 + \phi_3 + 2\phi_2}{4} \cong 0$$

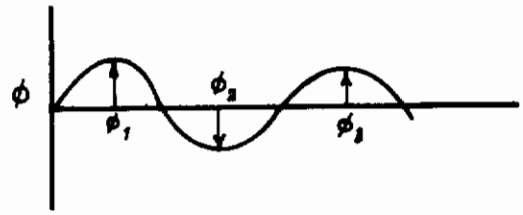

Example for large adverse yaw due to aileron.

The relationship between the $\frac{\phi_{osc}}{\phi_{AV}}$ and $\frac{\Delta\beta}{\phi_1}\left|\frac{\phi}{\beta}\right|_d$ metrics is illustrated in Figure 107 extracted from Reference 56, Figure 1(3.3.8), for a portion of the data in Reference 3. Other parameters intended to limit sideslip excursions or intended to ensure good heading control have been proposed in the literature. A number of these parameters are listed below with short discussions and appropriate references.

NASA Ames investigators have proposed the parameters β_1/ϕ_1 and $\Delta\beta/\Delta\phi$ in References 57, 58, and 59 where β_1 is the first peak in sideslip and ϕ_1 is the first peak in bank angle occurring in a rapid side step maneuver; $\Delta\beta$ and $\Delta\phi$ are similar measures from a rapid 10° bank and hold maneuver. Both maneuvers are performed using aileron alone, i.e., rudder pedals fixed or free. These metrics have merit but they are believed to be too subject to the manner in which the maneuvers are performed to permit their use as Military Specification requirements. A discussion of this approach is contained in Reference 56.

Investigators at Systems Technology Inc. have suggested or investigated the following parameters.

$\zeta_\phi \omega_\phi > 0.4$	Real part of roll-aileron numerator factors	Ref. 42
T_ψ	Heading delay parameter	Ref. 60
$\lvert r\rvert_d$ vs $\psi_{r_{IMPULSE}}$	Residue and phase of Dutch roll in yaw rate	Ref. 34
r_{osc}/r_{AV} vs $\psi_{r_{IMPULSE}}$	Analogous to $\frac{\phi_{osc}}{\phi_{AV}}$ in MIL-F-8785B	
ω_{ψ_c}	Pilot-airplane closed-loop heading crossover frequency for aileron control	
μT_R vs $\frac{N'_{\delta_a}}{\omega_d^2 L'_{\delta_a}}$	Aileron-to-rudder crossfeed to keep sideslip zero	
$-0.25 < N'_p - \frac{g}{V} < 0.15$	Additional requirement when $\frac{N'_{\delta_a}}{L'_{\delta_a}} \leq .04$	

The parameter $\zeta_\phi \omega_\phi$ was tested against the data of Reference 3 and found to be without merit.

The heading delay parameter τ_ψ is reviewed in References 54 and 34. The parameter is shown to have practical measurement problems and fails to correlate pilot rating data from experiments other than that for which it was developed.

The residue and phase of the Dutch roll component of yaw rate for an aileron step was briefly examined in Reference 34 but was not pursued because it would be difficult to measure in flight test and because a requirement would have to be made a function of Dutch roll damping and perhaps roll damping.

The closed-loop heading crossover frequency was studied at some length in Reference 34 and at least temporarily abandoned because of strong differences between proverse and adverse yaw cases and a dependence on Dutch roll frequency.

The parameter $\frac{r_{osc}}{r_{AV}}$ for an inpulse input was considered briefly in Reference 34 because it seemed analogous to ϕ_{osc}/ϕ_{AV} . The parameter was not studied in detail in Reference 34 because the author considered it unlikely that this parameter adequately included the effects of variations in Dutch roll damping and frequency or could cover aircraft with yaw dampers.

In development of the requirements in MIL-F-8785B(ASG) and MIL-F-83300, consideration was also given to formulating requirements based on the yaw rate response to aileron. This approach was discontinued because it was realized that the yaw rate response to aileron inputs is a strong function of the axis system in which the motion is measured. Because of this, preference was given to use of sideslip as the response parameter for which requirements would be formulated, partly because this parameter is independent of axis system inclination. In flight test, however, there are other problems associated with measurement of sideslip that could be more difficult to correct for than resolution of rate gyro signals into a particular axis system. In the current study it was decided to pursue the idea of using the yaw rate response to an impulse or pulse aileron input as the basis for a requirement to restrict Dutch roll excitation in yaw due to roll commands. There are several important differences between the yaw rate and the roll rate or bank response that must be accounted for in formulating r_{osc}/r_{AV} criteria. First, the yaw rate transfer function numerator is a cubic and the coefficient of the s^0 term is $(N'_{\delta_{AS}} + Y_{\delta_{AS}} N'_\beta)$. Applying the initial value theorem for an impulse aileron command shows that the yaw rate response will have an initial value equal to $(N'_{\delta_{AS}} + Y_{\delta_{AS}} N'_\beta)\ \delta_{AS}$. The time history may look like the following sketch.

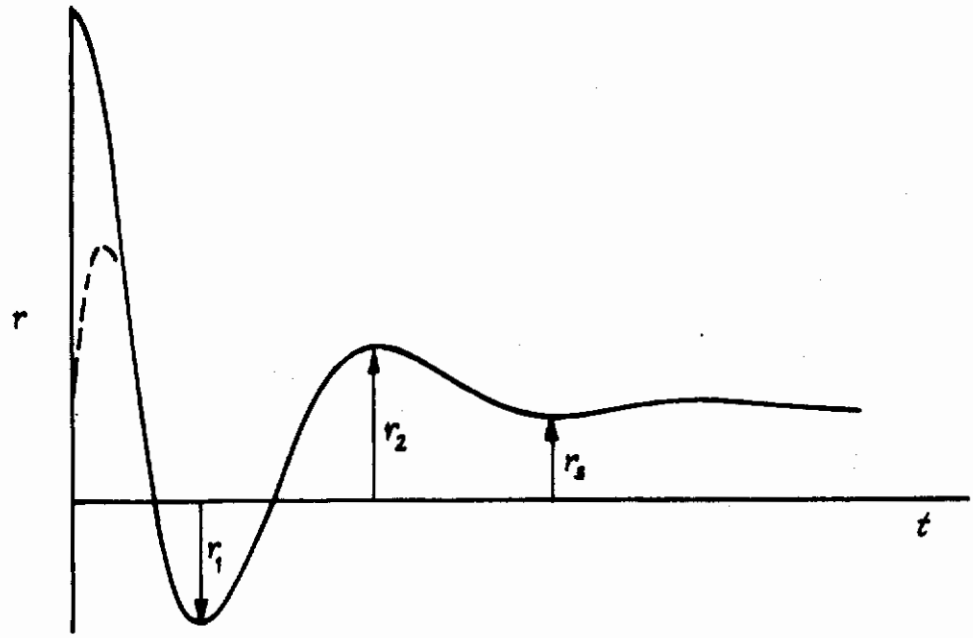

From this sketch it is seen that the first peak occurs at time zero. In general, this peak will not correspond to a peak of the Dutch roll oscillation, and further, the amplitude will be quite dependent on the detailed shape of the aileron input. If the aileron input is not an ideal impulse or if control system dynamics are recognized, the effect will be to attenuate the initial value approximately as indicated by the dashed line in the sketch. Because of these considerations it is advisable to ignore the initial value of the yaw rate response and to formulate the requirement based on succeeding peaks. A rule that required measurements to be taken from peaks occurring after a time interval equal to 1/5 the Dutch roll period has been used in analyzing data in this report. The following sketch indicates the result of such a rule.

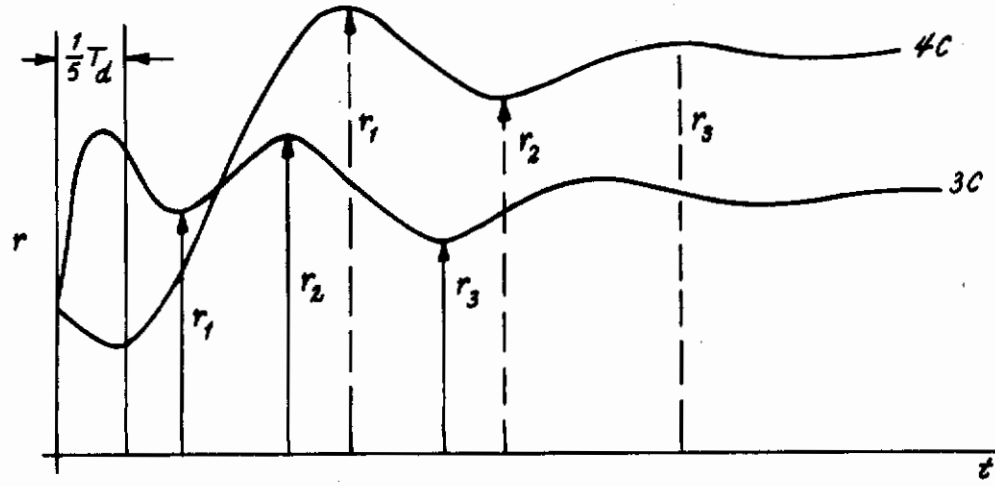

The rule accomplishes the intended purpose in case 3C, that is, the first peak is ignored and measurements would be taken from second, third, and fourth peaks as indicated by the solid vertical arrows. For case 4C, however, the Dutch roll is phased such that the initial maximum at $t = 0$ is excluded by the rule but so is the next peak, which because of the Dutch roll phasing, occurs at or slightly before $1/5\ T_d$. This situation will occur for any simple measurement rule expressed as a fraction of the Dutch roll period. The rather arbitrary choice of $1/5\ T_d$ as the interval to use is based on choosing a fraction less than $1/4\ T_d$ but large enough to provide the maximum time for control system effects to occur. The peaks to be used in the requirement for case 4C are indicated by the dashed vertical arrows. The following definitions for $\frac{r_{osc}}{r_{AV}}$ would be used by analogy with the roll oscillation requirements of MIL-F-8785B. The phase angle follows also from analogy with the roll oscillation requirement.

$$\frac{r_{osc}}{r_{AV}} = \frac{r_1 + r_3 - 2r_2}{r_1 + r_3 + 2r_2} \quad vs \quad \psi_{r_{IMPULSE}}$$

The sign of the yaw rate at the various peaks influences the sign of the ratio r_{osc}/r_{AV} in a different way than occurs for p_{osc}/p_{AV} or ϕ_{osc}/ϕ_{AV}. In the case of the roll responses, the first peak will always be positive for aileron commands to the right. This is not the case for yaw rate as can be seen from the cases illustrated in the preceding sketches. If, as in the first sketch the yaw rate at the first peak is negative, then the numerator for the r_{osc}/r_{AV} parameter will be negative and the ratio will be negative. Really this fact is redundant information about the phase of the Dutch roll which is measured directly by the parameter $\psi_{r_{IMPULSE}}$. There are cases where the denominator of the ratio r_{AV} can be negative for a right aileron command. This indicates that the steady bank angle has the opposite sign from the command, i.e., the airplane ended up rolled to the left after a right aileron impulse. From these considerations, it appears advisable to define

$$\frac{|r_{osc}|}{r_{AV}} = \frac{|r_1 + r_3 - 2r_2|}{r_1 + r_3 + 2r_2}$$

This will eliminate problems caused by sign changes of the numerator but retain the information conveyed by the occurrence of a negative sign from the denominator.

Carrying the analogy with the roll oscillation requirements a step further, it is obvious that the spiral mode will have a similar effect on the yaw rate time history as it has on bank angle and roll rate. Thus it is necessary to remove the spiral residue from the yaw rate time history by techniques analogous to those developed under 3.3.2.2. For the subtraction method, $\hat{r}$ is defined as follows

$$\hat{r}(t)\Big|_{\substack{\text{IMPULSE}\\ \delta_{AS}}} = r(t)\Big|_{\substack{\text{IMPULSE}\\ \delta_{AS}}} + K_s\left(1-e^{-\lambda_s t}\right)\delta_{AS}$$

K_s: RESIDUE OF SPIRAL MODE IN YAW RATE FOR AILERON IMPULSE COMMAND

δ_{AS}: MAGNITUDE

The following general discussion of transfer function forms and command input forms is instructive in understanding how the magnitude of the Dutch roll oscillation is related to the Dutch roll frequency. An understanding of this aspect is helpful in formulating parameters to be tested for efficiency in correlating pilot rating data.

The transfer functions of interest are listed below for convenient reference. The spiral mode is assumed to be at the origin.

$$\frac{\phi(s)}{\delta_{AS}(s)} = \frac{As^2+Bs+C}{s(s+\lambda_R)\left(s^2+2\zeta_d\omega_{n_d}s+\omega_{n_d}^2\right)} \qquad \frac{p(s)}{\delta_{AS}(s)} = \frac{s\left[As^2+Bs+C\right]}{\Delta}$$

$$\frac{r(s)}{\delta_{AS}(s)} = \frac{As^3+Bs^2+Cs+D}{\Delta} \qquad \frac{\dot{r}(s)}{\delta_{AS}(s)} = \frac{s\left[As^3+Bs^2+Cs+D\right]}{\Delta}$$

$$\frac{\beta(s)}{\delta_{AS}(s)} = \frac{As^3+Bs^2+Cs+D}{\Delta} \qquad \frac{\dot{\beta}(s)}{\delta_{AS}(s)} = \frac{s\left[As^3+Bs^2+Cs+D\right]}{\Delta}$$

The Laplace transform for a step command is $1/s$ and the transform for an impulse command is unity. As a result the inverse transform of a variable to an impulse input is identical to the inverse transform of the derivative of the variable for a step input.

Advantage is taken of this fact in stating the requirements for bank angle oscillations for an impulse input and the requirements for roll rate oscillations for a step input. In this example

$$\frac{p_{osc}}{p_{AV}}\Big|_{STEP} = \frac{\phi_{osc}}{\phi_{AV}}\Big|_{IMPULSE} \quad \text{and} \quad \psi_{p_{STEP}} = \psi_{\phi_{IMPULSE}}$$

Since ϕ_{osc} for the step and ϕ_{osc} for the impulse are related to the residue of the Dutch roll mode, it is of interest to see how this parameter is related to the Dutch roll frequency. The following expression for the Dutch roll residue in bank for an impulse is taken from Reference 61.

$$K_D = \frac{1}{\beta}\gamma\sqrt{\frac{\beta^2(a_1 - 2\alpha)^2 + (a_0 - a_1\alpha + \alpha^2 - \beta^2)^2}{(\alpha^2+\beta^2)\left[(\alpha-\gamma)^2+\beta^2\right]}}$$

Consider the following case

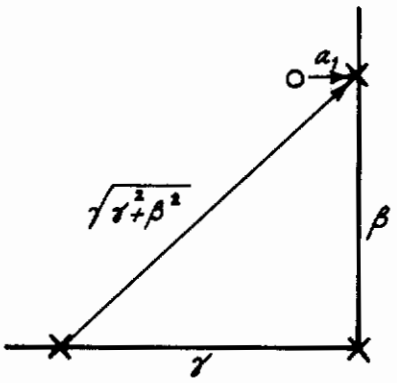

$$\zeta_d \omega_{n_d} = \alpha = 0$$

$$\omega_\phi^2 = \omega_{n_d}^2 = a_0 = \beta^2$$

$$\zeta_\phi \omega_\phi = a_1 \neq 0$$

$$\gamma = \lambda_R$$

Then:

$$K_D = \frac{1}{\beta}\gamma\sqrt{\frac{a_1^2}{\gamma^2+\beta^2}} \sim \frac{1}{\omega_{n_d}^2}$$

The residue of the Dutch roll mode in the bank angle (roll rate) response for an aileron inpulse (step) is roughly proportional to $\omega_{n_d}^{-2}$.

A similar exercise for the sideslip response to a step aileron shows the following. Assume that $Y_{\delta_{AS}} = 0$ and $\frac{g}{V}\left(N'_{\delta_{AS}} L'_r - L'_{\delta_{AS}} N'_r\right) \approx 0$ then the sideslip transfer function simplifies to

$$\beta(s)\Big|_{STEP} = \frac{s(s+a_0)}{s(s+\gamma)\left[(s+\alpha)^2+\beta^2\right]} \quad \frac{\delta_{AS}}{s}$$

The expression for the Dutch roll residue is

$$K_D = \frac{1}{\beta\sqrt{\alpha^2+\beta^2}}\sqrt{\frac{(a_o-\alpha)^2+\beta^2}{(\alpha-\gamma)^2+\beta^2}} \sim \frac{1}{\omega_{n_d}^2}$$

For a case with light Dutch roll damping and with $a_o \approx \gamma$ it turns out that the residue in sideslip for an aileron step is roughly proportional to $\omega_{n_d}^{-2}$. It follows that the residue in sideslip for an impulse input will be roughly proportional to $\omega_{n_d}^{-1}$. Also the residue of sideslip rate for an aileron step input is proportional to $\omega_{n_d}^{-1}$.

These points are significant because if one were to claim that good correlations had been obtained between pilot rating and some measure of the oscillatory component of sideslip for a step input and then for some reason it was desirable to change to an impulse input (to reduce the spiral residue for example), it would be necessary to divide the measure of the sideslip oscillatory component resulting from the impulse by ω_{n_d} to preserve the correlation with pilot rating. To clarify this point, assume that pilot rating is found by experiment to be a function of $\beta_{\text{oscillatory}}$ for a step aileron input

$$P.R. = f(\beta_{osc})_{STEP}$$

Then it follows that pilot rating should be correlated with $\beta_{\text{oscillatory}}$ divided by ω_{n_d} if an impulse aileron input is used. If it were desired to correlate the pilot ratings with a measure of $\dot{\beta}_{\text{oscillatory}}$ for a step input, the $\dot{\beta}_{\text{oscillatory}}$ measure should be divided by ω_{n_d}.

$$P.R. = f\left(\frac{\beta_{osc}}{\omega_{n_d}}\right)_{IMPULSE} \quad \text{or} \quad P.R. = f\left(\frac{\dot{\beta}_{osc}}{\omega_{n_d}}\right)_{STEP}$$

For conventional configurations, the yaw rate and sideslip rate responses are proportional and 180° out of phase in the Dutch roll mode. Therefore the residue of the Dutch roll mode in the yaw rate response for a step input is analogous to the residue of sideslip rate for a step input.

$$K_D \text{ for yaw rate} \sim \omega_{n_d}^{-1} \text{ for step input}$$
$$\sim \omega_{n_d}^{0} \text{ for impulse input}$$

The following summary indicates how the residue of the Dutch roll mode is related to the Dutch roll frequency for various responses, and their derivatives, for both step and impulse aileron commands.

Residue of Dutch Roll in:	Step	Impulse
ϕ	$f(\omega_{n_d}^{-3})$	$f(\omega_{n_d}^{-2})$
p	$f(\omega_{n_d}^{-2})$	$f(\omega_{n_d}^{-1})$
β	$f(\omega_{n_d}^{-2})$	$f(\omega_{n_d}^{-1})$
$\dot{\beta}$	$f(\omega_{n_d}^{-1})$	$f(\omega_{n_d}^{0})$
r	$f(\omega_{n_d}^{-1})$	$f(\omega_{n_d}^{0})$
$\dot{r}$	$f(\omega_{n_d}^{0})$	$f(\omega_{n_d}^{+1})$

A numerical example (two cases from Reference 34) will illustrate the relative magnitudes of the Dutch roll oscillation in sideslip and $\dot{r}$ for two configurations with equal $N'_{\delta_{AS}}$, λ_R and ζ_d but with different Dutch roll frequencies, $\omega_{n_d} = 0.5$ and $\omega_{n_d} = 2.0$. The responses in Figure 108 are for unit step aileron commands. Since the control inputs are equal and $N'_{\delta_{AS}}$ is equal for the two cases, the initial yaw accelerations are equal but the amplitude of the resulting Dutch roll oscillation in sideslip is greatly different, roughly inversely proportional to the ratio of $\omega_{n_d}^2$. The amplitude of the Dutch roll oscillation in yaw acceleration is larger for the case with the higher Dutch roll frequency.

$$\frac{\Delta\beta_{\delta A}}{\Delta\beta_{10A}} = \frac{1.12}{0.09} = 12.4 \; ; \qquad \frac{\omega_{n_{d\,\delta A}}}{\omega_{n_{d\,10A}}} = \frac{\left(\frac{1}{2}\right)^2}{(2^2)} = 16 \; ; \qquad \frac{\Delta\dot{r}_{\delta A}}{\Delta\dot{r}_{10A}} = \frac{0.14}{0.22} = 0.64$$

If the $\dot{r}$ values are divided by the Dutch roll frequency squared, their ratio is then nearly the same as the ratio of sideslip measurements.

$$\frac{\left(\Delta\dot{r}/\omega_{n_d}^2\right)_{\delta A}}{\left(\Delta\dot{r}/\omega_{n_d}^2\right)_{10A}} = \frac{0.14/\left(\frac{1}{2}\right)^2}{0.22/(2)^2} = 10.2$$

These observations coupled with an assumption: "pilot rating is reasonably well correlated by the $\frac{\Delta\beta_{max}}{k}$ parameter for a step aileron input in MIL-F-8785B(ASG)" suggests that if one were to attempt correlation of pilot rating with a measure of the oscillatory component in yaw rate for an impulse input, the measure representing the oscillatory component of yaw rate should be divided by $\omega_{n_d}^2$.

Thus if pilot ratings are to be correlated with r_{osc}/r_{AV} type measures it is probably best to start by trying the following parameters

$$\frac{1}{\omega_{n_d}^2}\ \frac{\hat{r}_{osc}\Big|_{t>0.2T_d}}{\hat{r}_{AV}} \quad VS \quad \psi_{r_{IMPULSE}}$$

or

$$\frac{1}{\omega_{n_d}^2}\ \frac{\hat{\dot{r}}_{osc}\Big|_{t>0.2T_d}}{\hat{\dot{r}}_{AV}} \quad VS \quad \psi_{\dot{r}_{STEP}}$$

where yaw rate is referenced to stability axes.

At the beginning of the discussion of the new paragraphs 3.3.2.3 and 3.3.2.3.1 a number of undesirable features of the sideslip requirements in MIL-F-8785B were listed. The following discussion will address these problems and indicate potential solutions and alternate approaches.

The limitation on the size of control input that can be tested when requirements are based on responses to step aileron inputs can be alleviated by changing the specified input to an aileron impulse or in practical situations to an abrupt pulse. In view of the previous discussion of r_{osc}/r_{AV} type requirements however, attention must be given to multiplication of the Dutch roll oscillatory component by ω_{n_d} to the proper power when impulse inputs are used instead of step inputs so that correlation with pilot rating is retained. In this case the $\Delta\beta_{max}$ component resulting from an impulse aileron input should be divided by ω_{n_d} to maintain the correlation observed for $\Delta\beta_{max}$ resulting from a step input.

The use of an impulse aileron input instead of a step input will also reduce the residue of the spiral mode in the sideslip response and thus alleviate the problem of the $\Delta\beta_{max}$ measure being dominated by the residue of the spiral mode rather than by the Dutch roll mode. Consideration was also given to the possibility of removing the spiral residue from the sideslip response to a step input by both the factoring and the subtraction techniques.

The following equations indicate the factoring approach investigated. The complete transfer function of sideslip to aileron is cubic over fourth order

$$\beta(s)\Big|_{\substack{\delta_{AS}\\ STEP}} = \frac{As^3+Bs^2+Cs+D}{(s+\lambda_S)(s+\lambda_R)\ s^2+2\zeta_d\omega_{n_d}s+\omega_{n_d}^2}\ \frac{\delta_{AS}}{s}$$

For much of the data used to develop the requirement in MIL-F-8785B(ASG), however, the transfer function could be simplified because the D coefficient in the numerator was near zero and the spiral root was near the origin. Thus the applicable transfer function was as follows:

$$\beta(s)\Big|_{\substack{\delta_{AS}\\ STEP}} = \frac{As^2+Bs+C}{(s+\lambda_R)\ s^2+2\zeta_d\omega_{n_d}s+\omega_{n_d}^2}\ \frac{\delta_{AS}}{s}$$

and the sideslip response looked like the following sketches from which the Dutch roll excitation could easily be measured.

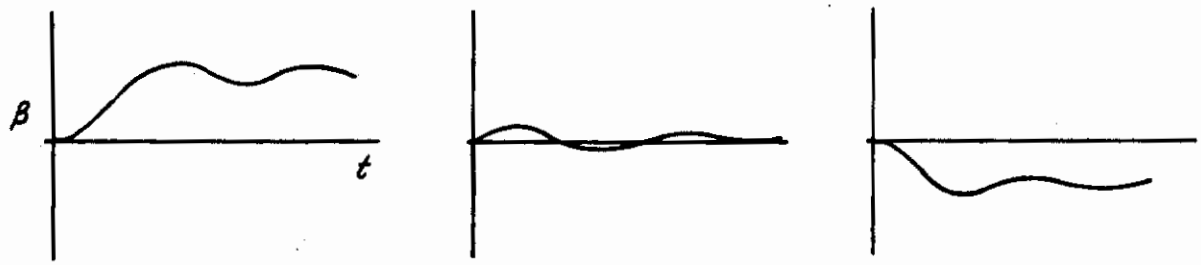

For the general case however, the sideslip response can appear as follows because the spiral mode residue is large. This can be the case even when the spiral root is at the origin if the D coefficient is not zero.

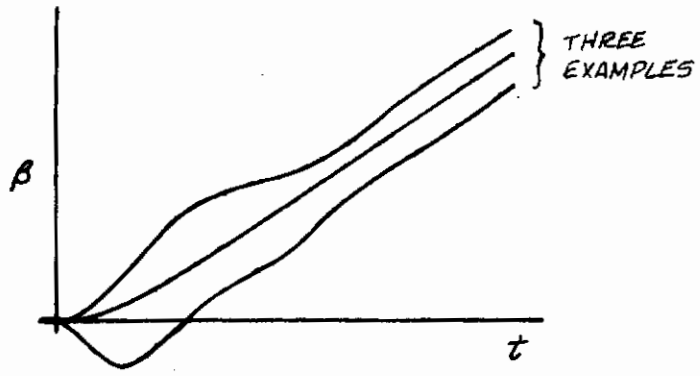

The general transfer function can be modified to the form of the simplified transfer function by the following operations.

1. Multiply both sides by $s + \lambda_s$
2. Divide both sides by s
3. Separate the numerator terms and transpose the constant term

$$\hat{\beta}(s)\Big|_{\substack{\delta_{AS}\\ STEP}} = \frac{s+\lambda_s}{s}\,\beta(s) - \frac{D\,\delta_{AS}}{s^2(s+\lambda_R)(s^2+2\zeta_d\omega_{n_d}s+\omega_{n_d}^2)} = \frac{s(As^2+Bs+C)}{s(s+\lambda_R)(s^2+2\zeta_d\omega_{n_d}s+\omega_{n_d}^2)}\,\frac{\delta_{AS}}{s}$$

Using the right hand part of this equation it is possible to calculate a $\hat{\beta}$ time history that will not exhibit the damping effect noted earlier. This method will give results similar to the subtraction method only when the Dutch roll root is far from the origin and when the numerator cubic has a factor fairly close to the origin. Otherwise the time histories from the two methods are considerably different because the residues and phase of the roll and Dutch roll modes are changed by the operations performed for the factoring method.

The subtraction method is detailed below. Two forms of the equations must be developed in this case because the inverse transform is different in form, depending on whether or not the spiral root is exactly at the origin.

Spiral root not at origin:

$$\beta(t)\Big|_{STEP} = \delta_{AS}\left[K_o + K_s e^{-\lambda_s t} + K_R e^{-\lambda_R t} + K_D e^{-\zeta_d \omega_{n_d} t}\cos(\omega t + \psi_\beta)\right]$$

This equation is modified by adding $K_s(1 - e^{-\lambda_s t})\delta_{AS}$ to both sides

$$\hat{\beta}(t)\Big|_{STEP} = \beta(t) + K_s(1-e^{-\lambda_s t})\delta_{AS} = \delta_{AS}\left[K_o + K_s + K_R e^{-\lambda_R t} + K_o e^{-\zeta_d \omega_{n_d} t}\cos\omega t + \psi_\beta\right]$$

where

$$K_o = \frac{D}{\lambda_s \lambda_R \omega_{n_d}^2}$$

$$K_s = \frac{-A\lambda_s^3 + B\lambda_s^2 - C\lambda_s + D}{\lambda_s(\lambda_s - \lambda_R)\left[(\zeta_d \omega_{n_d} - \lambda_s)^2 + \omega_{n_d}^2(1-\zeta_d^2)\right]}$$

Spiral root at the origin:

$$\beta(t)\Big|_{STEP} = \delta_{AS}\left[K_o + K_t t + K_R e^{-\lambda_R t} + K_D e^{-\zeta_d \omega_{n_d} t}\cos(\omega t + \psi_\beta)\right]$$

This equation is modified by subtracting $K_t t\, \delta_{AS}$ from both sides

$$\hat{\beta}(t)\Big|_{STEP} = \beta(t) - K_t t\, \delta_{AS} = \delta_{AS}\left[K_o + K_R e^{-\lambda_R t} + K_D e^{-\zeta_d \omega_{n_d} t}\cos(\omega t + \psi_\beta)\right]$$

where

$$K_o = \frac{D}{\lambda_R \omega_{n_d}^2}\left[\frac{C}{D} - \frac{1}{\lambda_R} - \frac{2\zeta_d \omega_{n_d}}{\omega_{n_d}^2}\right]$$

$$K_t = \frac{D}{\lambda_R \omega_{n_d}^2}$$

The subtraction method does not modify the residues and phase of the roll and Dutch roll modes.

The approach of subtracting the residue of the spiral mode from the sideslip time history for step aileron inputs is a possible solution to the problem of the poor correlation of pilot rating with $\Delta\beta_{max}$ when the sideslip results from the spiral residue rather than the Dutch roll residue.

From the study of landing approach data, however, it appears that a requirement based on the response to an impulse aileron input can be formulated and thus avoid the complication of identifying and subtracting the spiral residue from the sideslip response.

The $\Delta\beta_{max}$ requirement is tied to the bank angle response through the parameter $k = \frac{\phi_t \text{ command}}{\phi_t \text{ requirement}}$. There are a number of assumptions implicit in this requirement. First, the requirement assumes that a measure of the undesired response (sideslip excursion) resulting from an aileron input ratioed to the desired response (bank angle at a specific time) resulting from the aileron input will reflect flying qualities. The use of bank angle response as the measure of the desired response to aileron was intuitive, but to an extent arbitrary. In the roll oscillation requirements, the oscillatory component of roll rate or bank angle is ratioed to the average roll rate or bank angle resulting from the aileron input. This is a straightforward requirement relating an undesirable component of a response to the desirable component of the same response. In the case of the sideslip excursion requirement, the Dutch roll component of sideslip is identified as an undesirable component of the airplane's response to aileron commands but it is clearly an assumption to expect a measure of bank angle to be a universally valid parameter to use as the measure of the desired response to aileron. The situation is one of dividing "apples and oranges" so if a successful correlation parameter of this form does exist, its discovery will depend on intuition and empirical correlation. Using intuition one might argue that sideslip is a yawing motion and should therefore be ratioed with an aspect of the airplane heading or yaw rate response to aileron. Based on this intuition and examination of $\Delta\beta/\phi$ type measures from several experiments, it was determined that better correlation of several sets of data could be obtained by introducing the factor V_T/g. Specifically the following parameter has been found to have potential as a flying qualities parameter.

$$\frac{1}{\omega_{n_d}} \frac{V_T}{g} \frac{|\Delta\beta_{max}|_{t<1.2T_d}}{\hat{\phi}_1} \quad \text{versus} \quad \psi_{\beta_{IMPULSE}}$$

For an impulse aileron input, the sideslip response will consist mainly of the Dutch roll component with no problems from the spiral mode unless it is highly divergent. Thus the measure of sideslip is $\Delta\beta_{max}$ defined as the maximum peak-to-peak excursion occurring within $1.2\,T_d$ seconds. This time interval is stated to eliminate problems with an unstable Dutch roll mode or a highly unstable spiral mode. This measure of sideslip is divided by $\frac{g}{V_T}\hat{\phi}_1$, which can be viewed as a measure of the yaw rate response to the aileron input. $\hat{\phi}_1$ is the first peak of the bank angle response. A measure like $\hat{\phi}_{AV}$ could be specified to better reflect the yaw rate resulting from the steady bank angle but this was not considered likely to be significantly different from $\hat{\phi}_1$ for the low $|\phi/\beta|_d$ cases for which the sideslip excursion requirements are critical. The parameter $\hat{\phi}_1$ is proposed to eliminate the possibility that there would not be a peak if the spiral mode were unstable. The $\Delta\beta_{max}$ measure is divided by ω_{n_d} to preserve correlation observed for $\Delta\beta_{max}$ for a step aileron input.

Comment on effects of pilot location relative to c.g. and flight path

Two simulation facilities have recently been developed which permit simulation of lateral acceleration at the pilots' station during lateral-directional maneuvers. These facilities are the NASA FSAA ground simulator located at Ames Research Center and the Air Force TIFS variable stability airplane operated by Cornell Aeronautical Laboratory. Data from these two facilities are reported in References 34 and 35. The following quotation from Reference 34 describes observations concerning the effects of pilot location on lateral accelerations during turning maneuvers.

> "In a large aircraft approaching at high angles of attack the pilot can be situated several feet above the stability axes. If the aircraft is coordinated it will roll about the velocity vector or stability X axis. This can produce highly objectionable side accelerations at the cockpit, especially if the aileron roll acceleration is high. The only solutions are to reduce the aileron power below what is normally considered desirable or to degrade the degree of coordination. Both have deleterious effects so a design compromise must be made. The outcome of the proper compromises needs further investigation and definition."

Experience from Reference 35 also indicates noticeable lateral acceleration resulting from rolling and turning maneuvers when the pilot is located far ahead and above the center of gravity. Pilots were reluctant to believe that the simulation was proper because the lateral accelerations seem unnatural or nonairplane-like. The complaints or comments on this aspect were most pronounced for the configurations which lacked turn coordination, i.e., ones for which the aileron inputs, roll rate and bank angle caused the Dutch roll mode to be excited. Configurations with proverse yaw due to aileron were most noticeable in this regard. In the experiments reported in Reference 35, the cockpit was not as high above the flight path (line through c.g. parallel to relative wind) as it was for some of the configurations in Reference 34, thus the lateral acceleration resulting from roll acceleration about the flight path was not as large but the data of Reference 35 do not indicate a design compromise such as suggested above in the quotation from Reference 34.

If lateral accelerations at the cockpit result from roll control, it is thought that pilots will learn to understand and accept such accelerations and will modify their use of aileron (i.e., not make abrupt stick inputs) to ameliorate these accelerations. To suggest that an uncoordinated airplane for which the Dutch roll mode is excited by aileron inputs would be more preferable is thought to be incorrect.

Other parameters that were considered

As part of the work performed under this contract, a number of potential flying qualities parameters were studied. The parameters considered are listed below along with comments concerning their potential usefulness of limitations. Tabulated data and plots of pilot rating data for 8 of these parameters (indicated by asterisks in the right hand margin) are contained in Appendix III.

Step Aileron Input

$\frac{p_{osc}}{p_{AV}}$ vs $\psi_{\beta_{STEP}}$

For low frequency Dutch roll the amplitude of step must be small. Correlation with ψ_β is not good when L'_β is small. ψ_β is difficult to measure when $|\phi/\beta|_d$ is very large or the spiral residue is large in sideslip. Measurement is distorted when the spiral root is not at the origin. Except for the above difficulties, correlation is good.

$\frac{\hat{p}_{osc}}{\hat{p}_1}$ vs $\psi_{p_{STEP}}$

Discussed in text. Roll rate oscillation parameter. *

$\frac{\hat{p}_{osc}}{\hat{p}_{AV}}$ vs $\psi_{p_{STEP}}$

Roll rate oscillation parameter. Still must limit input size for low frequency Dutch roll to prevent excessive bank angle change. Phase angle correlation is improved, phase angle easier to measure. Spiral effect has been removed. Roll rate should be measured in stability axes. *

$\frac{\Delta\beta_{max}}{k}$ vs $\psi_{\beta_{STEP}}$ *

$k = \frac{\phi_{t\ command}}{\phi_{t\ required}}$

$\Delta\beta_{max}$ for $\begin{cases} t \leq 2 \text{ sec or } 1/2\ T_d \text{ whichever is greater} \\ t \leq 2 \text{ sec} \end{cases}$

ϕ_t required $\begin{cases} \text{for } t \text{ as specified in 3.3.4} \\ \text{for } t = 1.8 \end{cases}$

Correlation is poor when $\Delta\beta_{max}$ results from residue of spiral more rather than Dutch roll. Can only test for small aileron inputs. Relation to 3.3.4 complicates requirement. Attempts to reduce spiral problem by measuring $\Delta\beta_{max}$ within 2 sec only. Looked at all landing data for $\phi_t = 1.8$ rather than ϕ_t in 3.3.4.

Impulse Aileron Input

$\frac{\Delta\beta_{max}}{\phi_1}$ vs $\psi_{\beta_{IMPULSE}}$

$\Delta\beta_{max}$ for $\begin{cases} t \leq 1/2\ T_d \text{ or 6 sec whichever is less} \\ t \leq 2 \text{ sec} \end{cases}$

ϕ_1 first peak

ϕ_{max} within 2 sec, ϕ_{AV}, ϕ^* a weighted average were also considered.

Impulse input used to permit larger inputs and to reduce residue of spiral. Considered $t \leq 2$ sec to try to improve correlation of low frequency cases with good Dutch roll damping $\zeta_\phi > \zeta_d$.

$\frac{\Delta\beta_{max}}{\phi_1}\left|\frac{\phi}{\beta}\right|_d$ vs $\psi_{\beta_{IMPULSE}}$

$\Delta\beta_{max}$ for $t \leq 1/2\ T_d$ or 6 sec whichever is less

ϕ_1 first peak

$|\phi/\beta|_d$ Modal response vector magnitude, considered to be analogous with $\frac{\phi_{osc}}{\phi_{AV}}$. Did not work well for data in Reference 35 for low L'_β and high L'_r data.

$\frac{\Delta\beta_{max}}{\phi_1}$ vs $\psi_{\beta_{IMPULSE}}$	$\Delta\beta_{max}$ Largest value within $t \leq 1/4\ T_d$ Largest of first two peaks Largest Peak-Peak between first three peaks Search for simple sideslip measure for impulse input. Attempt to correlate low frequency high damped Dutch roll with $\zeta_\phi > \zeta_d$.	*
$\frac{1}{\omega_{n_d}} \frac{\Delta\beta_{max}}{\phi_1}$ vs $\psi_{\beta_{IMPULSE}}$	$\Delta\beta_{max}$ Largest Peak-Peak between first three peaks account for effect on Dutch roll residue of using impulse input instead of step input.	
$\frac{V_T}{g} \frac{\Delta\beta_{max}}{\phi_1}$ vs $\psi_{\beta_{IMPULSE}}$	$\Delta\beta_{max}$ Largest Peak-Peak of first three peaks explore idea of normalizing relative to yaw rate rather than bank angle response to aileron impulse.	*
$\frac{1}{\omega_{n_d}} \frac{V_T}{g} \frac{\Delta\beta_{max}}{\hat{\phi}_1}$ vs $\psi_{\beta_{IMPULSE}}$ $t < 1.2\ T_d$	Discussed in text. Uses impulse input to permit testing large inputs. Reduces residue of spiral mode. Divide by ω_{n_d} because impulse input used instead of step. Normalized to yaw rate rather than bank angle. $\Delta\beta_{max}$ is peak-peak so it is simple to measure. ψ_β is easy to measure for impulse input. $\hat{\phi}$ ~ residue of spiral mode is removed so first peak or steady state bank is definable.	*
$\frac{\lvert\hat{r}_{osc}\rvert_{t>.2T_d}}{\hat{r}_{AV}}$ vs $\psi_{r_{IMPULSE}}$	Yaw rate in stability axes. Spiral residue removed. $\hat{r}_{osc}$ and $\hat{r}_{AV}$ measured from Dutch roll peaks occurring after $1/5\ T_d$ are analogous to roll oscillation parameters. Delay of $1/5\ T_d$ is suggested because yaw rate has initial value for impulse input. Absolute value taken to avoid sign resulting from numerator. Information would be redundant with ψ_r . Sign of denominator indicates roll reversal. Correlation poor, Dutch roll frequency dependent.	
$\frac{1}{\omega_{n_d}} \frac{\lvert\hat{r}_{osc}\rvert_{t>.2T_d}}{\hat{r}_{AV}}$ vs $\psi_{r_{IMPULSE}}$	Divide by ω_{n_d} to improve correlation for different Dutch roll frequencies.	*
$\frac{1}{\omega_{n_d}^2} \frac{\lvert\hat{r}_{osc}\rvert_{t>.2T_d}}{\hat{r}_{AV}}$ vs $\psi_{r_{IMPULSE}}$	Yaw rate parameter discussed in text. Referenced to stability axes. Division by frequency squared should improve correlation for different Dutch roll frequencies.	*
$\frac{\hat{\phi}_{osc}}{\hat{\phi}_{AV}}$ vs $\psi_{\phi_{IMPULSE}}$	Roll oscillation parameter impulse input permits testing large inputs. Spiral residue is removed to eliminate distortion of ϕ_{osc}/ϕ_{AV} . Phase angle is referenced to Dutch roll in bank angle for impulse input. Bank angle should be attitude of flight path axis system.	
$\frac{\hat{\phi}_{osc}}{\hat{\phi}_1}$ vs $\psi_{\phi_{IMPULSE}}$	Discussed in text.	

Discussion of Roll Performance Requirements for Category C Flight Phases

In examining assumptions involved in the $\Delta\beta_{max}/k$ requirement, attention was directed at determining the validity of the roll performance numbers in Table IX of 3.3.4. For this purpose the roll performance requirements of Table IX were viewed as representing the minimum roll control authority necessary to perform maneuvers typical of the Class, Flight Phase and Level. They were not intended to cover all situations for which roll control authority might be required. For example, roll control authority in excess of the requirements of Table IX might be required in particular cases to balance unsymmetrical wing mounted stores, to trim high cross winds for airplanes with large dihedral or to counter gust effects for such airplanes.

Roll control usage data in the following reports was examined to establish roll control authority required for the landing approach Flight Phase.

Ref. 31	AFFDL-TR-70-145	Class IIL MIL-F-8785B(ASG)
Ref. 62	NASA TND-6339	Class II MIL-F-8785B(ASG)
Ref. 63	R&M 3347	Class IIL MIL-F-8785B(ASG)
Ref. 35	TIFS Phase I	Class III MIL-F-8785B(ASG)
Ref. 53	FAA 70-65	Class I MIL-F-8785B(ASG)
Ref. 33	NRC LTR FR-12	Class I MIL-F-83300

In References 31 and 62, in-flight experiments were performed in which roll control authority used in making landing approaches was measured. Tests were then repeated in which the roll control authority available to the pilot was limited to fractions of that used when the authority available was essentially unlimited.

The tests of Reference 31 showed that pilot ratings did not degrade beyond 3.5 until the control authority was reduced below $\phi_t = 16°$ in 1.8 sec. The roll control authority became unacceptable, P.R. = 6.5, when it was reduced below $\phi_t = 10°$ in 1.8 sec. These values were found to apply for configurations with the following characteristics

	Group 6	Group 11	Group 14	Group 16
ω_{n_d}	1.0	1.0	1.01	1.00
ζ_d	0.11	0.11	0.10	0.11
γ_R	0.40	0.35	1.10	2.0
γ_s	100.0	40.0	∞	∞
$\lvert\phi/\beta\rvert_d$	1.56	0.25	1.53	1.55

Note the factor of five range in roll damping (as approximated by $1/\tau_R$).

A case with higher L'_β and $|\phi/\beta|_d$ required considerably higher roll control authority for control in cross winds and turbulence.

The tests of Reference 62 showed that pilot ratings did not degrade beyond 3.5 until control authority was degraded below ϕ_t = 12° in 2 sec. The roll control authority became unacceptable, P.R. > 6.5, when it was reduced below ϕ_t = 6° in 2 sec. Turbulence and cross winds were not a major factor in the tests of Reference 62.

In Reference 63, the roll control authority and lateral-directional flying qualities of a number of Class II airplanes were investigated and evaluated for the landing approach task including sidestep maneuvers. A general result of this study was that roll control authority of ϕ_t = 20° in 1.8 sec was adequate for the task.

In the flight program of Reference 35, roll control power used in a number of landing approach, wave-off and go-around maneuvers was recorded. A brief analysis of this data shows that ϕ_t = 16° in 1.8 sec was not exceeded.

In the flight tests of Reference 53, roll control sensitivity and roll damping combinations were tested for a value of L'_β = -16. The data is discussed in terms of control authority available with no analysis of the control actually used in making the approaches. The report does include a number of time histories of approaches which indicate that the maximum control used for a configuration with τ_R = 0.4 did not exceed ϕ_t = 27° in 1.8 sec. If the extreme peaks are "clipped", a value of ϕ_t = 15° in 1.8 sec is indicated. This report shows that when the roll damping was reduced, τ_R > .4, the roll control authority required increased. The primary reason for this increase is believed to be the high L'_β used in the tests. The increased roll control authority was required to counter the gust-induced rolling motions.

In Reference 33 the roll control authority available for the $|\phi/\beta|_d$ = 0.20, τ_R = 0.25 cases was ϕ_t = 27° in 1.8 sec. Roll control actually used in the flight tests is not documented in the report but from pilot comments it can be observed that this control authority was adequate for the task.

From this review of roll control used in various experiments it is concluded that the roll control authority requirements in 3.3.4 for Category C Flight Phases are excessive for airplanes that do not have high sensitivity to cross wind and turbulence. Data in References 31, 53, 33, and 62 clearly indicate that there is an interaction between the roll control authority and the amount of roll damping and roll sensitivity to side velocity. A new requirement has been proposed which established minimum roll damping as a function of the parameter $\frac{|\phi/\beta|_d}{V_T \omega_{n_d}}$. Effort should also be directed toward establishing minimum control authority limits as a function of roll damping and sensitivity to side velocity.

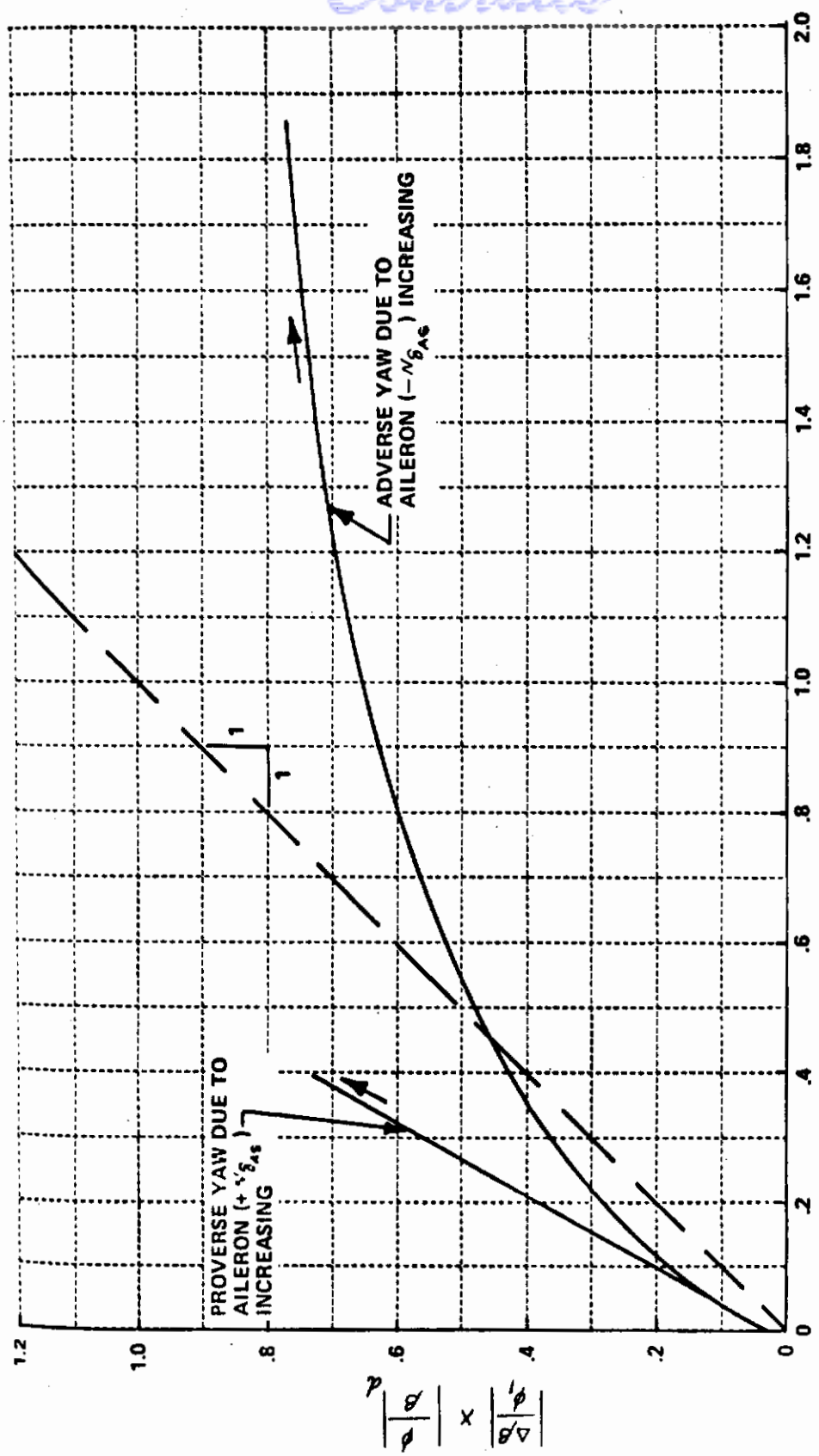

Figure 107 SENSITIVITY OF ROLL-SIDESLIP COUPLING PARAMETERS

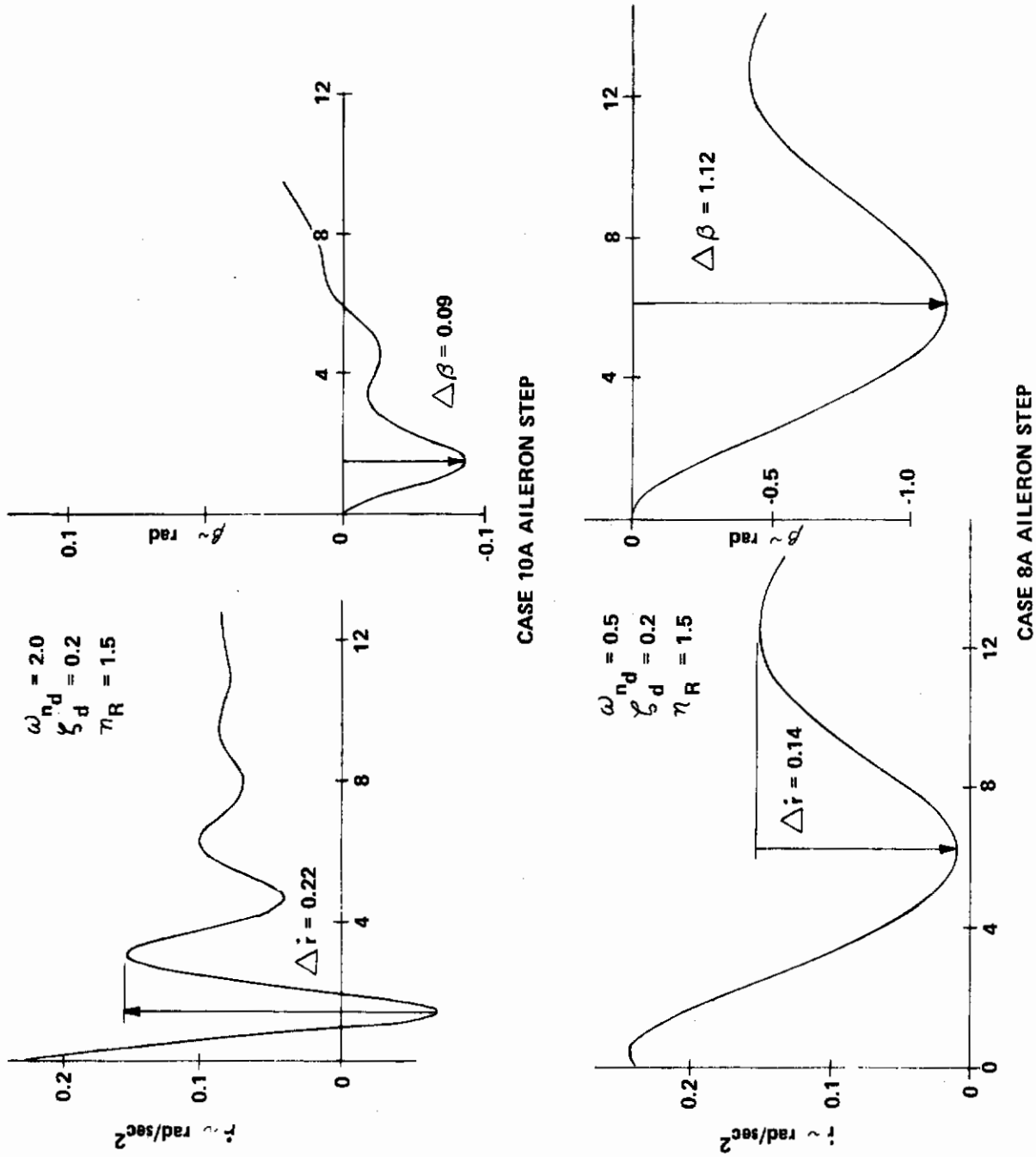

Figure 108 SIDESLIP AND YAW ACCELERATION RESPONSES TO STEP AILERON COMMAND

Discussion and Substantiation for 3.3.2.3 and 3.3.2.3.1

Several potential parameters were developed and discussed in the Motivation and Background Section for 3.3.2.1. The purpose was to develop a parameter to limit the amount of sideslip and to ensure good heading control and turn coordination for airplanes with low dihedral and low Dutch roll frequency. The data correlation achieved for the parameter

$$\frac{1}{\omega_{n_d}} \frac{V_T}{g} \frac{\Delta \dot{\beta}_{MAX}}{\hat{p}_1} \text{ vs. } \psi_{\dot{\beta}_{STEP}} \qquad \Delta \dot{\beta}_{MAX}\Big|_{t < 1.2\, T_d}$$

is shown in Figures 109 to 123 for the data in the references listed in the discussion of new Paragraphs 3.3.22 and 3.3.2.2.1. These plots are identical to what would be obtained for sideslip and bank angle for an impulse input,

$$\frac{1}{\omega_{n_d}} \frac{V_T}{g} \frac{\Delta \beta_{MAX}}{\ddot{\phi}_1} \text{ vs. } \psi_{\beta_{IMPULSE}} \qquad \Delta \beta_{MAX}\Big|_{t < 1.2\, T_d}$$

In establishing boundaries on Figures 109 to 123, emphasis was given to cases with low dihedral effect. The data from the various experiments is sufficient to define the Level 1 boundary reasonably well. The Level 2 boundary is less well defined because there are fewer data points, especially for phase angles other than $\psi_{\dot{\beta}_{STEP}} = -90°$ or $-270°$.

The data from the fifteen references have been grouped into three sets corresponding to Flight Phase Categories A, B and C. The Level 1 and 2 boundaries defined by the data for Flight Phase Category A were found to be greatly different from the boundaries defined by the data for Flight Phase Category C. The Flight Phase Category A boundaries are much more severe than the boundaries for Flight Phase Category C.

The data for Flight Phase Category B is limited but seemed to define a Level 1 boundary nearly the same as that defined by the data for Flight Phase Category C. Based on this observation, the Level 1 and 2 boundaries for Flight Phase Categories B and C have been made identical.

Figure 109 DATA FROM AFFDL-TR-67-98 (MEEKER-HALL)

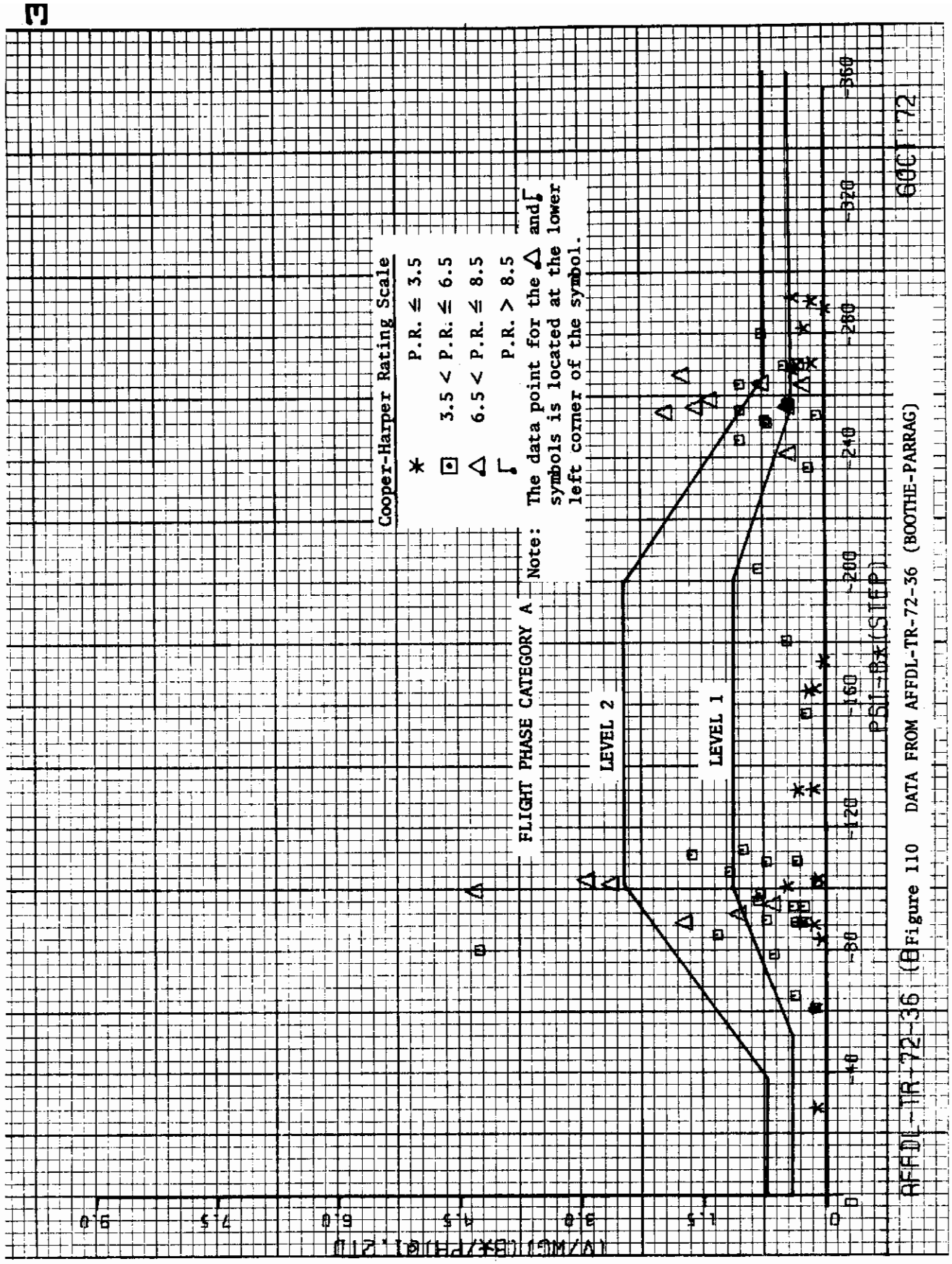

Figure 110 DATA FROM AFFDL-TR-72-36 (BOOTHE-PARRAG)

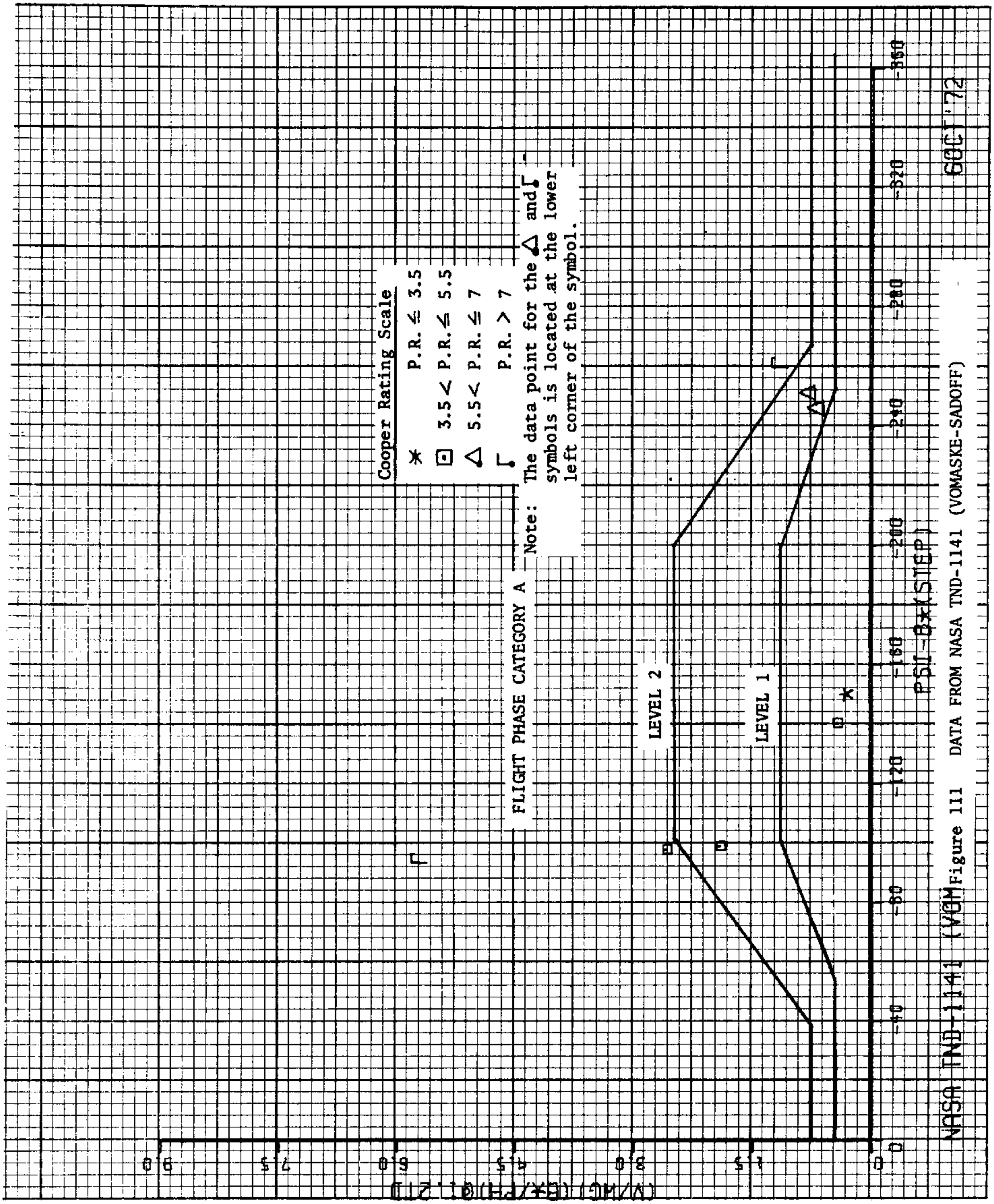

Figure 111 DATA FROM NASA TND-1141 (VOMASKE-SADOFF)

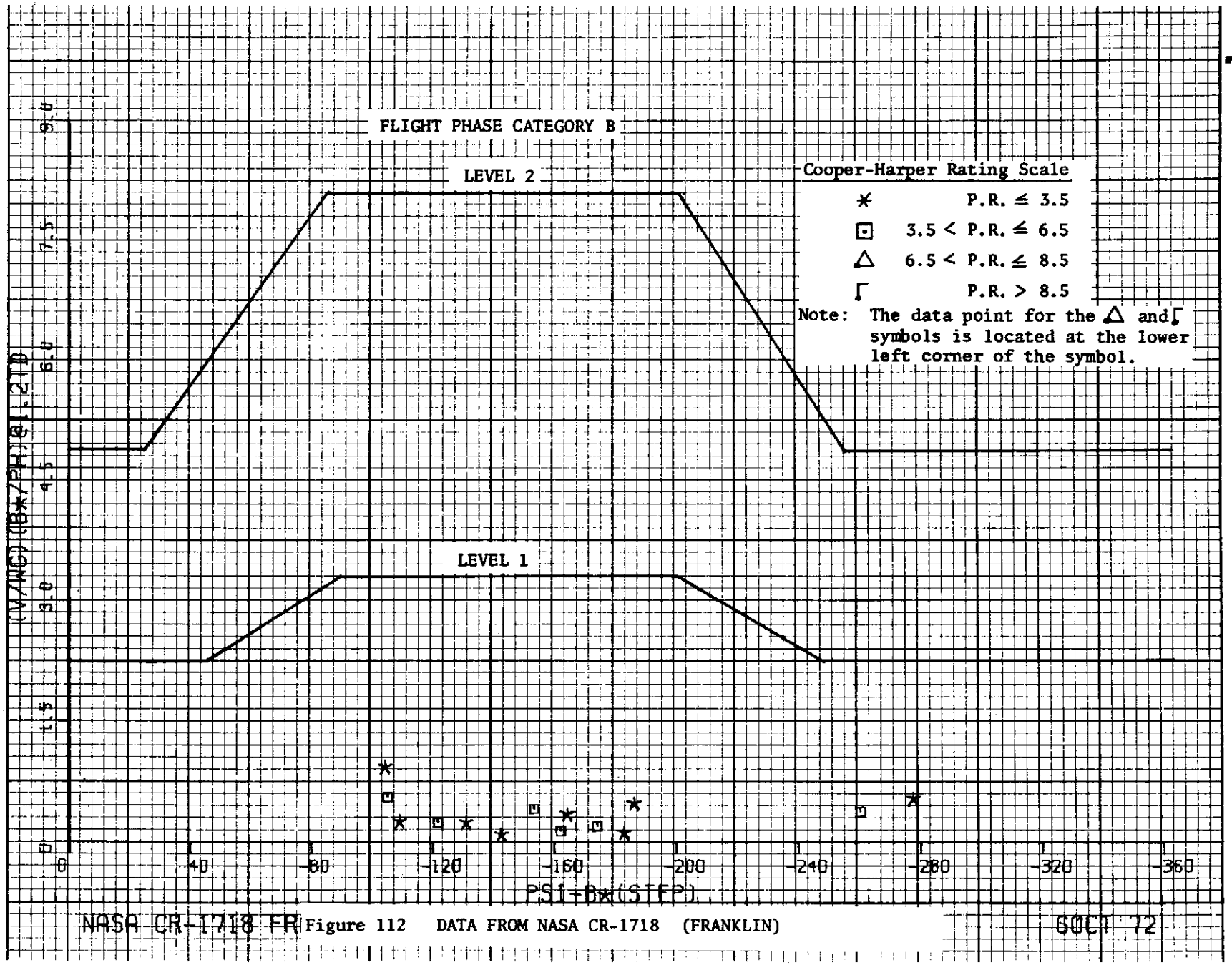

Figure 112 DATA FROM NASA CR-1718 (FRANKLIN)

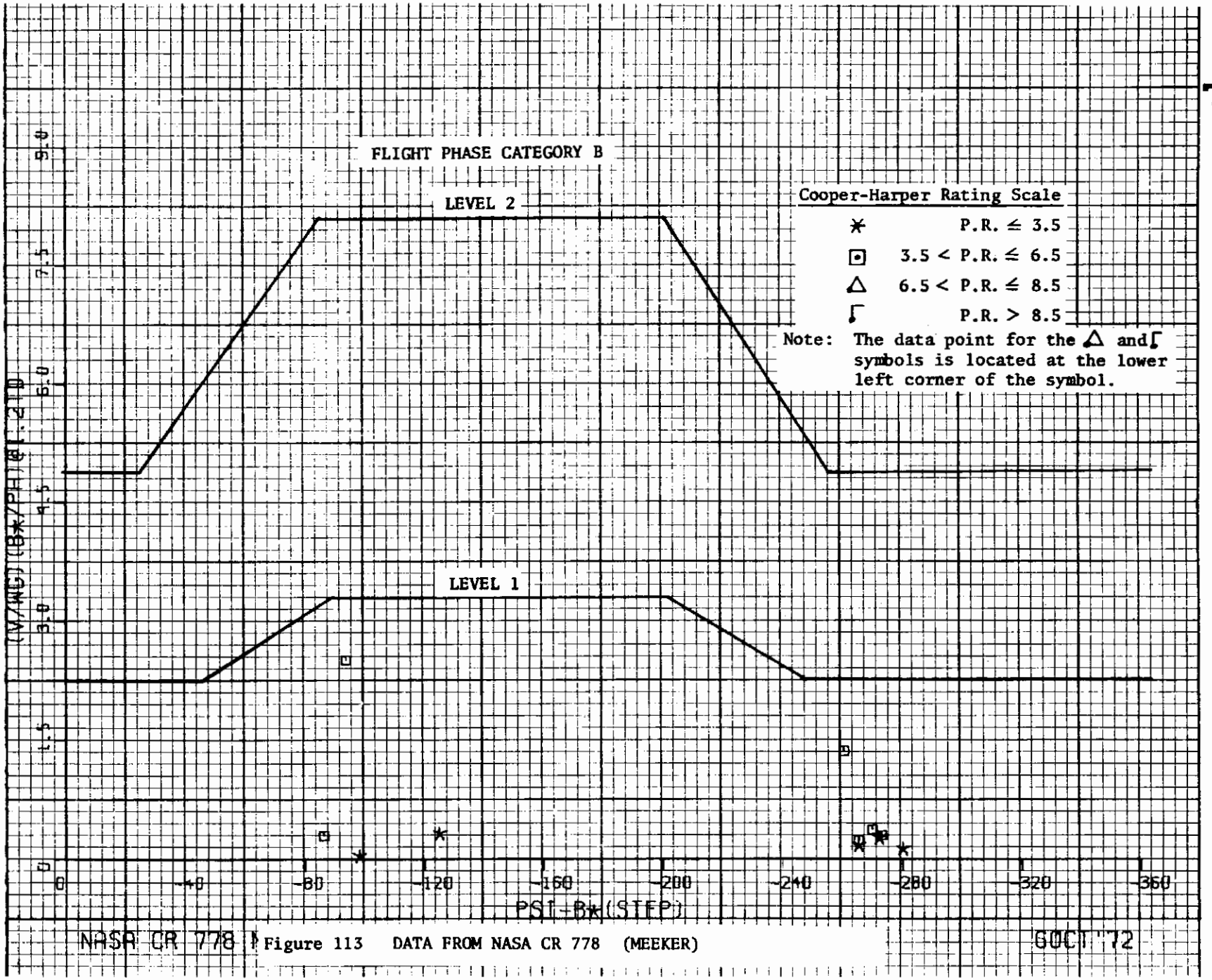

Figure 113 DATA FROM NASA CR 778 (MEEKER)

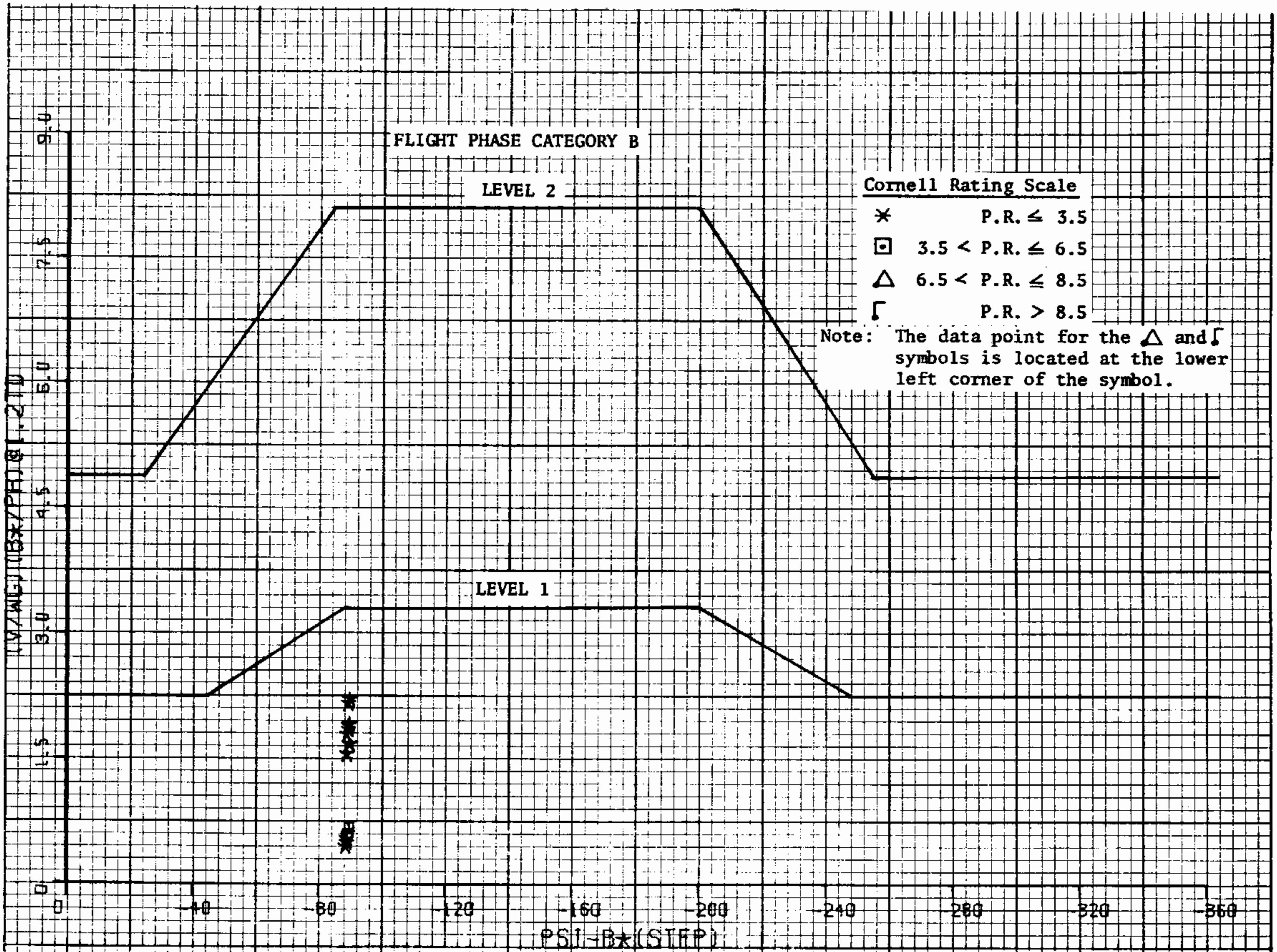

AFFDL TR-69-11 Figure 114 DATA FROM AFFDL TR-69-13 (HALL)

GOC1 '72

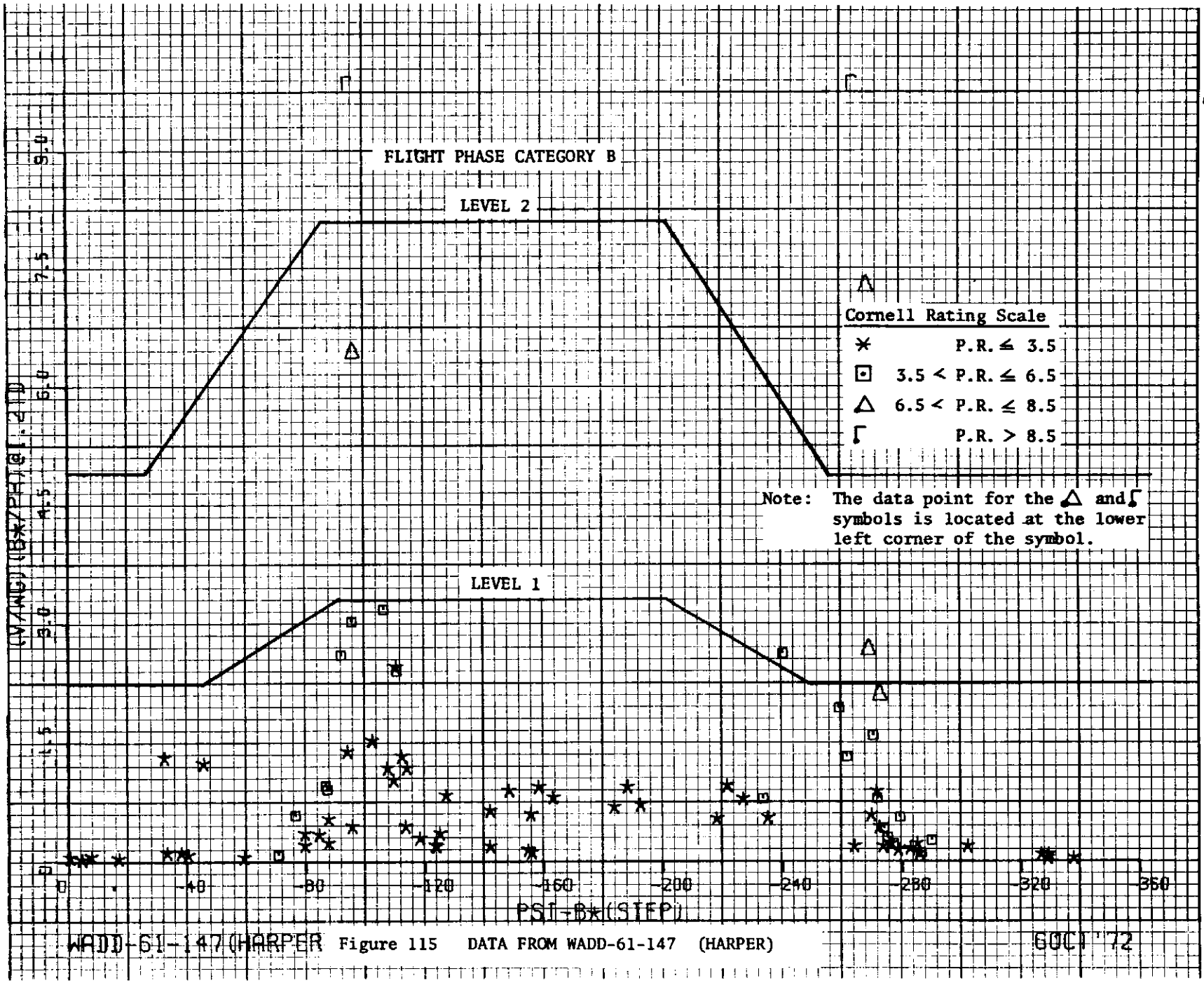

Figure 115 DATA FROM WADD-61-147 (HARPER)

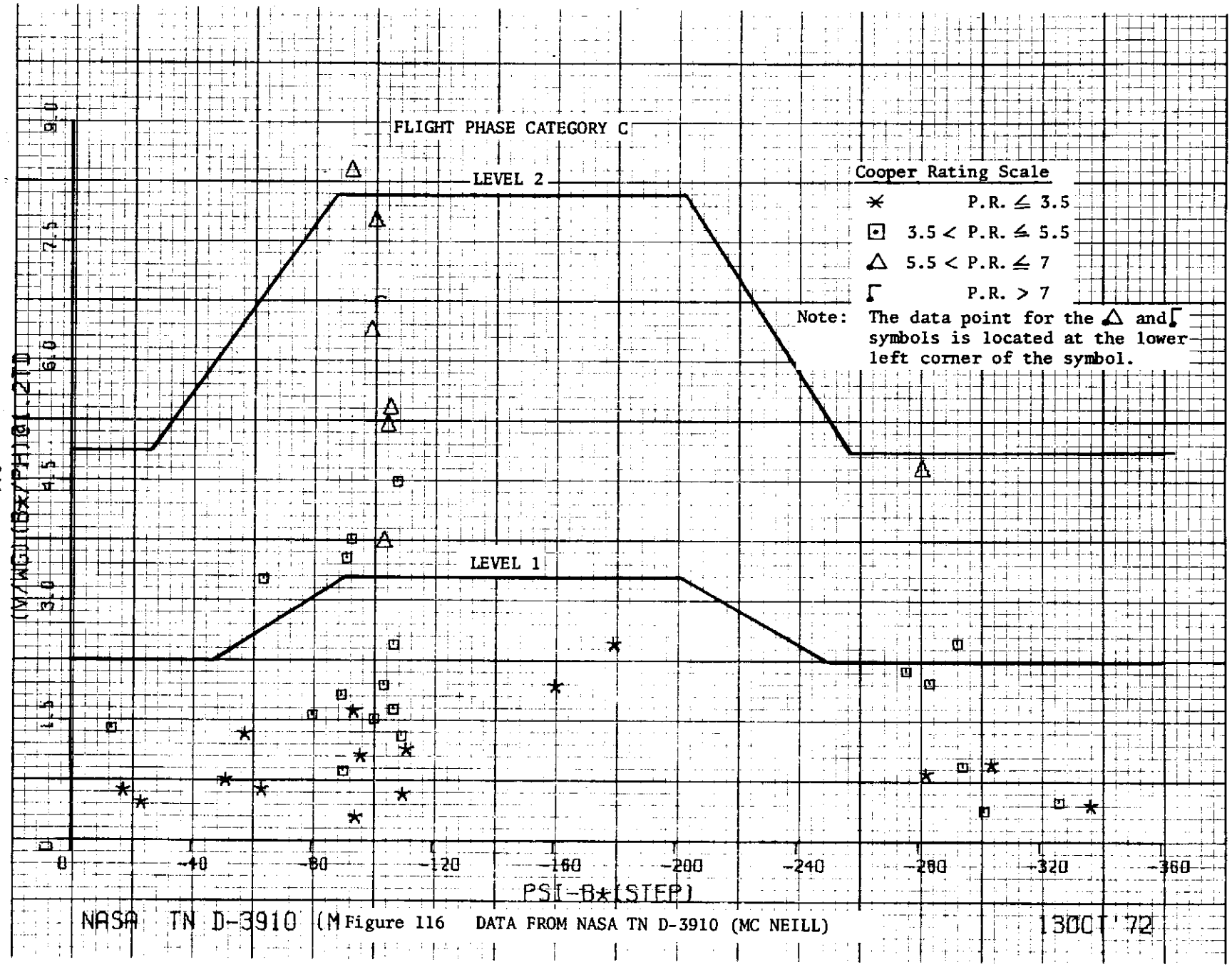

Figure 116 DATA FROM NASA TN D-3910 (MC NEILL)

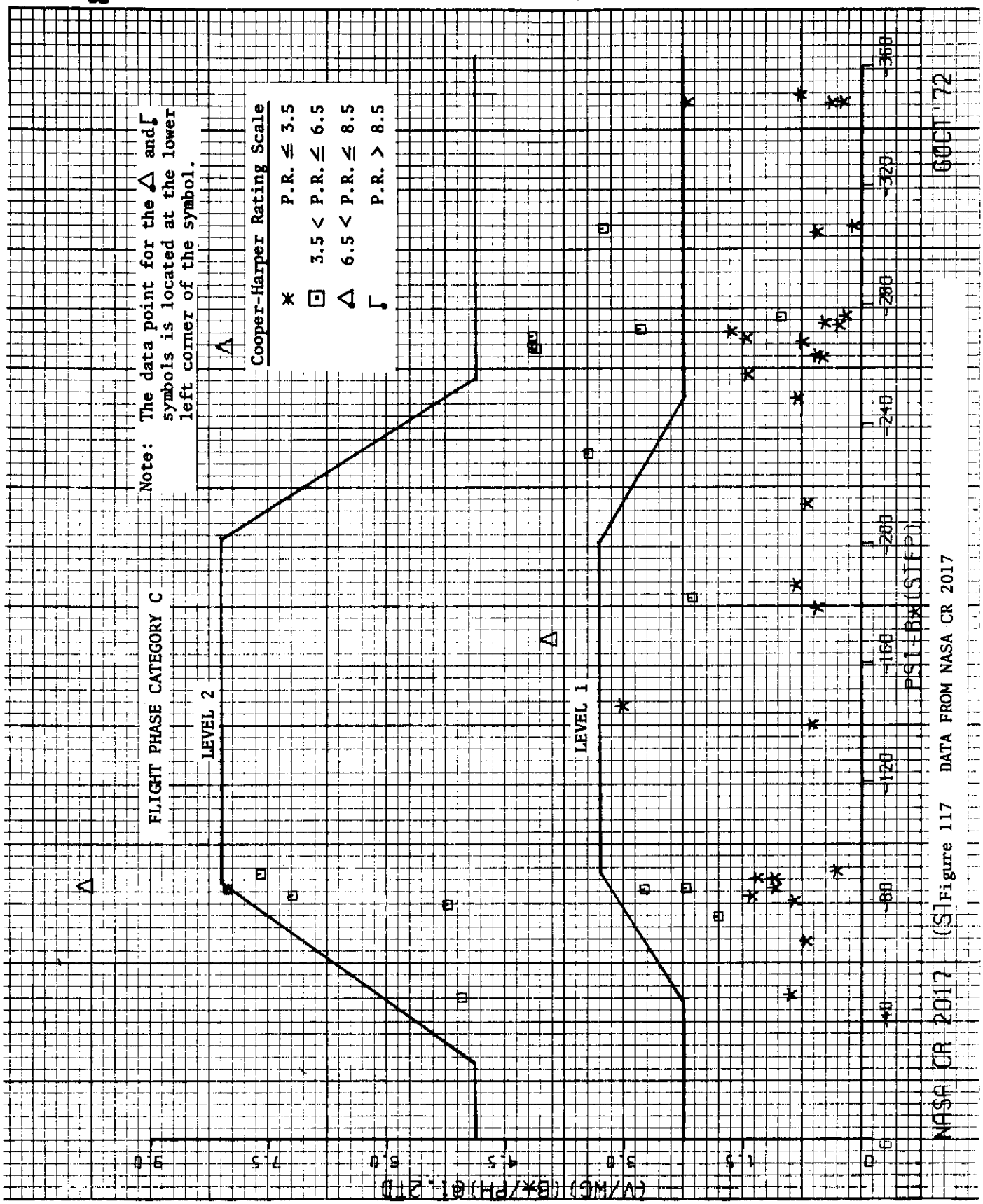

(S)Figure 117 DATA FROM NASA CR 2017

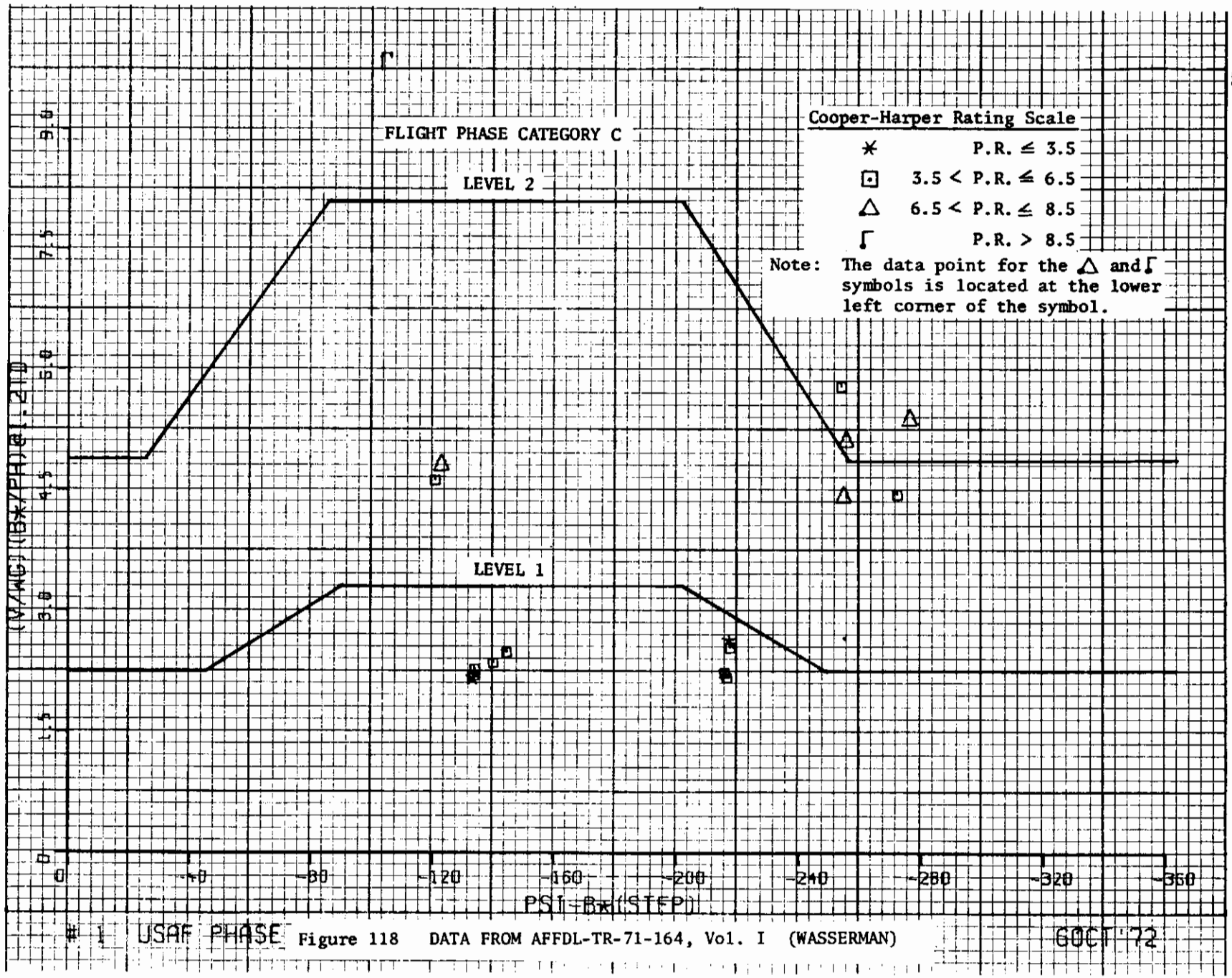

Figure 118 DATA FROM AFFDL-TR-71-164, Vol. I (WASSERMAN)

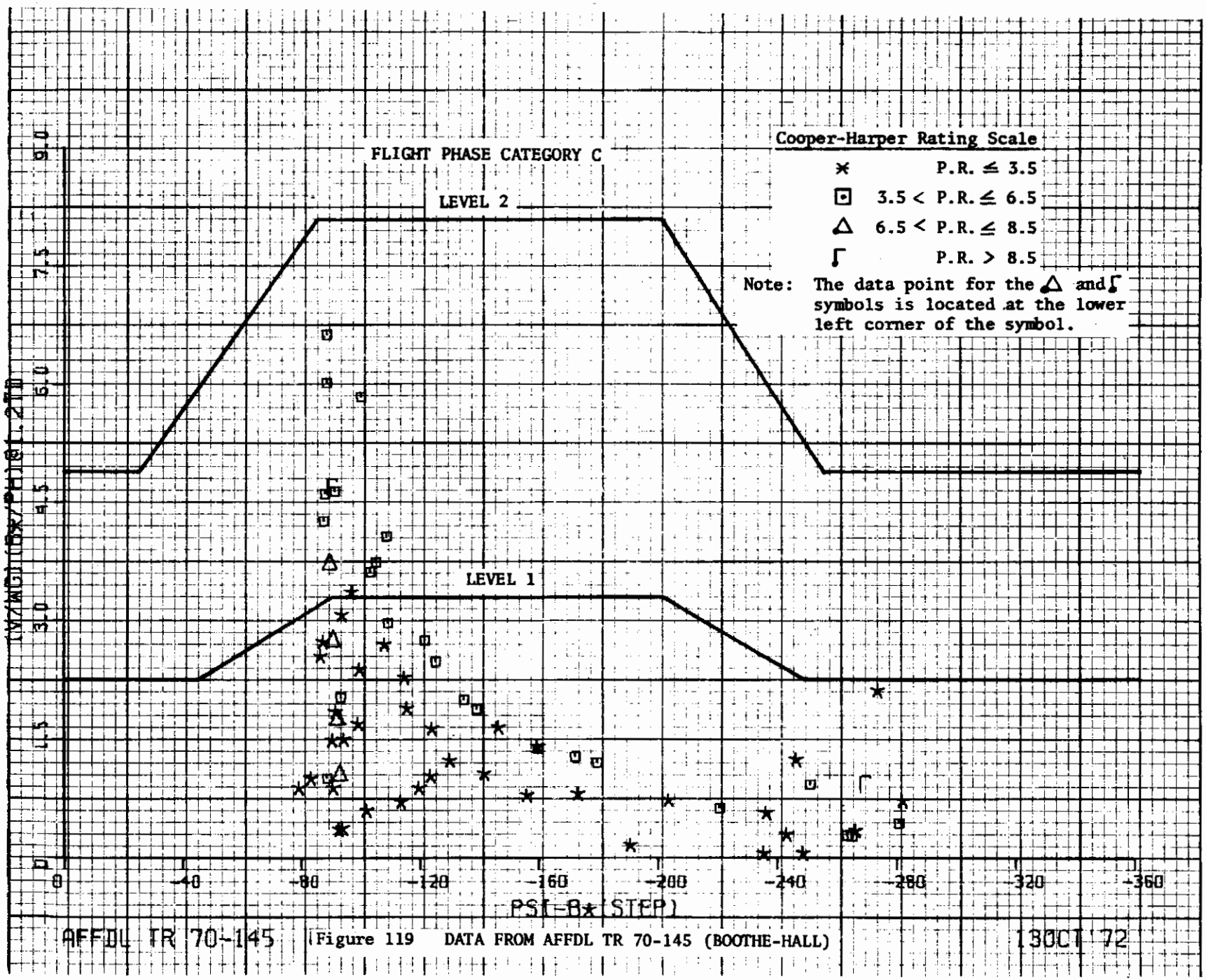

AFFDL TR 70-145 Figure 119 DATA FROM AFFDL TR 70-145 (BOOTHE-HALL) 130CT72

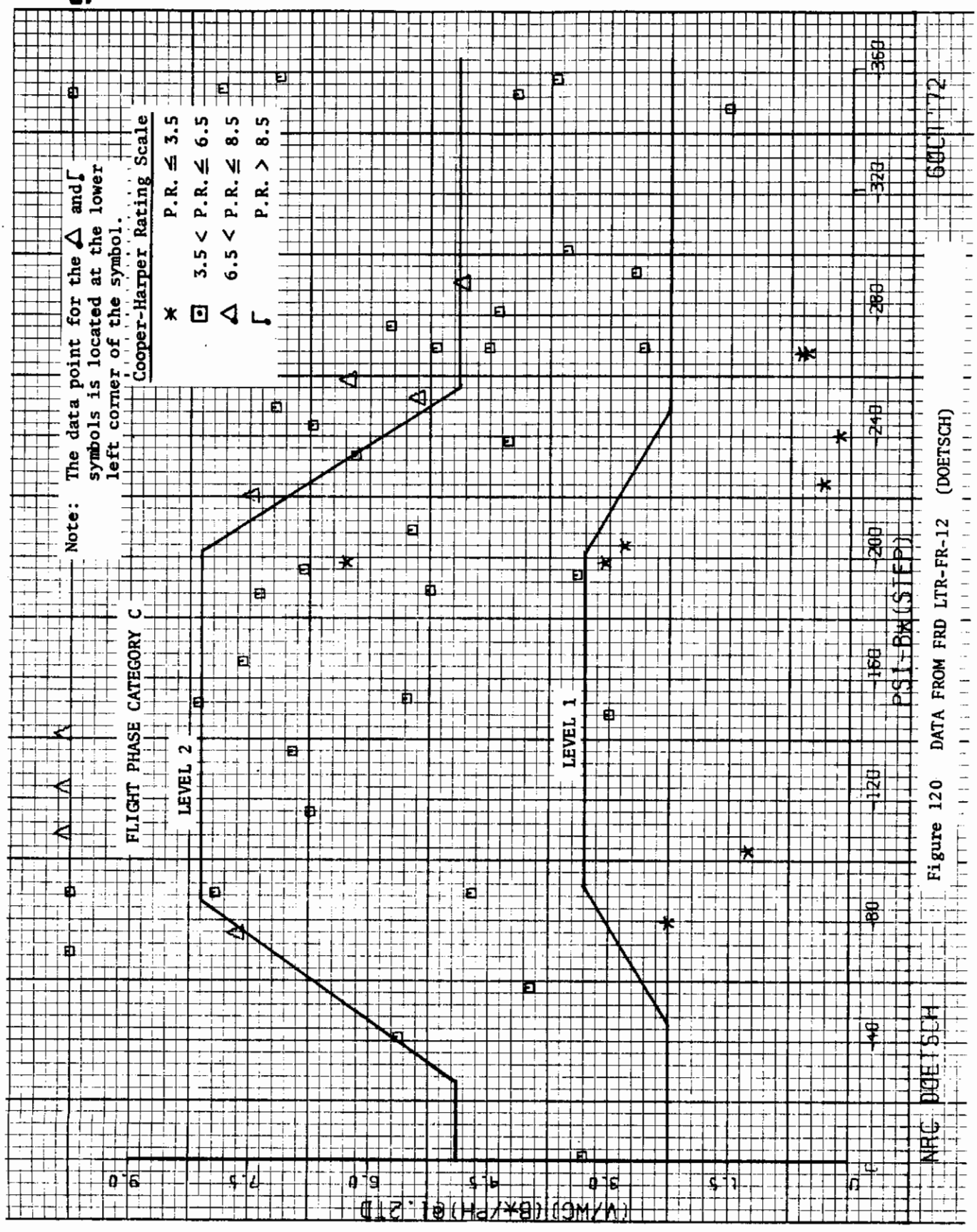

Figure 120 DATA FROM FRD LTR-FR-12 (DOETSCH)

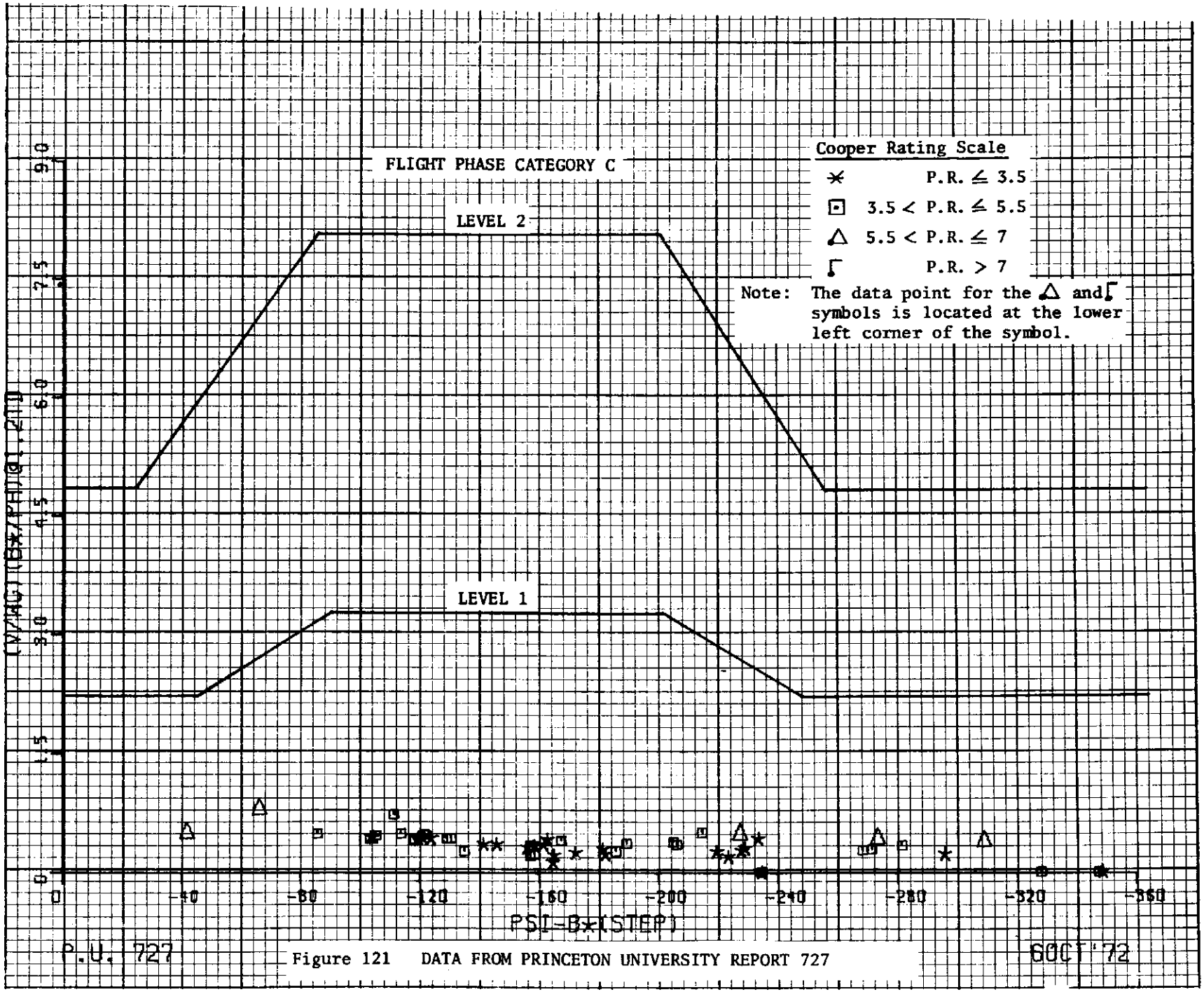

Figure 121 DATA FROM PRINCETON UNIVERSITY REPORT 727

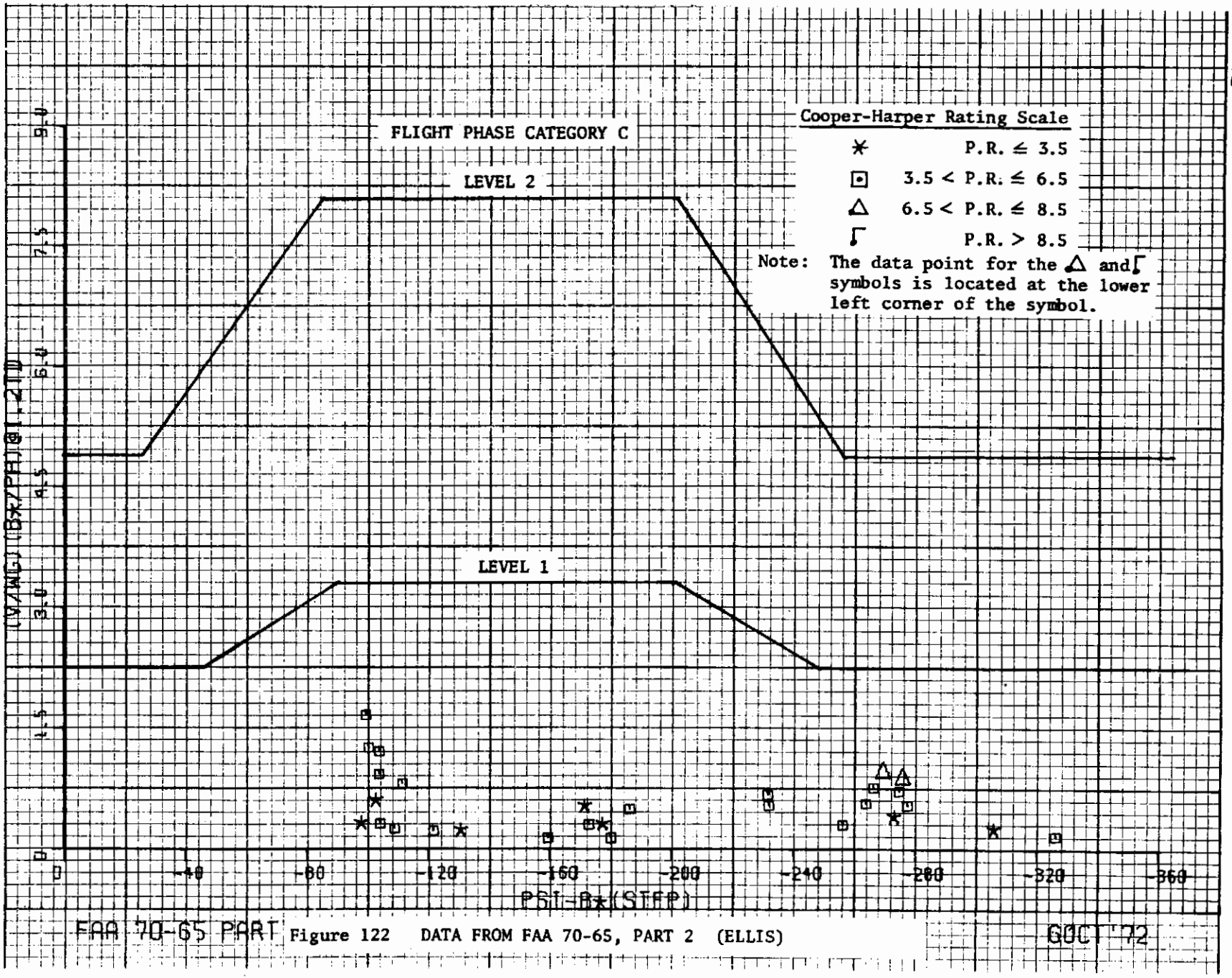

FAA 70-65 PART Figure 122 DATA FROM FAA 70-65, PART 2 (ELLIS)

GOCT 72

Figure 123 DATA FROM FAA RD-71-118 (ELLIS)

Action recommended for Pilot-induced oscillations, 3.3.3		No change
Action recommended for Roll-control effectiveness, 3.3.4		
3.3.4	Roll control effectiveness	No change - see discussion
3.3.4.1	Roll performance for class IV airplanes	
3.3.4.1.1	Air-to-air combat	
3.3.4.1.2	Ground attack with external stores	
3.3.4.1.3	Roll rate characteristics for ground attack	
3.3.4.1.4	Roll response	
3.3.4.2	Aileron control forces	
3.3.4.3	Linearity of roll response	
3.3.4.4	Wheel control throw	
3.3.4.5	Rudder-pedal-induced rolls	

Action recommended for Directional control characteristics, 3.3.5

3.3.5	Directional control characteristics	Not treated in this study; no change is recommended
3.3.5.1	Directional control with speed change	
3.3.5.1.1	Directional control with asymmetric loading	
3.3.5.2	Directional control in wave-off (go-around)	

Action recommended for Lateral-directional characteristics in steady sideslips, 3.3.6

3.3.6	Lateral-directional characteristics in steady sideslips	
3.3.6.1	Yawing moments in steady sideslips	Not treated in this study; no change is recommended
3.3.6.2	Side forces in steady sideslips	
3.3.6.3	Rolling moments in steady sideslips	
3.3.6.3.1	Exception for wave-off (go-around)	
3.3.6.3.2	Positive effective dihedral limit	

Action recommended for Lateral-directional control in cross winds, 3.3.7

3.3.7	Lateral-directional control in cross winds	Not treated in this study; no change is recommended
3.3.7.1	Final approach in cross winds	
3.3.7.2	Takeoff run and landing rollout in crosswinds	
3.3.7.2.1	Cold- and wet-weather operation	
3.3.7.2.2	Carrier-based airplanes	
3.3.7.3	Taxiing wind speed limits	

Action recommended for Lateral-directional control in dives, 3.3.8

3.3.8	Lateral-directional control in dives	No change

Action recommended for Lateral-directional control with asymmetric thrust, 3.3.9

3.3.9	Lateral-directional control with asymmetric thrust	Not treated in this study; no change is recommended
3.3.9.1	Thrust loss during takeoff run	
3.3.9.2	Thrust loss after takeoff	

3.3.9.3 Transient effects

3.3.9.4 Asymmetric thrust-rudder pedals free

3.3.9.5 Two engines inoperative

} Not treated in this study; no change is recommended.

Section IV

PROPOSED REVISIONS TO MISCELLANEOUS FLYING QUALITIES 3.4

No action is recommended at this time.

CAL participated in the Air Force in-house effort that resulted in Interim Amendment-1 (USAF) 31 March 1971 to MIL-F-8785B(ASG). CAL also reviewed the 22 February and 31 March draft versions of MIL-F-83691 (USAF).

The review comments prepared by CAL were transmitted to the Air Force in FRM No. 454 dated March 1971 and in a letter to AFFTC/TGEP 6510 dated 21 June 1971.

Section V

PROPOSED REVISIONS TO CHARACTERISTICS OF THE PRIMARY FLIGHT CONTROL SYSTEM 3.5

3.5.1	General characteristics	No Change
3.5.2	Mechanical characteristics	No Change
3.5.2.1	Control centering and breakout forces	No Change
3.5.2.2	Cockpit control free play	No Change
3.5.2.3	Rate of control displacement	No Change
3.5.2.4	Adjustable controls	No Change
3.5.3	Dynamic characteristics	Delete
3.5.3.1	Control feel	Delete
3.5.3.2	Damping	Renumber 3.5.3.1
3.5.4	Augmentation systems	No Change
3.5.4.1	Performance of augmentation systems	No Change
3.5.4.2	Saturation of augmentation systems	No Change
3.5.5	Failures	No Change
3.5.5.2	Trim changes due to failures	No Change
3.5.6	Transfer to alternate control mode	No Change
3.5.6.1	Transients	No Change
3.5.6.2	Trim changes	No Change

Introduction and Motivation for Action Recommended for 3.5

The requirements of 3.5.3 and 3.5.3.1 were included in MIL-F-8785B(ASG) in an attempt to quantify control system dynamic characteristics. Further analysis and more recent experimental data, Reference 8, indicate that the requirements as stated are not generally applicable and it is recommended that they be deleted. The new requirement for pitch dynamic response in maneuvering flight, 3.2.2.1, treats the combined airplane-control system-feel system combination and reduces the need for a separate quantitative requirement on the control system dynamics. It is proposed that the qualitative requirement from paragraph 6.11 of MIL-F-8785 amendment No. 4 dated 17 April 1959 be substituted.

Proposed New Paragraphs

3.5.3 Control system dynamic characteristics. So many arrangements of flight control systems are possible, considering direct mechanical, power-boosted, and fully powered controls, artificial feel, artificial stabilization, autopilot tie-in, etc., that a limited set of requirements such as those specified in paragraph 3.5 hardly can be expected to rule out all undesirable characteristics. Some of the known important variables, even in a simple system, are friction in the control valve; friction, flexibility, back-lash, gear ratio, and inertia in the control system; viscous damping and preload in the control system or valve; rate limiting of the control actuator; and the level of aircraft static and dynamic stability. The introduction of nonlinear linkages or valve characteristics further multiplies the important variables. In general, the designer should make every effort to provide a linear or smoothly varying response to cockpit control deflection and to control force for all amplitudes of control input, including values of stick force within the range of allowable breakout forces (table XII), and small control deflections such as those required in tracking. The phase lag between the cockpit control deflection or force and control surface deflection should be kept to a minimum for reasonably large amplitude motions at frequencies considerably above the airplane natural frequencies, and should not increase unduly at very small control amplitudes.

3.5.3.1 Damping [Same as 3.5.3.2 of MIL-F-8785B(ASG)].

Discussion and Substantiation

The quantitative requirements of 3.5.3 and 3.5.3.1 were based primarily on data in Reference 11. Since MIL-F-8785B(ASG) was adopted the experiment reported in Reference 8 has been performed and the data resulting from Reference 8 does not substantiate the requirement.

Studies reported in References 64 and 65 also cast doubt on the general validity of the quantitative requirement of 3.5.3 and 3.5.3.1 of MIL-F-8785B(ASG).

It is proposed that the requirements be deleted and the qualitative requirement of the proposed new 3.5.3 be substituted.

The new requirements of 3.2.2.1 and 3.2.2.3 should serve the purpose intended by the old 3.5.3 and 3.5.3.1 and are more general in application.

Section VI

PROPOSED REVISIONS TO 3.6, CHARACTERISTICS OF SECONDARY CONTROL SYSTEMS

Action Recommended for Characteristics of secondary control systems, 3.6

No changes are recommended.

SECTION VII

PROPOSED REVISIONS TO 3.7, ATMOSPHERIC DISTURBANCES

INTRODUCTION

The purpose of this section is to summarize a study that was made of the atmospheric turbulence requirements (Section 3.7) of MIL-F-8785B, and to present relevant conclusions. In particular, attention was focused upon the following items:

1. Development of a wind shear model.
2. New definition of the values for σ_u , σ_w , σ_v given in 3.7.3.
3. Interpretation of the ρ_g spectrum given in 3.7.5.
4. Interpretation of the q_g spectrum given in 3.7.5.

Items 2, 3, and 4 required study as a result of comments and correspondence received concerning Section 3.7 and Item 1 in an attempt to fill a gap in the current specification.

A fairly comprehensive literature survey was undertaken for the effort on Items 1 and 2, and a partial bibliography is given at the end of this section. A major portion of the survey concerned meteorological research of the so-called "atmospheric surface layer," and is material not originally used in the development of Section 3.7. This section will discuss these theories only in passing in the presentation of the wind shear and turbulence intensities models; a more complete discussion is given in References 66 and 67.

This section is organized as follows. Each subsection of 3.7 is listed in order. If no change in the section is required, either in the specification or the background discussion in Reference 3, this fact is noted; if a change in either the specification or the background discussion is necessary, the change is given, followed by a discussion of the philosophy behind the change. The wind shear model is introduced as Section 3.7.5, with the previous 3.7.5, Application of the turbulence models in analyses, changed to 3.7.6.

DISCUSSION OF SECTION 3.7 OF MIL-F-8785B(ASG)

3.7.1 Use of turbulence models. No change to either specification or BIUG.

3.7.2 Turbulence models. No change to specification. No change to BIUG except that "homogeneity" is consistently misspelled.

3.7.2.1, 3.7.2.2 Continuous random turbulence model.

A. Change requirements:

3.7.2.1 Continuous random model (von Karman form). The von Karman form of the spectra for the turbulence velocities is:

$$\Phi_{u_g}(\Omega) = \sigma_u^2 \frac{2L_u}{\pi} \frac{1}{\left[1+(1.339\,L_u\Omega)^2\right]^{5/6}}$$

$$\Phi_{v_g}(\Omega) = \sigma_v^2 \frac{2L_v}{\pi} \frac{1+\frac{8}{3}(2.678\,L_v\Omega)^2}{\left[1+(2.678\,L_v\Omega)^2\right]^{11/6}}$$

$$\Phi_{w_g}(\Omega) = \sigma_w^2 \frac{2L_w}{\pi} \frac{1+\frac{8}{3}(2.678\,L_w\Omega)^2}{\left[1+(2.678\,L_w\Omega)^2\right]^{11/6}}$$

3.7.2.2 Continuous random model (Dryden form). The Dryden form of the spectra for the turbulence velocities is:

$$\Phi_{u_g}(\Omega) = \sigma_u^2 \frac{2L_u}{\pi} \frac{1}{1+(L_u\Omega)^2}$$

$$\Phi_{v_g}(\Omega) = \sigma_v^2 \frac{2L_v}{\pi} \frac{1+12(L_v\Omega)^2}{\left[1+4(L_v\Omega)^2\right]^2}$$

$$\Phi_{w_g}(\Omega) = \sigma_w^2 \frac{2L_w}{\pi} \frac{1+12(L_w\Omega)^2}{\left[1+4(L_w\Omega)^2\right]^2}$$

B. Change BIUG:

1. Change last paragraph on page 425 to read: "Both the von Karman and Dryden forms of the one-dimensional spectra satisfy all the mathematical requirements for isotropic atmosphere turbulence. For isotropic turbulence, the characteristics of the one-dimensional spectra are related by:

$$\sigma^2 = \sigma_u^2 = \sigma_v^2 = \sigma_w^2$$

and

$$L = L_u = 2L_v = 2L_w$$

2. Change L_w to $2L_w$ in Figure 1 (3.7.2.1, 3.7.2.2).

C. Philosophy of the Changes:

The spectra and scales as defined in 3.7.2.1, 3.7.2.2 of MIL-F-8785B give the correct answers, but for the wrong reasons. In isotropic turbulence, the three longitudinal scales are all equal, the six lateral scales are all equal, and the longitudinal scales equal twice the lateral scales. Longitudinal and lateral here refer to the gust field, not the airplane. When we are

considering one-dimensional spectra, there is one longitudinal scale in the direction of the spatial frequency (L_u), and the other two scales (L_w and L_v) are lateral scales. This point is frequently confused; for explanation and derivation, see References 66 and 68. As presently written in 3.7.2.1 and 3.7.2.2, the equations are correct only if L_u is written in all of them. The change is merely adding the factor 2 to L_w and L_v where they appear.

3.7.2.3 Discrete model.

A. Change requirement:

The abscissa of Figure 7 of MIL-F-8785B (Magnitude of Discrete Gusts) should be changed to: "Normalized Discrete Gust Length $\frac{dx}{L_u}$, $\frac{dy}{2L_u}$, $\frac{dz}{2L_w}$."

B. No change required for BIUG.

C. Philosophy for the changes.

The change in the ordinate is a direct result of the change to 3.7.2.1, 3.7.2.2, and is consistent.

3.7.3 Scales and intensities (Clear air turbulence).

A. Change requirement:

1. Change the initial part of the requirement to read: "The root-mean-square intensity $\sigma_u = \sigma_v$ for clear air turbulence is defined on figure 8 as a function of altitude. The intensity σ_w may be obtained using the relationships:

$$\frac{\sigma^2}{L^{2/3}} = \frac{\sigma_u^2}{L_u^{2/3}} = \frac{\sigma_v^2}{(2L_v)^{2/3}} = \frac{\sigma_w^2}{(2L_w)^{2/3}} \quad \text{(von Karman form)}$$

$$\frac{\sigma^2}{L} = \frac{\sigma_u^2}{L_u} = \frac{\sigma_v^2}{2L_v} = \frac{\sigma_w^2}{2L_w} \quad \text{(Dryden form)}$$

2. Change the ordinate on Figure 8 of MIL-F-8785B (Intensity for Clear Air Turbulence) to:

"Root-Mean-Square Gust Intensities, $\sigma_u = \sigma_v$ ft/sec."

B. Change BIUG:

Change the last part of pg 438 (after (4)) to read: "The following procedure was therefore used to develop the intensity models for MIL-F-8785B. Using the isotropic assumption, so that $\sigma_u^2 = \sigma_v^2 = \sigma_w^2 = \sigma^2$ and $L = L_u = 2L_v = 2L_w$, and choosing an appropriate Dryden scale length, L, a large quantity of data was analyzed as outlined above to obtain σ^2. This probability density function is integrated to become the cumulative probability distribution, which is then multiplied by the probability of encountering turbulence

as a function of altitude, thereby yielding the probability of equalling or exceeding a given value of σ as a function of altitude, or "exceedance probability". By choosing an "exceedance probability", therefore, we determine σ as a function of altitude. However, MIL-F-8785B also specifically introduces anisotropy at low altitudes, and hence, for the σ just obtained, the relationship $\sigma^2 = \sigma_u^2 = \sigma_v^2 = \sigma_w^2$ is no longer valid below a given altitude. It is assumed that $\sigma^2 = \sigma_u^2 = \sigma_v^2$ remains valid, and then σ_w is determined by using the relationships given in 3.7.3, the scale lengths given in 3.7.3.1, 3.7.3.2, and the value in Figure 8 of MIL-F-8785B.

The following discussion gives in more detail the development of Figure 8. It starts with the determination of the statistical properties of σ, and then gives the determination of $\sigma_u = \sigma_v$ as a function of altitude."

2. Change σ_w to σ in all of the discussion Statistical properties of σ_w. Also delete "vertical" where it appears. (Pgs 437 to top of 440).

3. Discussion Specification of σ_w (pg 440) - change to read as follows: "Specification of σ_u $(= \sigma_v)$. With the statistics of σ determined as just discussed, it is now possible to provide a concrete value as a function of altitude. Recalling the assumption that $\sigma^2 = \sigma_u^2 = \sigma_v^2$ is valid even at low altitude, a value of $\sigma_u = \sigma_v$ is specified as a function of altitude for clear air turbulence that can only be equalled or exceeded with a probability of 0.01."

Change σ_w to $\sigma_u = \sigma_v$ in the rest of this first paragraph (pg 440).

Change $L_u = L_v = L_w$ to $L_u = 2L_v = 2L_w$ in the second paragraph (pg 440).

4. Change σ_w to σ in Figure 2 (3.7.3).

C. Philosophy of the changes:

The original requirements of 3.7.3 were first questioned by the Boeing Company (Reference 69). They noted that, using the value of σ_w from Figure 8 and the scales of 3.7.3.1, 3.7.3.2, σ_u and σ_v were forced to increase as altitude decreased, a situation which they questioned. In addition, other individuals using 3.7.3 of MIL-F-8785B for simulation work (e.g., NASA-Ames) have expressed the opinion that the value of σ_w given by Figure 8 is unrealistically high as the ground is approached. The proposed change is an attempt to cure these difficulties. The following discussion presents the evidence to partially substantiate the proposed change. It should be noted that the evidence is somewhat inconclusive, as the variation of turbulence intensity with height is dependent on the atmospheric stability, is therefore dependent on local conditions, and hence is difficult to specify in a general form.

Atmospheric stability is essentially defined by whether the temperature lapse rate is greater than (unstable), equal to (neutral), or less than (stable) the adiabatic lapse rate. The Monin-Obukhov similarity theory (References 66, 67, 70 and 71) predicts that in the atmospheric surface layer --

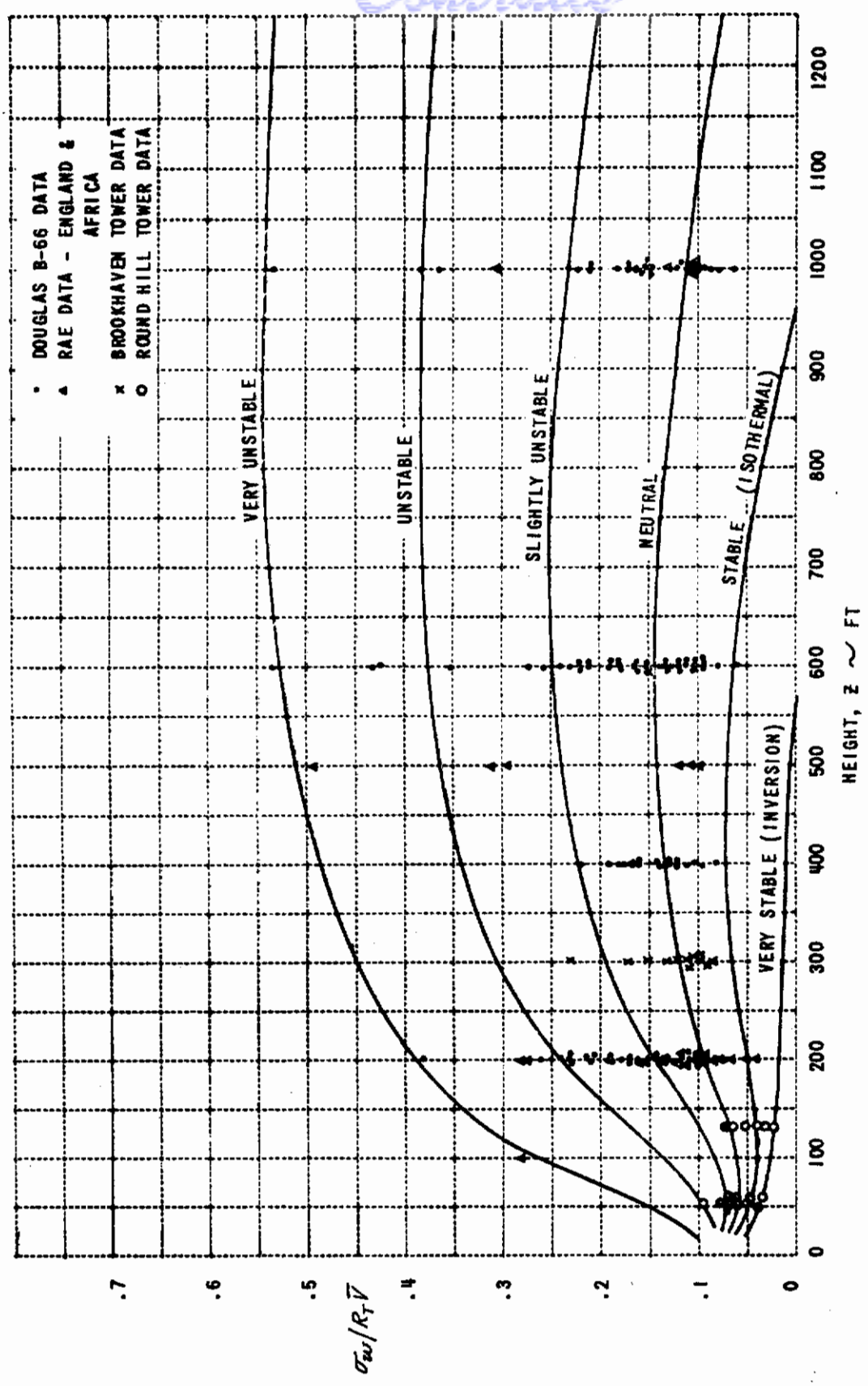

Figure 124 TERRAIN NORMALIZED RMS VERTICAL GUST VELOCITY vs. HEIGHT FOR VARIOUS STABILITIES

approximately 0-300 feet AGL -- the rms gust intensities are constant with altitude in neutral air. Although the ratio of the components is still questionable, general orders of magnitudes are $\sigma_u / \sigma_v / \sigma_w$ = 2 to 3/2 to 3/1.3. This approximate ratio somewhat substantiates the assumption that $\sigma_u = \sigma_v$ as the ground is approached, and that $\sigma_w < \sigma_u, \sigma_v$. Since the intensities are equal at some height that is assumed the onset of isotropy, the question is whether σ_w decreases below this height or σ_u and σ_v increase.

As we have noted, for neutral air the intensities are constant with height. For stable air, the production of turbulence is primarily mechanical through wind shear, and hence the characteristics of the surface layer might be expected to be similar to a wind tunnel boundary layer. In this case, experimental evidence (Reference 72) would indicate that the intensities are highest near the surface, and decrease with height. The original form of 3.7.3 results in this type of behavior for σ_u and σ_v, whereas we shall show the proposed change to 3.7.3 has the characteristic that σ_w will decrease as the surface is approached. This behavior is more realistic if the air is unstable.

In unstable air, the production of turbulence by heat convection becomes more dominant, and also the dissipation of the produced turbulence decreases. For MIL-F-8785B, this situation is considered as the general case. In general, for unstable conditions, σ_w <u>increases</u> with height through the surface layer (Reference 67); in particular, in very unstable air (free convection) Wyngaard and Cote (References 73 and 74) have shown : $\frac{\sigma_w}{u_*} \sim \left(-\frac{z}{L}\right)^{1/3}$, where u_* is "friction velocity" and L is a (negative) scaling length. This result is particularly interesting in light of the proposed change to 3.7.3, for it is easy to show that, using the scales of 3.7.3.1, 3.7.3.2, the variation of σ_w with altitude goes as:

$$\sigma_w \sim \sigma_u h^{1/3}$$

Experimental results given in Reference 75 (Reference M7 of the BIUG) support this type of behavior of σ_w with height. In particular, Figure 3 of that reference, reproduced as Figure 124 here, does indicate decreases in σ_w with decreasing height from 500 feet to at least 50 feet for unstable conditions, with the gradient becoming higher with increasing instability. Clearly, the proposed change gives the correct trend for very unstable air, whereas the original form of 3.7.3 did not and, since simulation results appear to warrant this trend, it is felt to be preferable.

3.7.3.1, 3.7.3.2 <u>Clear air turbulence (scales).</u>

A. Change requirements:

3.7.3.1 <u>Clear air turbulence (von Karman scales)</u>. The scales for clear air turbulence using the von Karman form are:

Above h = 2500 feet: $L_u = 2L_v = 2L_w$ = 2500 feet

Below h = 2500 feet: L_w = 0.5 h feet

$L_u = 2L_v = 184\ h^{1/3}$ feet

3.7.3.2 Clear air turbulence (Dryden scales). The scales for clear air turbulence using the Dryden form are:

Above h = 1750 feet: $L_u = 2L_v = 2L_w = 1750$ feet

Below h = 1750 feet: $L_w = 0.5\ h$ feet

$L_u = 2L_v = 145\ h^{1/3}$ feet

B. Change BIUG:

1. First sentence of first paragraph of Discussion (pg 444) is changed to read:

"The von Karman scale $L = L_u = 2L_v = 2L_w$ for isotropic turbulence is set at 2500 feet for isotropic turbulence above 2500 feet AGL."

2. Last sentence of first paragraph (pg 444) is changed to read:

"The formulae for the scales at low altitudes are adjusted to force them to be equal to the isotropic scales at 2500 feet AGL."

3. First sentence, second paragraph (pg 444) is changed to read:

"The low altitude formulae for the Dryden scales are adjusted to make them equal to the isotropic scales ($L = L_u = 2L_v = 2L_w$) at 1750 feet AGL."

4. Change σ_w to $\sigma_u = \sigma_v$ in third paragraph, pg 445.

5. Change formulae on pg 446 to read:

$$\frac{\sigma_u^2}{L_u} = \frac{\sigma_v^2}{2L_v} = \frac{\sigma_w^2}{2L_w} \qquad \text{(Dryden)}$$

$$\frac{\sigma_u^2}{L_u^{2/3}} = \frac{\sigma_v^2}{(2L_v)^{2/3}} = \frac{\sigma_w^2}{(2L_w)^{2/3}} \qquad \text{(von Karman)}$$

C. Philosophy for the changes:

These changes are required to correct the mistake made in the scales as previously noted.

3.7.4 Scales and intensities (thunderstorm turbulence).

A. No change to requirement.

B. Change BIUG:

"Thunderstorm turbulence is assumed to be completely isotropic; therefore, the rms intensities are equal ($\sigma_u = \sigma_v = \sigma_w$) and the scales follow the isotropic law ($L = L_u = 2L_v = 2L_w$)."

C. Philosophy for the changes:

As above.

3.7.4.1, 3.7.4.2 Thunderstorm turbulence (scales).

A. Change requirement:

3.7.4.1 Thunderstorm turbulence (von Karman scales). The scales for thunderstorm turbulence using the von Karman form are $L = L_u = 2L_v = 2L_w = 2500$ feet.

3.7.4.2 Thunderstorm turbulence (Dryden scales). The scales for thunderstorm turbulence using the Dryden form are $L = L_u = 2L_v = 2L_w = 1750$ feet.

B. No change to BIUG.

C. Philosophy of the changes.

As above.

3.7.5 Wind shear model. There is no section in the current version of MIL-F-8785B dealing with wind shear. The following items are the proposed requirement and BIUG discussion.

REQUIREMENT

3.7.5 Wind shear model. For Flight Phase Category C analyses, the mean wind used in conjunction with the turbulence analyses shall have the following characteristics (relative to the ground) for the three cases of headwind only, crosswind only, and tailwind only:

$$V_w = V_0 + 0.135h \quad \text{ft/sec}, \quad 0 \leq h \leq 300 \text{ feet}$$

Class I aircraft:

V_0 = 15 ft/sec headwind

V_0 = 6.8 ft/sec crosswind

V_0 = 0 ft/sec tailwind

Classes II, III, IV aircraft:

V_0 = 23.7 ft/sec headwind

V_0 = 23.7 ft/sec crosswind

V_0 = 0 ft/sec tailwind

For all other Flight Phase Categories, no wind shear need be used.

RELATED MIL-F-8785B PARAGRAPHS

None.

DISCUSSION

The wind shear model given in the requirement is a compromise between a more exact description of the wind profile and no consideration at all of the variation of mean wind with altitude. The approximation of a linear profile is made in the interest of simplicity for analytical studies.

In general, meteorological research has shown that, in the "atmospheric surface layer" ($0 < h \lesssim 300$ ft), the mean wind profile in neutral or stable air is given by an equation of the form (References 66 and 71):

$$V_w = \frac{V_*}{K}\left[\ln \frac{h}{h_0} + K_1(h-h_0)\right]$$

In this equation, K is a constant, K_1 depends upon the atmospheric stability, V_* is a scaling velocity related to the shearing stress and density at the surface, and h_0 is a "roughness" length to account for different surface characteristics. This equation is often approximated by a power law expression of the form (References 66, 76, 77)

$$V_w = V_1\left(\frac{h}{h_1}\right)^{\alpha}$$

where V_1 is the mean wind speed at height h_1, and α varies as a function of the surface characteristics (generally, $0.1 < \alpha < .5$).

Both of these models are more pleasing in terms of the physics of the problem than the linear model of the requirement. In addition, the "log-linear" model is a direct result of Monin-Obukhov similarity theory in the atmospheric surface layer (References 66, 70, 71). Therefore, by applying the theory, the rms gust intensities may be related to the wind profile for neutral or stable air, although not so easily for unstable air. While basing the requirement on this wind profile model would therefore give a more realistic overall picture, the incorporation of this model into the aircraft equations of motion is more involved, as shall be discussed and hence the linear model has been chosen, with values that give a reasonable representation of the profile characteristics.

The values given for the wind velocities and shears in the requirement are essentially those of References 78 and 79, with the steady wind velocities of those references selected to be at 200 ft AGL. These velocity values are relaxed somewhat in the requirement for Class I aircraft to maintain consistency with the remainder of MIL-F-8785B, particularly Section 3.3.7 (Lateral-Directional control in crosswinds), in which crosswind requirements are relaxed for Class I aircraft, but the gradient with height remains the same. The value of the gradient corresponds to .135 ft/sec/ft, a value which is about the extreme value found in the atmospheric surface layer (Reference 77).

The intent of this requirement is to ensure that the aircraft has sufficient performance flexibility in the approach subphase of Category C to counteract the effects of a wind shear on its ground track. As demonstrated in Reference 77, a headwind shear similar to that of the requirement will cause the pilot to either undershoot (constant power, angle of attack, airspeed) or overshoot (constant angle of attack, pitch attitude, and airspeed) the point on the runway he would reach in a steady wind. The analyses required to demonstrate these points are quite straightforward in the case of a linear gradient, as then the equations of motion remain explicitly independent of altitude and only flight path angle relative to the ground needs to be redefined. This simplicity is the reason that a linear gradient model is used in the requirement.

3.7.6 Application of the turbulence models in analyses.

A. Change requirement:

1. The equation for Φ_{p_g} should read:

$$\Phi_{p_g}(\Omega) = \frac{\sigma_w^2}{L_w} \frac{0.4\left(\frac{\pi L_w}{2b}\right)^{1/3}}{1+\left(\frac{4b}{\pi}\Omega\right)^2} \qquad \text{where } b = \text{wing span.}$$

2. Change requirement number to 3.7.6.

B. Change BIUG:

1. Change all references to Section 3.7.5 to references to Section 3.7.6.

2. Change the second paragraph on pg 457 to read:

"Unlike the spectra for q_g and r_g, the spectrum for p_g is not obtained by a differentiation in the X direction, and hence cannot be simply obtained from the one-dimensional (in the X-direction) w_g spectrum. Therefore, the spectrum given in 3.7.6 for p_g is not a simple cascade of the w_g spectrum as is q_g, but is instead a curve-fit to the very complicated transcendental function given in Reference M37. The p_g spectrum is statistically independent of the other spectra as a result, and hence must be generated by an independent white noise source in simulations. It should not be generated by an approximate filter cascaded to the w_g spectrum."

3. Change the last three equations on pg 459 to read:

$$\phi_{v_g}(\omega):\ T_{v_g}(s) = \sigma_v \sqrt{\frac{2L_v}{\pi V}} \frac{1+\frac{2\sqrt{3}L_v}{V}s}{\left(1+\frac{2L_v}{V}s\right)^2} = -V T_{\beta_g}(s)$$

$$\Phi_{w_g}(\omega):\ T_{w_g}(s) = \sigma_w \sqrt{\frac{2L_w}{\pi V}}\ \frac{1+\frac{2\sqrt{3}L_w}{V}s}{\left(1+\frac{2L_w}{V}s\right)^2} \quad = -V T_{\alpha_g}(s)$$

$$\Phi_{\rho_g}(\omega):\ T_{\rho_g}(s) = \sigma_w \sqrt{\frac{1}{L_w V}}\ \sqrt{0.4\left(\frac{\pi L_w}{2b}\right)^{1/3}}\ \frac{1}{1+\frac{4b}{\pi V}s}$$

C. Philosophy of the changes:

The change in the requirement formula for ρ_g and the No. 3 change to the BIUG are required to correct the scale factors L_w and L_u as previously discussed. The changes to the requirement number (from 3.7.5 to 3.7.6) are necessary because of the inclusion of the wind shear requirement as 3.7.5. The change in the BIUG discussion of the ρ_g spectrum is necessary to emphasize the fact that ρ_g is independent of w_g in the formulation of the one-dimensional spectra for MIL-F-8785B. The emphasis appears necessary as a result of comments received in Reference 69. Although the form of the q_g spectrum has also been questioned, specifically the appearance of the wing span "b", it is correct as it stands. As explained in the BIUG, the factors multiplying w_g and v_g to obtain q_g and r_g, respectively, were obtained by curve fitting the results of M37, which include some effects of two-dimensional (in the y direction) spectra.

CONCLUDING REMARKS

To summarize this section on the study of Section 3.7 of MIL-F-8785B, the following major changes have been made:

1. The scale factors L_w and L_v were corrected to properly employ them. Although the relationships given in MIL-F-8785B did give the correct results throughout, the formulae for the spectra, for example, were not consistent with the rest of the literature on atmospheric turbulence.

2. The magnitudes of σ_u, σ_v, and σ_w at low altitude as a function of altitude were changed to more correctly describe the variation of gust intensities with altitude in unstable air.

3. A wind shear model with linear gradient was added as Section 3.7.5. The magnitude of the gradient was chosen to represent an extreme condition to be consistent with the rest of Section 3.7.

4. The analytic forms of all the rotational spectra (ρ_g , ϕ_g , r_g) were rechecked and found correct. The statistical independence of ρ_g was more heavily emphasized.

SELECTED BIBLIOGRAPHY

Batchellor, G.K., The Theory of Homogeneous Turbulence, Cambridge University Press, 1953.

Blackadar, A.K. et al., "Investigation of the Turbulent Wind Field Below 150M Altitude at the Eastern Test Range," NASA CR-1410, August 1969.

Businger, J.A. et al., "Flux-Profile Relationships in the Atmospheric Surface Layer," Journal of the Atmospheric Sciences, Vol. 28, 1971 (pp 181-189).

Chalk, C.R., Neal, T.P., Harris, T.M., Pritchard, F.E., and Woodcock, R.J., Background Information and User Guide for MIL-F-8785B(ASG), "Military Specification - Flying Qualities of Piloted Airplanes," AFFDL-TR-69-72, August 1969.

Chuang, H., and Cermak, J.E., "The Diabatic Wind and Temperature Profiles," Colorado State University, CER 69-70-HC-JEC-18.

Dobrolenskiy, Yu P., "Flight Dynamics in Moving Air," NASA TT F-600, July 1971.

Dutton, J.A. et al., "Statistical Properties of Turbulence at the Kennedy Space Center for Aerospace Vehicle Design," NASA CR-1889, August 1971.

Elderkin, C.E., "Experimental Investigation of the Turbulence Structure in the Lower Atmosphere," Battelle Memorial Institute Report BNWL-329, December 1966.

Etkin, B., Theory of the Flight of Airplanes in Isotropic Turbulence - Review and Extension, AGARD Report 372, April 1961.

Firebaugh, J.M., "Evaluations of a Spectral Gust Model Using VGH and V-G Flight Data," Journal of Aircraft, Vol. 4, No. 6, November-December 1967.

Flinn, E.H., "Low Altitude Turbulence and V/STOL Gust Response," AFFDL/FGC-TM-70-3, September 1970.

Franklin, J.A., "Turbulence and Lateral-Directional Flying Qualities," NASA CR-1718, April 1971.

Franklin, J.A., "Turbulence and Longitudinal Flying Qualities," NASA CR-1821, July 1971.

Friedlander, S.K., and Topper, Leonard (eds), Turbulence: Classic Papers on Statistical Theory, Interscience Publishers, Inc., New York 1961.

Gault, J.D., and Gunter, D.E., Jr., "Atmospheric Turbulence Considerations for Future Aircraft Designed to Operate at Low Altitudes," Journal of Aircraft, Vol. 5, No. 6, November-December 1968.

Gera, J., "The Influence of Vertical Wind Gradients on the Longitudinal Motion of Airplanes," NASA TN D-6430, September 1971.

Hanna, S.R., "Turbulence and Diffusion in the Atmospheric Boundary Layer Over Urban Areas," ARATDL COM-71-00562, 1970.

Haugen, D.A., Kaimal, J.C., and Bradley, E.F., "An Experimental Study of Reynolds Stress and Heat Flux in the Atmospheric Surface Layer," Quarterly Journal of the Royal Meteorological Society, Vol. 97, 1971, pp 168-180.

Hinze, J.O., Turbulence: An Introduction to its Mechanism and Theory, McGraw-Hill Book Company, Inc., 1959.

Houbolt, J.C., Steiner, R., and Pratt, K.G., "Dynamic Response of Airplanes to Atmospheric Turbulence Including Flight Data on Input and Response," NASA TR R-199, June 1964.

Jones, J.G., "Turbulence Models for the Assessment of Handling Qualities During Take-Off and Landing," RAE Technical Memorandum Aero 1347, August 1971.

Kaimal, J.C., et al., "Spectral Characteristics of Surface Layer Turbulence," submitted to the Quarterly Journal of the Royal Meteorological Society.

Kaynes, I.W., "Aircraft Centre of Gravity Response to Two-Dimensional Spectra of Turbulence," Aeronautical Research Council R&M No. 3665.

Laning, J.H., and Battin, R.H., Random Processes in Automatic Control, McGraw-Hill Book Company, Inc., 1956.

Lappe, U.O., and Davidson, Ben, "On the Range of Validity of Taylor's Hypothesis and the Kolmogoroff Spectral Law," Journal of the Atmospheric Sciences, Vol. 20, November 1963.

Lumley, J.L., Stochastic Tools in Turbulence, Academic Press, 1970.

Lumley, J.L., and Panofsky, H.A., The Structure of Atmospheric Turbulence, Interscience, 1964.

McCloskey, J.E., et al., "Statistical Analysis of LO-LOCAT Turbulence Data for Use in the Development of Revised Gust Criteria," AFFDL-TR-71-29, April 1971.

Monin, A.S., and Obukhov, A.M., "Basic Laws of Turbulent Mixing in the Ground Layer of the Atmosphere," Atcad. Nauk SSSR Geof. Institut Trudy, NO24(151), pp 163-187, 1954.

Pandolfo, J.P., "Wind and Temperature Profiles for Constant-Flux Boundary Layers in Lapse Conditions with a Variable Eddy Conductivity to Eddy Viscosity Ratio," Journal of the Atmospheric Sciences, Vol. 23, 1966 (pp 495-502).

Panofsky, H.A., and Press, Harry, "Meteorological and Aeronautical Aspects of Atmospheric Turbulence," Progress in the Aeronautical Sciences (ed. A. Farris, et al.) Pergamon Press, 1962.

Panofsky, H.A., and Prasad, B., "Similarity Theories and Diffusion," Int. J. of Air and Water Pollution, Vol. 9, 1965 (pp 419-430).

Papoulis, A., Probability, Random Variables, and Stochastic Processes, McGraw-Hill Book Company, 1965.

Peckham, C.G., "A Summary of Atmospheric Turbulence Recorded by NATO Aircraft," AGARD-R-586-71, September 1971.

Prasad, B.A., "Wind and Temperature Fluctuation in the Surface Layer," Pennsylvania State University, Dept. of Meteorology, Ph.D. Thesis, 1967.

Pritchard, F.E., Easterbrook, C.C., and McVehil, G.E., "Spectral and Exceedance Probability Models of Atmospheric Turbulence for Use in Aircraft Design and Operation," AFFDL TR-65-122, October 1965.

Reeves, P.M., A Non-Gaussian Turbulence Simulation, AFFDL-TR-69-67, November 1969.

Skelton, G.B., "Investigation of the Effects of Gusts on V/STOL Craft in Transition and Hover," AFFDL-TR-68-85, October 1968.

Teunissen, H.W., "Characteristics of the Mean Wind and Turbulence in the Planetary Boundary Layer," University of Toronto, UTIAS Review No. 32, October 1970.

Wyngaard, J.C., and Cote, O.R., "Co-spectral Similarity in the Atmospheric Surface Layer," submitted to the Quarterly Journal of the Royal Meteorological Society.

Wyngaard, J.C., Cote, O.R., and Izumi, Y., "Local-Free Convection, Similarity, and the Budgets of Shear Stress and Heat Flux," Journal of the Atmospheric Sciences, Vol. 28, 1971 (pp 1171-1182).

Yaglom, A.M., Stationary Random Functions, Prentice-Hall, Inc., 1962.

SECTION VIII

PROPOSED REVISIONS TO 4, QUALITY ASSURANCE

Action Recommended for Quality Assurance, 4

No changes are recommended.

Section IX

PROPOSED REVISIONS TO 6, NOTES

6.2 Definitions

6.2.1 General

Deletions: None

Additions: Definition of stability axes (see next page).

6.2.1 General - stability axes. Stability axes are specialized body axes in which the orientation of the "body axes" is determined by the initial flight condition. The x-axis is selected to be coincident with the velocity vector, V_o at the start of the motion. Consequently, the moment of inertia and product of inertia terms vary for each initial flight condition. However, they are then constant in the equations of motion.

6.2.2 Speeds

Deletions: None

Additions: V_T - True airspeed ft/sec

6.2.3 Thrust and power

Deletions: None

Additions: None

6.2.4 Control parameters

Deletions: None

Additions: None

6.2.5 Longitudinal parameters

Deletions: ζ_{sp}, ω_{sp}

Additions: Listed in following pages

Description of Coordinate System

Origin: vehicle center of gravity.

Reference plane: X_sZ_s, a plane of symmetry.

Positive X_s-axis: coincident with velocity vector at start of motion.

Positive Z_s-axis: toward bottom of vehicle.

Positive rotation: about Y_s-axis from Z_s to X_s, i.e., right-hand system.

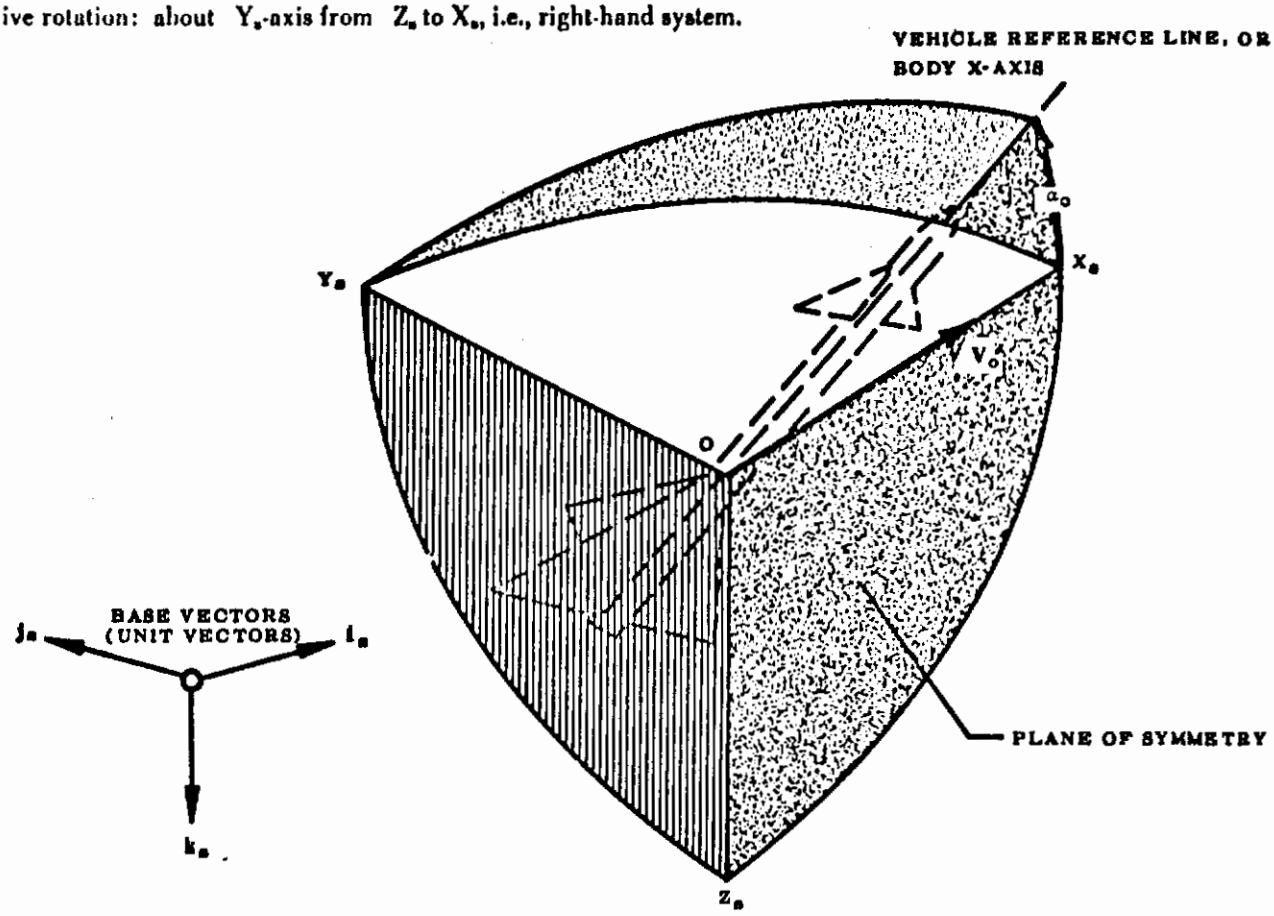

STABILITY AXES

The initial angle of attack α_o is the angle between the body X-axis and the steady relative velocity vector V_0 at the start of motion.

$\left[\frac{\Delta A}{\Delta \angle}\right]_\theta$ A parameter measured from the amplitude ratio-phase angle plot of the transfer function $\left[\frac{\theta(j\omega)}{F_s(j\omega)} e^{-0.3j\omega}\right]$. If the amplitude ratio, $\left|\frac{\theta(j\omega)}{F_s(j\omega)}\right|$, is plotted versus the phase, $\left[\angle \frac{\theta(j\omega)}{F_s(j\omega)} - 17.19\omega\right]$, then the parameter $\left[\Delta A/\Delta \angle_\theta\right]$ is defined as either:

a) The most negative <u>average</u> slope of a line drawn from ω_θ to any lower frequency than ω_θ for which the phase is more positive, or,

b) The most negative <u>local</u> tangent between ω_θ and the frequency for which the phase is (-180°), whichever is more negative. Units are dB/deg, see Figure 125.

$\Delta \angle_\theta$ A parameter measured from the amplitude-phase curve of $\left[\frac{\theta(j\omega)}{F_s(j\omega)} e^{-0.3j\omega}\right]$. It is defined as either:

a) The difference between the phase at ω_θ and -90°, or,

b) The difference between the phase at ω_θ and the first local phase maximum,

whichever results in the largest negative increment. If no well-defined local phase maximum exists, $\Delta \angle_\theta$ = (phase at ω_θ + 90°). Units are degrees, see Figure 125.

Note that a pure delay does not alter the amplitude ratio but it does alter the phase

$$\left|\frac{\theta(j\omega)}{F_s(j\omega)} e^{-0.3j\omega}\right| = \left|\frac{\theta(j\omega)}{F_s(j\omega)}\right|$$

$$\angle\left[\frac{\theta}{F_s} e^{-0.3j\omega}\right] = \left[\angle \frac{\theta}{F_s} - 0.3\omega\right] \sim rad$$

$$= \left[\angle \frac{\theta}{F_s} - 17.19\omega\right] \sim deg$$

ω_θ The reference frequency used for the maneuver response measurements of 3.2.2.1, rad/sec.

$\left|\frac{\ddot{\theta}}{F_s}\right|_{max}$ Pitch control sensitivity. The peak frequency-response amplitude of $\left|\frac{\ddot{\theta}(j\omega)}{F_s(j\omega)}\right|$, $\frac{rad/sec^2}{lb}$.

6.2.6 Lateral-directional parameters

Deletions:

ϕ

p

p_{osc}/p_{AV}

ϕ_{osc}/ϕ_{AV}

Figure 9

$\Delta\beta_{max}$

k

t_{n_β}

ψ_β

$\frac{p}{\beta}$

Paragraphs on Page 72 and 73.

Additions:

ϕ bank angle measured in the $y_s - z_s$ plane, between the y_s - stability axis and the horizontal (6.2.1)

p roll rate about the x_s stability axis (6.2.1)

r yaw rate about the z_s stability axis (6.2.1)

$\hat{\phi}(t) \equiv \phi(t) + K_{s_\phi}(1-e^{-\lambda_s t})\delta_{AS_{IMPULSE}}$ Bank angle response to an impulse aileron input with the spiral component subtracted.

$\hat{p}(t) \equiv p(t) + K_{s_p}(1-e^{-\lambda_s t})\delta_{AS_{STEP}}$ Roll rate response to a step aileron input with the spiral component subtracted.

$\hat{r}(t) \equiv r(t) + K_{s_r}(1-e^{-\lambda_s t})\delta_{AS_{IMPULSE}}$ Yaw rate response to an impulse aileron input with the spiral component subtracted.

$\dot{\hat{r}}(t) \equiv \dot{r}(t) + K_{s_{\dot{r}}}(1-e^{-\lambda_s t})\delta_{AS_{STEP}}$ Yaw acceleration response to a step aileron input with the spiral component subtracted.

$\frac{\hat{p}_{osc}}{\hat{p}_1}$ a measure of the ratio of the oscillatory component of roll rate to the roll rate at the first peak following a rudder-pedal-fixed aileron control command.

$$\frac{\hat{p}_{osc}}{\hat{p}_1} = \frac{\frac{1}{2}\left[\left(\hat{p}_1 - \hat{p}_2\right) + \left(\hat{p}_3 - \hat{p}_2\right)\right]}{\hat{p}_1}$$

where $\hat{p}_1$, $\hat{p}_2$ and $\hat{p}_3$ are roll rates at the first, second and third peaks, respectively (Figure 126).

$\frac{\hat{\phi}_{osc.}}{\hat{\phi}_1}$ a measure of the ratio of the oscillatory component of bank angle to the bank angle at the first peak following a rudder-pedal-free impulse aileron control command.

$$\frac{\hat{\phi}_{osc}}{\hat{\phi}_1} = \frac{\frac{1}{2}\left[(\hat{\phi}_1 - \hat{\phi}_2) + (\hat{\phi}_3 - \hat{\phi}_2)\right]}{\hat{\phi}_1}$$

where $\hat{\phi}_1$, $\hat{\phi}_2$ and $\hat{\phi}_3$ are bank angles at the first, second, and third peaks, respectively. (Figure 126)

$\frac{|\hat{r}_{osc}|}{\hat{r}_{AV}} t > .2T_d$ a measure of the ratio of the oscillatory component of yaw rate to the average component of yaw rate following a rudder-pedals-free impulse aileron control command:

$$\frac{|\hat{r}_{osc}|}{\hat{r}_{AV}} \; t > .2T_d = \frac{|\hat{r}_1 + \hat{r}_3 - 2\hat{r}_2|}{\hat{r}_1 + \hat{r}_3 + 2\hat{r}_2}$$

where $\hat{r}_1$, $\hat{r}_2$ and $\hat{r}_3$ are yaw rate at the first, second and third peaks respectively occurring after time $t = t_o + .2T_d$. (Figure 127)

$\frac{|\hat{\dot{r}}_{osc}|}{\hat{\dot{r}}_{AV}} t > .2T_d$ a measure of the ratio of the oscillatory component of yaw acceleration to the average component of yaw acceleration following a rudder-pedals-fixed step aileron control command:

$$\frac{|\hat{\dot{r}}_{osc}|}{\hat{\dot{r}}_{AV}} \; t > .2T_d = \frac{|\dot{r}_1 + \dot{r}_3 - 2\dot{r}_2|}{\dot{r}_1 + \dot{r}_3 + 2\dot{r}_2}$$

where $\hat{\dot{r}}_1$, $\hat{\dot{r}}_2$ and $\hat{\dot{r}}_3$ are yaw acceleration at the first, second and third peaks respectively occurring after time $t = t_o + .2T_d$. (Figure 127)

$\Delta\beta_{max}$ maximum sideslip excursion at the c.g., occurring within $1.2\ T_d$ sec following a rudder-pedals-free impulse aileron control command. Usually the peak to peak amplitude (Figure 128)

$\Delta\dot{\beta}_{max}$ maximum sideslip rate excursion at the c.g. occurring within $1.2\ T_d$ sec following a rudder-pedals-fixed step aileron control command (Figure 128).

$\psi_{\chi_{\substack{IMPULSE \\ or\ STEP}}}$ Phase angle expressed as a lag for a cosine representation of the Dutch roll oscillation in the (x) response resulting from an aileron impulse or an aileron step input

$$\psi_{\chi_{\substack{IMPULSE \\ or\ STEP}}} = -360\left[\frac{t_{n_\chi}}{T_d} + 1 - n\right] - \sin^{-1}\zeta_d \qquad deg$$

with n as in t_{n_χ} below. Where (χ) is bank angle, roll rate, yaw rate, yaw acceleration, sideslip or sideslip rate response with the spiral residue subtracted (Figures 126, 127, 128)

$\psi_{\chi_{\substack{IMPULSE \\ or\ STEP}}}$ phase angle expressed as a lag for a cosine representation of the Dutch roll oscillation in the (x) response resulting from an impulse or step aileron-control command

$$\psi_{\chi_{\substack{IMPULSE \\ or\ STEP}}} = \sum \theta_z - \sum \theta_p$$

where:

θ_z angles of line segments from zeros of $\frac{X(s)}{\delta_{AS}(s)}$ transfer function numerator to the positive conjugate Dutch roll root, for δ_{AS} impulse or step.

θ_p angles of line segments from poles of $\frac{X(s)}{\delta_{AS}(s)}$ transfer function denominator to the positive conjugate Dutch roll root, for δ_{AS} impulse or step (Reference 3).

t_{n_χ} time for the Dutch roll oscillation in the (x) response to reach the nth local maximum for a right step or impulse aileron-control command, or the nth local minimum for a left command. In the event a step command is employed, the control shall be moved as abruptly as practical and, for purposes of this definition, initial time, t_o , shall be defined as the instant the cockpit control deflection passes through half the amplitude of the commanded value. For pulse inputs, time shall be measured from the point halfway through the duration of the pulse. Only peaks occurring after $t = 3\tau_R$ should be used to avoid distortion resulting from the roll mode.

K_{s_χ} Residue of spiral root in the (x) time history response to aileron impulse or aileron step input.

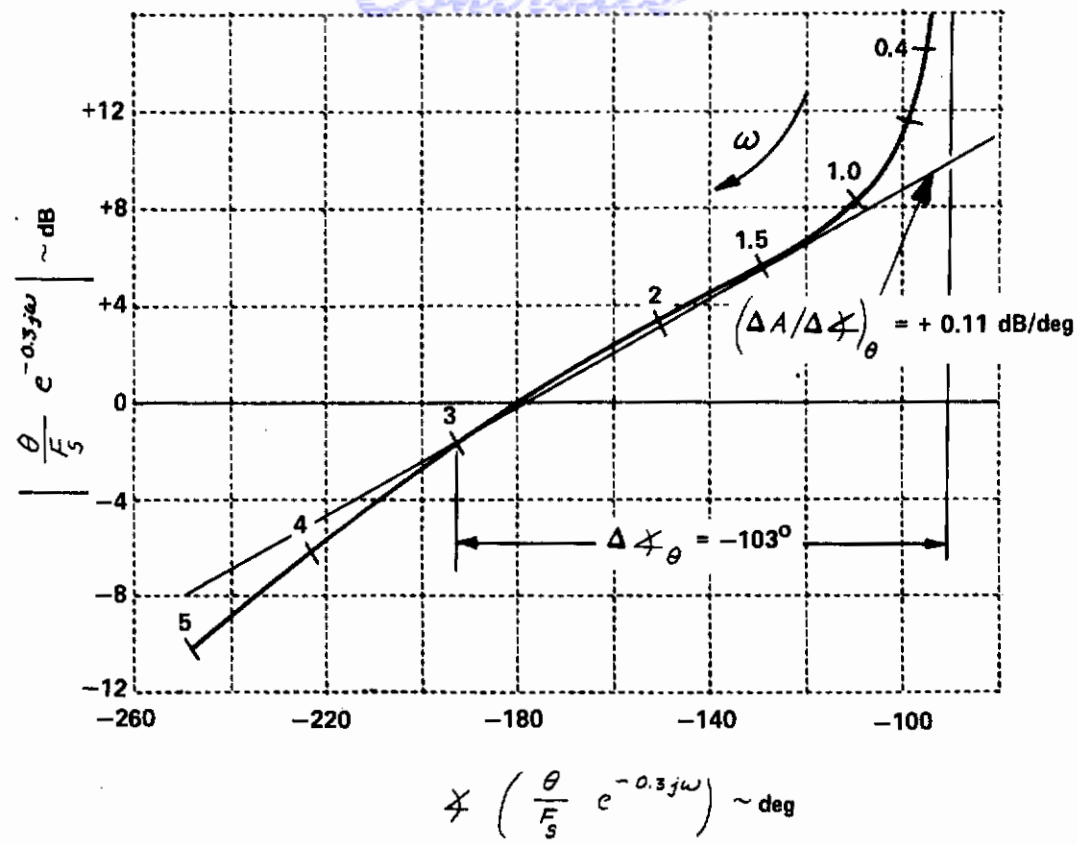

(a) LOW ω_{sp}, GOOD ζ_{sp}

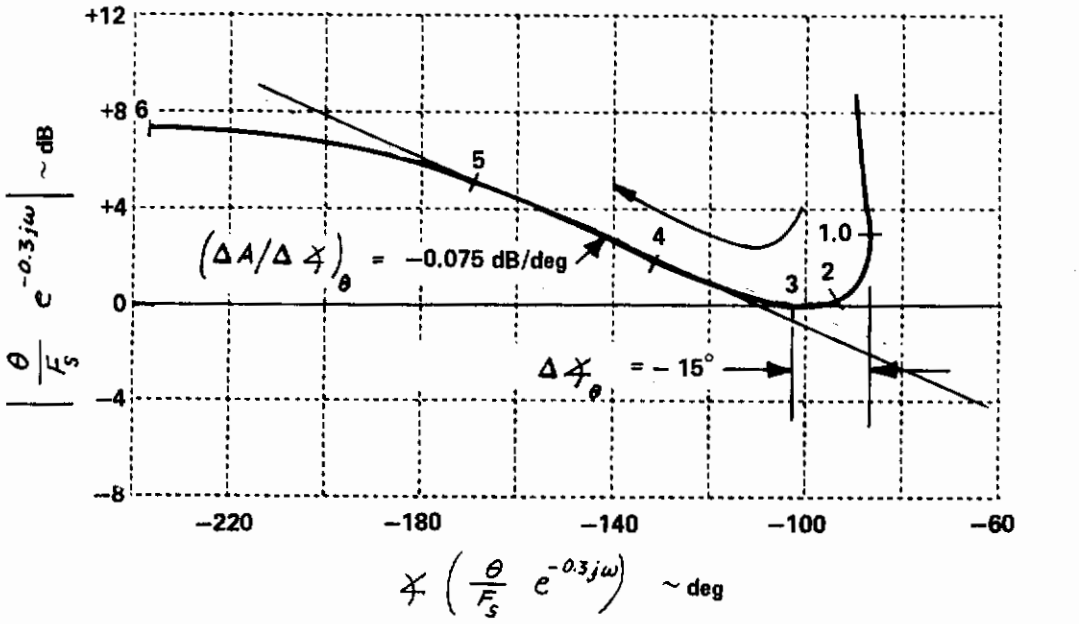

(b) MODERATE ω_{sp}, LOW ζ_{sp}

Figure 125 EXAMPLES OF MEASUREMENT OF MANEUVER RESPONSE PARAMETERS (ω_θ = 3.0 RAD/SEC)

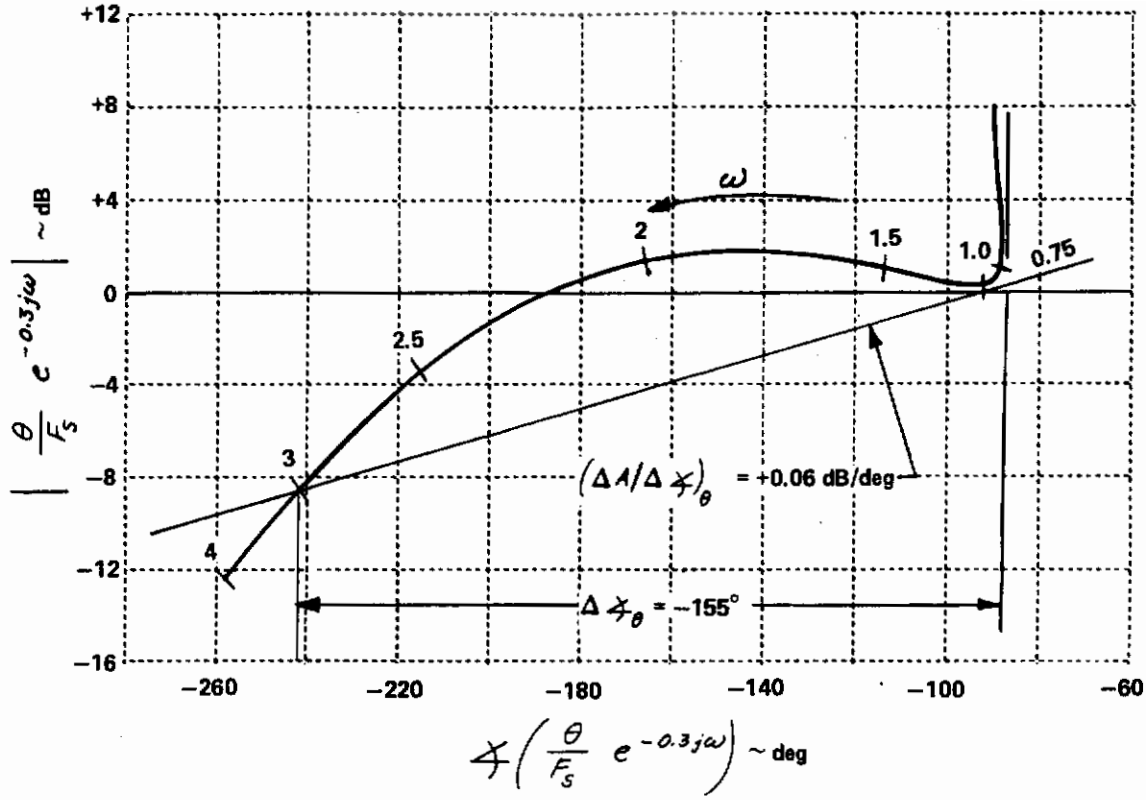

(c) LOW ω_{sp}, LOW ζ_{sp}

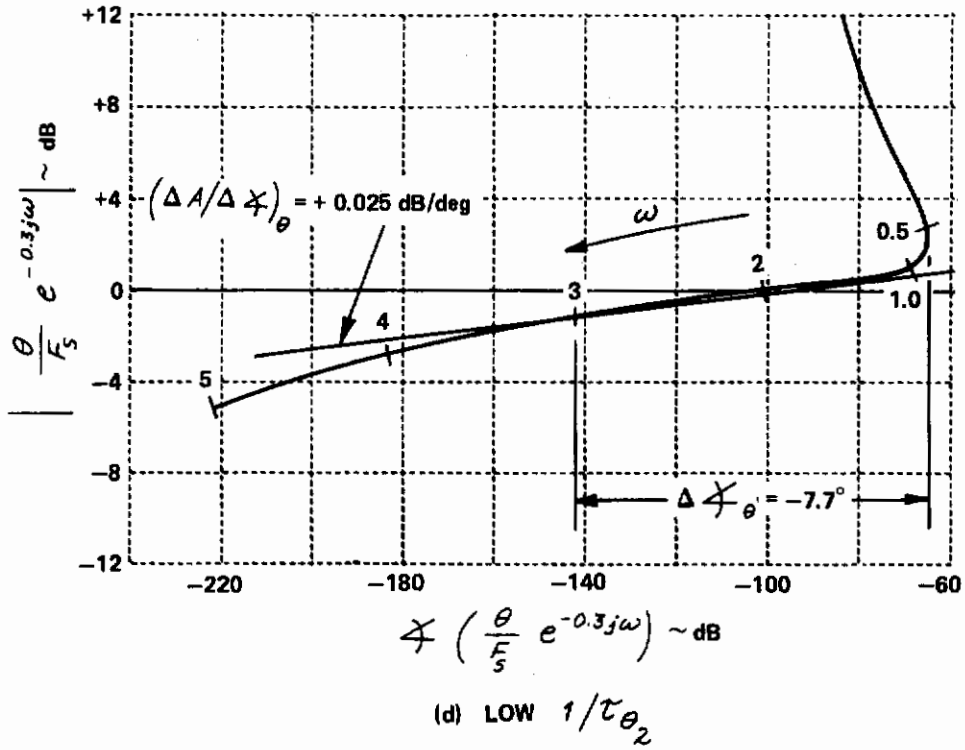

(d) LOW $1/\tau_{\theta_2}$

Figure 125 (Continued) EXAMPLES OF MEASUREMENT OF MANEUVER RESPONSE PARAMETERS (ω_θ = 3.0 RAD/SEC)

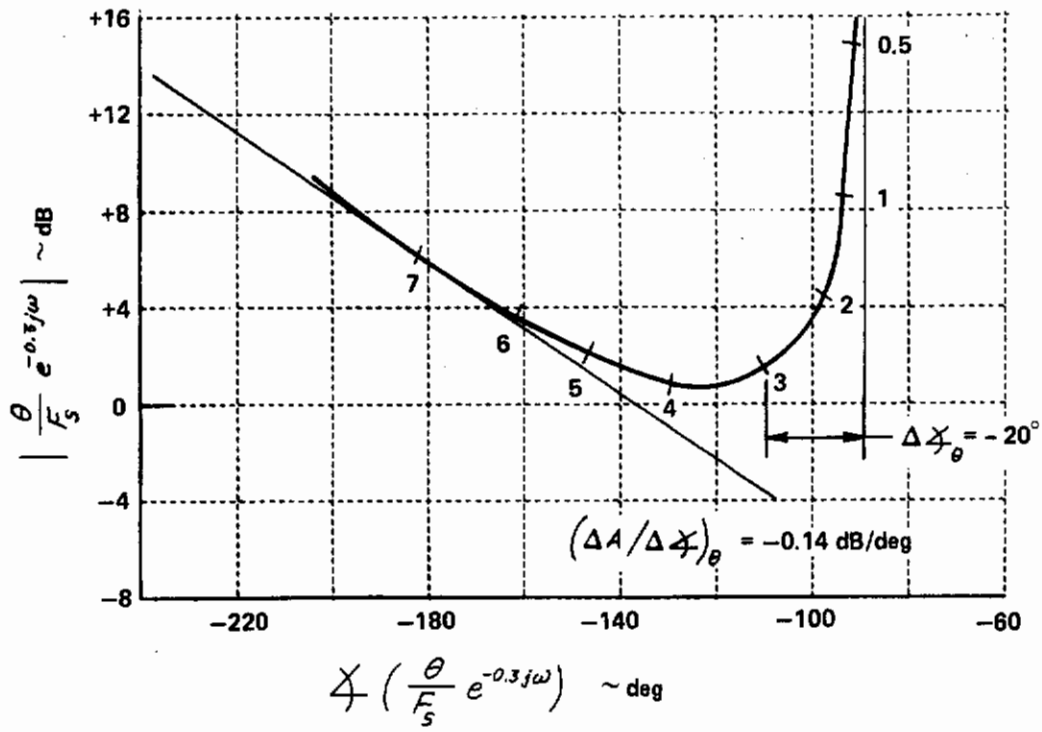

(e) HIGH ω_{sp}, LOW ζ_{sp}, CONTROL SYSTEM LEAD AND AMPLIFICATION

Figure 125 (Concluded) EXAMPLE OF MEASUREMENT OF MANEUVER RESPONSE PARAMETERS (ω_θ = 3.0 RAD/SEC)

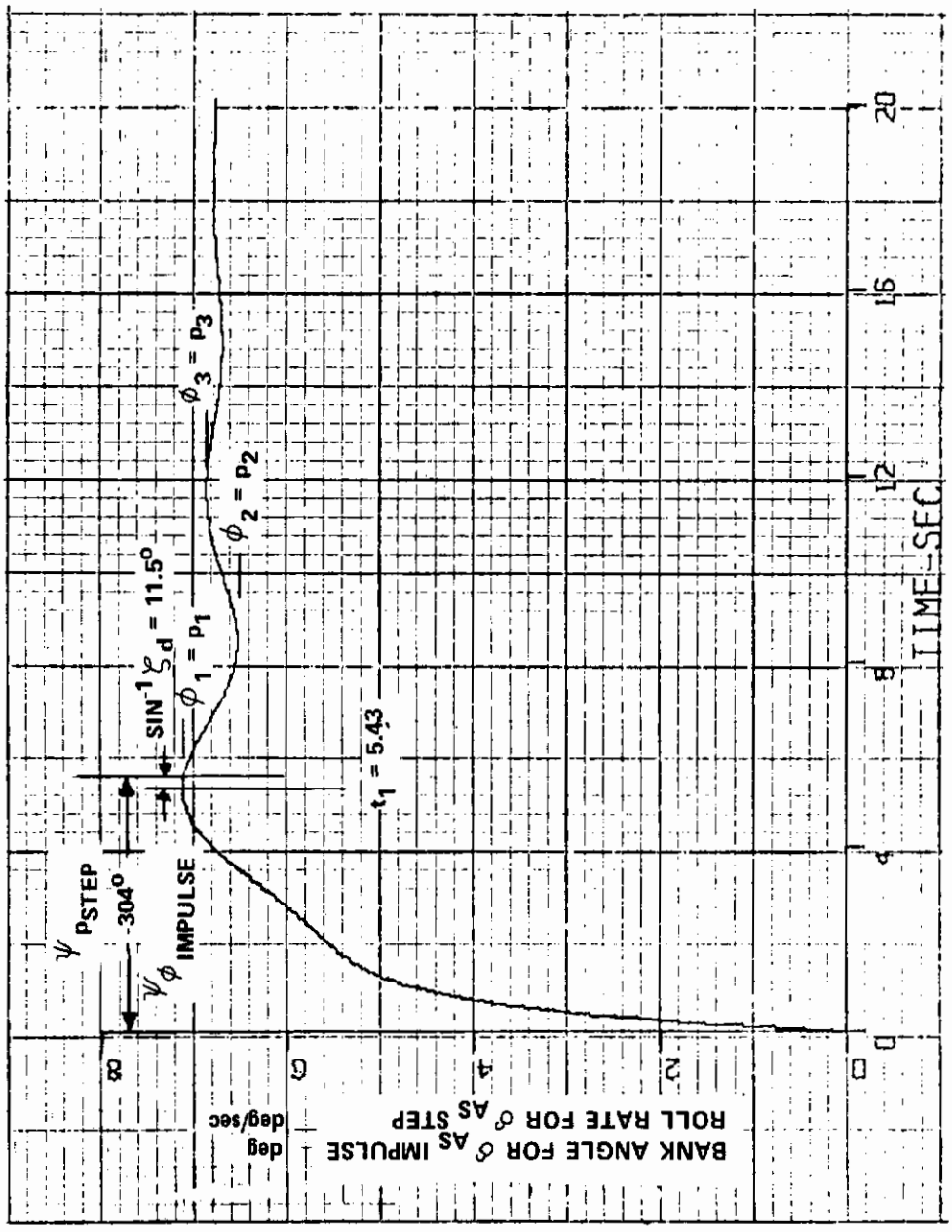

Figure 126 BANK ANGLE OR ROLL RATE RESPONSE TO AILERON IMPULSE OR STEP COMMAND

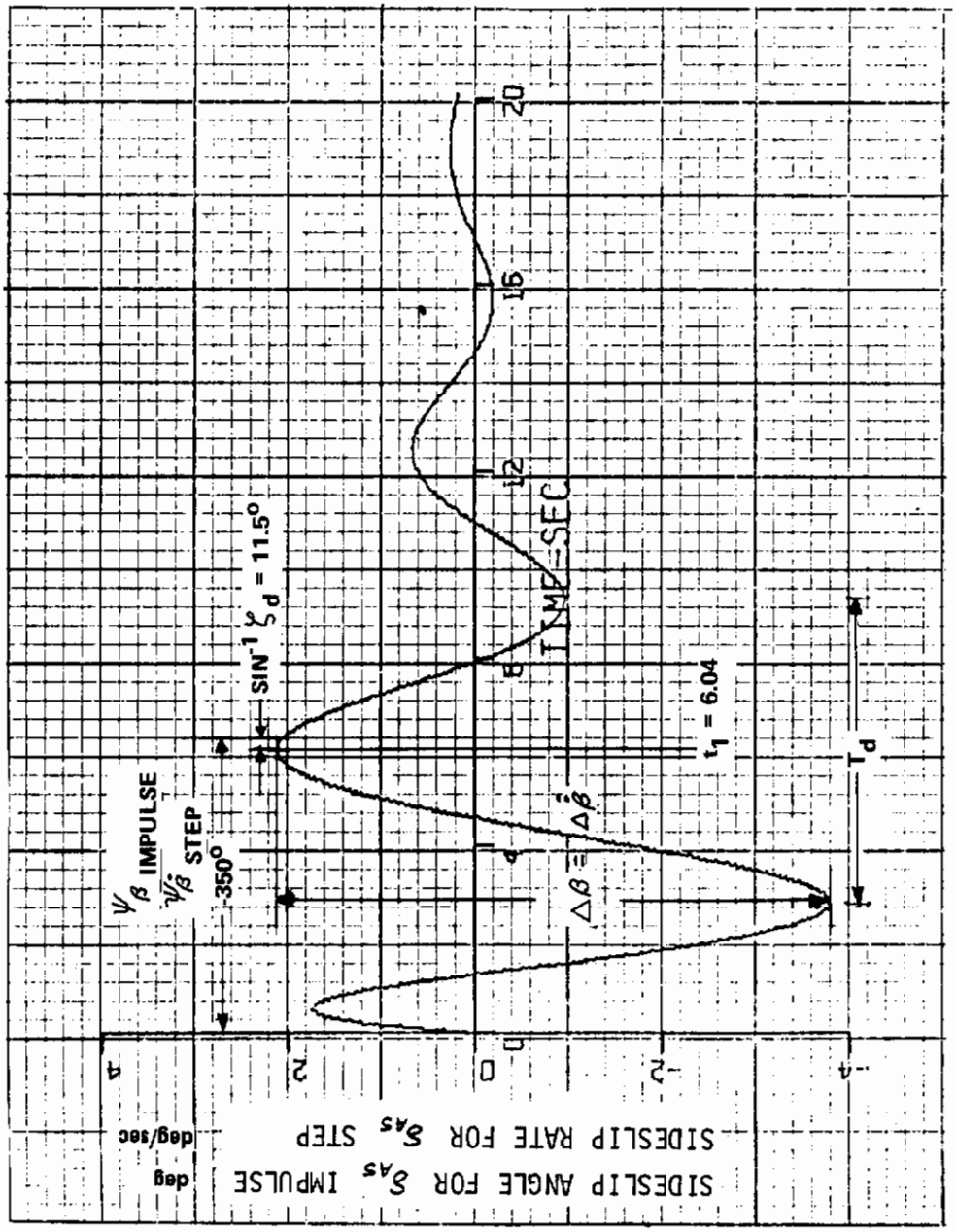

Figure 127 SIDESLIP OR SIDESLIP RATE RESPONSE TO AILERON IMPULSE OR STEP COMMAND

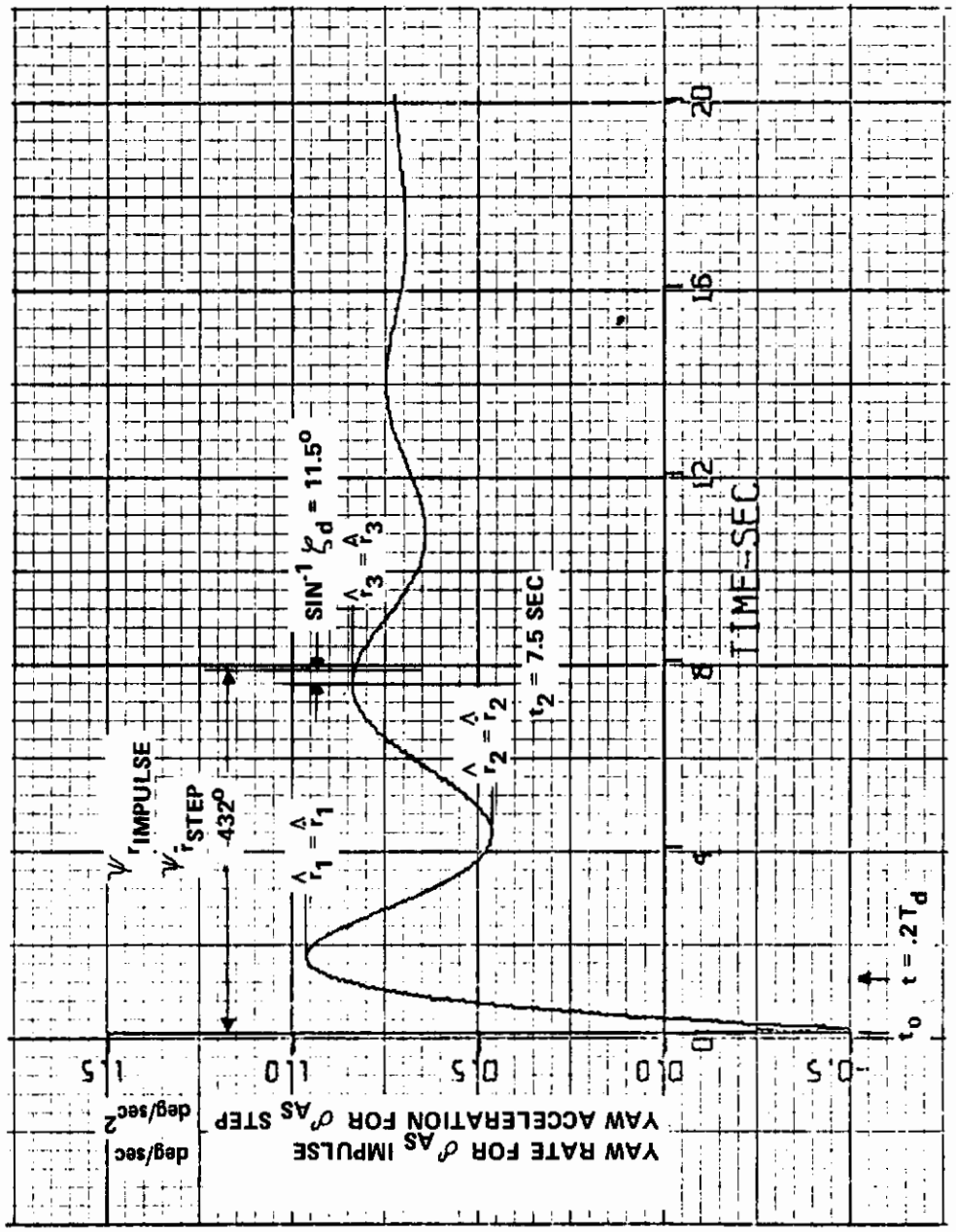

Figure 128 YAW RATE OR YAW ACCELERATION RESPONSE TO IMPULSE OR STEP AILERON COMMAND

APPENDIX I

TURBULENCE SIMULATION IN FLYING QUALITIES EXPERIMENTS

1. Experience with turbulence models and intensity levels in MIL-F-8785B indicates that the intensity specified for low altitude corresponds to rather severe turbulence. In Reference 3, it says the intensity level is supposed to represent the level that would be exceeded only 1% of the time, $P(\sigma_w) = P_1 \hat{P}(\sigma_w) = 0.01$.

The probability density function used in MIL-F-8785B for turbulence intensity, once turbulence has been encountered, is of the following form (Figure 1(3.7.3) of Reference 3).

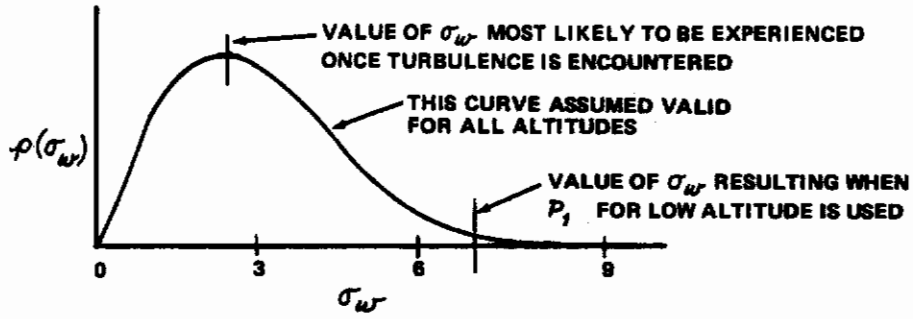

At low altitude, the $P(\sigma_w) = P_1 \hat{P}(\sigma_w) = 0.01$ requirement results in $\sigma_w \approx$ 6.7 ft/sec which is quite severe turbulence. If only this intensity is used in flying quality experiments, the results of the experiment will be highly colored by the aircraft's response to turbulence and the effects of dynamic parameters on response to control may be masked by the turbulence response. Thus the sensitivity of the experiment can be blunted if the evaluation is performed only in severe turbulence.

2. A better approach is probably to let the pilot see the airplane in smooth air and also in turbulence of an intensity that is the most probable to be encountered, i.e., the σ_w with the highest relative frequency in the above sketch. The pilot should be informed that this intensity represents light-to-moderate turbulence which he is quite likely to encounter. He should also be given the opportunity to evaluate the configuration in more severe turbulence and should be informed that the turbulence intensity represents severe turbulence which will be infrequently encountered. He should then be required to weigh his observations and give an overall rating to the configuration for the Flight Phase being evaluated. This method requires that the evaluation pilot have three "runs" with the configuration before it is rated.

3. An alternate approach used in experiments reported in the literature is to have the pilot perform separate evaluations in various turbulence intensities without any knowledge of the intensity being experienced. Thus each evaluation is done separately and the same performance standard and workload tolerance is applied during each evaluation. The experimenter is then left with the job of interpreting the results. You might imagine, for example, that a Level 1 airplane would be defined to be one that receives a PR $\leq$ 3.5 for smooth air and light-to-moderate turbulence and PR $\leq$ 6.5 for severe turbulence.

4. The approach outlined in (2) above is recommended for flying qualities experiments. Evaluations should be performed in the following environments:

a) Smooth air
b) Turbulence of most probable intensity
c) Severe turbulence

The pilot should be briefed on the Mission, the Mission Flight Phase and the environment appropriate to the Flight Phase. This introduces the probability of encountering turbulence which is a function of altitude and terrain, etc. Figure 3(3.7.3) of Reference 3, MIL-F-8785B BIUG, relates P_1 ~ probability of encountering turbulence to altitude.

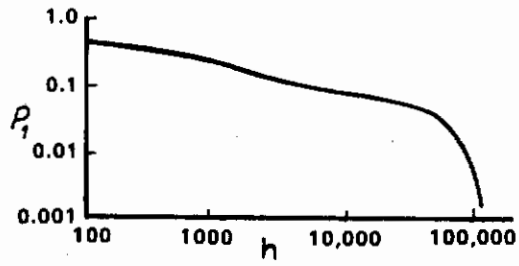

This relationship can be used to instruct the pilot as to the importance of turbulence effects to the overall evaluation. For example, in Landing Approach or Terrain Following Flight Phases the probability of encountering turbulence is high, $P_1 \approx .80$, thus the pilot would give high weighting to his observations in moderate turbulence (also spend most of his evaluation time examining the configuration in moderate turbulence) and considerable weight to his observations in severe turbulence when arriving at the overall rating for the configuration. In contrast, if the Flight Phase is cruise at h = 80,000 ft, the probability of encountering turbulence at this altitude is quite low, $P_1 \approx .02$, and also the pilot may have the option of changing altitude

to get out of the turbulent layer; thus he should give a relatively low weighting to his observations of the characteristics in turbulence in arriving at his overall rating. He should also spend most of his evaluation time examining the configuration in smooth air. Auxiliary rating scales indicating the degree of degradation in turbulence are useful in better defining the effect of turbulence on the flying qualities.

5. The turbulence intensity values specified in MIL-F-8785B, 3.7.3 and Figure 8, are to represent the intensity, at a given altitude, that can only be equaled or exceeded with a probability of 0.01.

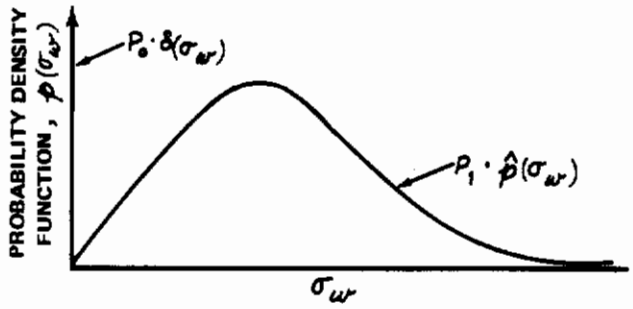

$$p(\sigma_w) = P_0 \cdot \delta(\sigma_w) + P_1 \cdot \hat{p}(\sigma_w)$$

where: P_0 and P_1 Function of Altitude

Cumulative Probability $\sigma_w \leq$ a given value:

$$P(\sigma_w \leq X) = P_0 \int_0^{\sigma_w = X} \delta(\sigma_w)\, d\sigma_w + P_1 \int_0^{\sigma_w = X} \hat{p}(\sigma_w)\, d\sigma_w = 0.99$$

$$= P_0 + P_1 \cdot \hat{\hat{P}}(\sigma_w \leq X) = 0.99 \qquad (1)$$

where $\hat{\hat{P}}(\sigma_w \leq X)$ = cumulative probability that σ_w is equal to or less than a given value, i.e. area under probability density curve between 0 and X.

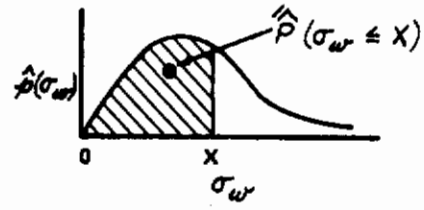

Since $P_0 = 1 - P_1$

Then

$$P(\sigma_w \le X) = 1 - P_1 + P_1 \hat{\hat{P}}(\sigma_w \le X) = 0.99$$

$$P_1\left[1 - \hat{\hat{P}}(\sigma_w \le X)\right] = 0.01$$

Define

$$\hat{\hat{P}}'(\sigma_w \ge X) \equiv 1 - \hat{\hat{P}}(\sigma_w \le X)$$

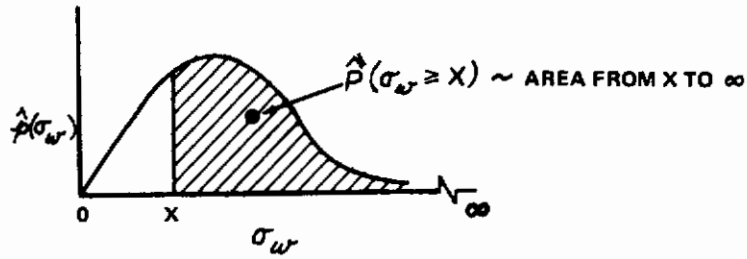

Then

$$P(\sigma_w \ge X) = P_1 \hat{\hat{P}}'(\sigma_w \ge X) = 0.01 \qquad (2)$$

This is the expression used in the BIUG. It is interpreted to mean that 99% of all time spent in flight at a given altitude will be spent in turbulence with less than the specified σ_w or in turbulence free air ($\sigma_w = 0$).

The turbulence intensity as a function of altitude resulting from this rule, Eq. (1) or (2), is given in Figure 8 of MIL-F-8785B.

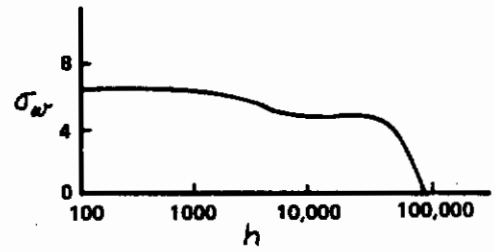

The result of the rule, $\begin{Bmatrix} P(\sigma_w \geq X) = .01 \\ P(\sigma_w \leq X) = .99 \end{Bmatrix}$ is that the turbulence intensity specified decreases with altitude. Above 50,000 ft, the intensity specified decreases rapidly, going to zero at 90,000 ft.

This result is not consistent with statements on page 438 of Reference 3 to the effect that the character of clear air turbulence, once it is encountered, is independent of altitude and is described by the Rayleigh distribution in Figure 1(3.7.3) of Reference 3.

Thus it appears that the rule, $P(\sigma_u \geq X) = .01$, has the effect of specifying turbulence of diminished intensity at altitude rather than specifying turbulence of a given character that is encountered less frequently at high altitude. This does not seem to be the right approach; but that reaction is tied to acceptance of the idea that turbulence (once encountered) does indeed have the same character independent of altitude.

MIL-F-8785B is not specific about how flying qualities simulation experiments are to be performed but it could be interpreted as saying the turbulence should be introduced with the intensity appropriate from Figure 8 for the altitude. Thus, Flight Phases requiring flight at low altitude would be done in severe turbulence and Flight Phases requiring flight at high altitude would be done in light turbulence. This is quite different from the procedure suggested in items 2 and 4 above.

Appendix II

Discussion of Aileron Stick-to-Rudder Crossfeed Required to Coordinate Rolling And Turning Maneuvers.

The aileron-to-rudder crossfeed required to keep sideslip zero is discussed in Reference 34 in terms of frequency response terminology, i.e., amplitude and phase characteristics of the shaping network between the aileron stick and the rudder surface that would be required to coordinate rolling and turning maneuvers. The discussion in Reference 34 will be presented later in this section but first the treatment of coordination of rolling maneuvers by Dolbin in Reference 80 is introduced. The problem is treated in the time domain working with the differential equations, time histories and rms rudder required to maintain zero sideslip. Similar treatments are to be found in Reference 81.

The following discussion is excerpted from Reference 80.

"Coordinating a Rolling Maneuver

"In view of the pilot's difficulty in maintaining sideslip small during roll maneuvers in the preliminary simulator studies, an analytical study was undertaken to examine the pilot's control tasks. The following two approaches are considered:

(a) The rudder pedal response required to maintain zero sideslip during a rolling maneuver is studied to indicate the amount of pilot effort and skill required for coordinated rolling maneuvers.

(b) The sideslip which results during a rolling maneuver with fixed rudder pedals is computed to indicate the consequences of the pilot not performing his coordination task.

"Approach (a) has the advantage that it is easy to study. But, since perfect coordination is assumed (defined by $\beta = 0$), no information of the influence of β stability derivatives can be obtained. In reality, however, the acceptability of an aircraft will improve with regard to the coordination problem if the sideslip excursions are reduced. Thus, the aerodynamic forces and moments resulting from β have a significant influence on the coordination problem.

"On the other hand, Approach (b) provides a tool for learning the influence of β stability derivatives; but, of course the assumption is made that the pilot takes no action. Therefore, consideration of only this approach may place severe requirements on the aircraft to achieve what would appear to be an acceptable aircraft.

"First, Approach (a) is considered in detail. The rudder pedal control response which is required to maintain zero sideslip is uniquely defined for any rolling maneuver achieved with the ailerons. The differential equation relating rudder pedal to bank angle is obtained by setting the sideslip to zero and then eliminating the yaw rate and the aileron stick terms with two of the three equations. Upon completion of this operation, one obtains the following expression (Y_p and Y_r are assumed to be zero):

$$Y_{\delta_{RP}} \dot{\delta}_{RP} - \left(N'_{\delta_{RP}} + N'_r Y_{\delta_{RP}} - \frac{N'_{\delta_{AS}}}{L'_{\delta_{AS}}} \left(L'_r Y_{\delta_{RP}} + L'_{\delta_{RP}}\right)\right) \delta_{RP} =$$

$$\frac{N'_{\delta_{AS}}}{L'_{\delta_{AS}}} \ddot{\phi} + \left(N'_p - \frac{g}{V} - \frac{N'_{\delta_{AS}}}{L'_{\delta_{AS}}} L'_p\right) \dot{\phi} + \frac{g}{V} \left(N'_r - \frac{N'_{\delta_{AS}}}{L'_{\delta_{AS}}} L'_r\right) \phi \qquad (1)$$

"The aileron input and the resulting yawing velocity are related to ϕ and its derivatives and δ_{RP} by the following expressions:

$$\left.\begin{aligned} \delta_{AS} &= \frac{1}{L'_{\delta_{AS}}} \left[\ddot{\phi} - L'_p \dot{\phi} - \frac{g}{V} L'_r \phi - \left(Y_{\delta_{RP}} L'_r + L'_{\delta_{RP}}\right) \delta_{RP}\right] \\ r &= \frac{g}{V} \phi + Y_{\delta_{RP}} \delta_{RP} \end{aligned}\right\} \qquad (2)$$

"Equation (1) is simply a first order differential equation forced with $\phi(t)$, the desired rolling maneuver, and its derivatives. For practical application the $\phi(t)$ function must be restricted to functions for which ϕ is continuous. If ϕ is not continuous then infinite amplitude control inputs will be demanded and, of course, these cannot be attained.

"Equation (1) can be further simplified to a good approximation since the coefficient of $\dot{\delta}_{RP}$ is very small with respect to the coefficient of the δ_{RP} term; thus, the time constant is very small. For the values of the reference X-19 configuration, the time constant

is .00972 seconds. Therefore, even if the amplitude of the transient term were large the contribution of this term would not be significant. Thus, dropping the term proportional to $\dot{\delta}_{RP}$, Equation (1) becomes an algebraic relation in ϕ and its derivatives.

$$\delta_{RP} = \frac{\frac{N'_{\delta_{AS}}}{L'_{\delta_{AS}}}\ddot{\phi} + \left(N'_p - \frac{g}{V} - \frac{N'_{\delta_{AS}}}{L'_{\delta_{AS}}}L'_p\right)\dot{\phi} + \frac{g}{V}\left(N'_r - \frac{N'_{\delta_{AS}}}{L'_{\delta_{AS}}}L'_r\right)\phi}{-N'_{\delta_{RP}} - Y_{\delta_{RP}}N'_r + \frac{N'_{\delta_{AS}}}{L'_{\delta_{AS}}}\left(L'_{\delta_{RP}} + L'_r Y_{\delta_{RP}}\right)} \qquad (3)$$

"If coordinating a rolling maneuver is a problem then the coefficients of Equation (3) are probably important parameters. Thus the primary parameters which influence the amount of rudder pedal required to maintain zero sideslip are $N'_{\delta_{AS}}/L'_{\delta_{AS}}$, N'_p, N'_r and $N'_{\delta_{RP}}$.

"If the denominator of Equation (3) is taken to the left hand side, then the entire left hand side represents the yawing moment which must be provided to trim the aircraft as a function of $\phi(t)$. From the coefficients of $\ddot{\phi}$, $\dot{\phi}$ and ϕ of Equation (3) it is seen that if $N'_{\delta_{AS}} = N'_r = 0$ and $N'_p = g/V$ then the aircraft is coordinated without a rudder pedal input, that is, the aircraft is said to be "two control."

"The subject of "two control" is discussed by Radt in Reference 4. Radt also points out that if β is maintained small with the rudder, then approximately the same rudder response is required regardless of how it is obtained.

"Time histories of the control inputs, $\delta_{RP}(t)$ and $\delta_{AS}(t)$ required to maintain zero sideslip for a $\phi(t)$ suggested by Etkin, Reference 5, are shown in Figure II-1. The aileron inputs for the two aircraft are similar but the amplitude of the reference X-19 configuration aileron response is greater as may be expected since the T-33 is a fighter-trainer aircraft and therefore requires greater roll response. However, the rudder time histories are significantly different. For the reference X-19 configuration rudder pedal opposite to the aileron stick input (cross-coordination) is required to maintain $\beta = 0$ throughout the transient of the rolling maneuver. However, in a steady turn moderate steady rudder pedal in the direction of the turn is needed. This change from rudder pedal opposite to the aileron stick to the steady rudder pedal application required proportional to yaw rate (which the pilot infers from bank angle) is generally difficult for the pilot to obtain because it requires precise timing and magnitude.

"An important factor which must be considered in coordinating a rolling maneuver, but which is not evident from Figure II-1, is the incentive to coordinate the aircraft. Even if the resulting β of the X-19 and the T-33 were the same, the lateral acceleration of the X-19 would be larger because of the larger n_y/β of the X-19. Therefore the consequence of not coordinating properly is more serious in the X-19. This fact may be clearly illustrated with Approach (b) which follows.

"With Approach (b) the β response is desired for the $\phi(t)$ used in Approach (a), but without a rudder input to coordinate the aircraft. Following the computation of the β response for that $\phi(t)$, the required aileron input can be computed from the given $\phi(t)$ and the β response. The differential equation relating β to ϕ for only aileron inputs can be obtained from the ratio of β/δ_{AS} to ϕ/δ_{AS} transfer functions. The solution of this differential equation for a prescribed rolling maneuver will yield the β response for that rolling maneuver. The differential equation may be written:

$$\ddot{\beta} + \left[\frac{N'_{\delta_{AS}}}{L'_{\delta_{AS}}} L'_r - (N'_r + Y_\beta)\right]\dot{\beta} + \left[N'_\beta + Y_\beta N'_r - \frac{N'_{\delta_{AS}}}{L'_{\delta_{AS}}}\left(L'_\beta + Y_\beta L'_r\right)\right]\beta =$$

$$-\frac{N'_{\delta_{AS}}}{L'_{\delta_{AS}}}\ddot{\phi} - \left(N'_p - \frac{g}{V} - \frac{N'_{\delta_{AS}}}{L'_{\delta_{AS}}} L'_p\right)\dot{\phi} - \frac{g}{V}\left(N'_r - \frac{N'_{\delta_{AS}}}{L'_{\delta_{AS}}} L'_r\right)\phi \qquad (4)$$

The δ_{AS} motion required to achieve the $\phi(t)$ rolling maneuver and $r(t)$ that results may be obtained from the following expressions:

$$\left.\begin{aligned} \delta_{AS} &= \frac{1}{L'_{\delta_{AS}}}\left[\ddot{\phi} - L'_p\dot{\phi} - \frac{g}{V}L'_r\phi + L'_r\beta - L'_\beta\beta\right] \\ r &= -\dot{\beta} + Y_\beta\beta + \frac{g}{V}\phi \end{aligned}\right\} \qquad (5)$$

"Equation (4) is a second order differential equation with $\phi(t)$ and its derivatives as the forcing function. The solution of Equation (4) for the $\phi(t)$ forcing function considered in Approach (a) is quite lengthy and, unfortunately, a simplifying approximation cannot be made. Therefore, an easier method was used to obtain the time histories for a rolling maneuver which would approximately yield the desired $\phi(t)$ function during the interval of the rolling maneuver. It is seen that the terms proportional to $\dot{\beta}$ and β in Equation (5) are fairly small in comparison with the other terms for the roll maneuver considered if the resulting sideslip is fairly small. Therefore, the aileron required to obtain this roll maneuver is nearly independent of sideslip for the particular rolling maneuver considered. And so, the time histories of the motion responses were computed with the digital computer program described earlier for the aileron input computed from Equation (5) assuming that the contribution from the β terms is negligible.

"The motion responses for this aileron input are given in Figure II-2. The roll response is a good approximation to the desired roll function for the first second but it departs from the desired function thereafter because the β terms of Equation (5) are no longer negligible. The β response indicates a large initial skid followed by a large slip. The lateral acceleration is computed in two ways:

$$n_y = \frac{V}{g}(\dot{\beta} + r) - \phi$$

$$\approx \frac{V}{g} Y_\beta \beta \qquad (6)$$

The difference between these two transients is the contribution of the $Y_p p$ and $Y_r r$ terms; thus, the importance of these terms can be assessed. The large lateral acceleration which develops whenever an uncoordinated rolling maneuver is attempted provides an incentive to coordinate the rolling maneuver.

"With the necessity for coordinating a rolling maneuver understood, an analytical investigation was undertaken to determine quantitatively the relative influence of parameter changes on the coordination problem. As a criterion, a scalar quantity indicating the "amount" of coordination difficulty encountered during a rolling maneuver is desired. Both the rms δ_{RP} (root-mean-square value of δ_{RP}) required to coordinate a specific rolling maneuver and the rms β resulting from no attempt to coordinate a specific rolling maneuver were hypothesized to be indicative of probable difficulties associated

with the coordination of a precognitive rolling maneuver. The rms δ_{RP} was selected for study for two reasons:

(1) The pilot does take action to coordinate the aircraft, and, therefore, the rms δ_{RP} would be indicative of the required effort and skill.

(2) It is much easier to study. But again the influence of β stability derivatives cannot be learned nor will it be indicative of the pilot's objection to cross-coordination.

"A question arises with regard to the specific rolling maneuver that should be considered for computation of the rms δ_{RP}. (A brief specific case is given in Appendix D of Reference 80). The rolling maneuver chosen for general study is the following:

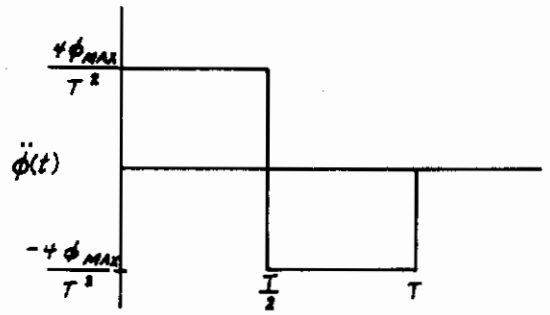

$$\ddot{\phi}(t) = \begin{cases} +\phi_{MAX}\frac{4}{T^2} & 0 < t < \frac{T}{2} \\ -\phi_{MAX}\frac{4}{T^2} & \frac{T}{2} < t < T \end{cases}$$

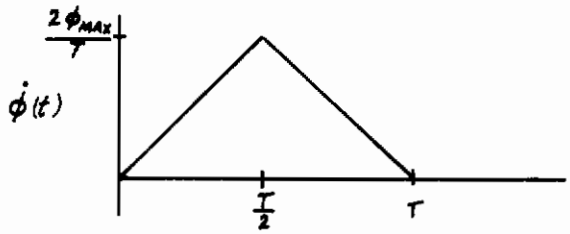

$$\dot{\phi}(t) = \begin{cases} \phi_{MAX}\frac{4T}{T^2} & 0 \le t \le \frac{T}{2} \\ \phi_{MAX}\frac{4(T-t)}{T^2} & \frac{T}{2} \le t \le T \end{cases}$$

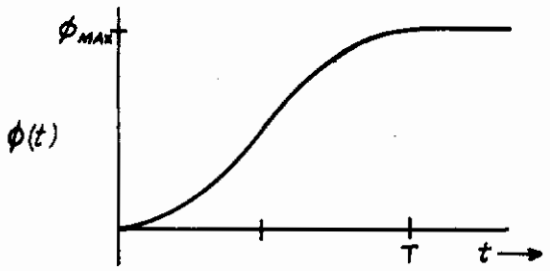

$$\phi(t) = \begin{cases} \phi_{MAX}\frac{2t^2}{T} & 0 \le t \le \frac{T}{2} \\ \phi_{MAX}\frac{2(T-t)^2}{T^2} & \frac{T}{2} \le t \le T \end{cases}$$

"The rms δ_{RP} is given by the following expressions:

$$rms\ \delta_{RP} = \sqrt{\frac{1}{T}\int_0^T \left[\delta_{RP}(t)\right]^2 dt} \qquad (7)$$

"Equation (3) provides the expression for δ_{RP} in terms of $\phi(t)$ and its derivatives. On the basis of experience from the preliminary simulator experiment, the primary objection to rudder pedal motion required to coordinate the rolling maneuver resulted from the magnitude during the transient and not the steady rudder pedal requirement. Therefore, the term proportional to ϕ in the expression for δ_{RP} was discarded to simplify the computation. With additional experience, this deletion is regretted because even δ_{RP} proportional to ϕ causes a significant problem. With the additional assumption that the other terms of the denominator are small compared to $N'_{\delta_{RP}}$ the expression for the rms δ_{RP} for the rolling given above is:

$$\text{rms}\ \delta_{RP} = \frac{4\phi_{MAX}}{T^2 N'_{\delta_{RP}}} \sqrt{\left(\frac{N'_{\delta_{AS}}}{L'_{\delta_{AS}}}\right)^2 + \frac{T^2}{12}\left(N'_p - \frac{g}{V} - \frac{N'_{\delta_{AS}}}{L'_{\delta_{AS}}} L'_p\right)^2} \qquad (8)$$

"The rms δ_{RP}/ϕ_{MAX} for variation in N'_p for selected constant values of $N'_{\delta_{AS}}/L'_{\delta_{AS}}$ are shown in Figure II-3 with values of other parameters taken to be reference X-19 configuration values and the time of the maneuver taken to be one second. The importance of maintaining small $N'_{\delta_{AS}}/L'_{\delta_{AS}}$ is evident since even the smallest rms δ_{RP} obtainable is large if $N'_{\delta_{AS}}/L'_{\delta_{AS}}$ is not small. In addition, it is important to have the proper N'_p for a given $N'_{\delta_{AS}}/L'_{\delta_{AS}}$ so that the rms δ_{RP} is small. If $N'_{\delta_{AS}} = 0$ and $N'_p = g/V$ then rudder will still be required proportional to ϕ since this term was discarded. The primary effect of including the term of δ_{RP} proportional to ϕ would be an upward shift of all the curves.

"The coefficients of the forcing function $\phi(t)$ and its derivatives in Equation (4) are exactly the same as the coefficients of the forcing function for δ_{RP} required to coordinate a rolling maneuver. These coefficients are the numerator terms of the β/δ_{AS} transfer function with $L'_{\delta_{AS}}$ factored out. Thus the same qualitative trends for the influence of the forcing function on δ_{RP} required to coordinate a

rolling maneuver and the β resulting from a δ_{AS} only rolling maneuver may be expected.

"Other important parameters in coordination of a rolling maneuver are the terms of the left-hand side of Equation (4). The important stability derivatives appearing in these coefficients are N'_β , L'_β , N'_r and $N'_{\delta_{AS}}$. An additional stability derivative (assumed zero in the derivation of Equation (3)) should appear in these coefficients: $N'_{\dot\beta}$. If $N'_{\dot\beta}$ is included, then the term + $N'_{\dot\beta}\dot\beta$ will be added to the left-hand side of Equation (4). In order to view the influence of the coefficients of β and its derivatives, β and $\emptyset$ were computed for the same $\delta_{AS}(t)$ used to obtain the desired $\emptyset(t)$ for a perfectly coordinated rolling maneuver as discussed previously. Changes were made to N'_β and $N'_{\dot\beta}$ and the time histories for the resulting configurations are given in Figure II-4. As pointed out previously, the $\emptyset(t)$ attained does appraoch the desired $\emptyset(t)$ whenever the $\beta(t)$ response becomes small.

"As seen from comparing Figures II-4a and II-4b with Figure II-2, roughly doubling N'_β reduces the maximum β only 17% and tripling N'_β reduces it only 35%; and in addition, the damping ratio is noticeably decreased. A significant reduction in β can be achieved with the addition of $N'_{\dot\beta}$ as shown in Figures II-4c and II-4d. A combination of N'_β = 6 and $N'_{\dot\beta}$ = 5 yields a 63% reduction of maximum β and N'_β = 10 and $N'_{\dot\beta}$ = 10 reduces maximum β by 72% and also the responses are smooth."

The time histories in Figure II-4 from Reference 80 illustrate that the Dutch roll frequency and damping strongly affect the amount of sideslip that will result from a given aileron time history. There is also an effect of roll damping on the relative amount of sideslip and roll rate resulting from aileron application through the term $\frac{N'_{\delta_{AS}}}{L'_{\delta_{AS}}} L'_p$ multiplying the roll rate in Equation 8 of Reference 80.

From the analysis of Reference 80, it is shown that it is easy to calculate the rudder required to maintain sideslip zero, but it is not obvious whether or not the pilot will be capable or willing to provide this coordination. It is also shown that the consequences, in terms of sideslip, of the pilot not performing the coordination task are interrelated with the Dutch roll and roll mode roots. Because of this it is considered necessary to develop measurements that include these influences and to experimentally correlate these measurements with pilot rating.

In the following paragraphs, the aileron-to-rudder crossfeed criterion suggested in Reference 34 is presented and discussed.

The recommended criterion is based on the aileron-to-rudder crossfeed which would be required to coordinate turns, i.e., keep sideslip equal to zero. The criterion involves two parameters. One is the ratio of aileron yaw to roll acceleration, $N'_{\delta a} / L'_{\delta a}$, measured in stability axes, divided by Dutch roll frequency squared. The second parameter, μ, defines the shape of the required crossfeed. This parameter is computed as follows:

- Compute the ideal rudder/aileron crossfeed, Y_{cf}, required to keep zero sideslip. This computation can be based on the measured or estimated sideslip/stick and sideslip/rudder pedal frequency responses, i.e.,

$$Y_{cf} = \frac{\text{- sideslip/stick frequency response}}{\text{sideslip/rudder pedal frequency response}}$$

  where the frequency responses are those of the airplane plus appropriate augmentation systems.

- Over the frequency range 0.2 - 5 rad/sec, approximate the ideal crossfeed by a filter of the form

$$- \frac{N'_{\delta a}}{N'_{\delta r}} \frac{(s+z)}{(s+p)}$$

- μ is given by

$$\mu = \frac{z}{p} - 1$$

The value of μ and $\frac{N'_{\delta a}}{L'_{\delta a}} \frac{1}{\omega_d^2}$ should then fall within the contours shown in Figure II-5 for Level 1 [as defined in MIL-F-8785B(ASG)].

It was found in Reference 34 that the above was not appropriate if the magnitude of aileron yaw became quite small. Then the yaw due to roll rate is assumed the critical parameter. It is therefore recommended that if $\left| N'_{\delta a} / L'_{\delta a} \right| \leq 0.04$, the following be used instead of Figure II-5 (N'_p also measured in stability axes):

$$-0.25 < N'_p - \frac{g}{U_0} < 0.15 \text{ sec}^{-1}$$

The following discussion of the development of the crossfeed is given in Reference 34.

"The basic idea was that the rudder which would be required to coordinate turns might be indicative of heading control and turn coordination problems. If an aileron-to-rudder crossfeed is used, i.e.,

$$\delta_r = Y_{c.f.}\ \delta_a$$

the condition for zero sideslip turns is given by the following ratio of numerators:

$$Y_{c.f.} = -\frac{N^{\beta}_{\delta a}}{N^{\beta}_{\delta r}}$$

For most configurations, $N^{\beta}_{\delta a}$ and $N^{\beta}_{\delta r}$ look like first-order polynomials in* the frequency range of interest; therefore

$$Y_{c.f.} \doteq -\frac{N'_{\delta a}\left(s + 1/T_{\beta}\right)}{N'_{\delta r}\left(s + 1/T_{R}\right)}$$

When $\left| Y_{\delta a} \right|$ is small and

$$\left[N'_{\delta a} L'_p + L'_{\delta a}\left(g/V - N'_p\right)\right]^2 >> \left| g/V\ N'_{\delta a}\left(N'_{\delta a} L'_r - L'_{\delta a} N_r\right)\right|$$

the sideslip/aileron zero can be approximated by:

$$\frac{1}{T_{\beta}} \doteq \frac{1}{T_R} + \frac{N'_p - g/V}{N'_{\delta a}/L'_{\delta a}}$$

This approximation is given only to demonstrate that the crossfeed parameter is sensitive to $N'_p - g/V$ and $N'_{\delta a}/L'_{\delta a}$. These two parameters are recognized as the key ones in evaluating turn coordination.

"If we define a crossfeed shaping parameter, μ, by:

$$\mu \equiv \frac{T_R}{T_{\beta}} - 1 \approx -\frac{L'_{\delta a}}{N'_{\delta a}}\frac{\left(N'_p - g/V\right)}{L'_p}$$

then the asymptotes of Y_{cf} take on the values shown in Figure II-6. The rudder sensitivity ($N'_{\delta r}$) is removed

*This assumption is examined in the following discussion.

from the crossfeed shaping since it can be separately optimized. Figure II-7 is a summary of the crossfeed shaping required on a plot of the shaping parameter μ versus the ratio of high frequency yawing to rolling acceleration with aileron inputs $N'_{\delta a}/L'_{\delta a}$. Moving vertically on this plot changes the shape of the crossfeed keeping the high frequency gain constant. Moving horizontally produces a change in the crossfeed gain at all frequencies without changing the shape.

"An initial correlation of the Reference 33 data and that obtained in the two heading control experiments (Reference 34) with μ and $N'_{\delta a}/L'_{\delta a}$ was excellent except for the low Dutch roll frequency cases. These were rated much poorer than the others for similar values of μ and $N'_{\delta a}/L'_{\delta a}$. It was found that this effect could be removed by changing from $N'_{\delta a}/L'_{\delta a}$ to $N'_{\delta a}/L'_{\delta a}\omega_d^2$. In this manner the effects of aileron yaw are reduced roughly proportional to the aircraft directional stability. The ratio of aileron excitation to directional stiffness is a better correlating parameter than aileron excitation alone.

"If the high frequency crossfeed parameter $N'_{\delta a}/L'_{\delta a}$ is very near zero, the required aileron rudder crossfeed takes the form shown in Figure II-8. The parameter $\frac{g}{V} - N'_p$ clearly defines the rudder requirements in this case.

From Figures II-7 and II-5 the following observations can be made:

- Moderately high proverse (positive) $N'_{\delta a}/L'_{\delta a}$ is acceptable in the region where $\mu = -1$. Physically, this corresponds to a sudden initial heading response in the direction of turn followed by decreasing rudder requirement.* (Required dc rudder is zero when $\mu = -1$, see Figure II-7. It is felt that the pilots are accepting the initial proverse yaw as a heading lead and are not attempting to use cross control rudder to coordinate the turn entry. The allowable values of proverse yaw decrease rapidly as μ becomes greater than -1. Physically this corresponds to an increase in the requirement for low frequency cross control rudder activity (see Figure II-7) which is highly objectionable.

*Figure II-7 shows that in these cases a washout or lead/lag crossfeed is necessary. The high frequency asymptote is rudder out of the turn so if the pilot does not use the rudder he will initially experience proverse yaw or heading into the turn. As the turn progresses little rudder is required as the low-frequency crossfeed gain is low.

The ratings are less sensitive to μ becoming less than -1 since this represents a requirement for low frequency rudder into the turn which is consistent with normal flying technique.

- The maximum allowable values of adverse $N'_{\delta a}/L'_{\delta a}$ occur in the region where μ is slightly greater than -1. This corresponds to decreasing rudder requirements as the turn progresses. As μ becomes greater than -1 the allowable adverse yaw decreases rapidly because of the increase in required dc rudder. The rapid decrease in ratings that occurs when μ becomes less than -1 is due to the rudder reversal required (first rudder into, then out of the turn) during rolling maneuvers. This type of rudder control is virtually impossible to learn and is therefore totally unacceptable.

- Increasing the required rudder-aileron shaping so that $\mu > 1$ results in appreciable reduction in allowable $N'_{\delta a}$. (The "knee of the curve" is at $\mu \doteq 1$.)"

The preceding approach to the coordination problem is interesting and again reveals the fundamental elements as $N'_{\delta a}$, $N'_p - g/V$, N'_r, $N'_{\delta r}$, ω_d^2, ζ_d and λ_r . The recommended criterion, however, is not considered to be practical for the following reasons.

1. It requires evaluating control derivatives $L'_{\delta a}$, $N'_{\delta a}$, $N'_{\delta r}$ and under certain circumstances the stability derivatives N'_p .

2. It requires obtaining two frequency response functions which must then be ratioed to obtain the required crossfeed shaping function in both amplitude and phase.

3. It requires approximating the ideal crossfeed which may be of third-order in both numerator and denominator with a simplified filter form consisting of a fixed high frequency gain equal to $\frac{-N_{\delta a}}{N'_{\delta r}}$ and a first-order over first-order shaping function.

That this step of the procedure can be quite inadequate and would require subjective judgment is demonstrated by the example shown in Figure II-9. The amplitude ratio data is completely incompatible with the shape of a first order lead-lag or lag-lead filter. Also the phase indicates 180 degrees lead in going from low frequency to high frequency. This would imply a zero in the left half plane and a pole in the right half plane. This example is case (LH-100-20-20) from Reference 33. The average pilot rating given was 2.4

based on six evaluations. The value of $\left| N'_{\delta_{AS}} / L'_{\delta_{AS}} \right| = 0.132$ was larger than 0.04, therefore the configuration would be required to meet the crossfeed requirement. The crossfeed required for case LH100+20+30 from Reference 33 is shown in Figure II-10. Again the amplitude ratio data can not be fit by a first order filter. This example has approximately 45° phase lag.

It should be noted that both of the cases cited above were used by the authors of Reference 34 to develop the criteria boundary of Figure II-5. It seems obvious that the points must have been plotted by evaluating the values of $\frac{N'_{\delta_{AS}}}{L'_{\delta_{AS}} \omega_d^2}$ and $\mu = \frac{L'_{\delta_{AS}}}{N'_{\delta_{AS}}} \frac{(N'_p - g/V)}{L'_p}$ rather than through curve fitting the crossfeed frequency response. These cases illustrate the consequence of the assumption that the crossfeed would be first-order over first-order in the frequency band 0.2 - 5 rad/sec.

Additional points can be made regarding the practical problems of computing the parameter μ . Under the assumptions required to reduce the β/δ_{AS} and β/δ_{RP} transfer function numerators from third order to first order, the crossfeed is:

$$\frac{\delta_R(s)}{\delta_{AS}(s)} = \frac{-N'_{\delta_{AS}} \left[s - \left(L'_p - \frac{L'_{\delta_{AS}}}{N'_{\delta_{AS}}} (N'_p - g/V) \right) \right]}{N'_{\delta_{RP}} (s - L'_p)}$$

The denominator is essentially the roll mode root which for the following example will be assumed constant. An s plane plot for the transfer function for several values of the numerator can be related to the μ parameter:

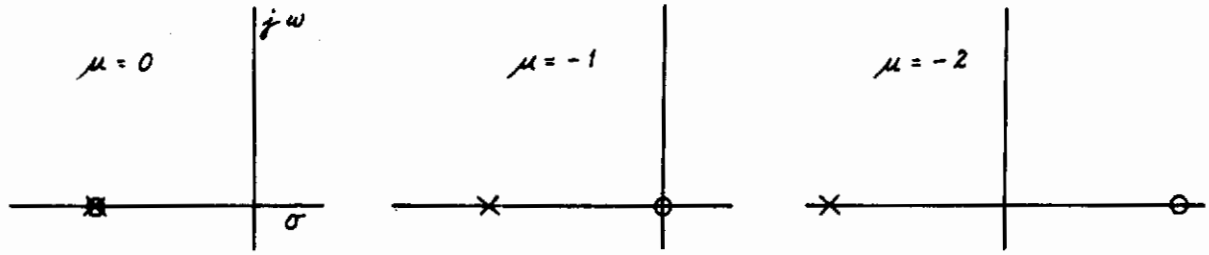

Figure II-7 indicates that the amplitude ratio is constant for all frequencies for both $\mu = 0$ and $\mu = -2$. The question is how does one recognize whether $\mu = 0$ or $\mu = -2$ from looking at frequency response data. Apparently the decision would depend on the shape of the phase plot as seen from the sketches on the following page.

In the discussion of Reference 34 the crossfeed shape with frequency is associated quite directly with control activity during a turn entry, i.e., the high frequency part of the crossfeed Bode diagram is directly associated with rudder activity at the start of the turn and the low frequency part of the Bode diagram is directly associated with the steady rudder required in the turn. (See footnote in preceding discussion). Such a direct association of time and frequency information is questioned.

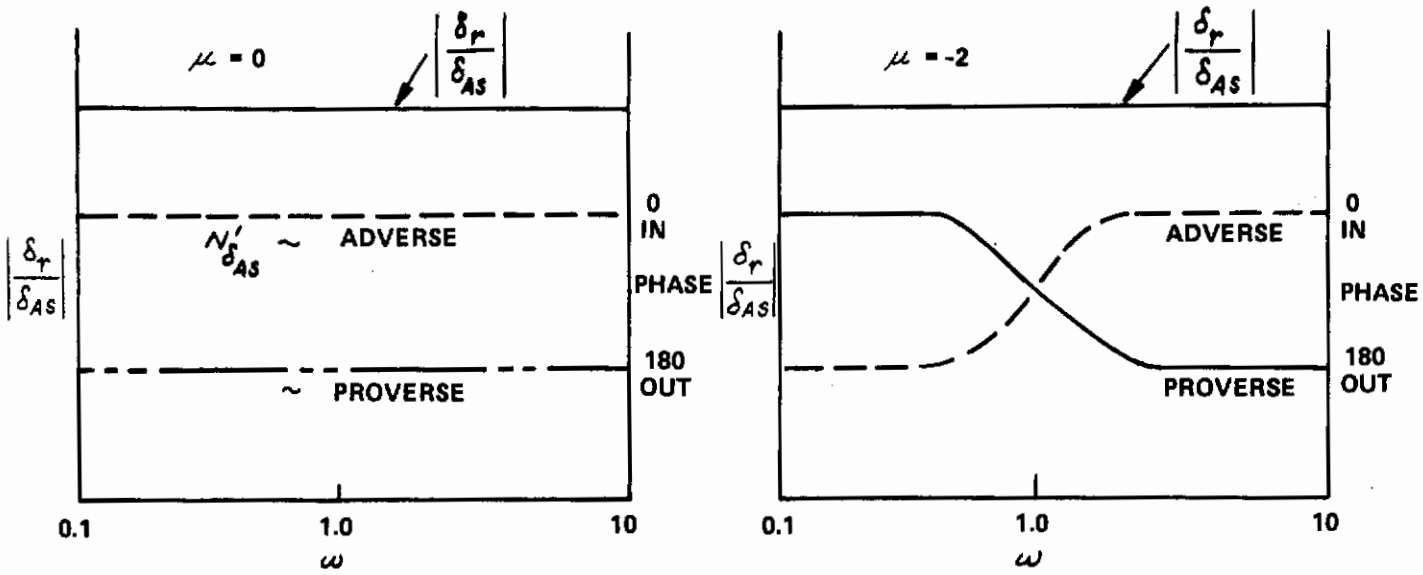

In summary, the aileron-to-rudder crossfeed approach proposed in Reference 34 is considered to be an interesting way to look at the turn coordination problem but the simplifications made in its development which required subjective approximations to be made in application makes the criterion inadequate for use in the military specification. Without the simplifying assumptions, however, the crossfeed description would become too complicated to be useful.

Referring again to equation (3) from Reference 80, it is seen that the rudder required to coordinate is a function of the rolling maneuver to be executed ($\ddot{\phi}$, $\dot{\phi}$ and ϕ) and the stability derivative dependent coefficients. This suggests the possibility of defining a catalog of rolling maneuvers representative of different Classes and Flight Phases. For each maneuver, one could construct three-dimensional plots of the coefficients of equation (3) to define acceptable volumes in which points defined by the three coefficients must occupy. These volumes could be analytically defined also.

P.R. = f (coefficients of eq. (3) for each maneuver cataloged).

This approach assumes that sideslip is being kept zero at all times. It would not recognize the situation where the airplane dynamic characteristics (Dutch roll frequency and damping and roll damping) are such that the sideslip resulting from uncoordinated maneuvers is acceptable.

Because of this latter consideration it is thought that the better approach for formulating specification requirements is to limit the sideslip or roll and yaw oscillations resulting from aileron inputs. Hopefully the parameters selected to indicate the consequence of not coordinating the maneuver will also be capable of reflecting the difficulty of coordinating or the complexity of the rudder coordination if it were attempted. The parameters used in MIL-F-8785B(ASG) are designed to have this characteristic by including a measure of the Dutch roll phase angle.

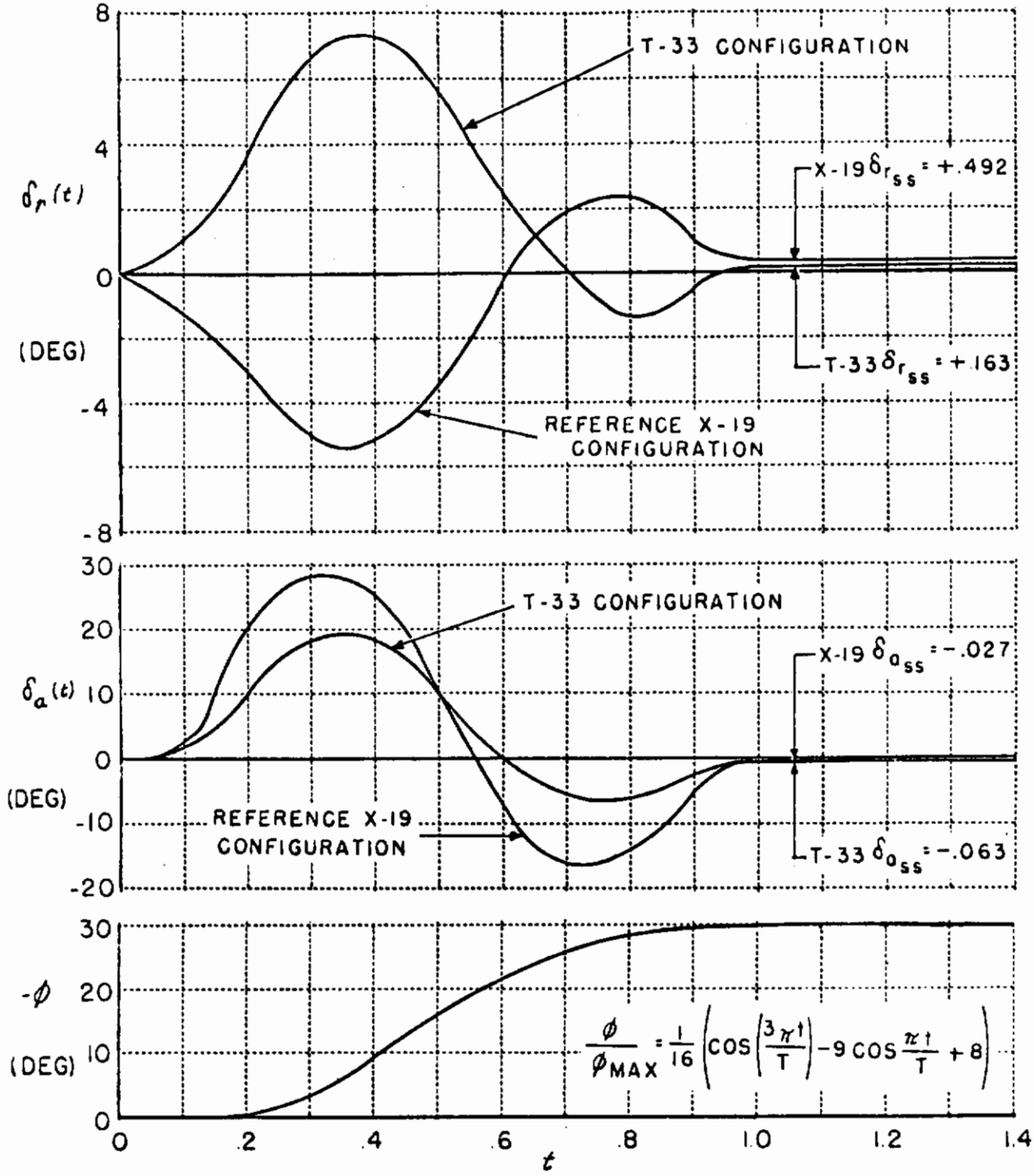

Figure II-1 COMPARISON OF THE CONTROL INPUT TIME HISTORIES TO COORDINATE THE GIVEN ROLL MANEUVER FOR THE REFERENCE X-19 CONFIGURATION WITH THE T-33 CONFIGURATION

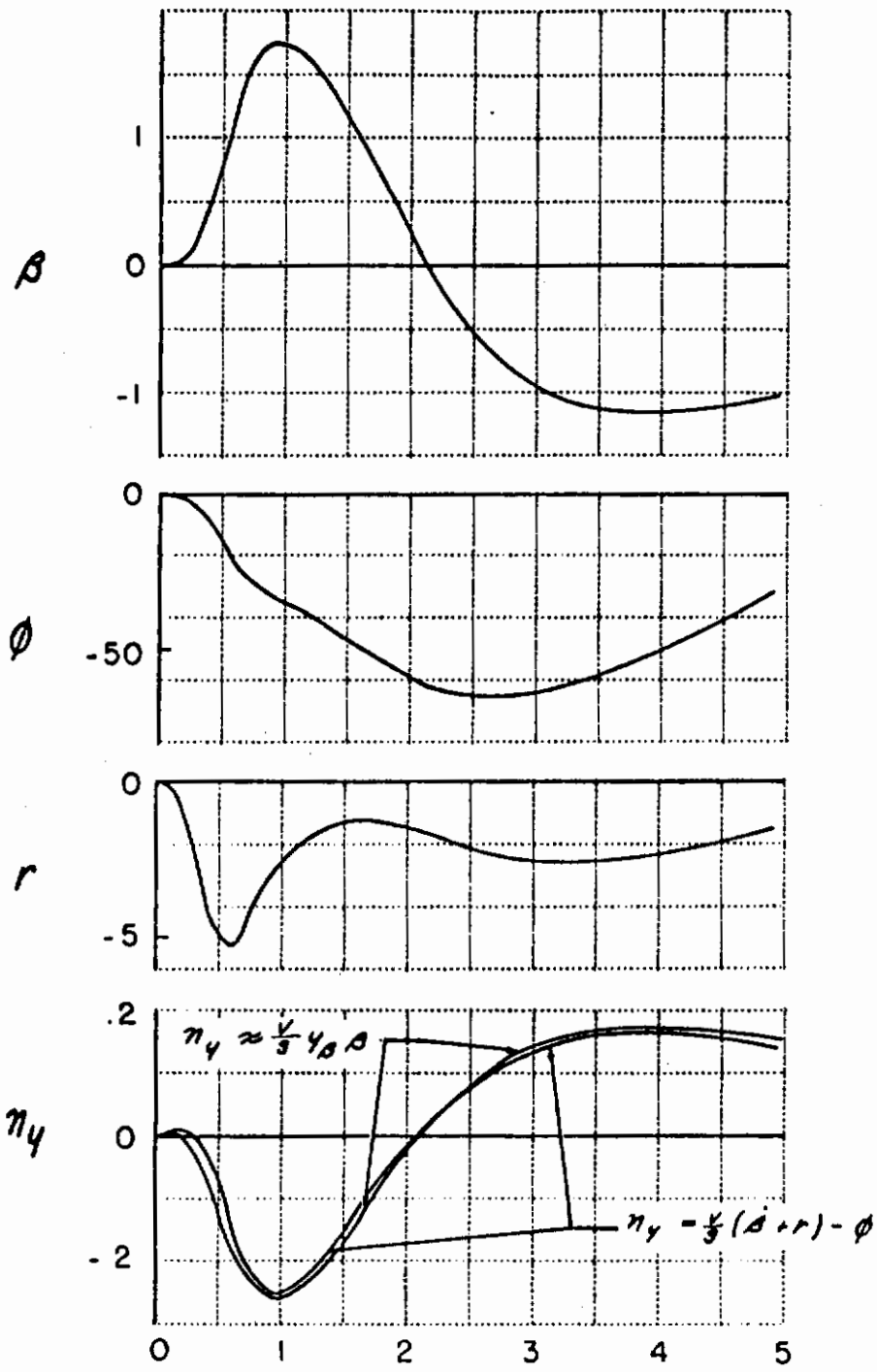

Figure II-2 MOTION RESPONSES OF THE REFERENCE X-19 CONFIGURATION FOR THE GIVEN ROLL MANEUVER FOR ONLY AN AILERON INPUT

NOTE : TERM OF δ_{RP} PROPORTIONAL TO ϕ WAS DISCARDED FOR THE COMPUTATION OF R.M.S. δ_{RP}

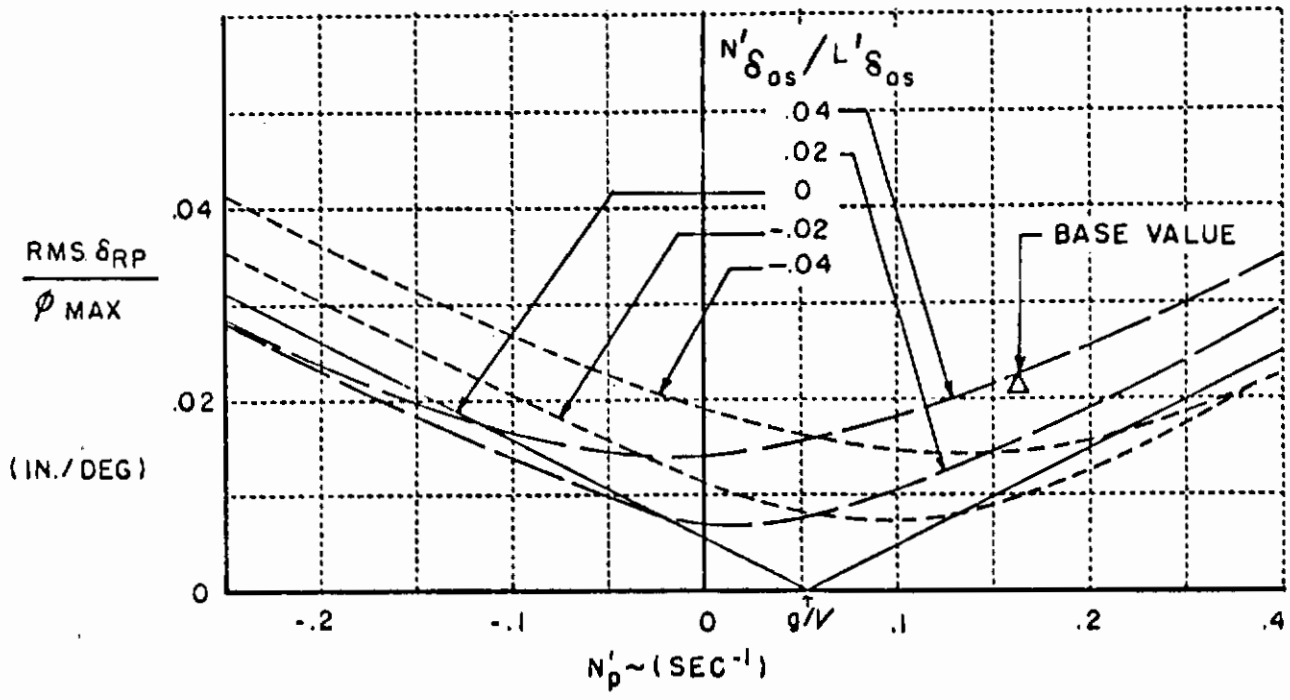

$$\frac{\delta_R}{\delta_{RP}} = \frac{5^\circ}{IN.}$$

$N'_{\delta_R} = -2.27$

$L'_p = -1.75$

$g/V = .0557$

Figure II-3 RMS RUDDER PEDAL REQUIRED TO COORDINATE A ROLL MANEUVER BY $\dot{\phi}$ = CONSTANT FOR 1/2 SECOND AND $\dot{\phi}$ = -CONSTANT FOR ANOTHER 1/2 SECOND

REFERENCE CONFIGURATION DATA A EXCEPT FOR VALUES OF N_β AND $N_{\dot\beta}$

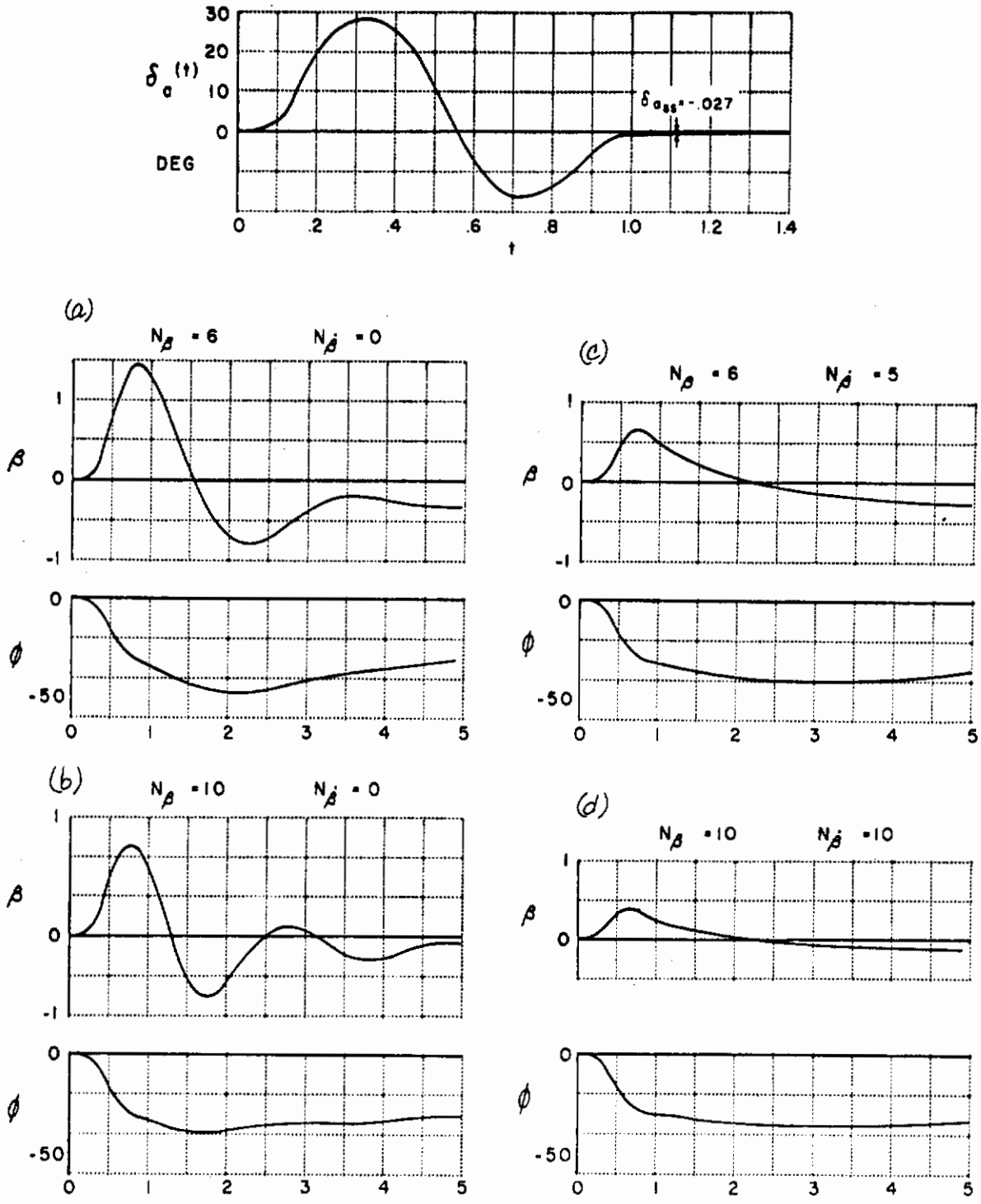

Figure II-4 TIME HISTORIES FOR A ROLL MANEUVER WITH CHANGES MADE TO N_β AND $N_{\dot\beta}$

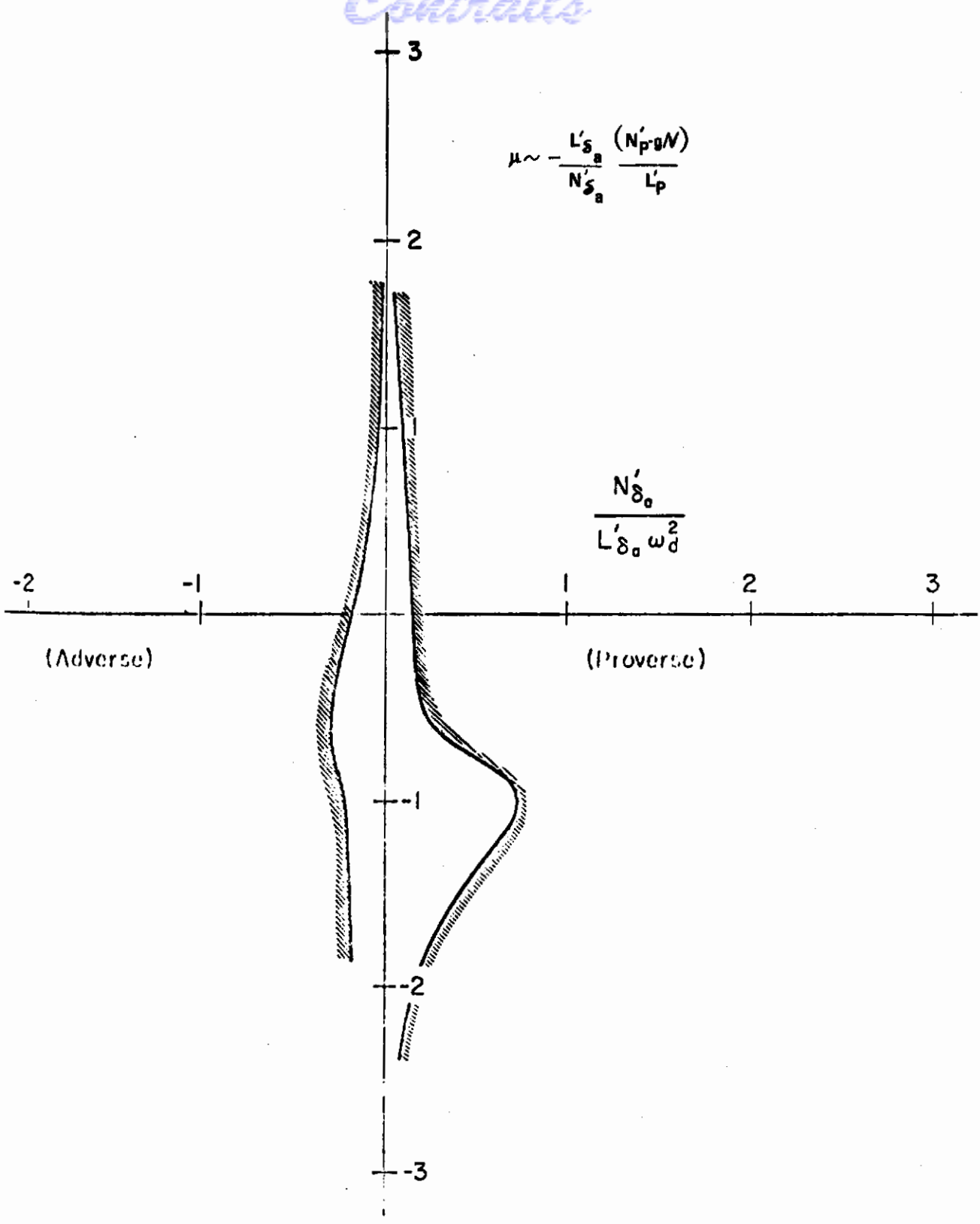

Figure II-5 RECOMMENDED HEADING CONTROL CRITERION FOR $\left|N_{\delta_a}/L_{\delta_a}\right| > 0.04$

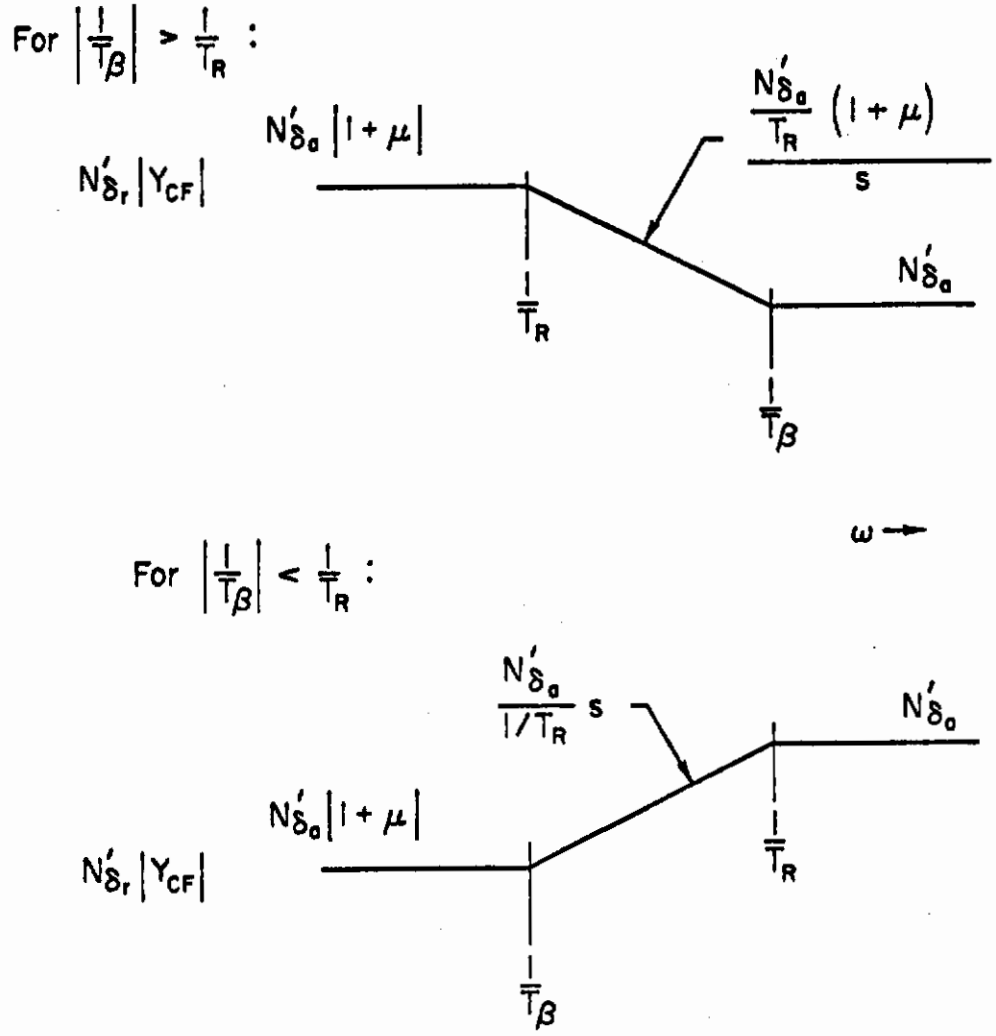

Figure II-6 ASYMPTOTES OF AILERON-RUDDER CROSSFEED

NOTE: TO KEEP μ CONSTANT AS N_{δ_a} APPROACHES ZERO, IT IS NECESSARY THAT $(N'_p \cdot g/V)$ APPROACH ZERO ALSO. THIS CRITERIA BREAKS DOWN IF N_{δ_a} GOES TO ZERO BUT $(N'_p \cdot g/V)$ STAYS LARGE.

$$\mu \approx -\frac{L_{\delta_a}}{N'_{\delta_a}} \frac{N'_p \cdot g/V}{L'_p}$$

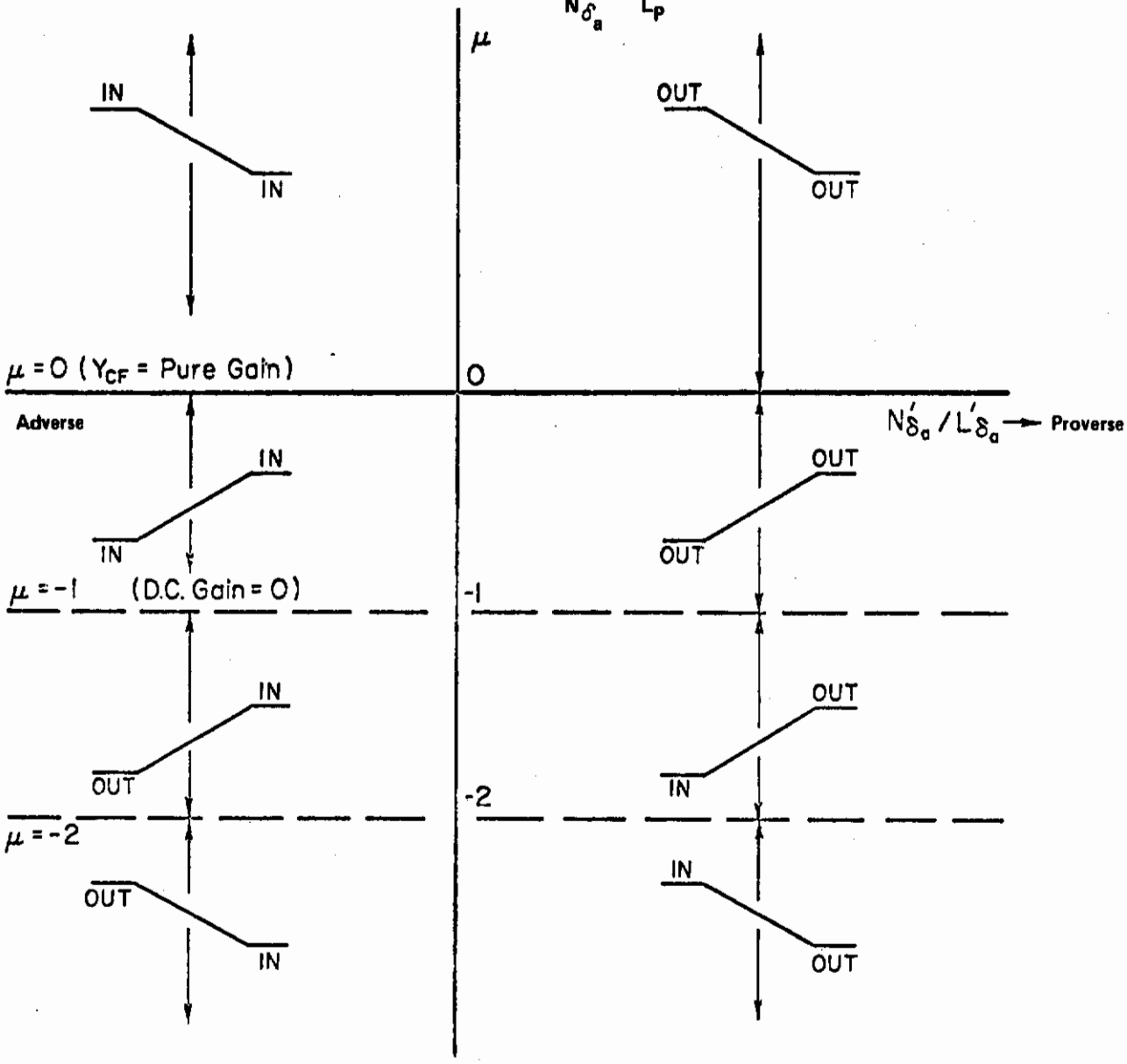

Note: "IN" means rudder into the turn
"OUT" means rudder out of the turn

Figure II-7 CROSSFEED VARIATION WITH SHAPING PARAMETER

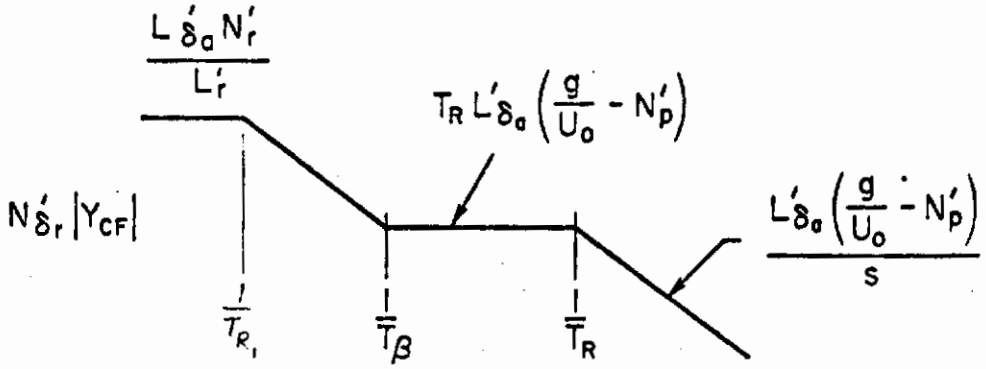

$$\frac{1}{T_{R_1}} \doteq \frac{g}{V} \frac{L'_r}{L'_p} \qquad \frac{1}{T_\beta} \doteq \frac{-\frac{g}{U_o} N_r}{\left(\frac{g}{U_o} - N'_p\right)} \qquad \frac{1}{T_R} \doteq L'_p$$

Figure II-8 REQUIRED CROSSFEED FOR $N'_{\delta_a} = 0$

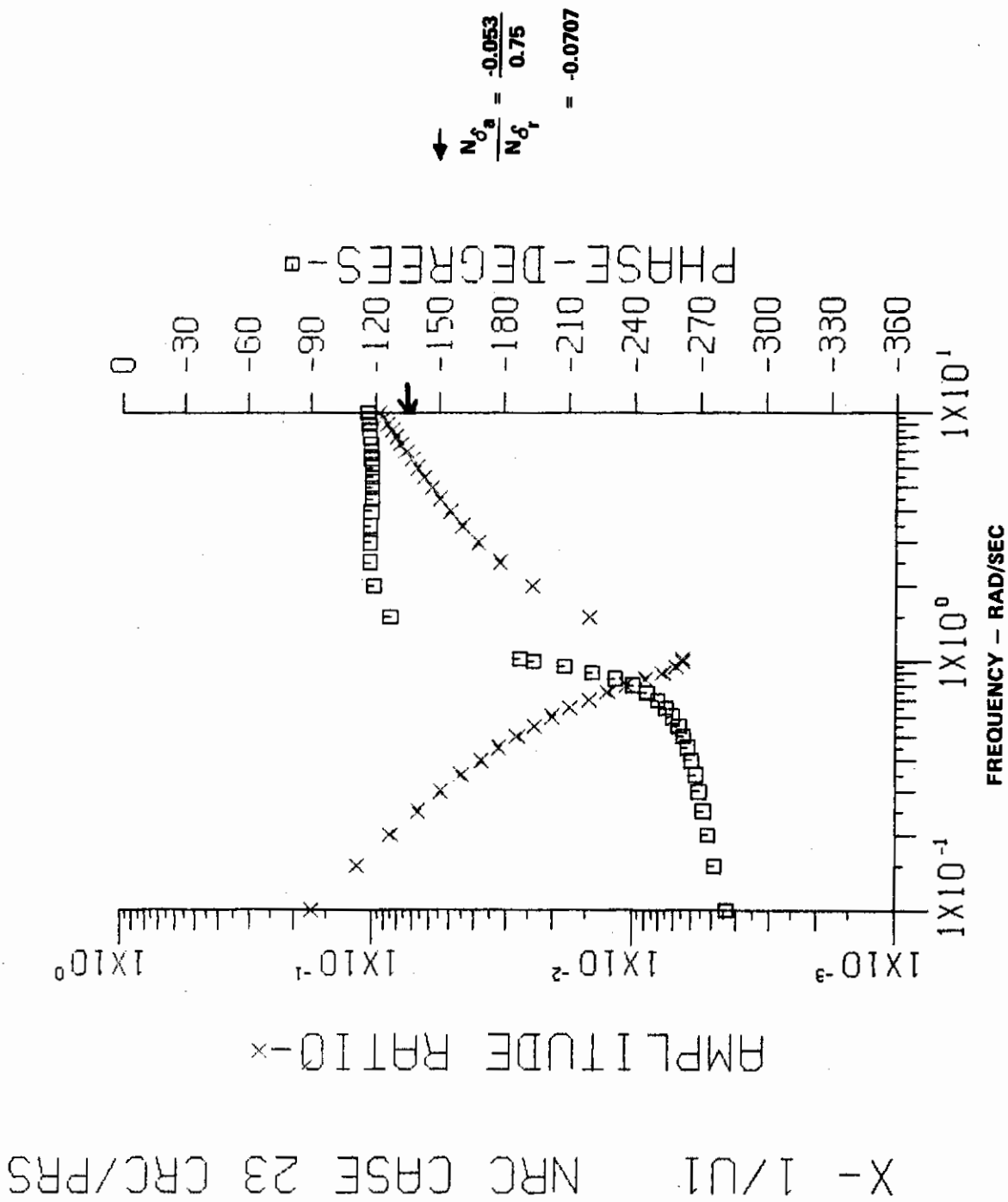

Figure II-9 AILERON-TO-RUDDER CROSSFEED REQUIRED FOR CASE LH100+20+20

Figure II-10 AILERON-TO-RUDDER CROSSFEED REQUIRED FOR CASE LH100+20+30

APPENDIX III

LATERAL-DIRECTIONAL COUPLING DATA

Data for the roll sideslip coupling parameters $\frac{\hat{p}_{osc}}{\hat{p}_1}$ vs. $\psi_{p_{STEP}}$ and $\frac{V_T}{g}\frac{1}{\omega_{n_d}}\frac{\Delta\dot{\beta}_{MAX}}{\hat{p}}$ vs. $\psi_{\dot{\beta}_{STEP}}$ for the fifteen reports considered in this study are listed on computer output sheets in columns 3 and 4 and columns 9 and 10. Additional parameters were computed and are listed in the tables also. The plotted data for these additional parameters are also included in this Appendix.

The additional parameters evaluated are identified at the top of each computer output data sheet. The plots for these parameters have been reviewed and compared visually with the plots of $\frac{\hat{p}_{osc}}{\hat{p}_1}$ and $\frac{V_T}{g}\frac{1}{\omega_{n_d}}\frac{\Delta\dot{\beta}_{MAX}}{\hat{p}_1}$. As a result of this review it is the authors' opinion that the best correlation is obtained by the selected parameters. Also the selected parameters are thought to be the most straightforward to evaluate in general and the most practical to evaluate from flight test data.

The parameters on the tables and plots are coded in computer language. The key to the parameters is as follows. The complete definitions are given on pages 230 and 231.

# 1	PHAT-OS/AV	$\frac{\hat{p}_{osc}}{\hat{p}_{AV}}$
# 2	PSI-P(STEP)	ψ_p (STEP)
# 3	(V/WG)(B*/PH)@1.2TD	$\frac{1}{\omega_{n_d}}\frac{V_T}{g}\frac{\Delta\dot{\beta}_{MAX}\mid t<1.2T_d}{\hat{p}_1}$
# 4	PSI-B*(STEP)	$\psi_{\dot{\beta}}$ (STEP)
# 5	(1/W2)R*HAT-OS/AV	$\frac{1}{\omega_{n_d}^2}\frac{\mid\hat{\dot{r}}_{osc}\mid t>.2T_d}{\hat{\dot{r}}_{AV}}$
# 6	PSI-R*(STEP)	$\psi_{\dot{r}}$ (STEP)
# 7	(DB)TD/2 OR 2/K	$\frac{\Delta\beta_{MAX}}{k}$

# 8	PSI-B(STEP)	ψ_β (STEP)
# 9	PHAT-1/2 OS/PEAK#1	$\frac{\hat{p}_{osc}}{\hat{p}_1}$
# 10	PSI-P(STEP)	ψ_p (STEP)
# 11	(V/G)(B*/PH)@1.2TD	$\frac{V_T}{g} \quad \frac{\Delta\dot{\beta}\,\vert_{t<1.2\,T_d}}{\hat{p}_1}$
# 12	PSI-B*(STEP)	$\psi_{\dot{\beta}}$ (STEP)
# 13	(1/W)R*HAT-OS/AV	$\frac{1}{\omega_{n_d}} \quad \frac{\vert\hat{r}_{osc}\vert\ t>.2T_d}{\hat{r}_{AV}}$
# 14	PSI-R*(STEP)	$\psi_{\dot{r}}$ (STEP)
# 15	(DB*/PH)@TD/4	$\frac{\Delta\dot{\beta}_{MAX}\,\vert_{t<\frac{1}{4}T_d}}{\hat{p}_1}$
# 16	PSI-B*(STEP)	$\psi_{\dot{\beta}}$ (STEP)

1=PHAT-OS/AV
2=PSI-P(STEP)
3=(V/WG)(B*/PH)@1.2TD
4=PSI-B*(STEP)
5=(1/W2)R*HAT-OS/AV
6=PSI-R*(STEP)
7=(DB)TD/2 OR 2/K
8=PSI-B(STEP)
9=PHAT-1/2 OS/PEAK#1
#10=PSI-P(STEP)
#11=(V/G)(B*/PH)@1.2TD
#12=PSI-B*(STEP)
#13=(1/W)R*HAT-OS/AV
#14=PSI-R*(STEP)
#15=(DB*/PH)@TD/4
#16=PSI-B*(STEP)

PR	# 1	# 2	# 3	# 4	# 5	# 6	# 7	# 8
7.0	0.144	-26.0	2.739	-75.2	0.765	-162.3	17.899	-172.0
7.0	0.105	-22.8	2.223	-72.1	0.626	-159.1	14.203	-168.8
7.0	0.070	-16.6	1.588	-65.8	0.465	-152.9	9.765	-162.6
6.5	0.034	-357.2	0.662	-46.5	0.280	-133.6	4.580	-143.3
7.0	0.024	-316.5	0.417	-5.7	0.203	-92.8	4.155	-102.5
8.0	0.028	-283.0	0.492	-332.3	0.174	-59.3	5.473	-69.0
7.0	0.265	-47.3	3.118	-91.1	0.965	-179.1	7.654	-186.8
4.0	0.150	-47.9	2.143	-91.7	0.651	-179.7	5.342	-187.4
3.0	0.044	-50.4	0.853	-94.1	0.266	-182.1	2.374	-189.9
4.0	0.026	-52.7	0.477	-96.4	0.172	-184.4	1.620	-192.2
3.0	0.015	-57.2	0.280	-101.0	0.100	-189.0	1.050	-196.7
3.0	0.003	-96.3	0.066	-140.1	0.023	-228.1	0.448	-235.8
3.0	0.013	-212.5	0.228	-256.3	0.084	-344.3	0.534	352.0
4.5	0.038	-220.8	0.539	-264.5	0.208	-352.5	1.542	-0.3
7.0	0.064	-222.9	0.847	-266.7	0.345	-354.7	2.720	-2.4
7.0	0.280	-63.3	3.499	-110.1	1.019	-197.7	29.685	-206.3
6.0	0.173	-71.2	2.473	-118.0	0.745	-205.6	22.142	-214.2
5.5	0.102	-85.7	1.608	-132.5	0.494	-220.1	15.741	-228.7
4.0	0.064	-115.9	0.984	-162.7	0.345	-250.3	10.532	-258.9
6.0	0.061	-147.9	0.834	-194.8	0.357	-282.3	9.119	-291.0
8.0	0.071	-167.3	0.932	-214.2	0.420	-301.7	9.460	-310.4
7.0	2.010	-44.5	2.368	-86.7	1.312	-174.1	18.876	-182.4
5.2	0.412	-41.6	1.283	-83.7	0.427	-171.1	9.027	-179.5
7.0	0.321	-40.6	1.114	-82.8	0.354	-170.2	7.757	-178.5
4.5	0.144	-36.3	0.672	-78.4	0.196	-165.8	4.581	-174.2
6.0	0.033	-11.6	0.154	-53.8	0.060	-141.1	1.172	-149.5
8.0	0.082	-241.9	0.330	-284.0	0.115	-11.4	3.852	-19.8
7.5	-1.898	-23.3	3.552	-87.9	-1.746	-181.9	268.901	-182.5
6.0	10.240	-21.9	1.902	-86.5	2.838	-180.5	21.260	-181.1
6.5	1.278	-20.4	1.284	-85.0	0.773	-179.0	10.885	-179.6
3.5	0.217	-13.0	0.480	-77.6	0.171	-171.6	3.173	-172.2
2.5	0.082	-224.4	0.199	-289.0	0.071	-23.0	1.517	-23.6
2.0	0.174	-212.6	0.384	-277.2	0.153	-11.2	3.584	-11.8

# 9	#10	#11	#12	#13	#14	#15	#16	----
0.291	-26.0	6.465	-75.2	1.806	-162.3	0.203	-75.2	
0.220	-22.8	5.248	-72.1	1.478	-159.1	0.164	-72.1	
0.150	-16.6	3.750	-65.8	1.098	-152.9	0.115	-65.8	AB-1
0.065	-357.2	1.563	-46.5	0.660	-133.6	0.044	-46.5	
0.046	-316.5	0.984	-5.7	0.480	-92.8	0.014	-5.7	
0.053	-283.0	1.162	-332.3	0.410	-59.3	0.024	-332.3	
0.461	-47.3	7.828	-91.1	2.422	-179.1	0.251	-91.1	
0.289	-47.9	5.380	-91.7	1.634	-179.7	0.174	-91.7	
0.092	-50.4	2.142	-94.1	0.668	-182.1	0.071	-94.1	
0.051	-52.7	1.196	-96.4	0.431	-184.4	0.041	-96.4	
0.030	-57.2	0.702	-101.0	0.251	-189.0	0.025	-101.0	AB-2
0.007	-96.3	0.166	-140.1	0.059	-228.1	0.007	-140.1	
0.026	-212.5	0.572	-256.3	0.211	-344.3	0.015	-256.3	
0.072	-220.8	1.353	-264.5	0.522	-352.5	0.039	-264.5	
0.118	-222.9	2.125	-266.7	0.866	-354.7	0.064	-266.7	
0.459	-63.3	8.924	-110.1	2.598	-197.7	0.294	-110.1	
0.309	-71.2	6.306	-118.0	1.900	-205.6	0.205	-118.0	
0.192	-85.7	4.101	-132.5	1.261	-220.1	0.124	-132.5	AB-3
0.122	-115.9	2.510	-162.7	0.881	-250.3	0.056	-162.7	
0.116	-147.9	2.126	-194.8	0.910	-282.3	0.031	-194.8	
0.131	-167.3	2.378	-214.2	1.072	-301.7	0.051	-214.2	
1.350	-44.5	5.896	-86.7	3.266	-174.1	0.186	-86.7	
0.649	-41.6	3.194	-83.7	1.064	-171.1	0.101	-83.7	
0.545	40.6	2.773	-82.8	0.883	-170.2	0.087	-82.8	BB-1
0.287	-36.3	1.674	-78.4	0.487	-165.8	0.053	-78.4	
0.064	-11.6	0.385	-53.8	0.149	-141.1	0.012	-53.8	
0.148	-241.9	0.822	-284.0	0.287	-11.4	0.025	-284.0	
3.220	-23.3	9.023	-87.9	-4.435	-181.9	0.276	-87.9	
1.677	-21.9	4.831	-86.5	7.208	-180.5	0.148	-86.5	
1.099	-20.4	3.262	-85.0	1.964	-179.0	0.100	-85.0	BA-2
0.369	-13.0	1.220	-77.6	0.434	-171.6	0.038	-77.6	
0.148	-224.4	0.507	-289.0	0.180	-23.0	0.014	-289.0	
0.286	-212.6	0.977	-277.2	0.389	-11.2	0.029	-277.2	

1=PHAT-OS/AV
2=PSI-P(STEP)
3=(V/WG)(B*/PH)@1.2TD
4=PSI-B*(STEP)
5=(1/W2)R*HAT-OS/AV
6=PSI-R*(STEP)
7=(DB)TD/2 OR 2/K
8=PSI-B(STEP)
9=PHAT-1/2 OS/PEAK#1
#10=PSI-P(STEP)
#11=(V/G)(B*/PH)@1.2TD
#12=PSI-B*(STEP)
#13=(1/W)R*HAT-OS/AV
#14=PSI-R*(STEP)
#15=(DB*/PH)@TD/4
#16=PSI-B*(STEP)

PR	# 1	# 2	# 3	# 4	# 5	# 6	# 7	# 8
5.0	0.260	-209.1	0.527	-273.8	0.230	-7.8	5.752	-8.4
7.0	0.300	-208.2	0.586	-272.9	0.266	-6.8	6.853	-7.4
6.5	0.649	-43.3	1.683	-89.0	0.667	-177.0	12.669	-184.6
3.0	0.224	-43.0	0.916	-88.7	0.292	-176.7	6.771	-184.3
2.0	0.039	-41.2	0.247	-86.9	0.075	-174.9	2.183	-182.5
4.0	0.044	-226.1	0.201	-271.9	0.069	-359.9	1.582	-7.5
7.0	0.107	-224.6	0.433	-270.4	0.164	-358.4	4.053	-6.0
7.5	226.525	-48.6	3.184	-95.3	4.384	-185.0	30.695	-190.0
4.0	0.660	-56.5	1.544	-103.2	0.649	-192.9	12.779	-197.9
3.0	0.184	-74.2	0.672	-120.9	0.225	-210.6	6.437	-215.6
2.0	0.079	-119.5	0.299	-166.3	0.113	-256.0	3.755	-260.9
4.0	0.097	-173.5	0.317	-220.3	0.135	-310.0	3.740	-315.0
3.5	0.145	-194.4	0.469	-241.1	0.200	-330.8	4.705	-335.8
5.5	0.202	-204.6	0.625	-251.3	0.279	-341.0	6.127	-346.0
9.0	-1.697	-47.2	2.204	-88.2	-0.668	-173.9	32.447	-183.9
7.0	3.376	-43.0	1.153	-84.1	0.725	-169.8	9.389	-179.8
6.5	0.127	-20.6	0.286	-61.6	0.062	-147.3	1.531	-157.3
7.0	0.048	-313.0	0.087	-354.0	0.027	-79.8	1.059	-89.8
9.0	0.110	-253.5	0.187	-294.5	0.050	-20.3	2.801	-30.3
9.9	-1.366	-49.0	2.205	-88.2	-0.410	-170.1	43.915	-184.1
5.5	13.578	-49.9	1.102	-89.0	1.204	-171.0	9.704	-185.0
5.5	0.158	-54.4	0.256	-93.5	0.056	-175.4	2.448	-189.4
8.0	0.086	-221.7	0.135	-260.8	0.035	-342.7	1.355	-356.7
7.5	-3.014	-43.3	1.527	-90.4	-1.147	-181.0	16.591	-185.1
6.0	0.482	-55.1	0.457	-102.2	0.124	-192.8	4.126	-196.8
5.5	0.113	-182.8	0.142	-229.9	0.037	-320.5	1.978	-324.6
8.0	0.192	-201.2	0.218	-248.4	0.061	-338.9	2.453	-343.0
8.0	0.251	-207.1	0.270	-254.2	0.079	-344.8	2.958	-348.8
6.7	-1.830	-22.1	3.441	-86.8	-1.551	-180.3	266.956	-181.9
4.0	6.093	-19.3	1.762	-83.9	2.081	-177.4	19.007	-179.0
2.5	0.128	-354.9	0.350	-59.5	0.109	-153.0	1.974	-154.7
4.0	0.076	-242.3	0.188	-307.0	0.064	-40.5	1.524	-42.1
5.3	0.197	-215.8	0.427	-280.4	0.168	-13.9	4.504	-15.6

# 9	#10	#11	#12	#13	#14	#15	#16	
0.393	-209.1	1.340	-273.8	0.585	-7.8	0.041	-273.8	BA-2
0.436	-208.2	1.487	-272.9	0.676	-6.8	0.045	-272.9	
0.839	-43.3	4.190	-89.0	1.660	-177.0	0.134	-89.0	
0.403	-43.0	2.281	-88.7	0.726	-176.7	0.074	-88.7	
0.080	-41.2	0.615	-86.9	0.187	-174.9	0.022	-86.9	BB-2
0.083	-226.1	0.502	-271.9	0.171	-359.9	0.013	-271.9	
0.189	-224.6	1.077	-270.4	0.408	-358.4	0.032	-270.4	
1.867	-48.6	8.281	-95.3	11.400	-185.0	0.259	-95.3	
.837	-56.5	4.016	-103.2	1.688	-192.9	0.130	-103.2	
0.329	-74.2	1.748	-120.9	0.586	-210.6	0.051	-120.9	
0.1.0	-11[illegible].5	0.777	-166.3	0.295	-256.0	0.016	-166.3	BB-3
0.176	-173.5	0.824	-220.3	0.352	-310.0	0.016	-220.3	
0.248	-194.4	1.220	-241.1	0.520	-330.8	0.030	-241.1	
0.325	-204.6	1.625	-251.3	0.726	-341.0	0.043	-251.3	
3.166	-47.2	5.445	-88.2	-1.650	-173.9	0.172	-88.2	
1.526	-43.0	2.848	-84.1	1.791	-169.8	0.089	-84.1	
0.268	-20.6	0.705	-61.6	0.154	-147.3	0.020	-61.6	CB-1
0.090	-313.0	0.215	-354.0	0.066	-79.8	0.004	-354.0	
0.193	-253.5	0.461	-294.5	0.125	-20.3	0.014	-294.5	
3.755	-49.0	5.469	-88.2	-1.017	-170.1	0.168	-88.2	
1.729	-49.9	2.734	-89.0	2.986	-171.0	0.087	-89.0	CB-2
0.304	-54.4	0.635	-93.5	0.139	-175.4	0.024	-93.5	
0.155	-221.7	0.335	-260.8	0.087	-342.7	0.007	-260.8	
2.609	-43.3	3.725	-90.4	-2.798	-181.0	0.113	-90.4	
0.690	-55.1	1.116	-102.2	0.303	-192.8	0.039	-102.2	
0.201	-182.8	0.347	-229.9	0.090	-320.5	0.005	-229.9	CB-3
0.312	-201.2	0.531	-248.4	0.148	-338.9	0.011	-248.4	
0.384	-207.1	0.658	-254.2	0.193	-344.8	0.015	-254.2	
3.179	-22.1	8.601	-86.8	-3.877	-180.3	0.268	-86.8	
1.573	-19.3	4.405	-83.9	5.203	-177.4	0.137	-83.9	
0.240	-354.9	0.875	-59.5	0.274	-153.0	0.027	-59.5	BA-1
0.139	-242.3	0.469	-307.0	0.160	-40.5	0.013	-307.0	
0.315	-215.8	1.068	-280.4	0.420	-13.9	0.033	-280.4	

1=PHAT-OS/AV
2=PSI-P(STEP)
3=(V/WG)(B*/PH)@1.2TD
4=PSI-B*(STEP)
5=(1/W2)R*HAT-OS/AV
6=PSI-R*(STEP)
7=(DB)TD/2 OR 2/K
8=PSI-B(STEP)
9=PHAT-1/2 OS/PEAK#1
#10=PSI-P(STEP)
#11=(V/G)(B*/PH)@1.2TD
#12=PSI-B*(STEP)
#13=(1/W)R*HAT-OS/AV
#14=PSI-R*(STEP)
#15=(DB*/PH)@TD/4
#16=PSI-B*(STEP)

PR	# 1	# 2	# 3	# 4	# 5	# 6	# 7	# 8
7.0	0.270	-211.6	0.545	-276.2	0.233	-9.7	6.547	-11.3
7.0	-6.848	-22.2	2.190	-88.6	-15.202	-185.0	10.939	-181.9
6.0	0.425	-19.9	0.663	-86.3	0.285	-182.7	1.540	-179.6
4.0	0.178	-206.9	0.328	-273.3	0.134	-9.8	0.921	-6.6
5.5	0.343	-204.6	0.545	-271.0	0.261	-7.4	1.986	-4.3
7.0	0.441	-204.1	0.648	-270.5	0.338	-6.9	2.743	-3.8

# 9	#10	#11	#12	#13	#14	#15	#16	
0.402	-211.6	1.363	-276.2	0.583	-9.7	0.042	-276.2	BA-1
2.199	-22.2	5.672	-88.6	-39.375	-185.0	0.169	-88.6	
0.617	-19.9	1.717	-86.3	0.738	-182.7	0.052	-86.3	
0.295	-208.9	0.850	-273.3	0.348	-9.8	0.025	-273.3	BA-3
0.488	-204.6	1.411	-271.0	0.675	-7.4	0.041	-271.0	
0.580	-204.1	1.678	-270.5	0.875	-6.9	0.049	-270.5	

1=PHAT-OS/AV
2=PSI-P(STEP)
3=(V/WG)(B*/PH)@1.2TD
4=PSI-B*(STEP)
5=(1/W2)R*HAT-OS/AV
6=PSI-R*(STEP)
7=(DB)TD/2 OR 2/K
8=PSI-B(STEP)
9=PHAT-1/2 OS/PEAK#1
#10=PSI-P(STEP)
#11=(V/G)(B*/PH)@1.2TD
#12=PSI-B*(STEP)
#13=(1/W)R*HAT-OS/AV
#14=PSI-R*(STEP)
#15=(DB*/PH)@TD/4
#16=PSI-B*(STEP)

PR	# 1	# 2	# 3	# 4	# 5	# 6	# 7	# 8
6.5	0.003	-49.5	0.838	-96.5	0.181	-175.4	11.706	-201.2
3.5	0.002	-53.7	0.501	-100.8	0.114	-179.7	8.044	-205.4
3.0	0.0	-85.5	0.164	-132.5	0.029	-211.4	4.143	-237.1
2.0	0.0	-85.5	0.164	-132.5	0.029	-211.4	4.143	-237.1
6.0	0.002	-210.4	0.468	-257.4	0.138	-336.3	3.408	-2.0
3.5	0.002	-210.4	0.468	-257.4	0.138	-336.3	3.408	-2.0
7.0	0.004	-214.6	0.686	-261.6	0.211	-340.5	5.923	-6.2
8.5	0.069	-32.6	2.545	-99.4	0.607	-180.3	31.319	-202.7
4.5	0.024	-45.9	1.021	-112.7	0.251	-193.6	16.556	-216.0
4.5	0.009	-114.2	0.483	-181.0	0.074	-261.9	6.017	-284.3
6.0	0.020	-178.7	1.046	-245.4	0.300	-326.3	5.831	-348.7
8.0	0.029	-187.4	1.504	-254.1	0.445	-335.0	11.800	-357.4
6.0	0.009	-20.5	0.390	-65.1	0.106	-142.3	4.876	-170.1
3.0	0.004	-343.8	0.131	-28.4	0.052	-105.6	1.483	-133.5
3.5	0.013	-246.9	0.411	-291.5	0.110	-8.7	4.548	-36.6
6.0	0.029	-235.2	0.775	-279.8	0.247	-357.0	10.073	-24.9
3.0	0.007	-72.6	0.353	-132.0	0.079	-210.2	7.073	-236.4
3.5	0.004	-104.8	0.231	-164.2	0.047	-242.4	5.340	-268.7
3.5	0.004	-104.8	0.231	-164.2	0.047	-242.4	5.340	-268.7
4.0	0.052	-46.3	1.180	-105.8	0.207	-184.0	13.978	-210.2
6.0	0.032	-192.7	0.740	-252.1	0.257	-330.3	6.107	-356.6
6.0	0.012	-226.9	0.277	-94.4	0.070	-175.6	5.920	-199.1
2.0	0.002	-235.7	0.121	-103.1	0.020	-184.4	3.565	-207.8
3.0	0.002	-235.7	0.121	-103.1	0.020	-184.4	3.565	-207.8
3.0	0.010	-40.3	0.404	-267.8	0.122	-349.0	3.394	-12.5
8.0	0.120	-22.7	4.227	-97.4	0.588	-165.9	61.601	-212.3
7.0	0.070	-26.2	2.845	-100.8	0.416	-169.4	47.402	-215.8
5.0	0.029	-36.6	1.654	-111.2	0.213	-179.8	30.964	-226.1
4.5	0.009	-129.5	0.830	-204.1	0.041	-272.7	10.454	-319.0
8.0	0.021	-178.0	1.869	-252.6	0.435	-321.2	14.766	-7.5
4.0	0.009	-38.9	0.378	-89.0	0.095	-167.4	5.765	-192.9
3.0	0.003	-38.5	0.161	-88.6	0.039	-167.0	3.470	-192.5
2.5	0.0	-33.5	0.071	-83.6	0.003	-162.0	2.350	-187.6

# 9	#10	#11	#12	#13	#14	#15	#16	
0.007	-49.5	1.977	-96.5	0.428	-175.4	0.090	-96.5	
0.004	-53.7	1.181	-100.8	0.270	-179.7	0.058	-100.8	
0.001	-85.5	0.387	-132.5	0.069	-211.4	0.020	-132.5	Group 1
0.001	-85.5	0.387	-132.5	0.069	-211.4	0.020	-132.5	
0.005	-213.4	1.104	-257.4	0.325	-336.3	0.033	-257.4	
0.005	-210.4	1.104	-257.4	0.325	-336.3	0.033	-257.4	
0.008	-214.6	1.618	-261.6	0.499	-340.5	0.054	-261.6	
0.129	-32.6	3.050	-99.4	0.727	-180.3	0.137	-99.4	
0.046	-45.9	1.223	-112.7	0.301	-193.6	0.065	-112.7	Group 2
0.018	-119.2	0.578	-181.0	0.088	-261.9	0.019	-181.0	
0.039	-176.7	1.254	-245.4	0.359	-326.3	0.031	-245.4	
0.056	-187.4	1.803	-254.1	0.533	-335.0	0.053	-254.1	
0.017	-20.5	0.974	-65.1	0.265	-142.3	0.044	-65.1	
0.008	-243.8	0.327	-28.4	0.131	-105.6	0.016	-28.4	Group 5A
0.026	-248.9	1.022	-291.5	0.276	-8.7	0.035	-291.5	
0.056	-233.2	1.936	-279.8	0.616	-357.0	0.072	-279.8	
0.014	-72.6	0.888	-132.0	0.198	-210.2	0.045	-132.0	
0.008	-104.8	0.583	-164.2	0.119	-242.4	0.023	-164.2	Group 5B
0.008	-104.8	0.583	-164.2	0.119	-242.4	0.023	-164.2	
0.106	-46.5	2.972	-105.8	0.523	-184.0	0.135	-105.8	
0.062	-192.7	1.865	-252.1	0.646	-330.3	0.060	-252.1	
0.024	-226.9	0.665	-94.4	0.168	-175.6	0.036	-94.4	
0.004	-235.7	0.291	-103.1	0.047	-184.4	0.016	-103.1	Group 5ND
0.004	-235.7	0.291	-103.1	0.047	-184.4	0.016	-103.1	
0.019	-40.3	0.969	-267.8	0.293	-349.0	0.030	-267.8	
0.203	-28.7	4.953	-97.4	0.689	-165.9	0.266	-97.4	
0.127	-26.2	3.334	-100.8	0.487	-169.4	0.192	-100.8	Group 3
0.055	-36.6	1.933	-111.2	0.249	-179.8	0.112	-111.2	
0.017	-129.5	0.972	-204.1	0.048	-272.7	0.030	-204.1	
0.040	-178.0	2.190	-252.6	0.510	-321.2	0.066	-252.6	
0.017	-38.9	0.946	-89.0	0.236	-167.4	0.046	-89.0	
0.007	-38.5	0.402	-88.6	0.097	-167.0	0.023	-88.6	Group 5
0.001	-38.5	0.177	-83.6	0.008	-162.0	0.009	-83.6	

1=PHAT-OS/AV
2=PSI-P(STEP)
3=(V/WG)(B*/PH)@1.2TD
4=PSI-B*(STEP)
5=(1/W2)R*HAT-OS/AV
6=PSI-R*(STEP)
7=(DB)TD/2 OR 2/K
8=PSI-B(STEP)
9=PHAT-1/2 OS/PEAK#1
#10=PSI-P(STEP)
#11=(V/G)(B*/PH)@1.2TD
#12=PSI-B*(STEP)
#13=(1/W)R*HAT-OS/AV
#14=PSI-R*(STEP)
#15=(DB*/PH)@TD/4
#16=PSI-B*(STEP)

PR	# 1	# 2	# 3	# 4	# 5	# 6	# 7	# 8
2.5	0.0	-33.5	0.071	-83.6	0.003	-162.0	2.350	-167.6
3.0	0.013	-219.5	0.366	-269.6	0.105	-348.0	3.026	-13.6
3.0	0.013	-219.5	0.366	-269.6	0.105	-348.0	3.026	-13.6
5.0	0.020	-219.4	0.515	-269.5	0.156	-347.9	4.967	-13.5
7.0	0.098	-61.2	0.995	-89.6	0.152	-169.1	8.789	-192.8
3.0	0.011	-61.0	0.294	-89.4	0.072	-168.8	3.639	-192.6
5.0	0.011	-61.0	0.294	-89.4	0.072	-168.8	3.639	-192.6
1.5	0.0	-259.6	0.022	-288.0	0.001	-7.5	1.110	-31.3
1.5	0.008	-242.0	0.176	-270.4	0.054	-349.9	1.553	-13.6
4.0	0.017	-241.7	0.316	-270.1	0.108	-349.6	3.145	-13.3
8.0	0.161	-17.5	1.654	-86.9	0.382	-161.8	22.673	-191.4
5.0	0.039	-20.4	0.739	-89.8	0.118	-164.8	13.696	-194.3
4.0	0.016	-188.2	0.450	-257.6	0.059	-332.5	5.503	-2.1
4.0	0.016	-188.2	0.450	-257.6	0.059	-332.5	5.503	-2.1
4.0	0.060	-194.2	1.050	-263.6	0.257	-338.5	7.212	-8.1
8.0	0.103	-195.0	1.664	-264.5	0.454	-339.4	22.525	-8.9
6.0	2.530	-13.2	4.265	-80.3	1.188	-135.8	48.933	-198.3
5.0	0.069	-18.0	1.342	-85.1	0.131	-140.5	25.49	-203.1
5.0	0.021	-183.9	0.699	-251.0	0.118	-306.5	11.326	-9.1
4.0	0.038	-188.2	1.053	-255.3	0.204	-310.8	8.453	-13.4
7.5	0.050	-189.4	1.315	-256.5	0.273	-312.0	13.120	-14.5
5.0	0.233	-50.2	0.816	-98.2	0.195	-173.5	9.054	-200.9
4.0	0.071	-61.3	0.358	-109.3	0.081	-184.6	5.508	-212.0
3.5	0.016	-117.0	0.145	-165.1	0.022	-240.4	3.600	-267.8
4.5	0.034	-188.7	0.211	-236.7	0.067	-312.0	2.870	-339.4
7.0	0.070	-206.2	0.372	-254.2	0.121	-329.5	3.394	-356.9
5.5	0.147	-35.9	0.640	-79.0	0.147	-153.3	6.175	-182.3
4.5	0.016	-18.1	0.157	-61.1	0.046	-135.4	2.343	-164.4
2.0	0.016	-18.1	0.157	-61.1	0.046	-135.4	2.343	-164.4
2.5	0.026	-247.5	0.174	-290.5	0.046	-4.8	1.325	-33.8
3.5	0.043	-238.4	0.265	-261.4	0.075	-355.8	2.727	-24.7
5.0	0.251	-59.7	0.742	-109.0	0.176	-183.3	9.405	-212.3
5.0	0.050	-107.8	0.239	-157.1	0.046	-231.5	5.371	-260.4

# 9	#10	#11	#12	#13	#14	#15	#16	
0.001	-33.5	0.177	-83.6	0.008	-162.0	0.009	-83.6	
0.025	-219.5	0.915	-269.6	0.262	-348.0	0.028	-269.6	Group 5
0.025	-219.5	0.915	-269.6	0.262	-348.0	0.028	-269.6	
0.039	-219.4	1.288	-269.5	0.390	-347.9	0.043	-269.5	
0.207	-61.2	4.282	-89.6	0.656	-169.1	0.173	-89.6	
0.021	-61.0	1.265	-89.4	0.309	-168.8	0.054	-89.4	Group 7
0.021	-61.0	1.265	-89.4	0.309	-168.8	0.054	-89.4	
0.0	-259.6	0.093	-288.0	0.002	-7.5	0.002	-288.0	
0.016	-242.0	0.758	-270.4	0.233	-349.9	0.025	-270.4	
0.035	-241.7	1.362	-270.1	0.467	-349.6	0.049	-270.1	
0.270	-17.5	1.721	-86.9	0.398	-161.8	0.088	-86.9	
0.075	-20.4	0.769	-69.8	0.123	-164.8	0.044	-89.8	
0.031	-188.2	0.469	-257.6	0.061	-332.5	0.010	-257.6	Group 8
0.031	-188.2	0.469	-257.6	0.061	-332.5	0.010	-257.6	
0.109	-194.2	1.092	-263.6	0.268	-338.5	0.024	-263.6	
0.174	-195.0	1.732	-264.5	0.473	-339.4	0.051	-264.5	
0.895	-13.2	4.873	-80.3	1.358	-135.8	0.243	-80.3	
0.127	-18.0	1.533	-85.1	0.150	-140.5	0.089	-85.1	
0.039	-183.9	0.799	-251.0	0.135	-306.4	0.016	-251.0	Group 9
0.070	-188.2	1.204	-255.3	0.234	-310.8	0.021	-255.3	
0.090	-189.4	1.503	-256.5	0.312	-312.0	0.036	-256.5	
0.388	-50.2	1.992	-98.2	0.476	-173.5	0.088	-98.2	
0.139	-61.3	0.874	-109.3	0.197	-184.6	0.045	-109.3	Group 11
0.033	-117.0	0.353	-165.1	0.054	-240.4	0.014	-165.1	
0.066	-188.7	0.516	-236.7	0.163	-312.0	0.009	-236.7	
0.126	-208.2	0.908	-254.2	0.295	-329.5	0.025	-254.2	
0.274	-35.9	1.574	-79.0	0.361	-153.3	0.067	-79.0	
0.032	-18.1	0.387	-61.1	0.112	-135.4	0.020	-61.1	Group 11A
0.032	-18.1	0.387	-61.1	0.112	-135.4	0.020	-61.1	
0.050	-247.5	0.428	-290.5	0.114	-4.8	0.011	-290.5	
0.080	-238.4	0.652	-281.4	0.184	-355.8	0.020	-281.4	
0.399	-59.7	1.824	-109.0	0.434	-183.3	0.085	-109.0	Group 11B
0.096	-107.8	0.587	-157.1	0.113	-231.5	0.025	-157.1	

1=PHAT-OS/AV
2=PSI-P(STEP)
3=(V/WG)(B*/PH)@1.2TD
4=PSI-B*(STEP)
5=(1/W2)R*HAT-OS/AV
6=PSI-R*(STEP)
7=(DB)TD/2 OR 2/K
8=PSI-B(STEP)
9=PHAT-1/2 OS/PEAK#1
#10=PSI-P(STEP)
#11=(V/G)(B*/PH)@1.2TD
#12=PSI-B*(STEP)
#13=(1/W)R*HAT-OS/AV
#14=PSI-R*(STEP)
#15=(DB*/PH)@TD/4
#16=PSI-B*(STEP)

PR	# 1	# 2	# 3	# 4	# 5	# 6	# 7	# 8
4.5	0.050	-107.8	0.239	-157.1	0.046	-231.5	5.371	-260.4
7.0	0.075	-189.7	0.356	-239.0	0.120	-313.3	4.281	-342.3
7.0	0.234	-65.9	0.567	-93.0	0.106	-169.4	6.119	-196.8
6.0	0.130	-67.5	0.406	-94.6	0.074	-171.0	4.291	-198.4
4.0	0.012	-75.1	0.120	-102.3	0.029	-178.7	2.635	-206.1
2.0	0.001	-146.9	0.038	-174.0	0.004	-250.4	1.695	-277.8
5.0	0.015	-226.4	0.102	-253.5	0.032	-329.9	1.516	-357.3
8.0	0.033	-233.9	0.176	-261.0	0.058	-337.4	1.739	-4.9

# 9	#10	#11	#12	#13	#14	#15	#16	
0.096	-107.8	0.587	-157.1	0.113	-231.5	0.025	-157.1	Group 11B
0.135	-189.7	0.875	-239.0	0.295	-313.3	0.020	-239.0	
0.415	-65.9	2.462	-93.0	0.459	-169.4	0.104	-93.0	
0.263	-67.5	1.761	-94.6	0.321	-171.0	0.077	-94.6	
0.023	-75.1	0.520	-102.3	0.126	-178.7	0.026	-102.3	Group 13
0.003	-147.9	0.163	-174.0	0.019	-250.4	0.005	-174.0	
0.031	-226.4	0.443	-253.5	0.140	-329.9	0.011	-253.5	
0.065	-233.9	0.764	-261.0	0.252	-337.4	0.024	-261.0	

```
# 1=PHAT-OS/AV
# 2=PSI-P(STEP)
# 3=(V/WG)(B*/PH)@1.2TD
# 4=PSI-B*(STEP)
# 5=(1/W2)R*HAT-OS/AV
# 6=PSI-R*(STEP)
# 7=(DB)TD/2 OR 2/K
# 8=PSI-B(STEP)
# 9=PHAT-1/2 OS/PEAK#1
#10=PSI-P(STEP)
#11=(V/G)(B*/PH)@1.2TD
#12=PSI-B*(STEP)
#13=(1/W)R*HAT-OS/AV
#14=PSI-R*(STEP)
#15=(DB*/PH)@TD/4
#16=PSI-B*(STEP)
```

PR	# 1	# 2	# 3	# 4	# 5	# 6	# 7	# 8
5.0	0.852	-50.4	1.909	-99.2	0.728	-174.4	37.371	-201.5
3.0	0.066	-101.5	0.327	-150.4	0.083	-225.6	11.480	-252.6
6.0	0.089	-195.3	0.615	-244.1	0.213	-319.4	10.047	-346.4
8.0	-2.748	-36.7	5.607	-93.0	-9.535	-176.9	104.550	-188.5
5.0	1.279	-42.1	2.584	-98.4	1.575	-182.3	41.636	-193.9
4.0	0.095	-84.7	0.442	-141.0	0.159	-224.9	10.239	-236.5
6.0	0.157	-193.0	0.727	-249.3	0.319	-333.2	12.491	-344.8
8.0	0.249	-202.8	1.060	-259.1	0.514	-343.1	27.335	-354.7

# 9	#10	#11	#12	#13	#14	#15	#16	Fig. 5 of Ref. 47
0.766	-50.4	3.736	-99.2	1.424	-174.4	0.292	-99.2	
0.122	-101.5	0.639	-150.4	0.163	-225.6	0.054	-150.4	ζ =.22
0.155	-195.3	1.204	-244.1	0.416	-319.4	0.067	-244.1	
2.475	-36.7	11.278	-93.0	-19.179	-176.9	0.724	-93.0	
1.078	-42.1	5.197	-98.4	3.169	-182.3	0.338	-98.4	
0.174	-84.7	0.889	-141.0	0.319	-224.9	0.049	-141.0	ζ =.1
0.261	-193.0	1.463	-249.3	0.641	-333.2	0.081	-249.3	
0.376	-202.8	2.132	-259.1	1.035	-343.1	0.126	-259.1	

1=PHAT-OS/AV
2=PSI-P(STEP)
3=(V/WG)(B*/PH)@1.2TD
4=PSI-B*(STEP)
5=(1/W2)R*HAT-OS/AV
6=PSI-R*(STEP)
7=(DB)TD/2 OR 2/K
8=PSI-B(STEP)
9=PHAT-1/2 OS/PEAK#1
#10=PSI-P(STEP)
#11=(V/G)(B*/PH)@1.2TD
#12=PSI-B*(STEP)
#13=(1/W)R*HAT-OS/AV
#14=PSI-R*(STEP)
#15=(DB*/PH)@TD/4
#16=PSI-B*(STEP)

PR	# 1	# 2	# 3	# 4	# 5	# 6	# 7	# 8
3.2	0.070	-70.1	0.239	-131.0	0.082	-217.3	3.112	-226.8
4.0	0.088	-54.2	0.241	-122.1	0.059	-205.3	2.837	-217.8
3.5	0.016	-89.9	0.083	-142.8	0.028	-229.0	1.261	-238.6
3.8	0.043	-124.5	0.134	-162.3	0.041	-241.6	3.077	-258.9
3.2	0.035	-32.4	0.260	-109.3	0.093	-199.2	2.608	-204.9
3.8	0.097	-123.5	0.189	-174.3	0.039	-220.5	2.924	-269.9
3.3	0.092	-111.8	0.346	-164.3	0.034	-213.4	9.242	-277.7
3.0	0.007	-117.3	0.122	-183.1	0.007	-250.4	.816	-296.7
3.3	0.216	-123.0	0.486	-186.3	0.272	-272.8	6.460	-282.0
3.0	0.340	-42.4	0.923	-104.3	0.369	-190.9	10.985	- 00.0
3.2	0.141	-221.8	0.540	-277.5	0.219	-3.8	5.834	-13.2
4.0	0.277	-104.0	0.402	-153.5	0.099	-198.4	6.870	-249.
4.3	0.432	-54.4	0.558	-105.2	0.174	-151.4	7.185	-200.9
5.0	0.225	-210.5	0.372	-260.5	0.118	-303.6	4.833	-356.1

# 9	#10	#11	#12	#13	#14	#15	#16	Airplane Configuration.
0.132	-70.1	0.550	-131.0	0.188	-217.3	0.055	-131.0	1
0.160	-54.2	0.314	-122.1	0.077	-205.3	0.039	-122.1	2
0.081	-89.9	0.250	-142.8	0.085	-229.0	0.027	-142.8	3
0.085	-124.5	0.308	-162.3	0.093	-241.6	0.031	-162.3	4
0.087	-32.4	0.599	-109.3	0.215	-199.2	0.065	-109.3	5
0.173	-123.5	0.246	-174.3	0.050	-220.5	0.027	-174.3	6
0.154	-111.8	0.450	-164.3	0.044	-213.4	0.072	-164.3	7
0.015	-117.3	0.367	-183.1	0.022	-250.4	0.042	-183.1	8
0.339	-123.0	1.119	-186.3	0.[illegible]6	-272.8	0.058	-186.3	9
0.51[illegible]	-42.4	2.123	-104.3	0.849	-190.9	0.227	-104.3	10
0.238	-221.8	1.241	-277.5	0.504	-[illegible].8	0.127	-277.5	11
0.414	-104.0	0.525	-153.5	0.129	-198.4	0.051	-153.5	12
0.595	-54.4	0.727	-105.2	0.227	-151.4	0.095	-105.2	13
0.348	-210.5	0.485	-260.5	0.153	-303.6	0.042	-260.5	14

1=PHAT-OS/AV
2=PSI-P(STEP)
3=(V/WG)(B*/PH)@1.2TD
4=PSI-B*(STEP)
5=(1/W2)R*HAT-OS/AV
6=PSI-R*(STEP)
7=(DB)TD/2 OR 2/K
8=PSI-B(STEP)
9=PHAT-1/2 OS/PEAK#1
#10=PSI-P(STEP)
#11=(V/G)(B*/PH)@1.2TD
#12=PSI-B*(STEP)
#13=(1/W)R*HAT-OS/AV
#14=PSI-R*(STEP)
#15=(DB*/PH)@TD/4
#16=PSI-B*(STEP)

PR	# 1	# 2	# 3	# 4	# 5	# 6	# 7	# 8
6.0	0.056	-49.7	2.512	-94.1	0.771	-181.8	4.546	-190.0
2.0	0.007	-81.0	0.333	-125.3	0.117	-213.0	0.857	-221.2
5.0	0.040	-216.4	1.371	-260.8	0.576	-348.5	2.338	-356.7
4.5	0.100	-226.5	0.294	-273.3	0.096	-345.2	0.593	-13.0
2.5	0.041	-233.6	0.132	-280.5	0.040	-352.4	0.157	-20.1
2.5	0.089	-225.5	0.266	-272.3	0.086	-344.2	0.510	-12.0
4.0	0.136	-223.1	0.378	-269.9	0.131	-341.8	0.855	-9.5
5.5	0.159	-38.3	0.305	-86.3	0.086	-157.1	0.717	-183.8
3.5	0.002	-50.4	0.040	-98.4	0.001	-169.2	0.238	-195.9
3.5	0.090	-217.6	0.176	-265.6	0.060	-336.4	0.220	-3.1
4.5	0.133	-217.7	0.242	-265.7	0.087	-336.5	0.375	-3.2

Fixed Base Configurations Tables I-1, -2, -3, -4 } Ref. 29

# 9	#10	#11	#12	#13	#14	#15	#16	
0.114	-49.7	5.775	-94.1	1.773	-181.8	0.180	-94.1	A-1
0.014	-81.0	0.766	-125.3	0.269	-213.0	0.023	-125.3	-2
0.076	-218.4	3.152	-260.8	1.325	-348.5	0.091	-260.8	-3
0.174	-220.5	0.618	-273.3	0.203	-345.2	0.017	-273.3	A-4
0.077	-233.6	0.277	-280.5	0.033	-352.4	0.006	-280.5	-5
0.157	-225.5	0.559	-272.3	0.180	-344.2	0.015	-272.3	-6
0.225	-223.1	0.793	-269.9	0.276	-341.8	0.023	-269.9	-6A
0.297	-58.3	0.701	-86.3	0.198	-157.1	0.026	-86.3	A-7
0.004	50.1	0.093	-98.4	0.003	-169.2	0.004	-98.4	-8
0.160	-217.6	0.406	-265.6	0.138	-336.4	0.009	-265.6	-9
0.225	-217.7	0.556	-265.7	0.200	-336.5	0.014	-265.7	-9A

1=PHAT-OS/AV
2=PSI-P(STEP)
3=(V/WG)(B*/PH)@1.2TD
4=PSI-B*(STEP)
5=(1/W2)R*HAT-OS/AV
6=PSI-R*(STEP)
7=(DB)TD/2 OR 2/K
8=PSI-B(STEP)
9=PHAT-1/2 OS/PEAK#1
#10=PSI-P(STEP)
#11=(V/G)(B*/PH)@1.2TD
#12=PSI-B*(STEP)
#13=(1/W)R*HAT-OS/AV
#14=PSI-R*(STEP)
#15=(DB*/PH)@TD/4
#16=PSI-B*(STEP)

PR	# 1	# 2	# 3	# 4	# 5	# 6	# 7	# 8
2.5	0.104	-51.8	1.676	-90.1	0.599	-180.5	3.129	-183.0
2.5	0.104	-51.6	1.672	-90.0	0.598	-180.5	3.141	-183.0
3.0	0.092	-46.6	1.555	-89.2	0.571	-179.9	3.465	-182.3
2.5	0.091	-46.5	1.552	-89.2	0.571	-179.9	3.474	-182.3
4.0	0.033	-75.4	0.600	-89.7	0.262	-178.8	2.067	-182.8
3.0	0.029	-73.1	0.543	-89.3	0.240	-178.5	2.139	-182.4
3.0	0.026	-71.1	0.493	-89.0	0.221	-178.3	2.201	-182.2
3.0	0.026	-71.1	0.493	-89.0	0.221	-178.3	2.201	-182.2
3.0	0.023	-69.3	0.447	-88.7	0.203	-178.0	2.260	-181.9
2.5	0.023	-69.3	0.447	-88.7	0.203	-178.0	2.260	-181.9
3.0	0.358	-47.5	2.202	-90.0	0.903	-180.6	4.508	-182.7
3.0	0.334	-44.4	2.154	-89.6	0.876	-180.4	4.845	-182.4
6.0	0.078	-75.0	0.680	-89.9	0.307	-177.6	2.265	-182.6
6.0	0.078	-74.9	0.677	-89.9	0.306	-177.5	2.269	-182.6
6.0	0.062	-70.8	0.564	-89.3	0.258	-177.1	2.433	-182.1
2.0	0.117	-48.3	1.917	-89.9	0.696	-180.6	3.590	-183.0
1.5	0.114	-47.2	1.895	-89.8	0.691	-180.5	3.668	-182.8
1.5	0.109	-45.0	1.847	-89.4	0.680	-180.2	3.823	-182.5
2.0	0.103	-42.7	1.791	-89.1	0.669	-179.9	3.995	-182.2

# 9	#10	#11	#12	#13	#14	#15	#16		$1/\tau_s$
0.214	-51.8	3.391	-90.1	1.213	-180.5	0.109	-90.1		0
0.214	-51.8	3.384	-90.0	1.211	-180.5	0.109	-90.0		.005
0.192	-46.6	3.147	-89.2	1.156	-179.9	0.101	-89.2	Group	.153
0.191	-46.5	3.141	-89.2	1.155	-179.9	0.100	-89.2	I	.158
0.065	-75.4	1.113	-89.7	0.486	-178.8	0.036	-89.7		0
0.058	-73.1	1.007	-89.3	0.445	-178.5	0.033	-89.3		.062
0.051	-71.1	0.913	-89.0	0.409	-178.3	0.029	-89.0	Group	.116
0.051	-71.1	0.913	-89.0	0.409	-178.3	0.029	-89.0	II	.120
0.046	-69.3	0.828	-88.7	0.376	-178.0	0.027	-88.7		.165
0.046	-69.3	0.828	-88.7	0.376	-178.0	0.027	-88.7		.170
0.596	-47.5	4.287	-90.0	1.758	-180.6	0.137	-90.0	Group	0
0.571	-44.4	4.195	-89.6	1.706	-180.4	0.134	-89.6	III	.092
0.148	-75.0	1.294	-89.9	0.584	-177.6	0.042	-89.9		.003
0.147	-74.9	1.289	-89.9	0.582	-177.5	0.041	-89.9	Group	.005
0.119	-70.8	1.073	-89.3	0.492	-177.1	0.034	-89.3	IV	.122
0.235	-48.3	3.690	-89.9	1.339	-180.6	0.120	-89.9		0
0.230	-47.2	3.647	-89.8	1.329	-180.5	0.118	-89.8	Group	.033
0.221	-45.0	3.554	-89.4	1.308	-180.2	0.114	-89.4	VI	.095
0.210	-42.7	3.446	-89.1	1.287	-179.9	0.111	-89.1		.160

WADD-61-147(HARPER)

1=PHAT-OS/AV
2=PSI-P(STEP)
3=(V/WG)(B*/PH)@1.2TD
4=PSI-B*(STEP)
5=(1/W2)R*HAT-OS/AV
6=PSI-R*(STEP)
7=(DB)TD/2 OR 2/K
8=PSI-B(STEP)
9=PHAT-1/2 OS/PEAK#1
#10=PSI-P(STEP)
#11=(V/G)(B*/PH)@1.2TD
#12=PSI-B*(STEP)
#13=(1/W)R*HAT-OS/AV
#14=PSI-R*(STEP)
#15=(DB*/PH)@TD/4
#16=PSI-B*(STEP)

PR	# 1	# 2	# 3	# 4	# 5	# 6	# 7	# 8
2.0	0.011	-77.9	0.452	-113.6	0.081	-187.9	1.469	-222.5
1.5	0.008	-91.3	0.205	-123.7	0.038	-198.4	0.871	-231.6
3.0	0.009	-86.9	0.193	-123.9	0.035	-197.9	0.809	-232.6
3.0	0.045	-352.9	1.242	-45.6	0.133	-119.9	2.448	-162.2
2.0	0.008	-70.2	0.296	-118.3	0.095	-204.6	1.095	-216.3
2.0	0.0	-141.6	0.126	-155.8	0.013	-228.0	0.798	-266.2
3.0	0.0	-134.5	0.156	-154.8	0.011	-228.4	1.142	-263.6
9.9	0.046	-245.2	29.544	-92.5	3.896	-174.1	166.863	-204.1
9.0	0.070	-60.0	11.409	-261.4	3.604	-339.1	18.736	-17.2
7.0	0.003	-278.2	6.365	-93.9	0.525	-154.1	24.590	-21.3
6.0	0.014	-51.4	2.618	-240.3	0.299	-297.7	3.034	-13.5
8.0	0.030	-93.0	7.203	-266.4	1.953	-328.9	18.097	-31.9
5.0	0.044	-13.5	3.177	-106.5	0.651	-188.2	8.665	-212.3
2.0	0.040	-43.0	1.329	-112.5	0.346	-196.7	3.742	-214.5
2.0	0.024	-84.5	0.939	-158.5	0.174	-240.6	2.353	-263.0
5.0	0.033	-188.1	1.940	-259.3	0.532	-340.8	2.984	-4.2
2.0	0.020	-39.3	1.534	-102.3	0.156	-161.7	5.765	-227.1
2.0	0.011	-46.7	1.032	-109.6	0.093	-169.2	4.141	-234.3
1.0	0.0	-349.0	1.324	-32.3	0.014	-94.6	4.330	-162.8
2.0	0.003	-155.2	0.954	-221.8	0.014	-278.9	1.100	-349.3
3.0	0.090	-34.5	2.457	-110.6	0.575	-192.8	6.714	-214.9
4.0	0.121	-40.1	2.394	-110.6	0.599	-193.2	6.450	-214.0
3.0	0.012	-31.2	0.457	-95.5	0.066	-178.4	1.753	-198.3
4.0	0.021	-162.5	0.790	-233.4	0.202	-314.6	0.767	-338.1
3.0	0.031	-159.8	0.801	-226.9	0.239	-311.6	0.578	-328.1
3.0	0.033	-116.4	0.938	-187.8	0.328	-270.3	1.439	-291.4
1.0	0.006	-167.5	0.543	-217.8	0.013	-277.5	0.975	-339.9
2.0	0.008	-97.0	0.598	-155.5	0.035	-216.2	1.996	-278.5
2.0	0.006	-135.1	0.718	-192.3	0.017	-249.8	1.540	-318.3
2.0	0.006	-128.6	0.683	-183.7	0.020	-241.4	1.702	-309.0
4.5	0.921	-32.5	3.025	-95.4	1.357	-181.6	7.325	-194.6
2.5	0.194	-44.6	1.178	-107.8	0.347	-193.9	2.960	-206.8
3.0	0.087	-76.1	0.906	-148.2	0.241	-231.5	2.522	-249.8

# 9	#10	#11	#12	#13	#14	#15	#16	Config.
0.023	-77.9	0.991	-113.6	0.178	-187.9	0.047	-113.6	2
0.016	-91.3	0.488	-123.7	0.090	-198.4	0.024	-123.7	3
0.019	-86.9	0.481	-123.9	0.086	-197.9	0.024	-123.9	4
0.085	-352.9	3.226	-45.6	0.347	-119.9	0.146	-45.6	7
0.015	-70.2	0.689	-118.3	0.221	-204.6	0.029	-118.3	8
0.001	-141.6	0.344	-155.8	0.036	-228.0	0.016	-155.8	9
0.0	-134.5	0.357	-154.8	0.026	-228.4	0.016	-154.8	10
0.081	-245.2	17.920	-92.5	2.363	-174.1	0.789	-92.5	11
0.121	-60.0	6.698	-261.4	2.116	-339.1	0.221	-261.4	13
0.005	-278.2	5.892	-93.9	0.486	-154.1	0.312	-93.9	15
0.027	-51.4	2.059	-240.3	0.235	-297.7	0.056	-240.3	17
0.016	-93.0	6.298	-266.4	1.708	-328.9	0.272	-266.4	18
0.084	-13.5	3.496	-106.5	0.717	-188.2	0.155	-106.5	19
0.077	-43.0	1.487	-112.5	0.387	-196.7	0.066	-112.5	20
0.046	84.5	1.062	-158.5	0.197	-240.6	0.040	-158.5	21
0.062	-188.1	2.025	-259.3	0.556	-340.8	0.054	-259.3	22
0.038	-39.3	1.664	-102.3	0.169	-161.7	0.088	-102.3	23
0.021	-46.7	1.119	-109.6	0.101	-169.2	0.059	-109.6	24
0.001	-349.0	1.546	-32.3	0.016	-94.6	0.082	-32.3	25
0.006	-155.2	1.053	-221.8	0.015	-278.9	0.029	-221.8	26
0.161	-34.5	2.782	-110.6	0.651	-192.8	0.122	-110.6	27a
0.209	-40.1	2.761	-110.6	0.691	-193.2	0.117	-110.6	27b
0.024	-31.2	0.493	-95.5	0.071	-178.4	0.026	-95.5	28
0.040	-162.5	0.847	-233.4	0.216	-314.6	0.010	-233.4	29
0.059	-159.8	0.916	-226.9	0.273	-311.6	0.016	-226.9	30a
0.063	-116.4	1.087	-187.8	0.380	-270.3	0.026	-187.8	30b
0.012	-167.5	0.609	-217.8	0.014	-277.5	0.017	-217.8	31
0.015	-97.0	0.710	-155.5	0.041	-216.2	0.033	-155.5	32
0.011	-135.1	0.807	-192.3	0.019	-249.8	0.031	-192.3	33
0.013	-128.6	0.765	-183.7	0.023	-241.4	0.031	-183.7	34
0.841	-32.5	3.902	-95.4	1.750	-181.6	0.135	-95.4	35
0.313	-44.6	1.518	-107.8	0.448	-193.9	0.059	-107.8	36
0.155	-76.1	1.105	-148.2	0.295	-231.5	0.045	-148.2	37

WADD-61-147(HARPER)

1=PHAT-OS/AV
2=PSI-P(STEP)
3=(V/WG)(B*/PH)@1.2TD
4=PSI-B*(STEP)
5=(1/W2)R*HAT-OS/AV
6=PSI-R*(STEP)
7=(DB)TD/2 OR 2/K
8=PSI-B(STEP)
9=PHAT-1/2 OS/PEAK#1
#10=PSI-P(STEP)
#11=(V/G)(B*/PH)@1.2TD
#12=PSI-B*(STEP)
#13=(1/W)R*HAT-OS/AV
#14=PSI-R*(STEP)
#15=(DB*/PH)@TD/4
#16=PSI-B*(STEP)

PR	# 1	# 2	# 3	# 4	# 5	# 6	# 7	# 8
3.0	0.065	-92.3	0.803	-163.1	0.177	-246.8	1.956	-264.9
3.0	0.074	-61.1	1.181	-114.2	0.145	-172.3	4.474	-236.8
3.0	0.042	-76.0	0.837	-127.1	0.086	-185.7	3.270	-248.8
2.0	0.027	-89.8	0.652	-142.1	0.051	-200.4	2.430	-264.4
2.0	0.017	-188.2	0.550	-235.3	0.098	-294.4	0.546	-353.5
5.0	0.055	-39.9	2.604	-91.8	0.757	-179.8	4.570	-188.2
2.0	0.007	-81.1	0.355	-125.3	0.124	-213.5	0.906	-221.2
6.0	0.034	-219.7	1.317	-261.6	0.538	-349.8	2.272	-357.4
8.0	0.079	-221.9	2.600	-266.8	1.240	-355.0	4.975	-2.9
2.0	0.005	-29.1	1.398	-94.0	0.186	-166.5	3.908	-205.7
1.0	0.001	-94.4	0.201	-142.1	0.028	-213.9	0.912	-254.1
3.0	0.009	-201.8	0.882	-271.7	0.237	-346.3	1.783	-21.5
8.0	0.026	-198.8	2.031	-270.3	1.100	-344.8	4.662	-20.3
4.0	0.114	-41.6	0.961	-86.7	0.255	-172.6	1.868	-184.0
1.5	0.016	-355.8	0.127	-38.2	0.052	-125.0	0.184	-134.8
1.5	0.027	-258.7	0.196	-301.9	0.063	-28.8	0.366	-38.6
4.0	0.083	-237.4	0.561	-279.1	0.202	-5.9	1.205	-15.8
1.5	0.029	-45.1	0.534	-87.4	0.079	-155.6	1.599	-201.3
1.0	0.001	-357.0	0.089	-40.3	0.011	-112.2	0.483	-151.2
1.0	0.007	-236.2	0.160	-282.8	0.029	-356.4	0.222	-32.4
2.0	0.026	-224.0	0.428	-272.6	0.095	-346.0	0.789	-22.3
4.0	0.153	-30.7	0.587	-76.6	0.165	-162.1	1.091	-174.2
3.0	0.009	-14.0	0.064	-59.4	0.019	-143.0	0.249	-157.7
3.0	0.020	-285.1	0.096	-329.1	0.024	-50.6	0.113	-68.9
5.0	0.060	-248.4	0.263	-20.1	0.081	-15.3	0.566	-27.6
2.0	0.045	-36.6	0.354	-79.4	0.056	-148.6	1.142	-191.5
2.0	0.001	-354.6	0.115	-33.1	0.004	-55.4	0.651	-149.0
1.5	0.004	-245.4	0.104	-285.8	0.013	-351.1	0.372	-41.1
2.0	0.017	-234.8	0.226	-276.4	0.040	-345.7	0.303	-28.4
2.5	0.045	-47.4	0.236	-87.8	0.034	-151.0	0.886	-201.3
1.5	0.001	-329.0	0.068	-7.5	0.001	-71.0	0.407	-121.3
3.0	0.004	-285.6	0.083	-326.7	0.008	-32.5	0.378	-80.3
2.0	0.023	-222.0	0.200	-263.9	0.038	-327.2	0.258	-17.1

# 9	#10	#11	#12	#13	#14	#15	#16	Config.
0.119	-92.3	0.975	-163.1	0.215	-246.8	0.034	-163.1	38
0.126	-61.1	1.396	-114.2	0.172	-172.3	0.074	-114.2	39
0.076	-76.0	0.976	-127.1	0.100	-185.7	0.051	-127.1	40
0.050	-89.8	0.771	-142.1	0.060	-200.4	0.039	-142.1	41
0.033	-188.2	0.675	-235.3	0.121	-294.4	0.015	-235.3	42
0.111	-39.9	6.016	-91.8	1.750	-179.8	0.189	-91.8	43
0.014	-81.1	0.816	-125.3	0.284	-213.5	0.025	-125.3	44
0.066	-219.7	2.969	-261.6	1.213	-349.8	0.086	-261.6	45
0.144	-221.9	6.008	-266.8	2.865	-355.0	0.181	-266.8	46
0.011	-29.1	3.264	-94.0	0.435	-166.5	0.145	-94.0	47
0.001	-94.4	0.467	-142.1	0.066	-213.9	0.023	-142.1	48
0.018	-201.8	1.988	-271.7	0.535	-346.3	0.070	-271.7	49
0.050	-198.8	4.632	-270.3	2.509	-344.8	0.177	-270.3	40
0.217	-41.6	2.197	-86.7	0.651	-172.6	0.073	-86.7	51
0.032	-355.8	0.289	-38.2	0.118	-125.0	0.009	-38.2	52
0.052	-258.7	0.450	-301.9	0.145	-28.8	0.011	-301.9	53
0.149	-237.4	1.270	-279.1	0.458	-5.9	0.038	-279.1	54
0.059	-45.1	1.212	-87.4	0.179	-155.6	0.060	-87.4	55
0.002	-357.0	0.200	-40.3	0.024	-112.2	0.011	-40.3	56
0.014	-236.2	0.365	-282.8	0.066	-356.4	0.006	-282.8	57
0.049	-224.0	0.986	-272.6	0.219	-346.0	0.031	-272.6	58
0.285	-30.7	1.399	-76.6	0.393	-162.1	0.046	-76.6	59
0.017	-14.0	0.140	-59.4	0.041	-143.0	0.007	-59.4	60
0.039	-285.1	0.197	-329.1	0.050	-50.6	0.004	-329.1	61
0.111	-248.4	0.611	-290.1	0.188	-15.3	0.017	-290.1	62
0.089	-36.6	0.807	-79.4	0.128	-148.6	0.042	-79.4	63
0.001	-354.6	0.228	-33.1	0.008	-95.4	0.012	-33.1	64
0.008	-245.4	0.238	-285.8	0.029	-351.1	0.003	-285.8	65
0.033	-234.8	0.513	-276.4	0.090	-345.7	0.013	-276.4	66
0.087	-47.4	0.539	-87.8	0.079	-151.0	0.029	-87.8	71
0.001	-329.0	0.156	-7.5	0.003	-71.0	0.007	-7.5	72
0.007	-285.6	0.192	-326.7	0.018	-32.5	0.005	-326.7	73
0.044	-222.0	0.455	-263.9	0.087	-327.2	0.011	-263.9	74

WADD-61-147(HARPER)

1=PHAT-OS/AV
2=PSI-P(STEP)
3=(V/WG)(B*/PH)@1.2TD
4=PSI-B*(STEP)
5=(1/W2)R*HAT-OS/AV
6=PSI-R*(STEP)
7=(DB)TD/2 OR 2/K
8=PSI-B(STEP)
9=PHAT-1/2 OS/PEAK#1
#10=PSI-P(STEP)
#11=(V/G)(B*/PH)@1.2TD
#12=PSI-B*(STEP)
#13=(1/W)R*HAT-OS/AV
#14=PSI-R*(STEP)
#15=(DB*/PH)@TD/4
#16=PSI-B*(STEP)

PR	# 1	# 2	# 3	# 4	# 5	# 6	# 7	# 8
5.0	0.018	-43.0	0.911	-87.3	0.131	-165.0	2.099	-193.6
1.5	0.0	-294.5	0.040	-337.6	0.005	-49.3	0.328	-89.5
4.0	0.014	-228.3	0.425	-273.9	0.145	-352.9	0.832	-19.0
5.0	0.030	-229.1	0.802	-271.7	0.497	-349.5	1.723	-17.7
3.0	0.011	-333.7	0.064	-0.3	0.027	-87.5	0.119	-96.2
3.0	0.043	-257.8	0.222	-285.0	0.079	-11.6	0.459	-21.5
3.0	0.012	-54.9	0.352	-84.2	0.069	-161.0	0.897	-190.8
1.5	0.0	-357.5	0.043	-16.9	0.004	-86.0	0.402	-130.2
2.0	0.003	-251.3	0.147	-279.0	0.028	-346.9	0.387	-33.7
4.0	0.023	-240.6	0.301	-275.1	0.087	-352.1	0.622	-21.6
3.0	0.012	-44.4	0.204	-79.4	0.042	-154.9	0.600	-187.1
1.5	0.0	-302.3	0.041	-328.6	0.004	-36.0	0.367	-83.3
5.0	0.006	-257.2	0.112	-286.4	0.023	-0.8	0.289	-34.7
6.0	0.035	-236.3	0.224	-277.0	0.067	-356.7	0.435	-21.0
5.0	0.003	-44.2	0.092	-70.8	0.014	-134.8	0.619	-186.8
3.0	0.0	-346.2	0.036	-4.3	0.004	-69.6	0.402	-119.4
3.0	0.019	-248.4	0.189	-273.8	0.041	-338.1	0.460	-29.8
6.0	0.022	-208.0	1.591	-270.5	0.638	-344.7	3.622	-20.6
3.0	0.012	-216.8	0.586	-269.6	0.130	-338.9	1.201	-23.7

# 9	#10	#11	#12	#13	#14	#15	#16	Config.
0.035	-43.0	3.933	-87.3	0.565	-165.0	0.153	-87.3	79
0.0	-294.5	0.172	-337.6	0.020	-49.3	0.002	-337.6	80
0.026	-228.3	1.830	-273.9	0.625	-352.9	0.063	-273.9	81
0.058	-229.1	3.418	-271.7	2.117	-349.5	0.124	-271.7	82
0.021	-333.7	0.259	-0.3	0.109	-87.5	0.002	-0.3	84
0.082	-257.8	0.907	-285.0	0.323	-11.6	0.026	-285.0	85
0.024	-54.9	1.430	-84.2	0.282	-161.0	0.058	-84.2	87
0.0	-357.5	0.166	-16.9	0.015	-86.0	0.004	-16.9	88
0.007	-251.3	0.604	-279.0	0.116	-346.9	0.018	-279.0	89
0.045	-240.6	1.284	-275.1	0.372	-352.1	0.044	-275.1	90
0.024	-44.4	0.860	-79.4	0.179	-154.9	0.037	-79.4	95
0.0	-302.3	0.167	-328.6	0.018	-36.0	0.002	-328.6	96
0.012	-257.2	0.449	-286.4	0.091	-0.8	0.013	-286.4	97
0.068	-236.3	1.008	-277.0	0.301	-356.7	0.033	-277.0	98
0.005	-44.2	0.367	-70.8	0.054	-134.8	0.019	-70.8	103
0.0	-346.2	0.143	-4.3	0.015	-69.6	0.004	-4.3	104
0.036	-248.4	0.755	-273.8	0.163	-338.1	0.026	-273.8	105
0.043	-208.0	3.642	-270.5	1.461	-344.7	0.137	-270.5	110
0.024	-216.8	1.337	-269.6	0.296	-338.9	0.048	-269.6	111

1=PHAT-OS/AV
2=PSI-P(STEP)
3=(V/WG)(B*/PH)@1.2TD
4=PSI-B*(STEP)
5=(1/W2)R*HAT-OS/AV
6=PSI-R*(STEP)
7=(DB)TD/2 OR 2/K
8=PSI-B(STEP)
9=PHAT-1/2 OS/PEAK#1
#10=PSI-P(STEP)
#11=(V/G)(B*/PH)@1.2TD
#12=PSI-B*(STEP)
#13=(1/W)R*HAT-OS/AV
#14=PSI-R*(STEP)
#15=(DB*/PH)@TD/4
#16=PSI-B*(STEP)

PK	# 1	# 2	# 3	# 4	# 5	# 6	# 7	# 8
6.5	0.322	-2.0	7.687	-98.3	2.665	-188.6	31.795	-197.4
7.5	0.263	-3.5	6.597	-99.8	2.209	-190.2	26.071	-199.0
6.5	0.191	-6.6	5.115	-102.9	1.640	-193.2	23.009	-202.0
6.5	0.243	-1.5	6.300	-97.1	2.085	-188.3	26.865	-195.8
7.0	0.342	-356.0	8.311	-90.5	2.775	-183.2	32.618	-188.7
5.5	0.126	-358.8	3.767	-93.3	0.811	-186.0	17.909	-191.4
2.7	0.024	-16.9	1.139	-111.4	0.140	-204.1	7.986	-209.6
4.5	0.028	-183.0	2.120	-276.4	0.493	-10.5	3.343	-14.1
4.5	0.088	-332.2	3.269	-64.1	0.566	-159.8	12.486	-161.5
3.6	0.024	-281.8	1.391	-13.7	0.234	-109.4	4.586	-111.1
5.0	0.033	-201.2	2.460	-293.1	0.429	-28.8	6.078	-30.5
6.0	0.069	-187.2	4.562	-279.1	0.915	-14.8	17.766	-16.5
5.7	0.116	-358.2	3.653	-101.7	1.069	-188.9	15.650	-201.4
5.0	0.076	-3.6	2.445	-107.1	0.717	-194.4	11.548	-206.8
5.0	0.048	-3.9	1.632	-107.2	0.486	-194.9	8.650	-206.5
5.0	0.103	-348.6	3.525	-91.4	1.050	-180.1	14.737	-190.2
3.5	0.043	-351.3	1.621	-94.1	0.484	-182.8	8.368	-192.9
3.5	0.028	-353.7	1.071	-96.6	0.325	-185.2	6.532	-195.4
3.0	0.009	-7.6	0.585	-110.4	0.112	-199.0	4.023	-209.2
3.7	0.037	-337.9	1.554	-80.4	0.465	-169.8	7.699	-178.7
3.0	0.009	-321.3	0.644	-63.8	0.161	-153.2	4.153	-162.1
2.5	0.004	-234.9	0.453	-337.4	0.057	-66.8	2.299	-75.7
3.0	0.019	-180.4	0.837	-282.9	0.242	-12.3	0.617	-21.2
3.5	0.026	-316.0	1.337	-58.1	0.403	-146.3	5.893	-156.0
3.0	0.012	-275.4	0.636	-17.5	0.231	-107.7	2.976	-115.4
3.0	0.022	-202.2	0.955	-304.3	0.283	-34.5	1.145	-42.1
4.5	0.049	-181.9	1.968	-284.0	0.628	-14.2	5.110	-21.8
5.0	0.051	-353.8	1.941	-103.8	0.560	-190.3	8.063	-202.6
4.7	0.034	-359.8	1.308	-109.8	0.386	-196.3	5.852	-208.7
4.5	0.037	-350.7	1.511	-100.7	0.446	-187.6	6.581	-199.3
5.0	0.042	-340.2	1.819	-90.1	0.537	-177.5	7.288	-188.2
4.0	0.018	-340.9	0.868	-90.9	0.267	-178.3	4.176	-189.0
3.0	0.004	-344.8	0.303	-94.7	0.073	-182.1	2.023	-192.8

# 9	#10	#11	#12	#13	#14	#15	#16		
0.459	-2.0	4.921	-98.3	1.706	-188.6	0.503	-98.3	1	
0.395	-3.5	4.223	-99.8	1.414	-190.2	0.441	-99.8	2	
0.308	-6.6	3.274	-102.9	1.050	-193.2	0.357	-102.9	3	
0.373	-1.5	3.846	-97.1	1.273	-188.3	0.402	-97.1	4	
0.484	-356.0	4.705	-90.5	1.571	-183.2	0.464	-90.5	5	
0.219	-358.8	2.132	-93.3	0.459	-186.0	0.243	-93.3	6	Nominal
0.047	-16.9	0.645	-111.4	0.079	-204.1	0.092	-111.4	7	Period
0.051	-183.0	1.115	-276.4	0.259	-10.5	0.067	-276.4	8	10 sec
0.164	-332.2	1.580	-64.1	0.273	-159.8	0.166	-64.1	9	
0.049	-281.8	0.673	-13.7	0.113	-109.4	0.084	-13.7	10	
0.060	-201.2	1.189	-293.1	0.207	-28.8	0.101	-293.1	11	
0.115	-187.2	2.205	-279.1	0.442	-14.8	0.173	-279.1	12	
0.209	-358.2	3.344	-101.7	0.979	-188.9	0.360	-101.7	13	
0.141	-3.6	2.239	-107.1	0.657	-194.4	0.257	-107.1	14	
0.092	-3.9	1.459	-107.2	0.434	-194.9	0.181	-107.2	15	
0.190	-348.6	3.037	-91.4	0.904	-180.1	0.320	-91.4	16	
0.084	-351.3	1.397	-94.1	0.417	-182.8	0.173	-94.1	17	
0.055	-353.7	0.923	-96.6	0.280	-185.2	0.130	-96.6	18	Nominal
0.019	-7.6	0.504	-110.4	0.097	-199.0	0.072	-110.4	19	Period
0.073	-337.9	1.296	-80.4	0.388	-169.8	0.157	-80.4	20	7 sec
0.019	-321.3	0.537	-63.8	0.134	-153.2	0.079	-63.8	21	
0.009	-234.9	0.378	-337.4	0.047	-66.8	0.042	-337.4	22	
0.037	-180.4	0.698	-282.9	0.202	-12.3	0.037	-282.9	23	
0.052	-316.0	1.077	-58.1	0.324	-148.3	0.130	-58.1	24	
0.024	-275.4	0.512	-17.5	0.186	-107.7	0.074	-17.5	25	
0.043	-202.2	0.769	-304.3	0.228	-34.5	0.058	-304.3	26	
0.091	-181.9	1.585	-284.0	0.506	-14.2	0.113	-284.0	27	
0.100	-353.8	2.483	-103.8	0.716	-190.3	0.260	-103.8	28	
0.067	-359.8	1.672	-109.8	0.494	-196.3	0.184	-109.8	29	
0.073	-350.7	1.906	-100.7	0.562	-187.6	0.205	-100.7	30	Nominal
0.084	-340.2	2.250	-90.1	0.664	-177.5	0.232	-90.1	31	Period
0.036	-340.9	1.073	-90.9	0.330	-178.3	0.127	-90.9	32	5 sec
0.008	-344.8	0.375	-94.7	0.090	-182.1	0.055	-94.7	33	

1=PHAT-OS/AV
2=PSI-P(STEP)
3=(V/WG)(B*/PH)@1.2TD
4=PSI-B*(STEP)
5=(1/W2)R*HAT-OS/AV
6=PSI-R*(STEP)
7=(DB)TD/2 OR 2/K
8=PSI-B(STEP)
9=PHAT-1/2 OS/PLAK#1
#10=PSI-P(STEP)
#11=(V/G)(B*/PH)@1.2TD
#12=PSI-B*(STEP)
#13=(1/W)R*HAT-OS/AV
#14=PSI-R*(STEP)
#15=(DB*/PH)@TD/4
#16=PSI-B*(STEP)

PR	# 1	# 2	# 3	# 4	# 5	# 6	# 7	# 8
4.0	0.010	-192.0	0.370	-301.8	0.115	-29.7	0.210	-39.5
3.5	0.016	-301.6	0.766	-51.6	0.267	-140.0	3.024	-149.0
3.5	0.011	-274.0	0.478	-23.8	0.188	-112.2	1.718	-121.1
4.0	0.013	-217.1	0.476	-326.9	0.153	-55.3	0.517	-64.2
4.2	0.027	-185.2	0.931	-295.0	0.314	-23.4	2.178	-32.3
6.0	0.322	-2.0	7.687	-98.3	2.665	-188.6	31.795	-197.4
6.0	0.206	-13.3	5.319	-103.5	1.299	-183.5	31.112	-210.1
5.5	0.138	-24.4	4.485	-108.4	0.695	-177.9	31.856	-223.1
2.8	0.024	-16.9	1.139	-111.4	0.140	-204.1	7.986	-209.6
3.0	0.027	-71.8	1.928	-160.8	0.118	-243.5	13.000	-265.9
3.5	0.025	-96.9	2.453	-179.9	0.097	-252.3	17.801	-292.1
5.0	0.046	-3.9	1.632	-107.2	0.486	-194.9	8.650	-206.5

# 9	#10	#11	#12	#13	#14	#15	#16	case	
0.020	-192.0	0.450	-301.8	0.140	-29.7	0.025	-301.8	34	
0.031	-301.8	0.917	-51.6	0.319	-140.0	0.101	-51.6	35	Nominal
0.022	-274.0	0.571	-23.8	0.224	-112.2	0.067	-23.8	36	Period
0.026	-217.1	0.569	-326.9	0.183	-55.3	0.040	-326.9	37	5 sec
0.052	-185.2	1.112	-295.0	0.374	-23.4	0.077	-295.0	38	
0.459	-2.0	4.921	-98.3	1.706	-188.6	0.503	-98.3	39	
0.307	-13.3	3.443	-103.5	0.841	-183.5	0.458	-103.5	40	10 sec
0.215	-24.4	2.903	-108.4	0.450	-177.9	0.424	-108.4	41	
0.047	-16.9	0.645	-111.4	0.079	-204.1	0.092	-111.4	42	
0.051	-71.8	1.105	-160.8	0.068	-243.5	0.134	-160.8	43	10 sec
0.048	-96.9	1.405	-179.9	0.055	-252.3	0.165	-179.9	44	
0.092	-3.9	1.459	-107.2	0.434	-194.9	0.181	-107.2	45	7 sec

1=PHAT-OS/AV
2=PSI-P(STEP)
3=(V/WG)(B*/PH)@1.2TD
4=PSI-B*(STEP)
5=(1/W2)R*HAT-OS/AV
6=PSI-R*(STEP)
7=(DB)TD/2 OR 2/K
8=PSI-B(STEP)
9=PHAT-1/2 OS/PEAK#1
#10=PSI-P(STEP)
#11=(V/G)(B*/PH)@1.2TD
#12=PSI-B*(STEP)
#13=(1/W)R*HAT-OS/AV
#14=PSI-R*(STEP)
#15=(DB*/PH)@TD/4
#16=PSI-B*(STEP)

PR	# 1	# 2	# 3	# 4	# 5	# 6	# 7	# 8
5.5	0.068	-357.9	5.054	-47.7	1.226	-135.2	10.657	-149.3
4.5	0.050	-256.4	3.259	-306.2	0.996	-33.7	15.657	-47.8
5.8	0.188	-37.5	7.602	-89.3	1.866	-176.7	23.575	-191.0
1.8	0.0	-224.5	0.214	-276.3	0.004	-3.6	1.283	-17.9
5.5	0.072	-217.6	4.153	-269.4	1.431	-356.8	18.666	-11.1
3.3	0.098	-74.6	3.023	-145.4	0.836	-234.0	10.957	-246.9
4.6	0.085	-159.6	3.450	-230.5	1.352	-319.0	7 475	-331.9
1.9	0.076	-1.6	0.908	-48.3	0.196	-119.0	2.121	-150.1
2.3	0.051	-257.5	0.568	-304.4	0.161	-15.4	2.376	-45.9
2.4	0.203	-42.2	1.332	-87.7	0.322	-164.3	4.360	-189.2
1.5	0.002	-260.9	0.101	-306.5	0.002	-22.8	0.572	-48.0
2.8	0.074	-222.1	0.747	-267.6	0.188	-343.7	2.818	-9.3
2.7	0.106	-88.2	0.640	-139.3	0.143	-216.5	3.378	-239.9
3.3	0.089	-161.6	0.700	-213.2	0.213	-289.5	1.769	-314.4
3.0	0.032	-303.9	2.208	-348.0	1.046	-75.4	6.441	89.5
1.5	0.035	-304.4	0.785	-350.2	0.322	-72.0	2.189	-91.7
1.0	0.034	-301.8	0.384	-347.6	0.123	-58.8	1.052	-88.9
2.1	0.035	-302.4	0.235	-348.1	0.056	-41.1	0.629	-89.4
5.5	0.188	-32.0	8.027	-83.9	1.934	-171.3	23.611	-185.4
4.0	0.198	-35.7	2.748	-84.0	0.724	-165.5	8.729	-185.4
1.9	0.197	-33.1	1.408	-81.4	0.345	-151.9	4.797	-183.0
2.3	0.198	-33.1	0.865	-79.9	0.204	-132.1	3.258	-181.4
5.8	0.075	-212.4	4.150	-265.9	1.453	-353.5	17.759	-7.4
3.5	0.077	-214.8	1.470	-268.7	0.425	-350.8	5.369	-10.2
1.8	0.074	-217.9	0.766	-267.6	0.199	-357.8	2.121	-9.3
2.3	0.079	-214.5	0.504	-262.3	0.064	-314.3	0.813	-3.6
6.8	0.055	-120.2	3.851	-165.7	2.064	-254.0	11.919	-267.5
3.8	0.058	-123.1	2.140	-182.0	1.027	-269.4	5.431	-283.9
2.3	0.055	-128.0	0.839	-185.8	0.151	-267.3	2.984	-287.8
2.0	0.055	-124.3	0.577	-178.3	0.073	-247.6	2.886	-280.3
4.5	0.094	-33.0	5.235	-78.9	0.741	-158.8	20.685	-192.6
3.8	0.097	-33.9	1.818	-74.6	0.290	-152.8	7.986	-188.3
2.8	0.101	-29.4	0.717	-66.6	0.109	-112.9	3.544	-180.0

# 9	#10	#11	#12	#13	#14	#15	#16	CASE	
0.142	-357.9	5.056	-47.7	1.227	-135.2	0.322	-47.7	1	First Experiment
0.092	-256.4	3.260	-306.2	0.996	-33.7	0.212	-306.2	2	
0.318	-37.5	7.604	-89.3	1.867	-176.7	0.546	-89.3	3	
0.0	-224.5	0.214	-276.3	0.004	-3.6	0.017	-276.3	4	
0.129	-217.6	4.154	-269.4	1.431	-356.8	0.270	-269.4	5	
0.175	-74.6	3.022	-145.4	0.836	-234.0	0.210	-145.4	6	
0.150	-159.6	3.450	-230.5	1.352	-319.0	0.182	-230.5	7	
0.156	-1.6	0.909	-48.3	0.196	-119.0	0.063	-48.3	8	
0.094	-257.5	0.567	-304.4	0.161	-15.4	0.033	-304.4	9	
0.335	-42.2	1.336	-87.7	0.323	-164.3	0.101	-87.7	10	
0.003	-260.9	0.101	-306.5	0.002	-22.8	0.008	-306.5	11	
0.132	-222.1	0.746	-267.6	0.188	-343.7	0.042	-267.6	12	
0.167	-88.2	0.635	-139.3	0.142	-216.5	0.058	-139.3	13	
0.156	-161.6	0.699	-213.2	0.213	-289.5	0.023	-213.2	14	
0.061	-303.9	2.212	-348.0	1.048	-75.4	0.124	-348.0	1A	Second Experiment
0.065	-304.4	0.784	-350.2	0.321	-72.0	0.043	-350.2	1B	
0.065	-301.8	0.383	-347.6	0.122	-58.8	0.021	-347.6	1C	
0.066	-302.4	0.234	-348.1	0.055	-41.1	0.013	-348.1	1D	
0.322	-32.0	8.037	-83.9	1.936	-171.3	0.569	-83.9	2A	
0.332	-35.7	2.751	-84.0	0.725	-165.5	0.203	-84.0	2B	
0.333	-33.1	1.406	-81.4	0.345	-151.9	0.111	-81.4	2C	
0.334	-33.1	0.865	-79.9	0.204	-132.1	0.074	-79.9	2D	
0.133	-212.4	4.152	-265.9	1.454	-353.5	0.266	-265.9	3A	
0.138	-214.8	1.469	-268.7	0.425	-350.8	0.083	-268.7	3B	
0.133	-217.9	0.767	-267.6	0.200	-337.8	0.035	-267.6	3C	
0.141	-214.5	0.503	-262.3	0.064	-314.3	0.016	-262.3	3D	
0.102	-120.2	3.857	-165.7	2.068	-254.0	0.238	-165.7	4A	
0.107	-123.1	2.138	-182.0	1.026	-269.4	0.110	-182.0	4B	
0.102	-128.0	0.837	-185.8	0.151	-267.3	0.045	-185.8	4C	
0.102	-124.3	0.577	-178.3	0.073	-247.6	0.040	-178.3	4D	
0.169	-33.3	5.243	-78.9	0.742	-158.8	0.478	-78.9	5A	
0.174	-33.9	1.820	-74.6	0.290	-152.8	0.180	-74.6	5B	
0.181	-29.4	0.716	-66.6	0.109	-112.9	0.076	-66.6	5D	

1=PHAT-OS/AV
2=PSI-P(STEP)
3=(V/WG)(B*/PH)@1.2TD
4=PSI-B*(STEP)
5=(1/W2)R*HAT-OS/AV
6=PSI-R*(STEP)
7=(DB)TD/2 OR 2/K
8=PSI-B(STEP)
9=PHAT-1/2 OS/PEAK#1
#10=PSI-P(STEP)
#11=(V/G)(B*/PH)@1.2TD
#12=PSI-B*(STEP)
#13=(1/W)R*HAT-OS/AV
#14=PSI-R*(STEP)
#15=(DB*/PH)@TD/4
#16=PSI-B*(STEP)

PR	# 1	# 2	# 3	# 4	# 5	# 6	# 7	# 8
5.0	0.025	-216.6	2.797	-271.9	0.641	-346.1	11.172	-25.5
3.8	0.024	-220.9	1.024	-275.9	0.188	-342.1	1.598	-29.5
7.0	0.253	-22.3	13.815	-82.6	3.708	-181.9	40.164	-183.7
5.0	0.266	-24.1	7.193	-82.2	1.430	-177.2	19.858	-183.0
3.8	0.247	-25.0	2.218	-84.3	0.198	-129.4	5.203	-185.3
3.3	0.254	-23.2	1.111	-84.3	0.206	-44.2	2.278	-186.0
6.9	0.057	-198.1	7.972	-264.1	1.852	2.8	40.108	-6.1
6.0	0.056	-203.6	4.109	-265.8	0.808	-359.7	20.349	-8.1
3.5	0.059	-197.1	1.457	-256.8	0.188	-302.9	4.613	-358.5
3.5	0.066	-192.7	0.827	-248.9	0.123	-219.4	1.222	-350.2
3.3	0.019	-56.8	1.132	-87.7	0.305	-169.8	4.435	-189.4
1.5	0.019	-58.3	0.336	-90.1	0.095	-167.9	1.727	-191.7
2.9	0.022	-235.9	1.659	-271.2	0.301	-353.6	22.884	-12.7
1.5	0.023	-237.6	0.481	-274.0	0.150	-354.6	1.364	-15.4
1.8	0.023	-238.1	0.304	-273.3	0.093	-351.3	0.695	-14.8
3.3	0.026	-220.2	0.566	-263.0	0.022	-301.3	2.780	-16.3

Second Experiment

# 9	#10	#11	#12	#13	#14	#15	#16	
0.047	-216.6	2.791	-271.9	0.640	-346.1	0.182	-271.9	6A
0.046	-220.9	1.026	-275.9	0.188	-342.1	0.034	-275.9	6B
0.381	-22.3	6.893	-82.6	1.850	-181.9	0.461	-82.6	7A
0.395	-24.1	3.594	-82.2	0.715	-177.2	0.231	-82.2	7B
0.373	-25.0	1.101	-84.3	0.098	-129.4	0.063	-84.3	7C
0.378	-23.2	0.557	-84.3	0.103	-44.2	0.029	-84.3	7D
0.098	-198.1	4.011	-264.1	0.932	-2.8	0.269	-264.1	8A
0.095	-203.6	2.056	-265.8	0.405	-359.7	0.134	-265.8	8B
0.101	-197.1	0.733	-256.8	0.095	-302.9	0.036	-256.8	8C
0.110	-192.7	0.412	-248.9	0.061	-219.4	0.012	-248.9	8D
0.036	-56.8	2.268	-87.7	0.611	-169.8	0.169	-87.7	9A
0.037	-58.3	0.671	-90.1	0.191	-167.9	0.060	-90.1	9C
0.043	-235.9	3.313	-271.2	0.602	-354.6	0.113	-271.2	10A
0.044	-237.6	0.961	-274.0	0.299	-354.6	0.054	-274.0	10B
0.044	-238.1	0.608	-273.3	0.186	-351.3	0.029	-273.3	10C
0.049	-220.2	0.565	-263.0	0.022	-301.3	0.022	-263.0	6D

1 USAF PHASE 1 WASSERMAN


```
# 1=PHAT-OS/AV
# 2=PSI-P(STEP)
# 3=(V/WG)(B*/PH)@1.2TD
# 4=PSI-B*(STEP)
# 5=(1/W2)R*HAT-OS/AV
# 6=PSI-R*(STEP)
# 7=(DB)TD/2 OR 2/K
# 8=PSI-B(STEP)
# 9=PHAT-1/2 OS/PEAK#1
#10=PSI-P(STEP)
#11=(V/G)(B*/PH)@1.2TD
#12=PSI-B*(STEP)
#13=(1/W)R*HAT-OS/AV
#14=PSI-R*(STEP)
#15=(DB*/PH)@TD/4
#16=PSI-B*(STEP)
```

PR	# 1	# 2	# 3	# 4	# 5	# 6	# 7	# 8
4.0	0.029	-6.1	2.274	-134.1	0.617	-220.4	12.124	-235.4
4.0	0.027	-89.6	2.551	-217.5	0.780	-303.8	3.449	-318.9
9.0	0.111	-334.2	9.167	-102.1	2.290	-188.4	39.071	-203.4
6.0	0.065	-125.9	5.792	-253.8	1.946	-340.1	17.583	-355.2
4.0	0.081	-45.5	2.205	-133.5	0.700	-219.4	10.486	-232.2
3.2	0.162	-55.1	2.180	-133.4	0.784	-219.0	9.000	-229.5
7.8	0.063	-352.5	4.736	-120.6	1.156	-204.3	23.536	-224.1
7.3	0.066	-146.2	5.305	-274.0	1.983	-5.8	17.938	-10.9
6.0	0.104	-32.2	4.617	-120.7	1.535	-205.7	18.997	-219.8
6.5	0.116	-186.0	4.438	-272.4	1.475	-359.9	19.317	-10.4
3.7	0.054	-128.5	2.169	-216.5	0.727	-302.3	3.218	-315.2
7.0	0.114	-164.3	4.345	-252.3	1.570	-338.2	15.122	-351.0
4.2	0.080	-2.4	2.484	-144.2	0.374	-230.3	11.893	-250.2
5.3	0.055	-0.2	2.359	-139.9	0.462	-225.9	12.076	-243.9
3.0	0.052	-77.6	2.633	-217.3	0.717	-303.3	4.193	-321.3
7.0	0.115	-113.4	5.033	-253.1	1.636	-339.1	13.594	-357.1
4.0	0.066	-109.3	2.234	-215.7	0.673	-301.2	3.502	-316.8

# 9	#10	#11	#12	#13	#14	#15	#16	
0.057	-6.1	1.693	-134.1	0.459	-220.4	0.210	-134.1	P-1
0.051	-89.6	1.899	-217.5	0.581	-303.8	0.107	-217.5	P-2
0.208	-334.2	6.824	-102.1	1.705	-188.4	0.714	-102.1	P-3
0.117	-125.9	4.312	-253.8	1.449	-340.1	0.340	-253.8	P-4
0.146	-45.5	1.750	-133.5	0.555	-219.4	0.196	-133.5	P-6
0.269	-55.1	1.858	-133.4	0.668	-219.0	0.174	-133.4	P-7
0.119	-352.5	3.663	-120.6	0.894	-204.3	0.436	-120.6	P-8
0.121	-146.2	3.652	-274.0	1.365	-5.8	0.285	-274.0	P-9
0.299	-32.2	3.990	-120.7	1.327	-205.7	0.394	-120.7	P-12
0.199	-186.0	2.830	-272.4	0.940	-359.9	0.219	-272.4	P-13
0.101	-128.5	1.722	-216.5	0.577	-302.3	0.097	-216.5	P-14
0.196	-164.3	3.449	-252.3	1.246	-338.2	0.258	-252.3	P-16
0.146	-2.4	1.976	-144.2	0.298	-230.3	0.224	-144.2	S-2
0.104	-0.2	1.816	-139.9	0.355	-225.9	0.224	-139.9	S-1
0.095	-77.6	2.027	-217.3	0 552	-303.3	0.098	-217.3	S-3
0.191	-113.4	3.874	-253.1	1.259	-339.1	0.291	-253.1	S-5
0.119	-109.3	1.826	-215.7	0.550	-301.2	0.090	-215.7	S-7

1=PHAT-OS/AV
2=PSI-P(STEP)
3=(V/WG)(B*/PH)@1.2TD
4=PSI-B*(STEP)
5=(1/W2)R*HAT-OS/AV
6=PSI-R*(STEP)
7=(DB)TD/2 OR 2/K
8=PSI-B(STEP)
9=PHAT-1/2 OS/PEAK#1
#10=PSI-P(STEP)
#11=(V/G)(B*/PH)@1.2TD
#12=PSI-B*(STEP)
#13=(1/W)R*HAT-OS/AV
#14=PSI-R*(STEP)
#15=(DB*/PH)@TD/4
#16=PSI-B*(STEP)

PR	# 1	# 2	# 3	# 4	# 5	# 6	# 7	# 8
8.0	1.251	-41.1	1.676	-89.9	0.704	-187.4	8.533	-185.9
8.0	0.390	-42.0	0.970	-90.9	0.277	-188.3	3.738	-186.8
3.5	0.100	-45.1	0.381	-93.9	0.092	-191.4	1.479	-189.9
3.0	0.013	-186.9	0.063	-235.7	0.013	-333.2	0.283	-331.7
6.0	0.086	-215.0	0.282	-263.8	0.077	-1.3	0.758	-359.8
2.5	0.283	-39.9	1.492	-90.3	0.476	-183.2	5.197	-186.0
2.5	0.132	-40.5	0.690	-90.9	0.262	-183.8	2.982	-186.6
2.0	0.041	-42.4	0.363	-92.8	0.105	-185.8	1.354	-188.6
1.5	0.007	-198.3	0.062	-248.7	0.016	-341.6	0.206	-344.4
1.5	0.053	-216.1	0.342	-266.5	0.110	-359.4	0.939	-2.2
3.0	0.029	-19.1	3.365	-97.0	0.593	-176.4	18.599	-206.9
2.5	0.019	-21.9	2.390	-99.8	0.437	-179.2	14.687	-209.7
2.0	0.005	-45.6	1.039	-123.6	0.126	-202.9	7.217	-233.4
2.0	0.003	-125.9	0.729	-203.8	0.149	-283.1	3.648	-313.6
2.0	0.007	-168.4	1.242	-246.3	0.275	-325.6	1.596	-356.1
4.2	0.037	-63.7	3.731	-105.3	1.182	-197.8	16.318	-201.1
4.5	0.028	-67.3	2.977	-109.0	0.950	-201.5	13.541	-204.8
3.5	0.021	-72.9	2.275	-114.6	0.732	-207.1	10.802	-210.4
3.0	0.015	-82.4	1.639	-124.1	0.533	-216.5	8.098	-219.8
3.0	0.010	-100.0	1.068	-141.6	0.367	-234.1	5.430	-237.4
3.0	0.008	-131.5	0.806	-173.1	0.361	-265.6	2.993	-268.9
8.5	4.140	-18.5	3.644	-87.1	2.226	-181.1	16.413	-191.6
3.5	0.461	-22.8	1.841	-91.5	0.420	-185.5	9.063	-196.0
3.0	0.076	-44.8	0.707	-113.4	0.078	-207.4	4.632	-217.9
3.5	0.051	-167.7	0.571	-236.3	0.093	-330.3	1.707	-340.8
4.0	0.091	-182.7	0.925	-251.3	0.169	-345.3	1.473	-355.8
5.0	0.081	-28.0	6.020	-88.3	2.112	-181.2	18.714	-184.5
4.0	0.054	-27.3	4.261	-87.7	1.485	-180.6	13.392	-183.8
3.5	0.029	-25.9	2.543	-86.2	0.883	-179.1	8.181	-182.4
3.0	0.008	-19.0	0.884	-79.3	0.309	-172.2	3.079	-175.5
2.0	0.008	-221.5	0.718	-281.9	0.257	-14.8	1.919	-18.0
3.0	0.024	-213.4	2.117	-273.8	0.787	-6.7	6.816	-9.9
9.0	-10.228	-25.6	4.586	-88.2	262.375	-191.2	18.077	-185.1

# 9	#10	#11	#12	#13	#14	#15	#16		
1.111	-41.1	3.374	-89.9	1.418	-187.4	0.261	-89.9	A1	
0.593	-42.0	1.954	-90.9	0.557	-188.3	0.156	-90.9	N0	
0.194	-45.1	0.768	-93.9	0.186	-191.4	0.067	-93.9	P1	Group
0.026	-186.9	0.127	-235.7	0.026	-333.2	0.002	-235.7	P2	4
0.154	-215.0	0.568	-263.8	0.154	-1.3	0.035	-263.8	P3	
0.472	-39.9	2.959	-90.3	0.945	-183.2	0.231	-90.3	A3	
0.252	-40.5	1.765	-90.9	0.520	-183.8	0.141	-90.9	A2	
0.083	-42.4	0.720	-92.8	0.209	-185.8	0.063	-92.8	N0	Group
0.013	-198.3	0.123	-248.7	0.032	-341.6	0.001	-248.7	P2	3
0.100	-216.1	0.678	-266.5	0.219	-359.4	0.044	-266.5	P3	
0.056	-19.1	3.305	-97.0	0.583	-176.4	0.398	-97.0	A2	
0.037	-21.9	2.348	-99.8	0.430	-179.2	0.303	-99.8	A1	
0.010	-45.6	1.020	-123.6	0.124	-202.9	0.131	-123.6	N0	Group
0.006	-125.9	0.716	-203.8	0.146	-283.1	0.054	-203.8	P1	12
0.013	-168.4	1.220	-246.3	0.270	-325.6	0.050	-246.3	P2	
0.074	-63.7	3.739	-105.3	1.184	-197.8	0.295	-105.3	A2	
0.057	-67.3	2.983	-109.0	0.952	-201.5	0.236	-109.0	A1	
0.043	-72.9	2.280	-114.6	0.734	-207.1	0.179	-114.6	N0	Group
0.031	-82.4	1.643	-124.1	0.534	-216.5	0.126	-124.1	P1	13
0.020	-100.0	1.070	-141.6	0.368	-234.1	0.072	-141.6	P2	
0.015	-131.5	0.808	-173.1	0.362	-265.6	0.039	-173.1	P3	
1.150	-18.5	3.761	-87.1	2.298	-181.1	0.349	-87.1	A1	
0.556	-22.8	1.900	-91.5	0.433	-185.5	0.207	-91.5	N0	
0.137	-44.8	0.730	-113.4	0.080	-207.4	0.094	-113.4	P1	Group
0.093	-167.7	0.590	-236.3	0.096	-330.3	0.016	-236.3	P2	10
0.157	-182.7	0.955	-251.3	0.175	-345.3	0.038	-251.3	P3	
0.151	-28.0	6.031	-88.3	2.116	-181.2	0.467	-88.3	A2	
0.103	-27.3	4.268	-87.7	1.488	-180.6	0.333	-87.7	A1	
0.057	-25.9	2.547	-86.2	0.865	-179.1	0.202	-86.2	N0	Group
0.016	-19.0	0.886	-79.3	0.309	-172.2	0.075	-79.3	P1	11
0.016	-221.5	0.720	-281.9	0.258	-14.8	0.047	-281.9	P2	
0.047	-213.4	2.121	-273.8	0.788	-6.7	0.154	-273.8	P3	
1.784	-25.6	5.007	-88.2	286.424	-191.2	0.388	-88.2	A1	Group 9

```
# 1=PHAT-OS/AV
# 2=PSI-P(STEP)
# 3=(V/WG)(B*/PH)@1.2TD
# 4=PSI-B*(STEP)
# 5=(1/W2)R*HAT-OS/AV
# 6=PSI-R*(STEP)
# 7=(DB)TD/2 OR 2/K
# 8=PSI-B(STEP)
# 9=PHAT-1/2 OS/PEAK#1
#10=PSI-P(STEP)
#11=(V/G)(B*/PH)@1.2TD
#12=PSI-B*(STEP)
#13=(1/W)R*HAT-OS/AV
#14=PSI-R*(STEP)
#15=(DB*/PH)@TD/4
#16=PSI-B*(STEP)
```

PR	# 1	# 2	# 3	# 4	# 5	# 6	# 7	# 8
8.3	1.178	-25.7	2.667	-88.3	1.073	-191.3	9.292	-185.2
5.5	0.205	-26.3	0.998	-88.9	0.228	-191.9	3.660	-185.8
5.0	0.040	-202.5	0.266	-265.1	0.055	-8.1	0.339	-2.0
9.0	0.142	-204.7	0.816	-267.3	0.197	-10.3	3.154	-4.2
4.0	0.350	-37.4	2.029	-93.1	0.428	-177.4	9.642	-196.9
3.0	0.207	-38.9	1.496	-94.6	0.304	-178.9	6.807	-198.4
2.0	0.056	-46.5	0.599	-102.2	0.121	-186.5	3.230	-206.0
2.5	0.006	-135.5	0.169	-191.0	0.033	-275.3	1.152	-294.8
3.0	0.023	-187.3	0.295	-243.0	0.069	-327.4	0.731	-346.8
5.3	1.899	-26.7	6.625	-88.4	4.531	-184.7	22.120	-184.8
4.0	0.723	-26.3	4.609	-86.0	2.034	-184.3	14.904	-184.3
2.8	0.293	-25.3	2.724	-87.0	0.917	-183.3	8.749	-183.4
2.0	0.076	-21.4	1.000	-83.2	0.285	-179.4	3.438	-179.5
4.0	0.032	-219.1	0.439	-260.0	0.128	-17.1	1.193	-17.2
4.0	0.767	-17.5	4.642	-91.2	1.325	-177.4	21.216	-198.1
2.5	0.358	-19.9	3.068	-93.7	0.714	-179.9	14.822	-200.5
2.3	0.143	-25.3	1.695	-99.1	0.347	-185.3	9.824	-205.9
2.0	0.043	-45.8	0.883	-119.5	0.113	-205.7	5.810	-226.4
4.0	0.024	-147.2	0.637	-221.0	0.120	-307.2	2.517	-327.8
4.0	0.328	-64.0	3.617	-103.0	1.146	-192.8	14.799	-198.8
2.0	0.211	-69.5	2.698	-107.9	0.791	-197.7	12.014	-203.6
1.0	0.131	-77.4	1.890	-115.8	0.530	-205.6	9.429	-211.5
2.0	0.078	-91.5	1.234	-129.9	0.339	-219.7	7.022	-225.6
3.0	0.050	-117.0	0.793	-155.9	0.221	-245.8	4.776	-251.7
6.5	-2.655	-45.0	5.839	-99.9	-4.028	-201.2	21.216	-195.1
5.5	79.306	-54.6	4.065	-106.7	7.233	-210.0	15.177	-203.9
5.0	1.775	-67.3	2.745	-121.5	1.410	-222.7	11.511	-216.7
4.5	0.765	-85.0	1.870	-139.2	0.678	-240.4	9.048	-234.3
4.5	0.489	-106.0	1.384	-160.2	0.548	-261.4	7.279	-255.3
5.0	0.400	-125.0	1.200	-179.7	0.462	-281.0	5.985	-274.9
4.5	0.172	-104.1	2.472	-125.2	0.668	-209.5	16.740	-221.5
4.0	0.130	-113.9	2.000	-134.9	0.527	-219.3	15.123	-231.3
3.2	0.103	-125.5	1.646	-146.5	0.430	-230.9	13.616	-242.9
3.3	0.087	-138.4	1.406	-159.4	0.370	-243.8	12.209	-255.8
4.0	0.080	-151.4	1.272	-172.5	0.337	-256.8	10.892	-268.8

# 9	#10	#11	#12	#13	#14	#15	#16		
1.000	-25.7	2.912	-88.3	1.171	-191.3	0.232	-88.3	N0	
0.342	-26.3	1.090	-88.9	0.249	-191.9	0.096	-88.9	P1	Group
0.076	-202.5	0.291	-265.1	0.061	-8.1	0.011	-265.1	P2	9
0.238	-204.7	0.893	-267.3	0.215	-10.3	0.059	-267.3	P3	
0.507	-37.4	4.086	-93.1	0.862	-177.4	0.390	-93.1	A1	
0.348	-38.9	3.011	-94.6	0.612	-178.9	0.297	-94.6	N0	
0.110	-46.5	1.207	-102.2	0.244	-186.5	0.139	-102.2	P1	Group
0.017	-135.3	0.341	-191.0	0.067	-275.3	0.026	-191.0	P2	2
0.044	-187.3	0.594	-243.0	0.139	-327.4	0.024	-243.0	P3	
1.176	-26.7	6.632	-88.4	4.536	-184.7	0.511	-88.4	A2	
0.797	-26.3	4.614	-88.0	2.037	-184.3	0.358	-88.0	A1	
0.449	-25.3	2.728	-87.0	0.918	-183.3	0.215	-87.0	N0	Group
0.145	-21.4	1.001	-83.2	0.285	-179.4	0.084	-83.2	P1	6
0.061	-219.1	0.440	-280.8	0.128	-17.1	0.027	-280.8	P2	
0.705	-17.5	4.698	-91.2	1.341	-177.4	0.474	-91.2	A2	
0.451	-19.9	3.106	-93.7	0.723	-179.9	0.337	-93.7	A1	
0.238	-25.3	1.716	-99.1	0.352	-185.3	0.217	-99.1	N0	Group
0.082	-45.8	0.894	-119.5	0.114	-205.7	0.115	-119.5	P1	7
0.046	-147.2	0.645	-221.0	0.122	-307.2	0.033	-221.0	P2	
0.523	-64.0	3.661	-103.0	1.160	-192.8	0.302	-103.0	A2	
0.371	-69.5	2.730	-107.9	0.801	-197.7	0.230	-107.9	A1	
0.245	-77.4	1.913	-115.8	0.536	-205.6	0.166	-115.8	N0	Group
0.152	-91.5	1.249	-129.9	0.343	-219.7	0.109	-129.9	P1	14
0.099	-117.6	0.802	-155.9	0.223	-245.8	0.060	-155.9	P2	
2.583	-45.8	6.605	-99.9	-4.556	-201.2	0.466	-99.9	A2	
1.780	-54.6	4.599	-108.7	8.182	-210.0	0.351	-108.7	A1	
1.198	-67.3	3.106	-121.5	1.595	-222.7	0.254	-121.5	N0	Group
0.824	-85.0	2.116	-139.2	0.767	-240.4	0.176	-139.2	P1	15
0.625	-106.0	1.566	-160.2	0.620	-261.4	0.117	-160.2	P2	
0.542	-125.6	1.358	-179.7	0.522	-281.0	0.080	-179.7	P3	
0.322	-104.1	2.476	-125.2	0.669	-209.5	0.242	-125.2	A2	
0.252	-113.9	2.003	-134.9	0.528	-219.3	0.197	-134.9	A1	Group
0.203	-125.5	1.649	-146.5	0.431	-230.9	0.158	-146.5	N0	16
0.173	-138.4	1.409	-159.4	0.371	-243.8	0.125	-159.4	P1	
0.157	-151.4	1.275	-172.5	0.338	-256.8	0.097	-172.5	P2	

NRC DOETSCH

1=PHAT-OS/AV
2=PSI-P(STEP)
3=(V/WG)(B*/PH)@1.2TD
4=PSI-B*(STEP)
5=(1/W2)R*HAT-OS/AV
6=PSI-R*(STEP)
7=(DB)TD/2 OR 2/K
8=PSI-B(STEP)
9=PHAT-1/2 OS/PEAK#1
#10=PSI-P(STEP)
#11=(V/G)(B*/PH)@1.2TD
#12=PSI-B*(STEP)
#13=(1/W)R*HAT-OS/AV
#14=PSI-R*(STEP)
#15=(DB*/PH)@TD/4
#16=PSI-B*(STEP)

PR	# 1	# 2	# 3	# 4	# 5	# 6	# 7	# 8
7.5	0.249	-103.7	7.391	-216.9	4.313	-299.4	43.626	-318.5
6.5	0.405	-51.3	7.589	-164.5	2.135	-246.9	48.232	-266.1
6.0	0.566	-37.5	8.138	-150.7	2.802	-233.2	67.311	-252.3
7.0	0.943	-24.9	9.781	-138.1	4.001	-220.6	98.819	-239.6
6.0	0.213	-144.9	7.190	-248.5	3.635	-329.9	72.955	-350.3
6.0	0.195	-139.0	6.725	-242.5	3.238	-324.0	60.387	-344.4
6.5	0.177	-128.9	6.176	-232.5	2.841	-313.9	46.029	-334.3
6.0	0.164	-104.6	5.476	-208.1	2.567	-289.6	27.282	309.9
6.0	0.177	-84.6	5.250	-188.1	2.788	-269.6	22.837	-289.9
6.0	0.281	-48.8	5.529	-152.3	1.594	-233.8	45.633	-254.1
5.0	0.459	-31.4	6.957	-135.0	2.416	-216.4	71.343	-236.8
7.0	1.080	-17.0	11.139	-120.5	4.315	-201.9	125.387	-222.3
7.0	0.169	-162.5	6.192	-255.3	2.735	-336.3	70.622	-356.9
7.0	0.140	-156.4	5.320	-249.3	2.161	-330.2	51.290	-350.9
6.0	0.109	-144.2	4.279	-237.1	1.597	-318.0	31.623	-338.6
3.0	0.084	-104.3	3.070	-197.2	1.193	-278.1	12.785	-298.7
4.5	0.127	-54.5	2.995	-147.4	0.826	-228.3	29.522	-248.9
5.0	0.371	-21.9	6.732	-114.8	2.182	-195.7	74.760	-216.3
7.0	0.947	-12.5	11.407	-105.4	4.173	-186.3	133.575	-206.9
5.5	0.128	-186.0	5.169	-267.9	2.035	-348.0	67.772	-9.5
6.5	0.109	-186.0	4.519	-267.9	1.681	-348.0	54.207	-9.5
4.5	0.058	-185.9	2.577	-267.8	0.824	-347.9	22.233	-9.4
2.5	0.0	-141.1	0.352	-223.2	0.002	-303.3	7.748	-324.7
5.0	0.179	-6.2	4.714	-88.1	1.323	-168.2	53.046	-189.7
6.5	0.384	-6.2	7.914	-88.1	2.385	-168.1	87.412	-189.6
6.0	0.756	-6.1	11.319	-88.1	3.753	-168.1	129.157	-189.6
6.5	0.143	-198.4	5.752	-275.2	2.358	-355.1	91.824	-16.6
6.0	0.103	-203.1	4.396	-280.0	1.608	-359.8	58.892	-21.3
5.0	0.059	-215.8	2.688	-292.6	0.864	-12.5	27.491	-34.0
5.0	0.025	-269.9	1.526	-346.8	0.345	-66.6	8.089	-88.1
5.0	0.106	-340.1	3.970	-56.9	1.026	-136.8	36.446	-158.3
7.5	0.111	-215.7	4.763	-287.3	1.792	-6.6	73.434	-28.8
6.5	0.079	-228.6	3.534	-300.2	1.206	-19.5	44.736	-41.7

# 9	#10	#11	#12	#13	#14	#15	#16	
0.355	-103.7	7.397	-216.9	4.317	-299.4	1.546	-216.9	1
0.494	-51.3	7.587	-164.5	2.135	-246.9	1.926	-164.5	2
0.605	-37.5	8.145	-150.7	2.804	-233.2	2.360	-150.7	3
0.782	-24.9	9.796	-138.1	4.007	-220.6	2.991	-138.1	4
0.316	-144.9	7.196	-248.5	3.638	-329.9	1.593	-248.5	5
0.296	-139.0	6.732	-242.5	3.242	-324.0	1.469	-242.5	6
0.275	-128.9	6.181	-232.5	2.844	-313.9	1.318	-232.5	7
0.259	-104.6	5.481	-208.1	2.570	-289.6	1.092	-208.1	8
0.275	-84.6	5.255	-188.1	2.790	-269.6	1.013	-188.1	9
0.390	-48.8	5.533	-152.3	1.595	-233.8	1.586	-152.3	10
0.5 1	-31.4	6.964	-135.0	2.419	-216.4	2.116	-135.0	11
0.836	17.0	11.142	-120.5	4.319	-201.9	3.052	-120.5	12
0.265	-16 .5	8.197	-255.3	2.737	-336.3	1.385	-255.3	13
0.228	-156.4	5.322	-249.3	2 162	-330.2	1.159	-249.3	14
0.185	-144.2	4.280	-237.1	1.598	-318.0	0.887	-237.1	15
0.148	-104.3	3.071	-197.2	1.194	-278.1	0.529	-197.2	16
0.213	-54.5	2.996	-147.4	0.826	-228.3	0.899	-147.4	17
0.483	-21.9	6.735	-114.8	2.183	-195.7	1.794	-114.8	18
0.807	-12.5	11.411	-105.4	4.175	-186.3	2.936	-105.4	19
0.213	-186.0	5.172	-267.9	2.036	-348.0	1.183	-267.9	20
0.186	-186.0	4.523	-267.9	1.682	-348.0	1.024	-267.9	21
0.106	-185.9	2.579	-267.8	0.824	-347.9	0.554	-267.8	22
0.001	-141.1	0.352	-223.2	0.002	-303.3	0.130	-223.2	23
0.29	-6.2	4.717	-88.1	1.324	-168.2	1.288	-88.1	24
0.509	-6.2	7.920	-88.1	2.387	-168.1	2.068	-88.1	25
0.745	-6.1	11.327	-88.1	3.756	-168.1	2.896	-88.1	26
0.232	-198.4	5.708	-275.2	2.340	-355.1	1.354	-275.2	27
0.177	-203.1	4.362	-280.0	1.595	-359.8	1.035	-280.0	28
0.108	-215.8	2.667	-292.6	0.857	-12.5	0.655	-292.6	29
0.048	-269.9	1.514	-346.8	0.343	-66.6	0.371	-346.8	30
0.195	-340.1	3.939	-56.9	1.018	-136.8	1.061	-56.9	31
0.188	-215.7	4.771	-287.3	1.795	-6.6	1.172	-287.3	32
0.140	-228.6	3.540	-300.2	1.208	-19.5	0.950	-300.2	33

```
# 1=PHAT-OS/AV
# 2=PSI-P(STEP)
# 3=(V/WG)(B*/PH)@1.2TD
# 4=PSI-B*(STEP)
# 5=(1/W2)R*HAT-OS/AV
# 6=PSI-R*(STEP)
# 7=(DB)TD/2 OR 2/K
# 8=PSI-B(STEP)
# 9=PHAT-1/2 OS/PEAK#1
#10=PSI-P(STEP)
#11=(V/G)(B*/PH)@1.2TD
#12=PSI-B*(STEP)
#13=(1/W)R*HAT-OS/AV
#14=PSI-R*(STEP)
#15=(DB*/PH)@TD/4
#16=PSI-B*(STEP)
```

PR	# 1	# 2	# 3	# 4	# 5	# 6	# 7	# 8
6.0	0.066	-285.0	3.680	-356.5	1.035	-75.8	15.723	-98.1
5.5	0.144	-329.0	5.623	-40.5	1.398	-119.8	42.267	-142.0
6.0	0.674	-357.0	12.029	-68.6	3.624	-147.9	123.935	-170.1
2.0	0.001	-179.0	0.562	-266.3	0.020	-340.4	11.083	-13.6
3.0	0.060	-104.7	2.832	-203.0	0.934	-277.8	11.535	-310.4
4.0	0.051	-284.8	3.321	-0.8	0 356	-74.0	19.775	-108.2
2.0	0.001	-161.9	0.152	-239.4	0.005	-325.5	3.142	-335.0
5.0	0.125	-105.1	3.403	-193.0	1.608	-279.9	12.838	-288.7
5.0	0.087	-284.3	4.172	-351.7	1.532	-77.0	19.129	-87.4
3.5	0.006	-348.0	2.269	-78.4	0.066	-154.3	49.805	-185.5
2.5	0.048	-96.6	6.312	-197.4	).656	-274.6	45.713	-304.8
6.0	0.062	-277.3	7.146	-357.0	0.450	-70.7	48.783	-104.6
2.5	0.001	-16.2	1.274	-102.0	0.011	-183.8	28.852	-203.5
4.5	0.083	-96.5	6.819	-194.6	2.042	-275.9	42.838	-298.4
6.5	0.079	-277.2	7.864	-353.2	0.722	-73.3	34.836	-94.7
3.5	0.004	-184.3	0.631	-266.0	0.137	-353.9	5.701	-1.7
5.5	0.128	-94.8	7.381	-186.6	3.009	-276.3	38.508	-282.4
5.0	0.107	-278.4	9.116	-351.4	2.909	-77.8	43.276	-87.1
7.5	0.300	-355.5	7.563	-72.4	2.126	-152.2	75.767	-173.7

# 9	#10	#11	#12	#13	#14	#15	#16	
0.138	-285.0	3.687	-356.5	1.037	-75.8	0.825	-356.5	34
0.262	-329.0	5.633	-40.5	1.400	-119.8	1.428	-40.5	35
0.725	-357.0	12.051	-68.6	3.630	-147.9	3.033	-68.6	36
0.003	-179.0	0.563	-266.3	0.020	-340.4	0.181	-266.3	82
0.108	-104.7	2.831	-203.0	0.934	-277.8	0.492	-203.0	108
0.106	-284.8	3.328	-0.8	0.356	-74.0	0.934	-0.8	114
0.001	-161.9	0.152	-239.4	0.005	-325.5	0.057	-239.4	104
0.216	-105.1	3.409	-193.0	1.611	-279.9	0.571	-193.0	109
0.183	284.3	4.171	-351.7	1.532	-77.0	0.806	-351.7	115
0.013	-348.0	1.141	-78.4	0.033	-154.3	0.435	-78.4	91
0.083	-96.6	3.153	-197.4	0.827	-274.6	0.645	-197.4	124
0.126	-277.3	3.572	-357.0	0.225	-70.7	1.154	-357.0	129
0.002	-16.2	0.637	-102.0	0.006	-183.8	0.243	-102.0	119
0.145	-96.5	3.424	-194.6	1.025	-275.9	0.689	-194.6	125
0.159	-277.2	3.929	-353.2	0.361	-73.3	0.969	-353.2	130
0.008	-184.3	0.315	-266.0	0.068	-353.9	0.062	-266.0	120
0.220	-94.8	3.699	-186.6	1.508	-276.3	0.674	-186.6	126
0.216	-278.4	4.454	-351.4	1.422	-77.8	1.006	-351.4	131
0.442	-355.5	7.503	-72.4	2.110	-152.2	1.935	-72.4	31B

Config. Number 1 - 36 Identified on Table 3-1a of Ref. 33

31b LH 79 + 20 + 13

82	LH 100 + 30 + 30	119	LM 50 + 20 + 20
108	+ 40	125	+ 30
114	+ 20	130	+ 10
104	LH 100 + 10 + 10	120	LM 50 + 10 + 10
109	+ 20	126	+ 20
115	+ 0	131	+ 0
91	LM 50 + 29 + 29		
124	30 + 40		
129	30 + 20		

1=PHAT-OS/AV
2=PSI-P(STEP)
3=(V/WG)(B*/PH)@1.2TD
4=PSI-B*(STEP)
5=(1/W2)R*HAT-OS/AV
6=PSI-R*(STEP)
7=(DB)TD/2 OR 2/K
8=PSI-B(STEP)
9=PHAT-1/2 OS/PEAK#1
#10=PSI-P(STEP)
#11=(V/G)(B*/PH)@1.2TD
#12=PSI-B*(STEP)
#13=(1/W)R*HAT-OS/AV
#14=PSI-R*(STEP)
#15=(DB*/PH)@TD/4
#16=PSI-B*(STEP)

PR	# 1	# 2	# 3	# 4	# 5	# 6	# 7	# 8
3.2	0.031	-26.4	0.455	-104.1	0.165	-196.0	3.604	-199.8
2.8	0.064	-56.4	0.434	-121.2	0.151	-210.8	4.359	-216.8
2.9	0.084	-99.1	0.365	-146.1	0.121	-230.2	5.490	-241.8
3.2	0.055	-148.6	0.249	-172.2	0.075	-250.9	6.529	-267.9
2.9	0.066	-26.4	0.457	-104.6	0.164	-196.0	3.688	-200.3
2.7	0.158	-56.9	0.439	-124.0	0.152	-210.7	4.697	-219.7
4.0	0.235	-106.3	0.345	-157.1	0.122	-230.0	6.269	-252.7
5.1	0.116	-163.7	0.268	-185.9	0.074	-251.0	7.151	-281.6
4.0	0.150	-26.4	0.462	-105.6	0.164	-196.0	3.892	-201.3
5.0	0.469	-58.3	0.441	-130.8	0.151	-210.8	5.440	-226.5
4.2	0.0	-254.6	0.018	-347.6	0.0	-79.9	0.468	-83.3
4.7	0.0	-315.1	0.428	-129.4	0.180	-225.1	4.409	-221.7
3.5	0.005	-306.5	0.019	-348.7	0.003	-63.0	0.208	-84.4
3.5	0.136	-134.3	0.244	-182.6	0.076	-256.0	4.184	-278.3
4.0	0.280	-134.6	0.377	-189.4	0.126	-262.0	6.124	-285.1
4.5	0.301	-74.0	0.483	-121.7	0.170	-194.8	6.791	-217.4
6.5	0.240	-173.9	0.413	-225.1	0.163	-291.2	4.013	-322.1
4.0	0.141	-88.9	0.277	-135.1	0.087	-208.3	4.783	-230.8
4.5	0.282	-150.3	0.397	-205.1	0.181	-277.7	5.584	-300.8
5.8	0.116	-0.6	0.431	-39.4	0.112	-114.2	2.087	-135.1
3.8	0.0	-120.8	0.018	-328.2	0.0	-60.5	0.408	-63.9
3.2	0.001	-173.0	0.021	-234.9	0.001	-320.3	0.397	-330.6
2.8	0.0	-29.7	0.142	-164.9	0.0	-245.4	3.217	-272.3
4.5	0.129	-229.4	0.301	-271.6	0.110	-346.0	4.711	-7.3
7.0	0.133	-267.8	0.326	-306.6	0.117	-21.4	9.183	-42.3
6.0	0.286	-25.2	0.736	-64.0	0.219	-138.8	3.940	-159.7
5.0	0.286	-67.8	0.492	-114.1	0.169	-187.2	6.376	-209.7
5.0	0.557	-63.2	0.729	-111.4	0.301	-184.8	8.485	-207.1
2.9	0.018	-77.4	0.345	-158.7	0.026	-230.3	5.956	-272.3
3.0	0.0	-196.0	0.268	-219.8	0.007	-283.9	7.520	-333.4
3.2	0.050	-78.4	0.365	-161.8	0.027	-230.2	6.182	-275.3
3.5	0.001	-206.4	0.278	-227.9	0.007	-283.9	7.668	-341.5
3.9	0.130	-80.1	0.399	-167.8	0.027	-230.1	6.607	-281.3

# 9	#10	#11	#12	#13	#14	#15	#16	
0.059	-26.4	0.819	-104.1	0.296	-196.0	0.089	-104.1	1
0.121	-56.4	0.782	-121.2	0.272	-210.8	0.080	-121.2	2
0.158	-99.1	0.657	-146.1	0.218	-230.2	0.064	-146.1	3
0.111	-148.6	0.448	-172.2	0.134	-250.9	0.044	-172.2	4
0.123	-26.4	0.822	-104.6	0.296	-196.0	0.090	-104.6	5
0.270	-56.9	0.790	-124.0	0.273	-210.7	0.084	-124.0	6
0.373	-106.3	0.620	-157.1	0.219	-230.0	0.067	-157.1	7
0.214	-163.7	0.482	-185.9	0.132	-251.0	0.040	-185.9	8
0.253	-26.4	0.830	-105.6	0.296	-196.0	0.092	-105.6	9
0.600	-58.3	0.792	-130.8	0.272	-210.8	0.090	-130.8	10
0.0	-254.6	0.033	-347.6	0.0	-79.9	0.005	-347.6	14
0.0	-315.1	0.763	-129.4	0.321	-225.1	0.054	-129.4	15
0.010	-306.5	0.035	-348.7	0.006	-63.0	0.003	-348.7	16
0.236	-134.3	0.440	-182.6	0.137	-256.0	0.032	-182.6	17
0.416	-134.6	0.678	-189.4	0.227	-262.0	0.043	-189.4	18
0.466	-74.0	0.869	-121.7	0.306	-194.8	0.108	-121.7	19
0.362	-173.9	0.689	-225.1	0.273	-291.2	0.025	-225.1	20
0.251	-88.9	0.498	-135.1	0.157	-208.3	0.064	-135.1	21
0.416	-150.3	0.715	-205.1	0.326	-277.7	0.031	-205.1	22
0.255	-0.6	0.775	-39.4	0.202	-114.2	0.047	-39.4	23
0.0	-120.8	0.033	-328.2	0.0	-60.5	0.006	-328.2	53
0.003	-173.0	0.038	-234.9	0.002	-320.3	0.005	-234.9	65
0.0	-29.7	0.256	-164.9	0.0	-245.4	0.045	-164.9	75
0.222	-229.4	0.542	-271.6	0.199	-346.0	0.053	-271.6	81
0.226	-267.8	0.587	-306.6	0.211	-21.4	0.067	-306.6	82
0.518	-25.2	1.325	-64.0	0.394	-138.8	0.112	-64.0	83
0.454	-67.8	0.886	-114.1	0.304	-187.2	0.109	-114.1	84
0.711	-63.2	1.312	-111.4	0.541	-184.8	0.156	-111.4	86
0.035	-77.4	0.621	-158.7	0.048	-230.3	0.092	-158.7	101
0.001	-196.0	0.481	-219.8	0.012	-283.9	0.043	-219.8	103
0.092	-78.4	0.656	-161.8	0.048	-230.2	0.095	-161.8	104
0.001	-206.4	0.500	-227.9	0.012	-283.9	0.041	-227.9	106
0.204	-80.1	0.716	-167.8	0.048	-230.1	0.100	-167.8	107

```
# 1=PHAT-OS/AV
# 2=PSI-P(STEP)
# 3=(V/WG)(B*/PH)@1.2TD
# 4=PSI-B*(STEP)
# 5=(1/W2)R*HAT-OS/AV
# 6=PSI-R*(STEP)
# 7=(DB)TD/2 OR 2/K
# 8=PSI-B(STEP)
# 9=PHAT-1/2 OS/PEAK#1
#10=PSI-P(STEP)
#11=(V/G)(B*/PH)@1.2TD
#12=PSI-B*(STEP)
#13=(1/W)R*HAT-OS/AV
#14=PSI-R*(STEP)
#15=(DB*/PH)@TD/4
#16=PSI-B*(STEP)
```

PR	# 1	# 2	# 3	# 4	# 5	# 6	# 7	# 8
3.8	0.054	-154.8	0.363	-206.6	0.019	-255.6	7.285	-320.2
3.3	0.0	-140.3	0.322	-156.2	0.027	-230.3	5.767	-269.8
3.0	0.0	-345.8	0.293	-181.7	0.019	-255.8	6.449	-295.3
3.8	0.001	-172.8	0.021	-234.8	0.001	-320.2	0.397	-330.5
3.8	0.0	-87.0	0.206	-157.2	0.0	-220.6	4.642	-270.8
3.0	0.0	-177.2	0.205	-223.5	0.0	-283.5	5.309	-337.1
3.0	0.026	-178.3	0.318	-229.4	0.014	-288.1	4.993	-342.9
3.0	0.048	-105.7	0.413	-162.8	0.028	-221.1	8.724	-276.4
4.8	0.054	-39.4	0.491	-86.0	0.059	-145.3	9.126	-199.6
4.0	0.025	-239.8	0.345	-281.6	0.073	-340.9	3.208	-35.2
3.0	0.015	-254.4	0.245	-296.0	0.048	-355.9	1.098	-49.6
4.0	0.019	-222.8	0.290	-268.4	0.062	-328.8	2.227	-21.9
3.3	0.051	-177.8	0.430	-233.4	0.112	-291.4	5.177	-347.0
4.5	0.100	-142.0	0.512	-214.7	0.144	-273.5	7.257	-328.4
5.7	0.160	-228.9	0.357	-271.1	0.135	-345.5	6.306	-6.8
4.5	0.0	-286.0	0.442	-103.8	0.162	-196.0	3.460	-199.4
4.5	0.0	-120.8	0.416	-118.5	0.151	-210.8	4.063	-214.2
4.5	0.0	-161.0	0.232	-158.7	0.074	-251.0	5.583	-254.4
3.5	0.027	-56.3	0.430	-119.8	0.151	-210.8	4.207	-215.4
3.2	0.031	-96.7	0.366	-141.7	0.121	-230.2	5.130	-237.4
3.3	0.018	-141.7	0.226	-165.0	0.075	-250.9	6.066	-260.7

# 9	#10	#11	#12	#13	#14	#15	#16	
0.097	-154.8	0.653	-206.6	0.034	-255.6	0.067	-206.6	108
0.0	-140.3	0.579	-156.2	0.048	-230.3	0.087	-156.2	109
0.0	-345.8	0.526	-181.7	0.034	-255.8	0.066	-181.7	110
0.003	-172.8	0.038	-234.8	0.002	-320.2	0.005	-234.8	112
0.0	-87.0	0.370	-157.2	0.0	-220.6	0.065	-157.2	113
0.0	-177.2	0.369	-223.5	0.0	-283.5	0.055	-223.5	115
0.050	-178.3	0.571	-229.4	0.026	-288.1	0.039	-229.4	116
0.088	-105.7	0.743	-162.8	0.051	-221.1	0.112	-162.8	117
0.106	-39.4	0.883	-86.0	0.106	-145.3	0.160	-86.0	118
0.048	-239.8	0.620	-281.6	0.132	-340.9	0.045	-281.6	119
0.030	-254.4	0.441	-296.0	0.087	-355.9	0.020	-296.0	120
0.036	-222.8	0.521	-268.4	0.111	-328.8	0.018	-268.4	121
0.092	-177.8	0.773	-233.4	0.202	-291.4	0.042	-233.4	122
0.165	-142.0	0.920	-214.7	0.258	-273.5	0.072	-214.7	123
0.265	-228.9	0.643	-271.1	0.244	-345.5	0.064	-271.1	126
0.0	-286.0	0.803	-103.8	0.295	-196.0	0.087	-103.8	127
0.0	-120.8	0.749	-118.5	0.273	-210.8	0.074	-118.5	128
0.0	-161.0	0.418	-158.7	0.134	-251.0	0.035	-158.7	130
0.052	-56.3	0.774	-119.8	0.273	-210.8	0.078	-119.8	132
0.061	-96.7	0.659	-141.7	0.217	-230.2	0.062	-141.7	133
0.036	-141.7	0.407	-165.0	0.134	-250.9	0.037	-165.0	134

1=PHAT-OS/AV
2=PSI-P(STEP)
3=(V/WG)(B*/PH)@1.2TD
4=PSI-B*(STEP)
5=(1/W2)R*HAT-OS/AV
6=PSI-R*(STEP)
7=(DB)TD/2 OR 2/K
8=PSI-B(STEP)
9=PHAT-1/2 OS/PEAK#1
#10=PSI-P(STEP)
#11=(V/G)(B*/PH)@1.2TD
#12=PSI-B*(STEP)
#13=(1/W)R*HAT-OS/AV
#14=PSI-R*(STEP)
#15=(DB*/PH)@TD/4
#16=PSI-B*(STEP)

PR	# 1	# 2	# 3	# 4	# 5	# 6	# 7	# 8
4.0	0.034	-32.5	0.260	-109.4	0.093	-199.2	1.700	-205.0
3.5	0.069	-69.9	0.240	-130.9	0.082	-217.3	2.049	-226.6
4.0	0.046	-120.4	0.141	-159.6	0.045	-240.1	2.062	-255.3
5.0	0.043	-162.2	0.137	-180.6	0.033	-257.8	2.862	-276.3
6.0	1.744	-28.0	1.664	-99.4	1.019	-184.8	10.824	-195.1
5.5	0.816	-32.4	1.218	-103.8	0.507	-189.2	8.083	-199.5
4.5	0.412	-40.2	0.813	-111.7	0.264	-197.1	5.718	-207.3
4.5	0.110	-37.1	0.322	-104.4	0.081	-187.7	2.222	-200.1
4.0	0.081	-54.2	0.228	-122.1	0.057	-205.9	1.738	-217.7
4.0	0.111	-101.6	0.299	-173.1	0.069	-258.5	1.922	-268.8
3.5	0.243	-101.6	0.542	-171.7	0.205	-256.1	3.604	-267.4
5.0	0.042	-262.7	0.161	-326.5	0.049	-48.7	1.407	-62.1
4.0	0.086	-189.2	0.303	-256.4	0.078	-339.8	1.701	-352.1
5.5	0.178	-196.9	0.566	-264.2	0.162	-347.5	4.744	-359.8
4.5	0.261	-161.7	0.682	-231.5	0.203	-313.2	3.297	-327.8
6.5	0.262	-199.2	0.764	-266.4	0.240	-349.8	8.506	-2.1
7.0	0.324	-200.1	0.892	-267.3	0.298	-350.7	12.326	-3.0
4.5	0.545	-38.6	1.254	-100.6	0.556	-187.3	9.139	-196.3
4.0	0.341	-42.2	0.935	-104.2	0.375	-190.8	6.609	-199.9
3.0	0.185	-42.5	0.618	-102.7	0.223	-189.2	4.237	-198.4
3.0	0.079	-39.5	0.333	-98.0	0.111	-184.4	2.271	-193.7
3.0	0.069	-69.9	0.240	-130.9	0.082	-217.3	2.049	-226.6
3.0	0.114	-111.2	0.310	-177.5	0.156	-264.5	2.722	-273.1
4.0	0.215	-123.1	0.491	-186.4	0.275	-272.9	4.214	-282.1
3.0	0.060	-251.0	0.262	-306.2	0.095	-32.5	1.969	-41.8
3.5	0.099	-216.2	0.408	-273.3	0.159	-359.8	2.794	-8.9
4.5	0.181	-163.3	0.538	-232.1	0.243	-319.5	2.879	-327.8
4.5	0.142	-221.8	0.547	-277.5	0.223	-3.8	4.389	-13.2
6.5	0.199	-218.9	0.719	-274.6	0.317	-1.0	6.357	-10.3
7.0	0.234	-217.8	0.814	-273.6	0.376	-359.9	7.616	-9.3

# 9	#10	#11	#12	#13	#14	#15	#16	
0.066	-32.5	0.599	-109.4	0.215	-199.2	0.065	-109.4	R1
0.131	-69.9	0.552	-130.9	0.189	-217.3	0.055	-130.9	R2
0.091	-120.4	0.325	-159.6	0.103	-240.1	0.031	-159.6	R3
0.090	-162.2	0.316	-180.6	0.077	-257.8	0.027	-180.6	R4
1.133	-28.0	2.160	-99.4	1.323	-184.8	0.234	-99.4	L7
0.829	-32.4	1.582	-103.8	0.658	-189.2	0.176	-103.8	L6
0.553	-40.2	1.056	-111.7	0.343	-197.1	0.123	-111.7	L5
0.197	-37.1	0.418	-104.4	0.106	-187.7	0.049	-104.4	L4
0.148	-54.2	0.302	-122.1	0.076	-205.9	0.035	-122.1	L3
0.194	-101.6	0.387	-173.1	0.090	-258.5	0.038	-173.1	L2
0.369	-101.6	0.707	-171.7	0.268	-256.1	0.067	-171.7	L1
0.079	-262.7	0.209	-326.5	0.063	-48.7	0.025	-326.5	L8
0.155	-189.2	0.394	-256.4	0.101	-339.8	0.035	-256.4	L9
0.279	-196.9	0.735	-264.2	0.211	-347.5	0.071	-264.2	L10
0.387	-161.7	0.834	-231.5	0.248	-313.2	0.057	-231.5	L13
0.390	-199.2	0.993	-266.4	0.312	-349.8	0.099	-266.4	L11
0.456	-200.1	1.161	-267.3	0.388	-350.7	0.117	-267.3	L12
0.701	-38.6	2.882	-100.6	1.279	-187.3	0.303	-100.6	H7
0.511	-42.2	2.150	-104.2	0.863	-190.8	0.227	-104.2	H6
0.318	-42.5	1.421	-102.7	0.512	-189.2	0.153	-102.7	H5
0.151	-39.5	0.765	-98.0	0.254	-184.4	0.087	-98.0	H4
0.131	-69.9	0.552	-130.9	0.189	-217.3	0.055	-130.9	H3
0.200	-111.2	0.714	-177.5	0.359	-264.5	0.042	-177.5	H2
0.338	-123.1	1.129	-186.4	0.631	-272.9	0.058	-186.4	H1
0.111	-251.6	0.602	-306.2	0.218	-32.5	0.050	-306.2	H8
0.176	-216.2	0.938	-273.3	0.365	-359.8	0.093	-273.3	H9
0.293	-163.3	1.236	-232.1	0.559	-319.5	0.100	-232.1	H13
0.239	-221.8	1.258	-277.5	0.513	-3.8	0.127	-277.5	H10
0.316	-218.9	1.653	-274.6	0.729	-1.0	0.169	-274.6	H11
0.358	-217.8	1.870	-273.6	0.864	-359.9	0.192	-273.6	H12

1=PHAT-OS/AV
2=PSI-P(STEP)
3=(V/WG)(B*/PH)@1.2TD
4=PSI-B*(STEP)
5=(1/W2)R*HAT-OS/AV
6=PSI-R*(STEP)
7=(DB)TD/2 OR 2/K
8=PSI-B(STEP)
9=PHAT-1/2 OS/PEAK#1
#10=PSI-P(STEP)
#11=(V/G)(B*/PH)@1.2TD
#12=PSI-B*(STEP)
#13=(1/W)R*HAT-OS/AV
#14=PSI-R*(STEP)
#15=(DB*/PH)@TD/4
#16=PSI-B*(STEP)

PR	# 1	# 2	# 3	# 4	# 5	# 6	# 7	# 8
5.0	0.893	-10.5	5.477	-91.8	2.799	-186.8	42.218	-187.4
3.5	0.030	-30.0	0.395	-111.3	0.131	-206.3	3.409	-206.9
3.5	0.047	-68.1	0.502	-149.4	0.175	-244.3	3.783	-245.0
3.0	0.135	-74.8	1.232	-156.0	0.659	-251.0	8.760	-251.7
4.5	0.114	-184.6	1.428	-265.6	0.540	-0.5	15.114	-1.4
5.5	0.196	-186.6	2.219	-267.9	0.951	-2.9	29.544	-3.6
3.5	0.005	-58.6	0.082	-284.0	0.035	-23.0	0.575	-19.6
3.5	0.001	-327.0	0.036	-115.5	0.013	-212.7	0.356	-211.2
4.0	0.089	-53.5	0.243	-121.6	0.060	-204.8	2.654	-217.1
4.5	0.022	-90.5	0.291	-328.4	0.156	-74.9	4.208	-64.1
4.0	0.006	-283.6	0.598	-71.1	0.194	-176.3	1.148	-166.7
4.3	0.115	-8.3	1.299	-88.8	0.336	-192.1	5.661	-184.4
5.0	0.695	-36.3	1.037	-108.3	0.158	-73.0	9.969	-203.7
5.0	0.0	-343.1	6.487	-80.5	1.665	-192.5	29.356	-175.6

# 9	#10	#11	#12	#13	#14	#15	#16	
0.918	-10.5	7.118	-91.8	3.637	-186.8	0.752	-91.8	A
0.059	-30.0	0.513	-111.3	0.170	-206.3	0.056	-111.3	B
0.090	-68.1	0.652	-149.4	0.227	-244.3	0.070	-149.4	C
0.231	-74.8	1.602	-156.0	0.857	-251.0	0.169	-156.0	D
0.199	-184.6	1.806	-265.6	0.683	-0.5	0.188	-265.6	E
0.313	-186.6	2.883	-267.9	1.236	-2.9	0.301	-267.9	F
0.011	-58.6	0.106	-284.0	0.045	-23.0	0.010	-284.0	G
0.001	-327.0	0.047	-115.5	0.017	-212.7	0.005	-115.5	H
0.162	-53.5	0.317	-121.6	0.078	-204.8	0.039	-121.6	J
0.042	-90.5	0.232	-328.4	0.125	-74.9	0.032	-328.4	K
0.012	-283.6	0.480	-71.1	0.156	-176.3	0.019	-71.1	L
0.206	-8.3	1.042	-88.8	0.269	-192.1	0.074	-88.8	M
0.741	-36.3	0.835	-108.3	0.127	-73.0	0.097	-108.3	N
0.0	-343.1	3.308	-80.5	0.849	-192.5	0.232	-80.5	O

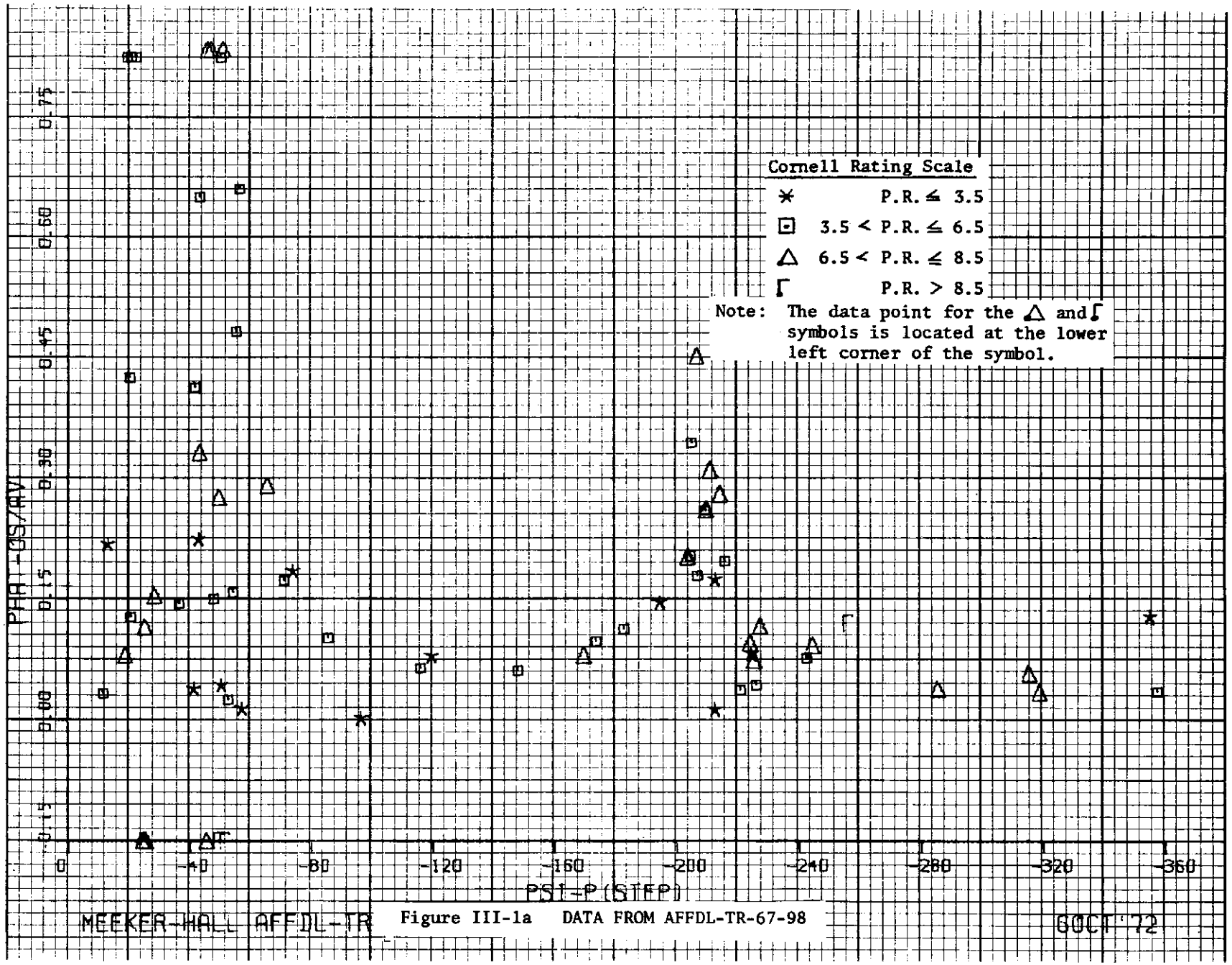

Figure III-1a DATA FROM AFFDL-TR-67-98

Figure III-1b DATA FROM AFFDL-TR-67-98

Figure III-1c DATA FROM AFFDL-TR-67-98

Figure III-1d DATA FROM AFFDL-TR-67-98

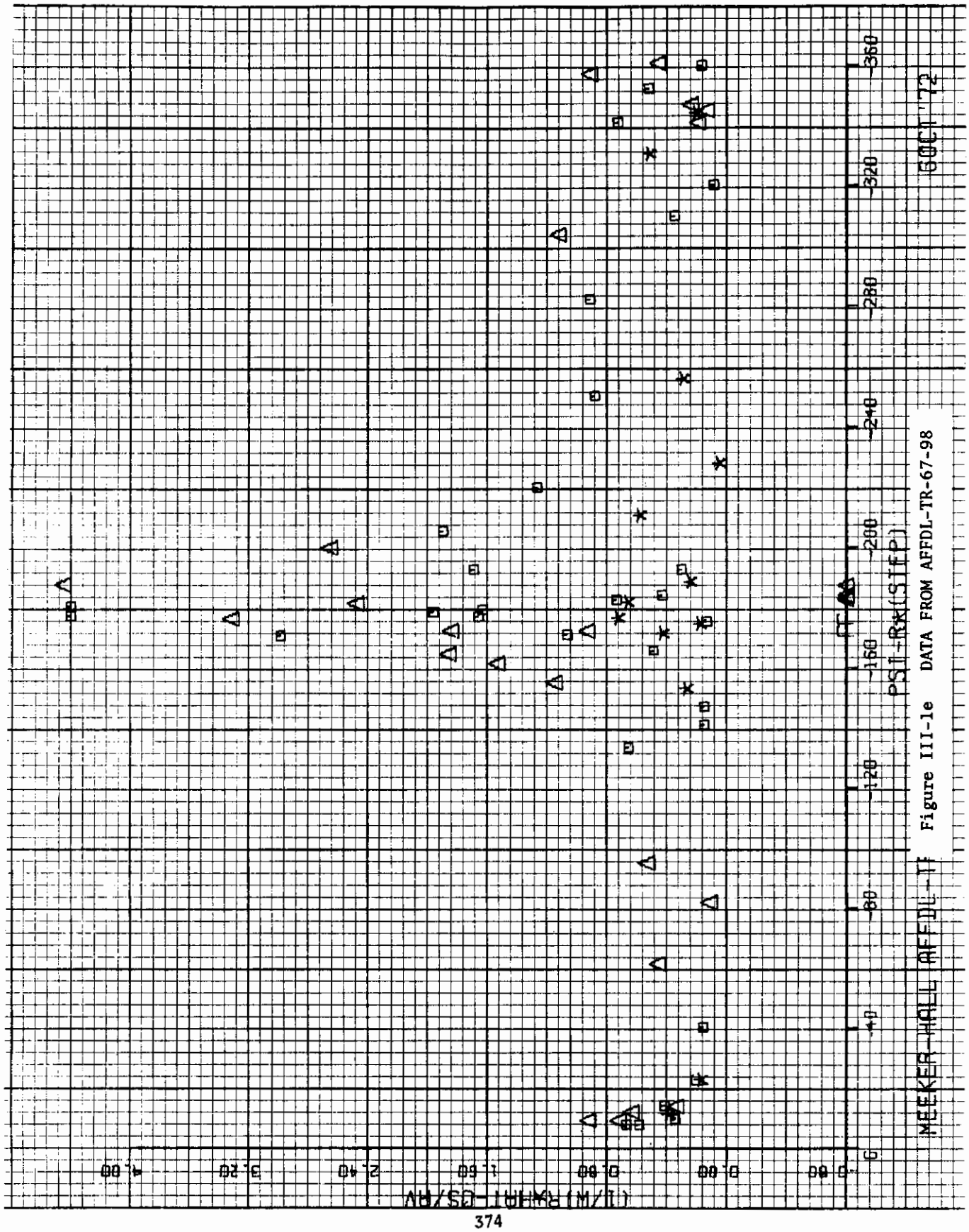

Figure III-1e DATA FROM AFFDL-TR-67-98

Figure III-1f DATA FROM AFFDL-TR-67-98

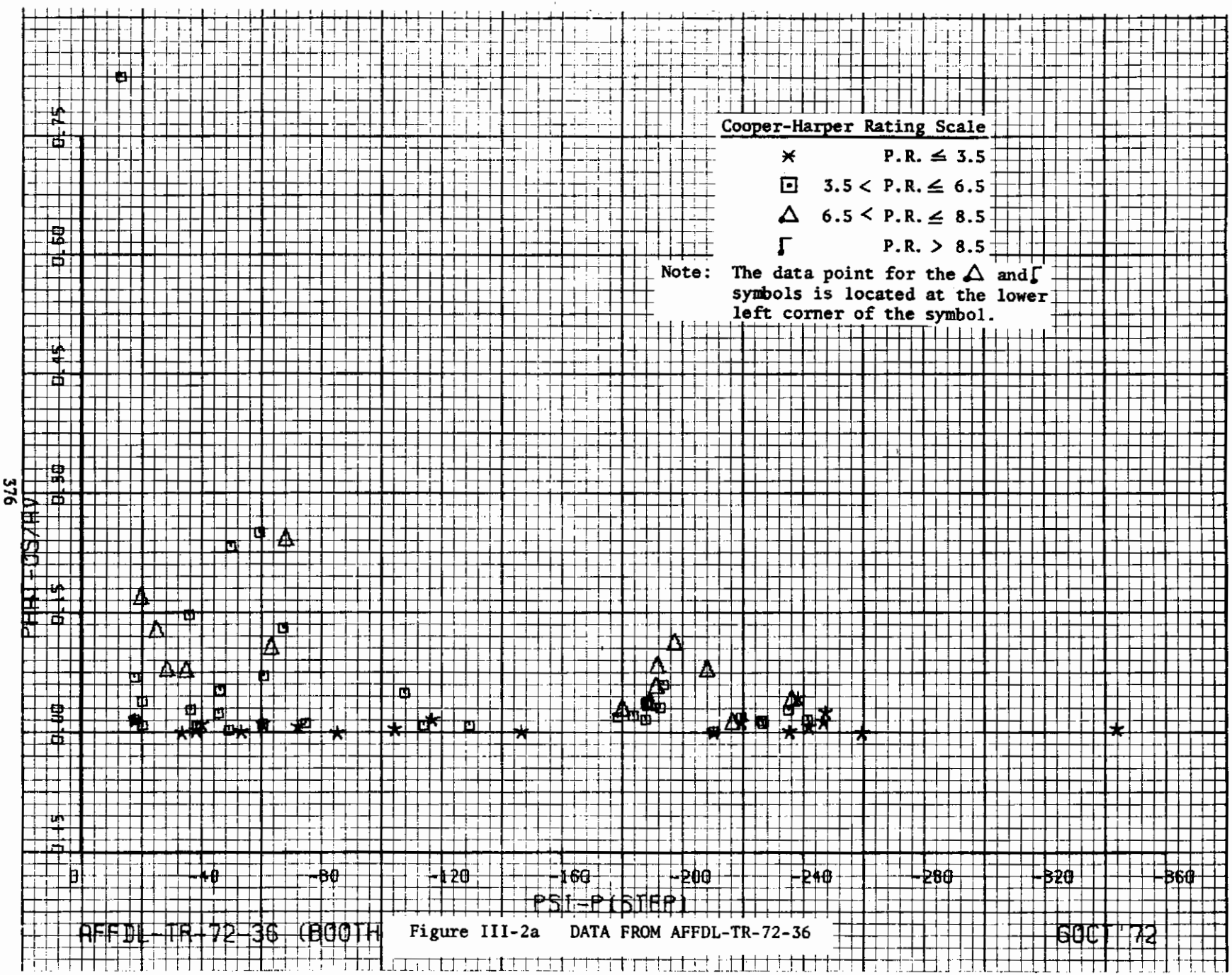

Figure III-2a DATA FROM AFFDL-TR-72-36

Figure III-2b DATA FROM AFFDL-TR-72-36

AFFDL-TR-72-36 (BOOT)

Figure III-2c DATA FROM AFFDL-TR-72-36

Figure III-2d DATA FROM AFFDL-TR-72-36

Figure III-2e DATA FROM AFFDL-TR-72-36

Figure III-2f DATA FROM AFFDL-TR-72-36

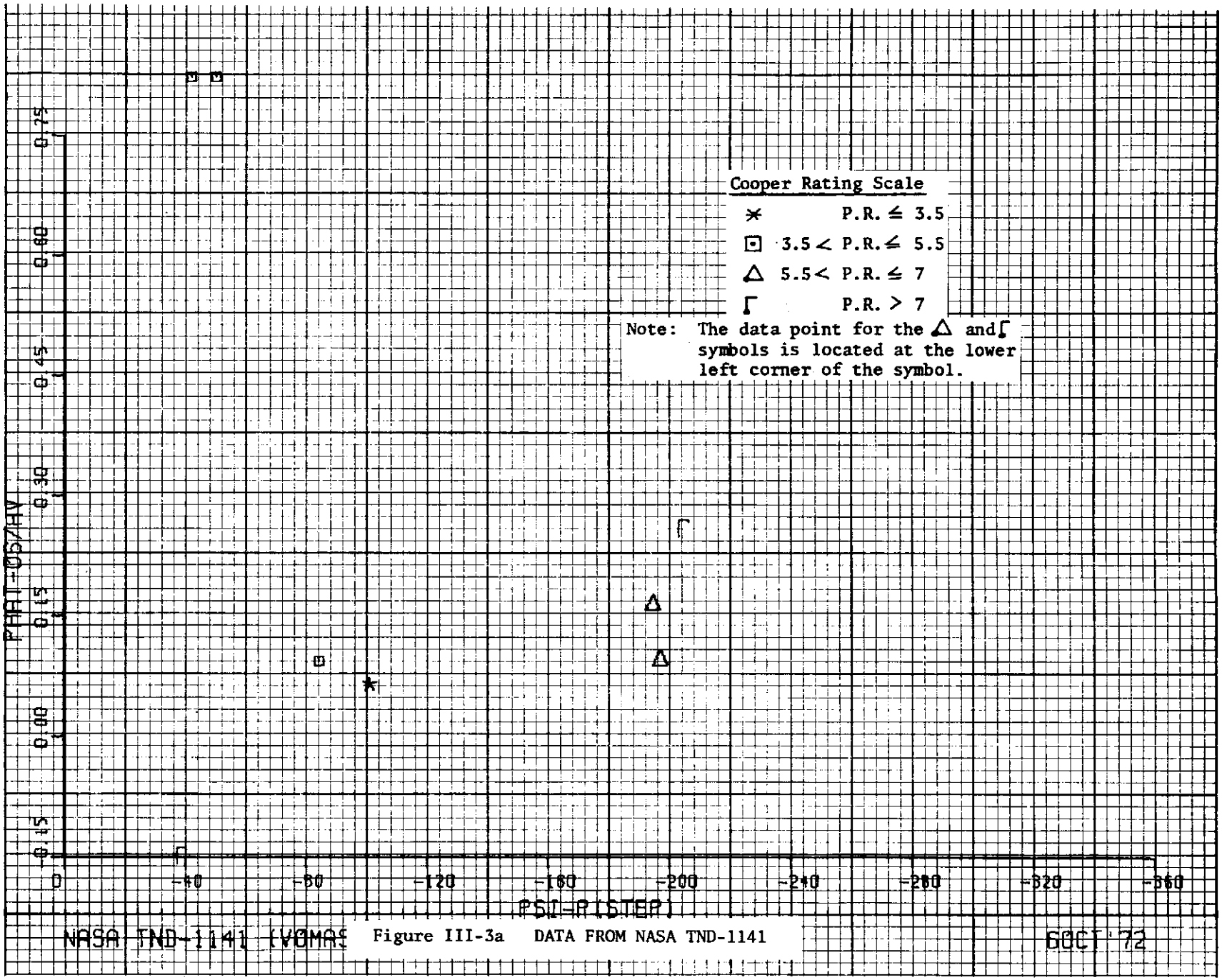

Figure III-3b DATA FROM NASA TDN-1141

Figure III-3c DATA FROM NASA TND-1141

Figure III-3e DATA FROM NASA TND-1141

Figure III-3f DATA FROM NASA TND-1141

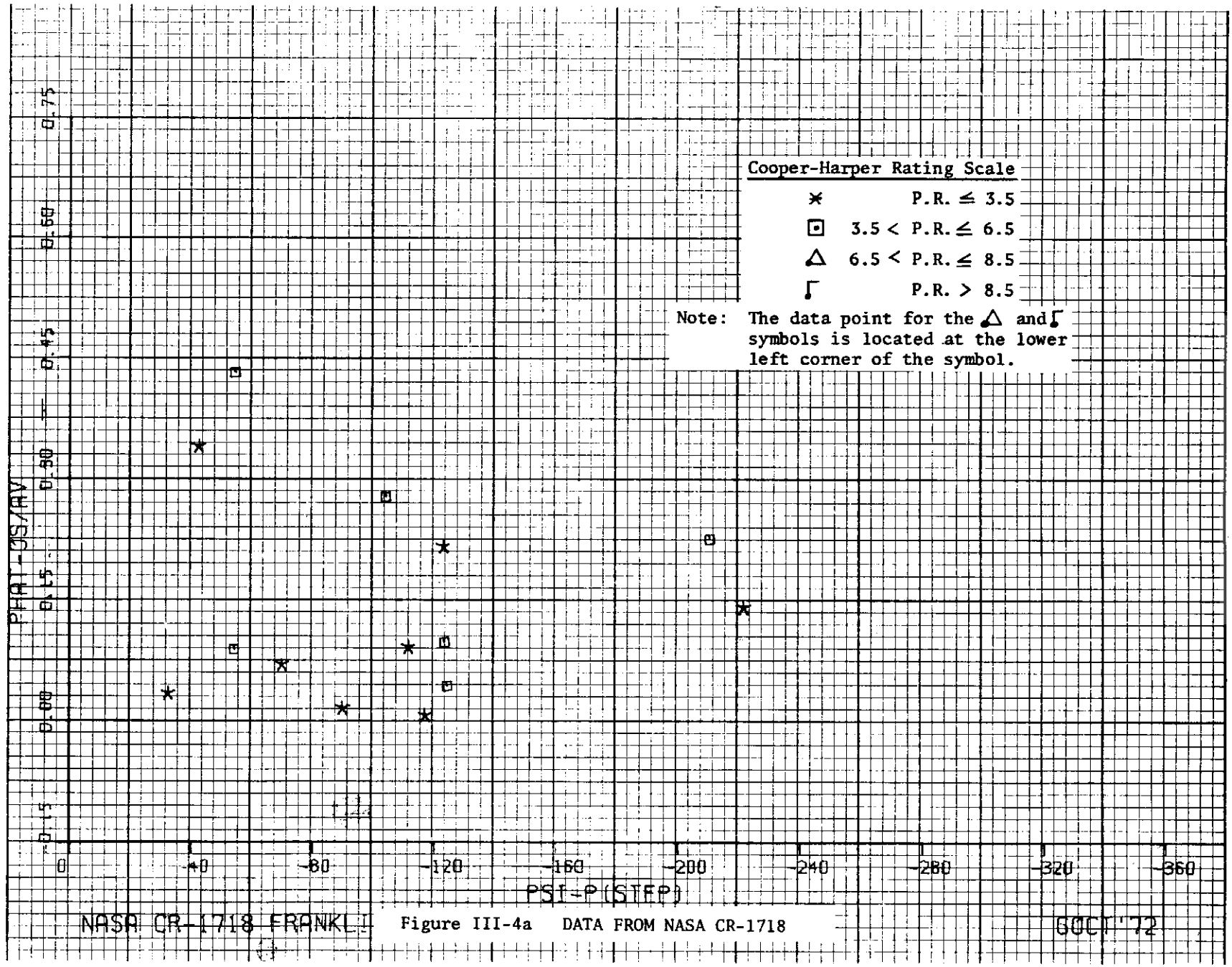

Figure III-4a DATA FROM NASA CR-1718

Figure III-4c DATA FROM NASA CR-1718

NASA CR-1718 FRANK Figure III-4d DATA FROM NASA CR-1718

Figure III-4e DATA FROM NASA CR-1718

NASA CR-1718 FRANK Figure III-4f DATA FROM NASA CR-1718

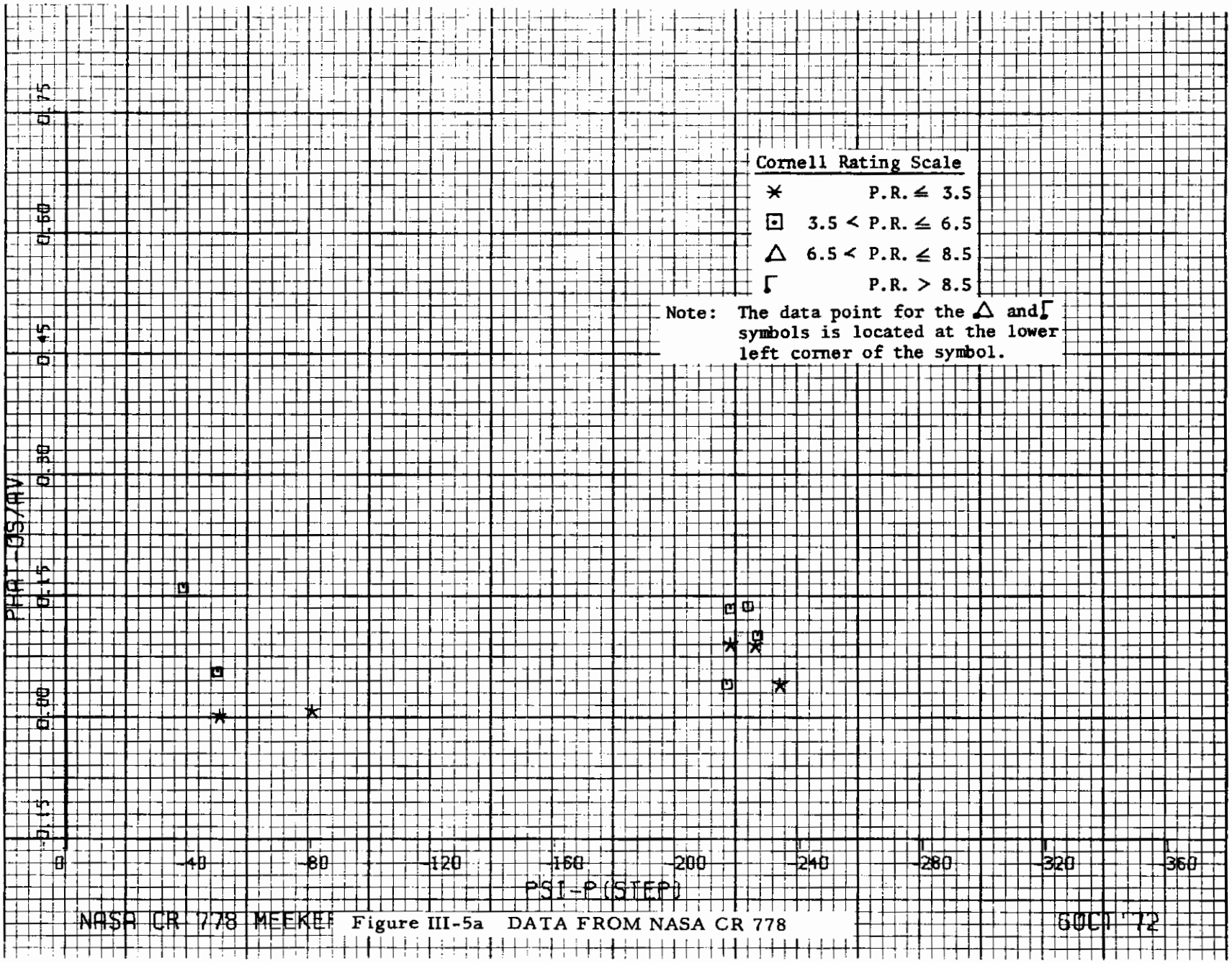

Figure III-5a DATA FROM NASA CR 778

Figure III-5c DATA FROM NASA CR 778

Figure III-5d DATA FROM NASA CR 778

Figure III-5f DATA FROM NASA CR 778

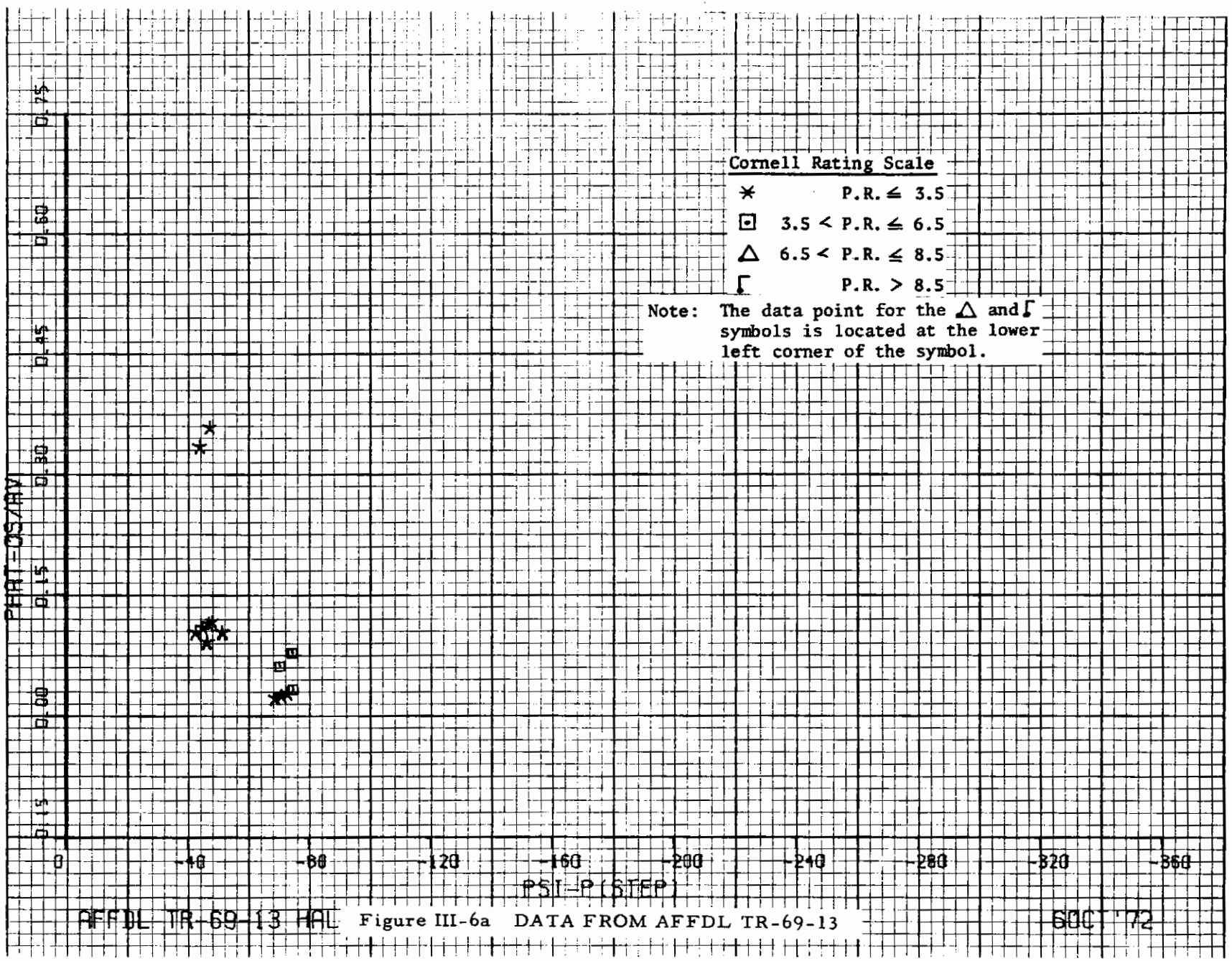

Figure III-6a DATA FROM AFFDL TR-69-13

Figure III-6c DATA FROM AFFDL TR-69-13

Figure III-6d DATA FROM AFFDL TR-69-13

Figure III-6e DATA FROM AFFDL TR-69-13

Figure III-6f

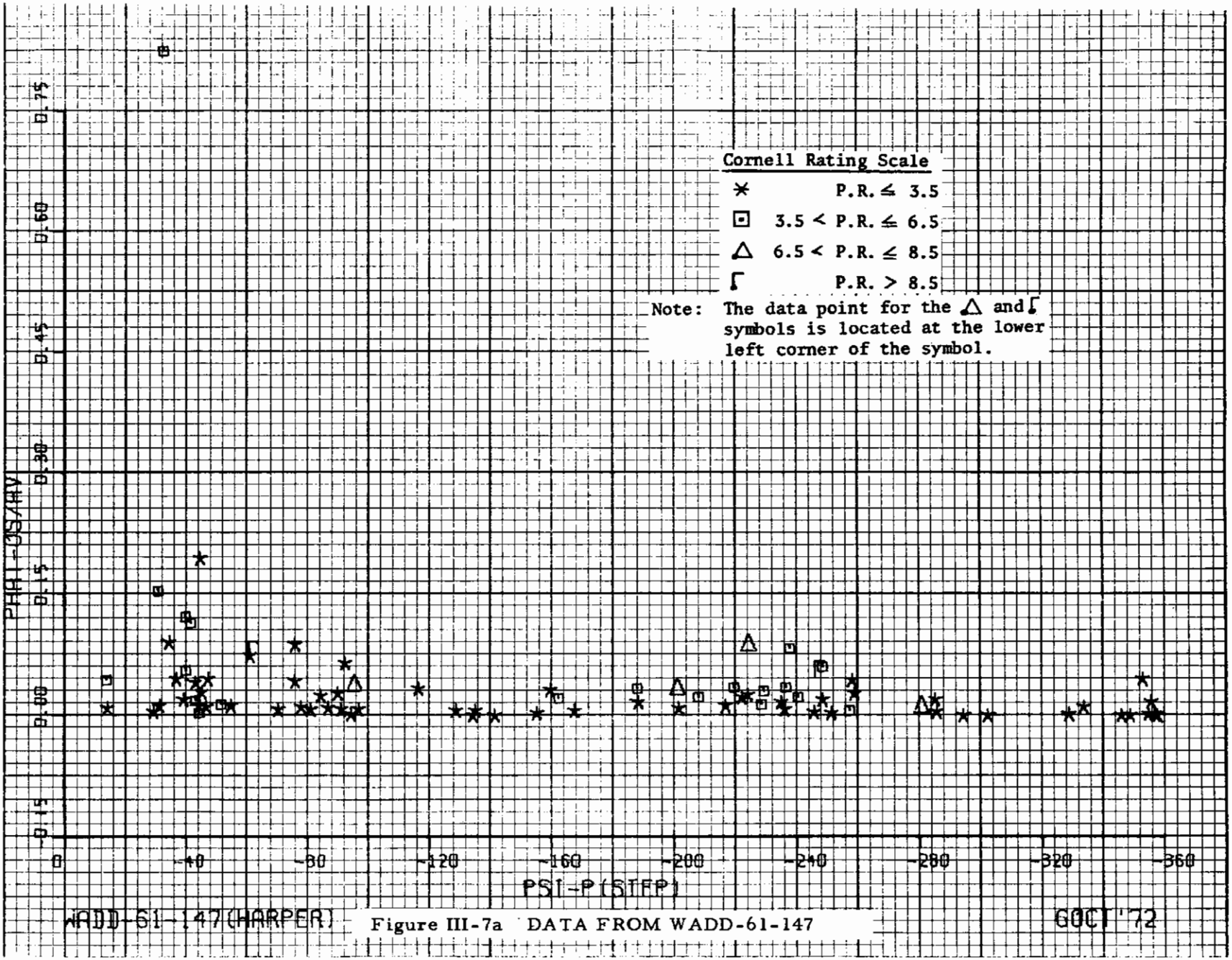

Figure III-7a DATA FROM WADD-61-147

Figure III-7b DATA FROM WADD-61-147

WADD-61-147(HARPER)

Figure III-7c DATA FROM WADD-61-147

Figure III-7d DATA FROM WADD-61-147

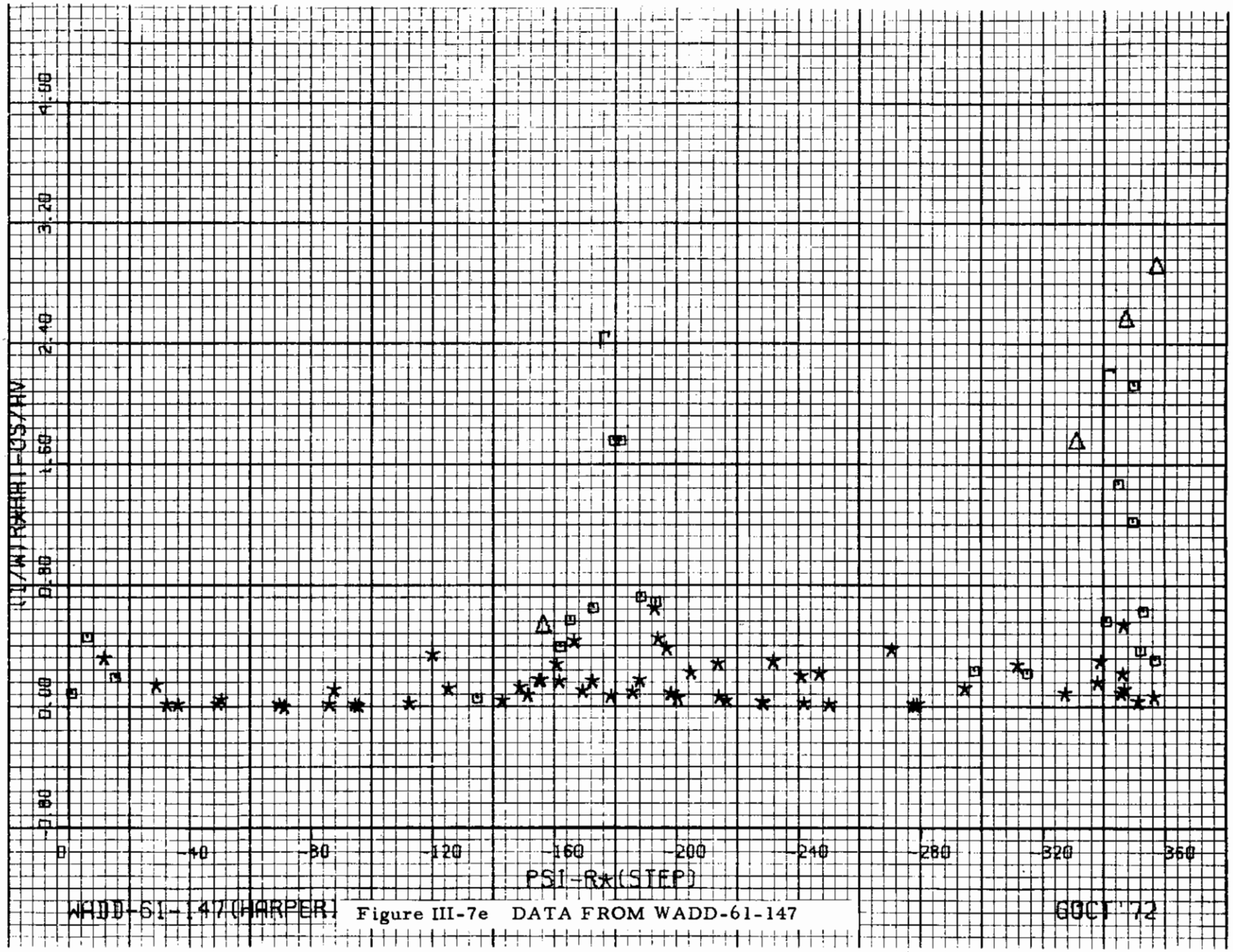

Figure III-7e DATA FROM WADD-61-147

Figure III-7f DATA FROM WADD-61-147

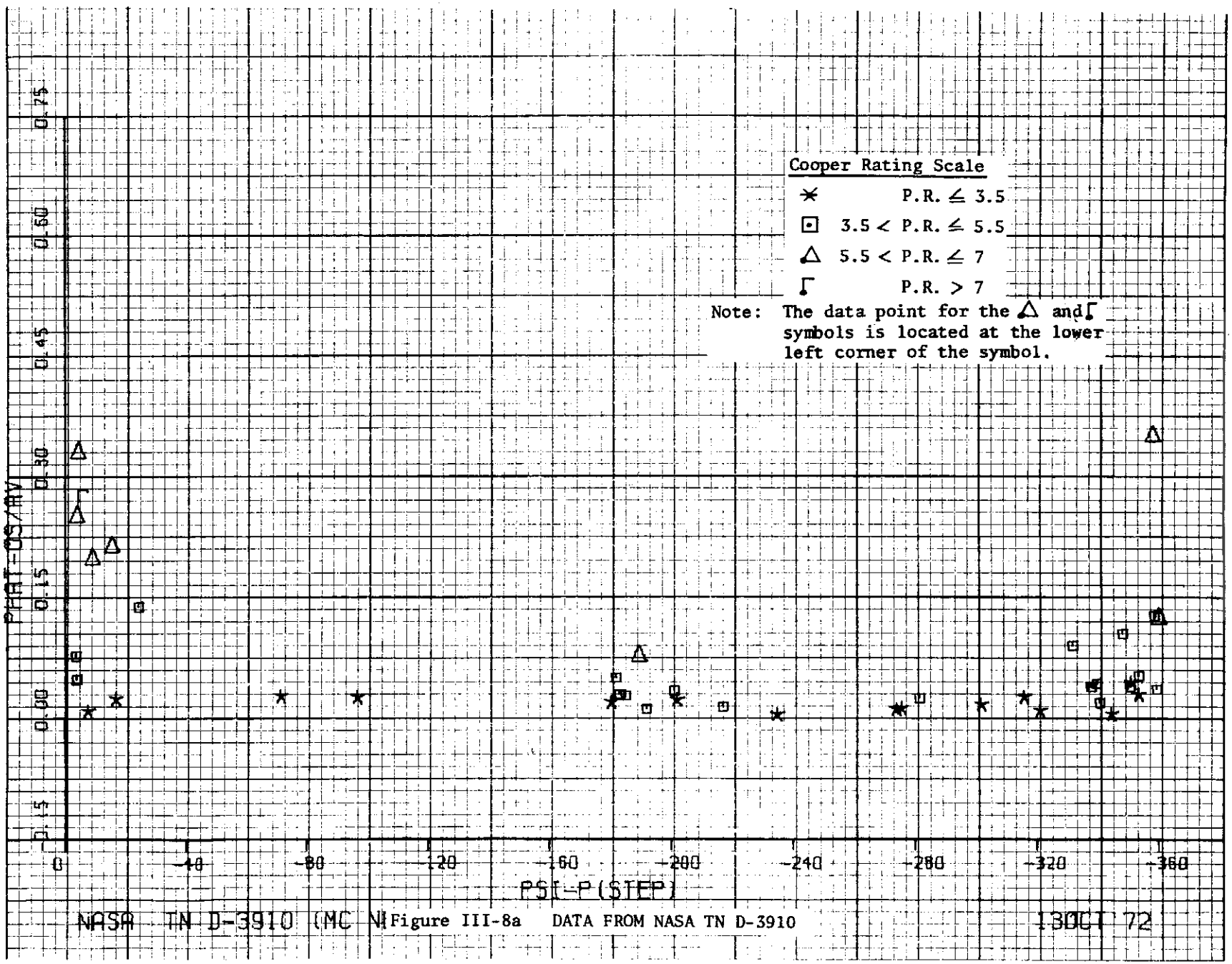

Figure III-8a DATA FROM NASA TN D-3910

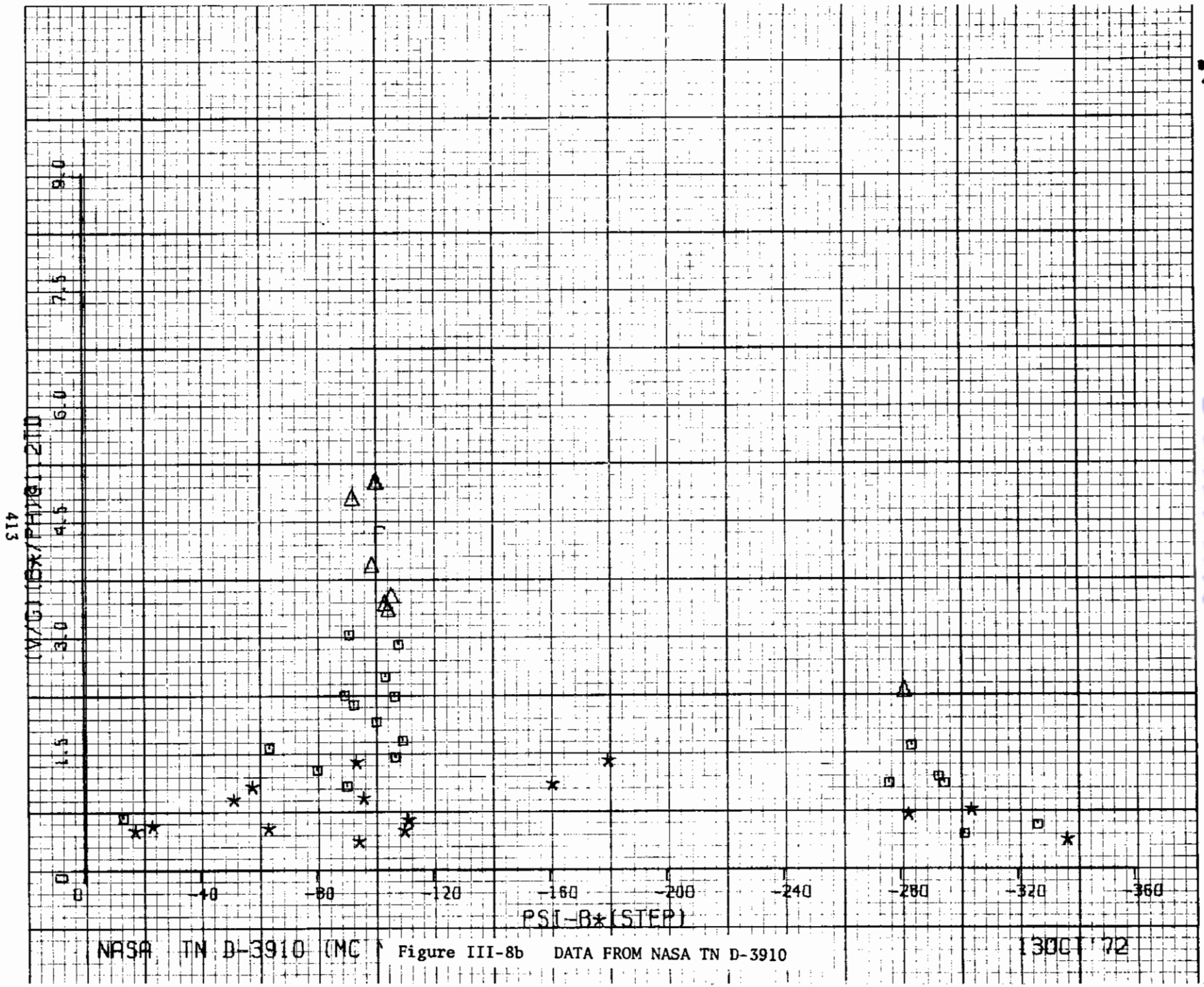

Figure III-8b DATA FROM NASA TN D-3910

Figure III-8c DATA FROM NASA TN D-3910

Figure III-8e DATA FROM NASA TN D-3910

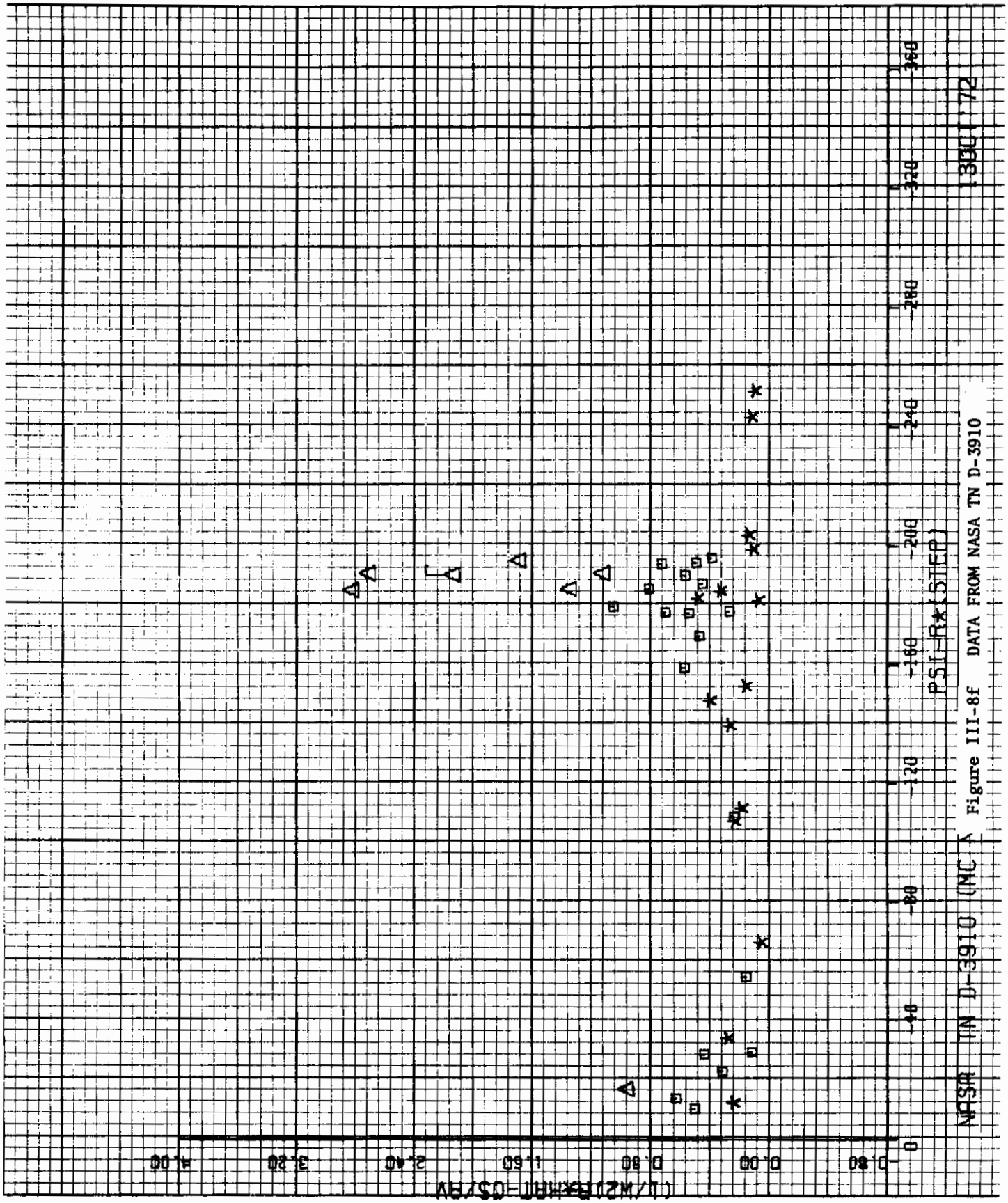

Figure III-8f DATA FROM NASA TN D-3910

NASA CR 2017 [SII] Figure III-9a DATA FROM NASA CR 2017

NHSA CR 2017 (STI) Figure III-9b DATA FROM NASA CR 2017

NASA CR 2017 (STI) Figure III-9c DATA FROM NASA CR 2017

NASA CR 2017 (STI) Figure III-9d DATA FROM NASA CR 2017

NASA CR 2017 (STI) Figure III-9e DATA FROM NASA CR 2017

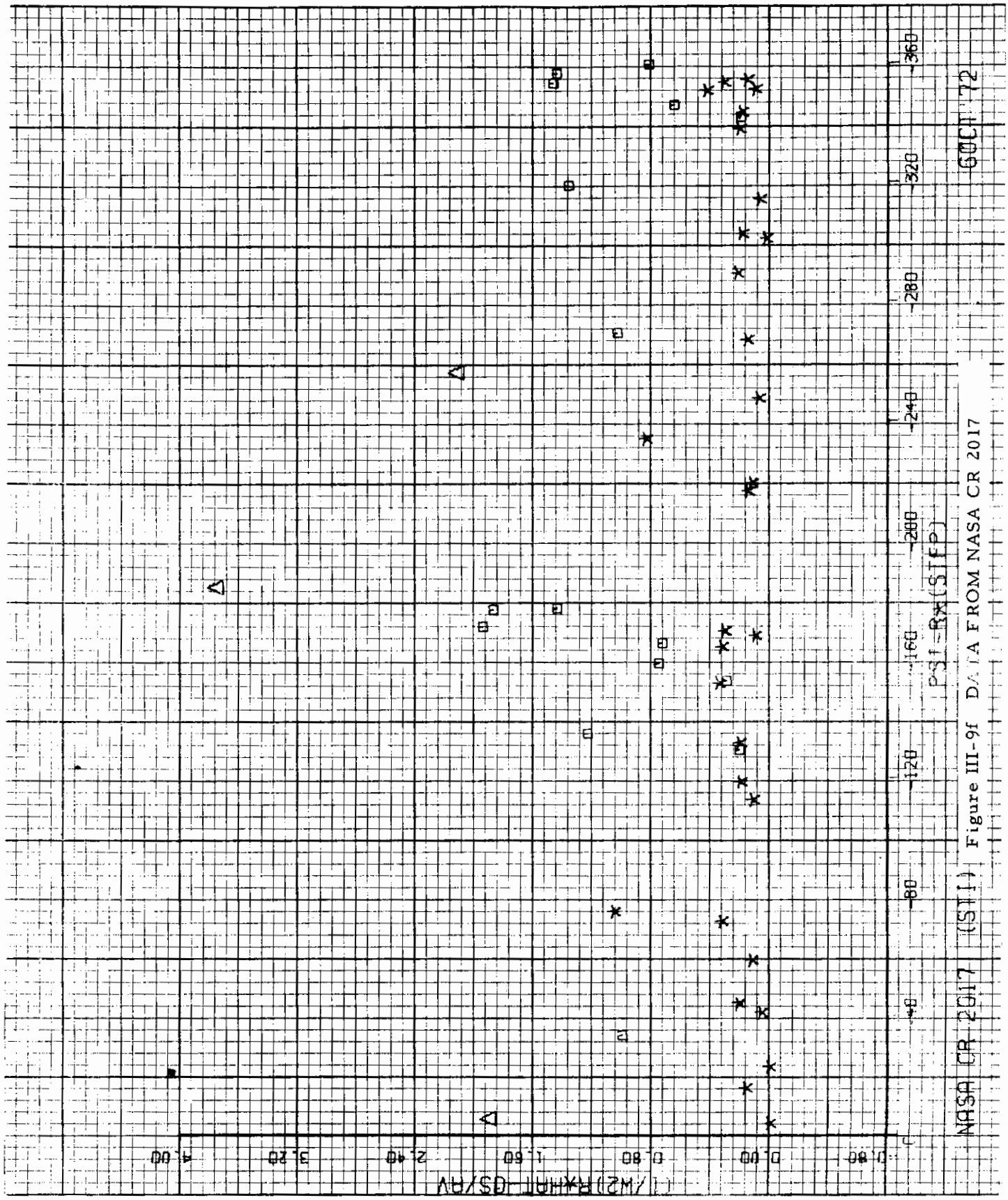

Figure III-9f

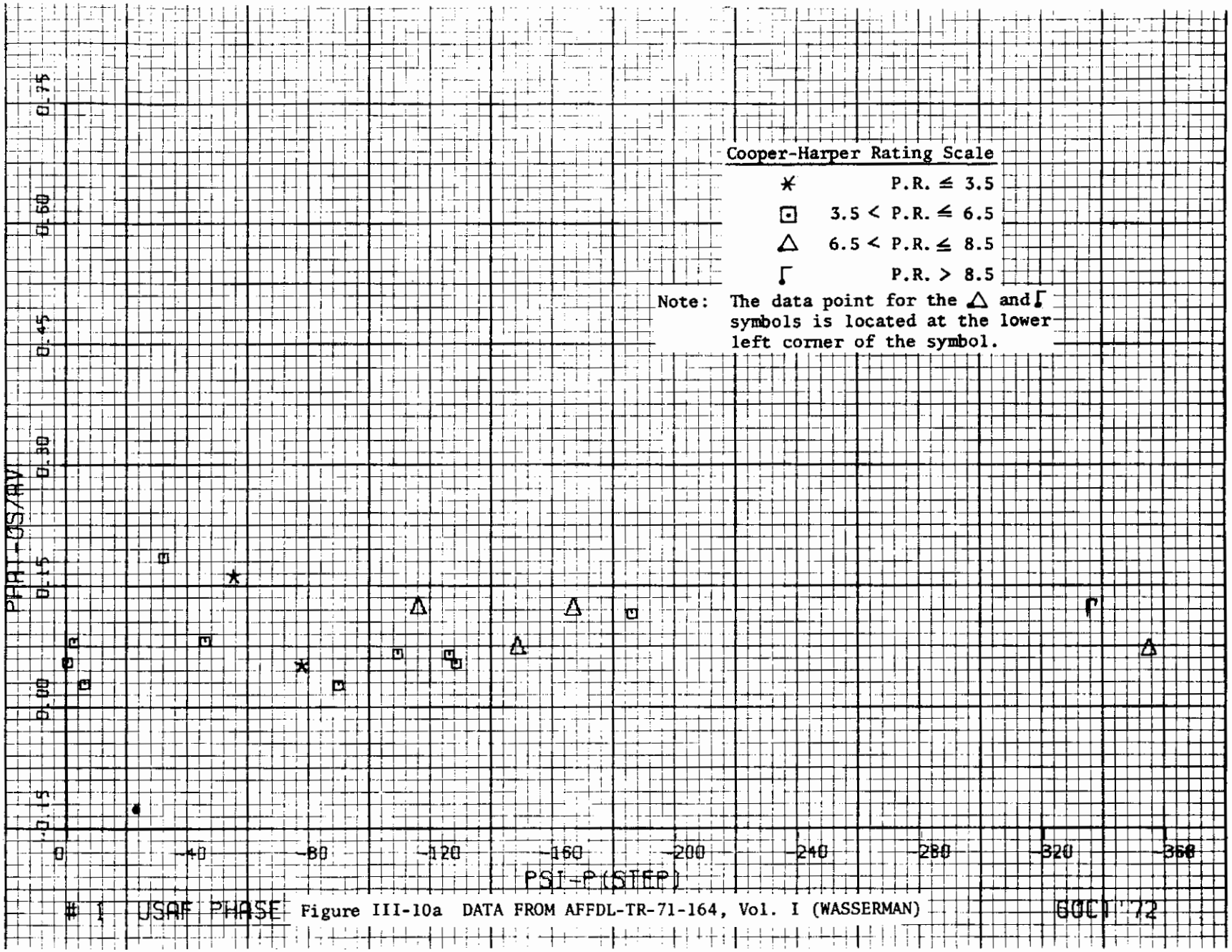

Figure III-10a DATA FROM AFFDL-TR-71-164, Vol. I (WASSERMAN)

Figure III-10b DATA FROM AFFDL-TR-71-164, Vol. I. (WASSERMAN)

Figure III-10c DATA FROM AFFDL-TR-71-164, Vol. I (WASSERMAN)

Figure III-10d DATA FROM AFFDL-TR-71-164, Vol. I (WASSERMAN)

Figure III-10e DATA FROM AFFDL-TR-71-164, Vol. I (WASSERMAN)

Figure III-10f DATA FROM AFFDL-TR-71-164, Vol. I (WASSERMAN)

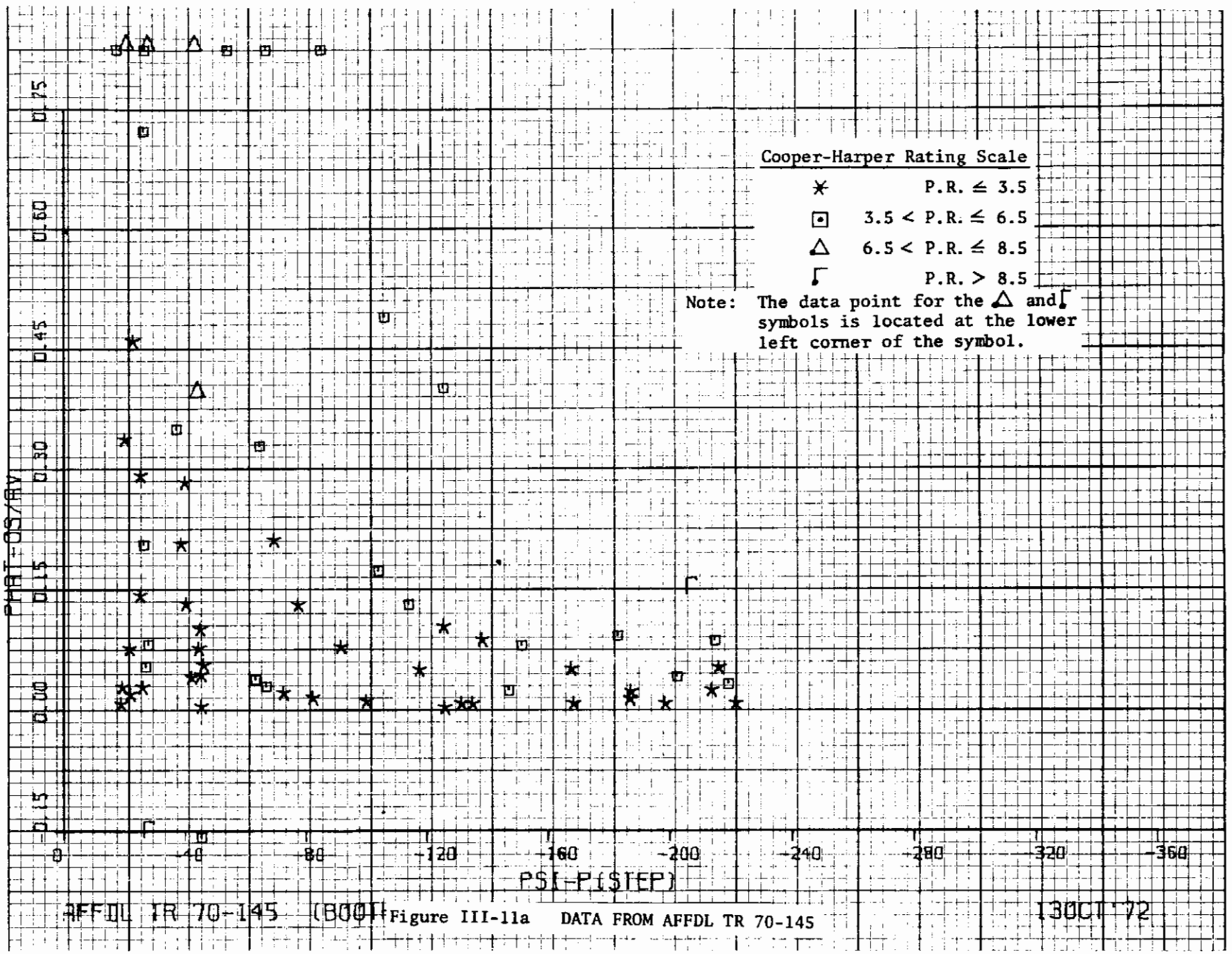

Figure III-11a DATA FROM AFFDL TR 70-145

Figure III-11b

Figure III-11c

Figure III-11d DATA FROM AFFDL TR 70-145

Figure III-11e DATA FROM AFFDL TR 70-145

Figure III-11f DATA FROM AFFDL TR 70-145

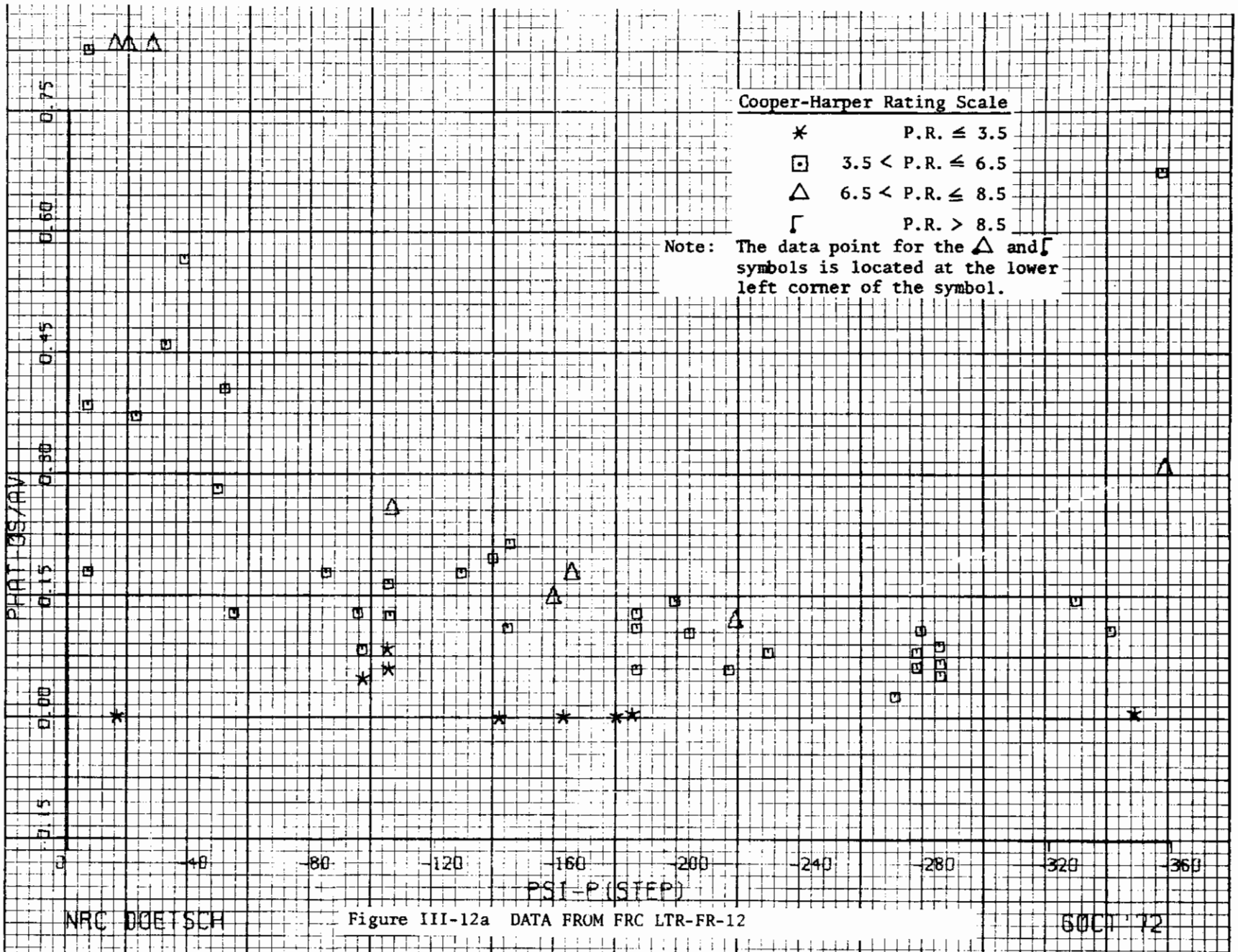

Figure III-12a DATA FROM FRC LTR-FR-12

Figure III-12b DATA FROM FRC LTR-FR-12

Figure III-12c DATA FROM FRC LTR-FR-12

Figure III-12d DATA FROM FRC LTR-FR-12

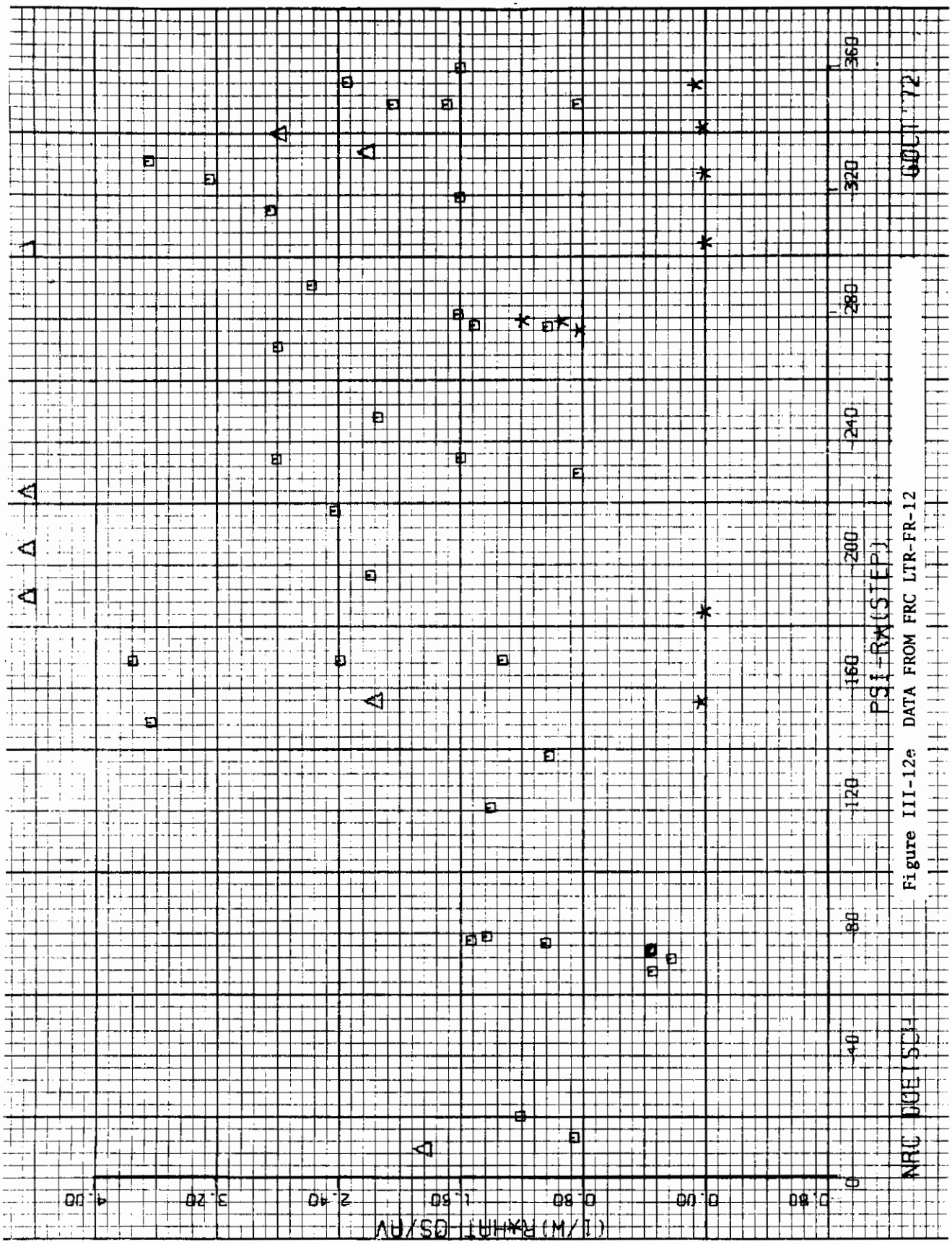

Figure III-12a DATA FROM FRC LTR-FR-12

Figure III-12f DATA FROM FRC LTR-FR-12

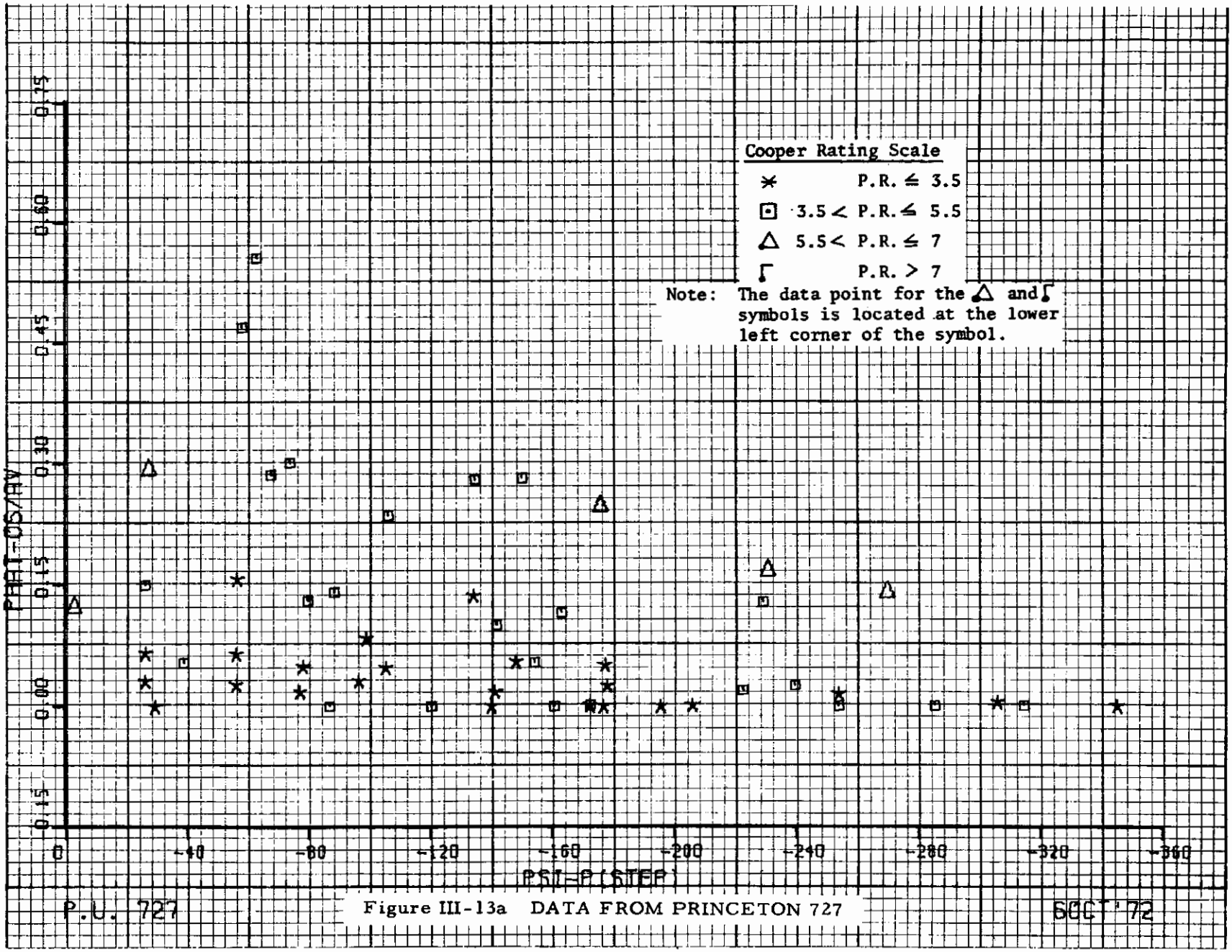

Figure III-13a DATA FROM PRINCETON 727

Figure III-13b DATA FROM PRINCETON 727

Figure III-13c DATA FROM PRINCETON 727

Figure III-13d DATA FROM PRINCETON 727

Figure III-13e DATA FROM PRINCETON 727

3i

Figure III-13f DATA FROM PRINCETON 727

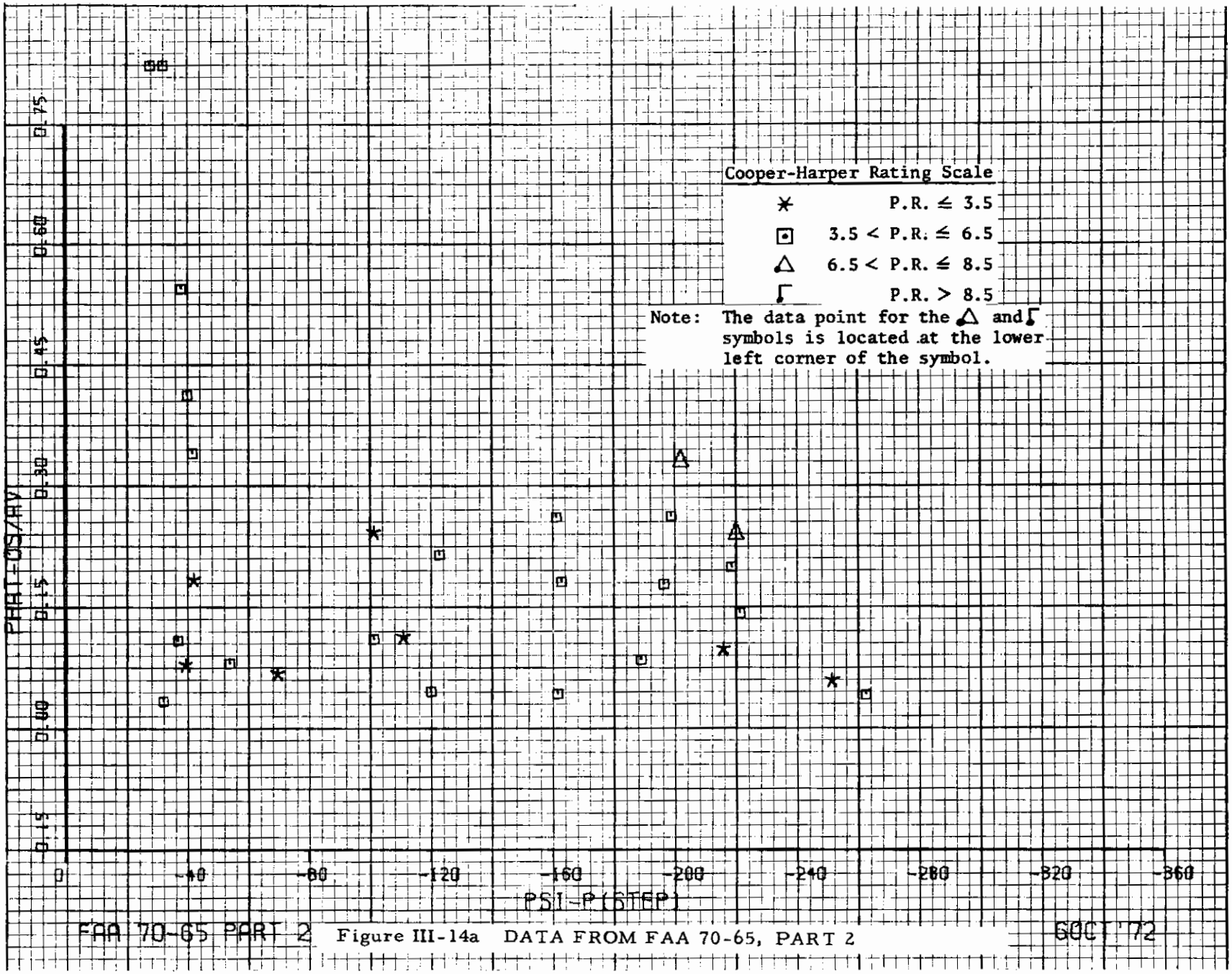

Figure III-14a DATA FROM FAA 70-65, PART 2

FAA 70-65 PAR Figure III-14b DATA FROM FAA 70-65, PART 2

Figure III-14c DATA FROM FAA 70665, PART 2

Figure III-14d DATA FROM FAA 70-65, PART 2

FAA 70-65 PART 2

Figure III-14e DATA FROM FAA 70-65, PART 2

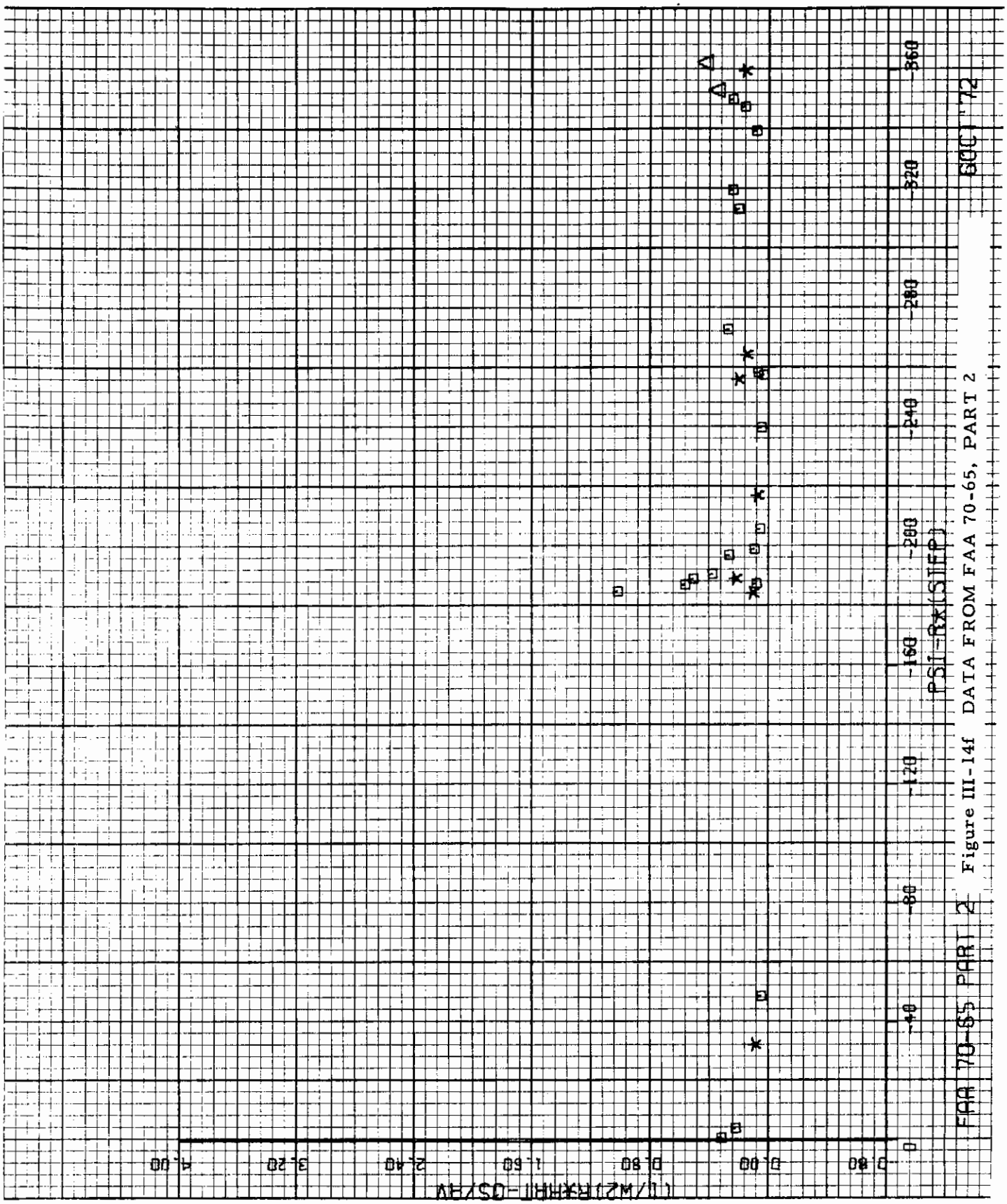

Figure III-14f DATA FROM FAA 70-65, PART 2

FAA RD-71-118 E Figure III-15a DATA FROM FAA RD-71-118

Figure III-15b DATA FROM FAA RD-71-118

Figure III-15c DATA FROM FAA RD-71-118

Figure III-15d DATA FROM FAA RD-71-118

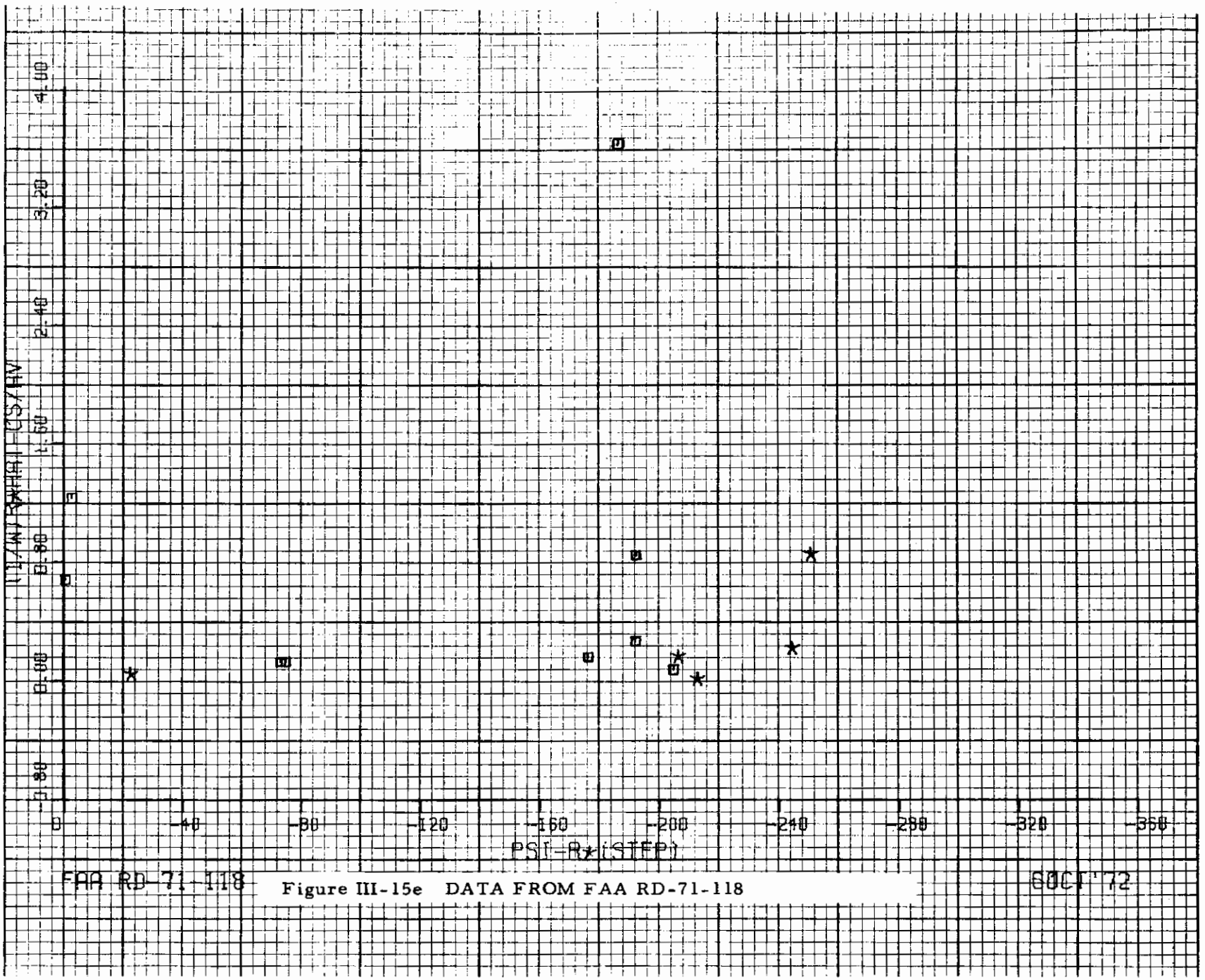

Figure III-15e DATA FROM FAA RD-71-118

Figure III-15f DATA FROM FAA RD-71-118

REFERENCES

1. Chalk, C.R., Neal, T.P., and Harris, T.M. : Final Report on the Revision of MIL-F-8785(ASG); "Military Specification - Flying Qualities of Piloted Airplanes." CAL No. BM-2238-F-6, July 1969. Also AFFDL-TR-69-45.

2. Anon. : Military Specification Flying Qualities of Piloted Airplanes. MIL-F-8785B(ASG), 7 August 1969.

3. Chalk, C.R. et al : Background Information and Users Guide for MIL-F-8785B(ASG) "Military Specification - Flying Qualities of Piloted Airplanes." AFFDL-TR-69-72, August 1969.

4. Neal, T.P.: Program Plan for Revision of MIL-F-8785B(ASG), "Flying Qualities of Piloted Airplanes." FRM No. 449, 19 February 1971.

5. Chen, R.T.N.: A New Development Toward Establishing a Unified Flying Qualities Theory of the Piloted Airplane in Landing Approach. FRM No. 465, 29 September 1971.

6. Neal, T.P.: Revision of Military Specification MIL-F-8785B(ASG), Flying Qualities of Piloted Airplanes. Memo No. 1 : Recommendations and Substantiation for Spin and Miscellaneous Requirements. FRM No. 454, March 1971.

7. Neal, T.P. : Revisions of Military Specification MIL-F-8785B(ASG) Flying Qualities of Piloted Airplanes. Memo No. 3: Proposed Longitudinal Maneuvering Requirements, With Substantiation. FRM No. 462, 23 July 1971.

8. Neal, T.P. and Smith R.E. : An In-Flight Investigation to Develop Control System Design Criteria for Fighter Airplanes. AFFDL-TR-70-74, Volume I and Volume II, June 1970.

9. Newell, F.D. and Wasserman, R. : In-Flight Investigation of Pitch Acceleration and Normal Acceleration Bobweights. AFFDL-TR-69-3, April 1969.

10. Kidd, E.A. and Bull, G. : Handling Qualities Requirements as Influenced by Pilot Evaluation Time and Sample Size. TB-1444-F-1, Cornell Aeronautical Laboratory, Inc., February 1962.

11. McFadden, N.M., Vomaske, R.F., and Heinle, D.R. :Flight Investigation Using Variable-Stability Airplanes of Minimum Stability for High-Speed, High-Altitude Vehicles. NASA TN D-779, April 1961.

12. Harper, R.P., Jr. : Flight Evaluations of Various Longitudinal Handling Qualities in a Variable-Stability Jet Fighter. WADC TR 55-299, July 1955.

13. Chalk, C.R. : Additional Flight Evaluations of Various Longitudinal Handling Qualities in a Variable-Stability Jet Fighter. WADC TR 57-719, July 1958.

14. Hall, G.W. : In-Flight Investigation of Longitudinal Short-Period Handling Characteristics of Wheel Control Airplanes. AFFDL-TR-68-91, July 1968.

15. DiFranco, D.A. : Flight Investigation of Longitudinal Short-Period Frequency Requirements and PIO Tendencies. AFFDL-TR-66-163, April 1967.

16. DiFranco, D.A. : In-Flight Investigation of the Effects of Higher-Order Control System Dynamics on Longitudinal Handling Qualities. CAL Report No. BM-2238-F-4 (AFFDL-TR-68-90), July 1968.

17. Eldridge, W. : A Simulator and Flight Evaluation of the Longitudinal and Lateral Control Requirements of the C-5A for the Landing Approach Task. Boeing Company D6-10725, 18 May, 1965.

18. Staff of Langley Research Center: Determination of Flight Characteristics of Supersonic Transports During the Landing Approach With a Large Jet Transport In-Flight Simulator. NASA TN D-3971, June 1967.

19. Chalk, C.R. : Flight Evaluation of Various Short-Period Dynamics at Four Drag Configurations for the Landing Approach Task. FDL-TDR-64-60, October 1964.

20. Eney, J.A. : Comparative Flight Evaluation of Longitudinal Handling Qualities in Carrier Approach. Report No. 777, Princeton University, May 1966.

21. A'Harrah, R.C. and Lockenour, J.L. : Wing Sizing Requirements Based on Flying Qualities in the Carrier Approach. North American Rockwell Report No. NR69H-178, March 1969.

22. Bull, G. : Minimum Flyable Longitudinal Handling Qualities of Airplanes. TB-1313-F-1, Cornell Aeronautical Laboratory, Inc. December, 1959.

23. Smith, R.E., Lebacqz, J.V., and Schuler, J.M. : Flight Investigation of Various Short-Term Dynamics for STOL Landing Approach Using the X-22A Variable Stability Aircraft. TB-3011-F-2, Cornell Aeronautical Laboratory, Inc., submitted to the Navy July 1972.

24. Powers, Bruce, G. : A Review of Transport Handling-Qualities Criteria in Terms of Preliminary XB-70 Flight Experience. NASA FRC TM-X-1584, May 1968.

25. Ashkenas, I.L., Jex, H.R., and McRuer, D.T. : Pilot-Induced Oscillations: Their Cause and Analysis. Norair Report NOR 64-143, 20 June 1964.

26. Terrill, W.H., Wong, J.G., and Springer, L.R. : Investigation of Pilot-Induced Longitudinal Oscillations in the Douglas Model A4D-2 Airplane. Report No. LB-25452, Douglas, 15 May 1957.

27. Hirsch, D.L. : Investigation and Elimination of PIO Tendencies in the Northrop T-38A. Northrop NORAIR Report,No number. SAE Paper for July 1964 Meeting, New York

28. ASD Review Board; Lt. Col. F. Finberg, Chairman : Report of the T-38 Flight Control System Pilot-Induced Oscillation (PIO) Review Board. Aeronautical Systems Div., No number, 15 February 1963.

29. Meeker, J.I. : Evaluation of Lateral-Directional Handling Qualities of Piloted Re-Entry Vehicles Utilizing Fixed-Base and In-Flight Evaluations. NASA CR-778, January 1966. Also CAL Report No. TC-1921-C-5.

30. Newell, F.D. : Ground Simulator Evaluations of Coupled Roll-Spiral Mode Effects on Aircraft Handling Qualities. AFFDL-TR-65-39, March 1965.

31. Hall, G.W. and Boothe, E.M. : An In-Flight Investigation of Lateral-Directional Dynamics and Roll-Control Power Requirement for the Landing Approach. AFFDL-TR-70-145, October 1971.

32. Seckel, E., et.al : Lateral-Directional Flying Qualities for Power Approach: Influence of Dutch-Roll Frequency. Princeton University Report No. 797, September 1967.

33. Doetsch, K.H. et.al : A Flight Investigation of Lateral-Directional Handling Qualities for V/STOL Aircraft in Low Speed Maneuvering Flight. National Research Council of Canada Report No. LTR-FR-12, 15 August 1969.

34. Stapleford, R.L. : Handling Qualities Criteria for the Space Shuttle Orbiter During the Terminal Phase of Flight. STI Technical Report No. 1002-1, August 1971.

35. Wasserman, R., et.al : In-Flight Investigation of an Unaugmented Class III Airplane in the Landing Approach Task, Phase I - Lateral-Directional Study. AFFDL-TR-71-164, Vol. I, January 1972.

36. Hall, G.W. : An In-Flight Investigation of Lateral-Directional Dynamics for Cruising Flight. FAA-ADS-69-13, December 1969.

37. Liddell, C.J., et.al: A Flight Study of Requirements for Satisfactory Lateral Oscillatory Characteristics of Fighter Aircraft. NACA RM A51E16, July 25, 1951.

38. Anon.: Analysis of Several Handling Quality Topics Pertinent to Advanced Manned Aircraft. AFFDL-TR-67-2, June 1967.

39. Kempel, R.W. : Analysis of a Coupled Roll-Spiral-Mode, Pilot-Induced Oscillation Experienced With the M2-F2 Lifting Body. NASA TN D-6496, September 1971.

40. Grantham, W.D. et.al: Simulator Study of Coupled Roll-Spiral Effects on Lateral-Directional Handling Qualities. NASA TN D-5466, March 1970.

41. Anon.: Critique of and Recommended Changes to July 1968 Draft of MIL-F-8785A. STI Working Paper No. 291-1, 30 September 1968.

42. Ashkenas, I.L. : A Study of Conventional Airplane Handling Quality Requirements, Part II - Lateral-Directional Oscillatory Handling Qualities. AFFDL-TR-65-138, Part II, November 1965.

43. Moore, N.B. : Artificial Stability Flight Tests of the XF-88A Airplane. WADC TR 52-298, July 1954.

44. Barnes, A.G. and Parsons, N.A. : A Flight Simulator Investigation of the Effect of Turbulence on Rolling Requirements at Low Speed. British Aircraft Corporation Ltd. Report No. Ae303, May 1970.

45. Meeker, J.I. and Hall, G.W. : In-Flight Evaluation of Lateral-Directional Handling Qualities for the Fighter Mission. CAL Report BM-2238-F-2. AFFDL-TR-67-87, July 1967.

46. Boothe, E.M. and Parrag, M.L. : Evaluation of Lateral-Directional Handling Qualities and Roll-Sideslip Coupling of Fighter-Class Airplanes. CAL Report BM-3053-F-2, AFFDL TR-72-36, May 1972.

47. Vomaske, R.F., Sadoff, M., and Drinkwater, F.J. III : The Effect of Lateral-Directional Control Coupling on Pilot Control of an Airplane as Determined in Flight and in a Fixed-Base Flight Simulator. NASA TN D-1141, November 1961.

48. Franklin, J.A. : Turbulence and Lateral-Directional Flying Qualities. NASA CR-1718, April 1971. Prepared by Princeton University .

49. Harper, R.P., Jr. : In-Flight Simulation of the Lateral-Directional Handling Qualities of Entry Vehicles. CAL Report TE-1243-F-2, WADC TR 61-147, February 1961.

50. McNeill W.E. and Innis, R.C. : A Simulator and Flight Study of Yaw Coupling in Turning Maneuvers of Large Transport Aircraft. Ames Research Center. NASA TN D-3910, May 1967.

51. Stapleford, R.L., Klein, R.H., and Hoh, R.H. : Handling Qualities Criteria for the Space Shuttle Orbiter During the Terminal Phase of Flight. Prepared by Systems Technology, Inc. NASA CR-2017, April 1972.

52. Seckel, E., Miller, G.E., and Nixon, W.G. : Lateral-Directional Flying Qualities for Power Approach. Princeton University Report No. 727, June 1965.

53. Ellis, D.R. : Flying Qualities of Small General Aviation Airplanes, Part 2, The Influence of Roll Control Sensitivity, Roll Damping, Dutch Roll Excitation, and Spiral Stability. FAA Report No. FAA-RD-70-65, April 1970.

54. Ellis, D.E. : Flying Qualities of Small General Aviation Airplanes, Part 4, Review of Recent In-Flight Simulation Experiments and Some Suggested Criteria. FAA RD-71-118, December 1971.

55. Anon. : Military Specification - Flying Qualities of Piloted V/STOL Aircraft. MIL-F-83300, 31 December 1970.

56. Chalk, C.R., et.al : Background Information and User Guide for MIL-F-83300 - Military Specification - Flying Qualities of Piloted V/STOL Aircraft. AFFDL-TR- 70-88, March 1971.

57. Quigley, H.C. et.al: Lateral-Directional Augmentation Criteria for Jet Swept-Wing Transport Airplanes Operating at STOL Airspeeds. Conference on V/STOL and STOL Aircraft, NASA SP-116, April 1966.

58. McNeill, W.E. and Innis, R.C.: The Effect of Yaw Coupling in Turning Maneuvers of Large Transport Aircraft. Conference on Aircraft Operating Problems, NASA SP-83, May 1965.

59. Anderson, S.B. et.al: Some Performance and Handling-Qualities Consideration for Operation of STOL Aircraft. Conference on Aircraft Operating Problems, NASA SP-83, May 1965.

60. Drake, D.E. et.al: A Flight Simulator Study of STOL Transport Lateral Control Characteristics. FAA-RD-70-61, September 1970.

61. Levy, E.C. : Table of Laplace Transforms. Douglas Aircraft Company, Inc. Report No. SM-14745, Rev. March 1953.

62. Holleman, E.C. and Gilyard, G.B. : In-Flight Evaluation of the Lateral Handling of a Four-Engine Jet Transport During Approach and Landing. NASA TN D-6339, May 1971.

63. Perry, D.H. et.al: A Flight Study of the Sidestep Manoeuvre During Landing. Aeronautical Research Council Report No. R. & M. No. 3347, 1964.

64. Stapelford, R.L. et.al: Outsmarting MIL-F-8785B(ASG), The Military Flying Qualities Specification. STI TR-190-1, August 1971.

65. Craig, S.J. and Ashkenas I.L.: Background Data and Recommended Revisions for MIL-F-8785B(ASG), Military Specification - Flying Qualities of Piloted Airplanes. STI TR-189-1, June 1970.

66. Teunissen, H.W.: Characteristics of the Mean Wind and Turbulence in the Planetary Boundary Layer. University of Toronto UTIAS Review No. 32, October 1970.

67. Lumley, J.L., and Panofsky, H.A. : "The Structure of Atmospheric Turbulence" Interscience, 1964.

68. Houbolt, J.C., Steiner, R., and Pratt, K.G. : Dynamic Response of Airplanes to Atmospheric Turbulence Including Flight Data on Input and Response. NASA TR R-199, June 1964.

69. Letter to F.E. Pritchard of the Cornell Aeronautical Laboratory from D.R. Schaeffer of the Boeing Company, April 29, 1970.

70. Monin, A.S., and Obukhov, A.M. : Basic Laws of Turbulent Mixing in the Ground Layer of the Atmosphere. Translated from Akademiia Nank SSSR, Leningrad, Geofizicheskii Institut Trudy, No. 24 (151), pp 163-187, 1954.

71. Businger, J.A., Wyngaard, J.C., Izumi, Y., and Bradley, E.F. : "Flux-Profile Relationships in the Atmospheric Surface Layer." Journal of the Atmospheric Sciences, Vol. 28, 1971 (pg 181-189).

72. Schlichting, H.: Boundary-Layer Theory. McGraw-Hill, 1968.

73. Wyngaard, J.C., and Cotē, O.R. : "Co-Spectral Similarity in the Atmospheric Surface Layer" , paper submitted to the Quarterly Journal of the Royal Meteorological Society.

74. Wyngaard, J.C., Cote, O.R., and Izumi, Y.: "Local Free Convection, Similarity, and the Budgets of Shear Stress and Heat Flux." Journal of the Atmospheric Sciences, Vol. 28, 1971, (pp 1171-1182).

75. Pritchard, F.E., Easterbrook, C.C., and McVehil, G.E.: Spectral and Exceedance Probability Models of Atmospheric Turbulence for Use in Aircraft Design and Operation. AFFDL TR 65-122, October 1965.

76. Dutton, J.A., Panofsky, H.A., Deaven, D.C., Kerman, B.R., and Mirabella, V. : Statistical Properties of Turbulence at the Kennedy Space Center for Aerospace Vehicle Design. NASA CR-1889, August 1971.

77. Gera, J. : The Influence of Vertical Wind Gradients on the Longitudinal Motion of Airplanes. NASA TND-6430, September 1971.

78. Graham, D. et.al: Investigation of Measuring System Requirements for Instrument Low Visibility Approach. AFFDL-TR-70-102, February 1971.

79. FAA Advisory Circular AC No. 20-57A, 12 January 1971.

80. Dolbin, B. and Eckhart, F.E. : Investigation of Lateral-Directional Handling Qualities of V/STOL Airplanes in Cruising Flight. CAL Report TB-1794-F-3, December 1963.

81. Walunas, J.: The Turn Entry Maneuver. Cornell Aeronautical Laboratory Flight Research Department VTOL H.Q. TM-21, December 1969.

Unclassified
Security Classification

DOCUMENT CONTROL DATA - R & D

(Security classification of title, body of abstract and indexing annotation must be entered when the overall report is classified)

1. ORIGINATING ACTIVITY (Corporate author) Calspan Corporation Box 235 Buffalo, New York 14221	2a. REPORT SECURITY CLASSIFICATION 2b. GROUP

3. REPORT TITLE
REVISIONS TO MIL-F-8785B(ASG) PROPOSED BY CORNELL AERONAUTICAL LABORATORY UNDER CONTRACT F33615-71-C-1254

4. DESCRIPTIVE NOTES (Type of report and inclusive dates)
FINAL REPORT

5. AUTHOR(S) (First name, middle initial, last name)
Chalk, Charles, R.; DiFranco, Dante A.; Lebacqz, J.Victor; Neal, T. Peter

6. REPORT DATE	7a. TOTAL NO. OF PAGES	7b. NO. OF REFS
April 1973	469	81

8a. CONTRACT OR GRANT NO.	9a. ORIGINATOR'S REPORT NUMBER(S)
AF33615-71-C-1254 b. PROJECT NO. 8219 c. Task No. 821905 d.	BM-3054-F-1 9b. OTHER REPORT NO(S) (Any other numbers that may be assigned this report) AFFDL-TR-72-41

10. DISTRIBUTION STATEMENT
Approved for public release; distribution unlimited

11. SUPPLEMENTARY NOTES	12. SPONSORING MILITARY ACTIVITY
	Air Force Flight Dynamics Laboratory Air Force Systems Command Wright-Patterson Air Force Base, 45433

13. ABSTRACT

In August 1969, the Air Force and the Naval Air Systems Command adopted MIL-F-8785B(ASG) as the official Military Specification for Flying Qualities of Piloted Airplanes. Since that time effort has been sponsored by the Air Force to further improve the specification document and to increase its applicability in the development of future weapons systems. Results of a study performed by Calspan (formerly Cornell Aeronautical Laboratory) are presented in this report. Changes to the requirements of MIL-F-8785B(ASG) are suggested in the following areas:

1. Longitudinal maneuvering dynamics and control gradients.
2. Lateral-directional maneuvering dynamics and roll-sideslip coupling.
3. Atmospheric disturbance models.
4. Stall-spin characteristics.
5. Numerous miscellaneous corrections and changes.
6. Additions to Background Information and Users Guide for MIL-F-8785B(ASG).

Substantiation data for the recommended changes is also presented.

DD FORM 1 NOV 68 1473

Unclassified
Security Classification

14. KEY WORDS	LINK A		LINK B		LINK C	
	ROLE	WT	ROLE	WT	ROLE	WT
Flying Qualities						
MIL-F-8785B(ASG), Revisions						
Longitudinal Dynamics						
Lateral-Directional Dynamics						
Atmospheric Disturbance Models						
Stall/Spin Characteristics						
Handling Qualities						
Flight Dynamics						
Airplane Design						

☆U.S.Government Printing Office: 1974 — 758-433/534